



**HAL**  
open science

# Study of the molecular mechanisms that maintain iron homeostasis in plants

Fei Gao

► **To cite this version:**

Fei Gao. Study of the molecular mechanisms that maintain iron homeostasis in plants. Plants genetics. Montpellier SupAgro, 2021. English. NNT : 2021NSAM0054 . tel-04041490

**HAL Id: tel-04041490**

**<https://theses.hal.science/tel-04041490>**

Submitted on 22 Mar 2023

**HAL** is a multi-disciplinary open access archive for the deposit and dissemination of scientific research documents, whether they are published or not. The documents may come from teaching and research institutions in France or abroad, or from public or private research centers.

L'archive ouverte pluridisciplinaire **HAL**, est destinée au dépôt et à la diffusion de documents scientifiques de niveau recherche, publiés ou non, émanant des établissements d'enseignement et de recherche français ou étrangers, des laboratoires publics ou privés.

# THÈSE POUR OBTENIR LE GRADE DE DOCTEUR DE MONTPELLIER SUPAGRO

En Biologie, Interactions, Diversité Adaptative des Plantes (BIDAP)

École doctorale GAIA – Biodiversité, Agriculture, Alimentation, Environnement, Terre, Eau

Portée par

Unité de recherche Biochimie et Physiologie Moléculaire des Plantes (BPMP)

## Étude des mécanismes moléculaires contrôlant l'homéostasie du fer chez les plantes

Présentée par Fei GAO

Le 22 juin 2021

Sous la direction de Christian DUBOS

Devant le jury composé de

Jacqueline GRIMA-PETTENATI, Directrice de recherche CNRS, LRSV, Toulouse

Sébastien THOMINE, Directeur de recherche CNRS, I2BC, Gif-sur-Yvette

José GENTILHOMME, Maître de conférence Université d'Angers, IRHS, Angers

Loïc LEPINIEC, Directeur de recherche INRAE, IJPB, Versailles

Gabriel KROUK, Directeur de recherche CNRS, BPMP, Montpellier

Rapporteur

Rapporteur

Examineur

Examineur

Président



UNIVERSITÉ  
DE MONTPELLIER

Montpellier  
SupAgro



# THÈSE POUR OBTENIR LE GRADE DE DOCTEUR DE MONTPELLIER SUPAGRO

En Biologie, Interactions, Diversité Adaptative des Plantes (BIDAP)

École doctorale GAIA – Biodiversité, Agriculture, Alimentation, Environnement, Terre, Eau

Portée par

Unité de recherche Biochimie et Physiologie Moléculaire des Plantes (BPMP)

## Study of the molecular mechanisms that maintain iron homeostasis in plants

Présentée par Fei GAO

Le 22 juin 2021

Sous la direction de Christian DUBOS

Devant le jury composé de

Jacqueline GRIMA-PETTENATI, Directrice de recherche CNRS, LRSV, Toulouse

Sébastien THOMINE, Directeur de recherche CNRS, I2BC, Gif-sur-Yvette

José GENTILHOMME, Maître de conférence Université d'Angers, IRHS, Angers

Loïc LEPINIEC, Directeur de recherche INRAE, IJPB, Versailles

Gabriel KROUK, Directeur de recherche CNRS, BPMP, Montpellier

Rapporteur

Rapporteur

Examineur

Examineur

Président



UNIVERSITÉ  
DE MONTPELLIER

Montpellier  
SupAgro



## ACKNOWLEDGEMENTS

It is my pleasure to express my deep sense of thanks and gratitude to several individuals who were instrumental for the completion of my PhD research.

First and foremost, I would like to express my sincere gratitude to my supervisor, **Christian DUBOS**. Thanks for his invaluable advices, continuous support and patience during my PhD study. His immense knowledge and plentiful experience have encouraged me in all the time of my academic research and daily life. His deep insights and creative ideas have quite often inspired me and helped me to unravel the questions raised during my Ph.D. research.

Second, I would like to express my appreciation to all the members of our laboratory for their wonderful collaboration. They are always enthusiastic to help me when I met problems in lab work or daily life. Special thanks to **Florence VIGNOLS** for her help in cloning, Y2H, BiFC and also for the proofreading of the publications. I am very grateful to **Nathalie BERGER** for her contribution to proteomic analysis and manuscript preparation. My thanks also go to **Ester IZQUIERDO ALEGRE** for her contribution to coumarin analysis. I would like to thanks **Brigitte TOURAINE** for her useful protocols and assistance in the Y2H experiments. I am deeply grateful to **Frédéric GAYMARD** for his kindly help in the preparation of my support letter. I would like to offer my special thanks to **Kevin ROBE** who helped me set up the experiment in the lab at the beginning, showed me how to use the machines and gave a lot of useful tips to live in Montpellier. I would like to thanks all the other students, **Maël TAUPIN-BROGGINI**, **Max STASSEN** and **Dennis BRANDT** for their help and discussion in research.

I would like to offer my special thanks to my Ph.D. committee members: **Thomas KROJ**, **David LATRASSE**, **Benjamin PERET** and **Hannetz ROSCHZTTARDTZ** for their insightful comments and suggestions for my Ph.D. project.

I am greatly thankful to **Carine ALCON** for her expertise and assistance with microscopy. I would like to thank **Sandrine CHAY** for technical support with plant iron determination. My gratitude extends to all people in BPMP who supported my research.

I would also like to thank the **Chinese Scholarship Council** for offering me the financial support to study in France for four years. I wish to thank **BPMP, INRAe** and **Supagro Montpellier** for hosting me and offering me the platform to carry out the experiments. Special thanks to **Elisabeth BOZSONYIK** for her generous help for the administrative stuff.

Then I would like to thank my master supervisors **Qi WU (吴琦)** and **Huipeng YAO (姚慧鹏)** as well as **Chenglei LI (李成磊)** for their help and advice for research. I would like to thank **Ning TANG (唐宁)**, **Shouyang LIU (刘守阳)**, **Jianfu LI (李建福)**, **Shuangjiang LI (李双江)**, **Yuechen BAI (白悦晨)**, **Xiaopeng LUO (雒晓鹏)**, **Weijie LAN (兰维杰)**, **Panfeng YAO (姚攀锋)** and **Yunji HUANG (黄云吉)** for their discussion and suggestion about both research and daily life.

I would like to offer my special thanks to **Jing ZHOU (周婧)** for her love, support, encouragement, patience and understanding. Words are powerless to express my gratitude to you. I am truly thankful for having you in my life. I have to thank my parents for their endless love and support throughout my life. My grandparents, sisters, brother, aunts and uncles deserve my wholehearted thanks as well.

# Table of contents

<b>ABBREVIATIONS</b> .....	v
<b>RESUME DE LA THESE EN FRANÇAIS</b> .....	vii
1) Objectifs de la thèse .....	viii
2) Résultats principaux .....	ix
3) Discussion .....	xi
4) Conclusion .....	xx
<b>CHAPTER I</b> .....	1
<b>INTRODUCTION GENERALE</b> .....	1
1.1 Research background .....	2
1.2 Role of iron in plants .....	2
1.2.1 Iron-sufur cluster proteins .....	4
1.2.2 Heme proteins .....	4
1.2.3 Non-heme iron proteins .....	7
1.3 Iron homeostasis in plants .....	7
1.4 Iron uptake in plants .....	12
1.4.1 Strategy I .....	12
1.4.2 Strategy II .....	15
1.5 Long distance iron translocation in plants .....	15
1.5.1 Xylem transport .....	17
1.5.2 Phloem transport .....	18
1.6 Subcellular transport of iron .....	22
1.6.1 Chloroplasts .....	22
1.6.2 Mitochondria .....	23
1.6.3 Vacuoles .....	24
1.7 Regulation of iron homeostasis .....	25
1.7.1 Article 1. Transcriptional integration of plant responses to iron availability .....	25
1.8 Objectives of the thesis .....	40
<b>CHAPTER II</b> .....	43
<b>ILR3 CONNECTS THE NEGATIVES AND POSITIVES OF IRON HOMEOSTASIS</b> .....	43



Article 2. Transcriptional integration of the responses to iron availability in arabidopsis by the bHLH factor ILR3 .....	44
<b>CHAPTER III</b> .....	87
<b>BHLH121 INTEGRATES IRON RESPONSES</b> .....	87
Article 3. The transcription factor bHLH121 interacts with bHLH105 (ILR3) and its closest homologs to regulate iron homeostasis in Arabidopsis.....	88
Article 4. Further insights into the role of bHLH121 in the regulation of iron homeostasis in <i>Arabidopsis thaliana</i> .....	131
<b>CHAPTER IV</b> .....	137
<b>BHLH121 AND CLADE IVC BHLH TFS FUNCTION SYNERGISTICALLY TO REGULATE IRON HOMEOSTASIS</b> .....	137
Article 5. bHLH121 and clade IVc bHLH transcription factors synergistically function to regulate iron homeostasis in <i>Arabidopsis thaliana</i> .....	138
<b>CHAPTER V</b> .....	184
<b>MATERIALS AND METHODS</b> .....	184
5.1 Plant materials .....	185
5.2 Plant growth conditions.....	185
5.2.1 Greenhouse conditions .....	185
5.2.2 <i>In vitro</i> cultures .....	185
5.2.3 Hydroponic cultures .....	186
5.3 Bacterial strains .....	186
5.3.1 DH5 $\alpha$ .....	186
5.3.2 DB3.1 .....	186
5.3.3 GV3101::pMP90 .....	186
5.4 Yeast strains .....	187
5.4.1 AH109 .....	187
5.5 Vectors .....	187
5.5.1 pDNOR207.....	187
5.5.2 pUBC-eGFP Dest .....	187
5.5.3 pGWB3.....	192
5.5.4 pGWB4.....	192
5.5.5 pDEST22.....	192
5.5.6 pDEST32.....	192

5.5.7	pUC-SPYCE and pUC-SPYNE .....	192
5.6	Arabidopsis transformation .....	193
5.7	Arabidopsis crossing .....	193
5.8	Extraction of Arabidopsis genomic DNA .....	194
5.9	DNA amplification by Polymerase Chain Reaction (PCR).....	194
5.10	Plasmid construction .....	195
5.10.1	Gateway cloning by recombination.....	195
5.10.2	Restriction enzyme cloning .....	196
5.11	Generation of <i>bhlh121</i> mutant lines by CRISPR-Cas9 system .....	199
5.12	Gene expression analysis by quantitative real time PCR .....	199
5.12.1	RNA extraction.....	199
5.12.2	Reverse-Transcription Reaction .....	200
5.12.3	Quantitative real time PCR.....	200
5.13	Yeast two-hybrid.....	201
5.13.1	Preparation of yeast competent cells .....	201
5.13.2	Transformation of yeast.....	202
5.14	Bimolecular fluorescence complementation (BiFC) Assays.....	205
5.14.1	Arabidopsis protoplast isolation.....	205
5.14.2	Arabidopsis protoplast transfection.....	205
5.15	Co-immunoprecipitation (Co-IP)/ LC-MS/MS Analyses.....	207
5.15.1	Co-immunoprecipitation (Co-IP) .....	207
5.15.2	LC-MS/MS analysis .....	208
5.15.3	Data analysis.....	209
5.16	Chromatin immunoprecipitation qPCR (ChIP-qPCR) assays.....	209
5.17	HPLC analysis of coumarins.....	212
5.18	Chlorophyll measurement .....	212
5.19	Ferric chelate reductase (FCR) activity assays.....	213
5.20	Metal measurements.....	213
5.21	Iron staining by Perls/DAB .....	213
5.22	Histochemical detection of $\beta$ -glucuronidase (GUS) activity.....	214
5.23	Measurement of root length .....	214
<b>DISCUSSIONS .....</b>		<b>215</b>

1. ILR3 connects the plant responses to both iron deficiency and iron excess .....	216
2. bHLH121 is required for the iron deficiency response in Arabidopsis.....	218
3. Post-translational regulation of bHLH121 .....	219
4. bHLH121 and clade IVc bHLH transcription factors function coordinately in the regulation of iron homeostasis.....	222
Conclusion.....	224
<b>REFERENCES</b> .....	225
<b>ANNEXES</b> .....	237

## ABBREVIATIONS

AHA	H <sup>+</sup> -ATPase
AHA2	PLASMA MEMBRANE PROTON ATPASE 2
BGLU42	β-GLUCOSIDASE 42
bHLH	Basic Helix-Loop-Helix
BiFC	Bimolecular fluorescence complementation
BTS	BRUTUS
BTSL	BRUTUS LIKE
cDNA	Complementary DNA
CIPK	CBL-INTERACTING PROTEIN KINASE
Co-IP	Co-immunoprecipitation
Col-0	Columbia-0
COSY	COUMARIN SYNTHASE
CYP82C4	CYTOCHROME P450 MONOOXYGENASE 82C4
DMA	Deoxymugineic acid
DMAS	DEOXYMUGINEIC ACID SYNTHASE
DNA	Deoxyribonucleic acid
dNTP	Deoxy-ribonucleoside triphosphate
DTT	Dithiothreitol
EDTA	Ethylenediaminetetraacetic acid
F6'H1	FERULOYL CoA ORTHO-HYDROXYLASE 1
FCR	Ferric-chelate reductase
Fe <sup>2+</sup>	Iron ferrous
Fe <sup>3+</sup>	Iron ferric
FER	FERRITIN
FIT	FE-DEFICIENCY INDUCED TRANSCRIPTION FACTOR
FRD3	FERRIC CHELATE REDUCTASE DEFECTIVE 3
FRO2	FERRIC REDUCTASE-OXIDASE 2
FW	Fresh weight
g	Gramme
GFP	GREEN FLUORESCENT PROTEIN
GUS	β-GLUCURONIDASE
H <sup>+</sup>	Proton
H <sup>+</sup> -ATPase	ATPase proton pump
HIS	Histidine
HPLC	High performance liquid chromatography
ILR3	IAA-LEU RESISTANT 3
IP	Immunoprécipitation

IREG1/FPN1	IRON REGULATED 1/FERROPORTIN 1
IRT1	IRON-REGULATED TRANSPORTER 1
ITP	IRON TRANSPORT PROTEIN
kb	Kilobase
LEU	Leucine
MA	Mugineic acid
MATE	MULTI DRUG AND TOXIN EFFLUX
MES	2-(N-morpholino)éthanesulfonic acid
mg	Milligramme
MIT1/2	MITOCHONDRIAL IRON TRANSPORTER 1/2
mL	Milliliter
mm	Millimeter
mM	Millimolarity
mRNA	Messenger RNA
MS	Murashige et Skoog
MS	Mass spectrometry
NA	Nicotiamine
NAAT	NICOTIANAMINE AMINOTRANSFERASE
NAS	NICOTIANAMINE SYNTHASE
NRAMP	NATURAL RESISTANCE-ASSOCIATED MACROPHAGE PROTEIN
OPT3	OLIGOPEPTIDE TRANSPORTER 3
PCR	Polymerase chain reaction
PDR9	PLEIOTROPIC DRUG RESISTANCE 9
PEG 4000	Polyethylene glycol 4000
pH	Potential of hydrogen
PIC1	PERMEASE IN CHLOROPLASTS 1
pUBI10	Ubiquitin 10 promoter
PYE	Popeye
qPCR	Quantitative real time PCR
RNA	Ribonucleic acid
ROS	Reactive oxygen species
S8H	SCOPOLETIN 8-HYDROXYLASE
SDS	Sodium dodecyl sulfate
T-DNA	Transfert DNA
TOM1	TRANSPORTER OF MUGINEIC ACID 1
Tris	2-amino-2-(hydroxymethyl)propane-1,3-diol
TRP	Tryptohan
URI	UPSTREAM REGULATOR OF IRT1
VIT1	VACUOLAR IRON TRANSPORTER 1
VTL	VACUOLAR IRON TRANSPORTER 1-LIKE
YS1	YELLOW STRIPE 1
YSL	YELLOW STRIPE 1-like

**RESUME DE LA  
THESE EN  
FRANÇAIS**



## 1) Objectifs de la thèse

Au début de ma thèse, notre compréhension des mécanismes moléculaires impliqués dans le contrôle transcriptionnel de l'homéostasie du fer chez *Arabidopsis thaliana* était relativement bien avancée. Par exemple, 16 facteurs de transcription de type bHLH (basic helix loop helix) avaient été caractérisés comme étant impliqués dans la régulation de l'homéostasie du fer chez *Arabidopsis* (Gao *et al.*, 2019b). Cependant, la manière dont ces facteurs bHLH agissaient de concert les uns avec les autres pour réguler l'homéostasie du fer restait à élucider. Des travaux antérieurs menés dans le groupe ont montré qu'ILR3/bHLH105 (IAA-LEUCINE RESISTANT 3 : un activateur transcriptionnel de la réponse à la carence en fer) pouvait se lier un élément *cis*-régulateur de type *G-Box* présent dans le promoteur de *FER1* (*FERRITIN 1* : gène marqueur de la réponse à l'excès de fer impliqué dans le stockage transitoire de ce dernier) et réprimer son expression dans les tissus végétatifs.

Cette découverte a soulevé une question importante, comment ILR3 agit à la fois comme activateur et répresseur dans la régulation de l'homéostasie du fer ? Par ailleurs, au début de ma thèse, des travaux additionnels réalisés dans l'équipe ont permis d'identifier un nouveau facteur de transcription de type bHLH capable d'interagir avec ILR3 appelée bHLH121. De cette découverte a émergé une deuxième question: quel est le rôle de bHLH121 dans la régulation de l'homéostasie du fer ?

Afin de répondre à ces deux questions, les objectifs suivants ont été formulés dans le cadre de ma thèse de doctorat :

- (i) Le premier objectif de ma thèse de doctorat était de déterminer comment ILR3 pouvait agir en tant que répresseur de l'homéostasie du fer. Notre hypothèse, sur la base de données d'interaction publiées (Long *et al.*, 2010), était qu'ILR3 interagit avec le répresseur transcriptionnel de type bHLH appelé PYE/bHLH47 (POPYE). Il s'agissait donc ici de vérifier l'interaction entre ILR3 et PYE, et de caractériser ce mécanisme de répression dans le contrôle de l'homéostasie du fer.
- (ii) Le deuxième objectif était de caractériser fonctionnellement bHLH121 et d'étudier son



rôle dans la régulation de l'homéostasie du fer.

- (iii) Le dernier objectif de ma thèse de doctorat était d'étudier l'interaction génétique entre bHLH121 et les facteurs bHLH de type IVc, auquel appartient ILR3, afin d'étudier comment ces facteurs de transcription sont coordonnés pour réguler l'expression des gènes impliqués dans l'homéostasie du fer.

## 2) Résultats principaux

Dans le premier axe, l'interaction entre ILR3 et le répresseur PYE a été confirmée par des expériences de complémentation de fluorescence bimoléculaire (BiFC) dans des protoplastes d'*Arabidopsis*. Des études d'expression associées à des tests d'immunoprécipitation de la chromatine couplée à la PCR quantitative (ChIP-qPCR) ont démontré qu'ILR3 pouvait réprimer l'expression de gènes impliqués dans le contrôle de l'homéostasie du fer par sa liaison directe avec leur promoteur et que l'activité répressive d'ILR3 était conférée par sa dimérisation avec PYE. La caractérisation phénotypique des mutants dominants et de perte de fonction d'ILR3, ainsi que du triple mutant ferritine (dépourvu de gènes *FER1*, *FER3* et *FER4* fonctionnels et donc de ferritines dans les parties végétatives), a mis en avant que plusieurs facettes de la croissance des plantes en réponse aux fluctuations de la disponibilité en fer (de la carence à l'excès) reposent sur les activités d'ILR3 et des ferritines. Ces résultats ont mis en évidence qu'ILR3 agit non seulement comme un activateur impliqué dans la réponse à la carence en fer, mais qu'il agit également comme un répresseur des réponses des plantes à l'excès de fer. Ces résultats sont présentés dans le chapitre II de cette thèse, à la manière d'un article publié dans *New Phytologist* dont je suis co-deuxième auteur (Tissot *et al.*, 2019).

Dans le deuxième axe de ma thèse, les études d'interaction ont montré que bHLH121 pouvait interagir avec bHLH34, bHLH104, bHLH115 et ILR3 (i.e. les quatre membres du clade IVc des facteurs de transcription de type bHLH). L'analyse phénotypique de mutant perte de fonction *bhlh121* (obtenus par CRISPR-Cas9) a permis de mettre en évidence que l'absence d'activité bHLH121 conduit à de graves défauts de croissance qui peuvent être inversés par un apport exogène en fer. Les études d'expression (i.e. qRT-PCR) couplées à des expériences de

ChIP-qPCR ont démontré que bHLH121 fonctionne comme un activateur transcriptionnel direct d'un ensemble de gènes importants impliqués dans le réseau de régulation de la carence en fer. Parmi les cibles directes de bHLH121 nous avons identifié la plupart des régulateurs impliqués dans le réseau transcriptionnel qui contrôle l'homéostasie du fer chez Arabidopsis (i.e. facteurs de transcription, E3-ubiquitine ligases, peptides signaux). Les tests de localisation cellulaire réalisés en microscopie confocale ont montrés que la disponibilité en fer affecte la localisation cellulaire de la protéine bHLH121 dans les tissus racinaires, bHLH121 étant préférentiellement localisé dans le cortex et l'épiderme en carence en fer et au niveau du cylindre central en suffisance en fer. Ces résultats présentés sous forme d'article dans le chapitre III ont été publiés dans The Plant Cell dans un article où je suis premier auteur(Gao *et al.*, 2020a). De plus, j'ai montré que bHLH121 pouvait également réguler l'expression des gènes de ferritine en se liant directement à leurs promoteurs, au même locus que le complexe répressif ILR3-PYE. Cette dernière observation indiquant que bHLH121, PYE et ILR3 forment une chaîne de commutateurs antagonistes qui régulent l'expression des gènes de ferritine. Ces résultats, également présentés sous forme d'article dans le chapitre III, ont été publiés dans Plant Signaling & Behavior dans un article où je suis premier auteur(Gao *et al.*, 2020b).

Dans le dernier axe, l'analyse phénotypique de doubles mutants entre bHLH121 et chacun des membres du clade IVc des facteurs bHLH a montré qu'ils présentaient des défauts de croissance associés à une carence en fer plus sévères que les mutants simples. Conformément à cela, nous avons observé par des analyses d'expression que les réponses à la carence en fer étaient altérées. L'expression constitutive de *bHLH34* et d'*ILR3*, mais pas de *bHLH104* ou de *bHLH115*, pouvait partiellement compléter les défauts de croissance associés à une carence en fer du mutant de perte de fonction *bhlh121* en activant l'expression à la fois de *bHLH39* et de *FIT/bHLH29* (deux facteurs de transcription cibles de bHLH121 qui conditionnent l'expression des gènes impliqués dans le prélèvement du fer). Ces résultats ont permis de mettre en évidence les rôles distincts des quatre membres du clade IVc des facteurs de transcription de type bHLH dans la régulation de l'homéostasie du fer. Par ailleurs, des études d'expression pour *bHLH121* et les quatre membres du clade IVc des facteurs bHLH indiquent qu'ils pourraient fonctionner de manières tissues spécifiques. Pris dans leur ensemble, ces résultats indiquent que bHLH121 et

les membres du clade IVc des facteurs bHLH fonctionnent de manière coordonnée dans la régulation de l'homéostasie du fer. Ces résultats sont présentés dans le chapitre IV, sous forme d'un article, dont je serai le premier auteur et que nous souhaitons soumettre à Journal of Experimental Botany.

### **3) Discussion**

Au cours des deux dernières décennies, des progrès remarquables ont été accomplis dans le décryptage des mécanismes moléculaires qui maintiennent l'homéostasie du fer chez les végétaux. Les recherches dans ce domaine ont mis en évidence que l'homéostasie du fer chez les végétaux est régulée au niveau transcriptionnel et implique plusieurs facteurs de transcription de type bHLH qui fonctionnent dans un réseau de régulation complexe (Gao and Dubos, 2020; Gao *et al.*, 2019b). Des études récentes suggèrent que, chez *Arabidopsis thaliana*, ce réseau de régulation complexe est composé de deux modules de régulation interconnectés, un où FIT (bHLH29) joue un rôle prédominant et l'autre où c'est ILR3 (bHLH105). Bien que dans leur ensemble les modules de régulation dépendant de FIT et d'ILR3 aient été bien caractérisés (Colangelo and Guerinot, 2004; Jakoby *et al.*, 2004; Li *et al.*, 2016; Liang *et al.*, 2017; Wang *et al.*, 2007a; Yuan *et al.*, 2008; Yuan *et al.*, 2005; Zhang *et al.*, 2015), il n'était toujours pas clairement établis comment ces deux sous-réseaux sont synchronisés pour réguler de manière coordonnée l'homéostasie du fer dans la plante.

#### **ILR3 connecte les réponses des plantes à la carence et à l'excès de fer.**

Chez les végétaux, la carence et l'excès de fer sont délétères. Ainsi, les niveaux de fer dans les cellules végétales doivent être étroitement régulés en réponse à la disponibilité en fer et aux besoins de la plante (Briat *et al.*, 2015). En cas de carence en fer, les plantes augmentent l'absorption du fer au niveau des racines et libèrent le fer stocké dans les différents compartiments cellulaires (e.g. vacuole) pour satisfaire les besoins du métabolisme cellulaire (Kobayashi and Nishizawa, 2012). En revanche, les plantes diminuent l'absorption du fer par les racines et séquestrent l'excès de fer pour éviter toute toxicité lorsque la concentration

en fer est élevée (Ravet *et al.*, 2009). Les ferritines jouent un rôle central dans ce processus pour maintenir l'équilibre intracellulaire du fer. Par conséquent, l'expression des ferritines est réprimée pour diminuer la séquestration du fer dans des conditions de faible approvisionnement en fer, tandis qu'avec un apport élevé en fer, l'expression des ferritines est induite pour augmenter la séquestration de ce micronutriment (Ravet *et al.*, 2009). Étant donné que l'absorption et la séquestration du fer sont régulées de manière opposés, il était attendu que la régulation de ces processus soit intégrée (Kobayashi *et al.*, 2019; Kroh and Pilon, 2019). Dans l'équipe, pour identifier les régulateurs clés qui pourraient coordonner la cascade de régulation transcriptionnelle associée aux réponses des plantes à la carence et à l'excès de fer, une stratégie basée sur la caractérisation fonctionnelle du promoteur de *FER1* (*FERRITIN 1*) a été retenue (Tissot *et al.*, 2019). Cela a permis de mettre en évidence qu'ILR3/bHLH105 (IAA-LEUCINE RESISTANT3), un facteur de transcription de type bHLH [basic helix loop helix] connu pour réguler positivement les réponses à la carence en fer, pouvait également réguler négativement l'expression des gènes de ferritine (i.e. *FER1*, *FER3* et *FER4*), intégrant ainsi les réponses à la carence et à l'excès de fer. Dans des études antérieures, ILR3 a été identifié comme un activateur des réponses à la carence en fer en ciblant les facteurs de transcription appartenant au clade Ib des bHLH (i.e. *bHLH38*, *bHLH39*, *bHLH100* et *bHLH101* ; Zhang *et al.*, 2015). La perte de fonction d'ILR3 chez *Arabidopsis* entraîne une altération de la réponse à la carence en fer, tandis que la surexpression d'ILR3 a un effet inverse et conduit à une accumulation excessive de fer (Zhang *et al.*, 2015). Néanmoins, certaines évidences suggèrent que la fonction d'ILR3 peut s'étendre au-delà de l'induction du mécanisme d'absorption du fer. Rampey *et al.* ont rapporté que l'expression de trois gènes impliqués dans le transport vacuolaires du fer (i.e. *VTL1*, *VTL2* et *VTL5* ; *VACUOLAR IRON TRANSPORTER-LIKE 1, 2 and 5*) et d'un gène codant pour une protéine chloroplastique impliquée dans le transfert de centre fer-soufre (i.e. *At-NEET*) était réprimée dans le mutant *ilr3-1* (mutation qui conduit à une forme stabilisée d'ILR3 ; Rampey *et al.* ., 2006). Par des expériences d'immunoprécipitation de la chromatine couplée à la PCR quantitative (ChIP-qPCR), nous avons en outre démontré qu'ILR3 pouvait se lier aux régions promotrices de *FER1*, *FER3*, *FER4*, *At-NEET*, *VTL2* ainsi que de *NAS4* (*NICOTIANAMINE SYNTHASE 4* codant pour une protéine impliquée dans la transport du fer), suggérant qu'ILR3 est un répresseur transcriptionnel direct de ces gènes cibles. PYE/bHLH47

(POPEYE), un facteur de transcription bHLH appartenant au clade IVb, a été identifié comme un régulateur négatif d'un ensemble de gènes impliqués dans la translocation et la mobilisation du fer (Long *et al.*, 2010). PYE contient dans sa région C-terminale un motif EAR typique (i.e. DLNxxP), l'une des formes les plus prédominantes de motif de répression transcriptionnelle identifiée chez les plantes (Kagale and Rozwadowski, 2011). Il a été démontré que PYE interagissait *in vivo* avec les protéines bHLH du clade IVc, y compris ILR3 (Long *et al.*, 2010; Zhang *et al.*, 2015). Au cours de ma thèse, nous avons démontré qu'ILR3 et PYE peuvent réprimer l'expression d'un ensemble commun de gènes et se lier directement à leur région promotrice au même locus. Nos travaux, à la lumière des travaux réalisés dans différents laboratoires, nous ont permis de mettre en évidence que l'activité de répresseur transcriptionnel d'ILR3 était certainement conférée par son hétérodimérisation avec PYE. Dans des conditions de carence en fer, les complexes dépendants d'ILR3 (i.e. bHLH34-ILR3, bHLH104-ILR3 et bHLH115-ILR3) agissent comme activateur pour favoriser l'absorption du fer (Li *et al.*, 2016; Zhang *et al.*, 2015) alors que le complexe ILR3-PYE agit comme un répresseur pour inhiber la séquestration du fer, ce qui est probablement important pour éviter une disponibilité réduite du fer dans les racines. On suppose que l'abondance relative des protéines bHLH de type IVc (i.e. bHLH34, bHLH104, bHLH115 et ILR3) et de PYE pourrait déterminer la quantité des deux types de complexes protéiques dépendant d'ILR3 (activateur et répresseur) dans les différents types cellulaires en fonction de la disponibilité de fer. Par conséquent, il serait intéressant d'étudier la co-localisation cellulaire de ces facteurs bHLH dans les tissus racinaires dans différentes conditions de fer. Il est à noter que PYE peut également former des hétérodimères avec bHLH104 et bHLH115 (Long *et al.*, 2010). Cependant, on ne sait pas si ces complexes jouent réellement un rôle dans la régulation de l'homéostasie du fer.

### **bHLH121 est nécessaire pour la réponse à la carence en fer chez Arabidopsis**

ILR3 joue un rôle essentiel dans la régulation de l'homéostasie du fer (Tissot *et al.*, 2019; Zhang *et al.*, 2015). Par conséquent, nous avons mené une expérience de co-immuno précipitation couplée à la spectrométrie de masse (Co-IP LC-MS/MS) pour identifier de nouveaux acteurs potentiels impliqués dans le contrôle de l'homéostasie du fer. Ainsi, bHLH121 (clade IVb) a été

identifié comme un facteur de transcription interagissant avec ILR3. Dans le cadre de ma thèse, j'ai pu mettre en évidence que la perte de fonction de bHLH121 provoque de graves symptômes de carence en fer qui peuvent être inhibés en fournissant un apport supplémentaire en fer. Des résultats similaires ont également été rapportés par deux autres groupes (Kim *et al.*, 2019; Lei *et al.*, 2020). Nous avons par ailleurs mis en évidence la position en amont de bHLH121 dans le réseau de régulation qui contrôle l'homéostasie du fer puisque les mutants *bhlh121* étaient affectés dans tous les aspects de la réponse à la carence en fer et que l'expression de plusieurs gènes codant pour des protéines régulatrices impliquées dans ce réseau était altérée (Gao *et al.*, 2020a; Gao *et al.*, 2020b; Kim *et al.*, 2019; Lei *et al.*, 2020). Nous avons par ailleurs démontré que bHLH121 pouvait se lier directement au promoteur des quatre facteurs bHLH appartenant au clade Ib (i.e. *bHLH38*, *bHLH39*, *bHLH100* et *bHLH101*) et activer leur expression. Il est à noter ici que ces quatre facteurs bHLH sont nécessaires pour activer, notamment, l'expression des gènes impliqués dans le prélèvement du fer présent dans le sol par les racines. Cependant, certaines incohérences entre dans ces trois études sont apparues. Tout d'abord, Lei *et al.*, en utilisant des approches de simple hybride en levure (Y1H), de gel retard (EMSA) et de ChIP-qPCR, suggèrent que bHLH121 peut se lier au promoteur de *FIT/bHLH29*, (bHLH qui interagit avec les facteurs bHLH du clade Ib pour activer, notamment, l'expression des gènes impliqués dans le prélèvement du fer présent dans le sol par les racines) alors que dans notre étude nous n'avons pas observé (ChIP-qPCR) de liaison entre bHLH121 le promoteur *FIT*. Cependant, Kim *et al.* sont parvenu à une conclusion similaire à la nôtre en utilisant une approche ChIP-seq (Kim *et al.*, 2019). Kim *et al.* ont aussi rapporté que la surexpression des facteurs bHLH de type Ib, mais pas la surexpression de *FIT*, pouvait compléter le mutant *bhlh121* et restaurer l'induction de l'expression de *IRT1* (*IRON-REGULATED TRANSPORTER 1*; transporteur haute affinité pour le fer permettant l'absorption de ce dernier par les racines) dans des conditions de carence en fer (Kim *et al.*, 2019). En revanche, Lei *et al.* ont montré que la surexpression de *FIT* pouvait partiellement compléter le mutant *bhlh121-5* (Lei *et al.*, 2020). Cependant, dans notre étude, ni la surexpression de *FIT* ni celle de *bHLH38* (clade Ib) n'a pu compléter les défauts de croissance de *bhlh121-2*. Il est à noter que différents mutants *bhlh121* ont été utilisés dans les trois études, ce qui peut expliquer les différents résultats. Malgré les incohérences observées, toutes ces études ont conclu que bHLH121 est nécessaire

pour la réponse à la carence en fer chez *Arabidopsis*.

### **Régulation post-traductionnelle de bHLH121**

Les modifications post-traductionnelles (e.g. la séquestration, l'ubiquitination ou la phosphorylation) peuvent affecter de manière significative l'activité des facteurs de transcription en contrôlant leurs niveaux de protéines actives (Schütze *et al.*, 2008). Il a été démontré que de tels mécanismes jouent un rôle essentiel dans le maintien de l'homéostasie du fer chez les plantes (Kobayashi *et al.*, 2019; Rodríguez-Celma *et al.*, 2019a; Spielmann and Vert, 2020; Wu and Ling, 2019).

Nous avons observé, ainsi que Kim *et al.*, que bHLH121 est exprimé dans l'ensemble des organes de la plante et que l'accumulation des transcrits et de la protéine ne sont pas affectés par la disponibilité du fer (Gao *et al.*, 2020a; Kim *et al.*, 2019). En revanche, nous avons constaté que la disponibilité du fer affectait la localisation cellulaire de la protéine bHLH121 dans les racines. En cas de carence en fer, bHLH121 a été principalement détecté dans le cortex racinaire et les cellules de l'épiderme, tandis que bHLH121 a été principalement observé dans les noyaux des cellules de la stèle lorsque les plantes étaient cultivées dans des conditions de suffisance en fer. Plusieurs hypothèses pourraient expliquer ces observations. Par exemple, un mécanisme post-traductionnel pourrait moduler la stabilité de la protéine bHLH121 d'une manière dépendant du type de cellule et de la disponibilité en fer pour déterminer sa localisation. Bien que les mécanismes précis de ces processus restent inconnus et doivent être étudiés dans le futur, ces résultats suggèrent que les gènes ciblés par bHLH121 diffèrent en fonction de la disponibilité du fer. En fait, la disponibilité du fer affecte non seulement la localisation cellulaire mais également la localisation sous-cellulaire de bHLH121. Lei *et al.* ont montré que bHLH121 est localisé à la fois dans le réticulum endoplasmique et dans le noyau des protoplastes d'*Arabidopsis* (Lei *et al.*, 2020). Dans les racines, nous avons montré (ainsi que Kim *et al.*) que bHLH121 était localisé dans le noyau que les plantes soient cultivées en condition de carence (0  $\mu\text{M}$  Fe) ou de suffisance (50  $\mu\text{M}$  Fe) en fer (Gao *et al.*, 2020a; Kim *et al.*, 2019). De manière très intéressante, Lei *et al.* ont rapporté que bHLH121 était observée à la fois dans le cytoplasme et le noyau lorsque la concentration en fer présent dans le milieu atteignait 100  $\mu\text{M}$  (Lei *et al.*,

2020). Ces résultats suggèrent qu'une faible disponibilité en fer favorise l'accumulation nucléaire de bHLH121. Cependant, il n'est toujours pas établi si la carence en fer peut faciliter la mobilité de bHLH121 vers le noyau ou si la carence en fer peut stabiliser bHLH121 dans le noyau et le déstabiliser dans le réticulum endoplasmique.

L'interaction du bHLH121 avec les facteurs bHLH de type IVc a été déterminée par différentes approches, notamment par double hybride en levure (Y2H), BiFC et Co-IP MS/MS (Gao *et al.*, 2020a; Kim *et al.*, 2019; Lei *et al.*, 2020). Lei *et al.* ont en outre démontré que ces interactions pouvaient faciliter l'accumulation nucléaire de bHLH121 (Lei *et al.*, 2020). Des études antérieures ont révélés que la carence en fer conduisait à une augmentation de l'accumulation des protéines bHLH de type IVc (Selote *et al.*, 2015; Tissot *et al.*, 2019). Par conséquent, on peut supposer que l'augmentation des niveaux de protéines appartenant au clade IVc des facteurs bHLH pourrait faciliter la mobilité de bHLH121 du réticulum endoplasmique vers le noyau lorsque le fer est limitant. Ce mécanisme post-traductionnel pour la partition intracellulaire des facteurs de transcription impliqués dans le contrôle de l'homéostasie du fer a déjà été rapporté. Par exemple, chez Arabidopsis, Trofimov *et al.* ont démontré que la localisation nucléaire de bHLH39 dépend de son interaction avec FIT, car dans des cellules dépourvues de FIT, bHLH39 se localise principalement dans le cytoplasme (Trofimov *et al.*, 2019). Des résultats similaires ont également été observés chez le riz pour lequel il a été montré que OsFIT/OsbHLH156 pouvait interagir avec OsIRO2/OsbHLH56 et faciliter son accumulation dans le noyau (Liang *et al.*, 2020; Wang *et al.*, 2020). Ainsi, il est probable que ce processus soit un mécanisme commun pour la séquestration des facteurs de transcription qui ne sont pas immédiatement requis par les cellules végétales.

La phosphorylation est l'un des types les plus répandus de modification post-traductionnelle qui affecte l'activité des protéines. Chez Arabidopsis, la protéine kinase CIPK11 (CBL-INTERACTING PROTEIN KINASE 11) peut phosphoryler FIT, ce qui régule positivement l'activité de la FIT en favorisant sa capacité d'accumulation nucléaire et de dimérisation avec bHLH39, favorisant ainsi l'absorption du fer dans des conditions de carence en fer (Gratz *et al.*, 2019). De même, Kim *et al.* ont rapporté que bHLH121 est phosphorylé dans des conditions de carence en fer (Kim *et al.*, 2019). Lorsque les plantes sont cultivées dans des conditions de carence en fer, la forme phosphorylée de bHLH121 est accumulée. Ceci a pour effet d'améliorer



la capacité de bHLH121 à s'hétérodimériser avec les membres du clade IVc des facteurs bHLH, ce qui augmente la capacité de bHLH121 à se lier au promoteur de ses gènes cibles, mettant en évidence le rôle positif de la phosphorylation sur l'activité de bHLH121 (Kim *et al.*, 2019). Cependant, on ne sait toujours pas quelle(s) kinase(s) est/sont impliquée(s) dans la phosphorylation de bHLH121. Des études futures pour caractériser le mécanisme de régulation précis menant à la phosphorylation de bHLH121 aideront à faire la lumière sur la façon dont ce facteur de transcription répond à la disponibilité en fer et active le réseau de régulation transcriptionnel localisé en aval.

Des études récentes ont démontrées que plusieurs E3 ubiquitine ligases à domaine hémérythrine (HHE) agissaient comme des régulateurs négatifs de l'homéostasie du fer pour éviter une surcharge en fer qui serait toxique pour la plante. Ces E3 ubiquitine ligases ciblant directement certains facteurs de transcription de type bHLH (Rodríguez-Celma *et al.*, 2019a). Il a notamment été rapporté, chez *Arabidopsis*, que BTS (BRUTUS) interagissait avec ILR3 et bHLH115 et facilitait ainsi leur dégradation *via* la voie du protéasome 26S, tandis que BRUTUS LIKE 1 et 2 (BTSL1 et BTSL2) facilitaient la dégradation FIT, permettant un réglage fin de l'expression des gènes impliqués dans la réponse à la carence en fer (Hindt *et al.*, 2017; Long *et al.*, 2010; Rodríguez-Celma *et al.*, 2019a; Rodríguez-Celma *et al.*, 2019b; Selote *et al.*, 2015). De même, OsHRZ1 et OsHRZ2 (HAEMERYTHRIN MOTIF CONTENANT UN NOUVEAU GÈNE [RING] VRAIMENT INTÉRESSANT [RING] ET ZINC-FINGER PROTEIN 1 et 2), deux homologues de BTS chez le riz, interagissent avec OsPRI1/OsbHLH60, OsPRI2/OsbHLH58 et OsPRI3/OsbHLH59 conduisant à leur dégradation *via* la voie du protéasome 26S (Zhang *et al.*, 2020; Zhang *et al.*, 2017). Comme mentionné précédemment, Kim *et al.* ont démontré que la forme phosphorylée de bHLH121 ne s'accumule qu'en condition de carence en fer. À l'inverse ils ont montré que la forme phosphorylée de bHLH121 est sujette à une dégradation *via* le protéasome lorsque le fer est réapprovisionné après une carence en fer. Ce mécanisme semble être lié à BTS car, contrairement à la forme non phosphorylée, la forme phosphorylée de bHLH121 est accumulée dans le mutant perte de fonction *bts-3* dans des conditions de suffisance en fer (Kim *et al.*, 2019). Cette dégradation de bHLH121 dépendante du fer permettrait de désactiver la cascade de signalisation liée à la carence en fer et d'éviter probablement une surcharge en ce micronutriment lorsque les plantes se retrouvent à nouveau

en conditions de suffisance en fer. Cependant, l'interaction directe entre bHLH121 et BTS, BTSL1 et BTSL2 n'a pas pu être démontrée par Y2H(Gao *et al.*, 2020a; Long *et al.*, 2010). D'autres approches seront nécessaires pour déterminer si BTS peut interagir directement avec bHLH121 ou s'il existe une protéine intermédiaire qui permet l'interaction entre ces deux protéines dans les cellules végétales.

### **Les facteurs de transcription bHLH121 et bHLH de type IVc fonctionnent de manière coordonnée pour réguler l'homéostasie du fer**

Comme nous l'avons vu précédemment, les quatre facteurs de transcription de type bHLH appartenant au clade IVc jouent un rôle critique en amont dans le réseau de régulation qui contrôle l'homéostasie du fer. Il a été démontré que ces quatre facteurs de transcription interagissent *in vivo* sous la forme d'homodimères ou d'hétérodimères et fonctionnent de manière similaire mais additive dans la régulation de l'homéostasie du fer(Li *et al.*, 2016; Liang *et al.*, 2017; Zhang *et al.*, 2015). Les mutants simple de chacun des facteurs bHLH de type IVc ont montré une plus grande sensibilité à la carence en fer par rapport aux plantes sauvages et les mutants d'ordre plus élevés ont présenté (i.e. double ou triple mutants) une augmentation des symptômes associés à la carence en fer fer(Li *et al.*, 2016; Liang *et al.*, 2017; Zhang *et al.*, 2015). En accord avec les phénotypes observés, l'induction de l'expression des gènes impliqués dans le prélèvement du fer, y compris celle des facteurs bHLH de type Ib et de *FIT*, est altérée chez ces mutants.

Il a été démontré que les facteurs bHLH de type IVc pouvaient se lier directement au promoteur des facteurs bHLH de type Ib mais pas à celui de *FIT* fer(Li *et al.*, 2016; Liang *et al.*, 2017; Zhang *et al.*, 2015). De manière intéressante, bHLH121 et les facteurs bHLH de type IVc partagent un ensemble de gènes cibles commun, avec notamment les quatre facteurs bHLH de type Ib (Gao *et al.*, 2020a; Kim *et al.*, 2019; Lei *et al.*, 2020). Néanmoins, nous ne connaissons pas encore l'ensemble des gènes cibles de ces facteurs de transcription. Récemment, Kim *et al.* ont utilisé des puces à ADN et une approche ChIP-seq pour révéler que bHLH121 pourrait réguler directement ou indirectement un ensemble de gènes cibles impliqués à la fois dans la voie dépendante de FIT et dans la voie indépendante de FIT(Kim *et al.*, 2019). Ainsi, étant

donné l'importance des facteurs bHLH de type IVc dans ce réseau de régulation, une analyse globale de l'expression génique et une analyse ChIP-seq seraient nécessaires pour décrypter l'ensemble des gènes cibles directs et indirects de ces facteurs de transcription, ce qui est nécessaire pour répondre à la question de savoir si les facteur bHLH de type IVc et bHLH121 présentent une divergence fonctionnelle qualitative et/ou quantitative dans la régulation des gènes cibles partagés.

Pour étudier plus en détail l'interaction génétique entre bHLH121 et les facteurs bHLH de type IVc, Lei *et al.* ont généré les doubles mutants *bhlh104 bhlh121* et *bhlh115 bhlh121* et comparé leurs phénotypes avec les mutants simples parentaux correspondants (Lei *et al.*, 2020). Par ce biais, Lei *et al.* ont montré que les phénotypes des doubles mutants *bhlh104 bhlh121* et *bhlh115 bhlh121* étaient similaires à ceux du mutant simple *bhlh121 (bhlh121-5)* et ils ont conclu que le bHLH121 agit en aval des facteurs bHLH de type IVc dans le réseau de régulation de l'homéostasie du fer (Lei *et al.*, 2020).

Cependant, des incohérences ont été identifiées lorsqu'on a comparé ces résultats à ceux obtenus durant ma thèse. En effet, dans notre étude les doubles mutants *bhlh121 bhlh34*, *bhlh121 bhlh104*, *bhlh121 bhlh105* et *bhlh121 bhlh115* ont montré des défauts de croissance plus sévère que ceux observés pour le mutant simple *bhlh121 (bhlh121-2)*, à la fois dans des conditions de carence et de suffisance en fer. En outre, nous avons démontré que ces doubles mutants présentaient une diminution des teneurs en fer et une augmentation des réponses géniques à la carence en fer par rapport au mutant *bhlh121-2*. Pris dans leur ensemble, nos données suggèrent que bHLH121 et les facteurs bHLH de type IVc jouent des rôles additifs, au moins en partie, dans l'homéostasie du fer chez Arabidopsis. Lei *et al.* ont montré que la surexpression de *bHLH104* et *bHLH115* pouvait restaurer l'expression des facteurs bHLH de type Ib mais pas celle FIT dans le mutant *bhlh121-5* (Lei *et al.*, 2020). Des résultats similaires ont été observés dans notre étude, où la surexpression de *bHLH105* et *bHLH115* permettait d'activer l'expression de *bHLH39* mais pas celle de *FIT* dans le mutant *bhlh121-2*, ce qui n'est pas suffisant pour activer les gènes situés en aval qui sont impliqués dans l'absorption du fer. Ces résultats suggèrent que bHLH121 est indispensable pour l'activation de *FIT* par *bHLH104* et *bHLH115*. En revanche, la surexpression de *bHLH34* et *bHLH105* peut partiellement compléter le phénotype associé au fer de *bhlh121* probablement via l'induction de

l'expression de *bHLH39* et de *FIT*, ce qui permet de reconstituer en partie la cascade de régulation impliquée dans l'absorption du fer en absence de *bHLH121*. Ces résultats ont également permis de mettre en évidence que des rôles distincts existent, dans la régulation de l'homéostasie du fer, pour les quatre membres du clade IVc des facteurs bHLH.

Zhang *et al.* ont utilisé une approche Chip-qPCR pour montrer qu'ILR3 ne pouvait pas se lier à la région *E-Box* du promoteur de *FIT* alors que Li *et al.* ont utilisé un test d'expression transitoire « rapporteur-effecteur » pour démontrer que *bHLH34* ne pouvait pas activer spécifiquement la transcription de *FIT* (Li *et al.*, 2016; Zhang *et al.*, 2015). Liang *et al.* ont également conclu que *FIT* n'est pas la cible directe des facteurs bHLH de type IVc (Liang *et al.*, 2017). Dans l'ensemble, ces conclusions soulèvent une question importante, quelle(s) protéine(s) agit(s) comme régulateur direct de l'expression de *FIT*. Comme indiqué précédemment, il a été proposé que *bHLH121* puisse interagir directement avec le promoteur de *FIT* même si cela nous semble peu probable (Gao *et al.*, 2020a; Kim *et al.*, 2019; Lei *et al.*, 2020). Ainsi, une recherche plus approfondie est nécessaire pour clarifier la relation entre *bHLH121* et *FIT* et pour déterminer si d'autres protéines connectent *FIT* avec *bHLH34* et ILR3.

#### **4) Conclusion**

L'objectif majeur de ma thèse était d'étudier le réseau de régulation transcriptionnel qui régule l'homéostasie du fer chez les végétaux en utilisant *Arabidopsis thaliana* comme modèle. Ces travaux ont révélé qu'ILR3 est au centre de ce réseau de régulation dans lequel il agit à la fois comme activateur et répresseur transcriptionnel. La découverte d'un nouveau facteur de transcription de type bHLH, *bHLH121*, qui joue un rôle essentiel dans l'homéostasie du fer, a considérablement amélioré notre compréhension des réseaux de régulation qui contrôlent l'homéostasie du fer chez les plantes et nous permet d'explorer davantage comment les facteurs de régulation connus et leurs partenaires protéiques contrôlent le statut du fer. Enfin, nos travaux indiquent que *bHLH121* et les facteurs bHLH appartenant au clade IVc jouent des rôles additifs et fonctionnent en synergie pour réguler l'homéostasie du fer. Cependant, beaucoup de travail reste à faire pour comprendre pleinement le réseau de régulation transcriptionnel qui contrôle l'homéostasie du fer chez les végétaux, en particulier si nous visons à utiliser ces facteurs de

transcription pour la sélection de plantes cultivées pouvant pousser de manière robuste dans des sols limités en fer et capable de produire des produits de haute qualité.

# **CHAPTER I**

## **INTRODUCTION GENERALE**



## **1. General introduction**

### **1.1 Research background**

Iron (Fe) is one of the most important microelement for almost all living organisms. It acts as enzyme cofactor and component in electron transport chains, which is crucial to metabolic functions, including DNA synthesis, respiration, energy production, and cell proliferation (Connorton *et al.*, 2017; Hentze *et al.*, 2010). In humans, iron deficiency is the most common micronutrient deficiency in the world, often leading in iron deficiency chronic disease and/or iron deficiency anemia (WHO, 2001). Iron deficiency anemia afflicts about 1 billion people worldwide, especially in developing countries (Miller, 2013). The WHO estimates that about 27% of children and 41% of women suffer from iron deficiency anemia (Stoltzfus, 2011) (Figure 1-1). To prevent iron deficiency anemia, two suitable prevention strategies have been recommend by WHO: dietary iron improvement and iron supplementation. Among them, the food fortification is often considered as the most cost-effective and long-term approach to solve this worldwide health problem. Human food depends almost directly or indirectly from plants. Therefore, the biofortification of iron content in plants, especially in cereals, have enormous benefits to feed humans safely with sufficient iron directly within their diet. To achieve this, the first critical goal is to decipher the mechanisms of iron uptake, translocation and storage in plants.

### **1.2 Role of iron in plants**

Like in humans, iron is also of great importance for plant growth and development. Under physiological conditions, iron exists in the two most common oxidation states,  $\text{Fe}^{2+}$  (ferrous) and  $\text{Fe}^{3+}$  (ferric), and can interconvert between these two forms (Hell and Stephan, 2003) (Figure 1-2). Based on this reversible redox reactions, iron functions to accept and donate electrons and serves as the essential enzyme cofactor or component of electron transport chains in various metabolic processes, including photosynthesis, mitochondrial respiration, nitrogen fixation, hormone biosynthesis and pathogen defense (Hänsch and Mendel, 2009).  $\text{Fe}^{2+}$  and  $\text{Fe}^{3+}$  are most frequently found to form octahedral complexes having six-coordinate with



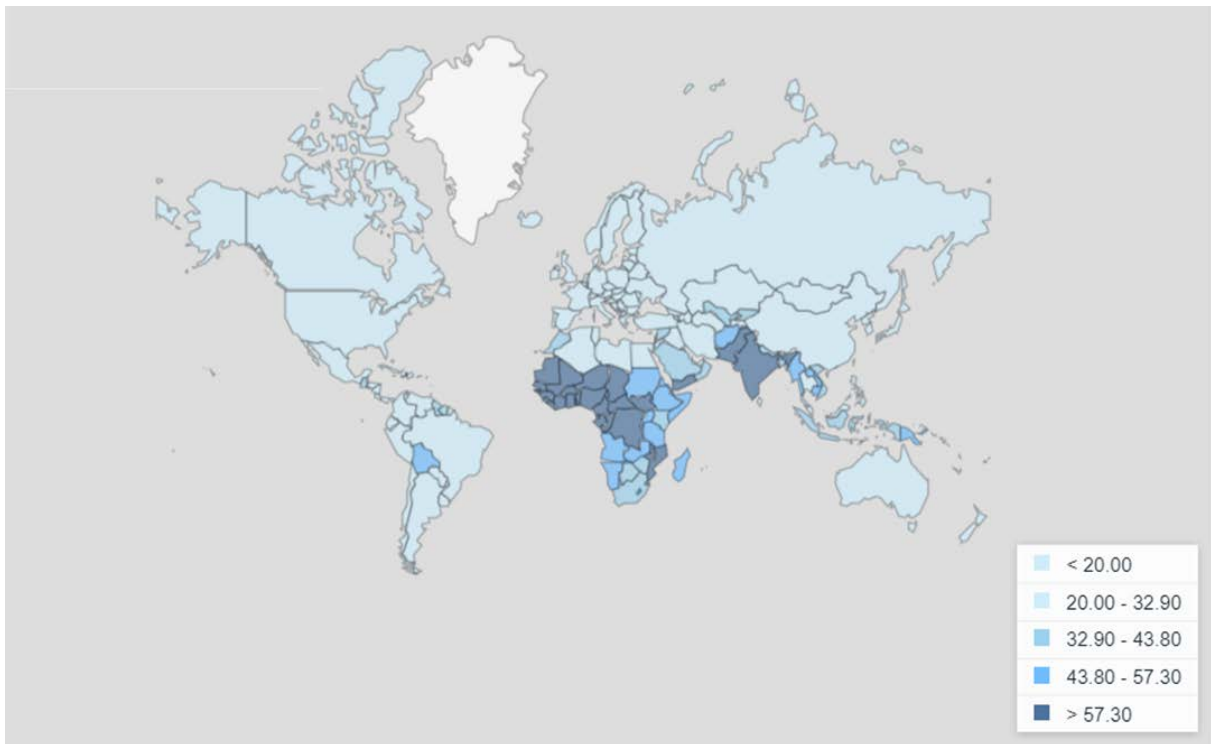


**Figure 1-1. Prevalence of anemia among children.** The map shows how prevalence of anemia among children (% of children under 5 year old) varies by country. The shade of the country corresponds to the magnitude of the indicator. The darker the shade, the higher the value.

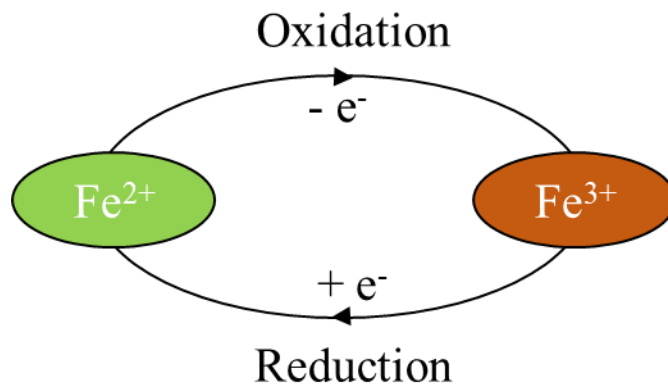


**Figure 1-2. The oxidation states of iron.** Ferric iron (Fe<sup>3+</sup>) can be reduced to ferrous iron (Fe<sup>2+</sup>) by gaining an electron (-e<sup>-</sup>), and ferrous iron can be oxidized to ferric iron by losing an electron (+e<sup>-</sup>).

various ligands. Depending on the type of iron ligand, iron containing protein can be divided into three groups, iron-sulfur cluster proteins, heme proteins and non-heme proteins (Hell and Stephan, 2003).

### **1.2.1 Iron-sulfur cluster proteins**

Iron-sulfur (Fe-S) clusters are ancient and ubiquitous cofactors that are arguably the most abundant use of iron. (Balk and Schaedler, 2014). As the name suggests, iron-sulfur clusters are formed by iron and sulfur atoms, which are generally coordinated in proteins *via* cysteinyl residues (Beinert, 2000). Diamond [2Fe-2S] and the cubane [4Fe-4S] clusters are more commonly encountered, although other different types of clusters have been described, such as [2Fe-2S] Rieske-type, [2Fe-2S] NEET-type or the [3Fe-4S] type clusters (Figure 1-3A) (Beinert, 2000; Couturier *et al.*, 2013). The primary role of iron-sulfur cluster containing proteins is to participate in electron transfer reactions, generally as one-electron carriers. Hence, iron-sulfur clusters mainly contribute to electron transfer in photosynthetic and respiratory electron transport chain in chloroplasts and mitochondria, respectively (Couturier *et al.*, 2013). Secondly, iron-sulfur clusters also act as the crucial component of reaction center of many enzymes, which is required for the substrate binding and/or activation, or funneling electrons to the substrate.

### **1.2.2 Heme proteins**

Heme consists in a tetrapyrrole ring that holds a central iron atom. Four of the six coordination sites of iron are occupied by the heme pyrrole nitrogens, forming a flat, rigid and highly stable structure (Figure 1-3B) (Balk and Schaedler, 2014). The function of heme depends on the iron ligands perpendicular to the tetrapyrrole ring. Like in hemoglobin, myoglobin and guanylate cyclase, one axial coordination is occupied by proximal histidines of the proteins, and another one is open to bind the exogenous ligands, such as dioxygen (O<sub>2</sub>) and nitric oxide (NO). These heme proteins are commonly involved in ligand transport, storage, sensing, scavenging and detoxification (Hoy and Hargrove, 2008). In the very large group of cytochrome P450 enzymes, another free coordination site could bind water to catalyze hydroxylations and other reactions

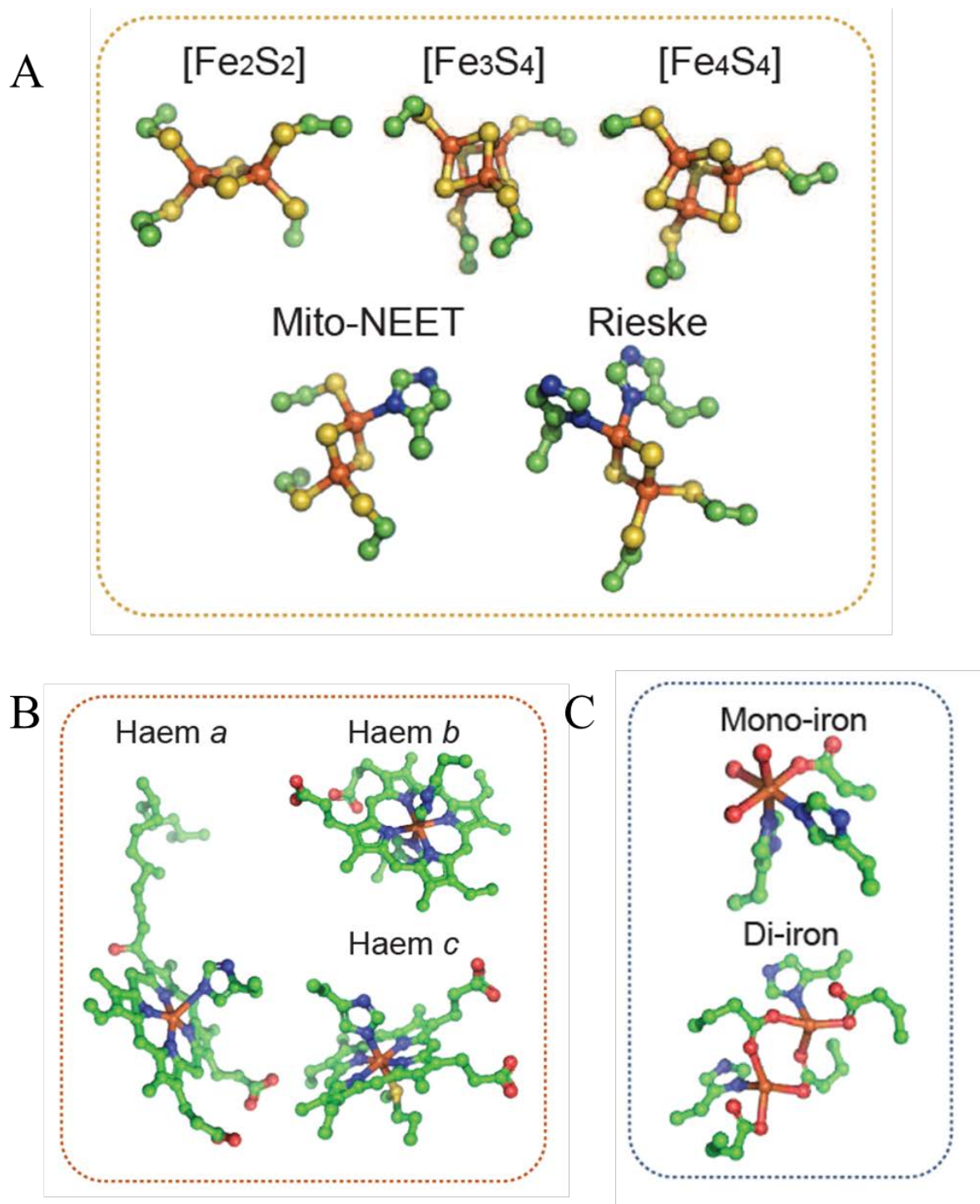


**Figure 1-3. Canonical Fe-binding structures found in Fe-S proteins(A), Heme proteins (B) and Non-Heme proteins (C).** Structures are represented as sticks with iron atoms in brown, sulfur in yellow, nitrogen in blue, carbon in green, and oxygen in red (From (Przybyla-Toscano *et al.*)).

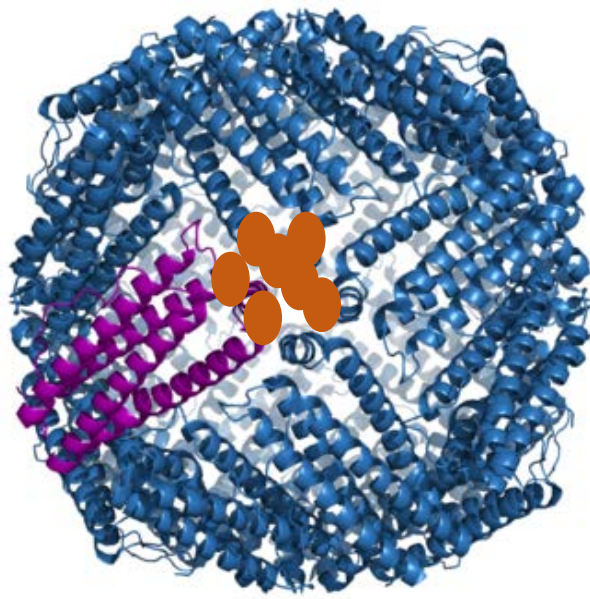


Figure 1-4. Ferritins in *Arabidopsis thaliana*.

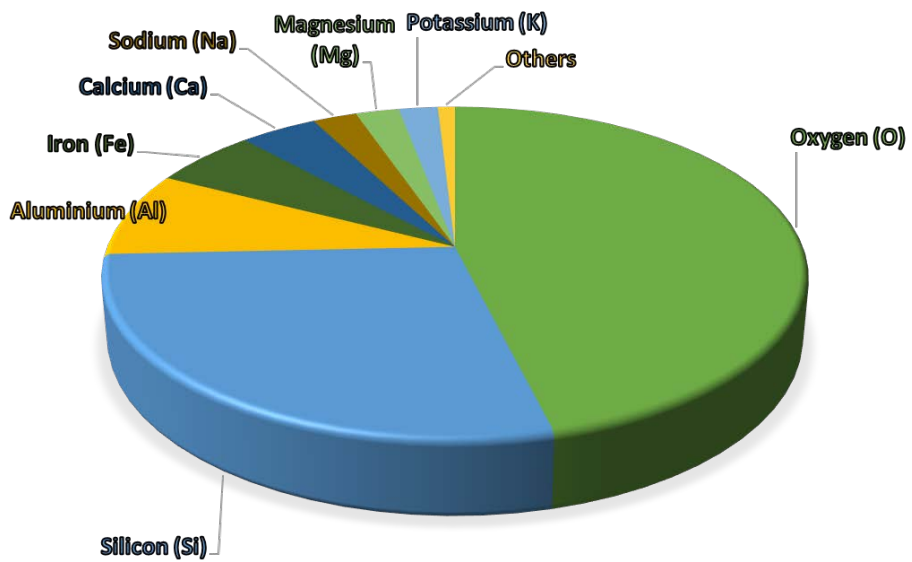


Figure 1-5. Abundance of elements in Earth's crust.

(Ortiz de Montellano, 2010). In photosynthetic and respiratory cytochromes, with an electron transfer function, the two axial coordination sites are occupied by two histidines or one histidine plus one methionine. In addition, in siroheme containing proteins sulfite reductase and nitrite reductase, one axial coordination site binds to cysteinyl of protein *via* a 4Fe-4S cluster bridge (Balk and Schaedler, 2014).

### **1.2.3 Non-heme iron proteins**

Non-heme iron proteins can also directly bind to the iron ion but neither in the iron-sulfur cluster nor in the heme form (Figure 1-3). Among these proteins, ferritins are most prominent and have a high capacity for iron storage. In plants, Ferritin is a hollow globular protein with high molecular weight comprising 24 subunits that can store up to 4500 iron atoms in a bioavailable form (Briat *et al.*, 2010) (Figure 1-4). Another example is the non-heme iron-dependent oxygenases, a widespread family of functionally diverse enzymes that contains a mononuclear non-heme iron centre which plays an important role in incorporating O<sub>2</sub> into a wide range of biological molecules (White and Flashman, 2016).

## **1.3 Iron homeostasis in plants**

Iron is the fourth abundant element in the earth crust, accounting for more than 5.6 % of its mass (Guerinot and Yi, 1994) (Figure 1-5) . Despite its abundance in the soil, its solubility and availability are very changeable depending on the soil eH-pH (Figure 1-6). Most of the iron present in the soil exists as ferric oxyhydrates that are practically insoluble under aerobic conditions. Therefore, iron is one of the limiting factors for the plant growth and development in neutral-to-alkaline soils, which is prevalent in over 30% of arable land, worldwide (Shenker and Chen, 2005) (Figure 1-7).

Iron deficiency is known to affect various physiological processes in higher plants (Briat *et al.*, 2015). The most notable symptom of iron deficiency is yellowing between the veins of the young leaves, known as chlorosis (Figure 1-8). The chlorosis phenotype could be explained by the deleterious effect of iron deficiency on chlorophyll synthesis, reducing the chlorophyll contents in the leaves (Tottey *et al.*, 2003). In addition, iron deficiency reduce the protein

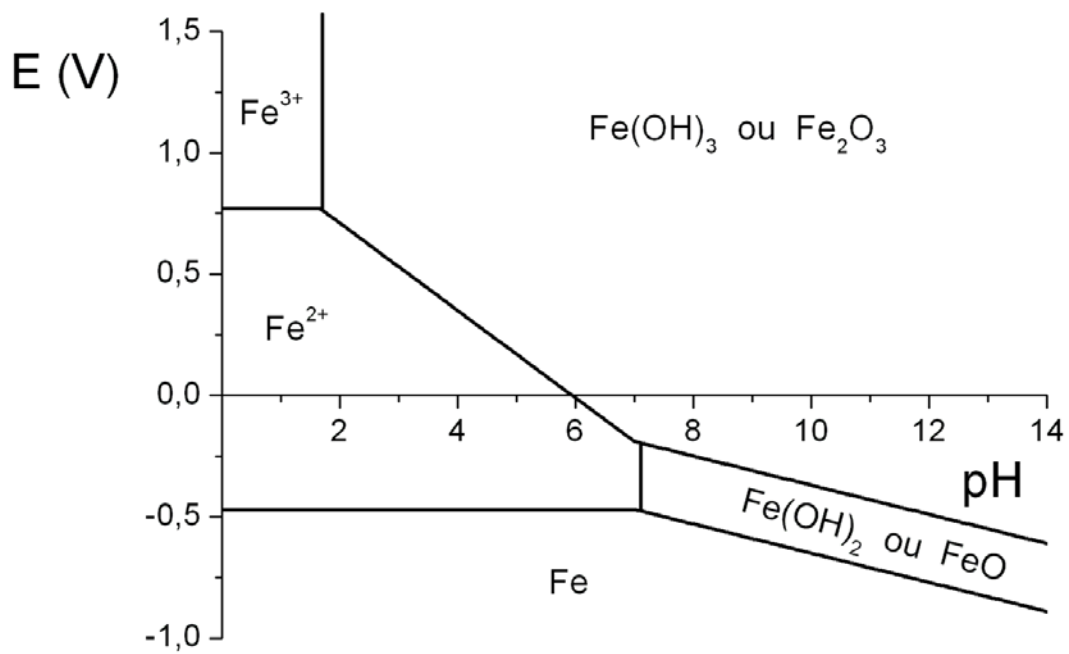


Figure 1-6.  $E_H$ -pH diagram of iron.

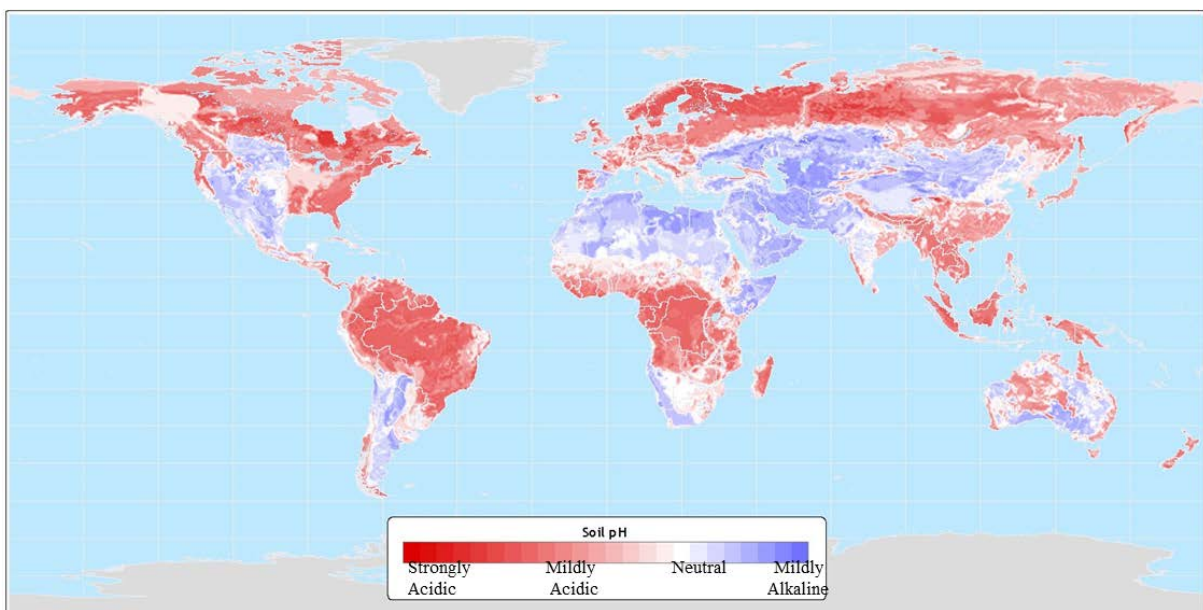
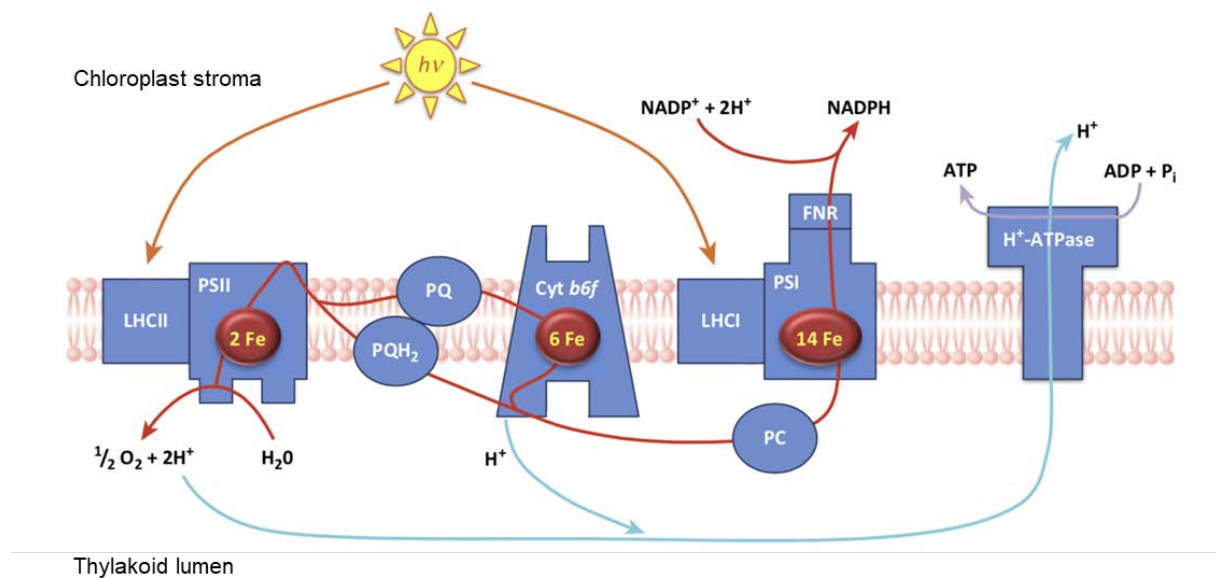


Figure 1-7. Global variation in soil pH.



**Figure 1-8. Fe deficiency-mediated chlorosis in different plant species.** Plants grown in iron sufficient conditions: (A) *Arabidopsis thaliana*, (B) tomato (*Solanum lycopersicum*), (C) sugar beet (*Beta vulgaris*), (D) lupine (*Lupinus albus*), and (E) peach tree (*Prunus persica*). Plants grown in Fe-deficient conditions: (F) Arabidopsis, (G) tomato, (H) sugar beet, (I) lupine, and (J) peach trees (Pictures B to E and G to H are from (Rellán-Álvarez *et al.*, 2011)).



**Figure 1-9. The role of iron in structure and/or function of the photosynthetic electron transfer chain at the thylakoid membrane (From (Briat *et al.*, 2015)).**

contents of electron transfer chain components (including the core and light-harvesting components of the PSI and PSII protein complexes) as well as cytochrome b6/f, thus decreasing electron transport between the photosystems (PSI and PSII) in both dicotyledonous and monocotyledonous plants (Briat *et al.*, 2015) (Figure 1-9). In legumes, iron deficiency also affects the nodule initiation and development as well as the nitrogenase activity (Brear *et al.*, 2013). In addition, iron deficiency also causes heavy metal accumulation (e.g. Mn, Zn) in plant tissues, which is toxic for the plants. As results, iron deficiency causes decreases in vegetative growth as well as marked yield and quality losses.

However, Plants can also suffer from iron toxicity when too much of iron is applied under acidic or submerged/anaerobic conditions. Among soil types, mainly acid clay soil, acid sulfate soil, and peat soil cause iron toxicity (Becker and Asch, 2005). Therefore, one of the most important abiotic stress in agriculture worldwide arises from high iron availability due to lower soil pH, with more than 50% of arable land too acid for optimal crop production, particularly in south China, southeast Asia, west and central Africa and Brazil (Aung and Masuda, 2020) (Figure 1-6). Excess free iron shows potential detrimental effects on plant cells because of its propensity to react with hydrogen peroxide, generating harmful free radicals through the Fenton reaction (Winterbourn, 1995) (Figure 1-10). The hydroxyl radical (OH•) is a highly reactive molecular specie with an unpaired electron, which can disrupt the antioxidant defense system in plant cells and damage cell membranes and cellular macromolecules such as proteins and nucleic acids thereby leading to cell death (Cho and Seo, 2005). The first symptom of iron excess is the appearance of necrotic spots and the bronzing of the leaves, which can ultimately stunt plant growth and result in crop yield loss or complete crop failure (Sperotto *et al.*, 2010) (Figure 1-11).

Consequently, plants have to quickly react to iron availability in soils and keep the iron homeostasis to avoid iron deficiency as well as iron overload in plant cells. It is noteworthy that the ability of plants to respond to iron availability not only affects crops yield and the quality of their derived products, but also affect the human nutrition. Therefore, elucidating the mechanisms of iron homeostasis is the first critical step to breed crops that are more nutrient rich and more capable of withstanding iron-limited soils.



# Fenton Reaction

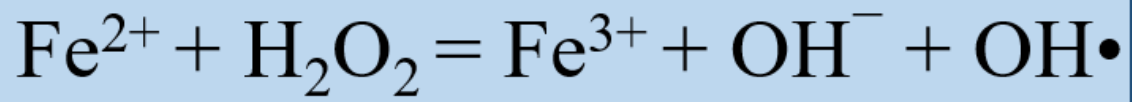


**Figure 1-10. Fenton reaction.** Free Iron ( $\text{Fe}^{2+}$ ) reacts with hydrogen peroxide, leading to the generation of very reactive and damaging hydroxyl radicals ( $\text{OH}\bullet$ ).



**Figure 1-11. Iron excess causes leaf bronzing in different plant species.** A: rice (*Oriza sativa*), B: marigold (*Targetes* spp.), C: *Rotala rotundifolia*

## 1.4 Iron uptake in plants

To adapt to different soil conditions, plants have developed two specific strategies to secure iron uptake. Most the higher plants, including *Arabidopsis thaliana*, employ a reduction based strategy (Strategy I), that includes three main steps: iron solubilization; reduction of  $\text{Fe}^{3+}$  into  $\text{Fe}^{2+}$ ; and subsequent  $\text{Fe}^{2+}$  transport into the root epidermal cells (Hell and Stephan, 2003) (Figure 1-12). Plants from gramineae family, including rice and other important crops utilize the chelation strategy (Strategy II) to chelate the  $\text{Fe}^{3+}$  and form more soluble complexes, which are then taken up by the root (Römheld and Marschner, 1986) (Figure 1-12).

### 1.4.1 Strategy I

Components of the reduction based iron uptake strategy (Strategy I) have been studied in various non-graminaceous plant species, but it is best characterized in *Arabidopsis* (Eckhardt *et al.*, 2001; Li *et al.*, 2004; Römheld and Marschner, 1983; Waters *et al.*, 2007). In *Arabidopsis*, iron absorption is achieved through three main processes step by step, which depend on the action of proteins present in plasma membrane of root epidermis cells. In response to iron deficiency, firstly, plants are able to release protons into the rhizosphere through  $\text{H}^+$ -ATPases expressed in the root epidermis cells, which would acidify the rhizosphere and promote iron solubility (Santi *et al.*, 2005; Santi and Schmidt, 2009). Although three plasma membrane  $\text{H}^+$ -ATPases family members (i.e. AHA1, AHA2 and AHA7) are induced under iron deficiency, AHA2 was identified as the dominant gene responsible for the local rhizosphere acidification during iron deficiency (Santi and Schmidt, 2009) (Figure 1-12).

Once solubilized,  $\text{Fe}^{3+}$  is subsequently reduced to  $\text{Fe}^{2+}$  through an enzymatic process performed by the NADPH-dependent FERRIC REDUCTASE-OXIDASE 2 (FRO2)(Robinson *et al.*, 1999) (Figure 1-12). FRO2 was identified based on its sequence similarity to the yeast ferric reductase FRE1 and a subunit of the human NADPH oxidase, NOX2 (Robinson *et al.*, 1999; Vignais, 2002). As expected for an enzyme involved in iron uptake from the soil, FRO2 is a plasma membrane-localized protein that is expressed at the root epidermis and whose expression is strongly induced by iron deficiency (Connolly *et al.*, 2003). The *frd1* mutant (*FRO2* loss-of-function) displays reduced activity of root surface ferric-chelate reductase activity, resulting in

impaired plant growth under iron deficiency as compared with wild type (Robinson *et al.*, 1999). In contrast, overexpression of ferric chelate reductase genes could enhance the iron deficiency tolerance in different plant species (Connolly *et al.*, 2003; Ishimaru *et al.*, 2007; Vasconcelos *et al.*, 2006). These studies highlighted that the reduction of Fe<sup>3+</sup> to Fe<sup>2+</sup> is the rate-limiting step in iron acquisition in plants, at least when the pH of the surrounding media is lower than 6.

In the last step, Fe<sup>2+</sup> can be transported from the rhizosphere, across the plasma membrane, into epidermal cells by the high-affinity divalent iron transporter IRT1 (Henriques *et al.*, 2002; Korshunova *et al.*, 1999; Vert *et al.*, 2002) (Figure 1-12). *IRT1* is expressed in the external cell layers of the root and is strongly induced by iron limitation (Vert *et al.*, 2002). *irt1-1* knockout mutant show severe iron deficiency chlorosis and growth defects together with reduced iron contents in the leaves when grown in soil (Vert *et al.*, 2002). In yeast complementation assay, IRT1 not only complement the yeast mutant *fet3fet4* (defective in iron uptake), but also complement the *smfΔ* (defective in manganese uptake) and *zrt1zrt2* (defective in zinc uptake) (Eide *et al.*, 1996; Korshunova *et al.*, 1999). Further experiments lead to the conclusion that IRT1 can also transport divalent heavy metals potentially toxic to plants such as zinc (Zn), manganese (Mn), cadmium (Cd) and cobalt (Co).

The secretion of iron-mobilizing coumarins as chelators and/or reductants of Fe<sup>3+</sup> has recently been identified as an additional component of Strategy I, which can positively affect plant iron uptake at neutral to alkaline conditions, when iron is only present in the form of insoluble oxides and hydroxides (Robe *et al.*, 2020a; Robe *et al.*, 2020b; Stassen *et al.*, 2020) (Figure 1-12). The expressions of the structural genes of the iron-mobilizing coumarin biosynthesis pathway, including *COSY* (*COUMARIN SYNTHASE*; Vanholme *et al.*, 2019), *F6'H1* (*FERULOYL-CoA 6'-HYDROXYLASE 1*; (Schmid *et al.*, 2014), *S8H* (*SCOPOLETIN 8-HYDROXYLASE*; Siwinska *et al.*, 2018; Tsai *et al.*, 2018) and *CYP82C4* (*CYTOCHROME P450, FAMILY 82, SUBFAMILY C, POLYPEPTIDE 4*; (Murgia *et al.*, 2011) are responsive to iron deficiency. Mutants defective in the expression of *COSY*, *F6'H1* or *SH8* showed increased sensitivity to iron limitation growth conditions and display decreased total iron accumulation (Schmid *et al.*, 2014; Siwinska *et al.*, 2018; Tsai *et al.*, 2018; Vanholme *et al.*, 2019). In addition, the coumarin transporter PLEIOTROPIC DRUG RESISTANCE 9/ATP-BINDING CASSETTE G37 (PDR9/ABCG37) transporter, that can transport the coumarins from the cortex to the

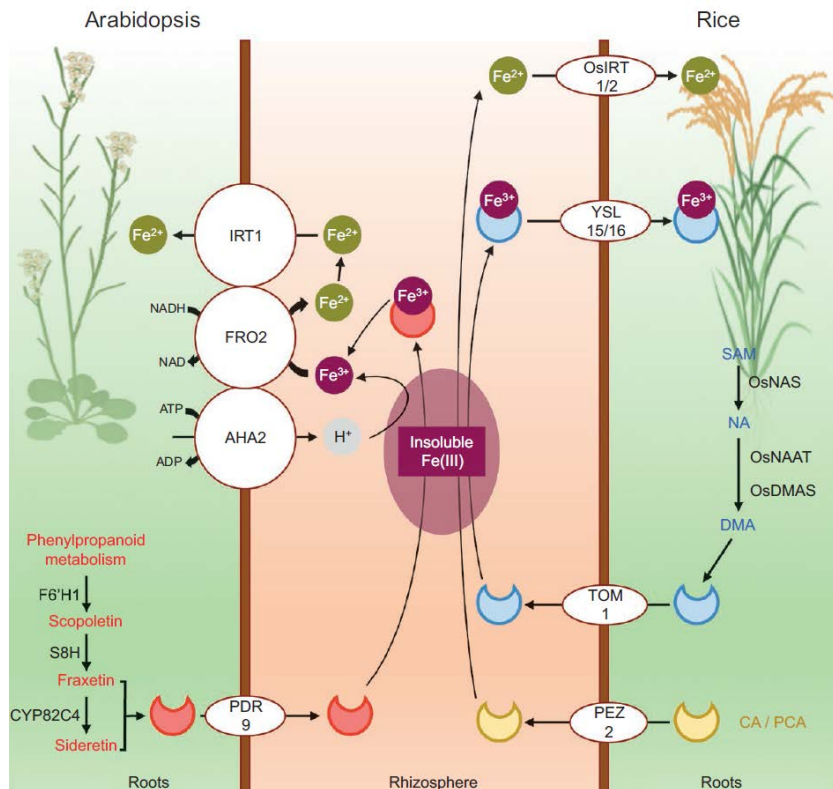


**Figure 1-12. Schematic diagram of iron uptake strategies in Arabidopsis and rice.** In Arabidopsis, AHA2 secretes protons into the rhizosphere to increase  $\text{Fe}^{3+}$  solubility; PDR9 secretes Fe-mobilizing coumarins (*i.e.* fraxetin and sideretin) to mobilize and chelate  $\text{Fe}^{3+}$ .  $\text{Fe}^{3+}$  is reduced into  $\text{Fe}^{2+}$  and is subsequently transported into the root epidermal cells by FRO2 and IRT1, respectively. AHA2, FRO2 and IRT1 form a protein complex optimizing Fe acquisition by creating a local environment with low pH and high  $\text{Fe}^{2+}$  concentration. Rice biosynthesizes and secretes DMA to chelate  $\text{Fe}^{3+}$ .  $\text{Fe}^{3+}$ -DMA complexes are transported into root cells *via* YSL15 and YSL16. In addition, rice also uptake  $\text{Fe}^{2+}$  from the soil through the activity of two  $\text{Fe}^{2+}$  transporters, OsIRT1 and OsIRT2 under waterlogged soil condition. The secretion of CA and PCA via the PEZ2 phenolics efflux transporter participates to  $\text{Fe}^{3+}$  mobilization and reduction into  $\text{Fe}^{2+}$ . AHA2:  $\text{H}^+$ -ATPase 2; PDR9: PLEIOTROPIC DRUG RESISTANCE 9/ATP-BINDING CASSETTE G37; FRO2: Ferric Reduction Oxidase 2; IRT1: Iron-Regulated Transporter 1, F6'H1: Feruloyl CoA 6' hydroxylase 1; S8H: Scopoletin 8-hydroxylase; CYP82C4: Fraxetin 5-hydroxylase; TOM1: Transporter of Mugineic acid 1; YSL15/16: Yellow Stripe-Like 15/16; OsIRT1/2: Rice Iron-Regulated Transporter 1/2; PEZ2: PHENOLICS EFFLUX ZERO 2; SAM: S-adenosyl Methionine; NA: nicotianamine; CA: caffeic acid; PCA: protocatechuic acid (From Gao and Dubos, 2021).

rhizosphere, is also required for improving iron uptake under the iron deficiency conditions (Fourcroy *et al.*, 2014; Fourcroy *et al.*, 2016; Robe *et al.*, 2020a). Although the precise mechanism of the coumarins in iron uptake is still unknown, it is believed that the secretion of coumarins increase  $\text{Fe}^{3+}$  mobilization and iron uptake.

#### **1.4.2 Strategy II**

In the plants from gramineae family, Strategy II iron uptake relies on biosynthesis and secretion of mugineic acid (MA)-family phytosiderophres (Hell and Stephan, 2003). In response to iron deficiency, MA-family phytosiderophres are synthesized through a conserved pathway from methionine (Bashir *et al.*, 2006; Ma *et al.*, 1999; Mori and Nishizawa, 1987; Shojima *et al.*, 1990) (Figure 1-12). In this pathway, the production of 2-deoxymugineic acid (DMA), the precursor of all the MAs, is mediated by three sequential enzymatic reactions catalyzed by nicotianamine synthase (NAS), nicotianamine aminotransferase (NAAT), and deoxymugineic acid synthase (DMAS) enzymes (Bashir *et al.*, 2006; Higuchi *et al.*, 1999; Takahashi *et al.*, 1999) (Figure 1-12). The expression of the corresponding genes is strongly induced by iron deficiency. Then, the plasma membrane located transporter TOM1 (TRANSPORTER OF MUGINEIC ACID 1) releases phytosiderophres into the rhizosphere, which can solubilize and chelate the  $\text{Fe}^{3+}$  to form  $\text{Fe}^{3+}$ -MA complexes (Nozoye *et al.*, 2011). The soluble and stable  $\text{Fe}^{3+}$ -MA complexes are subsequently taken up into root epidermis cells via a high affinity uptake system mediated by the YELLOW STRIPE 1 (YS1) and YELLOW STRIPE 1-like (YSL) transporters (Curie *et al.*, 2001; Inoue *et al.*, 2009; Lee *et al.*, 2009; Murata *et al.*, 2006) (Figure 1-12). In addition, MAs are also play a role in the chelation and uptake of non-iron metals such as Zn as a form of  $\text{Zn}^{2+}$ -MAs complexes (Suzuki *et al.*, 2006).

#### **1.5 Long distance iron translocation in plants**

In contrast to the abundant data on root iron uptake and its regulation (Gao and Dubos, 2020; Gao *et al.*, 2020a; Gao *et al.*, 2020b; Gao *et al.*, 2019b; Morrissey and Guerinot, 2009), relatively little is known regarding iron translocation in plants. Briefly, iron translocation in plants involves several steps, including the symplastic transport of iron toward the vasculature

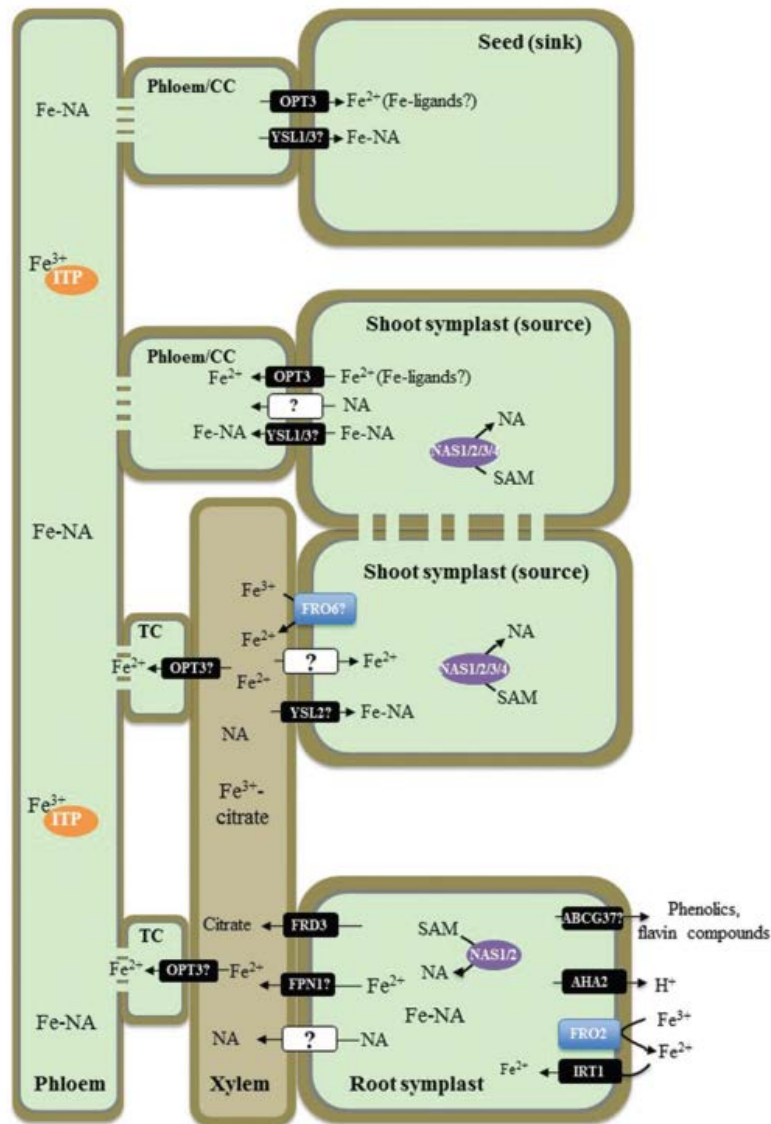


**Figure 1-13. Overview of iron transport in *Arabidopsis thaliana*.** Once transported into the root epidermal cells, iron is chelated, probably with the nicotianamine (NA). Then, Fe-NA complexes move symplastically in interconnected cytoplasm of the root toward the vasculature. IREG1/FPN1 (IRON REGULATED1/FERROPORTIN 1) is implicated in loading iron into the xylem, while FRD3 (FERRIC REDUCTASE DEFECTIVE 3) provides citrate. Once in the xylem, iron is bound by citrate to form (tri)Fe<sup>3+</sup>-(tri)citrate complexes, which move toward the shoot via the transpiration stream. In phloem sap, iron is chelated by NA. Phloem is specifically used to transport iron to the developing organs, such as the apex and the seeds. OPT3 (OLIGOPEPTIDE TRANSPORTER 3), YSL 1 and YSL3 play a role in loading iron into the seeds, while YSL2 is proposed to transport Fe-NA complexes to mesophyll cells (YSL1, 2 and 3: YELLOW STRIPE-LIKE 1, 2 and 3).

*via* plasmodesmata in root tissues, the loading of iron into the xylem, the long-distance transport of iron to the shoot via the xylem sap and its unloading, the transfer of iron from the xylem to the phloem, the loading of iron into the phloem, the transport of iron into the phloem sap, the unloading of iron and the symplastic transport to the places of highest demand (Gayomba *et al.*, 2015; Kim and Guerinot, 2007; Kobayashi and Nishizawa, 2012) (Figure 1-13). To avoid precipitation and potential cellular damage by the generation of harmful reactive oxygen species (ROS) through the Fenton reaction, iron translocation inside the plant body relies on suitable chelators such as citrate and nicotianamine (NA) (Grillet *et al.*, 2014; Hell and Stephan, 2003).

### 1.5.1 Xylem transport

After entering the root epidermal cells, it is almost certain that iron is chelated by unknown chelator(s). The iron complex moves symplastically in interconnected cytoplasm of the root, and perhaps diffuses down a concentration gradient, from areas of higher concentration to areas of lower concentration (Marschner, 1995). At the pericycle, iron is effluxed into the xylem sap *via* one or more transporters. To date, the most promising transporter contributing to this process is IREG1/FPN1 (IRON REGULATED1/FERROPORTIN 1), although its transport activity has not been identified (Morrissey *et al.*, 2009). Once transported into the xylem, iron is known to be chelated by citrate to form a (tri)Fe<sup>3+</sup>-(tri)citrate complex, which moves toward the shoot via the transpiration stream (Curie *et al.*, 2009; Gayomba *et al.*, 2015; Rellán-Alvarez *et al.*, 2010) (Figure 1-14). FRD3 (FERRIC REDUCTASE DEFECTIVE 3), a MULTIDRUG AND TOXIN EFFLUX (MATE) transporter, is proposed to mediate citrate loading into xylem vessels (Durrett *et al.*, 2007; Green and Rogers, 2004; Rogers and Guerinot, 2002; Roschzttardtz *et al.*, 2011). *FRD3* is expressed in the root pericycle and vascular cylinder and is induced by iron deficiency (Green and Rogers, 2004; Rogers and Guerinot, 2002). The loss of *FRD3* function results in leaf chlorosis and constitutive iron deficiency response. In addition, *frd3* mutant showed significant iron accumulation in the central vascular cylinder of roots and failure to transport iron to shoot, indicating that *FRD3* plays a role in long distance iron transport in xylem vessels (Durrett *et al.*, 2007; Green and Rogers, 2004; Rogers and Guerinot, 2002; Roschzttardtz *et al.*, 2011).

### 1.5.2 Phloem transport

Like the xylem, the phloem is also required for the iron long distance transport to support the plant growth and development. It is particularly used to transport this metal to the developing organs, such as apex and seeds, in which the transpiration flow in the xylem vessels is inefficient (Morrissey and Guerinot, 2009). In addition, iron remobilization from old leaves to young leaves also relies on the phloem transport. The pH of the phloem sap is more basic than that of the xylem sap. It is between 7 and 8, thus iron needs to be chelated in order to remain soluble. Nicotianamine (NA) has been proposed to act as iron chelator in the phloem based on its ability to form stable complexes with  $\text{Fe}^{2+}$  at alkaline pH (von Wiren *et al.*, 1999) (Figure 1-15). The important role of these complexes in iron long distance transport was demonstrated by the study of the tomato *chl*n mutant (*chloronerva*) (Herbik *et al.*, 1996; Ling *et al.*, 1996). This mutant is altered in a *NAS* gene (*NICOTIANAMINE SYNTHASE*) and shows strong interveinal chlorosis on young leaves, while its root iron uptake system is constitutively activated, and results in iron accumulation in the roots and leaves (Ling *et al.*, 1996). In Arabidopsis, there are four *NAS* genes, among them, the expression of *NAS2* and *NAS4* can be induced in the roots under iron deficiency conditions (Klatte *et al.*, 2009). The quadruple Arabidopsis loss of function mutant *nas4x-2* showed a chloronerva-like phenotype with strong leaf chlorosis and was sterile (Klatte *et al.*, 2009). Conversely, overexpression of a *Thlaspi caerulescens* *NAS* gene in Arabidopsis results in 100 times over accumulation of NA, decreased iron content and constitutive *IRT1* and *FRO2* induction in the roots (Cassin *et al.*, 2009). Thus, NA seems to be a preponderant element in allocation of iron to the organs that use it. In addition to NA, an iron binding protein, ITP (IRON TRANSPORT PROTEIN) has been identified in the phloem sap of castor bean (*Ricinus communis*) and proposed to participate to the transport of this micronutrient (Kruger *et al.*, 2002). The ITP protein was shown to bind  $\text{Fe}^{3+}$  but not  $\text{Fe}^{2+}$  (Kruger *et al.*, 2002).

The main transporters involved in the phloem loading and unloading of iron belong to the OLIGOPEPTIDE TRANSPORTER (OPT) family that includes the YELLOW STRIPE-LIKE



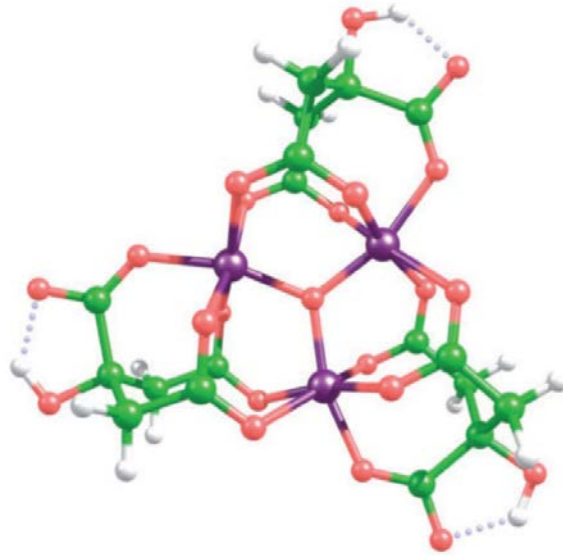


**Figure 1-14. Proposed structure of (tri)Fe<sup>3+</sup>-(tri)citrate complex in the plant xylem.** Iron, oxygen, carbon and hydrogen atoms are shown in purple, red, green and white, respectively (From(Rellán-Alvarez *et al.*, 2010)).



**Figure 1-15. Proposed chemical structure for nicotianamine-metal complexes.**

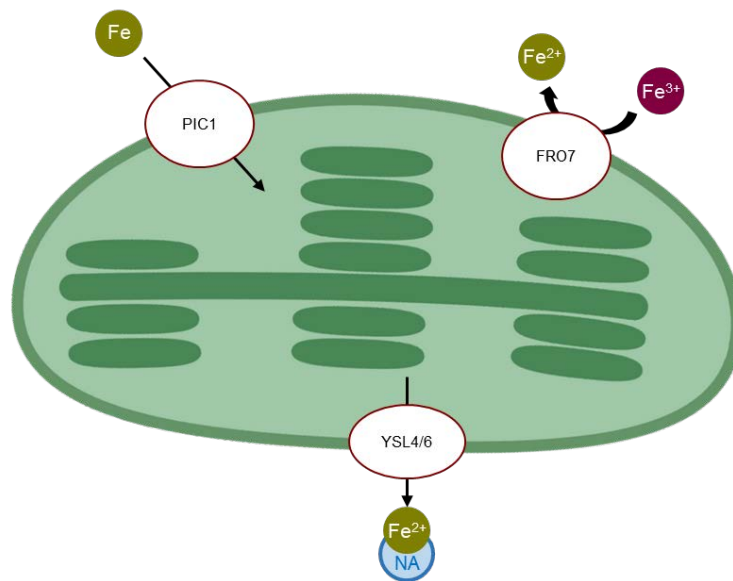


**Figure 1-16. Summary of the known iron transport mechanisms in Arabidopsis chloroplasts.** PIC1: PERMEASE IN CHLOROPLASTS 1, FRO7: FERRIC REDUCTION OXIDASE 7, YSL4 and 6: YELLOW STRIPE-LIKE 4 and 6. NA: nicotianamine.

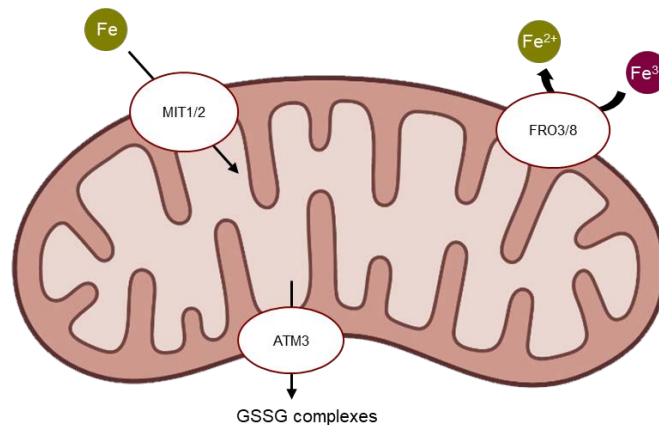


**Figure 1-17. Summary of the known iron transport mechanisms in Arabidopsis mitochondria.** MIT1 and 2: MITOCHONDRIAL IRON TRANSPORTER 1 and 2, FRO3 and 8: FERRIC REDUCTION OXIDASE 3 and 8, ATM3: ABC TRANSPORTER OF THE MITOCHONDRION 3. GSSG: oxidized glutathion.

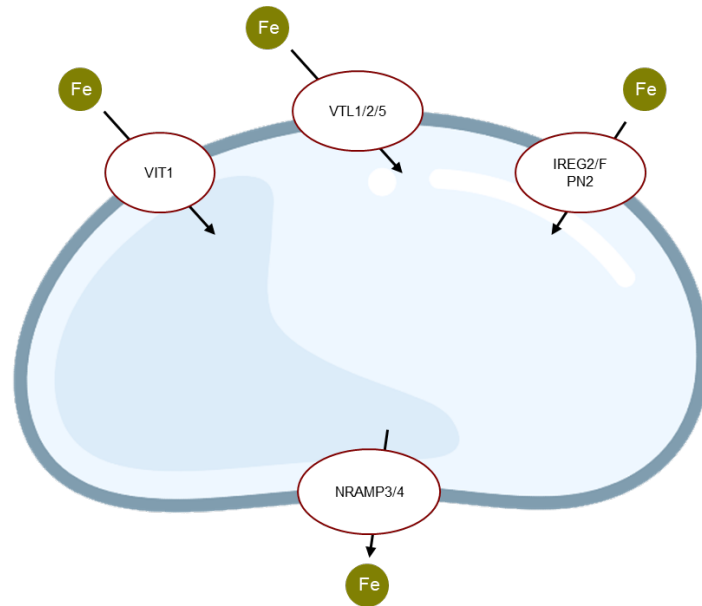


**Figure 1-18. Summary of the known iron transport mechanisms in Arabidopsis vacuoles.**

VIT1: VACUOLAR IRON TRANSPORTER 1, VTL1, 2 and 5: VIT1-LIKE 1, 2 and 5,  
 IREG2/FPN2: IRON REGULATED 2/ FERROPORTIN 2, NRAMP3 and 4: NATURAL  
 RESISTANCE ASSOCIATED MACROPHAGE 4 and 6

(YSL) proteins (Chu *et al.*, 2010; Curie *et al.*, 2009; DiDonato Jr *et al.*, 2004; Jean *et al.*, 2005; Lubkowitz, 2011; Schaaf *et al.*, 2005; Waters *et al.*, 2006). In Arabidopsis, YSL transporters are proposed to be involved in the transport of Fe<sup>2+</sup>-NA complexes (Waters *et al.*, 2006). Among the 8 YSL genes in Arabidopsis, YSL1, YSL2 and YSL3 could complement the iron uptake defect of the *fet3fet4* yeast mutant when Fe<sup>2+</sup>-NA was provided as a substrate (Chu *et al.*, 2010; DiDonato Jr *et al.*, 2004; Waters *et al.*, 2006). YSL1 and YSL3 were found to be expressed in a broad range of tissues, especially in the vasculature, and the *ysl1* and *ysl3* single loss-of-function mutants show decreased iron accumulation in seed, suggesting that these two genes play a partly redundant role in loading iron into the seeds (Chu *et al.*, 2010; Waters *et al.*, 2006). OPT3 plays also an essential role in loading iron into the seeds (Mendoza-Cózatl *et al.*, 2014; Stacey *et al.*, 2008; Zhai *et al.*, 2014). Studies in *Xenopus* oocytes demonstrated that OPT3 mediates uptake of Fe<sup>2+</sup> and Cd<sup>2+</sup> without ligands, suggesting that OPT3 is a transition metal transporter (Zhai *et al.*, 2014). Studies in Arabidopsis indicate that OPT3 could load iron into the phloem, facilitate iron recirculation from the xylem to the phloem and iron redistribution from mature to developing tissues (Mendoza-Cózatl *et al.*, 2014; Stacey *et al.*, 2008; Zhai *et al.*, 2014). In contrast, YSL2 has been proposed to function in lateral iron movement in the vasculature because of its specific expression in xylem parenchyma cells (DiDonato Jr *et al.*, 2004; Schaaf *et al.*, 2005).

## **1.6 Subcellular transport of iron**

Plants absorb iron from the soil and deliver it to specific subcellular compartments such as chloroplast or mitochondria where they participate in various metabolic processes, whereas vacuoles act as reservoirs to keep iron for later use and regulate the cell iron concentration balance.

### **1.6.1 Chloroplasts**

It is believed that chloroplasts are the largest iron pool in plant cells, holding nearly 80% to 90% of cellular iron in leaves (Marschner, 2011; Terry and Abadía, 1986). Chloroplast has a high demand for iron that is involved in photosynthesis, heme biosynthesis, and iron-sulfur cluster

assembly (Briat *et al.*, 2007). However, little is known about how iron is transported in and out of the chloroplast. The permease PIC1 (PERMEASE IN CHLOROPLASTS 1) has been identified, in Arabidopsis, to transport iron into the chloroplast (Duy *et al.*, 2007). PIC1 is localized in the inner envelope of the chloroplast and is able to complement the growth of the iron uptake defective yeast mutant *fet3fet4*. Loss-of-function of PIC1 leads to severe chlorosis, dwarfism and altered iron homeostasis, suggesting PIC1 plays a role in iron compartmentalization (Duy *et al.*, 2007) (Figure 1-16). However, it is still unknown whether Fe<sup>2+</sup> or Fe<sup>3+</sup> is transported by PIC1 and whether a ferric-chelate reductase is required. FRO7, a ferric-chelate reductase, is localized to the chloroplast. Chloroplasts of *fro7* loss-of-function mutant showed lower ferric chelate reductase activity and lower iron contents than those of wild-type chloroplasts, suggesting that the ferric chelate reductase activity is required for iron import into the chloroplasts (Jeong *et al.*, 2008) (Figure 1-16). In addition, it was reported that the YSL4 and YSL6 play a fundamental role in releasing chloroplastic Fe-NA complexes during plastid dedifferentiation occurring during the embryogenesis and the senescence (Divol *et al.*, 2013) (Figure 1-16).

## 1.6.2 Mitochondria

The mitochondrion is another important iron-requiring organelle in the plant cells. Indeed, iron is required for respiration, assembly of iron-sulfur clusters, biosynthesis of heme and other cofactors such as lipoic acid (Balk and Lobréaux, 2005; Lill *et al.*, 2015). However, iron transport in this organelle has not been fully clarified. In Arabidopsis, ATM3 (ABC TRANSPORTER OF THE MITOCHONDRION 3) localize to the mitochondria and can rescue the *Δatm1p* yeast mutant that over accumulates iron and non-heme proteins and lacks cytochromes (Chen *et al.*, 2007; Kushnir *et al.*, 2001). ATM3 loss-of-function mutant *stal* (*starik 1*) showed dwarf and chlorotic phenotype. The mitochondria of the *stal* mutant contain higher non-heme proteins than those of the wild-type, suggesting that ATM3 plays a role in export of glutathione polysulphide for the assembly of cytosolic iron-sulfur clusters in Arabidopsis (Kushnir *et al.*, 2001; Schaedler *et al.*, 2014) (Figure 1-17). Two ferric reduction oxidases, FRO3 and FRO8 localize to the mitochondria, thereby influencing the mitochondrial

iron homeostasis (Jain *et al.*, 2014) (Figure 1-17). Recently, two mitochondrial iron transporters, MIT1 and MIT2, belonging to the MITOCHONDRIAL CARRIER FAMILY (MCF) of transport proteins has been identified to play an important role in mitochondrial iron acquisition/import (Jain *et al.*, 2019). MIT1 and MIT2 (MITOCHONDRIAL IRON TRANSPORTER 1 and 2) could rescue the phenotype of the mitochondrial iron transport defective yeast mutant *mrs3mrs4*. Double loss-of-function *mit1mit2* mutant display decrease iron content in mitochondria, indicating that MIT1 and MIT2 mediate mitochondrial iron uptake in Arabidopsis (Jain *et al.*, 2019) (Figure 1-17).

### 1.6.3 Vacuoles

The vacuole serves as the most important reservoir to deposit the excess iron to avoid metal toxicity, and release iron in response to changes in cytosolic iron levels. In Arabidopsis, several vacuolar efflux and influx transporters from different transporter families have been identified. VACUOLAR IRON TRANSPORTER 1 (VIT1) and VIT1-LIKE (VTL) proteins have been characterized to mediate iron import into the vacuole (Gollhofer *et al.*, 2014; Kim *et al.*, 2006b; Roschttardt *et al.*, 2009) (Figure 1-18). *vit1* mutants show misdistribution of iron in seeds and strong chlorotic phenotype when grown on alkaline soil (Kim *et al.*, 2006a). The Arabidopsis VTL1, VTL2 and VTL5 could complement the yeast vacuolar iron transport mutant *Δccc1*. VTL1 and VTL2 are localized at the vacuolar membrane. These three VTL proteins are functional iron transporters that play a role in regulating cellular iron homeostasis, likely by acting as vacuolar iron transporters (Gollhofer *et al.*, 2014). In addition, IREG2/FPN2 (IRON REGULATED 2/ FERROPORTIN 2) localizes to the vacuole where it mediates nickel (Ni), Co and most probably iron transport into the vacuole to detoxify the root epidermal cells (Morrissey *et al.*, 2009; Schaaf *et al.*, 2006) (Figure 1-18). In contrast, two NATURAL RESISTANCE ASSOCIATED MACROPHAGE proteins, NRAMP3 and NRAMP4, that function oppositely to VIT1, are proposed to efflux iron from the vacuole to the cytosol under iron limiting conditions or when demand increases (Lanquar *et al.*, 2005; Mary *et al.*, 2015; Pottier *et al.*, 2015) (Figure 1-18).

## **1.7 Regulation of iron homeostasis**

Gene regulation is a crucial step for plants to adapt to fluctuating environmental conditions. To maintain iron homeostasis, plants have evolved regulatory mechanisms to control, at transcriptional and posttranslational levels, iron uptake, transport, storage and use.

### **1.7.1 Article 1. Transcriptional integration of plant responses to iron availability**

In this article, figure numbers are numbered independently of the rest of manuscript starting with Figure 1.

REVIEW PAPER

# Transcriptional integration of plant responses to iron availability

Fei Gao<sup>ID</sup> and Christian Dubos<sup>\*</sup><sup>ID</sup>

BPMP, Univ Montpellier, CNRS, INRAE, Institut Agro, Montpellier, France

\* Correspondence: [christian.dubos@inrae.fr](mailto:christian.dubos@inrae.fr)

Received 20 November 2020; Editorial decision 10 November 2020; Accepted 23 November 2020

Editor: Janneke Balk, John Innes Centre, UK

## Abstract

**Iron is one of the most important micronutrients for plant growth and development. It functions as the enzyme co-factor or component of electron transport chains in various vital metabolic processes, including photosynthesis, respiration, and amino acid biosynthesis. To maintain iron homeostasis, and therefore prevent any deficiency or excess that could be detrimental, plants have evolved complex transcriptional regulatory networks to tightly control iron uptake, translocation, assimilation, and storage. These regulatory networks are composed of various transcription factors; among them, members of the basic helix-loop-helix (bHLH) family play an essential role. Here, we first review recent advances in understanding the roles of bHLH transcription factors involved in the regulatory cascade controlling iron homeostasis in the model plant *Arabidopsis*, and extend this understanding to rice and other plant species. The importance of other classes of transcription factors will also be discussed. Second, we elaborate on the post-translational mechanisms involved in the regulation of these regulatory networks. Finally, we provide some perspectives on future research that should be conducted in order to precisely understand how plants control the homeostasis of this micronutrient.**

**Keywords:** *Arabidopsis thaliana*, basic helix-loop-helix, bHLH, iron homeostasis, rice, transcription factor.

## Introduction

Iron (Fe) is an essential micronutrient for almost all living organisms. In humans, iron deficiency anemia is a major global health issue, affecting about one billion people worldwide (Camaschella, 2015). Increasing the iron content of plants, especially crops (a process known as biofortification), would therefore have enormous benefits for human health. A critical step in achieving this goal is to uncover the mechanisms controlling iron homeostasis in plants. As in humans, iron is an essential microelement for plant growth and development. It functions in various vital metabolic processes (e.g. photosynthesis, respiration, and amino acid biosynthesis) by acting as a cofactor for several metalloproteins or a component of electron transport chains (Hänsch and Mendel, 2009; Touraine *et al.*,

2019). However, excess iron is deleterious to plants because of its capacity to interact with oxygen, generating reactive oxygen species via the Fenton reaction. Thus, the levels of iron in plant cells must be tightly regulated to avoid iron deficiency or iron excess, both of which severely affect the yield of crops and the quality of their derived products (Briat *et al.*, 2015).

Although iron is the fourth most abundant element on Earth, much of it is not readily available for plant use due to the poor solubility of its main oxides/hydroxides, especially in neutral to alkaline soils (Guerinot and Yi, 1994; Colombo *et al.*, 2018). To adapt to low-iron conditions and acquire iron from soil, higher plants have evolved two different strategies (Marschner and Römheld, 1994) (Fig. 1). Dicots and non-graminaceous



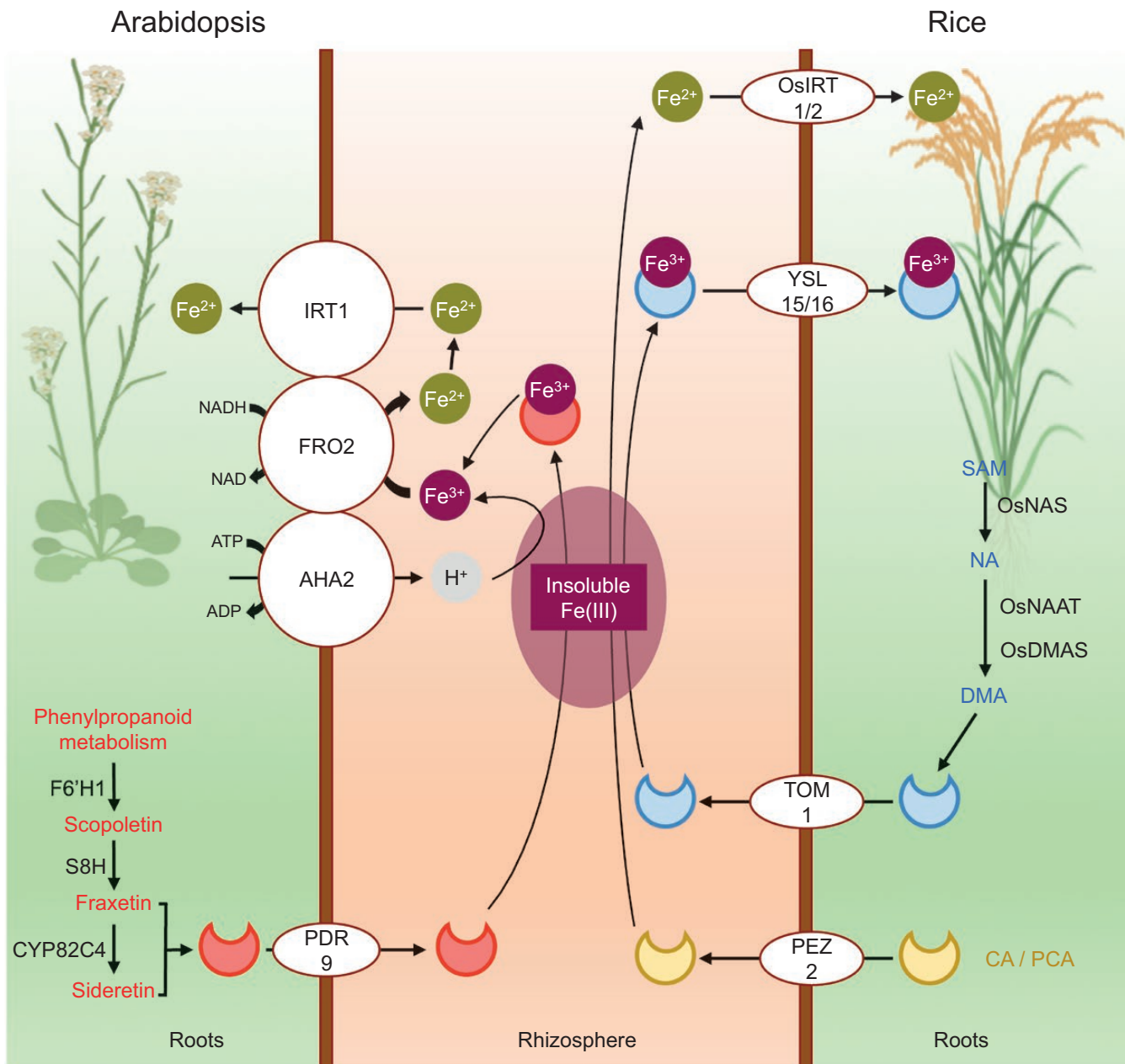


**Fig. 1.** Schematic diagram of iron uptake strategies in Arabidopsis and rice. In Arabidopsis, AHA2 secretes protons into the rhizosphere to increase  $\text{Fe}^{3+}$  solubility, and PDR9 secretes Fe-mobilizing coumarins (fraxetin and sideretin) to mobilize and chelate  $\text{Fe}^{3+}$ .  $\text{Fe}^{3+}$  is reduced into  $\text{Fe}^{2+}$  by FRO2 and is subsequently transported into the root epidermal cells by IRT1. AHA2, FRO2, and IRT1 form a protein complex that optimizes Fe acquisition by creating a local environment with low pH and high  $\text{Fe}^{2+}$  concentration. Rice biosynthesizes and secretes 2-deoxymugineic acid (DMA) to chelate  $\text{Fe}^{3+}$ .  $\text{Fe}^{3+}$ -DMA complexes are transported into root cells via YSL15 and YSL16. In addition, rice also takes up  $\text{Fe}^{2+}$  from the soil through the activity of two  $\text{Fe}^{2+}$  transporters, OsIRT1 and OsIRT2, under waterlogged soil conditions. The secretion of caffeic acid (CA) and protocatechuic acid (PCA) via the phenolics efflux transporter PEZ2 participates in  $\text{Fe}^{3+}$  mobilization and reduction into  $\text{Fe}^{2+}$ . AHA2,  $\text{H}^+$ -ATPase 2; CYP82C4, FRAXETIN 5-HYDROXYLASE; F6'H1, FERULOYL CoA 6' HYDROXYLASE 1; FRO2, FERRIC REDUCTION OXIDASE 2; IRT1, IRON-REGULATED TRANSPORTER 1; NA, nicotianamine; OsDMAS, DEOXYMUGINEIC ACID SYNTHASE; OsIRT1/2, rice IRON-REGULATED TRANSPORTER 1/2; OsNAAT, NICOTIANAMINE AMINOTRANSFERASE; OsNAS, NICOTIANAMINE SYNTHASE; PDR9, PLEIOTROPIC DRUG RESISTANCE 9/ATP-BINDING CASSETTE G37; PEZ2, PHENOLICS EFFLUX ZERO 2; S8H, SCOPOLETIN 8-HYDROXYLASE; SAM, S-adenosyl methionine; TOM1, TRANSPORTER OF MUGINEIC ACID 1; YSL15/16, YELLOW STRIPE-LIKE 15/16.

monocots (non-grass species) employ the reduction strategy, named Strategy I. The graminaceous species utilize the chelation strategy, named Strategy II.

In Strategy I, plants are able to acidify the rhizosphere to promote iron solubility through the release of protons, and mobilize  $\text{Fe}^{3+}$  through the secretion of coumarins (i.e. fraxetin and

sideretin) or riboflavins (Santi and Schmidt, 2009; Fourcroy et al., 2016; Robe et al., 2020). Following iron mobilization,  $\text{Fe}^{3+}$  is reduced to the more soluble form,  $\text{Fe}^{2+}$ , which is subsequently transported into the root epidermal cells via high-affinity iron transporters from the Zrt/Irt-like protein (ZIP) family. In *Arabidopsis thaliana*, the release of protons into the

rhizosphere is ensured by the H<sup>+</sup>-ATPASE 2 (AHA2; Santi and Schmidt, 2009), while the reduction of iron and its translocation into the roots are ensured by FERRIC REDUCTION OXIDASE 2 (FRO2) and IRON-REGULATED TRANSPORTER1 (IRT1), respectively (Brumbarova et al., 2015; Connorton et al., 2017). AHA2, FRO2, and IRT1 associate into a complex at the surface of the root epidermal cells, most likely allowing optimal iron acquisition and uptake (Martín-Barranco et al., 2020). Secretion of coumarins is ensured by the PLEIOTROPIC DRUG RESISTANCE 9/ATP-BINDING CASSETTE G37 (PDR9/ABCG37) transporter (Fourcroy et al., 2014; Fourcroy et al., 2016).

In Strategy II, plants biosynthesize and secrete phytosiderophores of the mugenic acid (MA) family into the rhizosphere to chelate Fe<sup>3+</sup> (Kobayashi et al., 2014). Fe<sup>3+</sup>-MAs complexes are then transported into root cells by transporters of the YELLOW STRIPE 1 (YS1) and YELLOW STRIPE 1-like (YSL) family (Murata et al., 2006; Inoue et al., 2009).

Interestingly, it was recently shown that some plant species might use both strategies. For instance, when grown in water-logged soil conditions, rice (*Oryza sativa*), a graminaceous species, acquires Fe<sup>2+</sup> from the soil through the activity of two Fe<sup>2+</sup> transporters, OsIRT1 and OsIRT2 (Ishimaru et al., 2006). The secretion of caffeic and protocatechuic acids via the PHENOLICS EFFLUX ZERO 2 (PEZ2) transporter participates in the mobilization of Fe<sup>3+</sup> and its reduction into Fe<sup>2+</sup> (Bashir et al., 2011). Iron acquisition is the first step in the maintenance of iron homeostasis in plants, and it should be noted that it is not the sole mechanism involved in this process. Iron translocation, compartmentalization, assimilation, and storage are also important processes required for the maintenance of iron homeostasis at the cellular and subcellular levels throughout the whole plant body (Kobayashi and Nishizawa, 2012; Kobayashi et al., 2019).

Gene regulation is a crucial step for coping with fluctuations in iron. For instance, *FRO2* and *IRT1* expression is induced when iron availability is low, whereas the expression of the genes encoding the iron storage ferritin proteins (i.e. *FER1*, *FER3*, and *FER4*) is induced in response to iron excess (Tissot et al., 2019). How plants control iron homeostasis by regulating the expression of genes involved in the various facets of this complex mechanism was a critical question for the past three decades. To address this question, several studies mostly based on forward and reverse genetic approaches were conducted, leading to the identification and characterization of several transcription factors (TFs). These studies, mostly conducted in *Arabidopsis* and rice, allowed regulatory networks controlling iron homeostasis to be established, in which basic helix-loop-helix (bHLH) TFs play a predominant role (Gao et al., 2019; Li et al., 2019; Gao et al., 2020a) (Fig. 2, Table 1). The bHLH proteins form one of the largest families of TFs (Heim et al., 2003) and are known to modulate several facets of plant growth and development, including cell differentiation, secondary metabolite biosynthesis, hormone signaling, and responses to environmental factors (Carretero-Paulet et al., 2010). Indeed, additional TFs and proteins regulating the activity of TFs were also identified (Palmer et al., 2013; Yan et al., 2016; Rodríguez-Celma et al., 2019a).

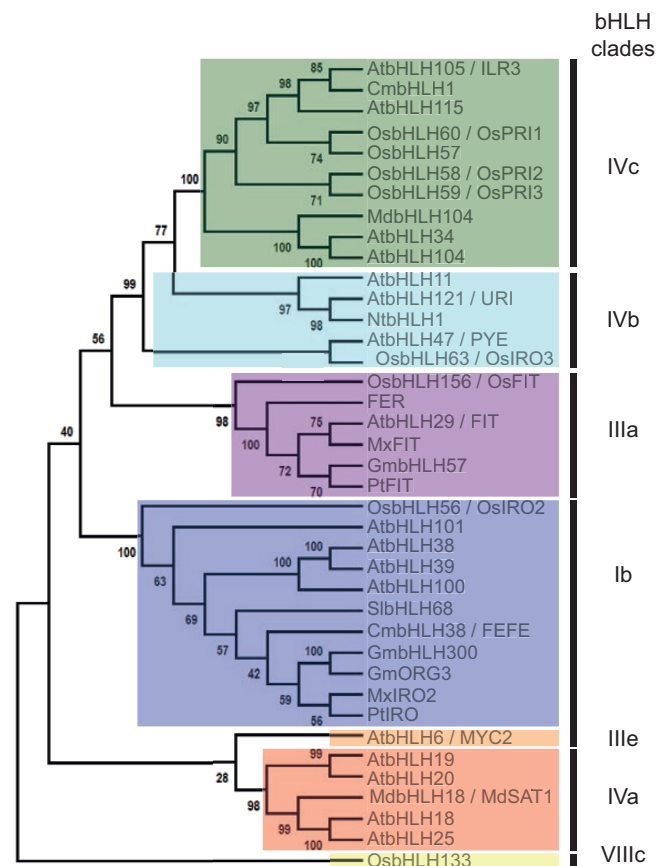


**Fig. 2.** Phylogenetic tree of bHLH TFs involved in the regulation of iron homeostasis in plants. The tree was constructed by using the neighbor-joining method with MEGA software (v10.0.5) using full-length bHLH amino acid sequences. The bootstrap analysis was carried out with 1000 replicates. Sequences were aligned before the construction of the phylogenetic tree using ClustalX software (v2.0.11). The different bHLH clades are designated as previously reported (Heim et al., 2003). Species abbreviations: At, *Arabidopsis thaliana*; Cm (CmbHLH1), *Chrysanthemum morifolium*; Cm (CmbHLH38), *Cucumis melo*; Gm, *Glycine max*; Md, *Malus domestica*; Mx, *Malus xiaojinensis*; Nt, *Nicotiana tabacum*; Os, *Oryza sativa*; Pt, *Populus tremula*; Sl, *Solanum lycopersicum*.

In this review, current knowledge on the control of iron homeostasis by TFs, especially those from the bHLH family, will be presented and discussed, with particular emphasis on the latest findings. The transcriptional and post-translational regulation of the iron homeostasis regulatory networks will also be described. Finally, some perspectives on future research to be conducted in order to improve our understanding of this complex mechanism will be provided.

## Transcriptional regulation of iron homeostasis in Strategy I plants: a predominant role for bHLH TFs

Studies in the model plant *Arabidopsis* have allowed the identification of several factors involved in the regulation of iron homeostasis, notably by investigating its response to iron deficiency. Such studies highlighted that the regulation of iron

**Table 1.** bHLH TFs involved in the regulation of iron homeostasis in plants

Name	Clade	Species	Interacting proteins	References
AtbHLH38 <sup>a</sup>	lb	<i>A. thaliana</i>	FIT/AtbHLH29, DELLAS	Yuan <i>et al.</i> , 2008; Wang <i>et al.</i> , 2013b
AtbHLH39 <sup>a</sup>	lb	<i>A. thaliana</i>	FIT/AtbHLH29, DELLAS	Yuan <i>et al.</i> , 2008; Wang <i>et al.</i> , 2013b
AtbHLH100 <sup>a</sup>	lb	<i>A. thaliana</i>	FIT/AtbHLH29	Wang <i>et al.</i> , 2013b
AtbHLH101 <sup>a</sup>	lb	<i>A. thaliana</i>	FIT/AtbHLH29	Wang <i>et al.</i> , 2013b
FIT/AtbHLH29 <sup>a</sup>	IIla	<i>A. thaliana</i>	AtbHLH38, AtbHLH39, AtbHLH100, AtbHLH101, AtbHLH18, AtbHLH19, AtbHLH20, AtbHLH25, BTSL1, BTSL2, CIPK11, DELLAS, EIL1, EIN3, MED16, ZAT12	Colangelo and Guerinot, 2004; Jakoby <i>et al.</i> , 2004; Yuan <i>et al.</i> , 2005
MYC2/AtbHLH6	IIle	<i>A. thaliana</i>		Cui <i>et al.</i> , 2018
AtbHLH18 <sup>a</sup>	IVa	<i>A. thaliana</i>	FIT/AtbHLH29	Cui <i>et al.</i> , 2018
AtbHLH19 <sup>a</sup>	IVa	<i>A. thaliana</i>	FIT/AtbHLH29	Cui <i>et al.</i> , 2018
AtbHLH20 <sup>a</sup>	IVa	<i>A. thaliana</i>	FIT/AtbHLH29	Cui <i>et al.</i> , 2018
AtbHLH25 <sup>a</sup>	IVa	<i>A. thaliana</i>	FIT/AtbHLH29	Cui <i>et al.</i> , 2018
AtbHLH11	IVb	<i>A. thaliana</i>	IDT1/AtbHLH34, AtbHLH104, ILR3/AtbHLH105, AtbHLH115	Tanabe <i>et al.</i> , 2019
PYE/AtbHLH47	IVb	<i>A. thaliana</i>	ILR3/AtbHLH105, AtbHLH115	Long <i>et al.</i> , 2010
URI/AtbHLH121	IVb	<i>A. thaliana</i>	IDT1/AtbHLH34, AtbHLH104, ILR3/AtbHLH105, AtbHLH115	Kim <i>et al.</i> , 2019; Gao <i>et al.</i> , 2020b; Lei <i>et al.</i> , 2020
IDT1/AtbHLH34	IVc	<i>A. thaliana</i>	IDT1/AtbHLH34, AtbHLH104, ILR3/AtbHLH105, AtbHLH115, AtbHLH11, URI/bHLH121	Li <i>et al.</i> , 2016
AtbHLH104	IVc	<i>A. thaliana</i>	IDT1/AtbHLH34, AtbHLH104, ILR3/AtbHLH105, AtbHLH115, AtbHLH11, URI/ bHLH121	Zhang <i>et al.</i> , 2015
ILR3/AtbHLH105	IVc	<i>A. thaliana</i>	IDT1/AtbHLH34, AtbHLH104, ILR3/AtbHLH105, AtbHLH115, AtbHLH11, PYE/ bHLH47, URI/bHLH121, BTS	Zhang <i>et al.</i> , 2015
AtbHLH115	IVc	<i>A. thaliana</i>	IDT1/AtbHLH34, AtbHLH104, ILR3/AtbHLH105, AtbHLH115, AtbHLH11, PYE/ bHLH47, URI/bHLH121, BTS	Liang <i>et al.</i> , 2017
OsIRO2/OsbHLH56	lb	<i>O. sativa</i>	OsFIT/OsbHLH156	Ogo <i>et al.</i> , 2006
OsIRO3/OsbHLH63	IVb	<i>O. sativa</i>		Zheng <i>et al.</i> , 2010
OsFIT/OsbHLH156	IIla	<i>O. sativa</i>	OsIRO2/OsbHLH56	Liang <i>et al.</i> , 2020; Wang <i>et al.</i> , 2020
OsPRI1/OsbHLH60	IVc	<i>O. sativa</i>	OshRZ1	Zhang <i>et al.</i> , 2017
OsPRI2/OsbHLH58	IVc	<i>O. sativa</i>	OshRZ1	Kobayashi <i>et al.</i> , 2019
OsPRI3/OsbHLH59	IVc	<i>O. sativa</i>	OshRZ1	Kobayashi <i>et al.</i> , 2019
OsbHLH133	VIIc	<i>O. sativa</i>		Wang <i>et al.</i> , 2013a
GmbHLH57	IIla	<i>G. max</i>	GmbHLH300	Li <i>et al.</i> , 2018
GmbHLH300	lb	<i>G. max</i>	GmbHLH57	Li <i>et al.</i> , 2018
FER	IIla	<i>S. lycopersicum</i>	SibHLH68	Ling <i>et al.</i> , 2002
SibHLH68	lb	<i>S. lycopersicum</i>	FER	Du <i>et al.</i> , 2015
MxIRO2	lb	<i>M. xiaojinensis</i>		Yin <i>et al.</i> , 2013
MxFIT	IIla	<i>M. xiaojinensis</i>	MxERF4	Yin <i>et al.</i> , 2014
PtFIT	IIla	<i>P. tremula</i>		Huang and Dai, 2015
PtIRO	lb	<i>P. tremula</i>		Huang and Dai, 2015
SAT1/MdbHLH18	IVa	<i>M. domestica</i>	MdMYB58	Wang <i>et al.</i> , 2018
MdbHLH104	IVc	<i>M. domestica</i>	MdbT1, MdBT2, MdbHLH104, MdbHLH105, MdbHLH115, MdbHLH11, MdbHLH121, MdPYE	Zhao <i>et al.</i> , 2016b
NtbHLH1	IVb	<i>N. tabacum</i>		Li <i>et al.</i> , 2020
CmbHLH1	IVc	<i>C. morifolium</i>		Zhao <i>et al.</i> , 2014
FEFE/CmbHLH38	lb	<i>C. melo</i>	CmFIT	Ramamurthy and Waters, 2017
GmORG3	lb	<i>G. max</i>		Xu <i>et al.</i> , 2017

<sup>a</sup> For details on post-translational regulation of FIT activity, see Schwarz and Bauer (2020) and Wu and Ling (2019).

homeostasis essentially occurs at the transcriptional level and involves several TFs, in particular those of the bHLH family. This topic has also been covered in recent reviews (Gao *et al.*, 2019; Kobayashi, 2019; Kobayashi *et al.*, 2019; Wu and Ling, 2019; Schwarz and Bauer, 2020). To date, at least six bHLH TF subfamilies (Heim *et al.*, 2003), encompassing 17 different proteins, are known to participate in the maintenance of iron homeostasis in Arabidopsis. These bHLH TFs form an intricate regulatory network composed of two interconnected regulatory modules (Fig. 3).

The first module relies on the activity of FIT/bHLH29 (FER-LIKE IRON DEFICIENCY INDUCED TRANSCRIPTION FACTOR), a clade IIIa bHLH TF (Colangelo and Guerinot, 2004; Jakoby *et al.*, 2004; Yuan *et al.*, 2005). FIT/bHLH29 is a direct regulator of *IRT1* and *FRO2* expression, highlighting its central role in the regulation of the iron uptake machinery (Wang *et al.*, 2013b). FIT/bHLH29 activity relies on its interaction with the four members of the Ib bHLH clade (bHLH38, bHLH39, bHLH100, and bHLH101), forming heterodimer complexes displaying partially redundant activities (Colangelo and Guerinot, 2004; Yuan *et al.*, 2008; Wang *et al.*, 2013b; Maurer *et al.*, 2014) (Fig. 3). Recently, the members of the IVa bHLH clade (bHLH18, bHLH19, bHLH20, and bHLH25) were identified as FIT/bHLH29-interacting proteins (Cui *et al.*, 2018). These interactions were shown to promote the degradation of FIT/bHLH29 via the 26S proteasome pathway, in a jasmonic acid-dependent manner (Cui *et al.*, 2018). It is noteworthy that the Ib bHLH and IVa bHLH TFs antagonize the activity of each other in regulating FIT/bHLH29 protein accumulation, to tightly regulate the iron uptake machinery in response to different environmental stimuli (Cui *et al.*, 2018) (Fig. 3).

The second module acts upstream from FIT/bHLH29. It involves the four members of the IVc bHLH clade, namely ILR3/bHLH105 (IAA-LEUCINE RESISTANT 3), IDT1/bHLH34 (IRON DEFICIENCY TOLERANT 1), bHLH104, and bHLH115. These four TFs play additive roles in the responses to iron deficiency and their activity is thought to rely at least in part on their ability to form homo- or heterodimers (Zhang *et al.*, 2015; Li *et al.*, 2016; Liang *et al.*, 2017) (Fig. 3). In response to iron deficiency, these TFs directly activate the expression of clade Ib bHLH genes and indirectly activate the expression of *FIT/bHLH29* (Zhang *et al.*, 2015; Li *et al.*, 2016; Liang *et al.*, 2017).

Clade IVb bHLH TFs (PYE/bHLH47, bHLH11, and URI/bHLH121) also participate in the regulation of iron homeostasis in Arabidopsis. PYE/bHLH47 is a negative regulator (Long *et al.*, 2010), which contains an EAR motif in its C-terminal region (DLNxxP; Kagale and Rozwadowski, 2011) that directly represses the expression of genes participating in the maintenance of iron homeostasis. Interaction studies highlighted the ability of PYE/bHLH47 to heterodimerize with ILR3/bHLH105 and bHLH115 (Long *et al.*, 2010; Zhang *et al.*, 2015; Tissot *et al.*, 2019). However, the role of these interactions was still a matter of debate until recently. In a recent study, ILR3/bHLH105 was found to play a central role in the regulation of iron homeostasis, where it acts as both a transcriptional activator of the plant responses to iron

deficiency and a repressor of the responses to iron excess (Kroh and Pilon, 2019; Tissot *et al.*, 2019). In this study, the authors showed that the repressive activity of ILR3/bHLH105 was conferred by its dimerization with PYE/bHLH47 (Fig. 3). They also highlighted that ILR3–PYE heterodimers might repress the expression of *PYE/bHLH47* when iron availability is not limiting via a negative feedback regulatory loop (Fig. 3). bHLH11 is another transcriptional repressor that also contains an EAR motif (LxLxL) in its C-terminal domain (Tanabe *et al.*, 2019). Overexpression studies suggest that bHLH11 inhibits plant tolerance of iron deficiency and the expression of *IRT1* and *FRO2*, most probably by indirectly repressing the expression of *FIT/bHLH29* (Tanabe *et al.*, 2019) (Fig. 3). In contrast to PYE/bHLH47 and bHLH11, URI/bHLH121 (UPSTREAM REGULATOR OF IRT1) has been recently identified and characterized by three different groups as a positive regulator of the plant responses to iron deficiency (Kim *et al.*, 2019; Gao *et al.*, 2020a; Lei *et al.*, 2020; Lockhart, 2020). URI/bHLH121 can form heterodimers with clade IVc bHLH TFs (Kim *et al.*, 2019; Gao *et al.*, 2020a; Lei *et al.*, 2020) (Fig. 3). These interactions participate in the relocation of URI/bHLH121 from the cytosol into the nucleus (Lei *et al.*, 2020). They also suggest that the transcriptional activation of clade IVc bHLH target genes requires, at least in part, URI/bHLH121 (Kim *et al.*, 2019; Gao *et al.*, 2020a; Lei *et al.*, 2020). In support of this assertion, it was demonstrated that several genes directly targeted by URI/bHLH121 are identical to those of clade IVc bHLH TFs (Fig. 3). The expression of *FIT/bHLH29* also relies on URI/bHLH121 activity, most probably via an indirect mechanism (Kim *et al.*, 2019; Gao *et al.*, 2020a). It is noteworthy that under iron-deficient conditions, URI/bHLH121 accumulates in its phosphorylated form (Fig. 3); phosphorylation increases its binding capacity to the promoter region of its target genes, such as those encoding the clade Ib bHLH TFs (Kim *et al.*, 2019). Interestingly, both URI/bHLH121 transcript and protein accumulate constitutively regardless of iron status (Kim *et al.*, 2019; Gao *et al.*, 2020a). In contrast, the cellular localization of URI/bHLH121 in roots differs depending on the availability of iron (Gao *et al.*, 2020a). When iron is not limiting, URI/bHLH121 mainly localizes in the stele and the endodermis, whereas under iron deficiency URI/bHLH121 is primarily observed in the cortex and the epidermis cells, where it promotes iron uptake (Gao *et al.*, 2020a). The thorough characterization of URI/bHLH121 indicates that it plays a key role in the control of plant iron homeostasis mainly because it directly or indirectly regulates the expression of most of the known genes involved in this regulatory network (Kim *et al.*, 2019; Gao *et al.*, 2020a) (Fig. 3). Interestingly, it was recently reported that URI/bHLH121 directly activates *FER1*, *FER3*, and *FER4* expression when iron is not in excess, indicating that URI/bHLH121 positively regulates the transient storage of iron as well as the iron deficiency response (Gao *et al.*, 2020b).

Functional homologs of most of the above-described Arabidopsis bHLH TFs have been characterized in several dicots (Fig. 2, Table 1), indicating that this regulatory mechanism is most likely conserved among Strategy I plants.

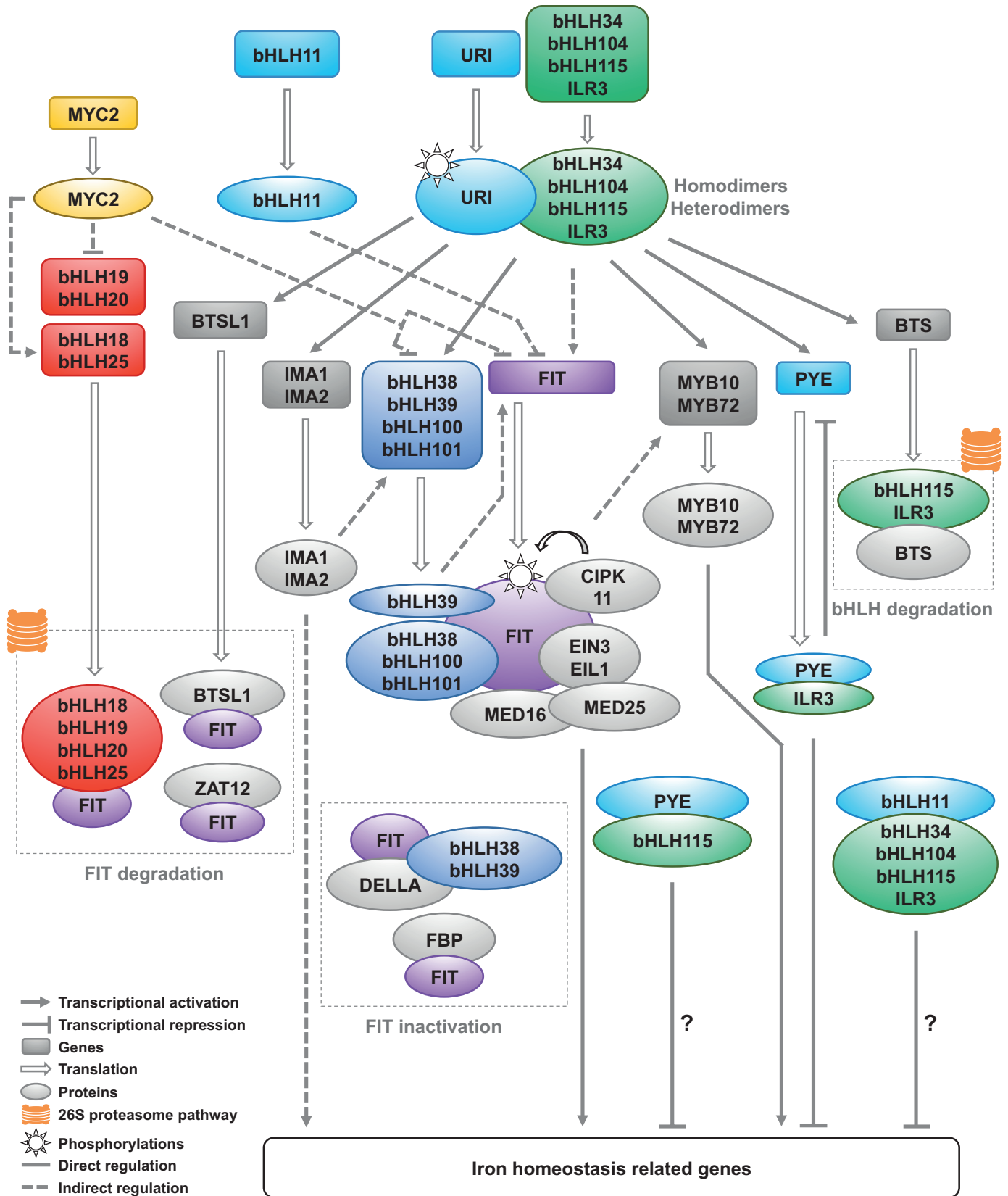


**Fig. 3.** The network of bHLH TFs that regulates iron homeostasis in Arabidopsis. Question marks indicate protein complexes for which transcriptional activities have not yet been clearly demonstrated. The color code for the bHLH TFs refers to the clades described in Fig. 2. Non-bHLH proteins are in grey. EIN3 and EIL1 favor FIT stability, whereas MED16 and MED25 mediate the FIT/bHLH29-dependent iron deficiency responses (for additional details on the post-translational regulation of FIT, see Kobayashi, 2019; Wu and Ling, 2019; Schwarz and Bauer, 2020; Spielmann and Vert, 2020). EIL1, ETHYLENE INSENSITIVE 3-LIKE1; EIN3, ETHYLENE INSENSITIVE 3; FBP, FIT-BINDING PROTEIN; MED16 and MED25, MEDIATOR SUBUNIT 16 and 25; ZAT12, ZINC FINGER OF ARABIDOPSIS THALIANA 12.

## bHLH TFs involved in the regulation of iron homeostasis in Strategy II plants

As stated above, plants have developed two different strategies to take up iron from the soil, distinguishing the non-graminaceous (Strategy I, reduction strategy) and graminaceous (Strategy II, chelation strategy) species (Fig. 1). However, the in-depth study of the responses to iron deficiency in rice has highlighted that the regulation of iron homeostasis in Strategy II plants involves the activity of several bHLH TFs belonging to the same clades as those identified in Strategy I plants (Figs 2, 4, Table 1) (Kobayashi, 2019; Kobayashi *et al.*, 2019).

OsFIT/OsbHLH156 was recently identified as a positive regulator of the iron deficiency response in rice (Liang *et al.*, 2020; Wang *et al.*, 2020). Loss of function of *OsFIT*/*OsbHLH156* resulted in strong symptoms of iron deficiency under upland conditions, whereas no such symptoms were observed when plants were grown in waterlogged soil (Wang *et al.*, 2020). These results imply that the Strategy II iron uptake system was impaired in the *Osfit* mutant, a hypothesis that is supported by disruption of the expression of Strategy II iron uptake-related genes. Among the Strategy II iron uptake-related genes are genes encoding enzymes involved in the biosynthesis of MAs [e.g. *NICOTIANAMINE SYNTHASE 1* and 2 (*NAS1* and *NAS2*)] or Fe<sup>3+</sup>-MA transport (e.g. *OsYSL15*,

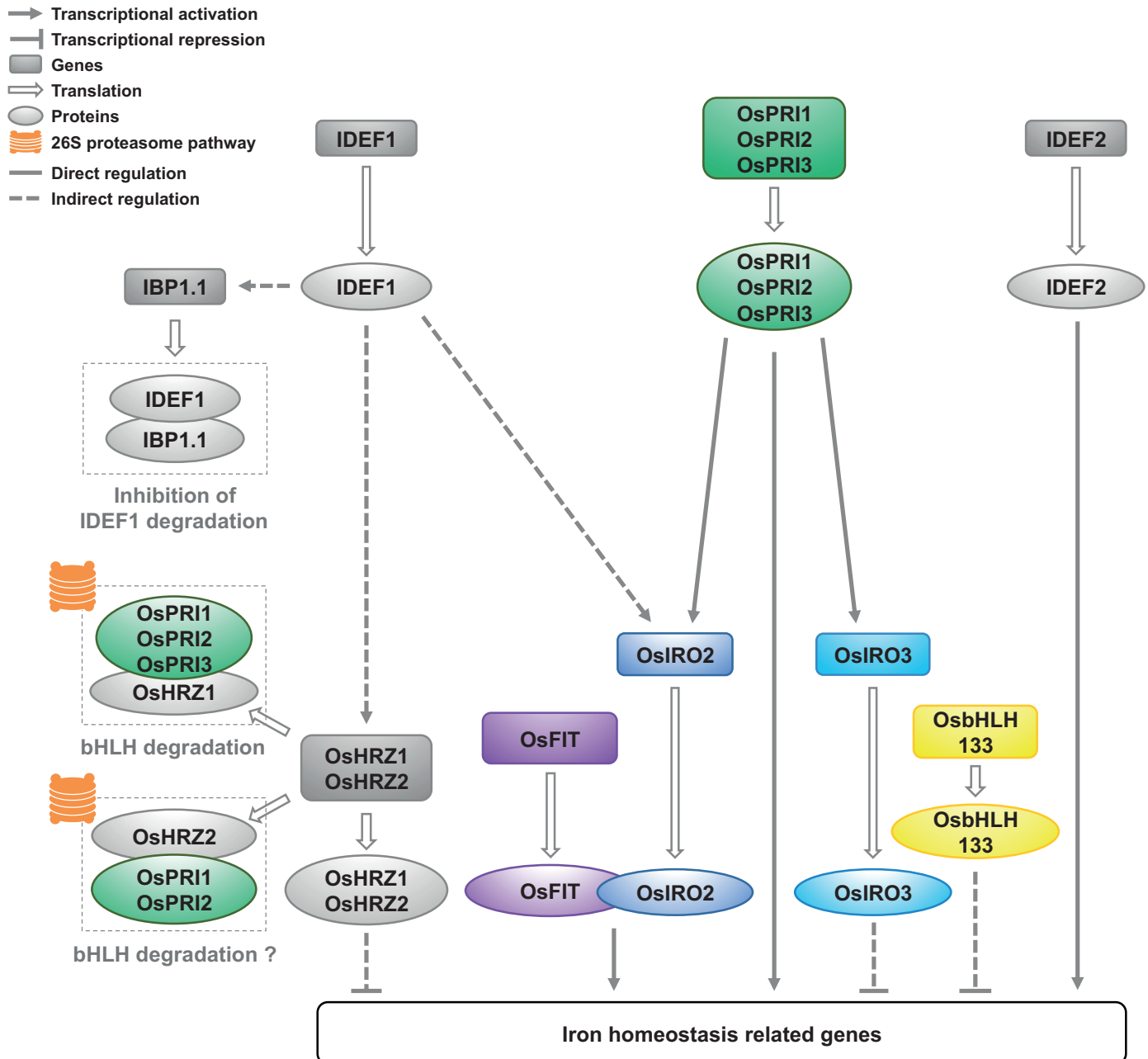


**Fig. 4.** The network of bHLH TFs that regulates iron homeostasis in rice. The question mark indicates the putative degradation mechanism for OsPRI1 and OsPRI2 via OsHRZ2. The color code for the bHLH TFs refers to the clades described in Fig. 2. Non-bHLH proteins are in grey. IBP1.1, IDEF1-BINDING PROTEINS 1.1.

*YELLOW STRIPE-LIKE 15* (Fig. 1) (Liang *et al.*, 2020; Wang *et al.*, 2020). Interestingly, it was demonstrated that OsFIT/OsbHLH156 regulates the expression of *OsIRT1* and therefore also participates in the regulation of the Strategy I iron uptake mechanism (Liang *et al.*, 2020) (Fig. 1). OsFIT/OsbHLH156 interacts with OsIRO2/OsbHLH56, a clade Ib bHLH, and promotes its nuclear accumulation (Fig. 4) (Liang *et al.*, 2020; Wang *et al.*, 2020). OsIRO2/OsbHLH56 was the first characterized bHLH TF involved in the control of iron homeostasis in rice, where it acts as a positive regulator of the iron deficiency response (Ogo *et al.*, 2006, 2007). Expression analysis indicated that the regulation of *OsIRT1* expression by OsFIT/OsbHLH156 might be different from the homologous regulatory system in Arabidopsis or that it might involve Ib bHLH TFs other than OsIRO2/OsbHLH56.

Three out of the four clade IVc bHLH TFs (OsPRI1/OsbHLH060, OsPRI2/bHLH058, OsPRI3/OsbHLH059; POSITIVE REGULATOR OF IRON HOMEOSTASIS 1, 2, and 3) have been identified as playing a positive role in the iron deficiency responses in rice (Zhang *et al.*, 2017; Kobayashi *et al.*, 2019; Zhang *et al.*, 2020b). The characterization of loss-of-function mutants suggested that these three TFs directly regulate the expression of *OsIRO2/OsbHLH56*, and indirectly regulate the expression of *OsNAS1*, *OsNAS2*, and *OsYSL15* via *OsIRO2/OsbHLH56* (Fig. 4) (Zhang *et al.*, 2017, 2020b). Among the potential direct targets of OsPRI1/OsbHLH060, OsPRI2/bHLH058, and OsPRI3/OsbHLH059, there is also *OsIRO3/OsbHLH63* (Fig. 4) (Zhang *et al.*, 2017, 2020b). *OsIRO3/OsbHLH63* is a member of clade IVb and is the functional homolog of PYE/bHLH47 (Zheng *et al.*, 2010). Like PYE/bHLH47, *OsIRO3/OsbHLH63* functions as a negative regulator of the iron deficiency responses (Zheng *et al.*, 2010). It is likely that *OsIRO3/OsbHLH63* activity might antagonize

OsIRO2/OsbHLH56 to tightly regulate iron uptake and avoid iron overload (Zhang *et al.*, 2012, 2010, 2017, 2020b). To date, there is no information on the role of OsbHLH057, the fourth member of the rice clade IVc bHLHs. Indeed, based on the information gathered in Arabidopsis, it is likely that OsbHLH057 participates in the control of iron homeostasis in rice. Whether OsbHLH057 exerts a minor role in specific cell types or in specific environmental conditions remains to be determined.

OsbHLH133 functions as a negative regulator of iron translocation from roots to shoots (Wang *et al.*, 2013a). It should be noted that OsbHLH133 is the only member of clade VIIIc reported to date as being involved in the regulation of iron homeostasis in plants. The other members of this clade in Arabidopsis play a positive role in root hair development but have not been associated with the maintenance of iron homeostasis (Bruex *et al.*, 2012). Whether these bHLHs have a similar and conserved role to that of OsbHLH133 in the regulation of iron homeostasis in Strategy II plants has yet to be investigated.

## The transcriptional regulation of iron homeostasis is not restricted to the activity of bHLH TFs

TFs from other families are involved in regulatory networks functioning in iron homeostasis in both Strategy I and Strategy II plants (Figs 3, 4, Table 2). Several R2R3-MYB TFs from different plant species have been shown to be involved in the regulation of iron deficiency responses. In Arabidopsis, MYB10 and MYB72 are two iron deficiency-inducible TFs required for proper iron uptake, whose expression is partially dependent on FIT/bHLH29 and URI/bHLH121 activities (Fig. 3) (Palmer *et al.*, 2013; Zamioudis *et al.*, 2014; Gao *et al.*, 2020a).

**Table 2.** TFs other than bHLHs involved in the regulation of iron homeostasis in plants

TF family	Gene name	Species	Interacting proteins	Reference
ABI3/VP1	<b>IDEF1</b>	<i>O. sativa</i>	IBP1	Kobayashi <i>et al.</i> , 2007
ARF	<b>OsARF12</b>	<i>O. sativa</i>		Qi <i>et al.</i> , 2012
ARF	<b>OsARF16</b>	<i>O. sativa</i>		Shen <i>et al.</i> , 2015
C2H2	<b>ZAT12<sup>a</sup></b>	<i>A. thaliana</i>	FIT/bHLH29	Le <i>et al.</i> , 2016
EIL	<b>EIN3<sup>a</sup></b>	<i>A. thaliana</i>	FIT/bHLH29	Lingam <i>et al.</i> , 2011
EIL	<b>EIL1<sup>a</sup></b>	<i>A. thaliana</i>	FIT/bHLH29	Lingam <i>et al.</i> , 2011
ERF	<b>ERF4</b>	<i>A. thaliana</i>		Liu <i>et al.</i> , 2017a
ERF	<b>ERF72</b>	<i>A. thaliana</i>		Liu <i>et al.</i> , 2017b
ERF	<b>ERF95</b>	<i>A. thaliana</i>		Sun <i>et al.</i> , 2020
ERF	<b>MxERF4</b>	<i>M. xiaojinensis</i>	MxFIT	Liu <i>et al.</i> , 2018
ERF	<b>MbERF4</b>	<i>M. baccata</i>	MbERF72	Zhang <i>et al.</i> , 2020a
ERF	<b>MbERF72</b>	<i>M. baccata</i>	MbERF4	Zhang <i>et al.</i> , 2020a
MYB (R2R3)	<b>MYB10</b>	<i>A. thaliana</i>		Palmer <i>et al.</i> , 2013
MYB (R2R3)	<b>MYB28</b>	<i>A. thaliana</i>		Coletto <i>et al.</i> , 2020
MYB (R2R3)	<b>MYB29</b>	<i>A. thaliana</i>		Coletto <i>et al.</i> , 2020
MYB (R2R3)	<b>MYB72</b>	<i>A. thaliana</i>		Palmer <i>et al.</i> , 2013
MYB (R2R3)	<b>MdMYB58</b>	<i>M. domestica</i>	MdSAT1/MdbHLH18	Wang <i>et al.</i> , 2018
MYB (R2R3)	<b>MxMYB1</b>	<i>M. xiaojinensis</i>		Shen <i>et al.</i> , 2008
NAC	<b>IDEF2</b>	<i>O. sativa</i>		Ogo <i>et al.</i> , 2008
NF-YC	<b>HAP5A/NF-YC1</b>	<i>A. thaliana</i>		Zhu <i>et al.</i> , 2020
WRKY	<b>WRKY46</b>	<i>A. thaliana</i>		Yan <i>et al.</i> , 2016

<sup>a</sup> For details on post-translational regulation of FIT activity, see Schwarz and Bauer (2020) and Wu and Ling (2019).

Furthermore, MYB72 has been identified as a transcriptional activator of genes associated with the biosynthesis and secretion of iron-mobilizing coumarins, highlighting its role in the Strategy I iron uptake system (Zamioudis *et al.*, 2014; Stringlis *et al.*, 2018) (Fig. 1). Recently, it was shown that Arabidopsis MYB28 and MYB29 are at the interface of the plant's sensitivity to ammonium stress and the modulation of iron homeostasis (Coletto *et al.*, 2020). Notably, the ammonium-dependent decrease of MYB28 and MYB29 expression (or the loss of function of both genes) leads to defects in iron translocation from roots to shoots and to the induction of the expression of *FIT/bHLH29*, clade Ib bHLHs, MYB72, and *IMA1/FEP3* and *IMA3/FEP1* in roots. MdMYB58, a close homolog of MYB72, was recently characterized as a positive regulator of iron uptake and translocation in apple (Wang *et al.*, 2018). Further investigation showed that MdMYB58 transcriptional activity is inhibited by its heterodimerization with MdSAT1/MdbHLH18, a IVa clade bHLH TF (Wang *et al.*, 2018). In contrast to the above-mentioned MYB TFs, MxMYB1 may function as a negative regulator of iron uptake and storage (Shen *et al.*, 2008).

In Arabidopsis, WRKY46 plays a role in iron translocation between root and shoot by directly regulating the expression of *VITL1* (*VACUOLAR IRON TRANSPORTER-LIKE 1*), a potential iron transporter involved in iron sequestration into the vacuole (Gollhofer *et al.*, 2014; Yan *et al.*, 2016). HAP5A/NF-YC1 is also involved in iron translocation between root and shoot by regulating the expression of *NAS1* (Zhu *et al.*, 2020). ERF4 and ERF72 are two Arabidopsis TFs belonging to the AP2/ERF family that have been reported as potential negative regulators of iron deficiency responses by repressing the expression of genes involved in iron uptake, such as *IRT1* (Liu *et al.*, 2017a, b). Similarly, MbERF4 and MbERF72 from *Malus baccata* and MxERF4 from *Malus xiaojinensis* act as negative regulators of the iron deficiency responses in these two apple species (Liu *et al.*, 2018; Zhang *et al.*, 2020a). In contrast, ERF95 was recently proposed to promote iron storage in Arabidopsis seeds (Sun *et al.*, 2020). However, how iron distribution is controlled in seeds is not clearly established, although it was recently proposed that B3 TFs, which are involved in the regulation of embryo development and seed maturation, might be good candidates (Roschztardt *et al.*, 2020).

IDEF1 and IDEF2 (*IRON DEFICIENCY-RESPONSIVE ELEMENT FACTOR 1 and 2*) are two rice TFs belonging to the ABI3/VP1 and NAC families, respectively (Fig. 4) (Kobayashi *et al.*, 2007; Ogo *et al.*, 2008). These two TFs participate in the regulation of iron homeostasis in rice. IDEF1 is required for the coordinated activation of genes related to iron uptake and translocation, including *OsIRT1*, *OsNAS1*, *OsNAS2*, and *OsYSL15* (Kobayashi *et al.*, 2007, 2009). In addition, IDEF1 positively regulates the expression of *OsIRO2*, indicating that IDEF1 functions upstream of *OsIRO2* in the iron deficiency regulatory network (Fig. 4) (Kobayashi *et al.*, 2007, 2009). Interestingly, it was shown that IDEF1 could bind to iron and zinc atoms and that this capacity was necessary for its activity (Kobayashi *et al.*, 2012). It was therefore proposed that IDEF1 could sense the cellular metal ion balance caused by changes in iron availability, suggesting that IDEF1 could

be a cellular iron sensor allowing the tight regulation of the iron deficiency responses (Kobayashi *et al.*, 2012). Similarly to IDEF1, IDEF2 plays a positive role in the plant response to iron deficiency (Ogo *et al.*, 2008).

A family of peptides named IMA/FEP (*IRONMAN/FE-UPTAKE-INDUCING PEPTIDE*) has been reported to play a positive role in iron deficiency responses in Arabidopsis, by regulating a set of deficiency-inducible genes including Ib bHLH TFs, a function that seems to be conserved across plant species (Grillet *et al.*, 2018; Hirayama *et al.*, 2018). Two recent studies showed that URI/bHLH121 is a direct positive regulator of *IMA1/FEP3* and *IMA2/FEP2* expression (Kim *et al.*, 2019; Gao *et al.*, 2020a). These results indicate that IMAs/FEPs are implicated in the bHLH-dependent regulatory network regulating iron homeostasis. However, the precise regulatory mechanisms by which IMAs/FEPs act are still unknown.

## Post-translational regulation of the iron homeostasis regulatory networks

Protein–protein interactions and post-translational modifications (i.e. ubiquitination, sumoylation, or phosphorylation) can significantly affect the regulatory activities of TFs. Such mechanisms have been shown to play an important role in the maintenance of iron homeostasis in plants. This topic has also been covered in recent reviews (Kobayashi, 2019; Rodríguez-Celma *et al.*, 2019a; Wu and Ling, 2019; Schwarz and Bauer, 2020; Spielmann and Vert, 2020).

As described earlier, the transcriptional activity of bHLH TFs involved in the control of iron homeostasis is extensively dependent on *in vivo* protein–protein interactions, in the form of homo- or heterodimers (Figs 3, 4, Tables 1, 2). For instance, heterodimerization of *FIT/bHLH29* with clade Ib bHLH TFs is required for its transcriptional activity and stability, whereas its interaction with clade IVa members promotes its degradation via the 26S proteasome pathway (Cui *et al.*, 2018). The nuclear localization of bHLH39 also depends on its interaction with *FIT/bHLH29*, since in cells lacking *FIT/bHLH29*, bHLH39 localizes predominantly in the cytoplasm (Trofimov *et al.*, 2019). Similarly, *OsFIT/OsbHLH156* facilitates the nuclear localization of *OsIRO2/OsbHLH156*, the functional homolog of bHLH39 in rice, suggesting that this post-translational regulatory mechanism is conserved within the plant kingdom (Liang *et al.*, 2020; Wang *et al.*, 2020). The activity and/or stability of *FIT/bHLH29* are also modulated by its interaction with several additional protein partners that do not belong to the bHLH family of TFs (Fig. 3, Table 1) (reviewed in Kobayashi, 2019; Wu and Ling, 2019; Schwarz and Bauer, 2020; Spielmann and Vert, 2020).

Several ubiquitin E3 ligases have been identified and characterized as negative regulators of iron uptake that function to avoid potential iron overload by targeting bHLH TFs for their degradation (for details, see Rodríguez-Celma *et al.*, 2019a; Spielmann and Vert, 2020) (Figs 3, 4). BTS (*BRUTUS*), whose expression is induced by iron deficiency in roots, is proposed to be a critical iron-sensing E3 ubiquitin ligase in Arabidopsis (Long *et al.*, 2010). BTS interacts with *ILR3/*



bHLH105 and bHLH115 to facilitate their degradation via the 26S proteasome pathway, allowing fine tuning of the expression of downstream iron deficiency response genes (Fig. 3) (Long *et al.*, 2010; Selote *et al.*, 2015). Similarly, OsHRZ1 and OsHRZ2 [HAEMERYTHRIN MOTIF-CONTAINING REALLY INTERESTING NEW GENE (RING) AND ZINC-FINGER PROTEIN 1 and 2], two rice ubiquitin E3 ligases displaying strong sequence similarities with BTS, have been reported as potential iron sensors that play a negative role in iron acquisition under iron-sufficient conditions (Kobayashi *et al.*, 2013). It was shown that OsHRZ1 could interact with OsPRI1/OsbHLH60, OsPRI2/OsbHLH58, and OsPRI3/OsbHLH59 and mediate their degradation via the 26S proteasome (Fig. 4) (Zhang *et al.*, 2017, 2020b). However, different results were reported in another study that only validated the sole interactions between OsHRZ1 and OsHRZ2 with OsPRI1/OsbHLH60 and OsPRI2/OsbHLH58 (Kobayashi *et al.*, 2019). Another *in vitro* ubiquitination study showed that neither OsPRI1/OsbHLH60 nor OsPRI2/OsbHLH58 or OsPRI3/OsbHLH59 were ubiquitinated by OsHRZ1 or OsHRZ2 (Kobayashi *et al.*, 2019). These discrepancies may be due to the different methodologies and materials used in these studies. Whether these interactions participate in the ubiquitination and degradation of OsPRI1/OsbHLH60, OsPRI2/OsbHLH58, and OsPRI3/OsbHLH59 remains to be further demonstrated and confirmed. IDEF1, whose activity is necessary for the expression of *HRZ* genes, is also degraded via the 26S proteasome pathway through an as yet uncharacterized mechanism (Zhang *et al.*, 2014). However, IDEF1 degradation is inhibited by its interaction with the IBP1.1 (IDEF1-BINDING PROTEINS 1.1) Bowman-Birk trypsin inhibitor protein (Fig. 4) (Zhang *et al.*, 2014). BTSL1 and BTSL2, two Arabidopsis homologs of BTS, function redundantly as negative regulators of the iron deficiency response (Hindt *et al.*, 2017). In addition, BTSL1 and BTSL2 were shown to directly target FIT/bHLH29 and promote its ubiquitination and subsequent degradation via the 26S proteasome pathway, thus negatively regulating the expression of iron uptake-related genes (Fig. 3) (Rodríguez-Celma *et al.*, 2019a, b). In apple, MdbT1 and MdbT2, two BTB-TAZ proteins, interact with MdbHLH104. MdbT proteins also interact with MdcUL3 (CULLIN-RING UBIQUITIN LIGASE 3) to form MdbT<sup>MdcUL3</sup> complexes required for MdbHLH104 ubiquitination and degradation via the 26S proteasome pathway (Zhao *et al.*, 2016a). In contrast, MdSIZ1, a SIZ/PIAS-type SUMO E3 ligase, directly sumoylates MdbHLH104, especially under iron deficiency, to enhance its stability (Zhou *et al.*, 2019). Recently, it was shown that the mutation of an alanine residue to valine in IDT1/bHLH34 enhances both its stability and its nuclear localization (Sharma and Yeh, 2020). Since this amino acid is conserved among clade IVc bHLH TFs in both monocots and dicots (Sharma and Yeh, 2020), one might speculate that it plays an important role in regulating the stability of clade IVc bHLHs and thus their degradation via the 26S proteasome.

Phosphorylation also plays an important role in determining the activity of TFs in the iron homeostasis networks (Fig. 3). In Arabidopsis, phosphorylation of FIT/bHLH29 by the calcium-dependent protein kinase CIPK11 (CBL-INTERACTING PROTEIN KINASE 11) positively regulates its activity by

favoring its nuclear accumulation and dimerization with bHLH39 (Gratz *et al.*, 2019). *CIPK11* is induced and activated via a CBL1/9-mediated  $\text{Ca}^{2+}$ -sensing pathway under iron deficiency. CIPK21 can also interact with FIT/bHLH29, indicating that this protein kinase might have a potential role in the regulation of the FIT/bHLH29-dependent iron deficiency response (Gratz *et al.*, 2019). Recently, the phosphorylation of URI/bHLH121 was also reported as a key mechanism that regulates its activity (Kim *et al.*, 2019). It was shown that the phosphorylated form of URI/bHLH121 accumulates only in response to iron deficiency, whereas the turnover of phosphorylated URI/bHLH121 is dependent on BTS activity (Kim *et al.*, 2019). Under iron deficiency, URI/bHLH121 showed enhanced capacity to heterodimerize with IVc bHLH TFs and increased ability to bind to the promoter of its target genes, indicating that the phosphorylation of URI/bHLH121 plays a positive role in the iron deficiency response (Kim *et al.*, 2019). Nevertheless, since URI/bHLH121 can activate the expression of *FER1*, *FER3*, and *FER4* in the stele when iron availability is not limiting (Gao *et al.*, 2020b), a growth condition in which the phosphorylated form of bHLH121 is degraded (Kim *et al.*, 2019), it is likely that URI/bHLH121 is transcriptionally active independently of its phosphorylation state. Interestingly, as stated earlier, the pattern of accumulation of URI/bHLH121 within the root cells is controlled by an iron-dependent mechanism. URI/bHLH121 preferentially accumulates in the epidermis and the cortex when plants are grown under iron deficiency, and in the stele when grown under iron sufficiency. From these observations, one might hypothesize that the cellular distribution of URI/bHLH121, rather than its transcriptional activity, is regulated by its phosphorylation state. However, the precise regulatory mechanism leading to the phosphorylation of URI/bHLH121 remains to be characterized.

## Conclusions and future prospects

In the past two decades, remarkable progress has been made in decrypting the molecular mechanisms that regulate iron homeostasis in both Strategy I and Strategy II plants (Fig. 1). Research in this area has highlighted that iron homeostasis in plants is regulated at the transcriptional level and involves several bHLH TFs that function in intricate regulatory networks (Figs 2–4).

The function of most of these bHLH TFs (i.e. clades Ib, IIIa, IVb, and IVc) is conserved among grass and non-grass species (Fig. 2), in contrast to the downstream target genes of the iron acquisition machinery, which are distinctive in Strategy I and Strategy II plants (Fig. 1). How these bHLH functional homologs evolved to target different genes is an intriguing question. bHLHs from clade IVa are involved in the regulation of iron homeostasis in Arabidopsis, but it remains to be investigated whether this clade of bHLH TFs has a similar role in other plant species. Additional investigations will also be necessary to determine whether the homologs of OsbHLH133 (clade VIIIc) in non-grass species play a role in the control of iron homeostasis. Other

regulatory proteins are also conserved among Strategy I and Strategy II plants; this is, for instance, the case for MYB and ERF TFs (Table 2) and for hemerythrin E3-ubiquitin ligases. Interestingly, BTB-TAZ-CUL3 ubiquitin ligase complexes participate in the degradation of clade IVc bHLH in apple. To date, this mechanism has been observed only in apple, raising the question of whether this regulatory mechanism is conserved in other plant species, from non-grasses to grasses and from perennials to annuals. Ubiquitination, as well as phosphorylation and sumoylation, are crucial post-translational modifications for regulation of key bHLH TF activities involved in the iron homeostasis networks, notably clade IVc bHLH FIT/bHLH29 and URI/bHLH121. Whether such modifications participate in the regulation of other TF activities within this network is still to be assessed. Determining the degree of conservation of this regulatory network between plants utilizing Strategy I and Strategy II, and between annual and perennial species, is another question that deserves to be addressed.

How plants sense iron status and switch on or repress the downstream regulatory network governing iron uptake, translocation, storage, or assimilation has remained elusive. To date, hemerythrin E3-ubiquitin ligases are the main candidates (Rodríguez-Celma *et al.*, 2019a). These E3-ubiquitin ligases are induced in response to iron deficiency, participate in the degradation of key bHLH TFs (i.e. clade IVc and FIT/bHLH29), and are destabilized by the binding of iron at their hemerythrin motifs. IDEF1, the rice iron-binding TF mentioned earlier, has also been proposed as a potential iron sensor (Kobayashi *et al.*, 2007, 2009, 2012). The characterization of functional homologs of IDEF1 in non-grass species would be an additional element in support of this hypothesis. Another important question concerns the regulation of the most upstream bHLH TFs. For instance, the main challenges would be to determine how the expression of clade IVc bHLHs is controlled and to identify which protein kinase modulates URI/bHLH121 activity.

Recently, epigenetic regulation has emerged as playing an important role in the control of iron homeostasis, by regulating the accessibility of promoters, and thus the expression of both TFs and iron uptake genes. This is, for instance, the case in *Arabidopsis*, in which the iron-dependent deposition of repressive marks on H3 histone (i.e. H3K27m3) at the promoter loci of *FIT/bHLH29*, *IRT1*, and *FRO2* has been identified (Park *et al.*, 2019). This additional layer of regulation in the transcriptional networks controlling iron homeostasis raises questions about the importance and the significance of such regulatory mechanisms in this process.

From the aspects covered in this review, it is possible to grasp the extent of the complexity of the regulatory networks that regulate iron homeostasis in plants. Nevertheless, another level of complexity that is still to be investigated concerns the apparent redundancies existing between several TFs, the localization of their target genes, and thus the physiological functions that are controlled by them. Unraveling this complexity will be achieved by the in-depth study of the tissue and cellular localization of the different TFs as well as the proteins involved in their regulation. Such knowledge will be necessary to fully decrypt and understand

the dynamics of this regulatory process. Unfortunately, such data are available for only a few of these proteins (Long *et al.*, 2010; Samira *et al.*, 2018; Gao *et al.*, 2020a). In conclusion, much work still lies ahead to fully comprehend the transcriptional regulatory network that regulates iron homeostasis in plants, which might offer novel opportunities for improving plant growth and health and for generating iron-fortified crops.

## Acknowledgements

This work was supported by grants from the Agence Nationale de la Recherche (ANR) to CD. Support was provided by the China Scholarship Council to FG. We thank Florence Vignols for help in preparing this article.

## Author contributions

FG and CD wrote the manuscript.

## References

- Bashir K, Ishimaru Y, Shimo H, *et al.* 2011. Rice phenolics efflux transporter 2 (PEZZ2) plays an important role in solubilizing apoplasmic iron. *Soil Science and Plant Nutrition* **57**, 803–812.
- Briat JF, Dubos C, Gaymard F. 2015. Iron nutrition, biomass production, and plant product quality. *Trends in Plant Science* **20**, 33–40.
- Bruex A, Kainkaryam RM, Wieckowski Y, *et al.* 2012. A gene regulatory network for root epidermis cell differentiation in *Arabidopsis*. *PLoS Genetics* **8**, e1002446.
- Brumbarova T, Bauer P, Ivanov R. 2015. Molecular mechanisms governing *Arabidopsis* iron uptake. *Trends in Plant Science* **20**, 124–133.
- Camaschella C. 2015. Iron-deficiency anemia. *New England Journal of Medicine* **372**, 1832–1843.
- Carretero-Paulet L, Galstyan A, Roig-Villanova I, Martínez-García JF, Bilbao-Castro JR, Robertson DL. 2010. Genome-wide classification and evolutionary analysis of the bHLH family of transcription factors in *Arabidopsis*, poplar, rice, moss, and algae. *Plant Physiology* **153**, 1398–1412.
- Colangelo EP, Guerinot ML. 2004. The essential basic helix-loop-helix protein FIT1 is required for the iron deficiency response. *The Plant Cell* **16**, 3400–3412.
- Coletto I, Bejarano I, Marín-Peña AJ, Medina J, Rioja C, Burow M, Marino D. 2020. *Arabidopsis thaliana* transcription factors *MYB28* and *MYB29* shape ammonium stress responses by regulating Fe homeostasis. *New Phytologist*. doi: 10.1111/nph.16918.
- Colombo C, Iorio ED, Liu Q, Jiang Z, Barrón V. 2018. Iron oxide nanoparticles in soils: environmental and agronomic importance. *Journal of Nanoscience and Nanotechnology* **18**, 761.
- Connorton JM, Balk J, Rodríguez-Celma J. 2017. Iron homeostasis in plants – a brief overview. *Metallomics* **9**, 813–823.
- Cui Y, Chen CL, Cui M, Zhou WJ, Wu HL, Ling HQ. 2018. Four IVa bHLH transcription factors are novel interactors of FIT and mediate JA inhibition of iron uptake in *Arabidopsis*. *Molecular Plant* **11**, 1166–1183.
- Du J, Huang Z, Wang B, Sun H, Chen C, Ling HQ, Wu H. 2015. SlbHLH068 interacts with FER to regulate the iron-deficiency response in tomato. *Annals of Botany* **116**, 23–34.
- Fourcroy P, Sisó-Terraza P, Sudre D, Savirón M, Rey G, Gaymard F, Abadía A, Abadía J, Alvarez-Fernández A, Briat JF. 2014. Involvement of the ABCG37 transporter in secretion of scopoletin and derivatives by *Arabidopsis* roots in response to iron deficiency. *New Phytologist* **201**, 155–167.
- Fourcroy P, Tissot N, Gaymard F, Briat JF, Dubos C. 2016. Facilitated Fe nutrition by phenolic compounds excreted by the *Arabidopsis* ABCG37/

- PDR9 transporter requires the IRT1/FRO2 high-affinity root  $\text{Fe}^{2+}$  transport system. *Molecular Plant* **9**, 485–488.
- Gao F, Robe K, Bettembourg M, et al.** 2020a. The transcription factor bHLH121 interacts with bHLH105 (ILR3) and its closest homologs to regulate iron homeostasis in *Arabidopsis*. *The Plant Cell* **32**, 508–524.
- Gao F, Robe K, Dubos C.** 2020b. Further insights into the role of bHLH121 in the regulation of iron homeostasis in *Arabidopsis thaliana*. *Plant Signaling & Behavior* **15**, 1795582.
- Gao F, Robe K, Gaymard F, Izquierdo E, Dubos C.** 2019. The transcriptional control of iron homeostasis in plants: a tale of bHLH transcription factors? *Frontiers in Plant Science* **10**, 6.
- Gollhofer J, Timofeev R, Lan P, Schmidt W, Buckhout TJ.** 2014. Vacuolar-Iron-Transporter1-Like proteins mediate iron homeostasis in *Arabidopsis*. *PLoS One* **9**, e110468.
- Gratz R, Manishankar P, Ivanov R, et al.** 2019. CIPK11-dependent phosphorylation modulates FIT activity to promote *Arabidopsis* iron acquisition in response to calcium signaling. *Developmental Cell* **48**, 726–740.e10.
- Grillet L, Lan P, Li W, Mokkapati G, Schmidt W.** 2018. IRON MAN is a ubiquitous family of peptides that control iron transport in plants. *Nature Plants* **4**, 953–963.
- Guerinot ML, Yi Y.** 1994. Iron: nutritious, noxious, and not readily available. *Plant Physiology* **104**, 815–820.
- Hänsch R, Mendel RR.** 2009. Physiological functions of mineral micronutrients (Cu, Zn, Mn, Fe, Ni, Mo, B, Cl). *Current Opinion in Plant Biology* **12**, 259–266.
- Heim MA, Jakoby M, Werber M, Martin C, Weisshaar B, Bailey PC.** 2003. The basic helix-loop-helix transcription factor family in plants: a genome-wide study of protein structure and functional diversity. *Molecular Biology and Evolution* **20**, 735–747.
- Hindt MN, Akmakjian GZ, Pivarski KL, Punshon T, Baxter I, Salt DE, Guerinot ML.** 2017. *BRUTUS* and its paralogs, *BTS LIKE1* and *BTS LIKE2*, encode important negative regulators of the iron deficiency response in *Arabidopsis thaliana*. *Metallomics* **9**, 876–890.
- Hirayama T, Lei GJ, Yamaji N, Nakagawa N, Ma JF.** 2018. The putative peptide gene *FEP1* regulates iron deficiency response in *Arabidopsis*. *Plant & Cell Physiology* **59**, 1739–1752.
- Huang D, Dai W.** 2015. Molecular characterization of the basic helix-loop-helix (bHLH) genes that are differentially expressed and induced by iron deficiency in *Populus*. *Plant Cell Reports* **34**, 1211–1224.
- Inoue H, Kobayashi T, Nozoye T, Takahashi M, Kakei Y, Suzuki K, Nakazono M, Nakanishi H, Mori S, Nishizawa NK.** 2009. Rice OsYSL15 is an iron-regulated iron (III)-deoxymugineic acid transporter expressed in the roots and is essential for iron uptake in early growth of the seedlings. *Journal of Biological Chemistry* **284**, 3470–3479.
- Ishimaru Y, Suzuki M, Tsukamoto T, et al.** 2006. Rice plants take up iron as an  $\text{Fe}^{3+}$ -phytosiderophore and as  $\text{Fe}^{2+}$ . *The Plant Journal* **45**, 335–346.
- Jakoby M, Wang HY, Reidt W, Weisshaar B, Bauer P.** 2004. *FRU (BHLH029)* is required for induction of iron mobilization genes in *Arabidopsis thaliana*. *FEBS Letters* **577**, 528–534.
- Kagale S, Rozwadowski K.** 2011. EAR motif-mediated transcriptional repression in plants: an underlying mechanism for epigenetic regulation of gene expression. *Epigenetics* **6**, 141–146.
- Kim SA, LaCroix IS, Gerber SA, Guerinot ML.** 2019. The iron deficiency response in *Arabidopsis thaliana* requires the phosphorylated transcription factor URI. *Proceedings of the National Academy of Sciences, USA* **116**, 24933–24942.
- Kobayashi T.** 2019. Understanding the complexity of iron sensing and signaling cascades in plants. *Plant & Cell Physiology* **60**, 1440–1446.
- Kobayashi T, Itai RN, Aung MS, Senoura T, Nakanishi H, Nishizawa NK.** 2012. The rice transcription factor IDEF1 directly binds to iron and other divalent metals for sensing cellular iron status. *The Plant Journal* **69**, 81–91.
- Kobayashi T, Itai RN, Ogo Y, Kakei Y, Nakanishi H, Takahashi M, Nishizawa NK.** 2009. The rice transcription factor IDEF1 is essential for the early response to iron deficiency, and induces vegetative expression of late embryogenesis abundant genes. *The Plant Journal* **60**, 948–961.
- Kobayashi T, Nagasaka S, Senoura T, Itai RN, Nakanishi H, Nishizawa NK.** 2013. Iron-binding haemerythrin RING ubiquitin ligases regulate plant iron responses and accumulation. *Nature Communications* **4**, 2792.
- Kobayashi T, Nakanishi Itai R, Nishizawa NK.** 2014. Iron deficiency responses in rice roots. *Rice* **7**, 27.
- Kobayashi T, Nishizawa NK.** 2012. Iron uptake, translocation, and regulation in higher plants. *Annual Review of Plant Biology* **63**, 131–152.
- Kobayashi T, Nozoye T, Nishizawa NK.** 2019. Iron transport and its regulation in plants. *Free Radical Biology & Medicine* **133**, 11–20.
- Kobayashi T, Ogo Y, Itai RN, Nakanishi H, Takahashi M, Mori S, Nishizawa NK.** 2007. The transcription factor IDEF1 regulates the response to and tolerance of iron deficiency in plants. *Proceedings of the National Academy of Sciences, USA* **104**, 19150–19155.
- Kobayashi T, Ozu A, Kobayashi S, An G, Jeon JS, Nishizawa NK.** 2019. OsbHLH058 and OsbHLH059 transcription factors positively regulate iron deficiency responses in rice. *Plant Molecular Biology* **101**, 471–486.
- Kroh GE, Pilon M.** 2019. Connecting the negatives and positives of plant iron homeostasis. *New Phytologist* **223**, 1052–1055.
- Le CT, Brumbarova T, Ivanov R, Stoof C, Weber E, Mohrbacher J, Fink-Straube C, Bauer P.** 2016. ZINC FINGER OF ARABIDOPSIS THALIANA12 (ZAT12) Interacts with FER-LIKE IRON DEFICIENCY-INDUCED TRANSCRIPTION FACTOR (FIT) linking iron deficiency and oxidative stress responses. *Plant Physiology* **170**, 540–557.
- Lei R, Li Y, Cai Y, Li C, Pu M, Lu C, Yang Y, Liang G.** 2020. bHLH121 functions as a direct link that facilitates the activation of FIT by bHLH IVc transcription factors for maintaining Fe homeostasis in *Arabidopsis*. *Molecular Plant* **13**, 634–649.
- Li Q, Chen L, Yang A.** 2019. The molecular mechanisms underlying iron deficiency responses in rice. *International Journal of Molecular Sciences* **21**, 43.
- Li L, Gao W, Peng Q, Zhou B, Kong Q, Ying Y, Shou H.** 2018. Two soybean bHLH factors regulate response to iron deficiency. *Journal of Integrative Plant Biology* **60**, 608–622.
- Li YY, Sui XY, Yang JS, Xiang XH, Li ZQ, Wang YY, Zhou ZC, Hu RS, Liu D.** 2020. A novel bHLH transcription factor, NtbHLH1, modulates iron homeostasis in tobacco (*Nicotiana tabacum* L.). *Biochemical and Biophysical Research Communications* **522**, 233–239.
- Li X, Zhang H, Ai Q, Liang G, Yu D.** 2016. Two bHLH transcription factors, bHLH34 and bHLH104, regulate iron homeostasis in *Arabidopsis thaliana*. *Plant Physiology* **170**, 2478–2493.
- Liang G, Zhang H, Li X, Ai Q, Yu D.** 2017. bHLH transcription factor bHLH115 regulates iron homeostasis in *Arabidopsis thaliana*. *Journal of Experimental Botany* **68**, 1743–1755.
- Liang G, Zhang H, Li Y, Pu M, Yang Y, Li C, Lu C, Xu P, Yu D.** 2020. *Oryza sativa* FER-LIKE FE DEFICIENCY-INDUCED TRANSCRIPTION FACTOR (OsFIT/OsbHLH156) interacts with OsIRO2 to regulate iron homeostasis. *Journal of Integrative Plant Biology* **62**, 668–689.
- Ling HQ, Bauer P, Bereczky Z, Keller B, Ganai M.** 2002. The tomato *fer* gene encoding a bHLH protein controls iron-uptake responses in roots. *Proceedings of the National Academy of Sciences, USA* **99**, 13938–13943.
- Lingam S, Mohrbacher J, Brumbarova T, Potuschak T, Fink-Straube C, Blondet E, Genschik P, Bauer P.** 2011. Interaction between the bHLH transcription factor FIT and ETHYLENE INSENSITIVE3/ETHYLENE INSENSITIVE3-LIKE1 reveals molecular linkage between the regulation of iron acquisition and ethylene signaling in *Arabidopsis*. *The Plant Cell* **23**, 1815–1829.
- Liu W, Karemera NJU, Wu T, Yang Y, Zhang X, Xu X, Wang Y, Han Z.** 2017a. The ethylene response factor *AtERF4* negatively regulates the iron deficiency response in *Arabidopsis thaliana*. *PLoS One* **12**, e0186580.
- Liu W, Li Q, Wang Y, Wu T, Yang Y, Zhang X, Han Z, Xu X.** 2017b. Ethylene response factor *AtERF72* negatively regulates *Arabidopsis thaliana* response to iron deficiency. *Biochemical and Biophysical Research Communications* **491**, 862–868.
- Liu W, Wu T, Li Q, Zhang X, Xu X, Li T, Han Z, Wang Y.** 2018. An ethylene response factor (*MxERF4*) functions as a repressor of Fe acquisition in *Malus xiaojinensis*. *Scientific Reports* **8**, 1–13.
- Lockhart J.** 2020. Personal trainer: bHLH121 functions upstream of a transcriptional network of heavy lifters involved in balancing iron levels. *The Plant Cell* **32**, 293–294.
- Long TA, Tsukagoshi H, Busch W, Lahner B, Salt DE, Benfey PN.** 2010. The bHLH transcription factor POPEYE regulates response to iron deficiency in *Arabidopsis* roots. *The Plant Cell* **22**, 2219–2236.

- Marschner H, Römheld V.** 1994. Strategies of plants for acquisition of iron. *Plant and Soil* **165**, 261–274.
- Martín-Barranco A, Spielmann J, Dubeaux G, Vert G, Zelazny E.** 2020. Dynamic control of the high-affinity iron uptake complex in root epidermal cells. *Plant Physiology* **184**, 1236–1250.
- Maurer F, Naranjo Arcos MA, Bauer P.** 2014. Responses of a triple mutant defective in three iron deficiency-induced *BASIC HELIX-LOOP-HELIX* genes of the subgroup Ib(2) to iron deficiency and salicylic acid. *PLoS One* **9**, e99234.
- Murata Y, Ma JF, Yamaji N, Ueno D, Nomoto K, Iwashita T.** 2006. A specific transporter for iron(III)-phytosiderophore in barley roots. *The Plant Journal* **46**, 563–572.
- Ogo Y, Itai RN, Nakanishi H, Inoue H, Kobayashi T, Suzuki M, Takahashi M, Mori S, Nishizawa NK.** 2006. Isolation and characterization of IRO2, a novel iron-regulated bHLH transcription factor in graminaceous plants. *Journal of Experimental Botany* **57**, 2867–2878.
- Ogo Y, Itai RN, Nakanishi H, Kobayashi T, Takahashi M, Mori S, Nishizawa NK.** 2007. The rice bHLH protein OsIRO2 is an essential regulator of the genes involved in Fe uptake under Fe-deficient conditions. *The Plant Journal* **51**, 366–377.
- Ogo Y, Kobayashi T, Nakanishi Itai R, Nakanishi H, Kakei Y, Takahashi M, Toki S, Mori S, Nishizawa NK.** 2008. A novel NAC transcription factor, IDEF2, that recognizes the iron deficiency-responsive element 2 regulates the genes involved in iron homeostasis in plants. *Journal of Biological Chemistry* **283**, 13407–13417.
- Palmer CM, Hindt MN, Schmidt H, Clemens S, Guerinot ML.** 2013. *MYB10* and *MYB72* are required for growth under iron-limiting conditions. *PLoS Genetics* **9**, e1003953.
- Park EY, Tsuyuki KM, Hu F, Lee J, Jeong J.** 2019. PRC2-mediated H3K27me3 contributes to transcriptional regulation of FIT-dependent iron deficiency response. *Frontiers in Plant Science* **10**, 627.
- Qi Y, Wang S, Shen C, Zhang S, Chen Y, Xu Y, Liu Y, Wu Y, Jiang D.** 2012. OsARF12, a transcription activator on auxin response gene, regulates root elongation and affects iron accumulation in rice (*Oryza sativa*). *New Phytologist* **193**, 109–120.
- Ramamurthy RK, Waters BM.** 2017. Mapping and characterization of the *fefe* gene that controls iron uptake in melon (*Cucumis melo* L.). *Frontiers in Plant Science* **8**, 1003.
- Robe K, Conejero G, Gao F, et al.** 2020. Coumarin accumulation and trafficking in *Arabidopsis thaliana*: a complex and dynamic process. *New Phytologist*. In press. doi: [10.1111/nph.17090](https://doi.org/10.1111/nph.17090)
- Rodríguez-Celma J, Chou H, Kobayashi T, Long TA, Balk J.** 2019a. Hemerythrin E3 ubiquitin ligases as negative regulators of iron homeostasis in plants. *Frontiers in Plant Science* **10**, 98.
- Rodríguez-Celma J, Connorton JM, Kruse I, Green RT, Franceschetti M, Chen YT, Cui Y, Ling HQ, Yeh KC, Balk J.** 2019b. Arabidopsis BRUTUS-LIKE E3 ligases negatively regulate iron uptake by targeting transcription factor FIT for recycling. *Proceedings of the National Academy of Sciences, USA* **116**, 17584–17591.
- Roschztardt H, Gaymard F, Dubos C.** 2020. Transcriptional regulation of iron distribution in seeds: a perspective. *Frontiers in Plant Science* **11**, 725.
- Samira R, Li B, Kliebenstein D, Li C, Davis E, Gillikin JW, Long TA.** 2018. The bHLH transcription factor ILR3 modulates multiple stress responses in *Arabidopsis*. *Plant Molecular Biology* **97**, 297–309.
- Santi S, Schmidt W.** 2009. Dissecting iron deficiency-induced proton extrusion in Arabidopsis roots. *New Phytologist* **183**, 1072–1084.
- Schwarz B, Bauer P.** 2020. FIT, a regulatory hub for iron deficiency and stress signaling in roots, and FIT-dependent and -independent gene signatures. *Journal of Experimental Botany* **71**, 1694–1705.
- Selote D, Samira R, Matthiadis A, Gillikin JW, Long TA.** 2015. Iron-binding E3 ligase mediates iron response in plants by targeting basic helix-loop-helix transcription factors. *Plant Physiology* **167**, 273–286.
- Sharma R, Yeh KC.** 2020. The dual benefit of a dominant mutation in Arabidopsis *IRON DEFICIENCY TOLERANT1* for iron biofortification and heavy metal phytoremediation. *Plant Biotechnology Journal* **18**, 1200–1210.
- Shen J, Xu X, Li T, Cao D, Han Z.** 2008. An MYB transcription factor from *Malus xiaojinensis* has a potential role in iron nutrition. *Journal of Integrative Plant Biology* **50**, 1300–1306.
- Shen C, Yue R, Sun T, Zhang L, Yang Y, Wang H.** 2015. OsARF16, a transcription factor regulating auxin redistribution, is required for iron deficiency response in rice (*Oryza sativa* L.). *Plant Science* **231**, 148–158.
- Spielmann J, Vert G.** 2020. The many facets of protein ubiquitination and degradation in plant root iron deficiency responses. *Journal of Experimental Botany*. doi: [10.1093/jxb/eraa441](https://doi.org/10.1093/jxb/eraa441).
- Stringlis IA, Yu K, Feussner K, de Jonge R, Van Bentum S, Van Verk MC, Berendsen RL, Bakker PAHM, Feussner I, Pieterse CMJ.** 2018. MYB72-dependent coumarin exudation shapes root microbiome assembly to promote plant health. *Proceedings of the National Academy of Sciences, USA* **115**, E5213–E5222.
- Sun Y, Li JQ, Yan JY, et al.** 2020. Ethylene promotes seed iron storage during *Arabidopsis* seed maturation via ERF95 transcription factor. *Journal of Integrative Plant Biology* **62**, 1193–1212.
- Tanabe N, Noshi M, Mori D, Nozawa K, Tamoi M, Shigeoka S.** 2019. The basic helix-loop-helix transcription factor, bHLH11 functions in the iron-uptake system in *Arabidopsis thaliana*. *Journal of Plant Research* **132**, 93–105.
- Tissot N, Robe K, Gao F, et al.** 2019. Transcriptional integration of the responses to iron availability in Arabidopsis by the bHLH factor ILR3. *New Phytologist* **223**, 1433–1446.
- Touraine B, Vignols F, Przybyla-Toscano J, et al.** 2019. Iron-sulfur protein NFU2 is required for branched-chain amino acid synthesis in Arabidopsis roots. *Journal of Experimental Botany* **70**, 1875–1889.
- Trofimov K, Ivanov R, Eutebach M, Acaroglu B, Mohr I, Bauer P, Brumbarova T.** 2019. Mobility and localization of the iron deficiency-induced transcription factor bHLH039 change in the presence of FIT. *Plant Direct* **3**, e00190.
- Wang FP, Wang XF, Zhang J, Ma F, Hao YJ.** 2018. MdMYB58 modulates Fe homeostasis by directly binding to the *MdMATE43* promoter in plants. *Plant & Cell Physiology* **59**, 2476–2489.
- Wang L, Ying Y, Narsai R, Ye L, Zheng L, Tian J, Whelan J, Shou H.** 2013a. Identification of OsbHLH133 as a regulator of iron distribution between roots and shoots in *Oryza sativa*. *Plant, Cell & Environment* **36**, 224–236.
- Wang N, Cui Y, Liu Y, Fan H, Du J, Huang Z, Yuan Y, Wu H, Ling HQ.** 2013b. Requirement and functional redundancy of Ib subgroup bHLH proteins for iron deficiency responses and uptake in *Arabidopsis thaliana*. *Molecular Plant* **6**, 503–513.
- Wang S, Li L, Ying Y, Wang J, Shao JF, Yamaji N, Whelan J, Ma JF, Shou H.** 2020. A transcription factor OsbHLH156 regulates Strategy II iron acquisition through localising IRO2 to the nucleus in rice. *New Phytologist* **225**, 1247–1260.
- Wu H, Ling HQ.** 2019. FIT-binding proteins and their functions in the regulation of Fe homeostasis. *Frontiers in Plant Science* **10**, 844.
- Xu Z, Liu X, He X, Xu L, Huang Y, Shao H, Zhang D, Tang B, Ma H.** 2017. The soybean basic helix-loop-helix transcription factor ORG3-like enhances cadmium tolerance via increased iron and reduced cadmium uptake and transport from roots to shoots. *Frontiers in Plant Science* **8**, 1098.
- Yan JY, Li CX, Sun L, Ren JY, Li GX, Ding ZJ, Zheng SJ.** 2016. A WRKY transcription factor regulates Fe translocation under Fe deficiency. *Plant Physiology* **171**, 2017–2027.
- Yin L, Wang Y, Yan M, Zhang X, Pan H, Xu X, Han Z.** 2013. Molecular cloning, polyclonal antibody preparation, and characterization of a functional iron-related transcription factor IRO2 from *Malus xiaojinensis*. *Plant Physiology and Biochemistry* **67**, 63–70.
- Yin L, Wang Y, Yuan M, Zhang X, Xu X, Han Z.** 2014. Characterization of MxFIT, an iron deficiency induced transcriptional factor in *Malus xiaojinensis*. *Plant Physiology and Biochemistry* **75**, 89–95.
- Yuan Y, Wu H, Wang N, Li J, Zhao W, Du J, Wang D, Ling HQ.** 2008. FIT interacts with AtbHLH38 and AtbHLH39 in regulating iron uptake gene expression for iron homeostasis in *Arabidopsis*. *Cell Research* **18**, 385–397.
- Yuan YX, Zhang J, Wang DW, Ling HQ.** 2005. *AtbHLH29* of *Arabidopsis thaliana* is a functional ortholog of tomato *FER* involved in controlling iron acquisition in strategy I plants. *Cell Research* **15**, 613–621.
- Zamioudis C, Hanson J, Pieterse CM.** 2014.  $\beta$ -Glucosidase BGLU42 is a MYB72-dependent key regulator of rhizobacteria-induced systemic resistance and modulates iron deficiency responses in *Arabidopsis* roots. *New Phytologist* **204**, 368–379.

- Zhang G, Liu W, Feng Y, et al.** 2020a. Ethylene response factors MBERF4 and MBERF72 suppress iron uptake in woody apple plants by modulating rhizosphere pH. *Plant & Cell Physiology* **61**, 699–711.
- Zhang H, Li Y, Pu M, Xu P, Liang G, Yu D.** 2020b. *Oryza sativa* POSITIVE REGULATOR OF IRON DEFICIENCY RESPONSE 2 (OsPRI2) and OsPRI3 are involved in the maintenance of Fe homeostasis. *Plant, Cell & Environment* **43**, 261–274.
- Zhang H, Li Y, Yao X, Liang G, Yu D.** 2017. POSITIVE REGULATOR OF IRON HOMEOSTASIS1, OsPRI1, facilitates iron homeostasis. *Plant Physiology* **175**, 543–554.
- Zhang J, Liu B, Li M, Feng D, Jin H, Wang P, Liu J, Xiong F, Wang J, Wang HB.** 2015. The bHLH transcription factor bHLH104 interacts with IAA-LEUCINE RESISTANT3 and modulates iron homeostasis in *Arabidopsis*. *The Plant Cell* **27**, 787–805.
- Zhang L, Nakanishi Itai R, Yamakawa T, Nakanishi H, Nishizawa NK, Kobayashi T.** 2014. The Bowman–Birk trypsin inhibitor IBP1 interacts with and prevents degradation of IDEF1 in rice. *Plant Molecular Biology Reporter* **32**, 841–851.
- Zhang X, Wang C, Zhang Y, Sun Y, Mou Z.** 2012. The *Arabidopsis* mediator complex subunit16 positively regulates salicylate-mediated systemic acquired resistance and jasmonate/ethylene-induced defense pathways. *The Plant Cell* **24**, 4294–4309.
- Zhao M, Song A, Li P, Chen S, Jiang J, Chen F.** 2014. A bHLH transcription factor regulates iron intake under Fe deficiency in chrysanthemum. *Scientific Reports* **4**, 6694.
- Zhao Q, Ren YR, Wang QJ, Wang XF, You CX, Hao YJ.** 2016a. Ubiquitination-related MdbT scaffold proteins target a bHLH transcription factor for iron homeostasis. *Plant Physiology* **172**, 1973–1988.
- Zhao Q, Ren YR, Wang QJ, Yao YX, You CX, Hao YJ.** 2016b. Overexpression of *MdbHLH104* gene enhances the tolerance to iron deficiency in apple. *Plant Biotechnology Journal* **14**, 1633–1645.
- Zheng L, Ying Y, Wang L, Wang F, Whelan J, Shou H.** 2010. Identification of a novel iron regulated basic helix-loop-helix protein involved in Fe homeostasis in *Oryza sativa*. *BMC Plant Biology* **10**, 166.
- Zhou LJ, Zhang CL, Zhang RF, Wang GL, Li YY, Hao YJ.** 2019. The SUMO E3 ligase MdSIZ1 targets MdbHLH104 to regulate plasma membrane H<sup>+</sup>-ATPase activity and iron homeostasis. *Plant Physiology* **179**, 88–106.
- Zhu XF, Wu Q, Meng YT, Tao Y, Shen RF.** 2020. AtHAP5A regulates iron translocation in iron-deficient *Arabidopsis thaliana*. *Journal of Integrative Plant Biology*. doi: [10.1111/jipb.12984](https://doi.org/10.1111/jipb.12984)

## 1.8 Objectives of the thesis

At the start of my PhD, our understanding of the transcriptional control of iron homeostasis in *Arabidopsis* was becoming clearer. As described in the introduction, at least 16 bHLH transcription factors have been characterized to regulate iron homeostasis in *Arabidopsis* (Gao *et al.*, 2019b). However, how these known bHLH transcriptional factors were acting in concert with each other to regulate iron homeostasis was still to be elucidated. Previous work conducted in the group showed that ILR3 could bind to the *G-Box* present in the promoter of *AtFER1* and repress its expression in vegetative tissues. This raised an important question, how the ILR3 act as both activator and repressor in the regulation of iron homeostasis? Previous work in the group has identified a novel ILR3 interacting protein named bHLH121. From this later finding arose a second question: what is the role of bHLH121 in the regulation of iron homeostasis? In order to answer these questions, the following objectives were formulated as a framework for this PhD thesis:

- (i) The first objective of this PhD thesis was to verify the interaction between ILR3 and PYE, and to characterize its repression mechanism in controlling iron homeostasis.
- (ii) The second objective was to functionally characterize the new ILR3 interacting protein bHLH121. To study the role of the bHLH121 in the regulation of iron homeostasis.
- (iii) The last objective of this PhD thesis was to investigate the genetic interaction between bHLH121 and the clade IVc bHLH transcriptional factors, to study how these transcription factors are coordinated to regulate the expression of genes involved in iron homeostasis.

In the first axis, the interaction between the ILR3 and PYE was confirmed by bimolecular fluorescence complementation (BiFC) experiment in *Arabidopsis thaliana* protoplasts. Expression studies together with chromatin immunoprecipitation (ChIP) assays demonstrated that ILR3 could repress the expression of genes involved in the control of iron homeostasis through the direct binding to their promoter and that ILR3 repressive activity was conferred by its dimerisation with another known repressor, PYE.

The phenotypic characterization of ILR3 dominant and loss-of-function mutants, as well as the triple ferritin mutant, indicated that several facets of plant growth in response to fluctuations in Fe availability, from deficiency to excess, rely on ILR3 and ferritin activities. These results highlighted that ILR3 not only acts as an activator involved in the iron deficiency response but also acts as a repressor of plant responses to iron excess. These results are presented in Chapter II, in the manner of an article published in *New Phytologist* where I am co-second author (Tissot *et al.*, 2019).

In the second axis, interaction studies showed that bHLH121 could interact with bHLH34, bHLH104, ILR3 and bHLH115. Loss-of-function of bHLH121 led to severe growth defects that could be reverted by exogenous iron supply. ChIP assays and expression studies demonstrated that bHLH121 functions as a direct transcriptional activator of a set of important genes involved in iron deficiency regulatory network. Cellular localization assays showed that iron availability affects the bHLH121 protein cellular localization within the root tissues. These results presented in Chapter III have been published in *The Plant Cell* (Gao *et al.*, 2020a). In addition, I found that bHLH121 could also regulate the expression of ferritin genes by directly binding to their promoters, at the same locus than the ILR3-PYE repressive complex, which highlight that bHLH121, PYE, and ILR3 form a chain of antagonistic switches that regulate the expression of ferritin genes. These results also presented in Chapter III have been published in *Plant Signaling & Behavior* (Gao *et al.*, 2020b).

In the last axis, phenotypical analysis showed that double mutants of bHLH121 and clade IVc bHLHs displayed more severe iron deficiency-associated growth defects compared to the single mutants. Consistent with this, enhanced impaired iron deficiency responses were observed by expression analysis. Constitutive expression of *bHLH34* and *bHLH105*, but not *bHLH104* or *bHLH115* could partially complement the iron deficiency associated growth defects of *bhlh121* loss-of-function mutant by activating the expression of both *bHLH39* and *FIT*. These results indicated the distinct roles of the four clade IVc bHLH members in the regulation of iron homeostasis. Meanwhile, the different spatial expression patterns of *bHLH121* and the clade IVc bHLHs implied that they might function in specific tissues. Taken together, these results indicated bHLH121 and clade IVc bHLHs function coordinately in the regulation of iron homeostasis. These results presented in Chapter IV, in a manner of an article that will be

submitted to Journal of Experimental Botany where I will be first author.





# **CHAPTER II**

## **ILR3 CONNECTS THE NEGATIVES AND POSITIVES OF IRON HOMEOSTASIS**



**Article 2. Transcriptional integration of the responses to iron  
availability in arabidopsis by the bHLH factor ILR3**



# Transcriptional integration of the responses to iron availability in *Arabidopsis* by the bHLH factor ILR3

Nicolas Tissot<sup>1</sup>, Kevin Robe<sup>1\*</sup>, Fei Gao<sup>1\*</sup> , Susana Grant-Grant<sup>3</sup>, Jossia Boucherez<sup>1</sup>, Fanny Bellegarde<sup>1</sup> , Amel Maghiaoui<sup>1</sup>, Romain Marcelin<sup>1</sup>, Esther Izquierdo<sup>1</sup> , Moussa Benhamed<sup>2</sup>, Antoine Martin<sup>1</sup> , Florence Vignols<sup>1</sup> , Hannetz Roschztardt<sup>3</sup> , Frédéric Gaymard<sup>1</sup>, Jean-François Briat<sup>1</sup> and Christian Dubos<sup>1</sup> 

<sup>1</sup>BPMP, Univ Montpellier, CNRS, INRA, SupAgro, 34060 Montpellier, France; <sup>2</sup>Institut of Plant Sciences Paris-Saclay (IPS2), UMR 9213/UMR1403, CNRS, INRA, Université Paris-Sud, Université d'Evry, Université Paris-Diderot, Sorbonne Paris-Cité, Bâtiment 630, 91405 Orsay, France; <sup>3</sup>Departamento de Genética Molecular y Microbiología, Pontificia Universidad Católica de Chile, 8331150 Santiago, Chile

## Summary

Author for correspondence:

Christian Dubos

Tel: +33 4 99 61 28 18

Email: Christian.dubos@inra.fr

Received: 8 November 2018

Accepted: 12 February 2019

*New Phytologist* (2019) **223**: 1433–1446

doi: 10.1111/nph.15753

**Key words:** *Arabidopsis thaliana*, basic helix–loop–helix, bHLH105, ferritins, homeostasis, ILR3, iron, PYE.

- Iron (Fe) homeostasis is crucial for all living organisms. In mammals, an integrated posttranscriptional mechanism couples the regulation of both Fe deficiency and Fe excess responses. Whether in plants an integrated control mechanism involving common players regulates responses both to deficiency and to excess is still to be determined.
- In this study, molecular, genetic and biochemical approaches were used to investigate transcriptional responses to both Fe deficiency and excess.
- A transcriptional activator of responses to Fe shortage in *Arabidopsis*, called bHLH105/ILR3, was found to also negatively regulate the expression of ferritin genes, which are markers of the plant's response to Fe excess. Further investigations revealed that ILR3 repressed the expression of several structural genes that function in the control of Fe homeostasis. ILR3 interacts directly with the promoter of its target genes, and repressive activity was conferred by its dimerisation with bHLH47/PYE. Last, this study highlighted that important facets of plant growth in response to Fe deficiency or excess rely on ILR3 activity.
- Altogether, the data presented herein support that ILR3 is at the centre of the transcriptional regulatory network that controls Fe homeostasis in *Arabidopsis*, in which it acts as both transcriptional activator and repressor.

## Introduction

The control of iron (Fe) homeostasis is essential in all living organisms. Perturbations of Fe uptake, circulation, metabolism or storage alter plant productivity and the quality of their derived products (Briat *et al.*, 2015). Although Fe is one of the most abundant elements found in soils, it is generally poorly available to plants because it is mainly present in the form of insoluble chelates. This is, for instance, found for calcareous soils that represent one-third of the world's cultivated lands (Guerinot & Yi, 1994). Therefore, decrypting the physiological and molecular mechanisms governing plant Fe uptake, transport and storage is a critical issue considering that all the Fe that is present in the human diet comes, directly or indirectly, from plants.

Plants respond to Fe shortage through different mechanisms (Kobayashi & Nishizawa, 2012). Nongraminaceous monocot as well as dicot species such as *Arabidopsis thaliana* have evolved a reduction-based strategy to solubilise and absorb Fe from the soil (Morrissey & Guerinot, 2009; Brumbarova *et al.*, 2015; Curie & Mari, 2016; Connorton *et al.*, 2017). It relies on the reduction of

Fe(III) chelates present in the soil by FRO2 (FERRIC REDUCTION OXIDASE 2) (Robinson *et al.*, 1999). The Fe<sup>2+</sup> ion generated is then transported across the rhizodermis cell membranes by IRT1 (IRON-REGULATED TRANSPORTER 1) (Eide *et al.*, 1996; Henriques *et al.*, 2002; Varotto *et al.*, 2002; Vert *et al.*, 2002). This process is facilitated by the activity of the AHA2 proton-ATPase, whose activity leads to rhizosphere acidification (Santi & Schmidt, 2009). In addition, Fe solubilisation is enhanced by the excretion (by the rhizodermis-specific PDR9/ABCG37 transporter) of Fe-mobilising phenolic compounds (Fourcroy *et al.*, 2004, 2014, 2016; Rodríguez-Celma *et al.*, 2013a; Schmid *et al.*, 2014). Fe transport, compartmentalisation and storage is also modulated in response to fluctuations in Fe availability (Morrissey & Guerinot, 2009; Kobayashi & Nishizawa, 2012; Brumbarova *et al.*, 2015; Curie & Mari, 2016; Connorton *et al.*, 2017).

Plant response to Fe deficiency is tightly regulated at the transcriptional level by a complex transcriptional regulatory cascade in which basic helix–loop–helix (bHLH) transcription factors (TFs) play a predominant role (Heim *et al.*, 2003; Gao *et al.*, 2019). In *Arabidopsis*, the main TFs involved have been characterised. At the top of this regulatory network, four bHLH TFs

\*These authors contributed equally to this work.

(bHLH34, bHLH104, bHLH105/ILR3 – IAA-LEUCINE RESISTANT3, and bHLH115) form homo- and heterodimers that regulate the expression of five additional bHLH TFs (Zhang *et al.*, 2015; Li *et al.*, 2016; Liang *et al.*, 2017). Targeted TFs consist of *bHLH38*, *bHLH39*, *bHLH100*, *bHLH101* and *bHLH47/PYE* (*POPEYE*) (Colangelo & Guerinot, 2004; Wang *et al.*, 2007, 2013; Yuan *et al.*, 2008; Zhang *et al.*, 2015). Once induced, bHLH38, bHLH39, bHLH100, bHLH101 can form heterodimers with bHLH29/FIT (FE-DEFICIENCY INDUCED TRANSCRIPTION FACTOR) (Colangelo & Guerinot, 2004; Jakoby *et al.*, 2004; Yuan *et al.*, 2008). Then, these FIT-dependent transcriptional complexes activate the transcription of genes encoding for the Fe uptake system (for example *FRO2*, *IRT1*) located at the root epidermis (Vert *et al.*, 2002; Yuan *et al.*, 2008; Wang *et al.*, 2013). Four additional bHLH partners of FIT (bHLH18, bHLH19, bHLH20, and bHLH25) promote its degradation in response to jasmonic acid induction, antagonising the activity of bHLH38, bHLH39, bHLH100, bHLH101 and hence Fe uptake (Cui *et al.*, 2018). By contrast, PYE is a transcriptional repressor that contains in its C-terminal part an EAR motif (DLNxxP), one of the most predominant form of transcriptional repression motif identified in plants (Kagale & Rozwadowski, 2011). For instance, in the root pericycle, PYE represses the expression of genes notably implicated in Fe transport such as *NAS4* (*NICOTIANAMINE SYNTHASE 4*), a key gene involved in phloem-based transport of Fe to sink organs (Klatte *et al.*, 2009; Long *et al.*, 2010). PYE was shown to heterodimerise *in vivo* with bHLH104, ILR3 and bHLH115 (Long *et al.*, 2010; Zhang *et al.*, 2015). However, it is still unclear if these interactions play a role in the plant response to Fe deficiency or in the control of Fe homeostasis.

Under aerobic conditions, Fe can react with H<sub>2</sub>O<sub>2</sub> (Fenton reaction) producing reactive oxygen species (ROS) that are deleterious to the cell. This property renders Fe excess detrimental for plant growth, severely affecting crop yield (Becker, 2005; Khabaz-Saberli, 2010). Regulation of Fe excess responses in plants has been studied at cellular and molecular levels mostly by using the *AtFER1* gene as a model. *AtFER1* encodes the most expressed Fe storage ferritin protein in Arabidopsis vegetative tissues whose expression and protein abundance is strongly induced in response to Fe excess (Petit *et al.*, 2001; Duc *et al.*, 2009; Briat *et al.*, 2010; Bournier *et al.*, 2013; Reyt *et al.*, 2015).

This is by contrast with the animal systems in which the balance between Fe uptake and storage is mainly achieved by the posttranscriptional regulation of ferritin and transferrin receptor synthesis by the iron-responsive protein element (IRE)/iron-responsive protein (IRP1)—cytosolic aconitase Fe switch (Hentze *et al.*, 2010). Briefly, specific sequences, named IREs and found in the 5'-untranslated region (UTR) of ferritin mRNA and in the 3'-UTR of transferrin receptor transcript, function as binding sites for related *trans*-acting factors, named IRPs. In the case of Fe deficiency, IRPs are bound to IREs. Consequently, the translation of the ferritin mRNA is inhibited, avoiding Fe storage, and the transferrin receptor mRNA is stabilised, leading to an increase in abundance of the corresponding protein, which promotes Fe uptake. By contrast, Fe excess leads to IRPs dissociation from IREs,

promoting ferritin mRNA translation and Fe storage on the one hand, and transferrin receptor mRNA degradation and Fe uptake inhibition on the other hand. Under Fe excess conditions, some IRPs contain a 4Fe–4S cluster, conferring to them a cytosolic aconitase activity, whereas others that do not contain such a cluster are degraded. If the Fe deficiency and Fe excess responses are controlled in plants by an integrated pathway involving common players, as it is the case in mammals (Hentze *et al.*, 2010), is therefore an important issue that remains to be addressed.

In this study, by combining molecular, genetic and biochemical approaches, ILR3 was found to act as a repressor of *AtFER1* gene expression in vegetative tissues. Expression studies together with chromatin immunoprecipitation (ChIP) assays highlighted that ILR3 represses the expression of structural genes involved in the control of Fe homeostasis through the direct binding to their promoter and that ILR3 repressive activity is conferred by its dimerisation with PYE. The use of *ilr3* mutants (loss-of-function and dominant mutations), as well as a triple ferritin mutant, indicated that several facets of plant growth in response to fluctuations in Fe availability, from deficiency to excess, rely on ILR3 and ferritin activities. Altogether, the data presented here indicate that ILR3 function extends beyond the sole control of bHLH TFs expression upstream of the Fe deficiency transcriptional regulatory network and therefore support the theory that ILR3 plays a critical role in the transcriptional regulatory network that controls Fe homeostasis in Arabidopsis, where it acts as both transcriptional activator and repressor.

## Materials and Methods

### Arabidopsis gene IDs

*APX1*, At1g07890; *AtFER1*, At5g01600; *AtFER3*, At3g56090; *AtFER4*, At2g40300; *At-NEET*, At5g51720; *bHLH34*, At3g23210; *bHLH39*, At3g56980; *bHLH47/PYE*, At3g47640; *bHLH104*, At4g14410; *bHLH105/ILR3*, At5g54680; *bHLH115*, At1g51070; *IRT1*, At4g19690; *PP2AA3*, At1g13320; *NAS4*, At1g56430; *VTL2*, At1g76800.

### Plant materials

*Arabidopsis thaliana* ecotype Columbia (Col-0) was used as the wild-type (WT). The following mutant lines were used in this study: *bhlh34* (Li *et al.*, 2016), *bhlh104-1* (Zhang *et al.*, 2015), *ilr3-1* (Rampey *et al.*, 2006), *ilr3-3* (Li *et al.*, 2016), *pye-1* (Long *et al.*, 2010), *ilr3-3 pye-1* (this study), *bhlh115-2* (Liang *et al.*, 2017) and *fer1,3,4* (Ravet *et al.*, 2009).

### Growth conditions

*In vitro* cultures: Seedlings were grown under long day conditions (16 h : 8 h, light : dark) on half strength Murashige and Skoog medium (½MS) with 0.05% MES, 1% sucrose, 0.7% agar for 7–10 d. Fe concentration was 50 µM and provided as Fe(III)-EDTA. For GUS experiments as well as for qRT-PCR, western and ChIP analyses, seedlings were transferred from agar plates to

liquid  $\frac{1}{2}$ MS medium for an additional 3 days of growth in the absence or presence of Fe (50  $\mu$ M Fe(III)-citrate), corresponding to the Fe deficiency ( $-$ Fe) or control (C) conditions, respectively. Fe excess (+Fe) treatment was applied by adding 500  $\mu$ M Fe-citrate for 6 h to the growth solution for plants grown in the absence of Fe. For root length and fresh weight measurements, seedlings were grown on solid  $\frac{1}{2}$ MS for 2 wk in the presence or absence of Fe(III)-EDTA (C,  $-$ Fe and +Fe). Root length was measured using the IMAGEJ software.

Detailed protocols for physiological, biochemical, molecular and cytological analyses are given in Supporting Information Methods S1. All the primers used are described in Table S1.

## Results

### Repression of *AtFER1* minimal promoter activity involves a *G-box* *cis*-regulatory sequence

To identify TFs that could link Fe deficiency and Fe excess responses, the promoter of *AtFER1* (*ProAtFER1*) was functionally characterised. The aim was to identify *cis*-regulatory sequences involved in *ProAtFER1* repression that could be used as baits in yeast one-hybrid (Y1H) screens. A deletion series of *ProAtFER1* fused to the *uidA* reporter gene (*ProAtFER1:GUS*) expressed in WT plants was carried out. This approach allowed the identification of a 496 bp minimal promoter (*ProAtFER1<sub>mini</sub>*) whose activity was still inducible in response to Fe excess, as does the endogenous gene (Figs 1a, S1) (Reyt *et al.*, 2015). Sequence comparison of *ProAtFER1<sub>mini</sub>* with the corresponding sequence of *ProAtFER3* and *ProAtFER4*, the two other ferritin genes expressed in vegetative tissues (Reyt *et al.*, 2015), highlighted some potential *cis*-regulatory motifs including a *G-box* (CACGTG) (Fig. S2) (Strozycki *et al.*, 2010). Because most of the master TFs regulating the Fe deficiency responses belong to the bHLH family (Li *et al.*, 2016; Cui *et al.*, 2018), and because bHLH TFs bind *G-box* sequences (and more generally *E-box*, *CANNTG*) that are usually localised within the promoter of their target genes (De Masi *et al.*, 2011), this potential *cis*-regulatory element was selected for further analysis. In support of this choice, the *G-box* sequences present in the promoter of the ferritin genes were located in nucleosome-free regions (NFR), suggesting the presence of regulatory proteins at these loci when Fe is not limiting (Fig. S3).

Site-directed mutagenesis revealed that the mutation of the *G-box* (*mG-box*) leads to an enhanced *ProAtFER1<sub>mini</sub>* activity in the control (C: 50  $\mu$ M Fe) condition (Fig. 1a). However, the effect of *mG-box* on *ProAtFER1<sub>mini</sub>* activity in the control condition was lower than that of the mutation of the well characterised repressive *IDRS* (*Iron-Dependent Regulatory Sequence*) regulatory element (Petit *et al.*, 2001). These observations indicate that this *G-box* plays a key role in the transcriptional repression of *ProAtFER1<sub>mini</sub>* when Fe is not in excess, and that part of the dynamic response of *AtFER1* expression to Fe availability relies on this specific *cis*-regulatory sequence.

Therefore, a 20 bp long DNA fragment containing the *G-box* (Element 5, Figs S2, S4a,b) present on *ProAtFER1<sub>mini</sub>* was used

as bait for Y1H experiments using a normalised TF cDNA library (Paz-Ares, 2002). This approach led to the identification of four TFs (Fig. S4c). Among these genes, there was only one bHLH TF, *bHLH105/ILR3* (*IAA-LEUCINE RESISTANT 3*), a well described transcriptional activator of plant responses to Fe shortage (Rampey *et al.*, 2006; Zhang *et al.*, 2015; Li *et al.*, 2016). In presence of 1 mM 3-AT (3-Amino-1,2,4-triazole), ILR3 was the sole TF still interacting with the bait DNA. ILR3 interaction in Y1H experiments was abolished when the *G-box* was mutated (Fig. 1b).

### ILR3 is a repressor of ferritin gene expression

To characterise the role of ILR3 in the transcriptional control of ferritin gene expression, a *ILR3* T-DNA insertion line (*ilr3-3*, knock down mutant) was studied together with another mutant expressing a dominant version of ILR3 (*ilr3-1*) and compared with WT seedlings (Fig. S5) (Rampey *et al.*, 2006; Meinke, 2013). The dominant *ilr3-1* allele displays conserved bHLH and leucine zipper domains, respectively involved in DNA binding and protein dimerisation, but lacks the C-terminal domain suspected to improve the stability of ILR3 homo- or heterodimers (Rampey *et al.*, 2006; Meinke, 2013).

Seedlings were grown with three different Fe concentrations in the growth media: control condition (C: 50  $\mu$ M), Fe deficiency ( $-$ Fe: 0  $\mu$ M) and Fe excess (+Fe: 500  $\mu$ M). By contrast to  $-$ Fe and +Fe, C condition corresponds to Fe concentration in the culture medium allowing optimal plant growth (repleteness). qRT-PCR analysis showed that in C and +Fe conditions the mRNA steady state level of *AtFER1* was increased in the *ilr3-3* mutant when compared with WT seedlings and decreased in *ilr3-1* (Fig. 1c). In  $-$ Fe condition, *AtFER1* transcript level was increased in *ilr3-3* compared with WT seedlings, whereas no difference was observed between WT and *ilr3-1* seedlings. For the two other ferritin genes expressed in vegetative tissues, namely *AtFER3* and *AtFER4*, comparable expression patterns to that of *AtFER1* were observed (Fig. S6).

Western blot analysis confirmed that ferritin protein (FER) abundance was, in comparison with WT seedlings, higher and lower in the *ilr3-3* and *ilr3-1* mutants, respectively (Fig. 1d). Under C conditions, the difference in *AtFER1* transcript levels between WT and *ilr3-3* was less pronounced when compared with the difference observed at the protein levels. Since the antibody used recognises all three ferritins, this observation suggests that ILR3 might regulate *AtFER1* and/or *AtFER3* and *AtFER4* protein abundance through a mechanism that expands beyond the sole regulation of their expression.

Then, WT plants carrying the *ProAtFER1<sub>mini</sub>:GUS* and *ProAtFER1<sub>mini</sub>-mG-box:GUS* constructs were crossed with the *ilr3-3* and *ilr3-1* mutants. Homozygous mutant plants harbouring the transgenes were selected, and the GUS activities analysed (Fig. 1e). As expected, *ProAtFER1<sub>mini</sub>:GUS* activity led to a more intense blue coloration in *ilr3-3* mutant when compared with both WT and *ilr3-1*. This result highlighted the repressive role of ILR3 on the activity of *ProAtFER1<sub>mini</sub>*. *ProAtFER1<sub>mini</sub>-mG-box*:



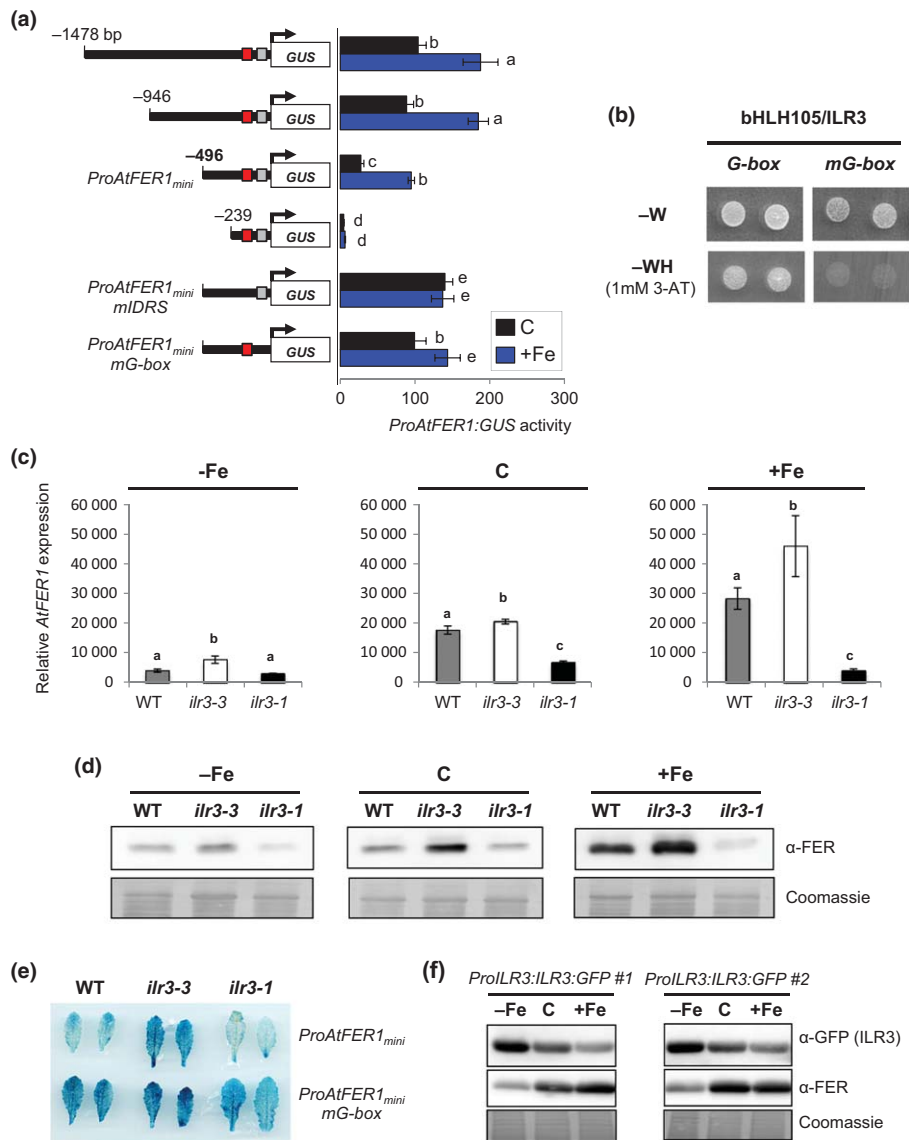


**Fig. 1** ILR3 is a repressor of ferritin genes expression. (a) Left panel, scheme of 5'-end deletion and site-directed mutagenesis constructs used for the functional characterisation of *ProAtFER1* as revealed by GUS ( $\beta$ -glucuronidase) activity in 2-wk-old wild-type (WT) *Arabidopsis thaliana* seedlings. Red boxes, *IDRS* (AGCACGAGGCCGCCACAGCCCC); grey boxes, *G-box* (CACGTG). *mIDRS*, mutated *Iron-Dependent Regulatory Sequence*; *mG-box*, mutated *G-box cis*-regulatory sequence. C and +Fe correspond to the control (50  $\mu$ M Fe) and Fe excess (500  $\mu$ M Fe) condition, respectively. Right panel, quantitative GUS analysis (nmol 4-MU  $\text{min}^{-1} \text{mg}^{-1}$  proteins) driven by *ProAtFER1* 5'-end deletion and site-directed mutagenesis constructs. Means with the same letter are not significantly different according to one-way analysis of variance (ANOVA) followed by post-hoc Tukey test,  $P < 0.05$  ( $n = 6$ , three biological repeats  $\times$  2 independent transgenic lines, from one representative experiment). Error bars show  $\pm$  SD. (b) Yeast one-hybrid experiment: yeasts were stably transformed with tetramers of a 20 bp long *ProAtFER1* DNA fragment containing the native *G-box* or a mutated version (*mG-box*) fused to *HIS3* (auxotrophic markers). These two yeast strains were then transfected with ILR3/bHLH105. Upper panel, growth on control media deprived of W amino acids. Lower panel, growth on selective media deprived of W and H amino acids. 3-AT, 3-amino-1,2,4-triazole. Two independent colonies per construct are shown. (c) Quantitative RT-PCR (qRT-PCR) analysis of *AtFER1* mRNA levels in 2-wk-old WT, *ilr3-3* (loss-of-function) and *ilr3-1* (dominant mutation) seedlings. -Fe, C and +Fe correspond to Fe deficiency (0  $\mu$ M Fe), control (50  $\mu$ M Fe), and Fe excess (500  $\mu$ M Fe) condition, respectively. Means with the same letter are not significantly different according to one-way ANOVA followed by post-hoc Tukey test,  $P < 0.05$  ( $n = 3$  biological repeats from one representative experiment). Error bars show  $\pm$  SD. (d) Abundance of ferritin proteins in 2-wk-old WT, *ilr3-3* and *ilr3-1* seedlings grown as in (a). (e) Histochemical detection of GUS activity driven by the *ProAtFER1<sub>mini</sub>* with the native or the mutated *G-box* (*mG-box*) in WT, *ilr3-3* and *ilr3-1* leaves. (f) Western blot analysis of ILR3 ( $\alpha$ -GFP) and ferritin proteins ( $\alpha$ -FER) in 2-wk-old WT seedlings expressing *pILR3::gILR3:GFP* (2 independent transgenic lines are shown, #1 and #2) grown as in (c).

*GUS* staining was stronger in all three genotypes tested when compared with WT plants expressing *ProAtFER1<sub>mini</sub>:GUS*, confirming the role of the *G-box* in the repression of *ProAtFER1<sub>mini</sub>*

activity. This experiment demonstrates, *in planta*, the genetic connection between ILR3 and the *G-box* present in *ProAtFER1<sub>mini</sub>*

Because of the repressive role of ILR3 on *AtFER1* expression, one would expect that a negative correlation exists *in planta* in term of protein accumulation between ILR3 and the FER proteins. Western blot analysis was carried out using WT plants expressing the *ProILR3:gILR3:GFP* construct. This experiment confirmed the negative correlation between ILR3 abundance and Fe availability (Fig. 1f).

In order to determine if ILR3 function in regulating ferritin gene expression is unique within the bHLH clade it belongs to (IVc), *AtFER1* mRNA abundance was measured in *bhlh34*, *bhlh104* and *bhlh115* loss-of-function mutants (Zhang *et al.*, 2015; Li *et al.*, 2016). No variation in *AtFER1* expression was found in *bhlh34*, *bhlh104* and *bhlh115* mutants when compared with WT seedlings for the three Fe conditions tested, by contrast to what is observed for the *ilr3-3* mutants (Fig. S7).

Taken together, these data demonstrate that ILR3 repression of ferritin gene expression is specific within the clade IVc bHLHs.

### ILR3 acts as both transcriptional activator and repressor to regulate Fe homeostasis

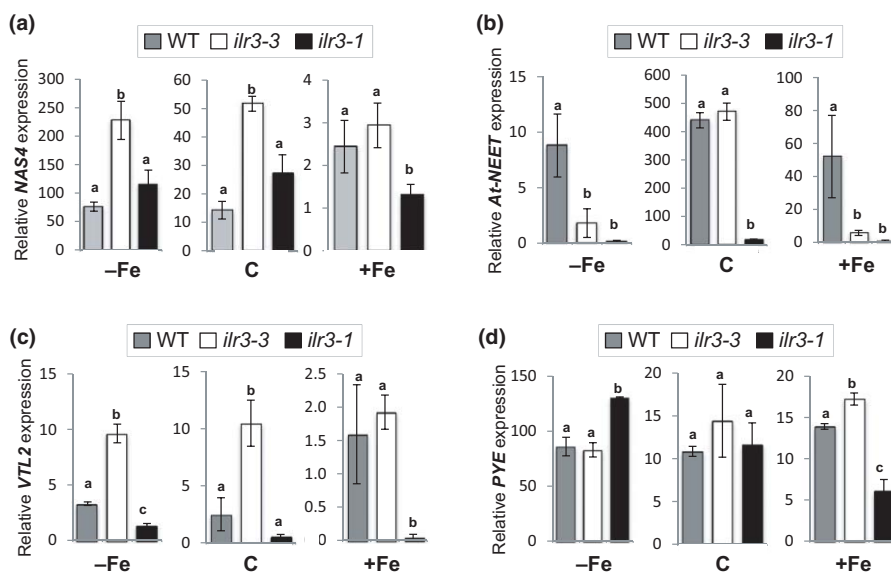
To determine if ILR3 repressive activity is specific to the ferritin genes, mRNA abundance of genes associated with Fe homeostasis and/or metabolism was measured by qRT-PCR under contrasting Fe conditions (C, -Fe and +Fe).

*APX1* is strongly induced in response to Fe excess and encodes the cytosolic ASCORBATE PEROXIDASE 1 that is, with the ferritin genes, another well known marker of the Arabidopsis response to Fe excess (Fourcroy *et al.*, 2004). *APX1* mRNA abundance was unaffected in the *ilr3-1* and *ilr3-3* mutant backgrounds when compared with WT seedlings regardless of the Fe condition (Fig. S8a). This observation indicates that the regulation of ferritin expression by ILR3 is related to the control of Fe homeostasis *per se*. As expected, *IRT1* expression was diminished in *ilr3-3* when compared with WT and *ilr3-1* seedlings in

response to -Fe (Fig. S8b; Zhang *et al.*, 2015). By contrast, *IRT1* mRNA level was higher in *ilr3-1* when compared with WT seedlings in C or +Fe conditions. Because *bHLH39* is a known target of ILR3 that participates to the transcriptional regulation of *IRT1* expression in response to Fe shortage (Zhang *et al.*, 2015), its mRNA steady state level was also analysed. This analysis confirmed that *bHLH39* expression is induced in response to -Fe in an ILR3-dependent manner (Fig. S8c). Last, *NAS4* expression was increased in *ilr3-3* when compared with WT and *ilr3-1* seedlings in -Fe or C conditions (Fig. 2a). These data indicate that ILR3, like PYE, represses *NAS4* expression when Fe is not in excess.

Three additional genes whose expression was previously reported to depend on ILR3 activity were assayed, namely *AtNEET*, *VTL2* (*VACUOLAR IRON TRANSPORTER-LIKE 2*) and *PYE*. *AtNEET* encodes a protein that is capable of transferring [Fe-S] cluster to an acceptor protein and that is thought to play a role in Fe homeostasis and/or metabolism (Nechushtai *et al.*, 2012). As previously described, *AtNEET* mRNA abundance was decreased in *ilr3-1* and unaffected in *ilr3* loss-of-function mutant when compared with WT seedlings grown in C condition (Fig. 2b) (Rampey *et al.*, 2006). Surprisingly, growth in -Fe or +Fe conditions led to a drastic decrease of *AtNEET* mRNA abundance in both mutants when compared with WT seedlings. These observations indicate that ILR3 represses *AtNEET* expression when plants are grown under Fe-replete condition. *VTL2* encodes a Fe vacuolar transporter whose expression was previously reported as increased in *ilr3-1* and decreased in *ilr3* loss-of-function mutant when compared with WT seedlings (Gollhofer *et al.*, 2011, 2014). This pattern of *VTL2* mRNA accumulation was conserved regardless of the Fe concentration in which seedlings were grown, with a less marked difference between WT and *ilr3-3* in +Fe condition (Fig. 2c). These data confirm that, like for the ferritin genes, ILR3 is a transcriptional repressor of *VTL2* expression. *PYE* mRNA abundance was then measured as *PYE* was proposed to be a target of ILR3

**Fig. 2** ILR3 acts as both transcriptional activator and repressor to regulate Fe homeostasis. Relative expression of (a) *NAS4* (*NICOTIANAMINE SYNTHASE 4*), (b) *AtNEET*, (c) *VTL2* (*VACUOLAR IRON TRANSPORTER-LIKE 2*) and (d) *PYE* (*POPEYE/bHLH47*) genes as revealed by quantitative RT-PCR analysis in 2-wk-old *Arabidopsis thaliana* wild type (WT), *ilr3-1* and *ilr3-3* seedlings. -Fe, C and +Fe correspond to Fe deficiency (0  $\mu$ M Fe), control (50  $\mu$ M Fe), and Fe excess (500  $\mu$ M Fe) conditions, respectively. Means within each condition with the same letter are not significantly different according to one-way ANOVA followed by post-hoc Tukey test,  $P < 0.05$  ( $n = 3$  biological repeats from one representative experiment). Error bars show  $\pm$  SD.



(Zhang *et al.*, 2015; Li *et al.*, 2016). This analysis revealed that *PYE* expression was higher in the *ilr3-1* mutant when compared with WT and *ilr3-3* in  $-Fe$  condition, confirming the positive role of ILR3 on *PYE* expression when Fe availability is low (Fig. 2d). By contrast, when Fe availability was not limiting, *PYE* expression appeared to be repressed in an ILR3-dependent manner, in particular in the  $+Fe$  condition. This later observation suggests that ILR3 acts as a transcriptional repressor of *PYE* expression when Fe is not limiting.

### ILR3 binds to *E-box* motifs present in the promoter of its target genes

In order to determine whether or not ILR3 interacts with the *E-box* motifs present in the promoter of the ferritins genes (*AtFER1*, *AtFER3* and *AtFER4*), as well as with the promoter of *At-NEET*, *VTL2* and *NAS4*, ChIP experiments were carried out (Fig. 3a). ChIP experiments were conducted on two independent transgenic lines expressing the *ProILR3:gILR3:GFP* construct using an anti-GFP antibody (Figs 1f, S9). A promoter fragment containing an *E-box* motif for both *bHLH39* and *FIT* was used as positive and negative control, respectively (Zhang *et al.*, 2015). As previously reported, ChIP-qPCR analyses showed that ILR3 bound to the promoter of *bHLH39* (*ProbHLH39*) and not to the

one of *FIT* (*ProFIT*) (Fig. 3b). The results presented Fig. 3c–e support the *in vivo* binding of ILR3 to the promoter of *AtFER1* (*ProFER1*), *AtFER3* (*ProFER3*) and *AtFER4* (*ProFER4*) with a higher affinity to the regions that contain the canonical *E-box* motif *CACGTG* also called *G-box* (Figs 1b, 3c–e). ILR3 also bind to the promoter of *At-NEET* (*ProAt-NEET*), *VTL2* (*ProVTL2*) and *NAS4* (*ProNAS4*) (Fig. 3f–h). Interestingly, ILR3 interacts with *ProNAS4* at the same locus than *PYE*, located on the main NFR region of *ProNAS4* that is about 3.2 kb upstream from the transcriptional initiation start (Fig. S10) (Long *et al.*, 2010).

These results indicate that ILR3 interacts with specific *E-box* motifs present in the promoter of its target genes to affect their transcription, in accordance with the amount of Fe that is present in the surrounding media.

### ILR3 and *PYE* repress the expression of a common set of genes

mRNA abundance of genes whose expression is repressed by ILR3 was measured in loss-of-function *pve-1* mutant grown by contrasting Fe conditions ( $-Fe$ , C and  $+Fe$ ) and compared with that of WT seedlings. *AtFER1*, *AtFER3* and *AtFER4* expression was induced in *pve-1* mutant regardless of the Fe condition in which seedlings were grown (not significantly for *AtFER1* in C

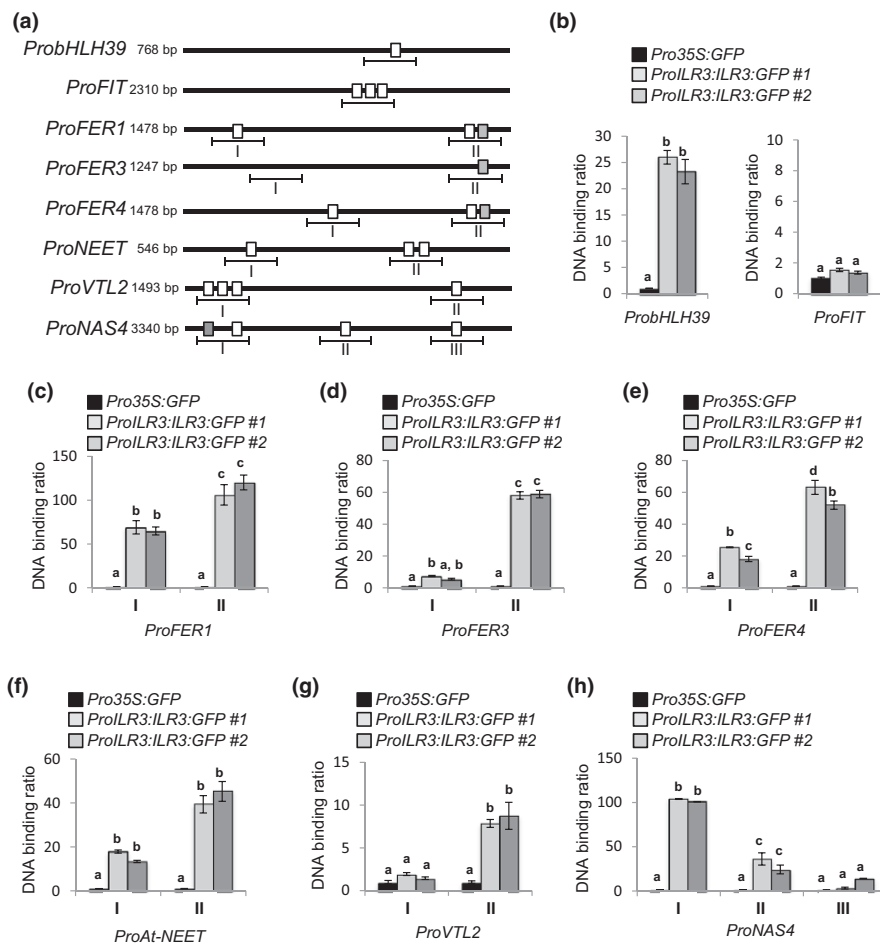


**Fig. 3** Chromatin immunoprecipitation (ChIP)-qPCR analysis of the binding of ILR3 to the promoter of selected Fe deficiency or excess responsive genes. (a) Promoter structure diagrams for the assayed genes. White boxes, *E-box* (*CANNTG*); grey boxes, *G-box* (*CACGTG*). Lines under the boxes indicate sequences detected by ChIP-qPCR assays. Chromatin from 2-wk-old wild-type *Arabidopsis thaliana* seedlings expressing *ProILR3:gILR3:GFP* (two independent transgenic lines) and grown under Fe deficiency was extracted using anti-GFP antibodies. Seedlings overexpressing GFP (*Pro35S:GFP*) were used as a negative control. qPCR was used to quantify enrichment of ILR3 to the selected gene promoters. Means within each condition with the same letter are not significantly different according to one-way ANOVA followed by post-hoc Tukey test,  $P < 0.05$  ( $n = 3$  technical repeats from one representative experiment). Error bars show  $\pm$  SD. (b) ILR3 DNA binding ratio (as revealed by GFP enrichment in ChIP experiments) to the promoter of *bHLH39* and *FIT* used as the positive or negative control, respectively (Zhang *et al.*, 2015). ILR3 binding ratio to the promoter of (c) *AtFER1*, (d) *AtFER3*, (e) *AtFER4*, (f) *At-NEET*, (g) *VTL2* and (h) *NAS4*.

condition), indicating that PYE acts as a transcriptional repressor of ferritin genes expression (Figs 4a, S11a,b). Similarly, *At-NEET*, *VTL2* and *NAS4* mRNA levels were increased in *pye-1* when compared with WT seedlings when grown in -Fe and C conditions. These observations indicate that PYE is a repressor of *At-NEET*, *VTL2* and *NAS4* expression when Fe is not in excess (Fig. 4b,d). By contrast, *ILR3* expression in *pye-1* mutant was unaffected when compared with WT seedlings regardless of the Fe condition, supporting the postulate that PYE is not a transcriptional regulator of *ILR3* expression (Fig. S11c).

ChIP experiments were then conducted on a transgenic line expressing the *ProPYE:gPYE:GFP* (in *pye-1*) using an anti-GFP antibody (Fig. 4e-j) (Long *et al.*, 2010). This approach revealed that PYE interacts *in planta* with the same promoter loci than *ILR3* on *ProFER1*, *ProFER3*, *ProFER4*, *ProAt-NEET*, *ProVTL2* and *ProNAS4*. Since *ILR3* could potentially act as a transcriptional repressor of *PYE* expression when Fe is not limiting (Fig. 2d), additional ChIP experiments were conducted in order to determine if *ILR3* and *PYE* interact at the same locus with the promoter of *PYE*. For this purpose, the above described *ProILR3:gILR3:GFP* (positive control; Zhang *et al.*, 2015) and *ProPYE:gPYE:GFP* transgenic lines were used revealing that *PYE* can

interact with its own promoter at the same locus than *ILR3* (Fig. 5a,b).

Altogether, these experiments show that *ILR3* and *PYE* repress the expression of a common set of genes (for example *AtFER1*, *AtFER3*, *AtFER4*, *VTL2*, *At-NEET* and *NAS4*) and that the transcriptional repressor activity of *ILR3* is likely conferred by its heterodimerisation with *PYE* (Long *et al.*, 2010). This later hypothesis is supported by BiFC experiments that show, *in planta*, the nuclear localisation of *ILR3* and *PYE* interaction *in planta* (Fig. 5c) (Zhang *et al.*, 2015).

### ILR3 and ferritin activities modulate Arabidopsis growth in a Fe-dependent manner

WT, *ilr3-3*, *pye-1*, *ilr3-3 pye-1*, and *ilr3-1* seedlings were grown under contrasting Fe concentrations in order to determine if *ILR3* activity could affect seedling growth in a Fe-dependent manner. In -Fe condition a strong reduction of *ilr3-3*, *pye-1*, and *ilr3-3 pye-1* root growth was observed when compared with WT seedlings, confirming observations made in previous studies (Fig. S12a,d) (Zhang *et al.*, 2015; Li *et al.*, 2016). Among the three mutants, *pye-1* was the less affected whereas *ilr3-3 pye-1*

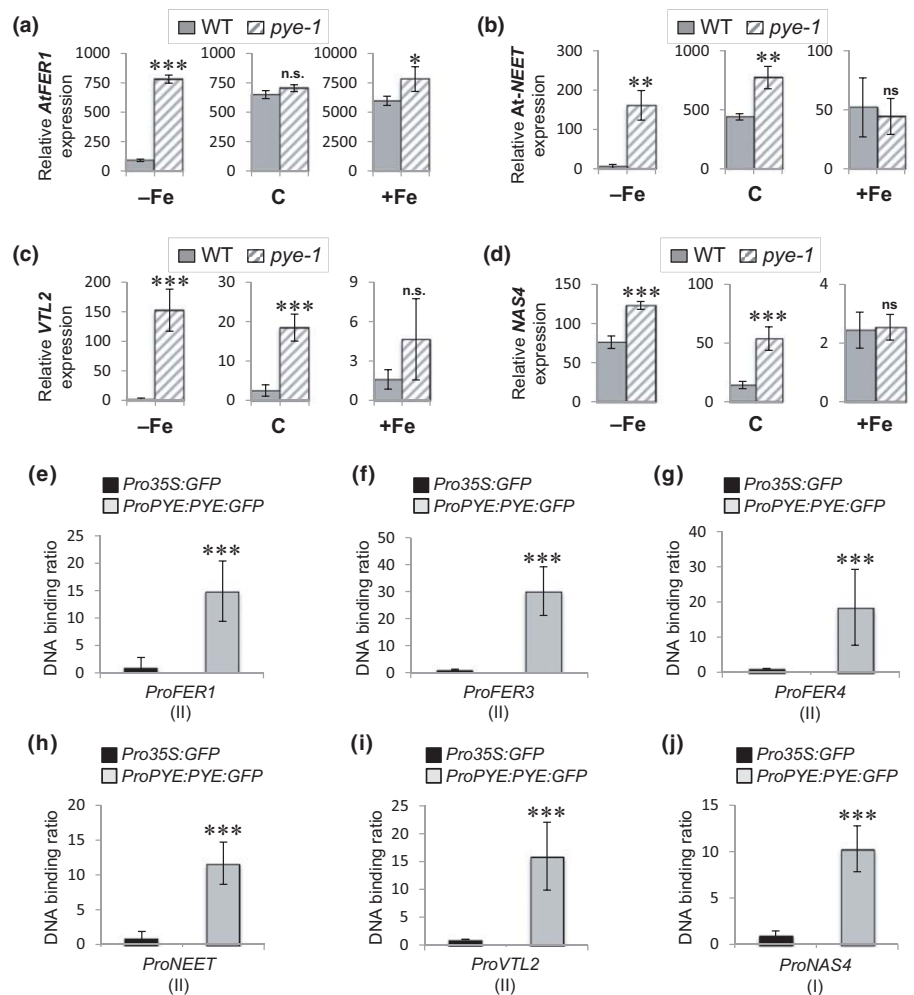


**Fig. 4** *ILR3* and *PYE* regulate common set of genes. Relative expression (qRT-PCR) of (a) *AtFER1*, (b) *At-NEET*, (c) *VTL2* and (d) *NAS4* genes as revealed by quantitative RT-PCR analysis in 2-wk-old *Arabidopsis thaliana* wild-type (WT) and *pye-1* seedlings. -Fe, C and +Fe correspond to the control (50 μM Fe), Fe deficiency (0 μM Fe) and Fe excess (500 μM Fe) conditions, respectively. *t*-test significance (compared with WT): \*,  $P < 0.05$ ; \*\*,  $P < 0.01$ ; \*\*\*,  $P < 0.001$ , ns not significant. Error bars show  $\pm$  SD. (e-j) Chromatin immunoprecipitation (ChIP)-qPCR analysis of the binding of *PYE* to the promoter of selected genes whose expression is repressed by *ILR3*. Chromatin from 2-wk-old *Arabidopsis* seedlings expressing *ProPYE:PYE:GFP* (Long *et al.*, 2010) and grown under Fe deficiency was extracted using anti-GFP antibodies. Seedlings overexpressing GFP (*Pro35S:GFP*) were used as the negative control. qPCR was used to quantify enrichment of *PYE* to promoter regions that are targeted by *ILR3* (Fig. 3). *PYE* DNA binding ratio (as revealed by GFP enrichment in ChIP experiments) to the promoter of (e) *AtFER1*, (f) *AtFER3*, (g) *AtFER4*, (h) *At-NEET*, (i) *VTL2* and (j) *NAS4*. *t*-test significance: ( $n = 2$  technical repeats from one representative experiment) \*\*\*,  $P < 0.001$ ; ns, not significant. Error bars show  $\pm$  SD.

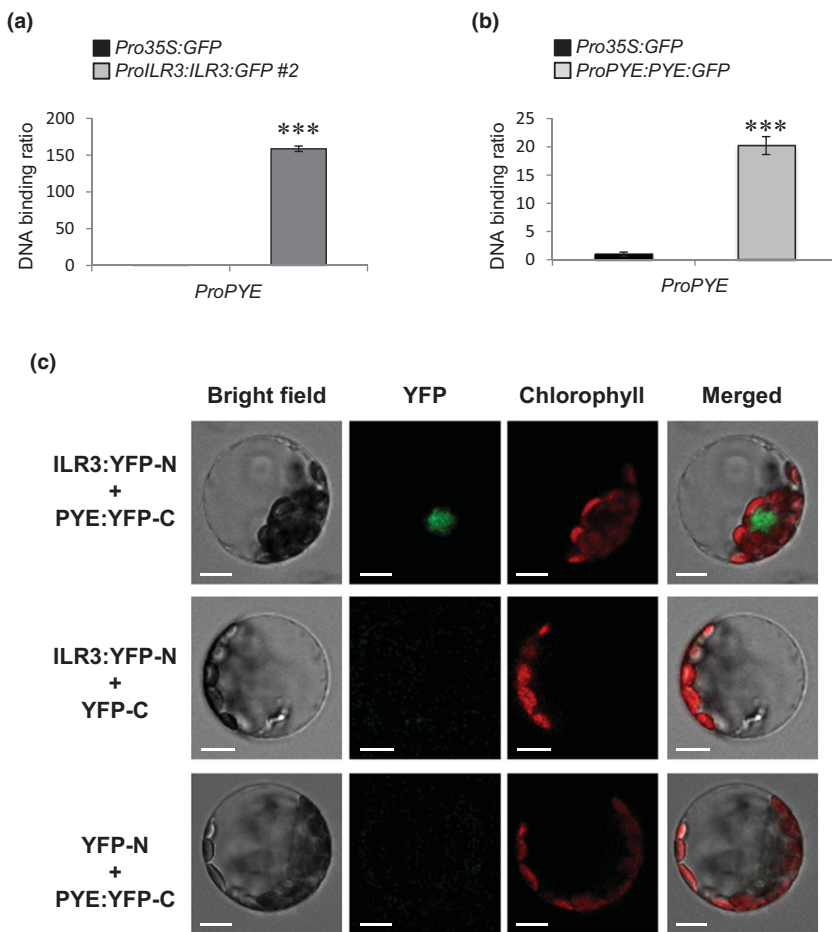


**Fig. 5** ILR3 and PYE directly interact, at the same locus, on *PYE* promoter. (a, b) Chromatin immunoprecipitation (ChIP)-qPCR analysis of the binding of ILR3 and PYE to the promoter of *PYE* (*ProPYE*). Chromatin from 2-wk-old wild-type (WT) *Arabidopsis thaliana* seedlings expressing *ProILR3:ILR3:GFP* or *ProPYE:PYE:GFP* (Long *et al.*, 2010) and grown under Fe deficiency was extracted using anti-GFP antibodies. Seedlings overexpressing GFP (*Pro35S:GFP*) were used as the negative control. qPCR was used to quantify enrichment of ILR3 and PYE to *PYE* promoter region that is targeted by ILR3 (Zhang *et al.*, 2015). ILR3 and PYE DNA binding ratio (as revealed by GFP enrichment in ChIP experiments) to the promoter *PYE* are presented in (a) and (b), respectively. *t*-test significance: ( $n = 3$  technical repeats from one representative experiment) \*\*\*,  $P < 0.001$ . Error bars show  $\pm$  SD. (c) Bimolecular fluorescence complementation labelled ILR3-PYE complexes in *Arabidopsis thaliana* protoplasts. Bars, 10  $\mu$ m.

displayed a similar phenotype to that of *ilr3-3*. Conversely, an opposite trend was observed for the *ilr3-1* mutant. Under Fe-replete condition, no significant difference in root length was observed between the mutants and WT seedlings (Fig. S12b,e). When seedlings were grown on Fe excess, root growth was drastically affected in all six genotypes. However, *ilr3-3*, *pye-1* and *ilr3-3 pye-1* on one hand and *ilr3-1* on the other displayed longer and shorter root length when compared with WT seedlings, respectively (Fig. S12c,f). Similarly to root growth, seedling fresh weight was also affected in a Fe-dependent manner (Fig. S13). These data suggest that ILR3 function extends beyond its role in the control of plant response to  $-Fe$  to a more central role in the transcriptional regulation of plant growth in response to Fe availability.

To investigate the possibility that the role of ILR3 in the Fe-dependent control of seedlings growth may involve ferritin activity, the triple *fer1,3,4* ferritin loss-of-function mutant was included in the analysis. Growth parameters of the *fer1,3,4* mutant were compared with those of the *ilr3-3*, *pye-1*, *ilr3-3 pye-1* and *ilr3-1* mutants and WT seedlings (Fig. S12). In all the conditions tested, the *fer1,3,4* and the *ilr3-1* mutants displayed similar growth parameters when compared with WT seedlings. These later observations suggest that part of ILR3 function relies on ferritin activity. In order to test this hypothesis, *ilr3-1* mutant overexpressing *AtFER1* lines (*Pro35S:FER1*) were generated and

grown as described above (Figs 6, S14). This approach revealed that the overexpression of *AtFER1* in *ilr3-1* was sufficient to revert the *ilr3-1* seedling root length and fresh weight phenotypes. Importantly, under Fe-replete condition, no significant difference was observed between the different genotypes. Altogether these experiments indicate that part of ILR3 function in the control of seedling growth, in response to Fe availability, relies on ferritin activity. Additional experiments also revealed that ILR3, by modulating ferritin expression, plays a key role in the response to Fe availability not only in seedlings but also in adult plants (Figs S15, S16).

#### ILR3 and PYE regulate Fe distribution in leaves

To characterise ILR3's role in the control of Fe homeostasis, Fe accumulation in rosette leaves was evaluated.

First, the Fe content present in the leaves of 6-wk-old plants grown under three different conditions was measured: Fe-replete condition (C, 50  $\mu$ M), Fe deficiency ( $-Fe$ : 20 d of Fe deficiency prior harvesting) and Fe excess ( $+Fe$ : 10 d of Fe deficiency followed by 10 d of Fe excess prior harvesting) (Fig. S17). This experiment revealed, for all genotypes, that the Fe content increased as the amount of Fe in the media rose. Under  $-Fe$  condition, no significant difference in Fe content was observed between the different genotypes. Under Fe-replete condition,

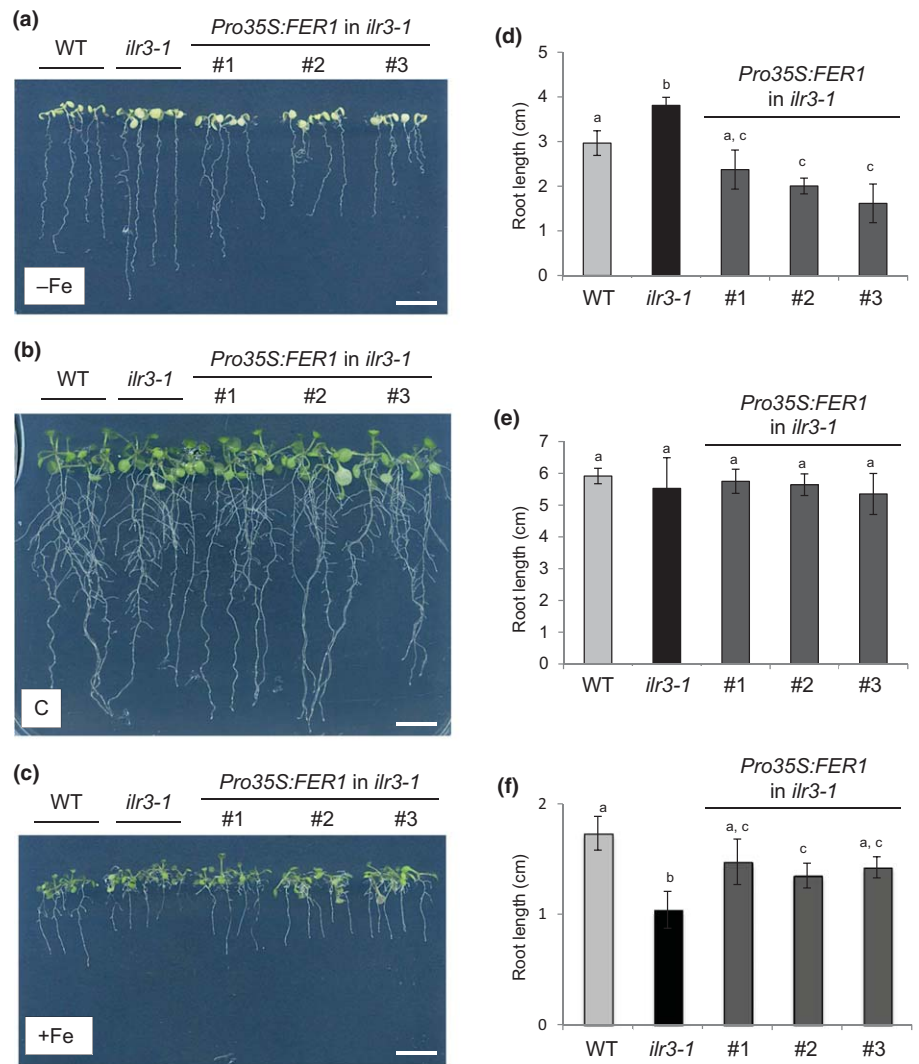


**Fig. 6** Complementation of *ilr3-1* seedling root growth phenotypes by overexpressing *AtFER1*. Seedling phenotypes of the wild-type (WT), *ilr3-1* and three independent *ilr3-1* lines overexpressing *AtFER1* (*Pro35S:FER1* in *ilr3-1*) grown for 2 wk in (a) Fe deficiency (0  $\mu$ M Fe), (b) control (50  $\mu$ M Fe), and (c) Fe excess (500  $\mu$ M Fe) conditions. Bar, 1 cm. Root length of WT, *ilr3-1* and three independent *ilr3-1* lines overexpressing *AtFER1* (*Pro35S:FER1* in *ilr3-1*) grown for 2 wk in (d) Fe deficiency (0  $\mu$ M Fe), (e) control (50  $\mu$ M Fe), and (f) Fe excess (500  $\mu$ M Fe) conditions. Means within each condition with the same letter are not significantly different according to one-way ANOVA followed by post-hoc Tukey test,  $P < 0.05$  ( $n = 16$  seedlings from one representative experiment). Error bars show  $\pm$  SD.

*ilr3-1* mutant accumulated more Fe than any other genotype. This later observation was more pronounced in Fe excess.

Fe localisation in leaves of 5-wk-old WT, *ilr3-3*, *pye-1*, *ilr3-3 pye-1* and *ilr3-1* plants grown in soil and watered or not with an excess of Fe was then determined (Fig. 7). For this purpose, the Perls/DAB histochemical staining method was used (Roschttardt et al., 2009, 2013). *ilr3-3*, *pye-1* and *ilr3-3 pye-1* Perls/DAB staining was similar to that of WT plants but displayed some more Fe-rich structures (black dots), in particular alongside the vasculature (that is vascular bundle and mesophyll cells) where the ferritins accumulate when Fe availability is in excess (Roschttardt et al., 2013). Interestingly, these Fe-rich dots are absent in *ilr3-1*. Instead, Fe accumulates in plaques in the vascular bundle and is nearly totally absent from the mesophyll cells. The absence of Fe-rich dots in *ilr3-1* is in agreement with the lack of induction of ferritin genes expression in response to Fe excess in this mutant as these structures are described as being Fe-ferritin (Roschttardt et al., 2013). In addition, these data support the hypothesis that ferritins play an important role in buffering the excess of Fe during xylem unloading (Roschttardt et al., 2013).

Taken together, these data highlight that ILR3 regulates, in addition to Fe uptake, the distribution of Fe at the tissue, cellular and subcellular levels.

## Discussion

ILR3/bHLH105 is a transcriptional regulator of ferritin genes expression

The ferritins are a class of ubiquitous Fe storage proteins found in all living kingdoms and that play a central role in the control of Fe homeostasis (Briat et al., 2010). In plants, the role of ferritins is to buffer Fe to maintain Fe concentration to levels that are optimal for metabolic purposes and to avoid the deleterious effects of free Fe-associated reactive oxygen species (ROS) (Ravet et al., 2009). The abundance of ferritins found in plants (mostly in chloroplasts) is transiently induced in response to Fe excess. The induction of ferritin mRNA levels is essentially regulated at the transcriptional level and involves the *cis*-regulatory element *IDRS* (*Iron-Dependent Regulatory Sequence*) through which ferritins expression is repressed (Petit et al., 2001). No *trans*-acting

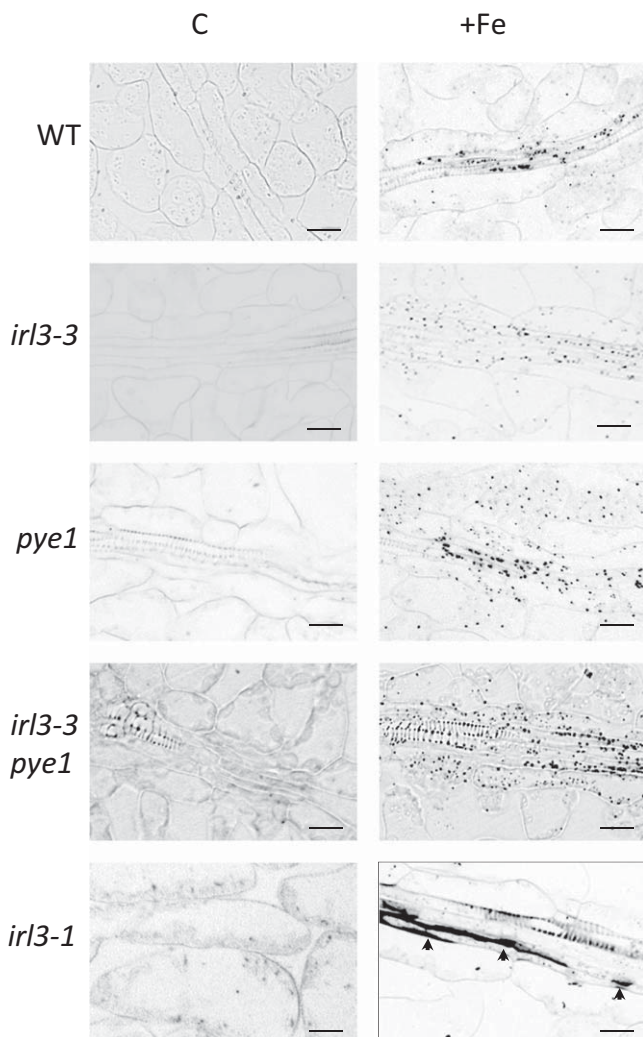


**Fig. 7** ILR3 regulates Fe storage in leaves. Fe localisation in rosette leaves as revealed by Perls/DAB histochemical staining of *Arabidopsis thaliana* wild-type (WT), *ilr3-3*, *pye-1*, *ilr3-3 pye-1* and *ilr3-1* plants grown in control (left panels, C) or Fe excess condition (right panels, +Fe). Arrows, Insoluble iron in vasculature; bars, 20  $\mu$ m.

factors interacting with the *IDRS* have been identified so far. Strikingly, all the studies aiming at decrypting the molecular mechanisms controlling ferritins expression have failed in identifying any actor repressing ferritin gene expression in response to Fe deprivation. Instead, it has been found that Fe is not the sole signal that directly modulates ferritin genes expression. Ferritin gene expression is under the control of the circadian clock and involves the nuclear factor TIC (TIME FOR COFFEE) (Fourcroy *et al.*, 2004; Duc *et al.*, 2009). Plant ferritin gene expression is also tightly connected to phosphate availability. In *Arabidopsis*, *AtFER1* expression (the most expressed ferritin gene present in vegetative tissues) is induced under phosphate starvation (Briat *et al.*, 2010; Bournier *et al.*, 2013). This induction relies on the interaction between two MYB-like TFs (PHOSPHATE STARVATION RESPONSE 1, PHR1 and PHR1-like 1, PHL1) and the *P1BS* (*PHR1 binding site*) *cis*-regulatory sequence present on *AtFER1* promoter. An *AtFER1*

promoter-based strategy was therefore developed with the aim to identify key molecular players that could coordinate the transcriptional regulatory cascade associated with the Fe acquisition from the soil and the Fe buffering activity of ferritins, connecting the plant responses to Fe deficiency and Fe excess. This approach led to the identification of both a *cis*-regulatory motif (*G-box*) through which *AtFER1* expression is repressed, and a cognate *trans*-acting factor, namely bHLH105/ILR3 (IAA-LEUCINE RESISTANT 3) (Fig. 1). ILR3 binding to this *G-box* was then confirmed *in planta* by ChIP experiments (Fig. 3) and its repressive role on *AtFER1* expression was validated using dominant (*ilr3-1*) and loss-of-function (*ilr3-3*) mutant alleles (Fig. 1). Importantly, ILR3 has been described as a master regulator of the plant responses to Fe shortage acting as a transcriptional activator (Zhang *et al.*, 2015; Li *et al.*, 2016). Therefore, it emerges that the role of ILR3 extends beyond the activation of the Fe acquisition machinery in response to Fe deficiency. Indeed, it connects the plant responses to both Fe deficiency and Fe excess, which are of central importance when plants are recovering from a period of Fe shortage or when Fe availability in the soil solution is fluctuating.

#### ILR3 integrates Fe signals to adjust plant growth

The transcriptional activity of ILR3 in coordinating the responses to Fe shortage is central for the plant survival. The ILR3-dependent transcriptional regulatory cascade is well characterised and most of the downstream targets participating to Fe assimilation from the soil by the plant have been identified (Brumbarova *et al.*, 2015; Li *et al.*, 2016). The specific role of ILR3 in the context of Fe deficiency is best exemplified by the extent of the growth defects that are observed in *ilr3-3* mutant when compared with WT plants (Figs S12, S13) (Zhang *et al.*, 2015; Li *et al.*, 2016). These growth defects are abolished in plants displaying increased ILR3 activity (*ilr3-1*). Nevertheless, some evidence suggests that ILR3 function may extend beyond the induction of the sole Fe acquisition machinery. ILR3 was first characterised as a potential regulator of metal homeostasis and (auxin) IAA-conjugate metabolism, whose activity was dependent on Fe availability (Rampey *et al.*, 2006). Rampey *et al.* (2006) found that ILR3 may regulate the expression of three vacuolar Fe transporter homologues (Gollhofer *et al.*, 2011, 2014) and a gene encoding a chloroplastic [Fe-S] cluster transfer protein called *At-NEET* (Nechushtai *et al.*, 2012). A recent study showed that ILR3 is involved in the salicylic acid-dependent defence signalling response in *Arabidopsis* and that ILR3 acts as transcriptional regulator of *At-NEET* expression (Aparicio & Pallas, 2016). Importantly, plant sensitivity to Fe availability is also dependent on *At-NEET* activity as its suppression renders mutant plants more susceptible to Fe deprivation and more resistant to Fe excess than WT plants (Nechushtai *et al.*, 2012). By contrast to its role in response to Fe deficiency, our data indicate that ILR3 functions as a repressor of the plant responses to high Fe concentrations, in agreement with an increased sensitivity of the *ilr3-1* mutant to an excess of Fe compared with WT plants (Figs S12, S13). Interestingly, it has recently been shown that ILR3 acts as a

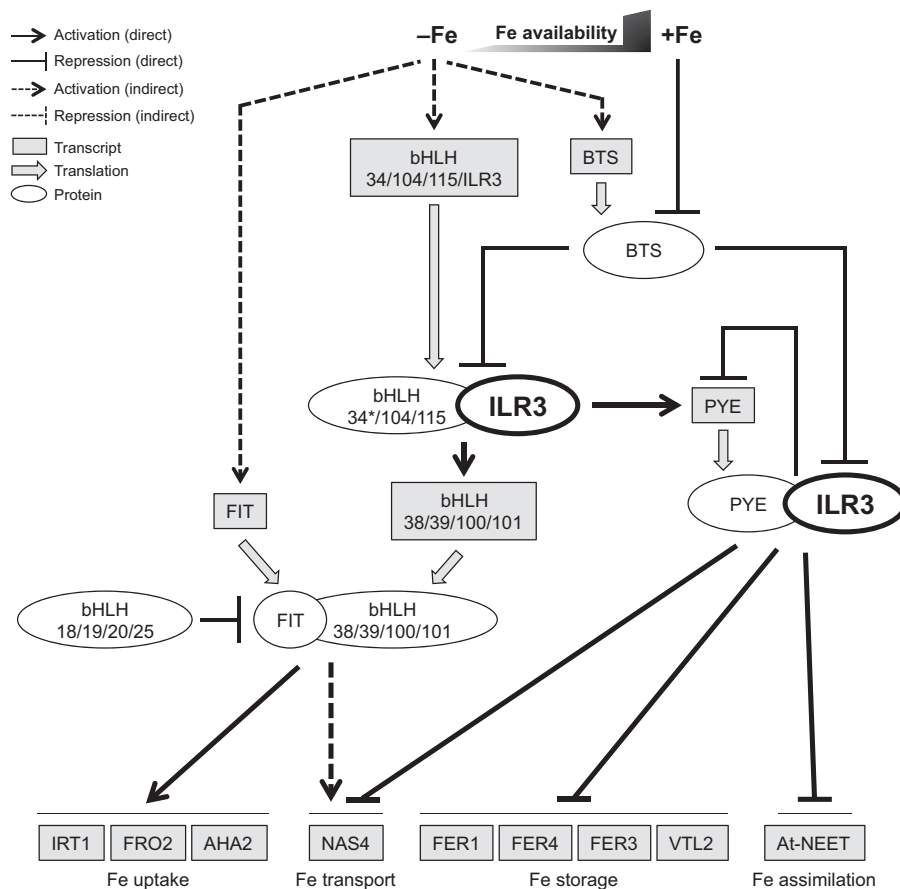


**Fig. 8** ILR3-mediated control of Fe homeostasis. The proposed model describes the dual role played by ILR3/bHLH105 in the control of the plant responses to fluctuations in Fe availability present in the growth medium. Depending on its interacting partner ILR3 acts as a transcriptional activator or repressor. Activating ILR3-dependent complexes relies on ILR3 heterodimerisation with bHLH34, bHLH104 and bHLH115. ILR3 as well as bHLH34, bHLH104 and bHLH115 belong to the bHLH clade IVc. ILR3 repressing activity relies on its heterodimerisation PYE/bHLH47 (clade IVb; Long *et al.*, 2010). PYE expression as well as expression of additional bHLH transcription factors regulating the plant response to Fe shortage (for example *bHLH39*, clade Ib) depends on activating ILR3-dependent complexes (Zhang *et al.*, 2015). A negative feedback regulatory loop involving the ILR3-PYE complex might repress the expression of *PYE* when Fe availability is not limiting. FIT/bHLH29 is another key transcriptional regulator of the plant response to Fe deficiency whose activity modulates the expression of structural or regulatory genes (for example *MYB10* and *MYB72*) required to maintain Fe homeostasis (Palmer *et al.*, 2013; Wang *et al.*, 2007, 2013). Part of FIT activity relies on its ability to form heterodimers with some clade Ib bHLH TFs (that is bHLH38, bHLH39, bHLH100 and bHLH101), and its stability is affected by its interaction with clade IVa bHLH TFs (that is bHLH18, bHLH19, bHLH20 and bHLH25) (Cui *et al.*, 2018). Structural genes whose expression is modulated by ILR3 are involved in Fe acquisition (for example *IRT1*, *FRO2*, *AHA2*), transport (for example *NAS4*), storage (for example *AtFER1*, *AtFER3*, *AtFER4*, *VTL2*) and assimilation (for example *At-NEET*). ILR3-dependent activities are modulated by the activity of BTS (BRUTUS; Selote *et al.*, 2015; Matthiadis & Long, 2016), an E3 ubiquitin ligase that specifically targets clade IVc bHLH transcription factors leading to their degradation through the 26S proteasome (\*, excluding bHLH34). BTS expression is induced in response to Fe deficiency in order to fine tune Fe uptake and avoid Fe excess that could be detrimental to the plant. BTS interaction with Fe, through its hemerythrin (HHE) domains, leads to its destabilisation. In this proposed model ILR3 and BTS play a central role in controlling the transcriptional machinery that regulates Fe homeostasis. Model adapted from Li *et al.* (2016).

repressor of glucosinolate biosynthesis, a class of secondary metabolites conferring resistance against several pathogens, confirming the dual role of ILR3 in regulating genes expression (Li *et al.*, 2014; Samira *et al.*, 2018).

The tight connection between ILR3 activity and ferritins accumulation, together with the strong similarity of *ilr3-1* and *fer1,3,4* (triple mutant deprived of ferritins in vegetative tissues) mutant responses to Fe availability (Figs S12, S13, S15), support that ILR3 integration of Fe signals to adjust plant development partly relies on ferritins. This hypothesis was confirmed by overexpressing *AtFER1* (*Pro35S:FER1*) in *ilr3-1* mutant (Figs 6, S14).

### ILR3 and BTS are central to the regulation of Fe homeostasis

Recent studies have shown the upstream position of ILR3, bHLH34, bHLH104 and bHLH115 in the Fe deficiency transcriptional regulatory network (Li *et al.*, 2016; Liang *et al.*, 2017). However, the peculiar nature of ILR3 in regulating Fe homeostasis was not fully assessed, most probably because ILR3 displays redundant activities with bHLH34, bHLH104 and bHLH115. The only evidence reported so far was that *ilr3* loss-of-function mutants displayed the strongest Fe deficiency phenotype when compared with the other class IVc bHLH mutants



when grown in low Fe availability (Zhang *et al.*, 2015; Li *et al.*, 2016; Liang *et al.*, 2017). BTS (BRUTUS), a Fe binding E3 ubiquitin ligase, specifically targets ILR3, bHLH104 and bHLH115 leading to their degradation through the 26S proteasome (Selote *et al.*, 2015; Matthiadis & Long, 2016). BTS contains a hemerythrin-like domain able to bind Fe. The binding of Fe to the hemerythrin-like domain of BTS participates in its destabilisation and subsequent degradation (Selote *et al.*, 2015; Matthiadis & Long, 2016). Therefore, BTS was seen as the main regulator of Fe homeostasis, even if the link between BTS and the plant response to Fe excess was not clearly established.

The data presented in this study support that, unlike its closet homologues, ILR3 represses the expression of the main markers of the plant response to Fe excess, the ferritin genes (Figs 1, S4). In addition, our data indicate that ILR3 and PYE repress the expression of a common set of target genes (Figs 2–4, S6, S11), most probably through the formation of heterodimers (Fig. 5; Long *et al.*, 2010; Zhang *et al.*, 2015). Last, our data suggest that the regulation of *PYE* expression might rely on a negative feedback regulatory loop involving the ILR3-PYE complex. Altogether, these findings highlight the dual and unique role played by ILR3 in regulating the plant responses to fluctuations in Fe availability in the growth medium.

*bHLH34*, *bHLH104*, *bHLH115*, *ILR3* and *PYE* are mainly expressed in the pericycle cells (Long *et al.*, 2010; Rodríguez-Celma *et al.*, 2013b), which is the place of accumulation of ferritins in response to Fe excess in roots (Reyt *et al.*, 2015), and consistent with the repressive role of *PYE* on ferritin genes expression under Fe deficiency. Interestingly, the extent of the induction of *bHLH34*, *bHLH104*, *bHLH115* and *ILR3* transcript abundance in response to Fe deficiency is less pronounced than that of *PYE* (Zhang *et al.*, 2015; Liang *et al.*, 2017) (Figs 2d, S5, S11c). By contrast, Fe excess had no striking effect on *ILR3* or *PYE* mRNA abundance, compared with control condition (Figs 2d, S5, S11c). Therefore, assuming that the relative mRNA abundance of the bHLH IVc on the one hand and *PYE* on the other reflects the amount of ILR3-dependent protein complexes acting as activator (that is bHLH34-ILR3, bHLH104-ILR3 and bHLH115-ILR3) or repressor (that is PYE-ILR3), it can be hypothesised that the stoichiometry between the two types of complex would be modified by the Fe conditions (deficiency vs excess). In this model, the formation of the PYE-ILR3 complex is triggered in response to Fe deficiency by the ILR3-dependent activating protein complexes favouring the repression of ILR3 target genes. The recent work, which shows that ILR3 and PYE function in a regulatory network that controls wounding pathogen response, clearly reinforces this hypothesis (Samira *et al.*, 2018).

Taken together, the data gathered herein and in previous studies suggest that ILR3 and BTS play a central role in the machinery controlling Fe homeostasis (Fig. 8). In this model ILR3, whose activity is regulated by BTS in a Fe-dependent manner, acts as both a transcriptional activator of plant responses to Fe shortage and as a repressor of plant responses to Fe excess. Such regulatory loops between ILR3 and BTS, through the modulation of the equilibrium between the different ILR3-dependent

protein complexes, most probably ensure the dynamic and balanced expression of genes involved in Fe homeostasis in accordance with Fe availability.








## Acknowledgements

*ilr3-1* seeds were kindly provided by Prof. Bonnie Bartel (Rice University, Houston, Texas, USA). The *ProPYE:gPYE:GFP* line was kindly provided by Prof. Terry A Long (North Carolina State University, Raleigh, North Carolina, USA). We thank Dr Carine Alcon and the Montpellier Rio-Imaging platform (Plateforme PHIV La Gaillarde) for expertise and assistance in microscopy and Sandrine Chay (BPMP, SAME platform) for technical support in plant Fe determination. NT and FB were supported by a fellowship from the French 'Ministère de l'Enseignement Supérieur et de la Recherche'. KR and FG were supported by a fellowship from the Agence Nationale pour la Recherche (ANR-17-CE20-0008-01) and from the China Scholarship Council (CSC), respectively. SG-G's work was supported by CONICYT-Chile grant 21170951. HR was funded by FONDECYT 1160334 (Chilean Government) grant. This work was also supported by the CONICYT-ECOS project C18B04. We thank Dr N. Berger for help in preparing this manuscript.

## Author contributions

Conceived and designed the experiments: NT, KR, FGao, SGG, FB, EI, AMartin, FV, HR, CD. Performed the experiments: NT, KR, SGG, FGao, JB, FB, AMaghiaoui, RM, EI, MB, FV, CD. Analysed the data: NT, KR, SGG, FGao, FB, EI, MB, AMartin, FV, HR, FGaynard, JFB, CD. Contributed reagents/materials/analysis tools: NT, KR, FGao, FB, EI, MB, AMartin, FV, HR, FGaynard, CD. Wrote the paper: NT, FGaynard, JFB, CD. KR and FGao contributed equally to this work.

## ORCID

Fanny Bellegarde  <https://orcid.org/0000-0001-7221-5033>  
 Christian Dubos  <https://orcid.org/0000-0001-5486-3643>  
 Fei Gao  <https://orcid.org/0000-0002-4347-8499>  
 Esther Izquierdo  <https://orcid.org/0000-0003-0448-4447>  
 Antoine Martin  <https://orcid.org/0000-0002-6956-2904>  
 Hannetz Roschztardt  <https://orcid.org/0000-0002-2614-2504>  
 Florence Vignols  <https://orcid.org/0000-0002-2031-0407>

## References

- Aparicio F, Pallas V. 2016. The coat protein of *Alfalfa mosaic virus* interacts and interferes with the transcriptional activity of the bHLH transcription factor ILR3 promoting salicylic-dependent defense signaling response. *Molecular Plant Pathology* 18: 173–186.
- Becker A. 2005. Iron toxicity in rice: conditions and management concepts. *Journal of Plant Nutrition and Soil Science* 168: 558–573.
- Bournier M, Tissot N, Mari S, Boucherez J, Lacombe E, Briat JF, Gaynard F. 2013. Arabidopsis ferritin 1 (AtFer1) gene regulation by the phosphate

- starvation response 1 (AtPHR1) transcription factor reveals a direct molecular link between iron and phosphate homeostasis. *Journal of Biological Chemistry* 288: 22670–22680.
- Briat JF, Dubos C, Gaymard F. 2015. Iron nutrition, biomass production, and plant product quality. *Trends in Plant Science* 20: 33–40.
- Briat JF, Duc C, Ravet K, Gaymard F. 2010. Ferritins and iron storage in plants. *Biochimica et Biophysica Acta* 1800: 806–814.
- Brumbarova T, Bauer P, Ivanov R. 2015. Molecular mechanisms governing Arabidopsis iron uptake. *Trends in Plant Science* 20: 124–133.
- Colangelo EP, Guerinot ML. 2004. The essential basic helix-loop-helix protein FIT1 is required for the iron deficiency response. *Plant Cell* 16: 3400–3412.
- Connorton JM, Balk J, Rodríguez-Celma J. 2017. Iron homeostasis in plants – a brief overview. *Metallomics* 9: 813–823.
- Cui Y, Chen CL, Cui M, Zhou WJ, Wu HL, Ling HQ. 2018. Four IVa bHLH transcription factors are novel interactors of FIT and mediate JA inhibition of iron uptake in Arabidopsis. *Molecular Plant* 11: 1166–1183.
- Curie C, Mari S. 2016. New routes for plant iron mining. *New Phytologist* 214: 521–525.
- De Masi F, Grove CA, Vedenko A, Alibes A, Gisselbrecht SS, Serrano L, Bulyk ML, Walhout AJ. 2011. Using a structural and logics systems approach to infer bHLH-DNA binding specificity determinants. *Nucleic Acids Research* 39: 4553–4563.
- Duc C, Cellier F, Lobreaux S, Briat JF, Gaymard F. 2009. Regulation of iron homeostasis in *Arabidopsis thaliana* by the clock regulator time for coffee. *Journal of Biological Chemistry* 284: 36271–36281.
- Eide D, Broderius M, Fett J, Guerinot ML. 1996. A novel iron-regulated metal transporter from plants identified by functional expression in yeast. *Proceedings of the National Academy of Sciences, USA* 93: 5624–5628.
- Fourcroy P, Siso-Terraza P, Sudre D, Saviron M, Rey G, Gaymard F, Abadia A, Abadia J, Alvarez-Fernandez A, Briat JF. 2014. Involvement of the ABCG37 transporter in secretion of scopoletin and derivatives by Arabidopsis roots in response to iron deficiency. *New Phytologist* 201: 155–167.
- Fourcroy P, Tissot N, Gaymard F, Briat JF, Dubos C. 2016. Facilitated Fe nutrition by phenolic compounds excreted by the Arabidopsis ABCG37/PDR9 transporter requires the IRT1/FRO2 high-affinity root Fe<sup>2+</sup> transport system. *Molecular Plant* 9: 485–488.
- Fourcroy P, Vansuyt G, Kushnir S, Inze D, Briat JF. 2004. Iron-regulated expression of a cytosolic ascorbate peroxidase encoded by the *APX1* gene in Arabidopsis seedlings. *Plant Physiology* 134: 605–613.
- Gao F, Robe K, Gaymard F, Izquierdo E, Dubos C. 2019. The transcriptional control of iron homeostasis in plants: a tale of bHLH transcription factors? *Frontiers in Plant Science* 10: 006.
- Gollhofer J, Schlawicke C, Jungnick N, Schmidt W, Buckhout TJ. 2011. Members of a small family of nodulin-like genes are regulated under iron deficiency in roots of *Arabidopsis thaliana*. *Plant Physiology and Biochemistry* 49: 557–564.
- Gollhofer J, Timofeev R, Lan P, Schmidt W, Buckhout TJ. 2014. Vacuolar-Iron-Transporter1-Like proteins mediate iron homeostasis in Arabidopsis. *PLoS ONE* 9: e110468.
- Guerinot ML, Yi Y. 1994. Iron: nutritious, noxious, and not readily available. *Plant Physiology* 104: 815–820.
- Heim MA, Jakoby M, Werber M, Martin C, Weisshaar B, Bailey PC. 2003. The basic helix-loop-helix transcription factor family in plants: a genome-wide study of protein structure and functional diversity. *Molecular Biology and Evolution* 20: 735–747.
- Henriques R, Jasik J, Klein M, Martinoia E, Feller U, Schell J, Pais MS, Koncz C. 2002. Knock-out of Arabidopsis metal transporter gene *IRT1* results in iron deficiency accompanied by cell differentiation defects. *Plant Molecular Biology* 50: 587–597.
- Hentze MW, Muckenthaler MU, Galy B, Camaschella C. 2010. Two to tango: regulation of Mammalian iron metabolism. *Cell* 142: 24–38.
- Jakoby M, Wang HY, Reidt W, Weisshaar B, Bauer P. 2004. FRU (BHLH029) is required for induction of iron mobilization genes in *Arabidopsis thaliana*. *FEBS Letters* 577: 528–534.
- Kagale S, Rozwadowski K. 2011. EAR motif-mediated transcriptional repression in plants: an underlying mechanism for epigenetic regulation of gene expression. *Epigenetics* 6: 141–146.
- Khabaz-Saberi R. 2010. Aluminium, manganese, and ion tolerance improves performance of wheat genotypes in waterlogged acidic soils. *Journal of Plant Nutrition and Soil Science* 173: 461–468.
- Klatte M, Schuler M, Wirtz M, Fink-Straube C, Hell R, Bauer P. 2009. The analysis of Arabidopsis nicotianamine synthase mutants reveals functions for nicotianamine in seed iron loading and iron deficiency responses. *Plant Physiology* 150: 257–271.
- Kobayashi T, Nishizawa NK. 2012. Iron uptake, translocation, and regulation in higher plants. *Annual Review of Plant Biology* 63: 131–152.
- Li B, Gaudinier A, Tang M, Taylor-Teeple M, Nham NT, Ghaffari C, Benson DS, Steinmann M, Gray JA, Brady SM *et al.* 2014. Promoter-based integration in plant defense regulation. *Plant Physiology* 166: 1803–1820.
- Li X, Zhang H, Ai Q, Liang G, Yu D. 2016. Two bHLH transcription factors, bHLH34 and bHLH104, regulate iron homeostasis in *Arabidopsis thaliana*. *Plant Physiology* 170: 2478–2493.
- Liang G, Zhang H, Li X, Ai Q, Yu D. 2017. bHLH transcription factor bHLH115 regulates iron homeostasis in *Arabidopsis thaliana*. *Journal of Experimental Botany* 68: 1743–1755.
- Long TA, Tsukagoshi H, Busch W, Lahner B, Salt DE, Benfey PN. 2010. The bHLH transcription factor POPEYE regulates response to iron deficiency in Arabidopsis roots. *Plant Cell* 22: 2219–2236.
- Matthiadis A, Long TA. 2016. Further insight into BRUTUS domain composition and functionality. *Plant Signal & Behavior* 11: e1204508.
- Meinke DW. 2013. A survey of dominant mutations in *Arabidopsis thaliana*. *Trends in Plant Science* 18: 84–91.
- Morrissey J, Guerinot ML. 2009. Iron uptake and transport in plants: the good, the bad, and the ionome. *Chemical Reviews* 109: 4553–4567.
- Nechushtai R, Conlan AR, Harir Y, Song L, Yogev O, Eisenberg-Domovich Y, Livnah O, Michaeli D, Rosen R, Ma V *et al.* 2012. Characterization of Arabidopsis NEET reveals an ancient role for NEET proteins in iron metabolism. *Plant Cell* 24: 2139–2154.
- Palmer CM, Hindt MN, Schmidt H, Clemens S, Guerinot ML. 2013. MYB10 and MYB72 are required for growth under iron-limiting conditions. *PLoS Genet* 9: e1003953.
- Paz-Ares J. 2002. REGIA, an EU project on functional genomics of transcription factors from *Arabidopsis thaliana*. *Comparative and Functional Genomics* 3: 102–108.
- Petit JM, van Wuytswinkel O, Briat JF, Lobreaux S. 2001. Characterization of an iron-dependent regulatory sequence involved in the transcriptional control of *AtFer1* and *ZmFer1* plant ferritin genes by iron. *Journal of Biological Chemistry* 276: 5584–5590.
- Rampey RA, Woodward AW, Hobbs BN, Tierney MP, Lahner B, Salt DE, Bartel B. 2006. An Arabidopsis basic helix-loop-helix leucine zipper protein modulates metal homeostasis and auxin conjugate responsiveness. *Genetics* 174: 1841–1857.
- Ravet K, Touraine B, Boucherez J, Briat JF, Gaymard F, Cellier F. 2009. Ferritins control interaction between iron homeostasis and oxidative stress in Arabidopsis. *The Plant Journal* 57: 400–412.
- Reyt G, Boudouf S, Boucherez J, Gaymard F, Briat JF. 2015. Iron- and ferritin-dependent reactive oxygen species distribution: impact on Arabidopsis root system architecture. *Molecular Plant* 8: 439–453.
- Robinson NJ, Procter CM, Connolly EL, Guerinot ML. 1999. A ferric-chelate reductase for iron uptake from soils. *Nature* 397: 694–697.
- Rodríguez-Celma J, Lin WD, Fu GM, Abadia J, Lopez-Millan AF, Schmidt W. 2013a. Mutually exclusive alterations in secondary metabolism are critical for the uptake of insoluble iron compounds by Arabidopsis and *Medicago truncatula*. *Plant Physiology* 162: 1473–1485.
- Rodríguez-Celma J, Pan IC, Li W, Lan P, Buckhout TJ, Schmidt W. 2013b. The transcriptional response of Arabidopsis leaves to Fe deficiency. *Frontiers in Plant Science* 4: 276.
- Roschttardt H, Conejero G, Curie C, Mari S. 2009. Identification of the endodermal vacuole as the iron storage compartment in the Arabidopsis embryo. *Plant Physiology* 151: 1329–1338.
- Roschttardt H, Conejero G, Divol F, Alcon C, Verdeil JL, Curie C, Mari S. 2013. New insights into Fe localization in plant tissues. *Frontiers in Plant Science* 4: 350.

- Samira R, Li B, Kliebenstein D, Li C, Davis E, Gillikin JW, Long TA. 2018. The bHLH transcription factor ILR3 modulates multiple stress responses in Arabidopsis. *Plant Molecular Biology* 97: 297–309.
- Santi S, Schmidt W. 2009. Dissecting iron deficiency-induced proton extrusion in Arabidopsis roots. *New Phytologist* 183: 1072–1084.
- Schmid NB, Giehl RF, Doll S, Mock HP, Strehmel N, Scheel D, Kong X, Hider RC, von Wiren N. 2014. Feruloyl-CoA 6'-Hydroxylase1-dependent coumarins mediate iron acquisition from alkaline substrates in Arabidopsis. *Plant Physiology* 164: 160–172.
- Selote D, Samira R, Matthiadis A, Gillikin JW, Long TA. 2015. Iron-binding E3 ligase mediates iron response in plants by targeting basic helix-loop-helix transcription factors. *Plant Physiology* 167: 273–286.
- Strozycki PM, Szymanski M, Szczurek A, Barciszewski J, Figlerowicz M. 2010. A new family of ferritin genes from *Lupinus luteus* – comparative analysis of plant ferritins, their gene structure, and evolution. *Molecular Biology and Evolution* 27: 91–101.
- Varotto C, Maiwald D, Pesaresi P, Jahns P, Salamini F, Leister D. 2002. The metal ion transporter IRT1 is necessary for iron homeostasis and efficient photosynthesis in *Arabidopsis thaliana*. *The Plant Journal* 31: 589–599.
- Vert G, Grotz N, Dedaldechamp F, Gaymard F, Guerinot ML, Briat JF, Curie C. 2002. IRT1, an Arabidopsis transporter essential for iron uptake from the soil and for plant growth. *Plant Cell* 14: 1223–1233.
- Wang HY, Klatte M, Jakoby M, Baumlein H, Weisshaar B, Bauer P. 2007. Iron deficiency-mediated stress regulation of four subgroup Ib BHLH genes in *Arabidopsis thaliana*. *Planta* 226: 897–908.
- Wang N, Cui Y, Liu Y, Fan H, Du J, Huang Z, Yuan Y, Wu H, Ling HQ. 2013. Requirement and functional redundancy of Ib subgroup bHLH proteins for iron deficiency responses and uptake in *Arabidopsis thaliana*. *Molecular Plant* 6: 503–513.
- Yuan Y, Wu H, Wang N, Li J, Zhao W, Du J, Wang D, Ling HQ. 2008. FIT interacts with AtbHLH38 and AtbHLH39 in regulating iron uptake gene expression for iron homeostasis in Arabidopsis. *Cell Research* 18: 385–397.
- Zhang J, Liu B, Li M, Feng D, Jin H, Wang P, Liu J, Xiong F, Wang J, Wang HB. 2015. The bHLH transcription factor bHLH104 interacts with IAA-LEUCINE RESISTANT3 and modulates iron homeostasis in Arabidopsis. *Plant Cell* 27: 787–805.

## Supporting Information

Additional Supporting Information may be found online in the Supporting Information section at the end of the article.

**Fig. S1** Histochemical detection of GUS activity in 2-wk-old seedlings driven by *ProAtFER1* 5'-end deletion and site-directed mutagenesis constructs.

**Fig. S2** Schematic representation of conserved DNA regions (elements) and *cis*-regulatory sequences present in the 500 bp upstream from the transcription initiation sequence of the three main ferritin genes expressed in vegetative tissues.

**Fig. S3** Genome Browser snapshots of ATAC-seq, and H3K9ac, H3K4me3 and H3K27me3 ChIP-seq peaks on the three main ferritin genes found in *Arabidopsis thaliana* vegetative tissues, namely *AtFER1*, *AtFER3* and *AtFER4*.

**Fig. S4** Yeast one-hybrid (Y1H) screen using *ProAtFER1* Element 5 as bait.

**Fig. S5** *ilr3-3* and *ilr3-1* express a loss-of-function and a dominant mutant allele of *ILR3*, respectively.

**Fig. S6** *ILR3* is a repressor of ferritin genes expression.

**Fig. S7** *ILR3* repression of ferritins expression is unique within the clade IVc bHLHs TFs implicated in the transcriptional control of iron deficiency responses.

**Fig. S8** *ILR3* acts as both transcriptional activator and repressor to regulate Fe homeostasis.

**Fig. S9** *ilr3-3* complementation experiment using *ProILR3:ILR3::GFP*.

**Fig. S10** Genome Browser snapshots of ATAC-seq, and H3K9ac, H3K4me3 and H3K27me3 ChIP-seq peaks on the *Arabidopsis thaliana* *NICOTIANAMINE SYNTHASE 4* gene (*NAS4*).

**Fig. S11** *ILR3* and *PYE* regulate common set of genes.

**Fig. S12** Fe-dependent seedling root growth involves *ILR3* and ferritins activity.

**Fig. S13** Fe-dependent seedling fresh weight involves *ILR3* and ferritins activity.

**Fig. S14** Complementation of *ilr3-1* seedling fresh weight phenotype by overexpressing *AtFER1*

**Fig. S15** *ILR3* participates to the plant response to Fe excess.

**Fig. S16** Overexpression of *AtFER1* rescue *ilr3-1* sensitivity to Fe excess.

**Fig. S17** *ILR3* modulates Fe content.

**Methods S1** Detailed protocols used in this study for physiological, biochemical, molecular and cytological analyses.

**Table S1** Primers used in this study.

Please note: Wiley Blackwell are not responsible for the content or functionality of any Supporting Information supplied by the authors. Any queries (other than missing material) should be directed to the *New Phytologist* Central Office.

See also the Commentary on this article by Kroh & Pilon, 223: 1052–1055.

## **New *Phytologist* Supporting Information**

**Article title:** Transcriptional integration of the responses to iron availability in *Arabidopsis* by the bHLH factor ILR3

**Authors:** Nicolas Tissot, Kevin Robe, Fei Gao, Susana Grant-Grant, Jossia Boucherez, Fanny Bellegarde, Amel Maghiaoui, Romain Marcelin, Esther Izquierdo, Moussa Benhamed, Antoine Martin, Florence Vignols, Hannetz Roschztardt, Frédéric Gaymard, Jean-François Briat, Christian Dubos.

**The following Supporting Information is available for this article:**

**Fig. S1.** Histochemical detection of GUS activity in 2 weeks old seedlings driven by *ProAtFER1* 5'-end deletion and site directed mutagenesis constructs.

**Fig. S2.** Schematic representation of conserved DNA regions (elements) and *cis*-regulatory sequences present in the 500bp upstream from the transcription initiation sequence of the three main ferritin genes expressed in vegetative tissues.

**Fig. S3.** Genome Browser snapshots of ATAC-seq, and H3K9ac, H3K4me3 and H3K27me3 ChIP-seq peaks on the three main ferritin genes found in *Arabidopsis thaliana* vegetative tissues, namely *AtFER1*, *AtFER3* and *AtFER4*.

**Fig. S4.** Yeast one-hybrid (Y1H) screen using *ProAtFER1* Element 5 as bait.

**Fig. S5.** *ilr3-3* and *ilr3-1* express a loss-of-function and a dominant mutant allele of *ILR3*, respectively.

**Fig. S6.** ILR3 is a repressor of ferritin genes expression.

**Fig. S7.** ILR3 repression of ferritins expression is unique within the clade IVc bHLHs TFs implicated in the transcriptional control of iron deficiency responses.

**Fig. S8.** ILR3 acts as both transcriptional activator and repressor to regulate Fe homeostasis.

**Fig. S9.** *ilr3-3* complementation experiment using *ProILR3:ILR3:GFP*.

**Fig. S10.** Genome Browser snapshots of ATAC-seq, and H3K9ac, H3K4me3 and H3K27me3 ChIP-seq peaks on the *Arabidopsis thaliana* NICOTIANAMINE SYNTHASE 4 gene (*NAS4*).

**Fig. S11.** ILR3 and PYE regulate common set of genes.

**Fig. S12. Fe-dependent seedling root growth involves ILR3 and ferritins activity.**

**Fig. S13.** Fe-dependent seedling fresh weight involves ILR3 and ferritins activity.

**Fig. S14.** Complementation of *ilr3-1* seedling fresh weight phenotype by overexpressing *AtFER1*.

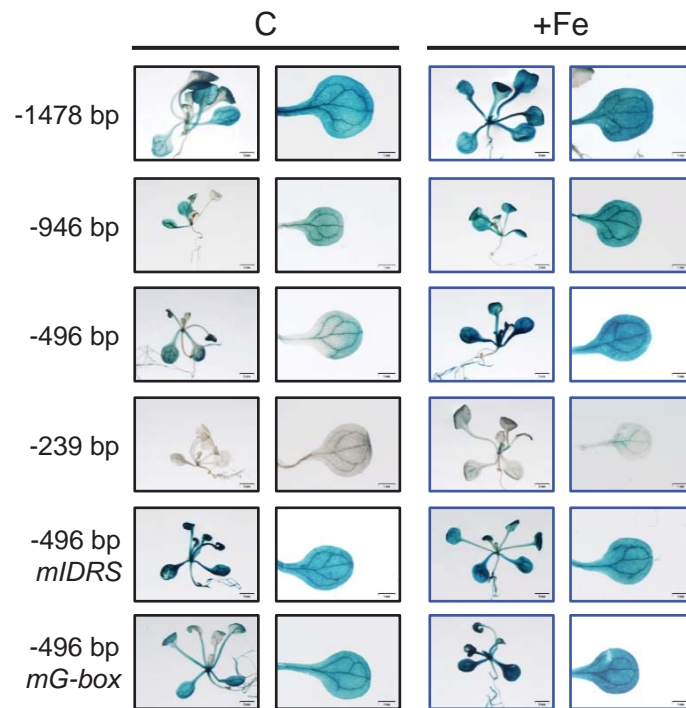
**Fig. S15.** ILR3 participates to the plant response to Fe excess.

**Fig. S16.** Overexpression of *AtFER1* rescue *ilr3-1* sensitivity to Fe excess.

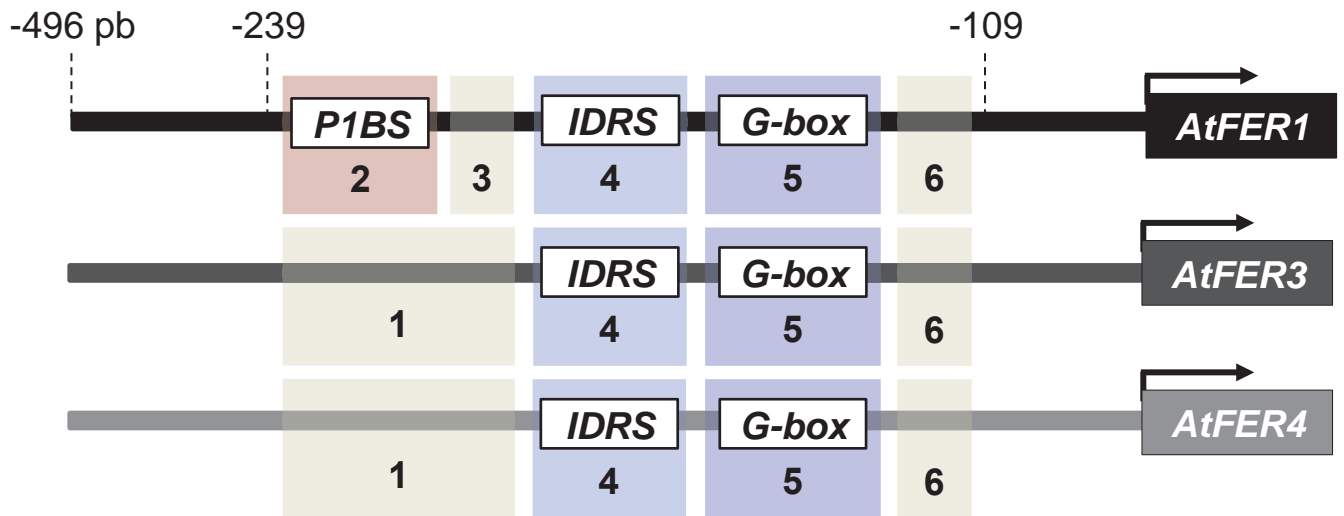
**Fig. S17.** ILR3 modulates Fe content.

**Table S1.** Primers used in this study.

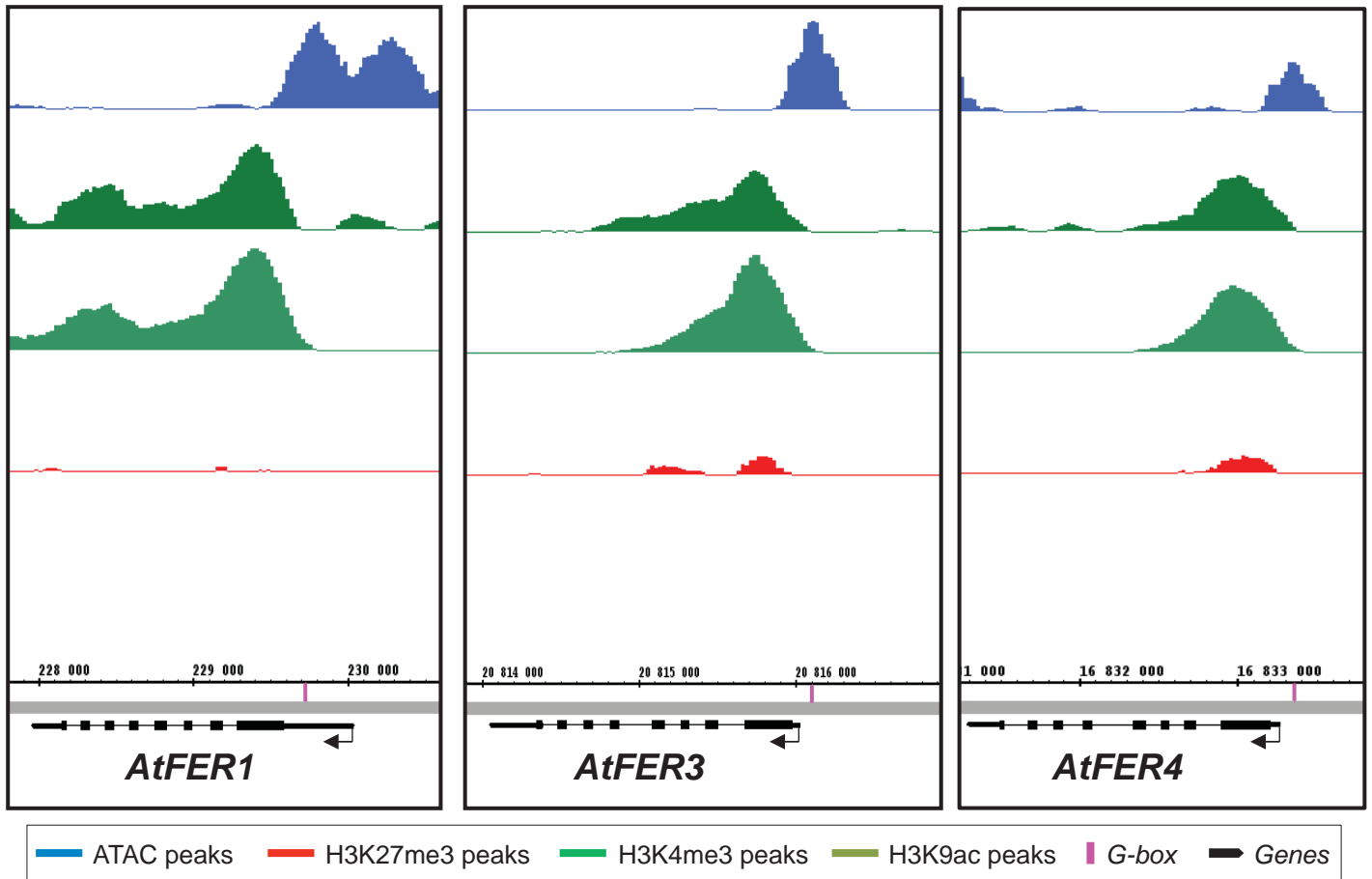
**Method S1.** Detailed protocols used in this study for physiological, biochemical, molecular and cytological analyses.



**Supporting Information Fig. S1. Histochemical detection of GUS activity in 2 weeks old seedlings driven by *ProAtFER1* 5'-end deletion and site directed mutagenesis constructs.** C and +Fe correspond to the control (50  $\mu$ M Fe) and Fe excess (500  $\mu$ M Fe) condition, respectively. *mIDRS*: mutated *Iron Dependent Regulatory Sequence*, *mG-box*: mutated *G-box cis-regulatory* sequence.



**Supporting Information Fig. S2.** Schematic representation of conserved DNA regions (Elements from 1 to 6) and *cis*-regulatory sequences present in the 500bp upstream from the transcription initiation sequence of the three main ferritin genes expressed in vegetative tissues. *P1BS*: *PHR1* binding site, *IDRS*: Iron Dependent Regulatory Sequence; adapted from Strozycki *et al.*, 2010.



**Supporting Information Fig. S3. Genome browser snapshots of ATAC-seq (blue peaks), and H3K9ac (dark green peaks), H3K4me3 (light green peaks) and H3K27me3 (red peaks) ChIP-seq peaks on the three main ferritin genes found in *Arabidopsis thaliana* vegetative tissues, namely *AtFER1*, *AtFER3* and *AtFER4*. Annotated genes are in black, and G-box motifs (CACGTG) in pink.** The analysis of publicly available ATAC-seq data (Assay for Transposase-Accessible Chromatin using sequencing) from wild-type seedlings grown in non-limiting Fe condition allows precise positioning of nucleosome-free regions (NFR) at the whole genome scale (Buenrostro *et al.*, 2013; Jegu *et al.*, 2017) and show that the G-box sequences present in the promoter of the ferritin genes were located in such regions, suggesting the presence of regulatory proteins at these loci. In addition, publicly available epigenomic profiles of histone modifications revealed that, in non-limiting Fe condition, ferritin gene loci are marked by histone 3 lysine 9 acetylation (H3K9ac) and histone 3 lysine 4 tri-methylation (H3K4me3) (two chromatin marks correlated with an active transcription), whereas the repressive marks H3K27me3 was barely detectable. These later observations indicate that the three ferritin genes are located in active chromatin regions in this growth condition.



(a)

NNNNAATTTCGACAAGAACACATATCCACCCTC**CACGTG**ATATCCACCCTC**CACGTG**  
ATATCCACCCTC**CACGTG**ATATCCACCCTC**CACGTG**GGTGCTCTTCTTCAACTAGNN  
NN

(b)

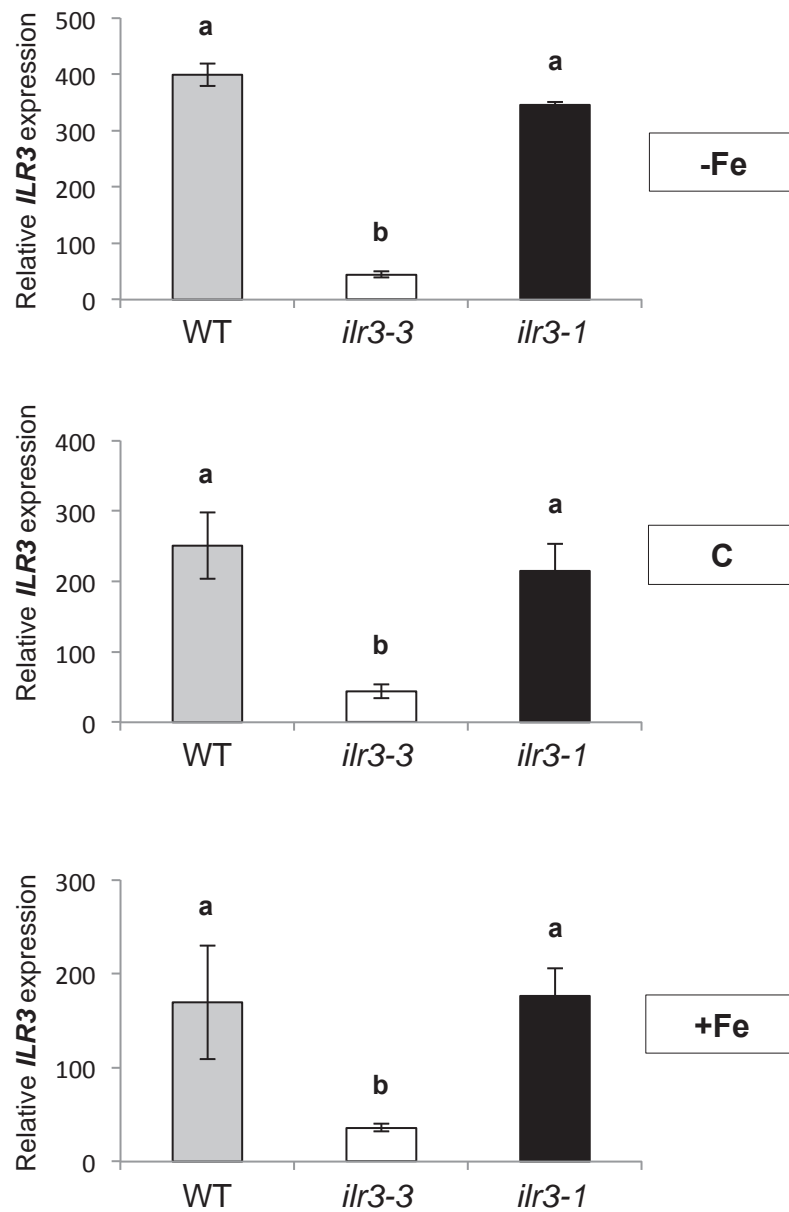
NNNNAATTTCGACAAGAACACATATCCACCCTC**ATGGAT**ATATCCACCCTC**ATGGAT**  
ATATCCACCCTC**ATGGAT**ATATCCACCCTC**ATGGAT**GTGCTCTTCTTCAACTAGNN  
NN

(c)

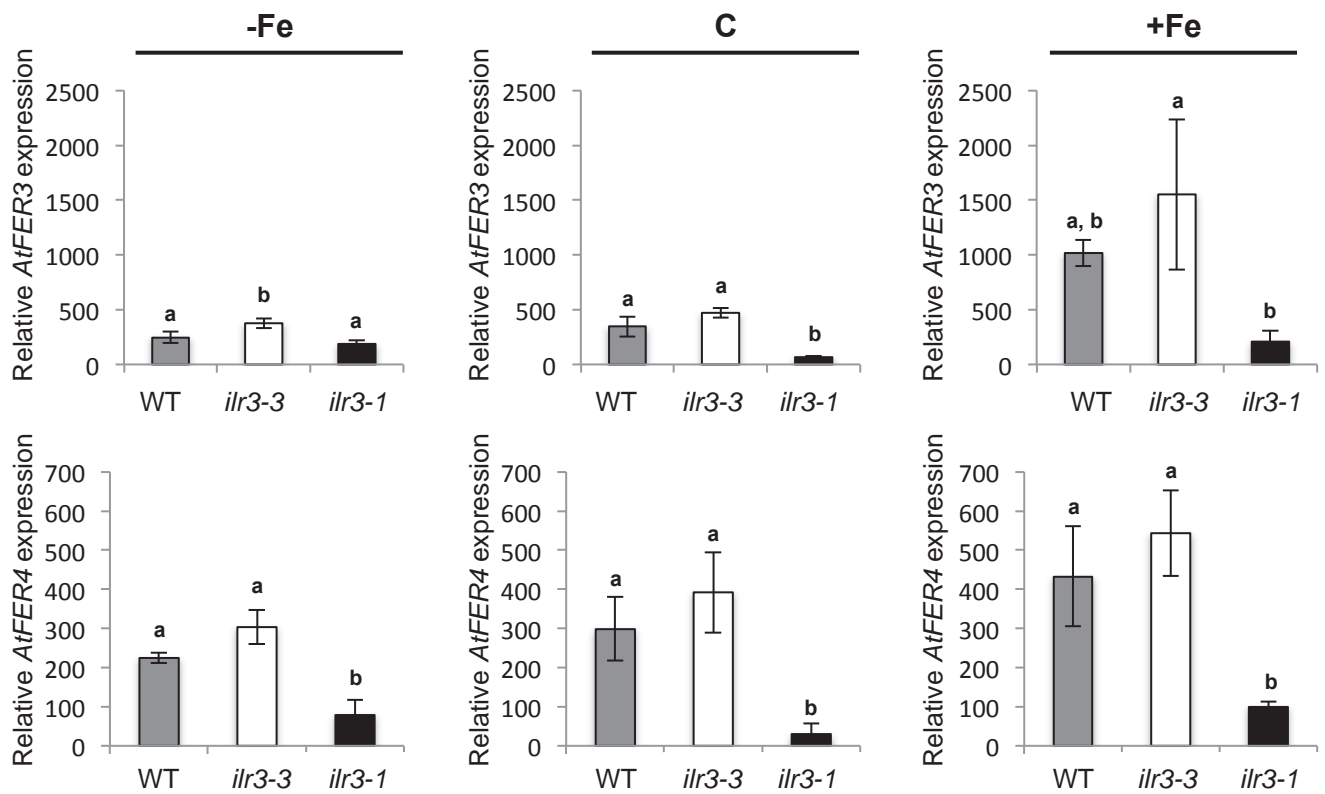
TF family	TF ID	Name
bHLH	At5g54680	BASIC HELIX-LOOP-HELIX 105
bZIP	At2g21230	BASIC LEUCINE-ZIPPER 30
MYB	At4g34990	MYB DOMAIN PROTEIN 32
NAC	At2g19520	NAC DOMAIN CONTAINING PROTEIN 64

**Supporting Information Fig. S4. Yeast one-hybrid (Y1H) screen using *ProAtFER1* Element 5 as bait.**

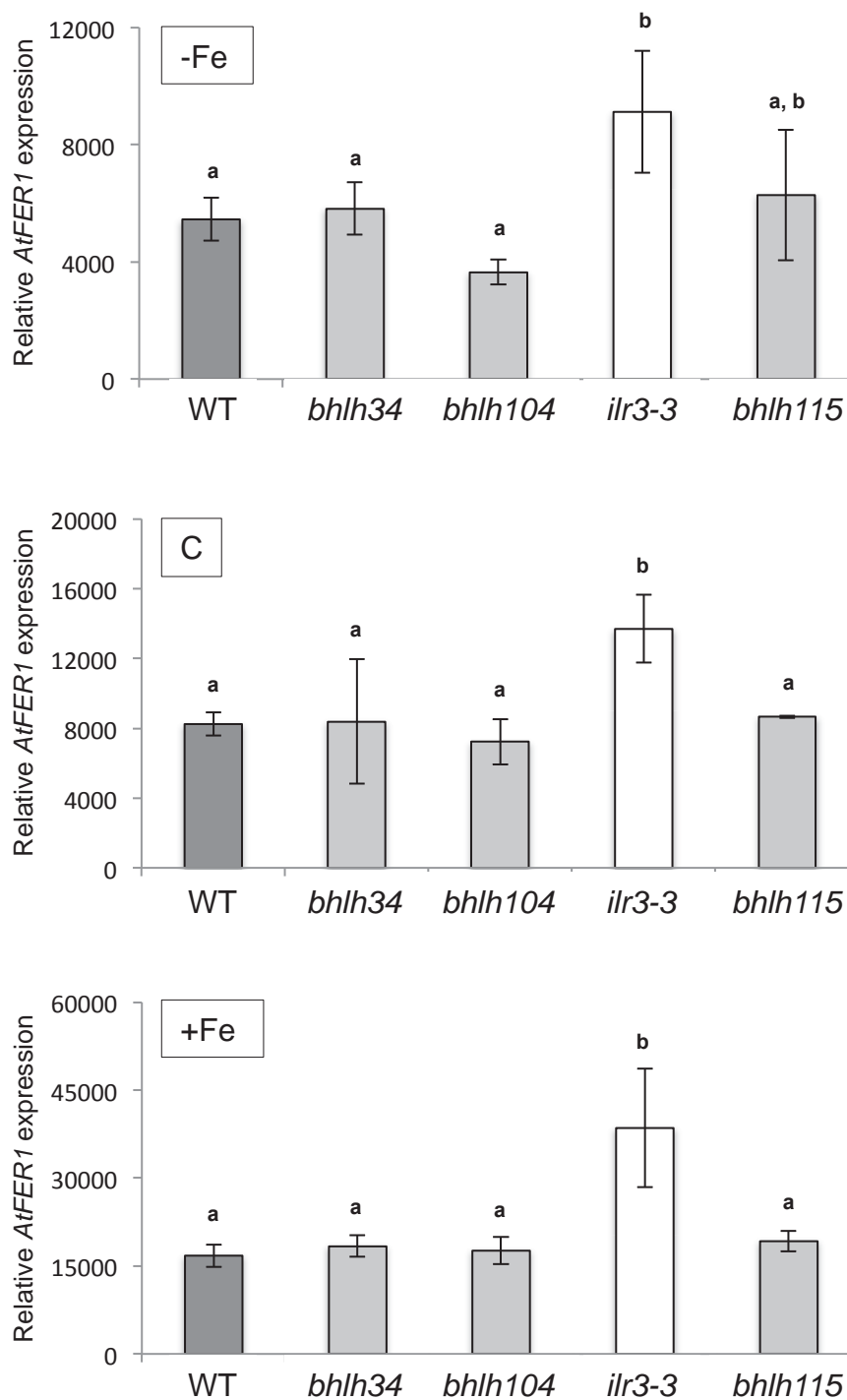
(a) Sequence of the bait DNA. The sequence used for the Y1H screen is a tetramer of *ProAtFER1* Element 5 (Supporting Information Fig. S2). Grey letter: pHISi-LIC vector sequence; black letters: *ProAtFER1* Element 5 sequence; blue letters: *G-box* sequence present in the Element 5. (b) Sequence of the mutated bait DNA used to confirm the interaction between ILR3 and the *G-box* present in *ProAtFER1* Element 5. The bait sequence used is as in (a) with the exception of the *G-box* that was mutated. Grey letter: pHISi-LIC vector sequence; black letters: *ProAtFER1* Element 5 sequence; red letters: mutated *G-box*. (c) List of candidate transcription factors (TFs) identified during the Y1H screen.



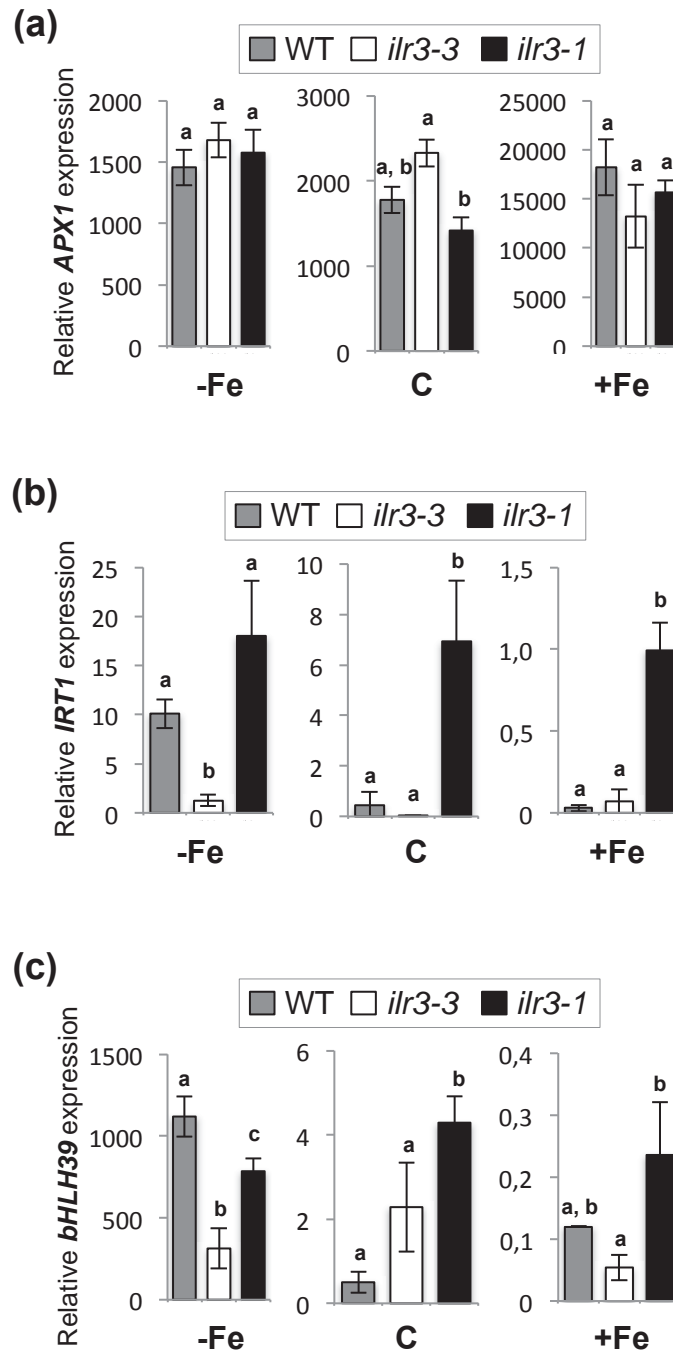
**Supporting Information Fig. S5. *ilr3-3* and *ilr3-1* express a loss-of-function and a dominant mutant allele of *ILR3*, respectively.** Relative expression of *ILR3* as revealed by quantitative RT-PCR analysis in 2 weeks old wild type (WT), *ilr3-1* and *ilr3-3* seedlings. -Fe, C and +Fe correspond to the Fe deficiency (0  $\mu$ M Fe), control (50  $\mu$ M Fe), and Fe excess (500  $\mu$ M Fe) conditions, respectively. Means within each condition with the same letter are not significantly different according to one-way ANOVA followed by post-hoc Tukey test,  $P < 0.05$  ( $n=3$  biological repeats from one representative experiment). Error bars show SD.



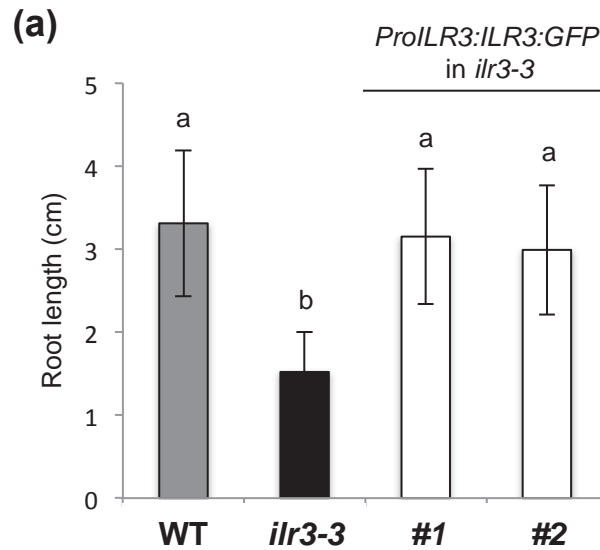
**Supporting Information Fig. S6. ILR3 is a repressor of ferritin genes expression.** Quantitative RT-PCR (qRT-PCR) analysis of the *AtFER3* and *AtFER4* mRNA levels in 2 weeks old wild type (WT), *ilr3-3* (loss-of-function) and *ilr3-1* (dominant mutation). -Fe, C and +Fe correspond to Fe deficiency (0  $\mu$ M Fe), control (50  $\mu$ M Fe), and Fe excess (500  $\mu$ M Fe) conditions, respectively. Means with the same letter are not significantly different according to one-way ANOVA followed by post-hoc Tukey test,  $P < 0.05$  (n=3 biological repeats from one representative experiment). Error bars show SD.



**Supporting Information Fig. S7. ILR3 repression of ferritins expression is unique within the clade IVc bHLHs TFs implicated in the transcriptional control of iron deficiency responses.** Quantitative RT-PCR (qRT-PCR) analysis of *AtFER1* mRNA levels in 2 weeks old wild type (WT), *bhlh34*, *bhlh104*, *ilr3-3* and *bhlh115* seedlings. -Fe, C and +Fe correspond to Fe deficiency (0  $\mu$ M Fe), control (50  $\mu$ M Fe) and Fe excess (500  $\mu$ M Fe) conditions respectively. Means with the same letter are not significantly different according to one-way ANOVA followed by post-hoc Tukey test,  $P < 0.05$  ( $n=3$  biological replicates from one representative experiment). Error bars show SD.



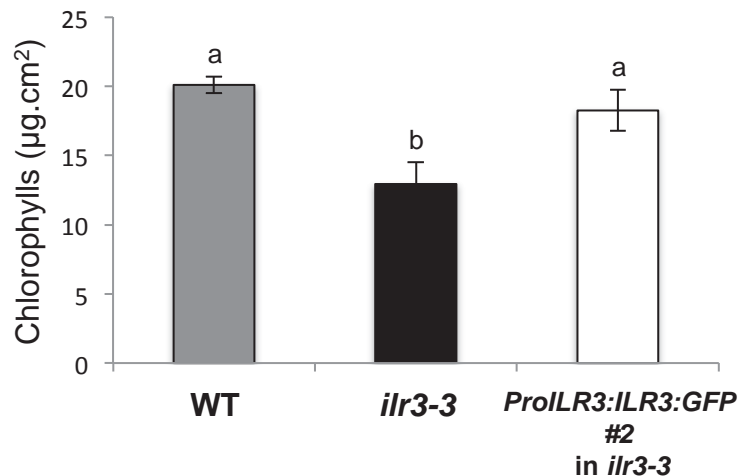
**Supporting Information Fig. S8. ILR3 acts as both transcriptional activator and repressor to regulate Fe homeostasis.** Relative expression of (a) *APX1* (*ASCORBATE PEROXIDASE 1*), (b) *IRT1* (*IRON-REGULATED TRANSPORTER 1*) and (c) *bHLH39* genes as revealed by quantitative RT-PCR (qRT-PCR) analysis in 2 weeks old wild type (WT), *ilr3-1* and *ilr3-3* seedlings. -Fe, C and +Fe correspond to Fe deficiency (0  $\mu$ M Fe), control (50  $\mu$ M Fe), and Fe excess (500  $\mu$ M Fe) condition, respectively. Means within each condition with the same letter are not significantly different according to one-way ANOVA followed by post-hoc Tukey test,  $P < 0.05$  ( $n=3$  biological repeats from one representative experiment). Error bars show SD.



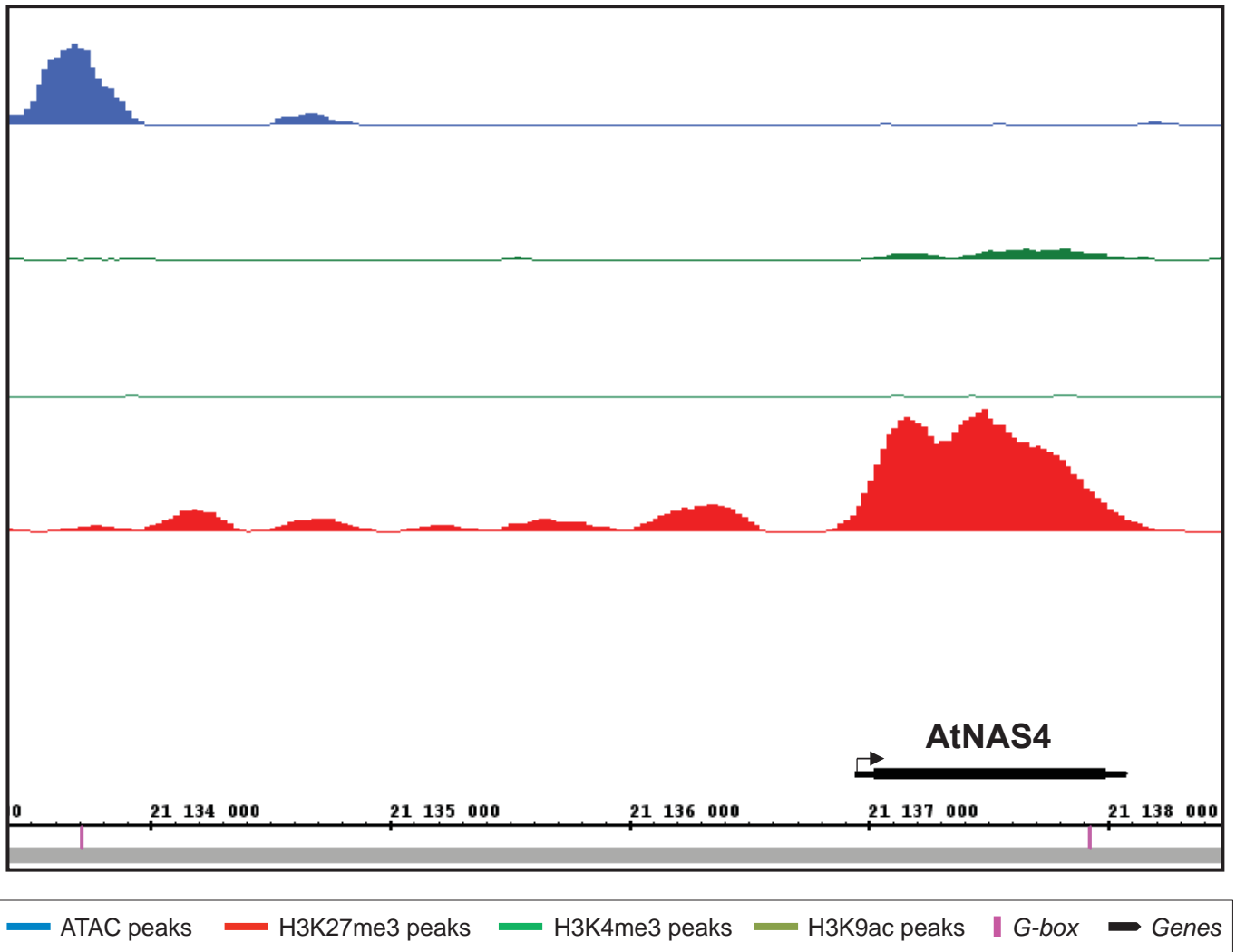
**(b)**



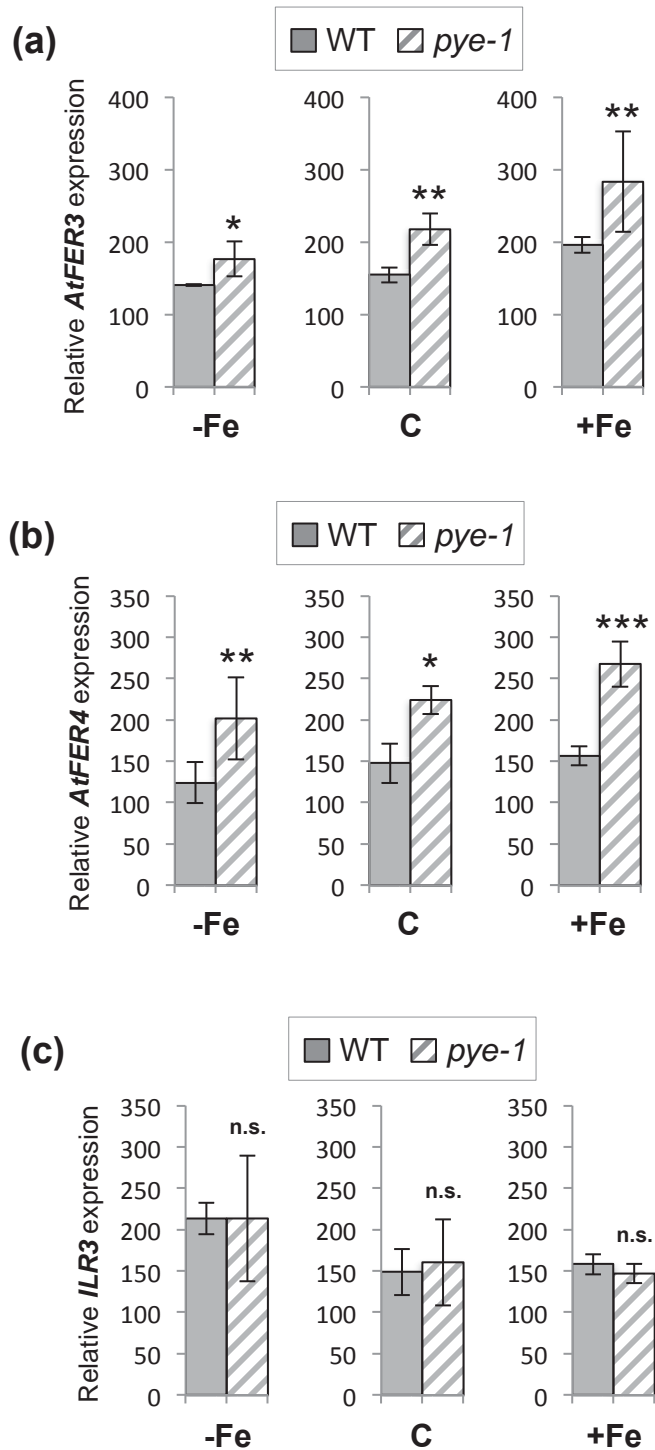
**(c)**



**Supporting Information Fig. S9. Complement of *ilr3-3* by *ProILR3:ILR3:GFP*.** (a) Root length of wild type (WT), *ilr3-3* and *ilr3-3* lines (#1 and #2) expressing *ProILR3:ILR3:GFP* grown for 10 days in Fe deficiency (0  $\mu\text{M}$  Fe). Means with the same letter are not significantly different according to one-way ANOVA followed by post-hoc Tukey test,  $P < 0.05$  ( $n=3$  biological repeats from one representative experiment). Error bars show SD. (b) Rosette phenotype of WT, *ilr3-3* and *ilr3-3* line #2 expressing *ProILR3:ILR3:GFP* grown for 2 weeks in soil. (c) Chlorophylls content measured in young leaves of WT, *ilr3-3* and *ilr3-3* line #2 expressing *ProILR3:ILR3:GFP* grown for 2 weeks in soil. Means with the same letter are not significantly different according to one-way ANOVA followed by post-hoc Tukey test,  $P < 0.05$  ( $n=3$  biological repeats from one representative experiment). Error bars show SD.

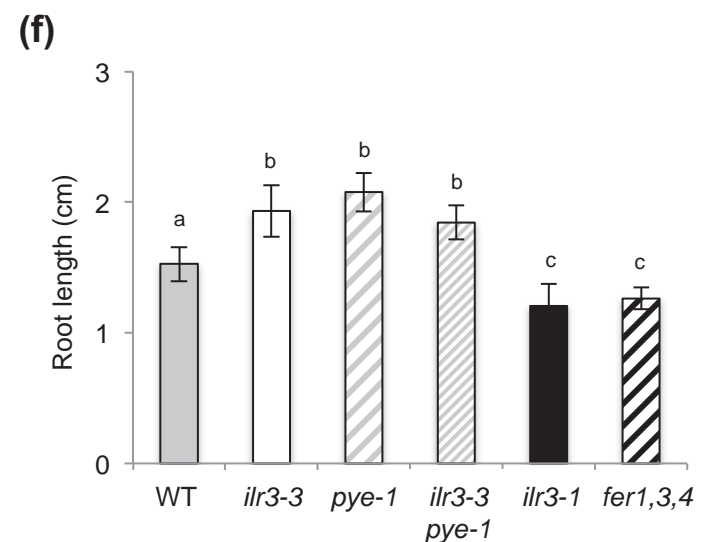
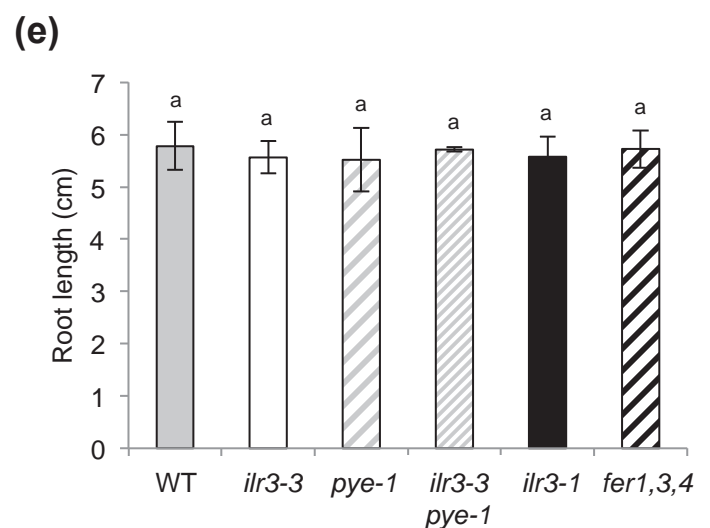
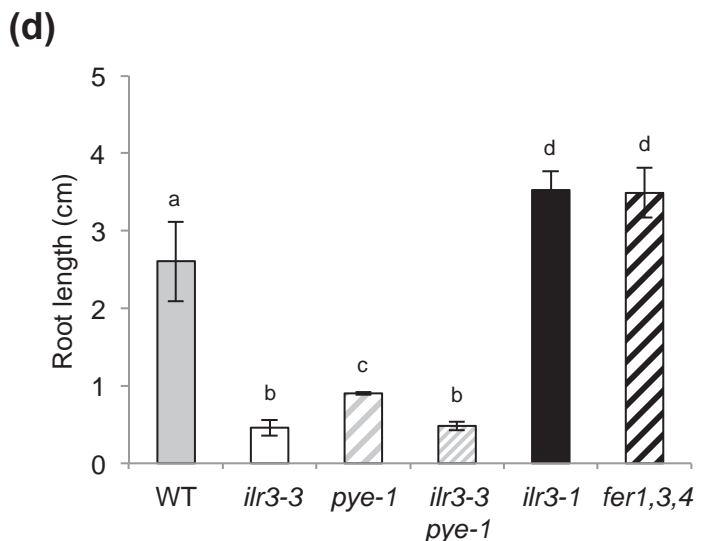
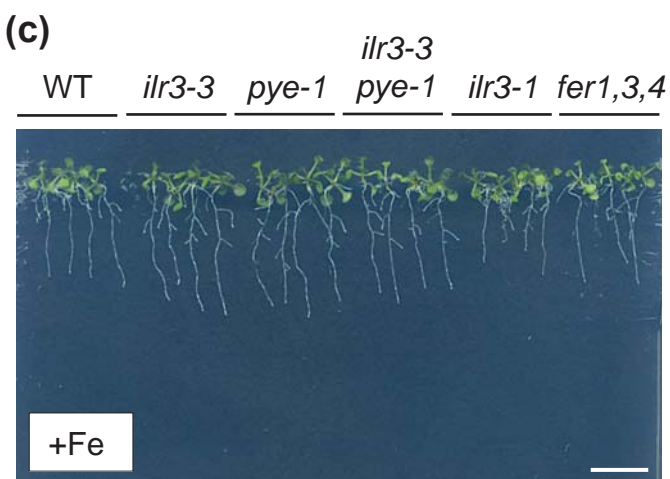
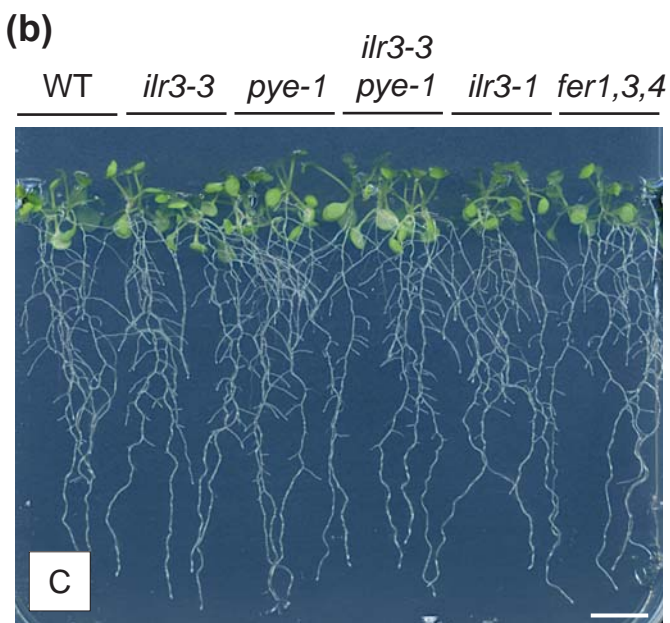
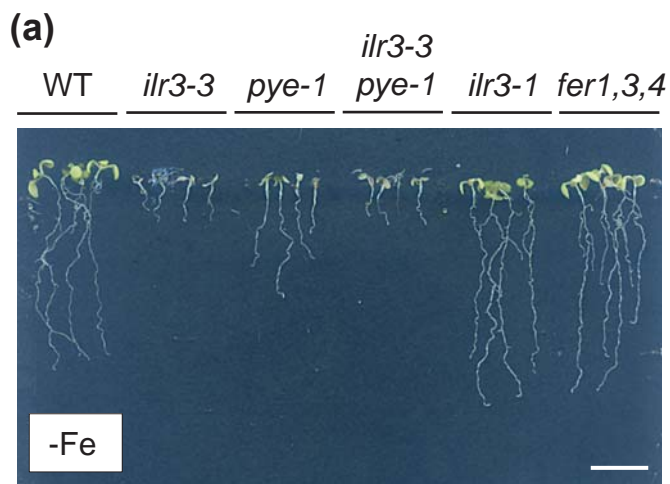


**Supporting Information Fig. S10. Genome Browser snapshots of ATAC-seq (blue peaks), and H3K9ac (dark green peaks), H3K4me3 (light green peaks) and H3K27me3 (red peaks) ChIP-seq peaks on the *Arabidopsis thaliana* NICOTIANAMINE SYNTHASE 4 gene (*NAS4*). Annotated gene is in black, and G-box motifs (*CACGTG*) in pink. Interestingly, the analysis of the publicly available ATAC-seq data carried out on WT seedlings grown on control Fe condition shows that ILR3/PYE binding site is located on the main NFR region on the promoter of *NAS4* (*ProNAS4*). In addition, publicly available epigenomic profiles of histone modifications show that, in control Fe condition, *NAS4* is enriched with the repressive marks H3K27me3 (inactive chromatin region), in support of its low expression level in this growth condition.**



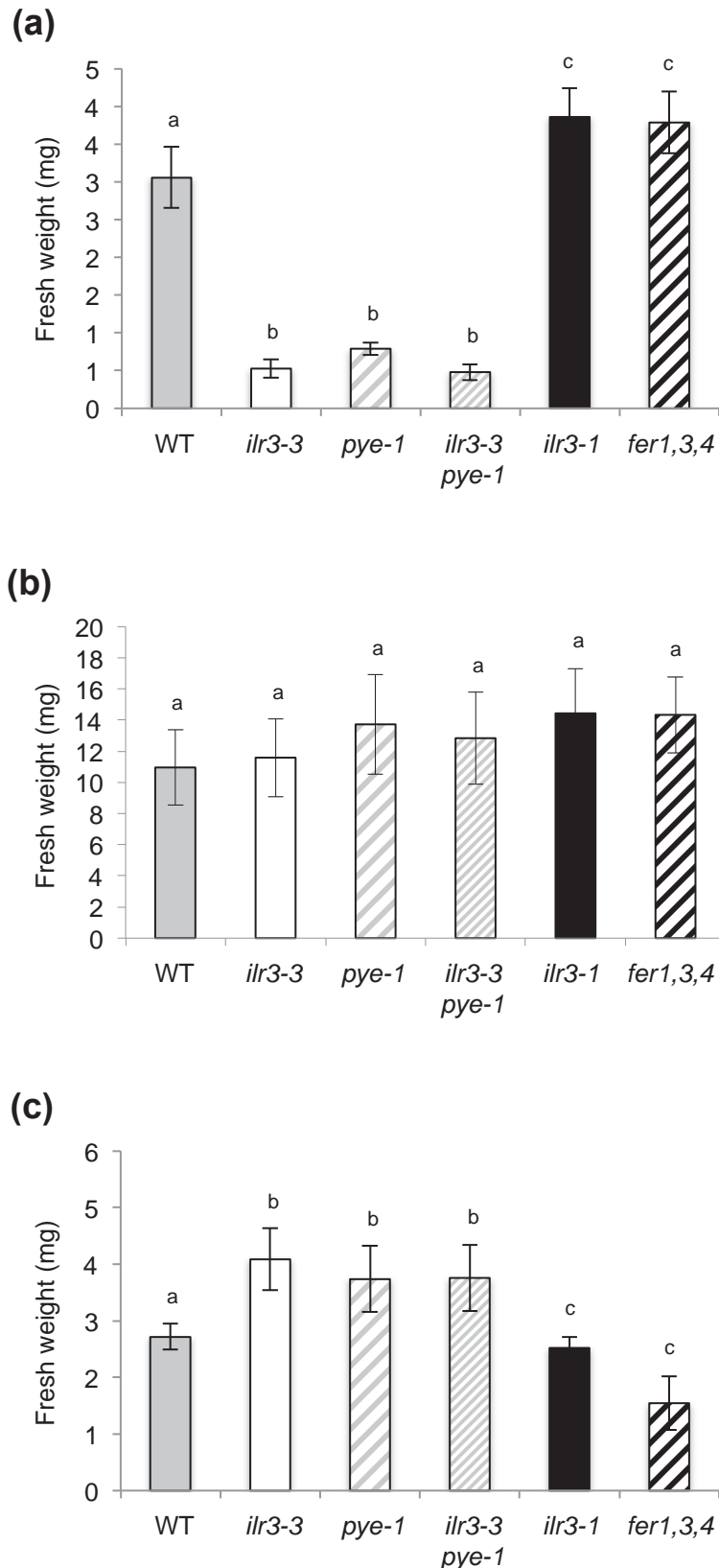
**Supporting Information Fig. S11. ILR3 and PYE regulate common set of genes.** Relative expression (qRT-PCR) of (a) *AtFER3*, (b) *AtFER4*, and (c) *ILR3* genes as revealed by quantitative RT-PCR analysis in 2 weeks old wild type (WT) and *pye-1* seedlings. *t*-test significance (n=3 biological repeats from one representative experiment): \*  $P < 0.05$ , \*\*  $P < 0.01$ , \*\*\*  $P < 0.001$  and n.s.: not significant. Error bars show SD. -Fe, C and +Fe correspond to the Fe deficiency (0  $\mu\text{M}$  Fe), control (50  $\mu\text{M}$  Fe) and Fe excess (500  $\mu\text{M}$  Fe) conditions, respectively.



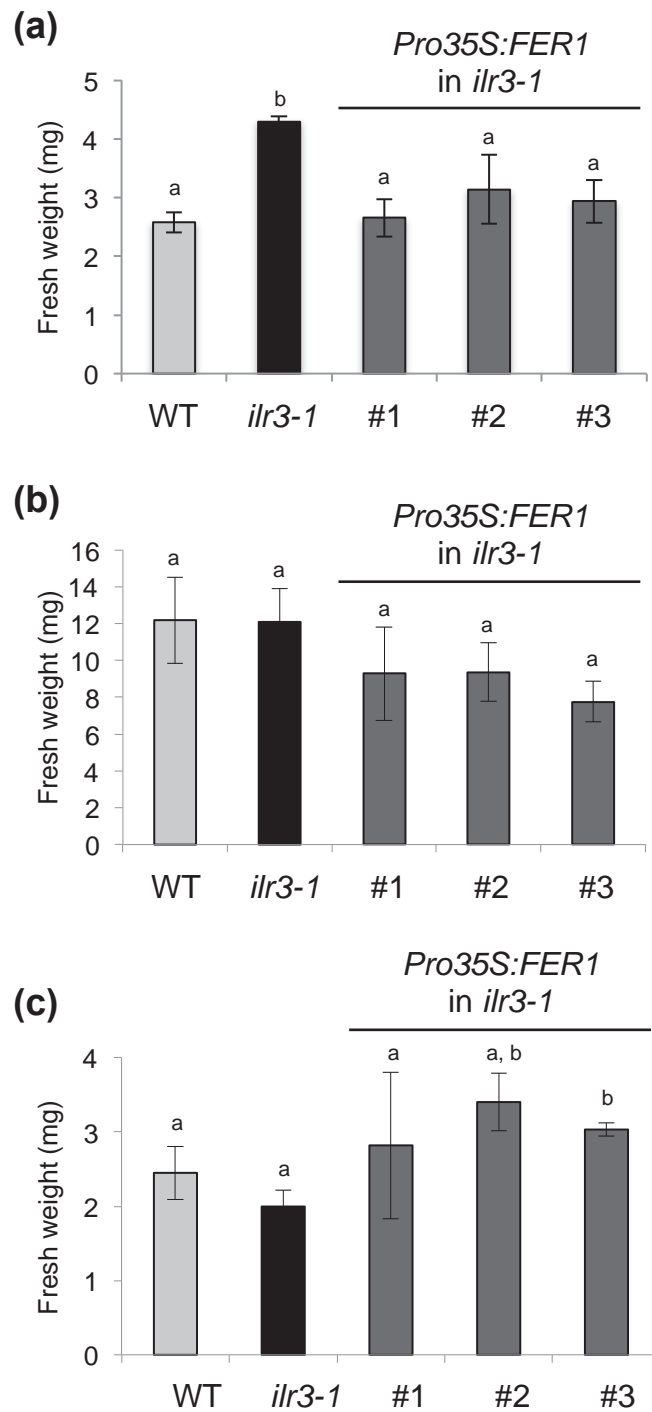


**Supporting Information Fig. S12. Fe-dependent seedling root growth involves ILR3 and ferritins activity.**

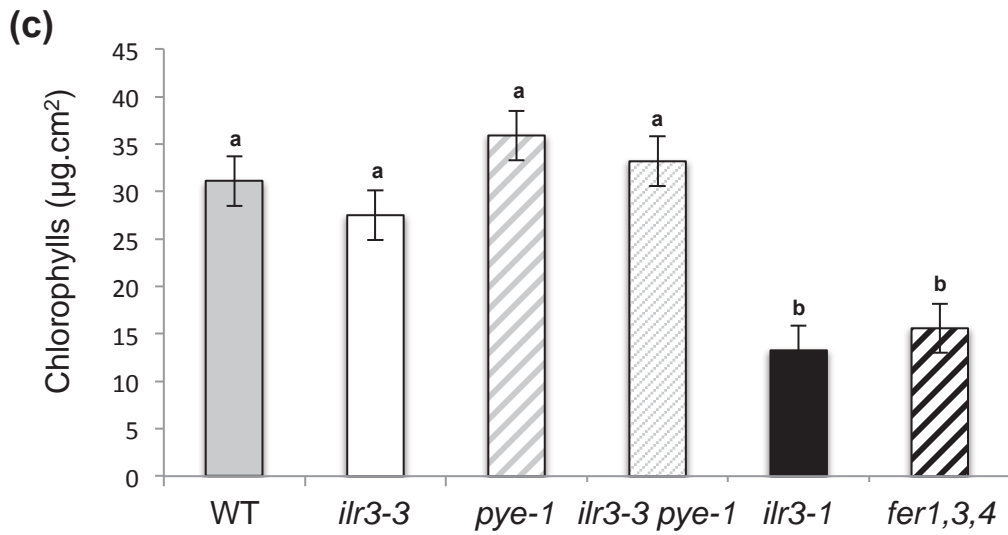
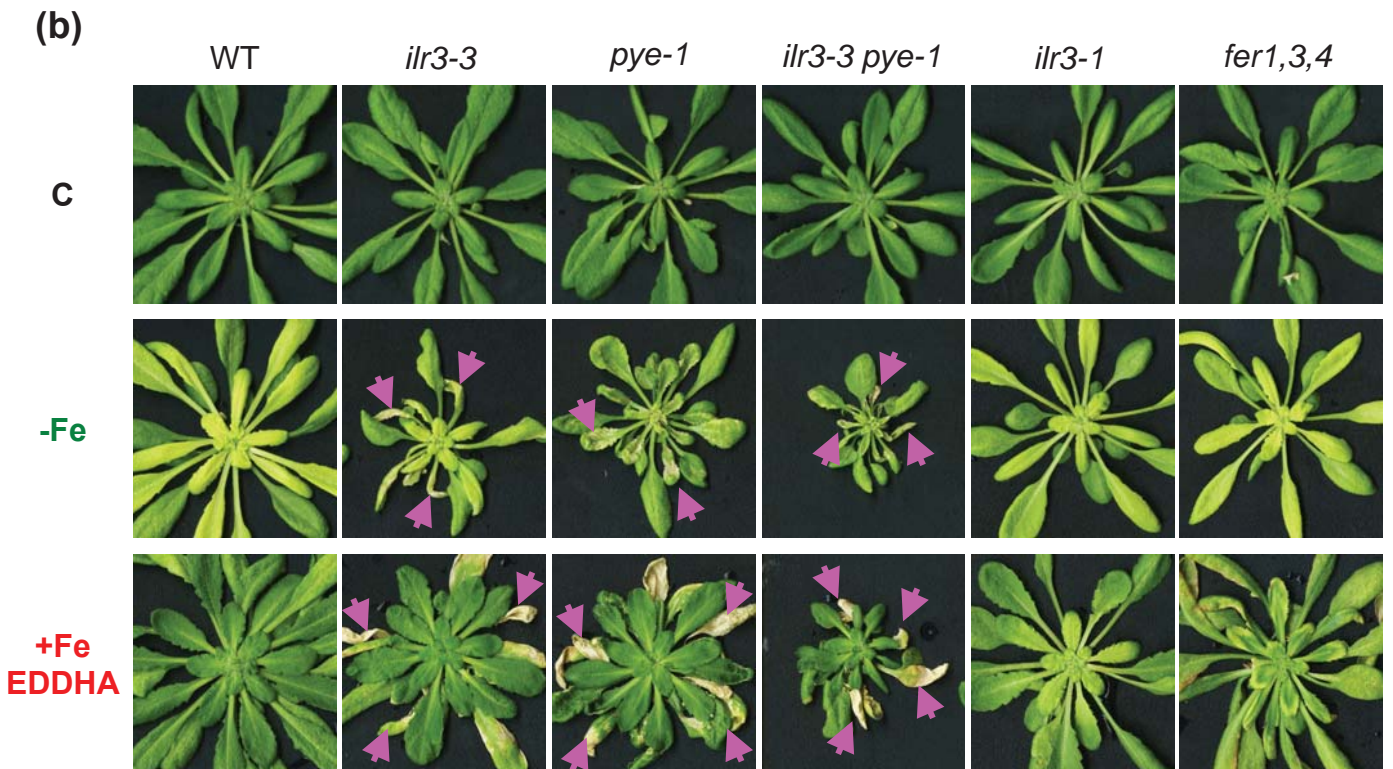
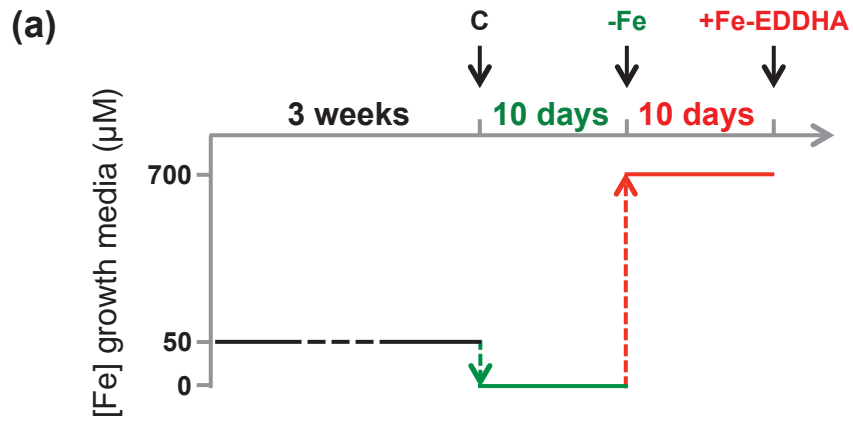
**(a-c)** Seedling phenotypes of the wild type (WT), *ilr3-3*, *pye-1*, *ilr3-3 pye-1*, *ilr3-1* and *fer1,3,4* mutants grown for 2 weeks in **(a)** Fe deficiency (0  $\mu$ M Fe), **(b)** control (50  $\mu$ M Fe), and **(c)** Fe excess (500  $\mu$ M Fe) conditions. Bar = 1 cm. **(d-f)** Root length of WT, *ilr3-3*, *pye-1*, *ilr3-3 pye-1*, *ilr3-1* and *fer1,3,4* mutants grown for 2 weeks in **(d)** Fe deficiency (0  $\mu$ M Fe), **(e)** control (50  $\mu$ M Fe), and **(f)** Fe excess (500  $\mu$ M Fe) conditions. Means within each condition with the same letter are not significantly different according to one-way ANOVA followed by post-hoc Tukey test,  $P < 0.05$  ( $n=16$  seedlings from one representative experiment). Error bars show SD.



**Supporting Information Fig. S13. Fe-dependent seedling fresh weight involves ILR3 and ferritins activity.** Seedling fresh weight of the wild type (WT), *ilr3-3*, *pye-1*, *ilr3-3 pye-1*, *ilr3-1* and *fer1,3,4* mutants grown for 2 weeks in (a) Fe deficiency (0  $\mu$ M Fe), (b) control (50  $\mu$ M Fe), and (c) Fe excess (500  $\mu$ M Fe) conditions. Means within each condition with the same letter are not significantly different according to one-way ANOVA followed by post-hoc Tukey test,  $P < 0.05$  (n=16 seedlings from one representative experiment). Error bars show SD.

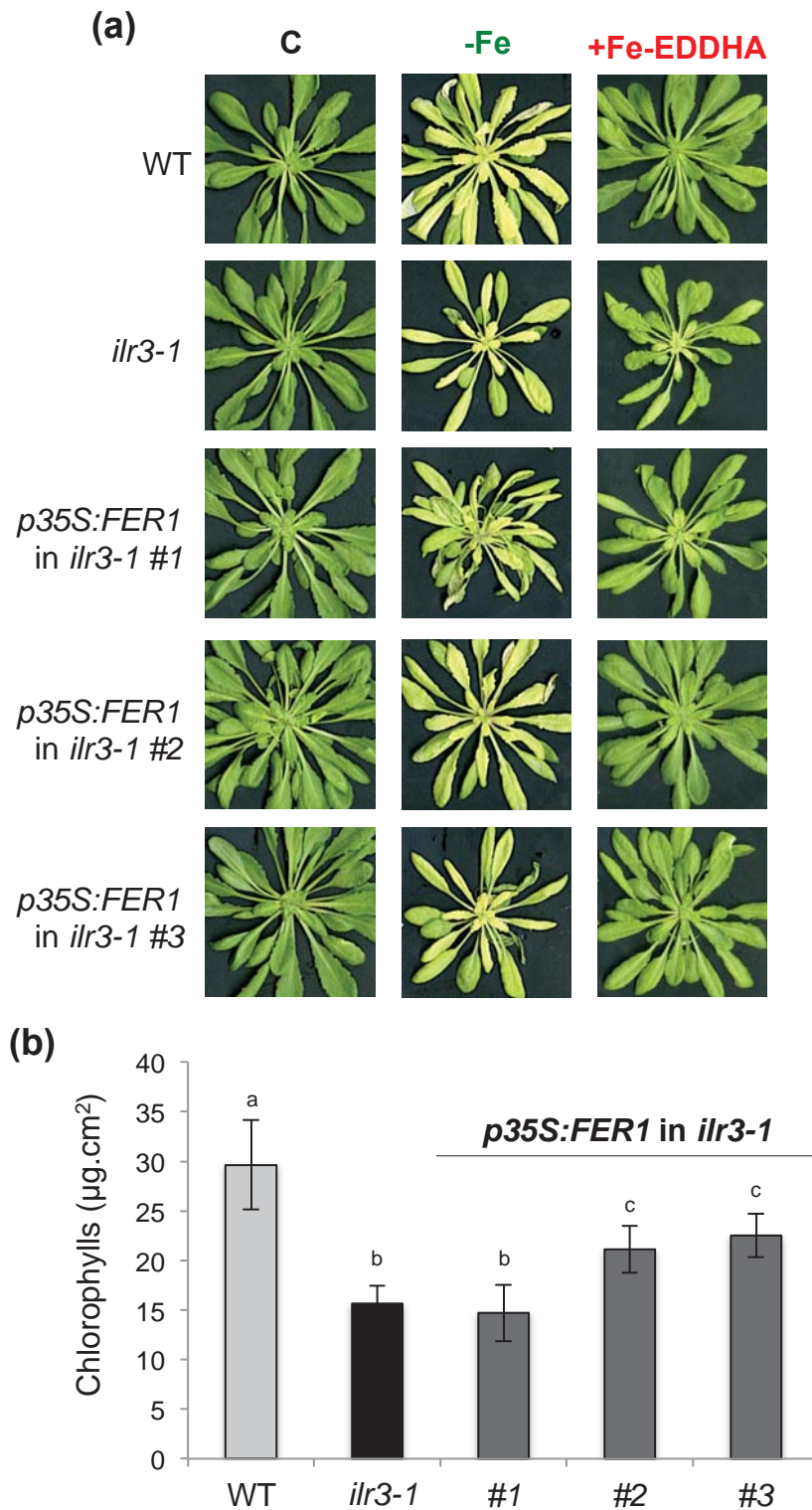


**Supporting Information Fig. S14. Complementation of *ilr3-1* seedling fresh weight phenotype by overexpressing *AtFER1*.** Seedling fresh weight of the wild type (WT), *ilr3-1* and three independent *ilr3-1* lines overexpressing *AtFER1* (*Pro35S:FER1* in *ilr3-1*) grown for 2 weeks in (a) Fe deficiency (0  $\mu$ M Fe), (b) control (50  $\mu$ M Fe), and (c) Fe excess (500  $\mu$ M Fe) conditions. Means within each condition with the same letter are not significantly different according to one-way ANOVA followed by post-hoc Tukey test,  $P < 0.05$  (n=16 seedlings from one representative experiment). Error bars show SD.

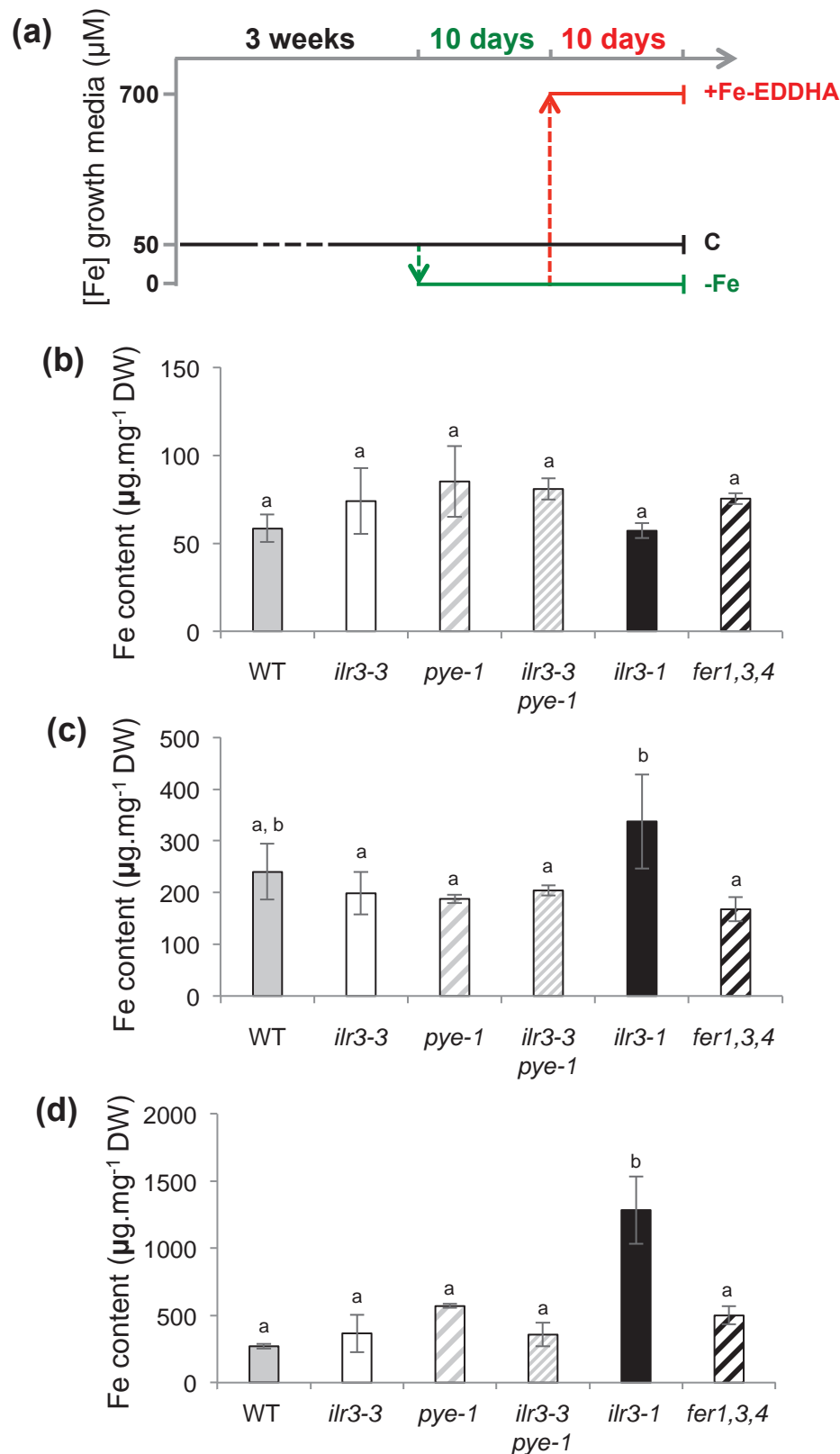


**Supporting Information Fig. S15. ILR3 participates to the plant response to Fe excess.**

(a) Experimental design used to highlight the role that ferritins play in the plant responses to Fe excess that relies on ILR3 activity. *ilr3-3*, *pye-1*, *ilr3-3 pye-1*, *ilr3-1*, *fer1,3,4* and WT plants were grown for three weeks under Fe replete (C) condition before Fe was removed from the nutrient solution (-Fe). After ten days of growth under -Fe, plants were subjected to Fe excess by supplementing the medium with 700 $\mu$ M ferric ethylenediamine di-(o-hydroxyphenylacetate) (+Fe-EDDHA), a form of Fe easily assimilated by the plant, and grown for an additional ten days. (b) Rosette phenotype of wild type (WT), *ilr3-3*, *pye-1*, *ilr3-3 pye-1*, *ilr3-1* and *fer1,3,4* mutants after 3 weeks of growth in Fe replete (C, 50  $\mu$ M Fe) condition followed by 10 days of Fe deficiency (-Fe) and then grown for an additional 10 days in Fe excess (+Fe: 700  $\mu$ M Fe-EDDHA). Magenta arrows indicate necrotic leaves. As expected, all genotypes were chlorotic after ten days of growth in -Fe with the *ilr3-3*, *pye-1* and *ilr3-3 pye-1* plants being the more affected as several leaves presented necrotic symptoms. This later observation was expected as previous studies have shown that among the clade IVc bHLH involved in Arabidopsis response to Fe deficiency, *ilr3* loss-of-function mutant was the most affected when Fe availability was scarce (Zhang *et al.*, 2015). In addition, *pye-1* is also a mutant that is severely affected by Fe deficiency (Long *et al.*, 2010). Following Fe(III)-EDDHA treatment, *ilr3-3*, *pye-1* and *ilr3-3 pye-1* mutants as well as WT plants were rescued as chlorosis and necrotic symptoms disappeared, except for the leaves that presented necrotic symptoms following -Fe treatment. In contrast, we observed that the re-greening of the *ilr3-1* and *fer1,3,4* plants was not homogenous and that young leaves (*i.e.* the one that developed during the treatment) displayed a patchy phenotype with chlorotic areas. (c) Chlorophylls content measured in young leaves of WT, *ilr3-3*, *pye-1*, *ilr3-3 pye-1*, *ilr3-1* and *fer1,3,4* mutants at the end of the experiment (*i.e.* following Fe-EDDHA treatment). Means with the same letter are not significantly different according to one-way ANOVA followed by post-hoc Tukey test,  $P < 0.05$  (n=3 biological repeats from one representative experiment). Error bars show SD. The chlorosis observed in *ilr3-1* and *fer1,3,4* plants following Fe(III)-EDDHA treatment is associated with a decrease in the overall chlorophyll content in young leaves indicating that the absence of ferritins was compromising the Fe(III)-EDDHA rescue of the chlorotic defects, and that ILR3 participates to the plant response to Fe excess.



**Supporting Information Fig. S16. Overexpression of *AtFER1* rescue *ilr3-1* sensitivity to Fe excess.** (a) Rosette phenotype of wild type (WT), *ilr3-1* and three independent *ilr3-1* lines overexpressing *AtFER1* (*Pro35S:FER1* in *ilr3-1*) after 3 weeks of growth in Fe replete (C, 50 µM Fe) condition followed by 10 days of Fe deficiency (-Fe) and then grown for an additional 10 days in Fe excess (+Fe: 700 µM Fe-EDDHA). The aim of this experiment was to clarify the role played by ferritins in the *ilr3-1* response to Fe excess. We found that the chlorotic defects still observed in *ilr3-1* when compared to WT plants upon Fe(III)-EDDHA treatment were, at least in part, rescued in the transgenic *ilr3-1* lines overexpressing *AtFER1*. This later results confirmed that part of the ILR3 function in the control of plant response to Fe availability relies on ferritin activity. (b) Chlorophylls content measured in young leaves of WT, *ilr3-1* and three independent *ilr3-1* lines overexpressing *AtFER1* at the end of the experiment (i.e. following Fe-EDDHA treatment). Means with the same letter are not significantly different according to one-way ANOVA followed by post-hoc Tukey test,  $P < 0.05$  ( $n=3$  biological repeats from one representative experiment). Error bars show SD.



**Supporting Information Fig. S17. ILR3 modulates Fe content.** (a) Experimental design used to highlight the role that ferritins play in the plant responses to Fe excess that relies on ILR3 activity. Fe content in rosette leaves of wild type (WT), *ilr3-3*, *pye-1*, *ilr3-3 pye-1*, *ilr3-1* and *fer1,3,4* mutants after (b) 3 weeks of growth in Fe replete (C, 50 µM Fe) condition followed by 20 days of Fe deficiency (-Fe), (c) 3 weeks of growth in C condition followed by an additional 20 days in C, and (d) 3 weeks of growth in C condition followed by 10 days of -Fe and then grown for an additional 10 days in Fe excess (+Fe: 700 µM Fe-EDDHA). Means with the same letter are not significantly different according to one-way ANOVA followed by post-hoc Tukey test,  $P < 0.05$  ( $n=3$  biological repeats from one representative experiment). Error bars show SD.

Table S1: Primer used in this study

Primer name	sequence (5' ->3')	Purpose	Sources
bhlh34-F	TGGAAATCTTCAGCAAGTTTGT	Mutant screening	Li et al, 2016 – Plant Physiol
bhlh34-R	ATCACATCAACAACAGAAATGG	Mutant screening	Li et al, 2016 – Plant Physiol
bhlh104-1-F	GGGGAAGGTTGTCTCTTTG	Mutant screening	Zhang et al, 2015 – Plant Cell
bhlh104-1-R	GCTGAGTCTTGATCACGAG	Mutant screening	Zhang et al, 2015 – Plant Cell
bhlh115-F	CGTGAGTAAATTCCTCTCC	Mutant screening	This study
bhlh115-R	CAGAGAACGTAAGCAAAACG	Mutant screening	This study
ir13-1-F	AGAAATCGCTATGGAATTTGTTATGGTTCT	Mutant screening	Rampey et al, 2006 – Genetics
ir13-1-R	CAATTTCAACAGATAACAGTTACGATGAT	Mutant screening	Zhang et al, 2015 – Plant Cell
ir13-3-F	TCAATCAATCCCGAATCAAG	Mutant screening	Zhang et al, 2015 – Plant Cell
ir13-3-R	CTTCCACTATACCGAATTTG	Mutant screening	This study
pFER1-1478bp-B1	GGGACAAGTTTGTACAAAAAAGCAGGCTTCTCTCGAAGAAAGGATAGAG	Promoter cloning	This study
pFER1-1kb-B1	GGGACAAGTTTGTACAAAAAAGCAGGCTTCGCTACCCCTTGTCTTTGTGC	Promoter cloning	This study
pFER1-500pb-B1	GGGACAAGTTTGTACAAAAAAGCAGGCTTCCTATGTCATATATGTGTACAGG	Promoter cloning	This study
pFER1-B2	GGGACACATTTGTACAGAAAGCTGGGTCCGTTGGAAAAATGTAGAAGAG	Promoter cloning	This study
pFER1-496bp-mIDRSF	ATCCTCAAGTTCCAGTAATCCATTTGGATGTAGCACGAGG	Promoter cloning	This study
pFER1-496bp-mIDRSR	GATTTACGGGAACCTTGAGGATATCGATCCACGTT	Promoter cloning	This study
pFER1-496bp-mboxF	ATGAGGCCGGGAAATCGCCCTTACATCTGGCTTTTC	Promoter cloning	This study
pFER1-496bp-mboxR	GGCGAATCCGGGCTCCATCTACATCAATGGATAGTG	Promoter cloning	This study
pIRL3-1.8kb-B1	GGGACAAGTTTGTACAAAAAAGCAGGCTTCCATAGTTTCAATTCGGTACATG	GFP fusion for ChIP analysis	This study
cILR3-B2	GGGACACATTTGTACAAAAAAGCTGGGTCTTAAAGCAACAGGAGGAGAAAG	GFP fusion for ChIP analysis	This study
ProAt-NEET-a-F	gcctatgaccaaatcccttgcga	ChIP-qPCR	This study
ProAt-NEET-a-R	ttgtctcaaatctogtctaaactaagt	ChIP-qPCR	This study
ProAt-NEET-b-F	acttagttagacgaatttgagaaaca	ChIP-qPCR	This study
ProAt-NEET-b-R	agcgtgtgatgagatggaaga	ChIP-qPCR	This study
ProBHLH39-F	CCAGTCTACTTTGACTAGACCTTG	ChIP-qPCR	Zhang et al, 2015 – Plant Cell
ProBHLH39-R	AACCAAACTTAAAAAATTCGCAAA	ChIP-qPCR	Zhang et al, 2015 – Plant Cell
ProFIT-F	GCCTGTGACAACTAACACAGTTGAC	ChIP-qPCR	Zhang et al, 2015 – Plant Cell
ProFIT-R	ATCGATCAGACCGTATTAATAAGGT	ChIP-qPCR	Zhang et al, 2015 – Plant Cell
ProFER1-a-F	tgcaactattcctgcagccaa	ChIP-qPCR	This study
ProFER1-a-R	agttgaaatgtggcaaggaca	ChIP-qPCR	This study
ProFER1-b-F	tcogatttccatgtcaatattgtg	ChIP-qPCR	This study
ProFER1-b-R	ATTTCCGGTTCCCTACTCTCCG	ChIP-qPCR	This study
ProFER1-c-F	CCTCACGTTCCACTATCCCA	ChIP-qPCR	This study
ProFER1-c-R	GATAGTTGAGCCGCCCTGA	ChIP-qPCR	This study
ProFER3-a-F	tcctgtctcttttgagcacagtga	ChIP-qPCR	This study
ProFER3-a-R	tgtgtgagcatttctcattcttaca	ChIP-qPCR	This study
ProFER3-b-F	gccaaaattacacaaataccaacag	ChIP-qPCR	This study
ProFER3-b-R	tgtgcaacgaatttggagga	ChIP-qPCR	This study
ProFER4-a-F	tcttcaatttgaggaatgtgcca	ChIP-qPCR	This study
ProFER4-a-R	agagtgcataaggaacaaatttgg	ChIP-qPCR	This study
ProFER4-b-F	agtgaagagattttgagctgca	ChIP-qPCR	This study
ProFER4-b-R	aggaagtttcttcgagga	ChIP-qPCR	This study
ProNAS4-a-F	tgagagtacacgtgccatcg	ChIP-qPCR	This study
ProNAS4-a-R	cgaaatgaagcaacacatgc	ChIP-qPCR	This study
ProNAS4-b-F	ggcaactctgtgcaatlgat	ChIP-qPCR	This study
ProNAS4-b-R	tcgtgcatatcgtgtg	ChIP-qPCR	This study
ProNAS4-c-F	tcaatgtattgttcttgaatgg	ChIP-qPCR	This study
ProNAS4-c-R	attdtaatttataccaagtgcag	ChIP-qPCR	This study
ProVTL2-a-F	cagtgtaacaagtgtatcaaacga	ChIP-qPCR	This study
ProVTL2-a-R	cgggtgagaaggtgatttatgg	ChIP-qPCR	This study
ProVTL2-b-F	tgtgactggattttggcaat	ChIP-qPCR	This study
ProVTL2-b-R	tttgtagctcgggtgcataacga	ChIP-qPCR	This study



<b>PtOPYE-C-F</b>	GAGATGAGCTTTAGTGGCACCG	ChIP-qPCR	Zhang et al, 2015 - Plant Cell
<b>PtOPYE-C-R</b>	GAAGTCCGAAGTTGAGGAGGG	ChIP-qPCR	Zhang et al, 2015 - Plant Cell
<b>APX1-F</b>	GGTGCAATGGACATCAAAACC	qRT-PCR	This study
<b>APX1-R</b>	ACAGGGTCCTCCAAATAGTGC	qRT-PCR	This study
<b>At-NEET-F</b>	TCGTTGTCACCGAGCTTTCC	qRT-PCR	Rampey et al, 2006 - Genetics
<b>At-NEET-R</b>	ACGTCCCGACCTCCAA	qRT-PCR	Rampey et al, 2006 - Genetics
<b>bHLH39-F</b>	GACGGTTTCGGAAGCTTG	qRT-PCR	Hong et al, 2013 - Plant Physiol
<b>bHLH39-R</b>	GGTGGCTGCTTAACGTTACAT	qRT-PCR	Hong et al, 2013 - Plant Physiol
<b>FER1-F</b>	TCGTTGAGAGTGAATTTCTGG	qRT-PCR	Reyt et al, 2015 - Mol Plant
<b>FER1-R</b>	ACCCCAACATTTGGTCACTG	qRT-PCR	Reyt et al, 2015 - Mol Plant
<b>FER3-F</b>	AGAATGTGTTCTGAACGAAC	qRT-PCR	Reyt et al, 2015 - Mol Plant
<b>FER3-R</b>	CCAACTGCAGATACAGC	qRT-PCR	Reyt et al, 2015 - Mol Plant
<b>FER4-F</b>	AGAGCGAGTTCTGCACAGAG	qRT-PCR	Reyt et al, 2015 - Mol Plant
<b>FER4-R</b>	CACAGTAGACACAAGACTCC	qRT-PCR	Reyt et al, 2015 - Mol Plant
<b>ILR3-F</b>	GCAACCATTGGTGTCTTCTTAATC	qRT-PCR	This study
<b>ILR3-R</b>	CCAGGTTCTTTGGCTPAGCTTCTGA	qRT-PCR	This study
<b>IRT1-F</b>	CGGTTGGACTTCTAAATGC	qRT-PCR	Reyt et al, 2015 - Mol Plant
<b>IRT1-R</b>	CGATAATCGACATTTCCACCG	qRT-PCR	Reyt et al, 2015 - Mol Plant
<b>NAS4-F</b>	GGCTTCGACGTTGTTCTTT	qRT-PCR	This study
<b>NAS4-R</b>	AGCAAGCACCCAGGAGACAT	qRT-PCR	This study
<b>PP2AA3-F</b>	TAAGGTGCCAAATATGTC	qRT-PCR	Reyt et al, 2015 - Mol Plant
<b>PP2AA3-R</b>	GTTCTCCACACCCCTTGGT	qRT-PCR	Reyt et al, 2015 - Mol Plant
<b>PYE-F</b>	CAGGACTTCCCATTTTCCAA	qRT-PCR	This study
<b>PYE-R</b>	CTTGTGTTGGGATCAGGT	qRT-PCR	This study
<b>VTL2-F</b>	GATGGAGTTGGAGCTGNAA	qRT-PCR	Rampey et al, 2006 - Genetics
<b>VTL2-R</b>	CCTCGAATCCGGAGAGAA	qRT-PCR	Rampey et al, 2006 - Genetics
<b>pAtFER1-g-box-LIC-F</b>	CGACAAGAACACATATCCACCCTCCACCGTGATATCCACCCTCCACCGTGATATCCACCCTCCACCGTG	Yeast one-hybrid experiments	This study
<b>pAtFER1-g-box-LIC-R</b>	GAAAGAGACACACATCCAGGTGGGGTGGATATCAGGTGGGGTGGATATCAGGTGGGGTGGATATCAGGTGGGGTGGATATCAGGTGGGGTGGATAT	Yeast one-hybrid experiments	This study
<b>pAtFER1-mg-box-LIC-F</b>	CGACAAGAACACATATCCACCCTCATGGATATATCCACCCTCATGGATATATCCACCCTCATGGATATATCCACCCTCATGGAT	Yeast one-hybrid experiments	This study
<b>pAtFER1-mg-box-LIC-R</b>	GAAAGAGACACATCCATGAGGGTGGATATATCCATGAGGGTGGATATATCCATGAGGGTGGATATATCCATGAGGGTGGATAT	Yeast one-hybrid experiments	This study
<b>PYE-BiFC-F</b>	CGCGGATCCATGGTATCGAAAATCCTTTCC	BiFC experiments	This study
<b>PYE-BiFC-R</b>	CGGGGTACCTTCACTGGTTTCAGCCGCTC	BiFC experiments	This study
<b>ILR3-BiFC-F</b>	GGACTAGTATGGTGTACCCGAAACCG	BiFC experiments	This study
<b>ILR3-BiFC-R</b>	CGGGGTACCAACACAGGAGCACGAAGGAC	BiFC experiments	This study

## **Supplemental Method S1. Detailed protocols for physiological, biochemical, molecular and cytological analyses**

### **Generation of transgenic lines**

*AtFER1* promoter (*ProAtFER1*) fusion to *GUS* (pGWB3 binary vector; Nakagawa et al., 2007) was carried out as described in (Xu et al., 2013). *ProAtFER1* mutations were obtained by PCR reactions. The same procedure was used to fuse the *ILR3* promoter and genomic region (without stop codon) to the *GFP* (pGWB4 binary vector; *ProILR3::gILR3:GFP*). Following *Arabidopsis* transformation (wild type plants through agroinfiltration), 24 independent lines were assayed for GUS activity (for each construct) and 17 for GFP. All the PCR products were obtained using high-fidelity Phusion DNA polymerase and each construct was sequenced to ensure its integrity. All the primers used are described in Supplemental Table S1. Generation of *ilr3-3* and *ilr3-1* mutant plants expressing *ProAtFER1<sub>mini</sub>:GUS* and *ProAtFER1<sub>mini</sub>mG-box:GUS* was obtained by crossing these mutants with wild type plants expressing these constructs. The *ilr3-1* lines overexpressing *AtFER1* were obtained by transforming (agroinfiltration) the corresponding mutant allele with the previously described *Pro35S:AtFER1* binary vector (Duc et al., 2009).

### **Biochemical analyses**

**Chlorophyll content:** Chlorophylls from 25 mg of leaves (FW: fresh weight) were extracted in 1 mL 100% acetone in the dark under agitation. The absorbance (A) at 661.8 and 644.8 nm was then measured. Total chlorophyll content was assessed using the following equations:  $\text{Chl a} + \text{Chl b} = 7.05 * A_{661.6} + 18.09 * A_{644.8}$  and expressed as  $\mu\text{g} \cdot \text{g}^{-1}$  FW (Lichtenthaler, 1987).  
**Iron determination:** 20 mg of ground seedlings (DW: dry weight) per sample were mixed with 750  $\mu\text{L}$  nitric oxide (65%) and 250  $\mu\text{L}$  hydrogen peroxide 30% before homogenization. Following 10 min at room temperature, samples were mineralized using the Microwave digestion system (Berghof, Eningen, Germany). Once mineralized, the nitric oxide proportion present in the samples was adjusted to 5 to 10% of the final volume by adding ultrapure water. Fe content present in the samples was then measured by microwave plasma atomic emission spectroscopy (MP-AES, Agilent, Les Ulis, France).

### **Analysis of GUS activity**

**Histochemical detection:** seedlings expressing the various *ProAtFER1:GUS* gene fusions were transferred into a 100 mM phosphate buffer (pH 7.5) solution containing 2 mM 5-

bromo-4-chloro-3-indolyl- $\beta$ -D-glucuronide, 0.1% Triton X-100, 10 mM Na<sub>2</sub>-EDTA. Prior to incubating the samples at 37°C in the dark (over night), a 1 h vacuum treatment (room temperature) was applied. Following GUS staining, chlorophylls were removed by gently shaking the samples in a clearing solution of acetic acid:ethanol (14:86). Prior to observation under a light microscope, samples were kept in 70% ethanol.

Quantitative analysis (adapted from Jefferson *et al.*, 1987): 5 seedlings per condition were homogenized in 1 mL 50 mM phosphate buffer (pH 7.0) solution containing 0.1% Triton X-100, 10 mM Na<sub>2</sub>-EDTA, 0.1% sodium sarcosine and 10 mM  $\beta$ -mercaptoethanol. Following centrifugation, 40  $\mu$ L of supernatant were mixed with 160  $\mu$ L of the above-described buffer supplemented with 1 mM 4-methylumbelliferyl- $\beta$ -d-glucuronide (4-MUG). Samples were then incubated at 37°C and the production of 4-methylumbelliferone (4-MU) was determined using a luminescence spectrometer (Perkin Elmer Wallac 1420 Victor2 Microplate Reader, Waltham, Massachusetts, USA) at 355 nm excitation and 460 nm emission. Samples were measured once every 8 min during 2 h. Protein content was determined using the Pierce 660 nm protein assay (Thermo scientific, Waltham, Massachusetts, USA) according to manufacturer instructions in order to calculate enzyme activity (nmol 4-MU. min<sup>-1</sup>. mg<sup>-1</sup> proteins).

### **Perls/DAB staining**

Seeds were sowed in MS medium and grown for two weeks under long day conditions (16h/8h light/dark). Seedlings were then planted in soil (3:1 vermiculite: turf) for three weeks. Five-week-old plants were then irrigated for two days with either 1% (w/v) DTPA (Diethylenetriaminepentaacetic acid) chelated iron or water. Collected leaves were fixated with 2% (w/v) paraformaldehyde in 1 mM phosphate buffer pH 7.0 for 45 min. The subsequent steps were conducted according to Roschztardt *et al.*, 2009 and Ibeas *et al.*, 2017.

### **Yeast one-hybrid assays**

Experiments were carried out as described in Dubos *et al.*, 2014, Kelemen *et al.*, 2015 and Kelemen *et al.*, 2016. Briefly, tetramers of target *AtFER1* promoter region (20bp long, Element 5 described Supporting Information Fig. S2) containing the *G-box cis*-regulatory sequence were cloned using the ligation independent cloning system into the pHisi-LIC vector. Following cDNA library screening (Paz-Ares, 2002) without the use of 3-AT (3-Amino-1,2,4-triazole), 4 interacting proteins were identified among which ILR3 was the sole

bHLH transcription factor. Proteins were then re-cloned and assayed against the target *AtFER1* promoter region that contains or not a mutated *G-box* in the presence of 1, 3, 5 and 10 mM 3-AT. Following this screen, ILR3 was the sole TF still interacting with the *AtFER1* promoter region that contains the *G-box* and not with the mutated version. All the primers used are described in Supplemental Table S1.

### **Bimolecular fluorescence complementation (BiFC)**

Experiments were carried out as described in Couturier *et al.*, 2014. All the PCR products were obtained using high-fidelity Phusion DNA polymerase (New England Biolabs, Ipswich, Massachusetts, USA) and each construct was sequenced to ensure its integrity. All the primers used are described in Supplemental Table S1.

### **Chromatin immunoprecipitation (ChIP)**

Experiments were performed as described by Gendrel *et al.*, 2002 with modifications: (i) nuclei were isolated with the following buffer: 20 mM PIPES-KOH pH 7.6, 1 M hexylene glycol, 10 mM MgCl<sub>2</sub>, 0.1 mM EGTA, 15 mM NaCl, 60 mM KCl, 0.5% Triton X100, 5 mM β-mercaptoethanol, protease inhibitor cocktail (complete tablets EASYpack, Roche, Bâle, switzerland), and (ii) after immunoprecipitation using antibodies raised against GFP (ab290, Abcam, Cambridge, United Kingdom), DNA was purified with IPURE Kit (Diagenode, Seraing, Belgium). Resulting DNA was analyzed by qPCR analysis using a LightCycler® 480 (Roche) and the LC480-SYBR-Green master I reaction mix (Roche). The binding measured in *Pro35S:GFP* line for each DNA fragment amplified was set to 1, and the DNA binding ratio was given as the fold increase in signal in *ProILR3:ILR3:GFP* (#1 and #2) or *ProPYE:PYE:GFP* lines relative to binding in *Pro35S:GFP* line. The seedlings used in these experiments were grown under Fe deficiency (-Fe). Two independent experiments were carried out for each line, and three technical repeat (n=3) were done for each experiment. All the primers used are described in Supplemental Table S1.

### **Gene expression analysis**

Total RNAs were extracted using the Tri-Reagent (Molecular Research Center, Cincinnati, Ohio, USA) method. Briefly, each sample was homogenized in 1 mL Tri-Reagent solution mixed with 160 μL of chloroform:isoamyl alcohol (24:1). Following centrifugation (10 min, 16.000 g, 4°C) total RNAs present in the aqueous phase were precipitated by the addition of 400 μL of isopropanol followed by another centrifugation. Pellets were then washed twice

with ethanol 70% and dried prior to resuspension in RNase-free water. For each sample 1 µg of total RNA treated with DNase was reverse transcribed into cDNA using the RevertAid kit (Thermo scientific). qRT-PCR analyses were performed as described earlier for ChIP experiments. *PP2AA3* (*PROTEIN PHOSPHATASE 2A SUBUNIT A3*) was used as reference gene (Czechowski *et al.*, 2005). Expression levels were calculated using the comparative threshold cycle method.

### Western blot analysis

Total proteins were extracted from 100 mg of samples grinded in liquid nitrogen and homogenized in 250 µL of 1x Laemmli buffer (62,5 mM Tris-HCl pH 6.8, 3% SDS, 100 mM DTT, 10% glycerol) preheated at 95°C and then incubated at 95°C for 5 min. Following two consecutive centrifugations the supernatant was collected and stored on ice prior use. Protein content was determined using the Pierce 660 nm protein assay (Thermo scientific) according to manufacturer's instructions. Proteins were separated by 12% SDS-PAGE and transferred to a PVDF membrane. Membranes were blocked for 1 h in TBST buffer (50 mM Tris pH 7.5, 150 mM NaCl, 0.1% Tween-20) containing 2% skimmed milk and then incubated overnight with primary antibody and then 1 h with secondary antibody, both diluted in TBST containing 1% skimmed milk. Dilutions of primary antibodies applied were: mouse anti-GFP (JL-8, Clontech, St-Germain-en-Laye, France) 1:4000, rabbit anti-AtFER1 that recognizing the four Arabidopsis ferritin proteins (Dellagi *et al.*, 2005) 1:10000. Dilutions of secondary antibodies applied were: goat anti-mouse HRP conjugated (W4021, Promega, Charbonnières-les-Bains, France) 1:10000, goat anti-rabbit HRP conjugated (W4011, Promega) 1:10000. Immunodetection was performed using the Clarity Western ECL substrate (Biorad, Marnes-la-Coquette, France). Coomassie blue was used as loading control.

### References

- Buenrostro JD, Giresi PG, Zaba LC, Chang HY, Greenleaf WJ. 2013.** Transposition of native chromatin for fast and sensitive epigenomic profiling of open chromatin, DNA-binding proteins and nucleosome position. *Nat Methods* **10**(12): 1213-1218.
- Couturier, J., Wu, H.C., Dhalleine, T., Pegeot, H., Sudre, D., Gualberto, J.M., Jacquot, J.P., Gaymard, F., Vignols, F., and Rouhier, N. 2014.** Monothiol glutaredoxin-BolA interactions: redox control of *Arabidopsis thaliana* BolA2 and SufE1. *Mol Plant* **7**:187-205.
- Czechowski, T., Stitt, M., Altmann, T., Udvardi, M.K., and Scheible, W.R. 2005.** Genome-wide identification and testing of superior reference genes for transcript normalization in Arabidopsis. *Plant Physiol* **139**:5-17.

- Dubos, C., Kelemen, Z., Sebastian, A., Bülow, L., Huep, G., Xu, W., Grain, D., Salsac, F., Brousse, C., Lepiniec, L., et al. 2014. Integrating bioinformatic resources to predict transcription factors interacting with *cis*-sequences conserved in co-regulated genes. *BMC Genomics* Apr **28**:317.
- Dellagi A, Rigault M, Segond D, Roux C, Kraepiel Y, Cellier F, Briat JF, Gaymard F, Expert D. 2005. Siderophore-mediated upregulation of Arabidopsis ferritin expression in response to *Erwinia chrysanthemi* infection. *Plant J* **43**:262-272.
- Duc C, Cellier F, Lobreaux S, Briat JF, Gaymard F. 2009. Regulation of iron homeostasis in *Arabidopsis thaliana* by the clock regulator time for coffee. *J Biol Chem* **284**(52): 36271-36281.
- Gendrel AV, Lippman Z, Yordan C, Colot V, Martienssen RA. 2002. Dependence of heterochromatic histone H3 methylation patterns on the Arabidopsis gene DDM1. *Science* **297**(5588):1871-1873.
- Hong S, Kim SA, Guerinot ML, McClung CR. 2013. Reciprocal interaction of the circadian clock with the iron homeostasis network in Arabidopsis. *Plant Physiol* **161**(2):893-903.
- Ibeas MA, Grant-Grant S, Navarro N, Perez MF, Roschttardt H. 2017. Dynamic subcellular localization of iron during embryo development in *Brassicaceae* seeds. *Front Plant Sci* **8**:2186.
- Jefferson RA, Kavanagh TA, Bevan MW. 1987. GUS fusions: beta-glucuronidase as a sensitive and versatile gene fusion marker in higher plants. *EMBO J* **6**(13):3901-3907.
- Jégu T, Veluchamy A, Ramirez-Prado JS, Rizzi-Paillet C, Perez M, Lhomme A, Latrassé D, Coleno E, Vicaire S, Legras S, Jost B, Rougée M, Barneche F, Bergounioux C, Crespi M, Mahfouz MM, Hirt H, Raynaud C, Benhamed M. 2017. The Arabidopsis SWI/SNF protein BAF60 mediates seedling growth control by modulating DNA accessibility. *Genome Biol* **18**(1):114.
- Kelemen Z, Przybyla-Toscano J, Tissot N, Lepiniec L, Dubos C. 2016. Fast and efficient cloning of *cis*-regulatory sequences for high-throughput yeast one-hybrid analyses of transcription factors. *Methods Mol Biol* **1482**:139-149.
- Kelemen Z, Sebastian A, Xu W, Grain D, Salsac F, Avon A, Berger N, Tran J, Dubreucq B, Lurin C, Lepiniec L, Contreras-Moreira B, Dubos C. 2015. Analysis of the DNA-binding activities of the arabidopsis R2R3-MYB transcription factor family by one-hybrid experiments in yeast. *PLoS One* **10**(10):e0141044.
- Li X, Zhang H, Ai Q, Liang G, Yu D. 2016. Two bHLH transcription factors, bHLH34 and bHLH104, regulate iron homeostasis in *Arabidopsis thaliana*. *Plant Physiol* **170**(4): 2478-2493.
- Lichtenthaler FW. 1987. Karl Freudenberg, Burckhardt Helferich, Hermann O. L. Fischer: a centennial tribute. *Carbohydr Res* **164**:1-22.
- Nakagawa T, Kurose T, Hino T, Tanaka K, Kawamukai M, Niwa Y, Toyooka K, Matsuoka K, Jinbo T, Kimura T. 2007. Development of series of gateway binary vectors, pGWBs, for realizing efficient construction of fusion genes for plant transformation. *J Biosci Bioeng* **104**(1): 34-41.
- Paz-Ares, J, Regia Consortium. 2002. REGIA, an EU project on functional genomics of transcription factors from *Arabidopsis thaliana*. *Comp Funct Genomics* **3**(32):102-108.
- Rampey RA, Woodward AW, Hobbs BN, Tierney MP, Lahner B, Salt DE, Bartel B. 2006. An Arabidopsis basic helix-loop-helix leucine zipper protein modulates metal homeostasis and auxin conjugate responsiveness. *Genetics* **174**(4): 1841-1857.
- Reyt G, Boudouf S, Boucherez J, Gaymard F, Briat JF. 2015. Iron- and ferritin-dependent reactive oxygen species distribution: impact on Arabidopsis root system architecture. *Mol Plant* **8**(3): 439-453.

- Roschzttardt H, Conejero G, Curie C, Mari S. 2009.** Identification of the endodermal vacuole as the iron storage compartment in the *Arabidopsis* embryo. *Plant Physiol* **151**(3): 1329-1338.
- Strozycki PM, Szymanski M, Szczurek A, Barciszewski J, Figlerowicz M. 2010.** A new family of ferritin genes from *Lupinus luteus* - comparative analysis of plant ferritins, their gene structure, and evolution. *Mol Biol Evol* **27**(1):91-101.
- Xu W, Grain D, Le Gourrierec J, Harscoet E, Berger A, Jauvion V, Scagnelli A, Berger N, Bidzinski P, Kelemen Z, Salsac F, Baudry A, Routaboul JM, Lepiniec L, Dubos C. 2013.** Regulation of flavonoid biosynthesis involves an unexpected complex transcriptional regulation of *TT8* expression in *Arabidopsis*. *New Phytol* **198**:59-70.
- Zhang J, Liu B, Li M, Feng D, Jin H, Wang P, Liu J, Xiong F, Wang J, Wang HB. 2015.** The bHLH transcription factor bHLH104 interacts with IAA-LEUCINE RESISTANT3 and modulates iron homeostasis in *Arabidopsis*. *Plant Cell* **27**(3): 787-805.

# **CHAPTER III**

## **BHLH121 INTEGRATES IRON RESPONSES**





**Article 3. The transcription factor bHLH121 interacts with  
bHLH105 (ILR3) and its closest homologs to regulate iron  
homeostasis in Arabidopsis**





# The Transcription Factor bHLH121 Interacts with bHLH105 (ILR3) and Its Closest Homologs to Regulate Iron Homeostasis in Arabidopsis

Fei Gao,<sup>a</sup> Kevin Robe,<sup>a</sup> Mathilde Bettembourg,<sup>a</sup> Nathalia Navarro,<sup>b</sup> Valérie Rofidal,<sup>a</sup> Véronique Santoni,<sup>a</sup> Frédéric Gaymard,<sup>a</sup> Florence Vignols,<sup>a</sup> Hannetz Roschztardt,<sup>b</sup> Esther Izquierdo,<sup>a</sup> and Christian Dubos<sup>a,1</sup>

<sup>a</sup>Biochimie et Physiologie Moléculaire des Plantes, University of Montpellier, Centre National de la Recherche Scientifique, Institut National de la Recherche Agronomique, SupAgro, 34060 Montpellier, France

<sup>b</sup>Departamento de Genética Molecular y Microbiología, Pontificia Universidad Católica de Chile, 8331150, Santiago, Chile

ORCID IDs: 0000-0002-4347-8499 (F.Gao); 0000-0001-7825-2142 (K.R.); 0000-0002-4214-0891 (M.B.); 0000-0002-1314-4391 (N.N.); 0000-0001-7666-7475 (V.R.); 0000-0002-1437-0921 (V.S.); 0000-0003-4278-2787 (F.Gaymard); 0000-0002-2031-0407 (F.V.); 0000-0002-2614-2504 (H.R.); 0000-0003-0448-4447 (E.I.); 0000-0001-5486-3643 (C.D.)

**Iron (Fe) is an essential micronutrient for plant growth and development. Any defects in the maintenance of Fe homeostasis will alter plant productivity and the quality of their derived products. In Arabidopsis (*Arabidopsis thaliana*), the transcription factor ILR3 plays a central role in controlling Fe homeostasis. In this study, we identified bHLH121 as an ILR3-interacting transcription factor. Interaction studies showed that bHLH121 also interacts with the three closest homologs of ILR3 (i.e., basic-helix-loop-helix 34 [bHLH34], bHLH104, and bHLH115). *bhlh121* loss-of-function mutants displayed severe defects in Fe homeostasis that could be reverted by exogenous Fe supply. bHLH121 acts as a direct transcriptional activator of key genes involved in the Fe regulatory network, including *bHLH38*, *bHLH39*, *bHLH100*, *bHLH101*, *POPEYE*, *BRUTUS*, and *BRUTUS LIKE1*, as well as *IRONMAN1* and *IRONMAN2*. In addition, bHLH121 is necessary for activating the expression of transcription factor gene *FIT* in response to Fe deficiency via an indirect mechanism. *bHLH121* is expressed throughout the plant body, and its expression is not affected by Fe availability. By contrast, Fe availability affects the cellular localization of bHLH121 protein in roots. Altogether, these data show that bHLH121 is a regulator of Fe homeostasis that acts upstream of *FIT* in concert with ILR3 and its closest homologs.**

## INTRODUCTION

Iron (Fe) is an essential micronutrient for plant growth and development, as it is a cofactor for several enzymes that participate in many fundamental biological processes (Hänsch and Mendel, 2009). Any defects in the maintenance of Fe homeostasis will alter plant productivity and the quality of their derived products (Briet et al., 2015). Efficient Fe uptake from soil is ensured, in dicot and nongraminaceous monocot species, by a reduction-based mechanism (Kobayashi and Nishizawa, 2012; Brumbarova et al., 2015). This process involves the reduction of Fe<sup>3+</sup> by Fe<sup>3+</sup>-reductases such as FERRIC REDUCTION OXIDASE2 (*FRO2*) and the subsequent transport of the reduced Fe<sup>2+</sup> across the rhizodermis cell plasma membrane via IRON-REGULATED TRANSPORTER1 (*IRT1*). Fe<sup>3+</sup> solubilization is facilitated by two distinct mechanisms that act in concert: the acidification of the rhizosphere and the secretion of Fe<sup>3+</sup>-mobilizing coumarins (Santi and Schmidt, 2009; Fourcroy et al., 2016).

Fe homeostasis is tightly regulated at the transcriptional level by a process involving numerous basic-helix-loop-helix (bHLH)

transcription factors (TFs) that form an intricate network (Gao et al., 2019). In Arabidopsis (*Arabidopsis thaliana*), 16 bHLH TFs (~12% of this gene family) have thus far been shown to participate in this network. Emerging evidence derived from analysis of the molecular and genetic relationships between these TFs indicates that FER-LIKE IRON DEFICIENCY-INDUCED TRANSCRIPTION FACTOR (*FIT*)/bHLH29 and IAA-LEUCINE RESISTANT3 (*ILR3*)/bHLH105 are two important nodes in this regulatory network (Ivanov et al., 2012; Zhang et al., 2015; Tissot et al., 2019).

*FIT* is the Arabidopsis ortholog of tomato (*Solanum lycopersicum*) *FER*, the first cloned regulatory gene involved in Fe homeostasis (Ling et al., 2002; Colangelo and Guerinot, 2004; Yuan et al., 2005). In Arabidopsis, the *fit* null mutation is lethal during early seedling development without an extra supply of Fe and the induction of the Fe uptake machinery in response to Fe shortage is abolished (Colangelo and Guerinot, 2004). Interactions of *FIT* with bHLH38, bHLH39, bHLH100, and bHLH101 are required for inducing the expression of its target genes, including *FRO2* and *IRT1* (Yuan et al., 2008; Wang et al., 2013). The activity of these heterodimers is counteracted by bHLH18, bHLH19, bHLH20, and bHLH25, whose interaction with *FIT* promotes its degradation via the 26S proteasome pathway (Cui et al., 2018). *BRUTUS LIKE1* (*BTSL1*) and *BTSL2*, two closely related RING E3 ubiquitin ligases, have also been recently proposed to negatively regulate Fe deficiency responses by directly targeting *FIT*, leading to its degradation via the 26S proteasome (Sivitz et al., 2011; Hindt et al., 2017; Rodríguez-Celma et al., 2019).

<sup>1</sup> Address correspondence to christian.dubos@inra.fr.

The author responsible for distribution of materials integral to the findings presented in this article in accordance with the policy described in the Instructions for Authors (www.plantcell.org) is: Christian Dubos (christian.dubos@inra.fr).

www.plantcell.org/cgi/doi/10.1105/tpc.19.00541

## IN A NUTSHELL

**Background:** Iron (Fe) is an essential micronutrient for plant growth and development since it is required for the activity of several enzymes involved in fundamental processes such as photosynthesis and respiration. The availability of this micronutrient for plants depends on the nature of the soil and the plant's ability to take it up. In order to avoid any deficiency or excess that could be detrimental, plants have evolved sophisticated molecular mechanisms to maintain Fe homeostasis. A cascade of transcription factors (TFs) controls this process by regulating the expression of genes involved in Fe uptake, transport, and storage. Understanding how this regulatory cascade is regulated might help improve food crop production without the use of Fe fertilizers, as these fertilizers are expensive and their sustainability in modern agriculture is questionable.

**Question:** Iron homeostasis in plants involves the activities of several TFs, but how these activities are coordinated remains a key question. As we already identify ILR3 as a TF that plays a critical role in the maintenance of Fe homeostasis in *Arabidopsis thaliana*, we used ILR3 as a target to reveal novel key players that participate in this process.

**Findings:** The bHLH121 TF interacts with ILR3 and its closest homologs. *bhlh121* loss-of-function mutants display severe Fe homeostasis defects that can be reverted by exogenous Fe supply, either in vitro or in soil. Importantly, bHLH121 acts upstream of the Fe homeostasis regulatory network by directly regulating the expression of genes encoding most TFs and associated regulatory proteins/peptides involved in this process. Finally, Fe availability does not modulate *bHLH121* expression but instead affects its protein localization within the root tissues.

**Next steps:** We proposed a model for the Fe homeostasis regulatory network. The validation of this model will require us to document how Fe availability affects the spatial distribution of bHLH121 together with the various actors involved in this regulatory network. Another important question to be addressed is how bHLH121 is regulated at the post-transcriptional and/or at post-translational levels.

ILR3 and its three closest homologs (i.e., bHLH34, bHLH104, and bHLH115) can form homo- and heterodimers. These four bHLH TFs positively regulate Fe homeostasis by directly activating the expression of *bHLH38*, *bHLH39*, *bHLH100*, and *bHLH101* (Heim et al., 2003; Zhang et al., 2015; Li et al., 2016; Liang et al., 2017). ILR3 also acts as a transcriptional repressor when interacting with POPEYE (PYE)/bHLH47, a TF originally described as playing a negative role in the Fe deficiency responses (Long et al., 2010; Tissot et al., 2019). *PYE* expression is induced in response to Fe shortage by ILR3 and its closest homologs (Zhang et al., 2015; Liang et al., 2017; Kroh and Pilon, 2019; Tissot et al., 2019). It is likely that a negative feedback regulatory loop involving the ILR3-PYE complex represses *PYE* expression when Fe availability is not limiting (Tissot et al., 2019). ILR3 and bHLH115 interact with BRUTUS (BTS), an Fe binding E3 ubiquitin ligase closely related to BTSL1 and BTSL2, leading to their degradation via the 26S proteasome, allowing fine tuning of Fe uptake (Selote et al., 2015; Matthiadis and Long, 2016). Interestingly, a family of peptides named IRON MAN/FE-UPTAKE-INDUCING PEPTIDE (IMA/FEIP) was recently shown to play a critical role in the acquisition and cellular homeostasis of Fe in plants by regulating the expression of *bHLH38* and *bHLH39* (Grillet et al., 2018; Hirayama et al., 2018).

In this study, we performed co-immunoprecipitation of ILR3 followed by liquid chromatography tandem-mass spectrometry (Co-IP LC-MS/MS) analyses and identified bHLH121 (a close homolog of PYE) as an ILR3-interacting TF. Interaction studies showed that bHLH121 also interacts with bHLH34, bHLH104, and bHLH115, but not with PYE, FIT, BTS, BTSL1, or BTSL2. Loss-of-function of bHLH121 (*bhlh121*) led to severe defects in Fe homeostasis, which were reverted by exogenous Fe supply. Expression studies and chromatin immunoprecipitation (ChIP) assays indicated that bHLH121 functions as a direct

transcriptional activator of key genes involved in the Fe regulatory network, including *bHLH38*, *bHLH39*, *bHLH100*, *bHLH101*, *PYE*, *BTS*, and *BTSL1* as well as *IMA1* and *IMA2*. In addition, bHLH121 is required for the activation of *FIT* expression in response to Fe deficiency via an indirect mechanism. *bHLH121* is expressed throughout the plant, and its expression is not affected by Fe availability. By contrast, Fe availability affects the cellular localization of bHLH121 in roots. Therefore, bHLH121 regulates Fe homeostasis in *Arabidopsis* by acting upstream of *FIT* together with ILR3 and its closest homologs.

## RESULTS

### bHLH121 Interacts with ILR3 in Vivo

ILR3 plays a key role in regulating Fe homeostasis in *Arabidopsis* (Zhang et al., 2015; Li et al., 2016; Tissot et al., 2019). We therefore conducted Co-IP LC-MS/MS to identify potential new actors involved in controlling Fe homeostasis. For this purpose, ILR3:GFP fusion protein was immunoprecipitated from *ilr3-3* knockdown mutant lines complemented with the *ProILR3:gILR3:GFP* construct and subjected to Fe starvation (Tissot et al., 2019). Co-IP LC-MS/MS analysis led to the identification of 13 proteins (Supplemental Table). Among the potential ILR3-interacting proteins, bHLH121, a close homolog of PYE and bHLH11 (Heim et al., 2003), was identified.

We conducted yeast two-hybrid (Y2H) assays using bHLH121 as bait (fused with the binding domain of GAL4) and ILR3 as prey (fused with the activation domain of GAL4) to confirm this interaction. We also used the closest homologs of ILR3 and bHLH121 as well as BTS, BTSL1, and BTSL2 as prey. This orientation was used since self-activation was observed for bHLH34 and bHLH104 when they were used as bait. These experiments

confirmed the interaction between bHLH121 and ILR3 (Figure 1A). They also showed that bHLH121 can interact *in vivo* with bHLH34, bHLH104, and bHLH115, but not with PYE, BTS, BTSL1, BTSL2, or itself (Figure 1A; Supplemental Figure 1A). We also detected a weak interaction with bHLH11 (Figure 1A).

We further analyzed these interactions using bimolecular fluorescence complementation (BiFC) assays in which bHLH121 was fused to the C-terminal part of the yellow fluorescent protein (YFP) reporter gene (Figure 1B). The other TFs were fused to the YFP N-terminal part. Strong signal was observed in the nucleus when bHLH121 was assayed with bHLH34, bHLH104, bHLH115, and ILR3, whereas no signal was observed with PYE, bHLH11, or itself. This approach confirmed the interactions observed by Co-IP LC-MS/MS and Y2H experiments.

To complete this study, we performed Y2H assays using bHLH11 and FIT as bait and prey, respectively. These experiments revealed that, like bHLH121, bHLH11 interacts *in vivo* with ILR3 and its three closest homologs (Supplemental Figure 1B). However, it also revealed that unlike bHLH121, bHLH11 can form homodimers. By contrast, no interaction between FIT and bHLH121 was observed (Supplemental Figure 1C).

Altogether, these data indicate that bHLH121 can form heterodimers with bHLH34, bHLH104, bHLH115, and ILR3, but not with PYE, bHLH11, or FIT. In addition, these data indicate that bHLH121 cannot form homodimers and suggest that BTS, BTSL1, and BTSL2 are likely not involved in the regulation of bHLH121 stability.

### *bhlh121* Knockout Mutants Have Altered Fe Homeostasis

To determine whether bHLH121 plays a role in controlling Fe homeostasis, we generated three independent loss-of-function mutant alleles using the clustered regular interspaced short palindromic repeats/associated protein 9 (CRISPR-Cas9) gene editing system. One allele displayed a 656-bp deletion (*bhlh121-2*) leading to a truncated protein, and the two other alleles contained a single nucleotide insertion (*bhlh121-1* and *bhlh121-4*) leading to premature stop codons (Supplemental Figure 2). All three mutations are located in the second exon, affecting the integrity of the bHLH DNA binding domain. In the absence of Fe (0  $\mu\text{M}$  Fe), the *bhlh121* mutants displayed a strong inhibition of primary root growth and ferric-chelate reductase (FCR) activity compared with

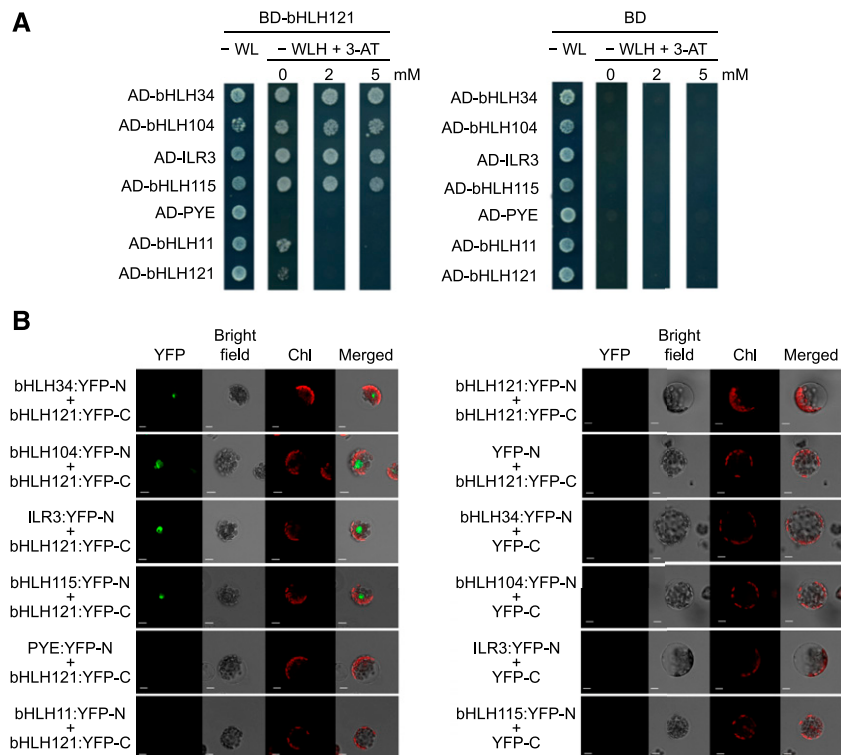


**Figure 1.** bHLH121 Interacts *In Vivo* with ILR3 and with Its Closest Homologs.

**(A)** Y2H assays. bHLH34, bHLH104, ILR3, bHLH115, PYE, bHLH11, and bHLH121 were fused with the GAL4 activation domain (AD) and bHLH121 with the GAL4 DNA binding domain (BD) into appropriate expression vectors prior to transfer into yeast (AH109 strain). The different yeast strains were plated on nonselective medium (-WL) or on selective medium lacking histidine (-WLH) and containing various concentration of 3-amino-1,2,4-triazole (3-AT). BD alone was used as a negative control. Growing colonies representative of positive Y2H interactions were identified after 6 d of growth. H, histidine; L, leucine; W, tryptophan.

**(B)** BiFC assays. bHLH34, bHLH104, ILR3, bHLH115, PYE, bHLH11, and bHLH121 were fused with the N-terminal part of YFP (YFP-N) and bHLH121 with the C-terminal part of YFP (YFP-C) into appropriate expression vectors prior to transfer into Arabidopsis protoplasts and analysis by confocal microscopy. YFP-C and YFP-N alone were used as negative controls. Chl, chlorophyll fluorescence. Bar = 10  $\mu\text{m}$ .

the wild type (Figures 2A to 2C). Fresh weight and chlorophyll contents were also lower in the mutants than in the wild type (Figures 2D and 2E). When the mutants were grown in the presence of 50  $\mu\text{M}$  Fe (control conditions), the root growth and fresh weight defects were partially rescued and the chlorosis symptoms were still visible. By contrast, when grown in the presence of 200  $\mu\text{M}$  Fe (mild Fe excess conditions), the mutants had no discernible differences from the wild type. However, at this concentration of Fe, the primary root length and fresh weight of the wild type were slightly reduced compared with control conditions. Interestingly, the mutants appeared to be a bit less affected than

the wild type by the presence of 500  $\mu\text{M}$  Fe in the medium (Fe excess conditions). Fe accumulation was also compromised in mutant plants grown under control conditions, suggesting limitations in Fe uptake (Figure 2F).

When grown in soil, the *bhlh121* mutants displayed severe growth defects (e.g., reduced rosette and stem size and flower number) and chlorosis symptoms that were rescued by exogenous supply of Fe (Figures 3A and 3C). We also observed a decrease in Fe accumulation in seeds (Figure 3D). This reduced accumulation of Fe in *bhlh121* seeds might explain the growth defects observed upon germination under Fe deficiency (Figure 2A).

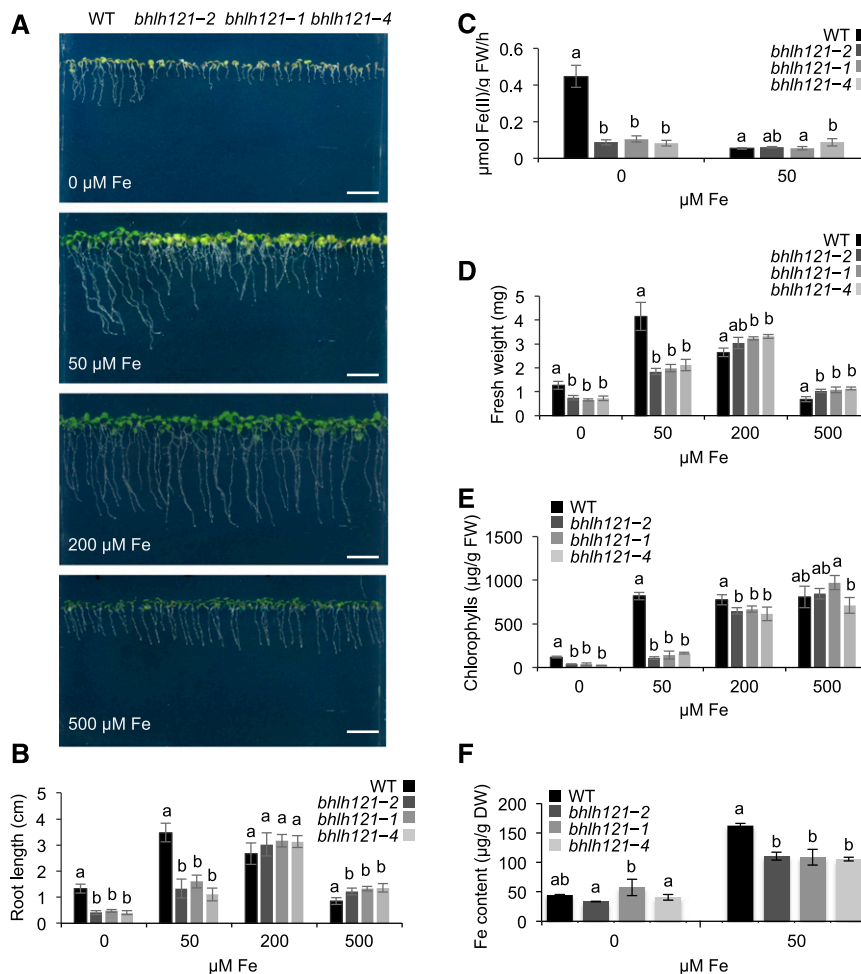


**Figure 2.** *bhlh121* Loss-of-Function Mutants Have Decreased Tolerance to Fe Deficiency.

**(A)** Phenotypes of the Arabidopsis wild type (WT) and the three *bhlh121* mutant alleles grown for 1 week on Fe-sufficient (50  $\mu\text{M}$  Fe), Fe-deficient (0  $\mu\text{M}$  Fe), or Fe-excess (200 and 500  $\mu\text{M}$  Fe) medium. Bar = 1 cm.

**(B)** Root length of the wild type (WT) and the *bhlh121* mutants grown on Fe-sufficient, Fe-deficient, and Fe-excess medium for 7 d.

**(C)** Ferric-chelate reductase activity of the wild type (WT) and the *bhlh121* mutants grown for 1 week under control conditions and transferred to Fe-sufficient or Fe-deficient medium for 3 d.

**(D)** and **(E)** Fresh weight (FW; see **[D]**) and chlorophyll content **(E)** of the wild type (WT) and the *bhlh121* mutants grown on Fe-sufficient, Fe-deficient, and Fe-excess medium for 7 d.

**(F)** Fe contents of the wild type (WT) and the *bhlh121* mutants grown on Fe-sufficient or Fe-deficient medium for 7 d.

**(B)** to **(F)** Means within each condition with the same letter are not significantly different according to one-way ANOVA followed by post hoc Tukey test,  $P < 0.05$  ( $n = 3$  biological repeats from one representative experiment). Error bars show  $\pm$ SD. A biological repeat comprised a pool of 12 seedlings in **(B)**, 40 seedlings in **(C)**, 5 seedlings in **(D)** and **(E)**, and  $\sim$ 80 to 100 seedlings in **(F)**. Each experiment was repeated three times.

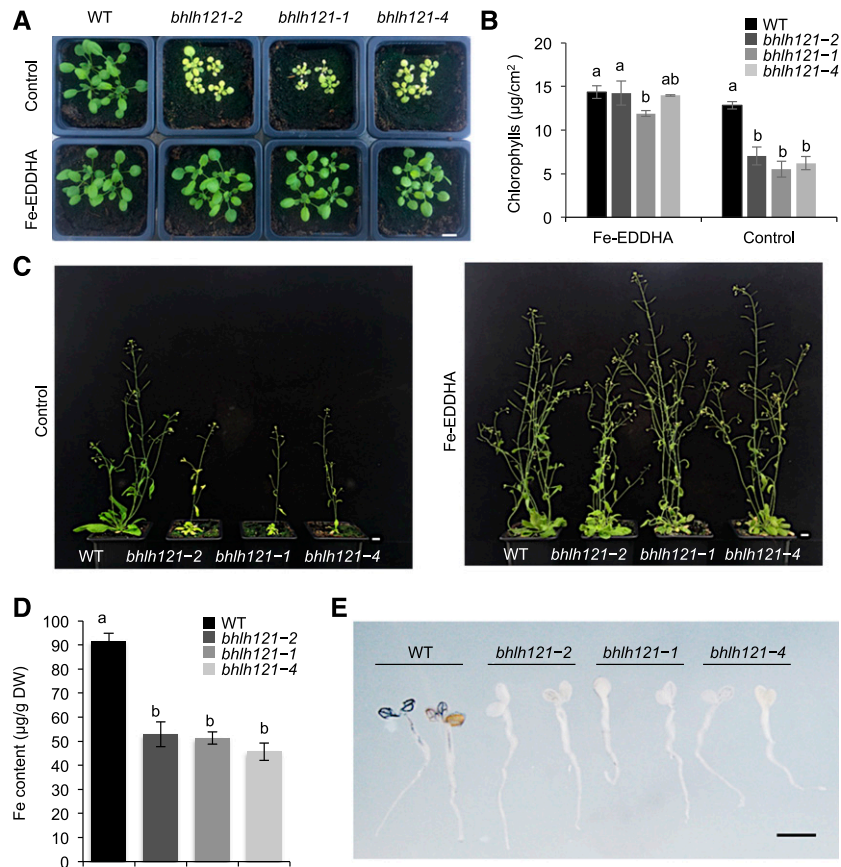


**Figure 3.** *bhlh121* Loss-of-Function Mutants Have Decreased Tolerance to Fe Deficiency and Accumulate Less Fe in Seeds Than the Wild Type.

(A) Phenotype of the wild-type (WT) and *bhlh121* loss-of-function mutant seedlings grown in soil for 3 weeks and watered or not with ferric ethylenediamine di-(*o*-hydroxyphenylacetate) [Fe-EDDHA, 1‰ (w/v)], a form of Fe easily assimilated by plants.

(B) Chlorophyll content of the wild type (WT) and *bhlh121* mutants grown in soil for 3 weeks and watered or not with ferric ethylenediamine di-(*o*-hydroxyphenylacetate) (Fe-EDDHA).

(C) Phenotypes of the wild type (WT) and *bhlh121* mutants grown in soil for 6 weeks and watered or not with ferric ethylenediamine di-(*o*-hydroxyphenylacetate) (Fe-EDDHA).

(D) Fe content in seeds of the wild type (WT) and *bhlh121* mutants grown in soil in the absence of ferric ethylenediamine di-(*o*-hydroxyphenylacetate) (Fe-EDDHA).

(E) Fe distribution (Perls/DAB staining) in 4-d-old wild-type (WT) and *bhlh121* seedlings. Fe accumulation appears in black.

(B) and (D) Means within each condition with the same letter are not significantly different according to one-way ANOVA followed by post hoc Tukey test,  $P < 0.05$  ( $n = 3$  biological repeats from one representative experiment). Error bars show  $\pm$ SD. A biological repeat comprised a pool of leaf disc samples from three seedlings in (B) and  $\sim 10$  mg of seeds in (D). Each experiment was repeated three times. Bar in (A) and (C) = 1 cm; bar in (E) = 1 mm.

In situ analysis of Fe accumulation in the embryo confirmed that Fe content (as revealed by a darker Perls and Perls/3'-Diaminobenzidine tetrahydrochloride [DAB] staining), and not Fe localization (near the vasculature), was altered in the mutants compared with the wild type (Supplemental Figure 3). Following germination, Perls/DAB staining confirmed the latter observation (Figure 3E).

To determine how the mutation of *bHLH121* affects Fe accumulation in roots and/or shoots, we grew the mutant and wild-type plants in hydroponic solution and subjected them to Fe deficiency or control conditions. A decrease in Fe accumulation was observed in the roots of the mutants regardless of whether the plants were grown in the presence or absence of Fe (Supplemental Figure 4A). Such a decrease was also observed in the shoots (but

to a lesser extent) of mutant plants grown under control conditions, whereas no difference was detected when grown under Fe deficiency (Supplemental Figure 4B).

### **bHLH121 Regulates the Biosynthesis of Fe-Mobilizing Coumarins**

Since Fe accumulation and FCR activity were compromised in the *bhlh121* mutant lines, we analyzed *IRT1* and *FRO2* expression. We used 1-week-old seedlings subjected or not to Fe deficiency for this experiment. As expected, RT-qPCR revealed that *IRT1* and *FRO2* expression was reduced in *bhlh121* seedlings grown under control conditions compared with the wild type and that Fe deficiency-induced expression of both genes was also compromised (Figure 4A).



We then investigated the expression of genes that participate in the coumarin biosynthesis and secretion pathway (Figures 4B and 4C). This analysis revealed that the induction of *F6'H1* (the first gene committed to the biosynthesis of coumarins) expression in response to Fe deficiency was reduced in all three *bhlh121* mutant alleles compared with the wild type (Rodríguez-Celma et al., 2013; Schmid et al., 2014). This was also observed for *S8H* and *CYP82C4*, encoding enzymes involved in the biosynthesis of the main Fe-mobilizing coumarins (fraxetin and sideretin, respectively; Rajniak et al., 2018; Siwinska et al., 2018; Tsai et al., 2018). We therefore assayed the expression of *PDR9* (ABCG transporter) and *BGLU42* ( $\beta$ -glucosidase), two genes necessary for the secretion of coumarins in the rhizosphere (Fourcroy et al., 2014; Zamioudis et al., 2014). *PDR9* expression in response to Fe deficiency was not significantly affected in the mutants compared with the wild type, whereas *BGLU42* expression was reduced. We also analyzed the expression of *MYB10* and *MYB72*, encoding two TFs required for plant growth under Fe deficiency, and the production and excretion of coumarins in the rhizosphere (by regulating for instance *BGLU42* expression; Figure 4D; Palmer et al., 2013; Zamioudis et al., 2014). Both genes displayed a lack of induction in response to Fe deficiency in the mutants. These data suggest that bHLH121 is a positive regulator of fraxetin and sideretin biosynthesis and excretion in the rhizosphere.

We measured coumarin accumulation in the roots of the wild type, *f6'h1-1*, *cyp82c4-1*, and *bhlh121-2* plants subjected to Fe deficiency at pH 5.5, the pH at which sideretin biosynthesis and secretion preferentially occurs (Rajniak et al., 2018). As expected, the wild-type plants grown under this condition accumulated more sideretin and sideretin-glycosides in their roots than the wild-type plants grown under control conditions (Figure 4E; Supplemental Figure 5). Similar defects that were previously described for coumarin accumulation in *cyp82c4-1* (i.e., increased fraxin [fraxetin glycoside] accumulation and the absence of sideretin and sideretin-glycosides) and in *f6'h1-1* (i.e., no coumarin accumulation) were also confirmed. In the roots of the *bhlh121-2* mutant, sideretin and sideretin-glycosides were not detected, and the accumulation of scopolin (scopoletin glycoside) was reduced. As expected, when grown at pH 7, Fe deficiency led to an increase in esculin and fraxin levels in the wild-type roots compared with the wild-type plants grown under control conditions (Supplemental Figure 6). By contrast, very little esculin and fraxin were detected in *bhlh121-2* at pH 7. Scopolin accumulation was also reduced at this pH. These coumarin measurements, which support the results of expression analysis, indicate that bHLH121 is a transcriptional activator of fraxetin and sideretin biosynthesis.

### **bHLH121 Is Required to Trigger the Transcriptional Regulatory Cascade That Controls Fe Deficiency Responses**

We performed RT-qPCR experiments to help decipher the positioning of bHLH121 within the transcriptional regulatory network that controls Fe homeostasis. This was achieved by analyzing the mRNA abundance of the major genes involved in controlling this pathway in 1-week-old seedlings subjected or not to Fe deficiency.

These experiments showed that the induction of *bHLH38*, *bHLH39*, *bHLH100*, *bHLH101*, and *PYE* expression in response to Fe deficiency was strongly reduced in all three mutants compared with the wild type, indicating that bHLH121 acts as an activator upstream of these TFs (Figure 5A; Supplemental Figure 7). By contrast, the expression levels of *bHLH34*, *bHLH104*, *bHLH115*, and *ILR3* in the mutants were similar to those of the wild type (Supplemental Figure 7). The induction of *FIT* expression in response to Fe deficiency was abolished in all three *bhlh121* mutant alleles, indicating that bHLH121 acts as an activator upstream of *FIT* (Figure 5A). The induction of *BTS*, *BTSL1*, *IMA1*, and *IMA2* expression in response to Fe deficiency was also reduced in the mutants compared with the wild type, whereas no difference was observed for *BTSL2* or *IMA3* (Figure 5A).

We generated transgenic plants overexpressing *bHLH121* under the control of the Arabidopsis *UBIQUITIN10* promoter (*ProUBI*). Based on root length measurements, we selected one representative line (*ProUBI:bHLH121-Ox3*) for gene expression analysis (Supplemental Figure 8). RT-qPCR highlighted the notion that *IRT1* and *FRO2* were expressed at higher levels in lines carrying the *ProUBI:bHLH121-Ox3* transgene under Fe deficiency than in the wild type (Supplemental Figure 9). A similar pattern of expression was observed for *FIT*, *bHLH38*, *bHLH39*, *bHLH101*, and *PYE*. Although not significant, *bHLH100* expression also appeared to follow the same trend. These results further support the notion that bHLH121 is a key transcriptional activator that acts upstream of the Fe homeostasis network.

We then performed ChIP-qPCR experiments to determine whether bHLH121 directly interacts with the promoters of its potential targets. These experiments were conducted on two *bhlh121-2* mutant lines carrying the *ProbHLH121:gbHLH121:GFP* transgene. These two lines were selected because the growth defects observed in *bhlh121-2* at the seedling and mature plant stages were rescued, indicating that the *ProbHLH121:gbHLH121:GFP* transgene was functional and sufficient to complement the *bhlh121-2* mutation (Supplemental Figures 10A, 11 and 12). The expression of *IRT1*, *FIT*, *bHLH39*, and *BGLU42* was also rescued in these two complemented lines (Supplemental Figure 10B). The results presented in Figure 5B and Supplemental Figure 13 support the in vivo binding of bHLH121 to the promoters of *bHLH38*, *bHLH39*, *bHLH100*, *bHLH101*, *PYE*, *BTS*, *BTSL1*, *IMA1*, *IMA2*, and *IMA3*. These results also suggest that bHLH121 does not likely interact with the promoter of *FIT*. Notably, these data also indicate that bHLH121 interacts with the promoters of *bHLH38*, *bHLH39*, *bHLH100*, *bHLH101*, and *PYE* at the same locus as *bHLH104*, *bHLH115*, and *ILR3* (Zhang et al., 2015; Liang et al., 2017). In addition, these data support the notion that bHLH121 directly interacts in vivo with the promoters of *MYB10* and *MYB72*. Indeed, these results also suggest that bHLH121 most likely does not interact with the promoters of *F6'H1*, *S8H*, or *CYP82C4*.

We conducted additional complementation experiments to further investigate the role of *bHLH121* within the Fe homeostasis regulatory network. For this purpose, *FIT* and *bHLH38* (coding sequences) were overexpressed in *bhlh121-2*. These two TFs, which are known to function as heterodimers, were selected since expression data suggested that both genes act downstream of bHLH121. None of the transgenic lines was able to overcome the

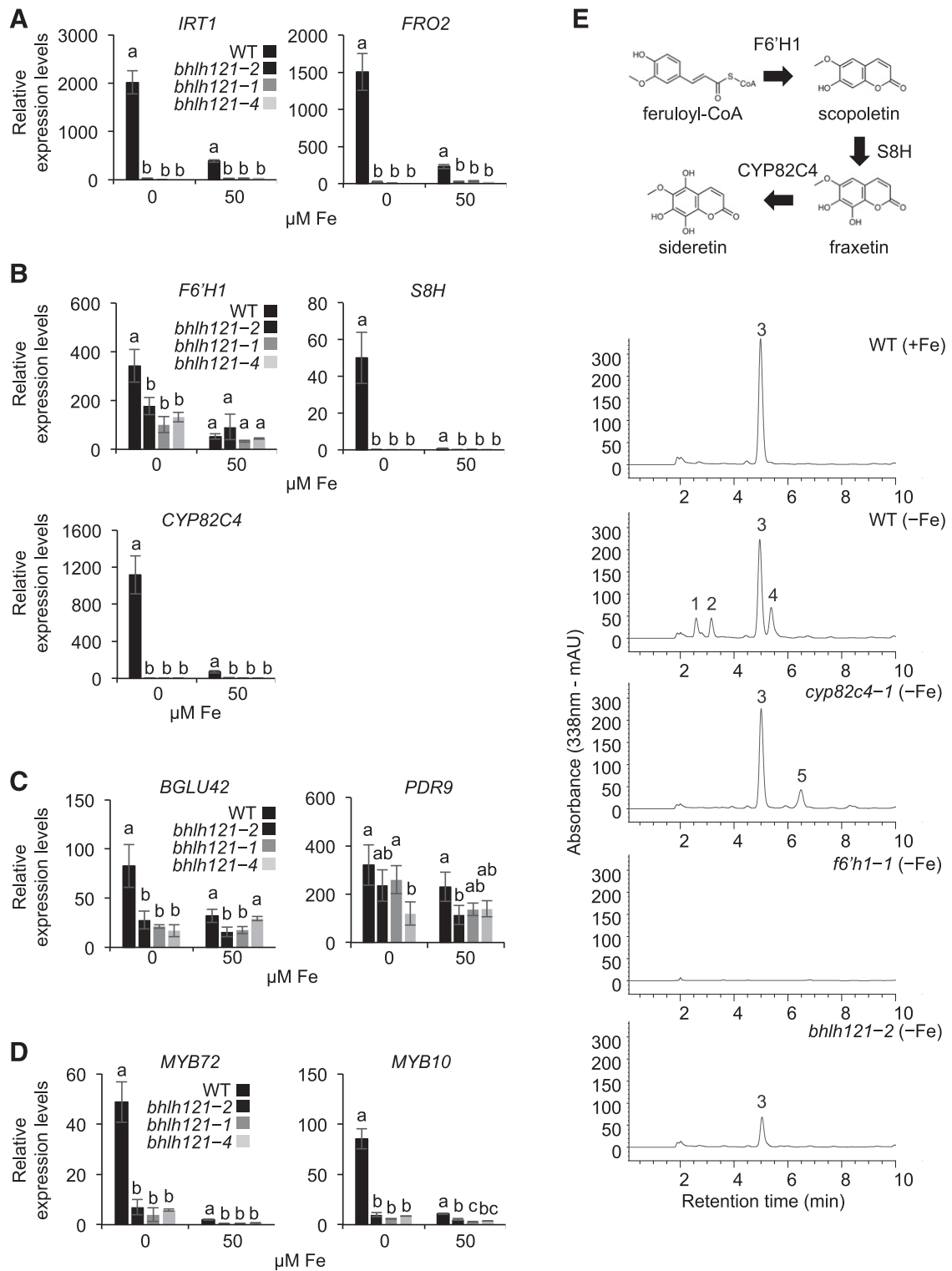


**Figure 4.** Coumarin Biosynthesis Is Affected in the *bhlh121* Loss-of-Function Mutants.

- (A) Relative expression of *IRT1* and *FRO2* (high-affinity Fe uptake system).
- (B) Relative expression of *F6'H1*, *S8H*, and *CYP82C4* (coumarin biosynthesis).
- (C) Relative expression of *BGLU42* and *PDR9* (coumarin secretion).
- (D) Relative expression of *MYB10* and *MYB72* (transcriptional control of coumarin biosynthesis and secretion).

*bhlh121-2* growth defects (Supplemental Figure 14). This observation further confirms the notion that bHLH121 acts as a transcriptional activator of both *FIT* and *bHLH38*.

Since bHLH121 interacts in vivo with bHLH34, bHLH104, bHLH115, and ILR3 and since these four TFs target similar regulatory loci, we performed comparative primary root growth analysis using the corresponding single mutants grown under control and Fe deficiency conditions. Under control conditions, *bhlh121-2* was the sole mutant that displayed growth defects (Supplemental Figure 15A). Under Fe deficiency, the growth defects observed in *bhlh121-2* were more pronounced than those in any other mutant (Supplemental Figure 15B).

Altogether, these results indicate that bHLH121 is a direct activator of *bHLH38*, *bHLH39*, *bHLH100*, *bHLH101*, *PYE*, *BTS*, *BTSL1*, *IMA1*, and *IMA2* expression and that bHLH121 regulates the biosynthesis and secretion of Fe-mobilizing coumarins, partly by directly regulating the expression of *MYB10* and *MYB72* and indirectly regulating the expression of *FIT*. Since bHLH121 binds to the promoter of *IMA3* based on ChIP-qPCR experiments, and since *IMA3* transcript levels in the *bhlh121* mutants are as high as in the wild type, these data also suggest that another TF might contribute to the regulation of *IMA3* expression alongside bHLH121.

#### Cellular Localization of bHLH121 Depends on Fe Availability

RT-qPCR analysis revealed that *bHLH121* expression is not restricted to any specific organ in mature plants (Figure 6A). The highest level of mRNA accumulation was detected in leaves, that is, approximately three times higher than that in roots. RT-qPCR analysis also revealed that *bHLH121* expression was not affected by any changes in Fe availability (i.e., deficiency or excess; Figure 6B).

To further describe the expression pattern of *bHLH121*, we cloned its promoter, fused it to the  $\beta$ -glucuronidase (*GUS*) reporter gene (*ProbHLH121:GUS*), and assessed the activity of *ProbHLH121* in seedlings grown under control, Fe deficiency, and Fe excess conditions. *GUS* analysis confirmed the ubiquitous expression of *bHLH121* (Figure 6C; Supplemental Figure 16). This analysis also suggested that *GUS* activity was, compared with control conditions, slightly enhanced in the cotyledons of seedlings grown under Fe deficiency and slightly repressed at the root tip when grown under Fe excess (Supplemental Figure 16).

To investigate whether bHLH121 protein accumulation and/or localization is affected by Fe availability, we subjected two independent complemented *bhlh121-2* lines carrying the *ProbHLH121:gbHLH121:GFP* transgene to GFP fluorescence

analysis by confocal microscopy. Under control conditions, GFP fluorescence in the root differentiation zone was mainly observed in the nuclei of cells localized to the central cylinder and endodermis (Figures 6D and 6E; Supplemental Figures 17 and 18). By contrast, under Fe deficiency, GFP fluorescence was primarily detected in nuclei of cells located at the rhizodermis and cortex. These experiments highlight the notion that the location of bHLH121 within the roots depends on Fe availability.

Notably, these experiments also suggested that the diffusion of propidium iodide (PI) within the root differentiation zone is affected by Fe availability, since xylem staining was observed under Fe deficiency and not under Fe replete conditions (Figures 6D and 6E; Supplemental Figures 17 and 18). Because the diffusion of PI into the stele is blocked upon the appearance of Casparian strips, Fe deficiency might alter the chemical or structural properties of this diffusion barrier, as has been shown for the suberization of the endodermis (Alassimone et al., 2010; Barberon et al., 2016). Whether there is a direct link between the diffusion properties of PI and the cellular localization of bHLH121, according to iron availability, remains to be elucidated.

Altogether, these results indicate that *bHLH121* is ubiquitously expressed within the plant and that its expression is not affected by Fe availability. However, bHLH121 protein localization within the roots is modulated by the availability of Fe.

## DISCUSSION

### bHLH121-Dependent Complexes Are Required to Maintain Fe Homeostasis in Arabidopsis

The regulation of Fe homeostasis in plants relies on an intricate regulatory network involving several bHLH TFs (Gao et al., 2019). Several studies suggest that this network is composed of two interconnected subnetworks in Arabidopsis, with *FIT* (bHLH29) playing a predominant role in one network and ILR3 (bHLH105) in the other. Although overall the molecular connection between the *FIT* and ILR3 subnetworks is well characterized (Yuan et al., 2008; Wang et al., 2013; Zhang et al., 2015; Li et al., 2016; Liang et al., 2017; Kroh and Pilon, 2019; Tissot et al., 2019), it is still unclear how the expression of both subnetworks is synchronized in order to adapt Fe uptake to plant requirements for this micronutrient to sustain its growth and development.

In this study, we conducted Co-IP LC-MS/MS using ILR3 as bait to identify proteins whose activity might modulate Fe homeostasis and reunite the *FIT* and ILR3 subnetworks. bHLH121, a close homolog of *PYE*, was identified as a potential ILR3 protein

**Figure 4.** (continued).

(A) to (D) Relative expression was determined by RT-qPCR in 1-week-old Arabidopsis seedlings grown on Fe-sufficient or Fe-deficient medium. Means within each condition with the same letter are not significantly different according to one-way ANOVA followed by post hoc Tukey test,  $P < 0.05$  ( $n = 3$  technical repeats from one representative experiment). Error bars show  $\pm$ SD. Each experiment (biological repeat) comprised pooled RNA extracted from  $\sim$ 30 seedlings and was independently repeated three times.

(E) (Top) Schematic representation of the coumarin biosynthetic pathway. (Bottom) Representative absorbance chromatograms obtained at 338 nm for root extracts of Arabidopsis wild type (WT), *cyp8c24-1*, *f6'h1-1*, and *bhlh121-2* mutant seedlings grown for 7 d on half-strength Murashige and Skoog medium agar plates at pH 5.5. +Fe, control; -Fe, Fe deficiency. Numbered peaks correspond to sideretin-glycosides (1 and 2), scopolin: scopoletin glycoside (3), sideretin (4), and fraxin: fraxetin glycoside (5).

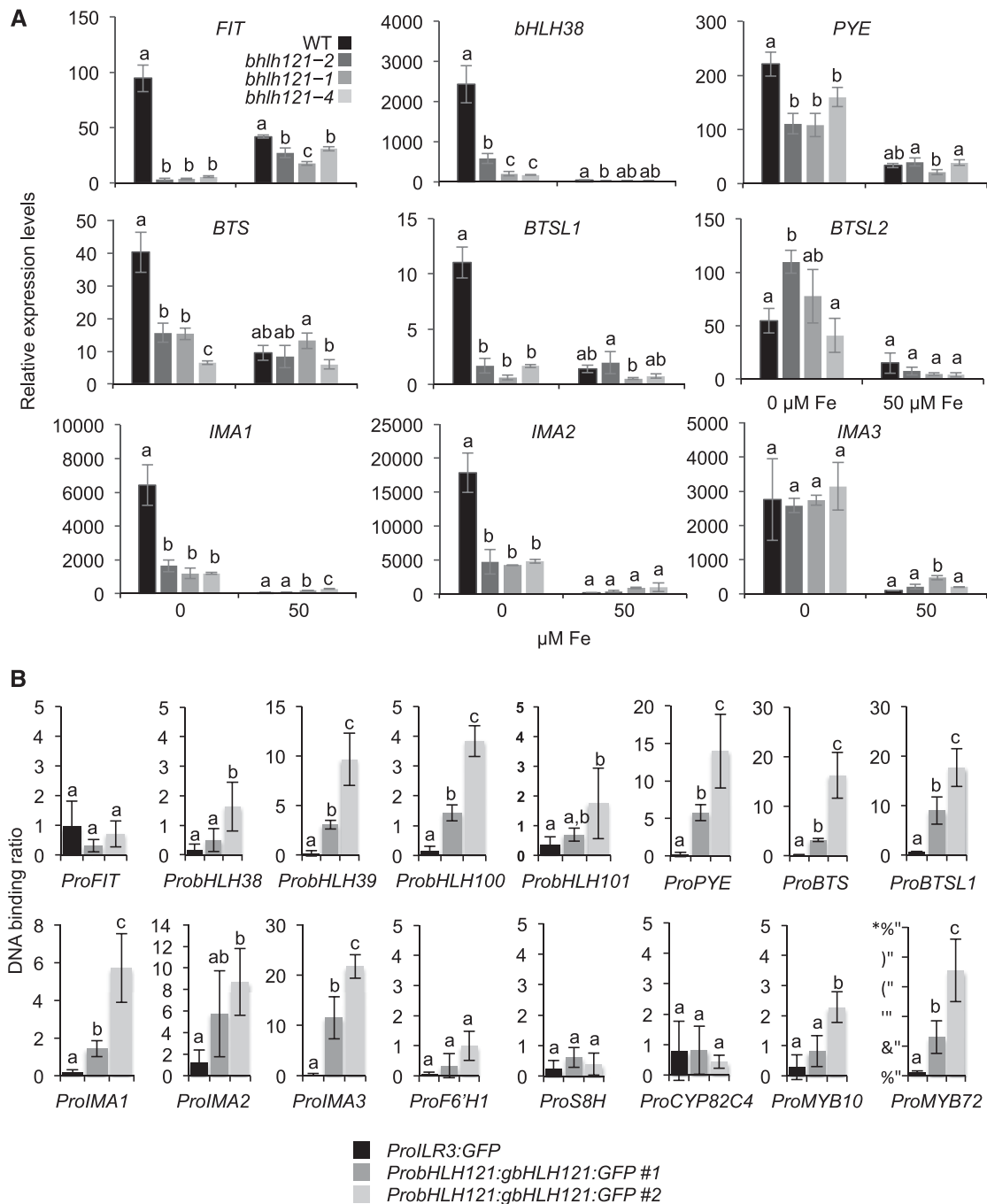


**Figure 5.** Expression of Several Genes Involved in the Fe Homeostasis Transcriptional Regulatory Network Is Compromised in the *bhlh121* Loss-of-Function Mutants.

**(A)** Relative expression of *FIT*, *bHLH38*, *PYE*, *BTS*, *BTSL1*, *IMA1*, *IMA2*, and *IMA3*. Relative expression was determined by RT-qPCR in 1-week-old *Arabidopsis* seedlings grown on Fe-sufficient or Fe-deficient medium. Means within each condition with the same letter are not significantly different according to one-way ANOVA followed by post hoc Tukey test,  $P < 0.05$  ( $n = 3$  technical repeats from one representative experiment). Error bars show  $\pm$ sd. Each experiment (biological repeat) comprised pooled RNA extracted from  $\sim 30$  seedlings and was independently repeated three times.

**(B)** ChIP-qPCR analysis of the binding of bHLH121 to the promoters of *FIT*, *bHLH38*, *bHLH39*, *bHLH100*, *bHLH101*, *PYE*, *BTS*, *BTSL1*, *IMA1*, *IMA2*, *IMA3*, *F6'H1*, *S8H*, *CYP82C4*, *MYB10*, and *MYB72*. Chromatin from the two complemented *bhlh121-2* lines expressing the *ProbHLH121:gbHLH121:GFP* construct subjected to Fe deficiency was extracted using anti-GFP antibodies. Seedlings expressing GFP under the control of the *ILR3* promoter (*ProILR3:GFP*) were used as a negative control. qPCR was used to quantify enrichment of bHLH121 on the selected gene promoters. Means within each condition with the same letter are not significantly different according to one-way ANOVA followed by post hoc Tukey test,  $P < 0.05$  ( $n = 4$  to 6 technical repeats from one representative experiment). Error bars show  $\pm$ sd. Each experiment (biological repeat) comprised pooled chromatin immunoprecipitated from  $\sim 500$  seedlings (2 g) and was independently repeated two times.

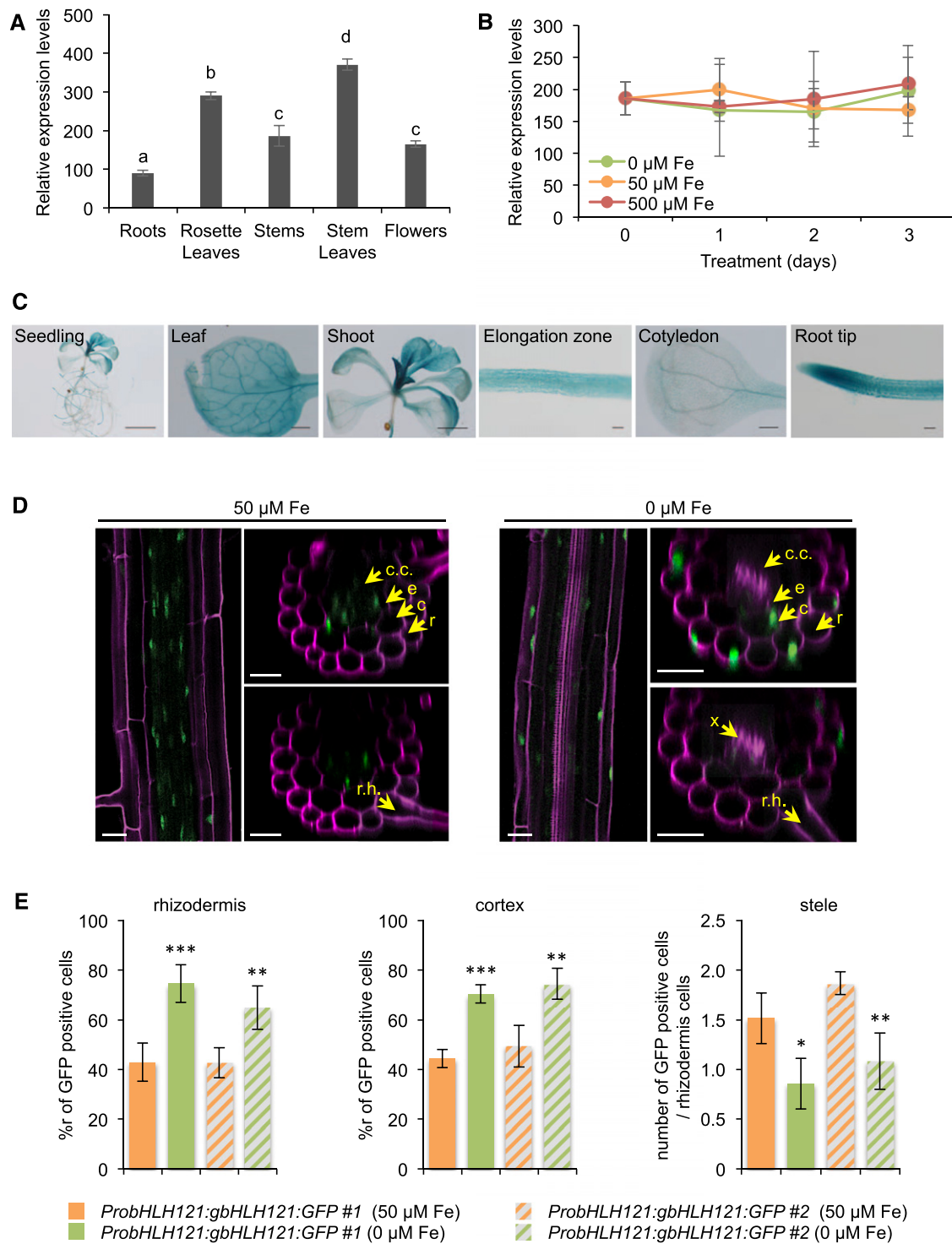


**Figure 6.** *bHLH121* Expression Pattern and Protein Localization.

(A) *bHLH121* expression pattern in 5-week-old Arabidopsis wild-type (WT) plants.

(B) Temporal expression pattern of *bHLH121* in 1-week-old wild-type (WT) seedlings grown under Fe deficiency (0  $\mu\text{M}$ ) or excess (500  $\mu\text{M}$ ) conditions.

(A) and (B) Relative expression was determined by RT-qPCR. Means within each condition with the same letter are not significantly different according to one-way ANOVA followed by post hoc Tukey test,  $P < 0.05$  ( $n = 3$  technical repeats from one representative experiment). Error bars show  $\pm$ sd. Each experiment (biological repeat) comprised pooled RNA extracted from tissues collected from three independent plants in (A) and from 30 seedlings in (B).

interaction partner. The study of three *bhlh121* loss-of-function mutant alleles revealed that bHLH121 is necessary to set up appropriate responses to Fe deficiency and to maintain Fe homeostasis during the entire life span of the plant (Figures 2 and 3; Supplemental Figures 3 to 6). bHLH121 acts as a transcriptional activator of key genes involved in controlling Fe homeostasis, including *FIT*, *bHLH38*, *bHLH39*, *bHLH100*, *bHLH101*, *PYE*, *MYB10*, *MYB72*, *BTS*, and *BTSL1* as well as *IMA1* and *IMA2* (Figures 4C and 5A; Supplemental Figure 7). By contrast, the effect of bHLH121 overexpression on plant growth and gene expression was weak, suggesting that bHLH121 activity requires partners whose abundance is limiting (Supplemental Figures 8 and 9).

Y2H and BiFC experiments revealed that bHLH121 can interact not only with ILR3 but also with its three closest homologs: bHLH34, bHLH104, and bHLH115 (Figure 1; Supplemental Figure 1). When we compared the phenotypes of the loss-of-function mutants of these five TFs, *bhlh121-2* presented stronger defects in root development than *bhlh34*, *bhlh104-1*, *ilr3-3*, and *bhlh115-2* (Supplemental Figure 15). Interestingly, a previous study showed that the *bhlh34 bhlh104 bhlh115* triple mutant displayed stronger defects in primary root growth than the single mutants in a manner similar to that of *bhlh121-2* (Liang et al., 2017). Previous studies also showed that the expression of *bHLH38*, *bHLH39*, *bHLH100*, *bHLH101*, *PYE*, *MYB10*, *MYB72*, and *BTS* was moderately reduced in the *bhlh34*, *bhlh104*, *bhlh115*, and *ilr3* single mutants and that this decrease was stronger in *bhlh34 bhlh104* double mutants (Zhang et al., 2015; Li et al., 2016; Liang et al., 2017). Similar observations were made for *FIT* except that *FIT* expression was not affected by the *bhlh115* mutation. These similarities between *bhlh121*, the *bhlh34 bhlh104* double mutant, and the *bhlh34 bhlh104 bhlh115* triple mutant suggest that bHLH121 might form heterodimers with bHLH34, bHLH104, bHLH115, and ILR3 that function in the same pathway as transcriptional activators. This hypothesis was further supported by ChIP-qPCR experiments that showed that ILR3 and its closest homologs, such as bHLH121, directly interact with the promoters of *bHLH38*, *bHLH39*, *bHLH100*, *bHLH101*, and *PYE* at the same locus. This approach also showed that bHLH121 directly interacts with the promoters of *MYB10*, *MYB72*, *BTS*, and *BTSL1* as well as the promoters of *IMA1* and *IMA2* (Figure 5B).

### Fe Availability Modulates the Cellular Localization of bHLH121

While the overall expression of bHLH121 is not significantly affected by the Fe status of the plant (Figures 6A to 6C; Supplemental

Figure 16), analysis of bHLH121:GFP fluorescence in roots revealed that Fe availability modifies the localization of bHLH121 to specific cell types within this tissue. When Fe was not limiting, GFP fluorescence was mainly detected in the nuclei of cells in the stele, whereas under Fe deficiency, the signal was mainly observed in the cortex and rhizodermis cells (Figures 6D to 6F; Supplemental Figures 17 and 18). Several hypotheses could explain why GFP fluorescence is preferentially observed in certain cell types depending on Fe availability. For example, some posttranscriptional mechanism could modulate the stability and/or translation of *bHLH121* mRNA in a cell type- and Fe-dependent manner, or perhaps some posttranslational mechanism regulates bHLH121 localization or cell-to-cell movement. Whether one or both of these mechanisms are involved in this process is still to be determined and should be studied in the future. Nevertheless, these results suggest that the genes that are targeted by bHLH121 differ depending on Fe availability.

Interestingly, ILR3 and PYE localization in roots also depends on Fe availability, as revealed by detecting GFP fluorescence from translational fusions. When Fe is not limiting, ILR3 is detected in all cell types, but at a lower level in the epidermis and cortex than in the stele, whereas only traces of PYE can be detected in the stele (Long et al., 2010; Samira et al., 2018; Gao et al., 2019). Under Fe deficiency, both proteins accumulate in all root cell types. Unlike *bHLH121* and *ILR3*, *PYE* expression and promoter activity are strongly induced in response to Fe deprivation (Long et al., 2010; Zhang et al., 2015; Li et al., 2016; Liang et al., 2017; Samira et al., 2018; Tissot et al., 2019). Notably, the overlap between ILR3, PYE, and bHLH121 accumulation patterns in root cells varies with Fe availability (Supplemental Figure 19). For instance, when Fe is not limiting, bHLH121 and ILR3 are mainly present in the stele. The precise function of this dimer in this tissue is still to be determined. However, based on the *bhlh121* mutant phenotypes, it is likely that the bHLH121-dependent dimers act to maintain the basal expression levels of genes potentially involved in Fe transport, partitioning, and/or storage. Indeed, since PYE is barely present in the stele when Fe is not limiting, the repressive activity of ILR3 must be low (Rampey et al., 2006; Tissot et al., 2019). This idea is in agreement with the expression patterns of ferritin genes: the expression of these genes alongside the vasculature is induced in the presence of Fe but repressed by ILR3/PYE dimers when Fe is limiting (Reyt et al., 2015; Kroh and Pilon, 2019; Tissot et al., 2019). By contrast, when Fe is not limiting, ILR3, PYE, and bHLH121 are barely detectable in the cortex and rhizodermis cells, which is consistent with the low levels of expression of genes encoding the Fe uptake machinery (Figure 4A; Kroh and Pilon, 2019). The accumulation of ILR3 and PYE in all root cell types when Fe

**Figure 6.** (continued).

**(C)** *bHLH121* promoter activity in seedlings grown under control conditions. Bar = 5 mm (seedling), 2 mm (shoot), 500  $\mu$ m (cotyledon and leaf), and 100  $\mu$ m (elongation zone and root tip).

**(D)** bHLH121:GFP localization in the roots (differentiation zone) of a complemented *bhlh121-2* line (*ProbHLH121:gbHLH121:GFP #1*) subjected or not to Fe deficiency. Bar = 25  $\mu$ m. c, cortex; c.c., central cylinder; e, endodermis; r, rhizodermis; r.h., root hair; x, xylem.

**(E)** (Left) Percentage of cells displaying GFP fluorescence in the rhizodermis cell layer (ratio between GFP-positive cells in the rhizodermis and total rhizodermis cells). (Middle) Percentage of cells displaying GFP fluorescence in the cortex cell layer (ratio between cortex GFP-positive cells and total cortex cells). (Right) Ratio between stele GFP-positive cells and total rhizodermis cells. The roots (differentiation zone) of four seedlings from two complemented *bhlh121-2* lines (*ProbHLH121:gbHLH121:GFP #1* and *#2*), subjected or not to Fe deficiency, were analyzed for each measurement. Error bars show  $\pm$ SD. *t* test significant difference: \*\*P < 0.01; \*\*\*P < 0.001.

availability is low likely allows the storage of Fe in vacuoles and ferritins to be inhibited, while the accumulation of bHLH121 in the cortex and rhizodermis favors Fe uptake.

### bHLH121 Acts Upstream of the Fe Homeostasis Network

The current results indicate that bHLH121 acts upstream of the Fe homeostasis network by forming heterodimers with ILR3 and its closest homologs to activate the expression of the large majority of genes encoding proteins and peptides involved in controlling Fe homeostasis (Figure 7). In the proposed model, when Fe availability is low, the bHLH121-dependent complexes activate the expression of *FIT* (indirectly) and the expression of *bHLH38*, *bHLH39*, *bHLH100*, and *bHLH101* (directly). Considering that the overexpression of *IMA3/FEP1* is sufficient to induce *bHLH38* and *bHLH39* expression, it could be hypothesized, given the structural similarity between the *IMA* peptides, that the concomitant induction of *IMA1* and *IMA2* expression (direct) by bHLH121 reinforces the induction of *bHLH38* and *bHLH39* expression (Grillet et al., 2018; Hirayama et al., 2018). Once induced, the encoded FIT protein heterodimerizes with bHLH38, bHLH39, bHLH100, and bHLH101 to promote the expression of structural genes involved in Fe uptake and transport. bHLH121-dependent complexes also directly activate the expression of *BTSL1*, whose encoded protein is predicted to target FIT to the 26S proteasome for degradation. The bHLH121-dependent complexes also directly induce *MYB10* and *MYB72* expression, enabling the biosynthesis and secretion of fraxetin and sideretin into the rhizosphere to improve Fe uptake.

On the other hand, the bHLH121-dependent complexes directly activate the expression of *PYE* (*bHLH47*) and *BTS* (E3 ubiquitin ligase). Once induced, *PYE* heterodimerizes with ILR3 to repress the expression of genes involved in Fe transport and storage, and likely *PYE* itself, in a negative feedback regulatory loop. By contrast, *BTS* specifically targets bHLH115 and ILR3, leading to their degradation via the 26S proteasome to fine tune Fe uptake and avoid Fe excess that could be detrimental to the plant.

Indeed, further experiments will be necessary to fully demonstrate this model, in particular colocalization analyses with all the major TFs, regulatory proteins (i.e., *BTS*, *BTSL1*, *BTSL2*) and peptides (i.e., *IMA1*, *IMA2*) involved in controlling Fe homeostasis to document the spatial distribution of the different actors depending on Fe availability. Another important question that will have to be addressed is how bHLH121 is regulated at the post-transcriptional and/or posttranslational level. Since the activity of bHLH121 depends on its interaction with ILR3 and its closest homologs, determining how the stability of bHLH34 and bHLH104 is modulated may help answer this question.

## METHODS

### Plant Materials

*Arabidopsis* (*Arabidopsis thaliana*) ecotype Columbia (Col-0) was used as the wild type. *bhlh121-1*, *bhlh121-2*, and *bhlh121-4* homozygous loss-of-function mutant alleles (CRISPR-Cas9 in Col-0) were generated during this study (Supplemental Figure 2). In addition, the following mutant lines were used: *bhlh34* (Li et al., 2016), *bhlh104-1* (Zhang et al., 2015), *ilr3-3* (Li et al., 2016; Tissot et al., 2019), and *bhlh115-2* (Liang et al., 2017).

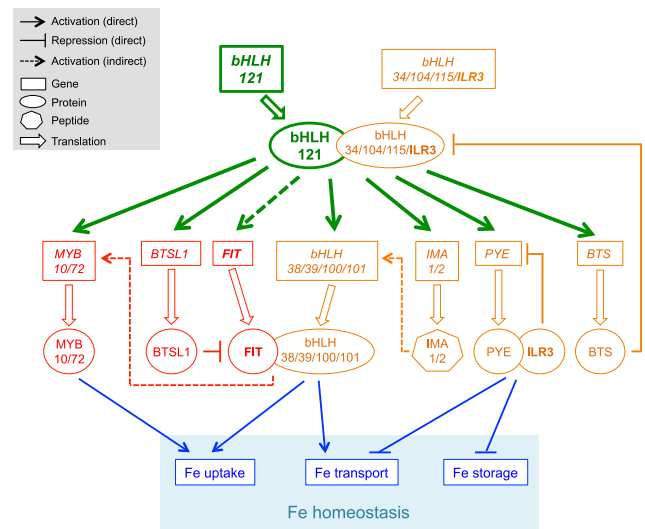


**Figure 7.** bHLH121 Acts Upstream of the Fe Homeostasis Network.

In *Arabidopsis*, two interconnected regulatory modules control Fe homeostasis: the first module (red) depends on the activity of FIT and the second module (orange) on the activity of ILR3 and its closest homologs (i.e., bHLH34, bHLH104, and bHLH115). The results presented in this study indicate that bHLH121 acts upstream of the Fe homeostasis network by forming heterodimers with ILR3 and its closest homologs to activate the expression of genes encoding several regulatory proteins belonging to both modules (green). In the proposed model, the bHLH121-dependent complexes indirectly activate *FIT* expression in response to Fe deficiency. Once induced, the encoded FIT protein heterodimerizes with bHLH38, bHLH39, bHLH100, and bHLH101 to induce the expression of structural genes involved in Fe uptake and transport (blue). bHLH121-dependent complexes are direct activators of *MYB10* and *MYB72* expression (two TFs regulating coumarin biosynthesis and secretion when Fe availability is limiting and whose expression is indirectly regulated by FIT). Another direct target of these bHLH121-dependent complexes is *BTSL1*. *BTSL1* is a RING E3 ubiquitin ligase that negatively regulates Fe deficiency responses by targeting FIT to the 26S proteasome for degradation. On the other hand, the bHLH121-dependent complexes directly activate the expression of *bHLH38*, *bHLH39*, *bHLH100*, and *bHLH101* in response to Fe deficiency. The direct induction of *IMA1* and *IMA2* expression in response to Fe deficiency by the bHLH121-dependent complexes might reinforce the induction of *bHLH38* and *bHLH39* expression. The potential role of bHLH121 in regulating *IMA3* expression remains to be elucidated. *PYE* (*bHLH47*) and *BTS* (E3 ubiquitin ligase) are two additional direct targets whose expression is also induced in response to Fe deficiency. Once induced, *PYE* heterodimerizes with ILR3 to repress the expression of genes involved in Fe transport and storage (blue) and most probably *PYE* itself, in a negative feedback regulatory loop. By contrast, *BTS* specifically targets bHLH115 and ILR3, leading to their degradation via the 26S proteasome to fine tune Fe uptake and avoid Fe excess that could be detrimental to the plant.

### Growth Conditions

#### *In Vitro* Culture

Seedlings were germinated and grown under long-day conditions (16-h-light/8-h-dark cycle; light intensity, 120  $\mu\text{mol}/\text{cm}^2/\text{s}$  provided by Osram 18-W 840 Lumilux neon tubes) on half-strength Murashige and Skoog medium containing 0.05% (w/v) MES, 1% (w/v) Suc, and 0.7% (w/v) agar for 7 d. The Fe concentration was 0  $\mu\text{M}$  (deficiency), 50  $\mu\text{M}$  (control), 200  $\mu\text{M}$  (mild

excess), or 500  $\mu\text{M}$  (excess), and it was provided as Fe(III)-EDTA. For the ChIP experiments, 1-week-old seedlings grown under control conditions were exposed to Fe deficiency for 3 d prior to analysis. For the GUS experiments, 1-week-old seedlings grown under control conditions were exposed to Fe deficiency for 5 d or Fe excess for 1 d prior to analysis (control seedlings were maintained at 50  $\mu\text{M}$  Fe).

### Hydroponic Culture

Plants were grown for 3 weeks under short-day conditions (8-h-light/16-h-dark cycle; light intensity, 120  $\mu\text{mol}/\text{cm}^2/\text{s}$  provided by a mix of sodium-vapor and metal halide 400-W lamps) in the presence of 50  $\mu\text{M}$  Fe-EDTA as described previously (Fourcroy et al., 2016). The plants were grown for 10 more days in the presence (50  $\mu\text{M}$ ) or absence of Fe.

### Measurement of Root Length

After the growing period, roots were scanned and measured using ImageJ 1.52a software (National Institutes of Health).

### Cloning

Homozygous *bhlh121* mutant alleles (loss-of-function in the Col-0 genetic background) were obtained by CRISPR-Cas9 gene editing. For this purpose, two single guide RNAs (sgRNAs) were designed and cloned into the pRM-Cas9 binary vector prior to plant transformation (Wang et al., 2015). For the design of the sgRNA, the data from four different websites were merged: CRISPRSCAN (<http://www.crisprscan.org/>), WU-Crispr (<http://crispr.wustl.edu/>), CHOP CHOP (<http://chopchop.cbu.uib.no/>), and CRISPR RGEN tool (<http://www.rgenome.net/cas-designer/>). The sgRNAs located in exons that were the most highly represented among these four databases and close to the translation initiation site (ATG) were manually selected. The number of potential off-targets of these selected sgRNAs was determined using the Cas-OFFinder tool of rgenome (<http://www.rgenome.net/cas-offinder/>). Finally, the two sgRNAs presenting the smallest number of putative off-targets were chosen. Three different homozygous mutant alleles were obtained following plant transformation (Bechtold et al., 1993), including one displaying a 78-bp deletion (*bhlh121-2*) in the coding sequence (656 bp at the genomic level) and two alleles with a single nucleotide insertion (*bhlh121-1* and *bhlh121-4*; Supplemental Figure 2A). To ensure that the generated constructs were not generating off-targets and thus affecting the integrity of key genes involved in the transcriptional regulation of Fe homeostasis, the regions between the start and stop codons of *bHLH11*, *bHLH34*, *bHLH104*, *bHLH115*, *ILR3*, and *FIT* were sequenced. No differences from the wild-type sequences were observed (Supplemental Figures 20 to 22).

The *bHLH121* promoter (ProbHLH121, 2586 bp prior to the start codon) was fused to GUS in the pGWB3 binary vector (Nakagawa et al., 2007) as described in Xu et al. (2013). The wild-type plants were transformed (agroinfiltration) with ProbHLH121:GUS, and nine independent lines were assayed for GUS activity. The same procedure was used to fuse the *bHLH121* promoter and genomic region (without the stop codon) to GFP (pGWB4 binary vector; ProbHLH121:gbHLH121:GFP). *bhlh121-2* mutant plants were transformed with ProbHLH121:gbHLH121:GFP, and complemented lines were selected for GFP fluorescence analysis and ChIP-qPCR experiments. To overexpress *FIT* and *bHLH38* in *bhlh121-2*, the corresponding coding sequences were cloned downstream of the strong, ubiquitous promoter of the Arabidopsis *UBIQUITIN10* gene (pUB-GFP-Dest binary vector; Grefen et al., 2010). Lines carrying ProUBI:FIT and ProUBI:bHLH38 transgenes (10 independent lines for each construct) were analyzed for *bhlh121-2* phenotypic complementation.

All PCR products were obtained using high-fidelity Phusion DNA polymerase, and each construct was sequenced to ensure its integrity. The

primers used and the sequences of the guide RNAs are described in Supplemental Data Set 1.

### Biochemical Analysis

#### Chlorophyll Content

Chlorophylls from 25 mg of leaf tissue (fresh weight) or five leaf discs (diameter, 0.35 cm) were extracted in 1 mL of 100% acetone in the dark under agitation. The absorbance (*A*) at 661.8 and 644.8 nm was then measured. Total chlorophyll content was assessed using the following equation:  $Chl\ a + Chl\ b = 7.05 \times A_{661.6} + 18.09 \times A_{644.8}$  and was expressed as micrograms per gram fresh weight or micrograms per square centimeter (Lichtenthaler, 1987).

#### Iron Measurements

Twenty milligrams of ground material (dry weight) per sample was mixed with 750  $\mu\text{L}$  of nitric oxide (65% [v/v]) and 250  $\mu\text{L}$  of hydrogen peroxide (30% [v/v]) prior to homogenization. Following 10 min of incubation at room temperature, the samples were mineralized using the Microwave digestion systems (Berghof). Once mineralized, the nitric oxide proportion present in the samples was adjusted to 5 to 10% of the final volume by adding ultrapure water. Fe content present in the samples was then measured by microwave plasma atomic emission spectroscopy (Agilent Technologies).

#### Histochemical GUS Detection

Seedlings expressing *ProbHLH121:GUS* gene fusions were transferred into a 100 mM phosphate buffer, pH 7.5, solution containing 2 mM 5-bromo-4-chloro-3-indolyl- $\beta$ -D-glucuronide, 0.1% (v/v) Triton X-100, and 10 mM  $\text{Na}_2\text{-EDTA}$ . Prior to incubating the samples at 37°C in the dark (overnight), a 1-h vacuum treatment (room temperature) was applied. Following GUS staining, chlorophylls were removed by gently shaking the samples in a clearing solution of acetic acid:ethanol (14:86). The samples were stored in 70% (v/v) ethanol prior to observation under a light microscope.

#### FCR Activity

Ten to 20 mg of fresh root tissue was incubated for 1 h in the dark with gentle shaking in 2 mL of FCR buffer (100  $\mu\text{M}$   $\text{Fe}^{3+}$ -EDTA, 300  $\mu\text{M}$  ferrozine, and 10 mM MES, pH 5.5). An identical assay without plant samples was used as a blank. The concentration of  $\text{Fe}^{2+}$ -ferrozine complex (which displays a purple coloration) was determined by reading absorbance at 560 nm using a Xenius microplate reader.

#### Iron Staining by Perls/DAB

Iron staining was performed according to Roschztardt et al. (2009). The embryos were dissected from dry seeds that were previously imbibed in distilled water for 3 h. Isolated embryos or 4-d-old seedlings were vacuum infiltrated with a solution containing 2% (v/v) HCl and 2% (w/v) potassium ferrocyanide for 15 min and incubated for 30 min at room temperature. After washing with distilled water, the embryos were incubated in a methanol solution containing 10 mM  $\text{NaN}_3$  and 0.3% (v/v)  $\text{H}_2\text{O}_2$  for 1 h and washed with 100 mM Na-phosphate buffer, pH 7.4. For the intensification reaction, the embryos were incubated for 10 min in 100 mM Na-phosphate buffer, pH 7.4, solution containing 0.025% (w/v) DAB hydrate, 0.005% (v/v)  $\text{H}_2\text{O}_2$ , and 0.005% (w/v)  $\text{CoCl}_2 \cdot 2\text{H}_2\text{O}$ . The reaction was stopped by rinsing with distilled water. The embryos were visualized under a stereoscopic microscope (Nikon SMZ800) and imaged with a Coolpix 4500 charge-coupled device (CCD) digital camera (Nikon).



### HPLC Analysis of Root Extracts

For HPLC analysis of coumarins, 30 mg of root material frozen in liquid nitrogen was ground in the presence of glass beads and extracted with 400  $\mu$ L of methanol:water [80:20 (v/v)]. The supernatants were vacuum dried and resuspended in 100  $\mu$ L of water:acetonitrile [90:10] containing 0.1% (v/v) of formic acid. HPLC-fluorescence analysis was performed using a 1220 Infinity II LC system (Agilent Technologies) coupled to a Prostar 363 fluorescence detector (Varian). Separation was done on an analytical HPLC column (Aeris 3.6  $\mu$ m WIDEPOR XB-C8 200  $\text{\AA}$ , 100  $\times$  2.1 mm; Phenomenex), with a gradient mobile phase made with 0.1% (v/v) formic acid in water (A) and 0.1% (v/v) formic acid in acetonitrile (B) and a flow rate of 0.25 mL/min. The gradient program started at 8% B for 2 min and increased linearly to 30% B in 13 min and then to 50% B in 1 min. This proportion was maintained for 4 min and returned linearly to initial conditions in 1 min. The column was allowed to stabilize for 9 min at the initial conditions. Absorbance was monitored at  $\lambda = 338$  nm. Fluorescence was monitored at  $\lambda_{\text{exc}}$  365 and  $\lambda_{\text{em}}$  460 nm. External calibration was done using commercial coumarins: esculin (Sigma), esculetin (Sigma), fraxetin (Sigma) scopoletin (Sigma), scopolin (TargetMol), and fraxin (TargetMol). Sideretin and sideretin-glycosides identification was confirmed by LC-MS/MS.

### Co-IP MS Analyses

#### Co-IP Analysis

Experiments were performed in triplicate for the bait *ProILR3:gILR3:GFP* and for the control *ProILR3:GFP*. For protein extraction, 0.7 g of root tissue was suspended in 1.5 mL of lysis buffer (50 mM Tris-HCl, pH 7.5, 150 mM NaCl, 10% [v/v] glycerol, 5 mM MgCl<sub>2</sub>, 0.1% [w/v] IGEPAL CA-630, 2 mM DTT, 1 $\times$  Complete Mini EDTA-Free Protease Inhibitor Cocktail Tablet [Roche], and 1 $\times$  Phosphatase Inhibitor Cocktail 3 [Sigma]). The lysates were cleared by centrifugation at 10,000g, and IPs were performed using an  $\mu$ MACS GFP isolation kit (MACS purification system, Milteny Biotech) according to the manufacturer's instructions, except that lysis buffer was used for all bead washes.

Eluted proteins were loaded for a short run (15 min at 100 V) on a 10% Mini-PROTEAN TGX pre-cast gel (Bio-Rad). The whole lane was manually excised and sequentially rinsed with water, 25 mM ammonium bicarbonate, and 50% (v/v) acetonitrile in 25 mM ammonium bicarbonate and then dehydrated with acetonitrile and dried at room temperature. Proteins were reduced with 10 mM DTT for 45 min at 56°C and then alkylated with 55 mM iodoacetamide for 30 min at room temperature in the dark. Excess iodoacetamide was removed, and gel slices were rinsed twice with 50% (v/v) acetonitrile in 25 mM ammonium bicarbonate, dehydrated with acetonitrile, and dried at room temperature. Proteins were digested by trypsin (Sequencing Grade Modified, Promega) in 25 mM ammonium bicarbonate overnight at 37°C. Peptides were eluted by step elutions with 2% (v/v) formic acid and twice with 50% (v/v) acetonitrile in 2% (v/v) formic acid. The supernatants were pooled and evaporated in a vacuum centrifuge. Peptides were resuspended in 8  $\mu$ L of 2% (v/v) formic acid, and 6  $\mu$ L samples were injected for LC-MS/MS analysis.

### MS Analysis

The LC-MS/MS analyses were performed using an Ultimate 3000 RSLC nano system (Thermo Fisher Scientific) interfaced online with a nano easy ion source and a Q Exactive Plus Orbitrap mass spectrometer (Thermo Fisher Scientific). The samples were analyzed in data-dependent acquisition mode. The protein digests were loaded onto a pre-column (PepMap 100 C18, 5- $\mu$ m particle size, 100- $\text{\AA}$  pore size, 300- $\mu$ m i.d.  $\times$  5-mm length; Thermo Fisher Scientific) at a flow rate of 10  $\mu$ L/min for 3 min. The peptides were separated in a reverse-phase column (PepMap C18, 2- $\mu$ m particle

size, 100- $\text{\AA}$  pore size, 75- $\mu$ m i.d.  $\times$  50-cm length; Thermo Fisher Scientific) at a flow rate of 300 nL/min.

The loading buffer (solvent A) was 0.1% (v/v) formic acid in water, and the elution buffer (solvent B) was 0.1% (v/v) formic acid in 80% (v/v) acetonitrile. The linear gradient used was 2 to 25% of solvent B in 103 min, followed by 25 to 40% of solvent B from 103 to 123 min and 40 to 90% of solvent B from 123 to 125 min. The total run time was 150 min, including a high organic wash step and re-equilibration step.

The Q Exactive Plus mass analyzer was operated in positive ESI mode at 1.8 kV. In data-dependent acquisition mode, the top 10 precursors were acquired between 375 and 1500  $m/z$  with a 2-Thomson selection window, dynamic exclusion of 40 s, normalized collision energy of 27, and resolutions of 70,000 for MS and 17,500 for MS2.

### Data Analysis

Spectra were recorded with Xcalibur software (4.3.31.9; Thermo Fisher Scientific). The raw files were analyzed with MaxQuant version 1.5.5.1 (Tyanova et al., 2016) using default settings. The minimal peptide length was set to 6. The criteria "Trypsin/P" was chosen as the digestion enzyme. Carbamidomethylation of Cys was selected as a fixed modification and oxidation of Met and acetylation (protein N terminus) as variable modifications. Up to two missed cleavages were allowed. The mass tolerance for the precursor was 20 and 4.5 ppm for the first and main searches, respectively, and that for the fragment ions was 20 ppm. The files were searched against an in-house modified Arabidopsis 10 database (35,417 entries). Identified proteins were filtered according to the following criteria: at least one different trypsin peptides with at least one unique peptide and at least one razor peptide. Minimum score for modified peptides was set to 20. A peptide-spectrum match false discovery rate and a protein false discovery rate below 0.05 were required. Using the above-mentioned criteria, the rates of false peptide sequence assignment and false protein identification were lower than 5%. Proteins were selected as potential ILR3 interactors if they were identified in the three IP replicates (i.e., ILR3:GFP) and if they were not identified in any of the control IPs (i.e., GFP).

### Y2H Assays

Experiments were performed as described in Touraine et al. (2019) using the yeast AH109 (*Saccharomyces cerevisiae*) reporter strain and the pDEST22 and pDEST32 vectors (Invitrogen).

### GFP Fluorescence Analysis by Confocal Microscopy

Roots of 7-d-old *bhlh121-2* seedlings expressing *ProbHLH121:gbHLH121:GFP* were imaged under an LSM 880 microscope (Zeiss) with a W Plan Aplanachromat 20 $\times$ /1.0 objective. Before imaging, roots were stained with PI for 5 min. GFP and PI were detected by excitation with an argon laser at 488 nm. The emission filter was set at 500 to 550 nm for GFP and 633 to 695 nm for PI.

### BiFC Assays

Experiments were performed as described in Couturier et al. (2014). Results are representative of the observations made on at least 20 cells. All PCR products were obtained using high-fidelity Phusion DNA polymerase, and each construct was sequenced to ensure its integrity. All primers used are described in Supplemental Data Set 1.

### Gene Expression Analysis

Total RNAs were extracted from the samples using the Tri-Reagent (Molecular Research Center) method. Briefly, each sample was homogenized

in 1 mL of Tri-Reagent solution mixed with 160  $\mu$ L of chloroform:isoamyl alcohol (24:1). Following centrifugation (10 min, 13,000 rpm, 4°C), total RNAs present in the aqueous phase were precipitated by the addition of 400  $\mu$ L of isopropanol followed by another centrifugation. The pellets were washed twice with 70% ethanol and dried prior to resuspension in RNase-free water. For each sample, 1  $\mu$ g of total RNA treated with DNase was reverse transcribed into cDNA using a RevertAid kit (Thermo Fisher Scientific). RT-qPCR analyses were performed using a LightCycler 480 (Roche) and LC480-SYBR-Green master I reaction mix (Roche). *PROTEIN PHOSPHATASE2A SUBUNIT A3 (PP2AA3)* was used as a reference gene (Czechowski et al., 2005). Expression levels were calculated using the comparative threshold cycle method. The primers used are described in Supplemental Data Set 1.

### ChIP Assays

Experiments were performed as described by Gendrel et al. (2002), with modifications: (1) nuclei were isolated with the following buffer: 20 mM PIPES-KOH, pH 7.6, 1 M hexylene glycol, 10 mM MgCl<sub>2</sub>, 0.1 mM EGTA, 15 mM NaCl, 60 mM KCl, 0.5% (v/v) Triton X100, 5 mM  $\beta$ -mercaptoethanol, protease inhibitor cocktail (complete tablets EASYpack, Roche), and (2) after immunoprecipitation using antibodies raised against GFP (1/1000 dilution; ab290, Abcam), DNA was purified with an IPURE Kit (Diagenode). The resulting DNA was analyzed by qPCR analysis using a LightCycler 480 (Roche) and LC480-SYBR-Green master I reaction mix (Roche). Data are presented as promoter target enrichment over input, using the following formula:  $(2 - (C_p IP - C_p Input) \times 100) \times 100$  (Supplemental Data Sets 2 and 3). All primers used are described in Supplemental Figure 23 and Supplemental Data Set 1.

### Accession Numbers

Sequence data from this article can be found in the GenBank/EMBL libraries under the following accession numbers: *bHLH11* (At4g36060); *bHLH29/FIT* (At2g28160); *bHLH34* (At3g23210); *BGLU42* (At5g36890); *bHLH38* (At3g56970); *bHLH39* (At3g56980); *bHLH47/PYE* (At3g47640); *bHLH100* (At2g41240); *bHLH101* (At5g04150); *bHLH104* (At4g14410); *bHLH105/ILR3* (At5g54680); *bHLH115* (At1g51070); *bHLH121* (At3g19860); *BTS* (At3g18290); *BTSL1* (At1g74770); *BTSL2* (At1g18910); *CYP82C4* (At4g31940); *FRO2* (At1g01580); *IMA1* (At1g47400); *IMA2* (At1g47395); *IMA3* (At2g30766); *IRT1* (At4g19690); *MYB10* (At3g12820); *MYB72* (At1g56160); *PDR9* (At3g53480); *PP2AA3* (At1g13320); *S8H* (At3g12900). All raw MS data and Maxquant files generated have been deposited to the ProteomeXchange Consortium via the PRIDE partner repository with the data set identifier PXD014620. The ANOVA tables are displayed in Supplemental Data Set 4.

### Supplemental Data

**Supplemental Figure 1.** bHLH11 interacts with ILR3 and with its closest homologs and forms homodimers.

**Supplemental Figure 2.** *bhlh121* loss-of-function mutations.

**Supplemental Figure 3.** Fe staining of wild type and *bhlh121* embryos.

**Supplemental Figure 4.** The *bhlh121* loss-of-function mutant plants have decreased accumulation of Fe in roots and shoots.

**Supplemental Figure 5.** Coumarin accumulation in wild type, *cyp8c24-1*, *f6'h1* and *bhlh121-2*.

**Supplemental Figure 6.** Coumarin accumulation in wild type and *bhlh121-2*.

**Supplemental Figure 7.** *bHLH34*, *bHLH104*, *bHLH115* and *ILR3* expression is not compromised in the *bhlh121* loss-of-function mutants.

**Supplemental Figure 8.** Phenotypes of *bHLH121* overexpressing lines.

**Supplemental Figure 9.** *bHLH121* overexpression induces the expression of several Fe homeostasis-related genes.

**Supplemental Figure 10.** Complementation of the *bhlh121-2* seedling defects with the *ProbHLH121:gbHLH121:GFP* transgene.

**Supplemental Figure 11.** Complementation of the *bhlh121-2* seedling defects with the *ProbHLH121:gbHLH121:GFP* transgene.

**Supplemental Figure 12.** Complementation of the *bhlh121-2* defects with the *ProbHLH121:gbHLH121:GFP* transgene.

**Supplemental Figure 13.** bHLH121 binding to the promoters of *FIT*, *bHLH38*, *bHLH39*, *bHLH100*, *bHLH101*, *PYE*, *BTS*, *BTSL1*, *IMA1*, *IMA2*, *IMA3*, *F6'H1*, *S8H*, *CYP82C4*, *MYB10* and *MYB72* by ChIP-qPCR.

**Supplemental Figure 14.** *bhlh121-2* complementation assays by overexpressing *FIT* and *bHLH38*.

**Supplemental Figure 15.** Root growth phenotypes of *bhlh121-2*, *bhlh34*, *bhlh104-1*, *ilr3-3* and *bhlh115-2*.

**Supplemental Figure 16.** *bHLH121* promoter activity.

**Supplemental Figure 17.** bHLH121 protein localization in longitudinal sections of roots.

**Supplemental Figure 18.** bHLH121 protein localization in transverse sections of roots.

**Supplemental Figure 19.** Schematic representation of the localization patterns of *PYE*, *ILR3* and bHLH121 (GFP translational fusion) in the presence or absence of Fe in the maturation zone of Arabidopsis roots.

**Supplemental Figure 20.** Blastn sequence comparisons between *bhlh121-2* and the wild type at the *bHLH11* and *bHLH34* loci (cds regions).

**Supplemental Figure 21.** Blastn sequence comparisons between *bhlh121-2* and the wild type at the *bHLH104* and *bHLH115* loci (cds regions).

**Supplemental Figure 22.** Blastn sequence comparisons between *bhlh121-2* and the wild type at the *ILR3* and *FIT* loci (cds regions).

**Supplemental Figure 23.** Promoter structure diagrams for the genes assayed in ChIP-qPCR experiments.

**Supplemental Table.** ILR3 interacting proteins identified by Co-IP LC-MS/MS.

**Supplemental Data Set 1.** Primers used in this study.

**Supplemental Data Set 2.** ChIP-qPCR experiment #1.

**Supplemental Data Set 3.** ChIP-qPCR experiment #2.

**Supplemental Data Set 4.** ANOVA tables.

### ACKNOWLEDGMENTS

We thank Carine Alcon, Geneviève Conejero, and the Montpellier Rio-Imaging platform (PHIV platform, La Gaillarde, Montpellier, France) for expertise and assistance with microscopy and Sandrine Chay (Biochimie et Physiologie Moléculaire des Plantes, SAME platform, Montpellier, France)

for technical support with plant Fe determination. We also thank Guillaume Cazals for LC-MS/MS analysis for the identification of coumarins (“Laboratoire de Mesures Physiques,” analytical facilities of Montpellier University, France). We thank Nathalie Berger and Alexandre Martinière for help in preparing this article. Support was provided by the Agence Nationale pour la Recherche (ANR-17-CE20-0008-01 to K.R.) and from the China Scholarship Council (to F.G.). This work was also supported by the Comisión Nacional de Investigación Científica y Tecnológica-Environmental Compliance Services (CONICYT-ECOS project C18B04).

#### AUTHOR CONTRIBUTIONS

F.Gao, K.R., M.B., F.V., E.I., and C.D. conceived and designed the experiments; F.Gao, K.R., M.B., N.N., H.R., V.R., F.V., and E.I. performed the experiments; F.Gao, K.R., M.B., F.Gaymard, H.R., F.V., E.I., and C.D. analyzed the data; V.S., F.Gaymard, F.V., E.I., and C.D. contributed reagents/materials/analysis tools; and F.Gao, K.R., F.Gaymard, F.V., E.I., and C.D. wrote the article.

Received July 17, 2019; revised November 4, 2019; accepted November 21, 2019; published November 27, 2019.

#### REFERENCES

- Alassimone, J., Naseer, S., and Geldner, N. (2010). A developmental framework for endodermal differentiation and polarity. *Proc. Natl. Acad. Sci. USA* **107**: 5214–5219.
- Barberon, M., Vermeer, J.E., De Bellis, D., Wang, P., Naseer, S., Andersen, T.G., Humbel, B.M., Nawrath, C., Takano, J., Salt, D.E., and Geldner, N. (2016). Adaptation of root function by nutrient-induced plasticity of endodermal differentiation. *Cell* **164**: 447–459.
- Bechtold, N., Ellis, J., and Pelletier, G. (1993). In planta *Agrobacterium*-mediated gene transfer by infiltration of adult *Arabidopsis thaliana* plants. *C. R. Acad. Sci. Paris* **316**: 1194–1199.
- Briat, J.F., Dubos, C., and Gaymard, F. (2015). Iron nutrition, biomass production, and plant product quality. *Trends Plant Sci.* **20**: 33–40.
- Brumbarova, T., Bauer, P., and Ivanov, R. (2015). Molecular mechanisms governing Arabidopsis iron uptake. *Trends Plant Sci.* **20**: 124–133.
- Colangelo, E.P., and Guerinot, M.L. (2004). The essential basic helix-loop-helix protein FIT1 is required for the iron deficiency response. *Plant Cell* **16**: 3400–3412.
- Couturier, J., Wu, H.C., Dhalleine, T., Pégeot, H., Sudre, D., Gualberto, J.M., Jacquot, J.P., Gaymard, F., Vignols, F., and Rouhier, N. (2014). Monothiol glutaredoxin-BolA interactions: Redox control of *Arabidopsis thaliana* BolA2 and SufE1. *Mol. Plant* **7**: 187–205.
- Cui, Y., Chen, C.L., Cui, M., Zhou, W.J., Wu, H.L., and Ling, H.Q. (2018). Four IVa bHLH transcription factors are novel interactors of FIT and mediate JA inhibition of iron uptake in Arabidopsis. *Mol. Plant* **11**: 1166–1183.
- Czechowski, T., Stitt, M., Altmann, T., Udvardi, M.K., and Scheible, W.R. (2005). Genome-wide identification and testing of superior reference genes for transcript normalization in Arabidopsis. *Plant Physiol.* **139**: 5–17.
- Fourcroy, P., Sisó-Terraza, P., Sudre, D., Savirón, M., Rey, G., Gaymard, F., Abadía, A., Abadía, J., Alvarez-Fernández, A., and Briat, J.F. (2014). Involvement of the ABCG37 transporter in secretion of scopoletin and derivatives by Arabidopsis roots in response to iron deficiency. *New Phytol.* **201**: 155–167.
- Fourcroy, P., Tissot, N., Gaymard, F., Briat, J.F., and Dubos, C. (2016). Facilitated Fe nutrition by phenolic compounds excreted by the Arabidopsis ABCG37/PDR9 transporter requires the IRT1/FRO2 high-affinity root Fe(2+) transport system. *Mol. Plant* **9**: 485–488.
- Gao, F., Robe, K., Gaymard, F., Izquierdo, E., and Dubos, C. (2019). The transcriptional control of iron homeostasis in plants: A tale of bHLH transcription factors? *Front. Plant Sci.* **10**: 6.
- Gendrel, A.V., Lippman, Z., Yordan, C., Colot, V., and Martienssen, R.A. (2002). Dependence of heterochromatic histone H3 methylation patterns on the Arabidopsis gene DDM1. *Science* **297**: 1871–1873.
- Grefen, C., Donald, N., Hashimoto, K., Kudla, J., Schumacher, K., and Blatt, M.R. (2010). A ubiquitin-10 promoter-based vector set for fluorescent protein tagging facilitates temporal stability and native protein distribution in transient and stable expression studies. *Plant J.* **64**: 355–365.
- Grillet, L., Lan, P., Li, W., Mokkapat, G., and Schmidt, W. (2018). IRON MAN is a ubiquitous family of peptides that control iron transport in plants. *Nat. Plants* **4**: 953–963.
- Hänsch, R., and Mendel, R.R. (2009). Physiological functions of mineral micronutrients (Cu, Zn, Mn, Fe, Ni, Mo, B, Cl). *Curr. Opin. Plant Biol.* **12**: 259–266.
- Heim, M.A., Jakoby, M., Werber, M., Martin, C., Weisshaar, B., and Bailey, P.C. (2003). The basic helix-loop-helix transcription factor family in plants: A genome-wide study of protein structure and functional diversity. *Mol. Biol. Evol.* **20**: 735–747.
- Hindt, M.N., Akmakjian, G.Z., Pivarski, K.L., Punshon, T., Baxter, I., Salt, D.E., and Guerinot, M.L. (2017). BRUTUS and its paralogs, BTS LIKE1 and BTS LIKE2, encode important negative regulators of the iron deficiency response in *Arabidopsis thaliana*. *Metallomics* **9**: 876–890.
- Hirayama, T., Lei, G.J., Yamaji, N., Nakagawa, N., and Ma, J.F. (2018). The putative peptide gene FEP1 regulates iron deficiency response in Arabidopsis. *Plant Cell Physiol.* **9**: 1739–1752.
- Ivanov, R., Brumbarova, T., and Bauer, P. (2012). Fitting into the harsh reality: Regulation of iron-deficiency responses in dicotyledonous plants. *Mol. Plant* **5**: 27–42.
- Kobayashi, T., and Nishizawa, N.K. (2012). Iron uptake, translocation, and regulation in higher plants. *Annu. Rev. Plant Biol.* **63**: 131–152.
- Kroh, G.E., and Pilon, M. (2019). Connecting the negatives and positives of plant iron homeostasis. *New Phytol.* **223**: 1052–1055.
- Li, X., Zhang, H., Ai, Q., Liang, G., and Yu, D. (2016). Two bHLH transcription factors, bHLH34 and bHLH104, regulate iron homeostasis in *Arabidopsis thaliana*. *Plant Physiol.* **170**: 2478–2493.
- Liang, G., Zhang, H., Li, X., Ai, Q., and Yu, D. (2017). bHLH transcription factor bHLH115 regulates iron homeostasis in *Arabidopsis thaliana*. *J. Exp. Bot.* **68**: 1743–1755.
- Lichtenthaler, F.W. (1987). Karl Freudenberg, Burckhardt Helferich, Hermann O. L. Fischer: A centennial tribute. *Carbohydr. Res.* **164**: 1–22.
- Ling, H.Q., Bauer, P., Bereczky, Z., Keller, B., and Ganai, M. (2002). The tomato fer gene encoding a bHLH protein controls iron-uptake responses in roots. *Proc. Natl. Acad. Sci. USA* **99**: 13938–13943.
- Long, T.A., Tsukagoshi, H., Busch, W., Lahner, B., Salt, D.E., and Benfey, P.N. (2010). The bHLH transcription factor POPEYE regulates response to iron deficiency in Arabidopsis roots. *Plant Cell* **22**: 2219–2236.
- Matthiadis, A., and Long, T.A. (2016). Further insight into BRUTUS domain composition and functionality. *Plant Signal. Behav.* **11**: e1204508.

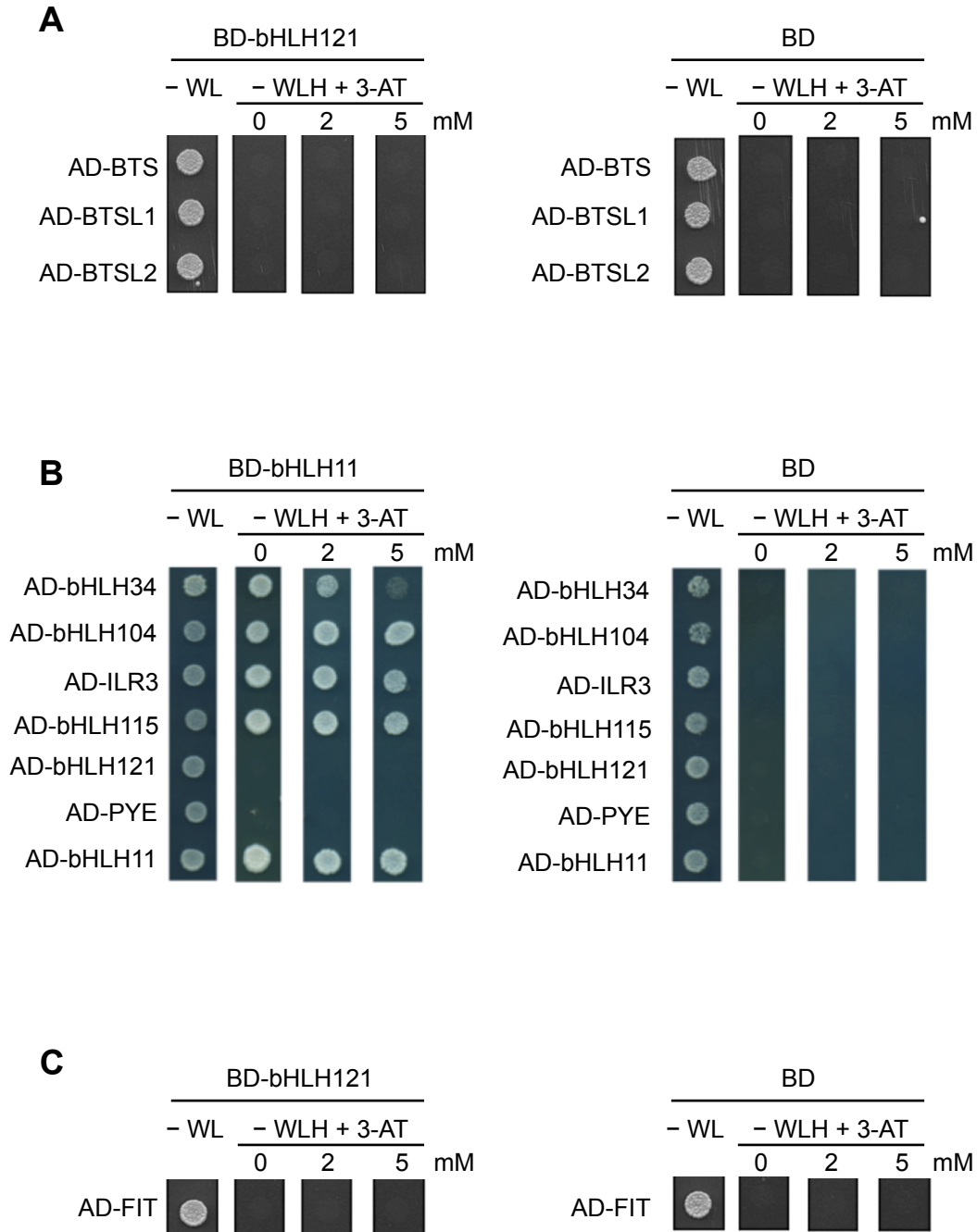
- Nakagawa, T., Kurose, T., Hino, T., Tanaka, K., Kawamukai, M., Niwa, Y., Toyooka, K., Matsuoka, K., Jinbo, T., and Kimura, T.** (2007). Development of series of gateway binary vectors, pGWBs, for realizing efficient construction of fusion genes for plant transformation. *J. Biosci. Bioeng.* **104**: 34–41.
- Palmer, C.M., Hindt, M.N., Schmidt, H., Clemens, S., and Guerinot, M.L.** (2013). MYB10 and MYB72 are required for growth under iron-limiting conditions. *PLoS Genet.* **9**: e1003953.
- Rajniak, J., Giehl, R.F.H., Chang, E., Murgia, I., von Wirén, N., and Sattely, E.S.** (2018). Biosynthesis of redox-active metabolites in response to iron deficiency in plants. *Nat. Chem. Biol.* **14**: 442–450.
- Rampey, R.A., Woodward, A.W., Hobbs, B.N., Tierney, M.P., Lahner, B., Salt, D.E., and Bartel, B.** (2006). An Arabidopsis basic helix-loop-helix leucine zipper protein modulates metal homeostasis and auxin conjugate responsiveness. *Genetics* **174**: 1841–1857.
- Reyt, G., Boudouf, S., Boucherez, J., Gaymard, F., and Briat, J.F.** (2015). Iron- and ferritin-dependent reactive oxygen species distribution: Impact on Arabidopsis root system architecture. *Mol. Plant* **8**: 439–453.
- Rodríguez-Celma, J., Connorton, J.M., Kruse, I., Green, R.T., Franceschetti, M., Chen, Y.T., Cui, Y., Ling, H.Q., Yeh, K.C., and Balk, J.** (2019). Arabidopsis BRUTUS-LIKE E3 ligases negatively regulate iron uptake by targeting transcription factor FIT for recycling. *Proc. Natl. Acad. Sci. USA* **116**: 17584–17591.
- Rodríguez-Celma, J., Lin, W.D., Fu, G.M., Abadía, J., López-Millán, A.F., and Schmidt, W.** (2013). Mutually exclusive alterations in secondary metabolism are critical for the uptake of insoluble iron compounds by Arabidopsis and *Medicago truncatula*. *Plant Physiol.* **162**: 1473–1485.
- Roschttardt, H., Conéjéro, G., Curie, C., and Mari, S.** (2009). Identification of the endodermal vacuole as the iron storage compartment in the Arabidopsis embryo. *Plant Physiol.* **151**: 1329–1338.
- Samira, R., Li, B., Kliebenstein, D., Li, C., Davis, E., Gillikin, J.W., and Long, T.A.** (2018). The bHLH transcription factor ILR3 modulates multiple stress responses in Arabidopsis. *Plant Mol. Biol.* **97**: 297–309.
- Santi, S., and Schmidt, W.** (2009). Dissecting iron deficiency-induced proton extrusion in Arabidopsis roots. *New Phytol.* **183**: 1072–1084.
- Schmid, N.B., Giehl, R.F., Döll, S., Mock, H.P., Strehmel, N., Scheel, D., Kong, X., Hider, R.C., and von Wirén, N.** (2014). Feruloyl-CoA 6'-Hydroxylase1-dependent coumarins mediate iron acquisition from alkaline substrates in Arabidopsis. *Plant Physiol.* **164**: 160–172.
- Selote, D., Samira, R., Matthiadis, A., Gillikin, J.W., and Long, T.A.** (2015). Iron-binding E3 ligase mediates iron response in plants by targeting basic helix-loop-helix transcription factors. *Plant Physiol.* **167**: 273–286.
- Sivitz, A., Grinvalds, C., Barberon, M., Curie, C., and Vert, G.** (2011). Proteasome-mediated turnover of the transcriptional activator FIT is required for plant iron-deficiency responses. *Plant J.* **66**: 1044–1052.
- Siwinska, J., Siatkowska, K., Olry, A., Grosjean, J., Hehn, A., Bourgaud, F., Meharg, A.A., Carey, M., Lojkowska, E., and Ichnatowicz, A.** (2018). Scopoletin 8-hydroxylase: a novel enzyme involved in coumarin biosynthesis and iron-deficiency responses in Arabidopsis. *J. Exp. Bot.* **69**: 1735–1748.
- Tissot, N., et al.** (2019). Transcriptional integration of the responses to iron availability in Arabidopsis by the bHLH factor ILR3. *New Phytol.* **223**: 1433–1446.
- Touraine, B., et al.** (2019). Iron-sulfur protein NFU2 is required for branched-chain amino acid synthesis in Arabidopsis roots. *J. Exp. Bot.* **70**: 1875–1889.
- Tsai, H.H., Rodríguez-Celma, J., Lan, P., Wu, Y.C., Vélez-Bermúdez, I.C., and Schmidt, W.** (2018). Scopoletin 8-hydroxylase-mediated fraxetin production is crucial for iron mobilization. *Plant Physiol.* **177**: 194–207.
- Tyanova, S., Temu, T., and Cox, J.** (2016). The MaxQuant computational platform for mass spectrometry-based shotgun proteomics. *Nat Protoc* **11**: 2301–2319.
- Wang, N., Cui, Y., Liu, Y., Fan, H., Du, J., Huang, Z., Yuan, Y., Wu, H., and Ling, H.Q.** (2013). Requirement and functional redundancy of Ib subgroup bHLH proteins for iron deficiency responses and uptake in *Arabidopsis thaliana*. *Mol. Plant* **6**: 503–513.
- Wang, Z.P., Xing, H.L., Dong, L., Zhang, H.Y., Han, C.Y., Wang, X.C., and Chen, Q.J.** (2015). Egg cell-specific promoter-controlled CRISPR/Cas9 efficiently generates homozygous mutants for multiple target genes in Arabidopsis in a single generation. *Genome Biol.* **16**: 144.
- Xu, W., et al.** (2013). Regulation of flavonoid biosynthesis involves an unexpected complex transcriptional regulation of TT8 expression, in Arabidopsis. *New Phytol.* **198**: 59–70.
- Yuan, Y., Wu, H., Wang, N., Li, J., Zhao, W., Du, J., Wang, D., and Ling, H.Q.** (2008). FIT interacts with AtbHLH38 and AtbHLH39 in regulating iron uptake gene expression for iron homeostasis in Arabidopsis. *Cell Res.* **18**: 385–397.
- Yuan, Y.X., Zhang, J., Wang, D.W., and Ling, H.Q.** (2005). AtbHLH29 of *Arabidopsis thaliana* is a functional ortholog of tomato FER involved in controlling iron acquisition in strategy I plants. *Cell Res.* **15**: 613–621.
- Zamioudis, C., Hanson, J., and Pieterse, C.M.** (2014).  $\beta$ -Glucosidase BGLU42 is a MYB72-dependent key regulator of rhizobacteria-induced systemic resistance and modulates iron deficiency responses in Arabidopsis roots. *New Phytol.* **204**: 368–379.
- Zhang, J., Liu, B., Li, M., Feng, D., Jin, H., Wang, P., Liu, J., Xiong, F., Wang, J., and Wang, H.B.** (2015). The bHLH transcription factor bHLH104 interacts with IAA-LEUCINE RESISTANT3 and modulates iron homeostasis in Arabidopsis. *Plant Cell* **27**: 787–805.

**The Transcription Factor bHLH121 Interacts with bHLH105 (ILR3) and Its Closest Homologs to Regulate Iron Homeostasis in Arabidopsis**

Fei Gao, Kevin Robe, Mathilde Bettembourg, Nathalia Navarro, Valérie Rofidal, Véronique Santoni, Frédéric Gaymard, Florence Vignols, Hannetz Roschzttardtz, Esther Izquierdo and Christian Dubos  
*Plant Cell* 2020;32;508-524; originally published online November 27, 2019;  
DOI 10.1105/tpc.19.00541

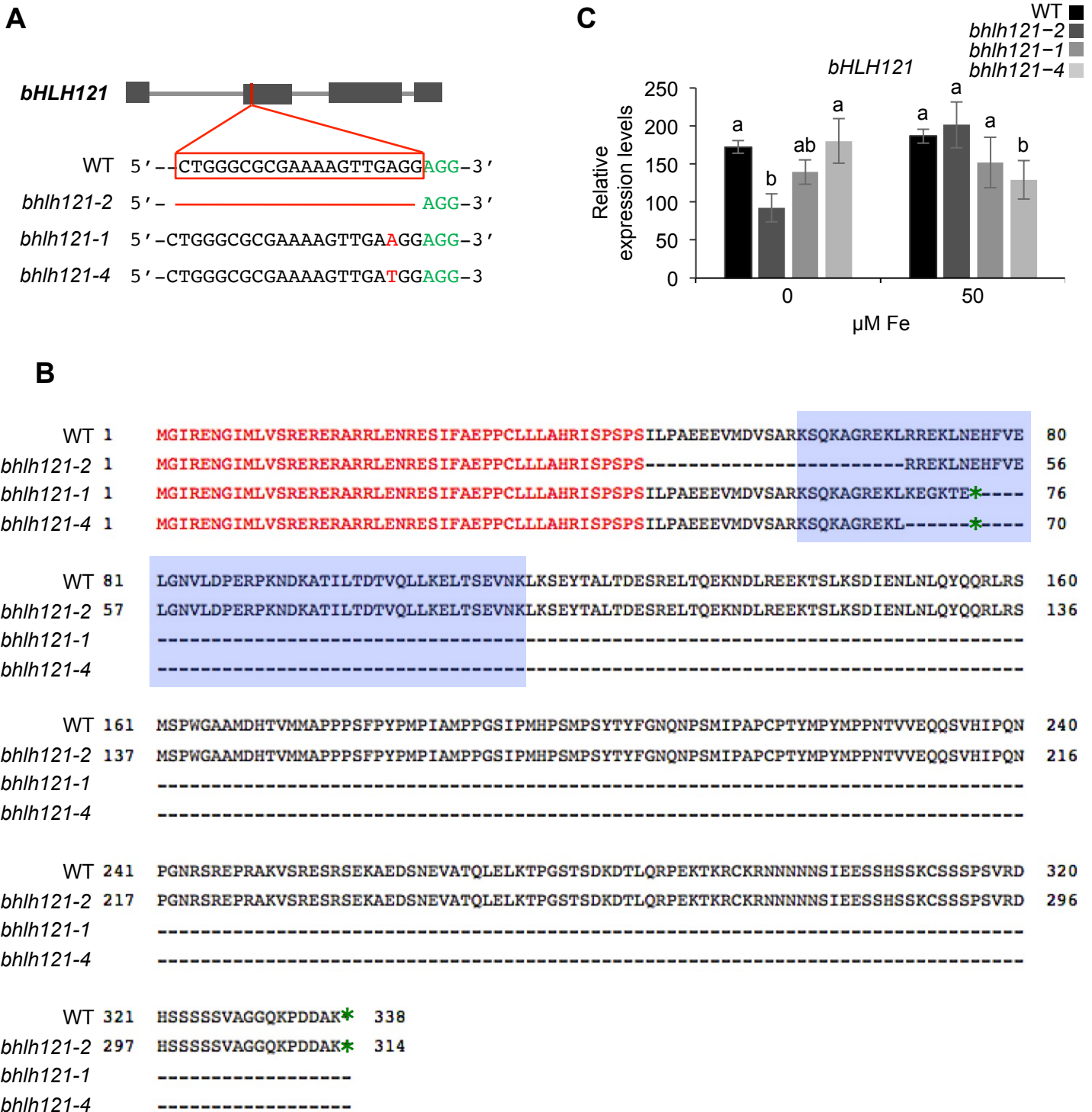
This information is current as of February 9, 2020

<b>Supplemental Data</b>	<a href="/content/suppl/2019/11/27/tpc.19.00541.DC1.html">/content/suppl/2019/11/27/tpc.19.00541.DC1.html</a>
<b>References</b>	This article cites 53 articles, 15 of which can be accessed free at: <a href="/content/32/2/508.full.html#ref-list-1">/content/32/2/508.full.html#ref-list-1</a>
<b>Permissions</b>	<a href="https://www.copyright.com/ccc/openurl.do?sid=pd_hw1532298X&amp;issn=1532298X&amp;WT.mc_id=pd_hw1532298X">https://www.copyright.com/ccc/openurl.do?sid=pd_hw1532298X&amp;issn=1532298X&amp;WT.mc_id=pd_hw1532298X</a>
<b>eTOCs</b>	Sign up for eTOCs at: <a href="http://www.plantcell.org/cgi/alerts/ctmain">http://www.plantcell.org/cgi/alerts/ctmain</a>
<b>CiteTrack Alerts</b>	Sign up for CiteTrack Alerts at: <a href="http://www.plantcell.org/cgi/alerts/ctmain">http://www.plantcell.org/cgi/alerts/ctmain</a>
<b>Subscription Information</b>	Subscription Information for <i>The Plant Cell</i> and <i>Plant Physiology</i> is available at: <a href="http://www.aspb.org/publications/subscriptions.cfm">http://www.aspb.org/publications/subscriptions.cfm</a>

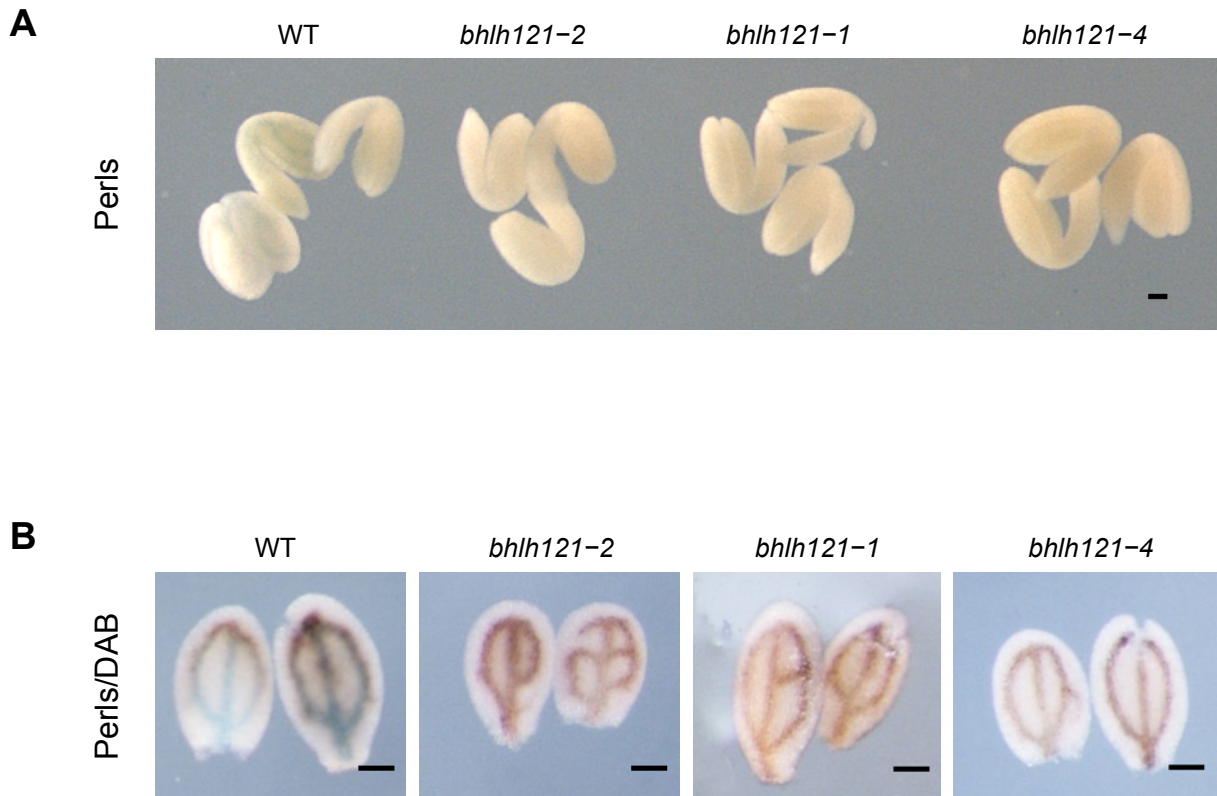


**Supplemental Figure 1. bHLH11 interacts with ILR3 and its closest homologous and form homodimers (Supports Figure 1).**

Yeast two-hybrid (Y2H) assays. bHLH34, bHLH104, ILR3, bHLH115, PYE, bHLH11, bHLH121, BTS, BTSL1, BTSL2 and FIT were fused with the GAL4 activation domain (AD) and bHLH11 and bHLH121 with the GAL4 DNA binding domain (BD) into appropriate expression vectors prior to transfer into yeast (AH109 strain). The different yeast strains were plated on nonselective medium (-WL) or on selective medium lacking histidine (-WLH) and containing various concentrations of 3-AT (3-Amino-1,2,4-triazole). BD alone was used as a negative control. Growing colonies representative of positive Y2H interactions were identified after 6 days of growth. W, tryptophan; L, leucine; H, histidine. **(A)** Interactions between bHLH121 and the E3-ubiquitin ligases involved in the control of Fe homeostasis. **(B)** Interactions between bHLH11 and the bHLH TF involved in the ILR3 subnetwork. **(C)** Interaction between bHLH121 and FIT.

**Supplemental Figure 2. *bhlh121* loss-of-function mutations (Supports Figure 2).**

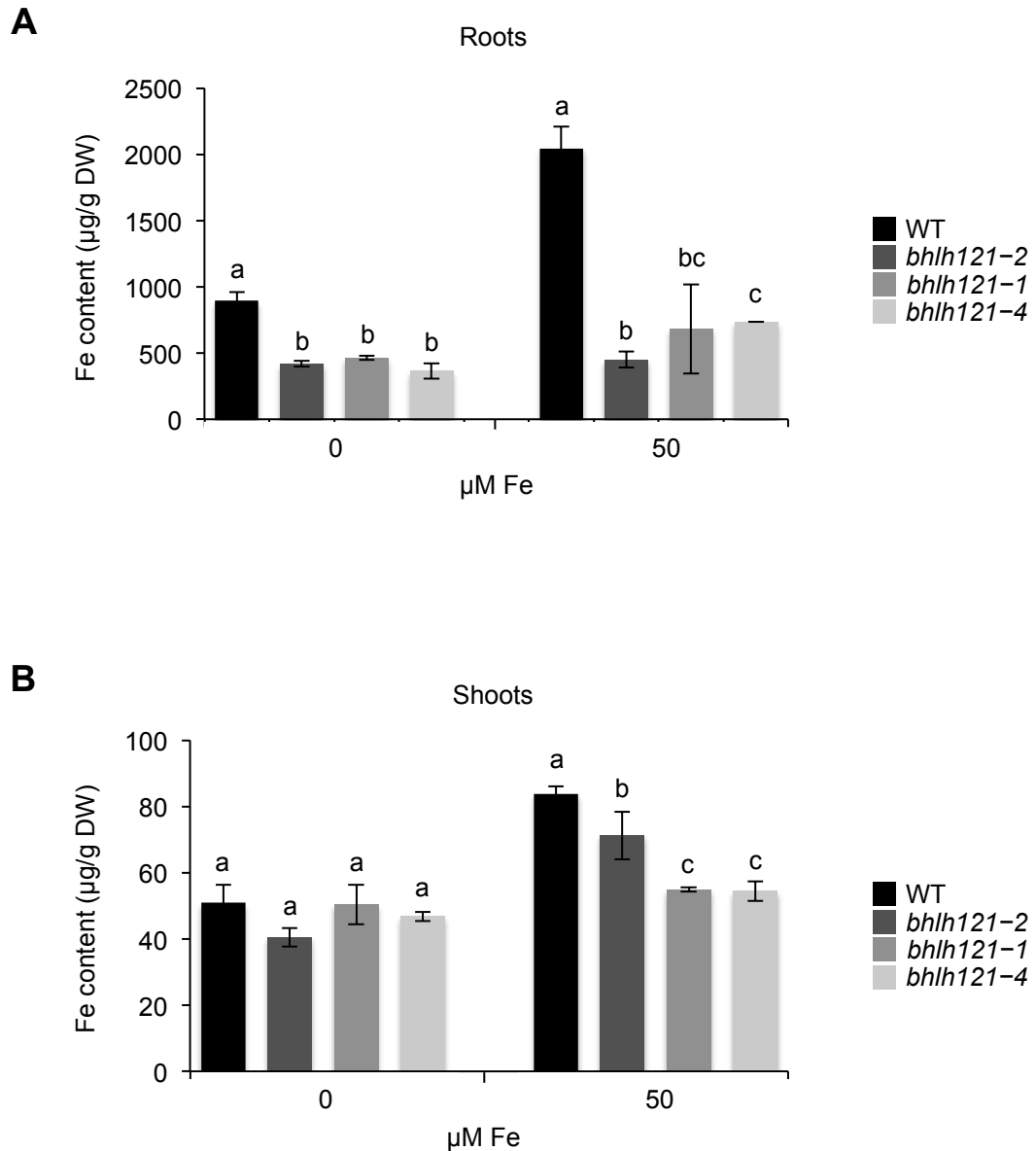
(A) Top part: schematic representation of *bHLH121* gene locus (grey box, exon; line, intron; red line: mutation site). Bottom part: localization of the RNA guides, within the second exon, selected for Crispr-Cas9 gene editing. In red are the mutations produced in the cds: a deletion for *bhlh121-2* (78 bp coding sequence) and single nucleotide insertions for *bhlh121-1* (A) and *bhlh121-4* (T). In green: NGG sequence. (B) Protein sequence alignment between the WT and the Crispr-Cas9 edited *bHLH121* sequences. In red: first exon; highlighted in blue: bHLH domain; green star: stop codon. (C) Relative expression of *bHLH121* was determined by qRT-PCR in 1-week-old *Arabidopsis thaliana* seedlings grown on Fe-sufficient (50 μM Fe) or Fe-deficient (0 μM Fe) medium. Means within each condition with the same letter are not significantly different according to one-way ANOVA followed by post-hoc Tukey test,  $p < 0.05$  ( $n = 3$  technical repeats from one representative experiment). Error bars show  $\pm$ SD. Each experiment (biological repeat) comprised pooled RNA extracted from approximately 30 seedlings and was independently repeated three times.



**Supplemental Figure 3. Fe staining of WT and *bhlh121* embryos (Supports Figure 3).**

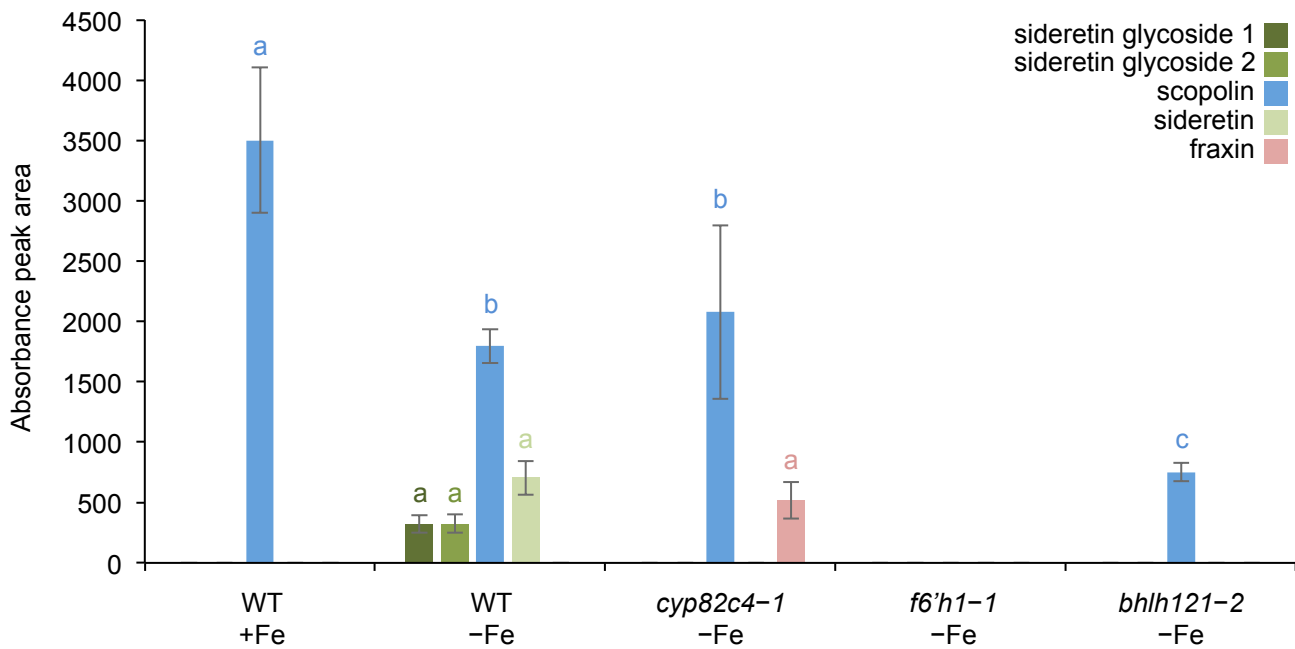
**(A)** Whole embryos following Perls staining. Fe appears in blue alongside the vasculature of WT embryos and is not visible in the *bhlh121* mutant embryos. **(B)** Perls/DAB staining of embryo cotyledons. Fe appears in brown/black. A darker staining indicates a higher amount of Fe in the concerned tissues. (A and B) Bars = 100  $\mu$ m.





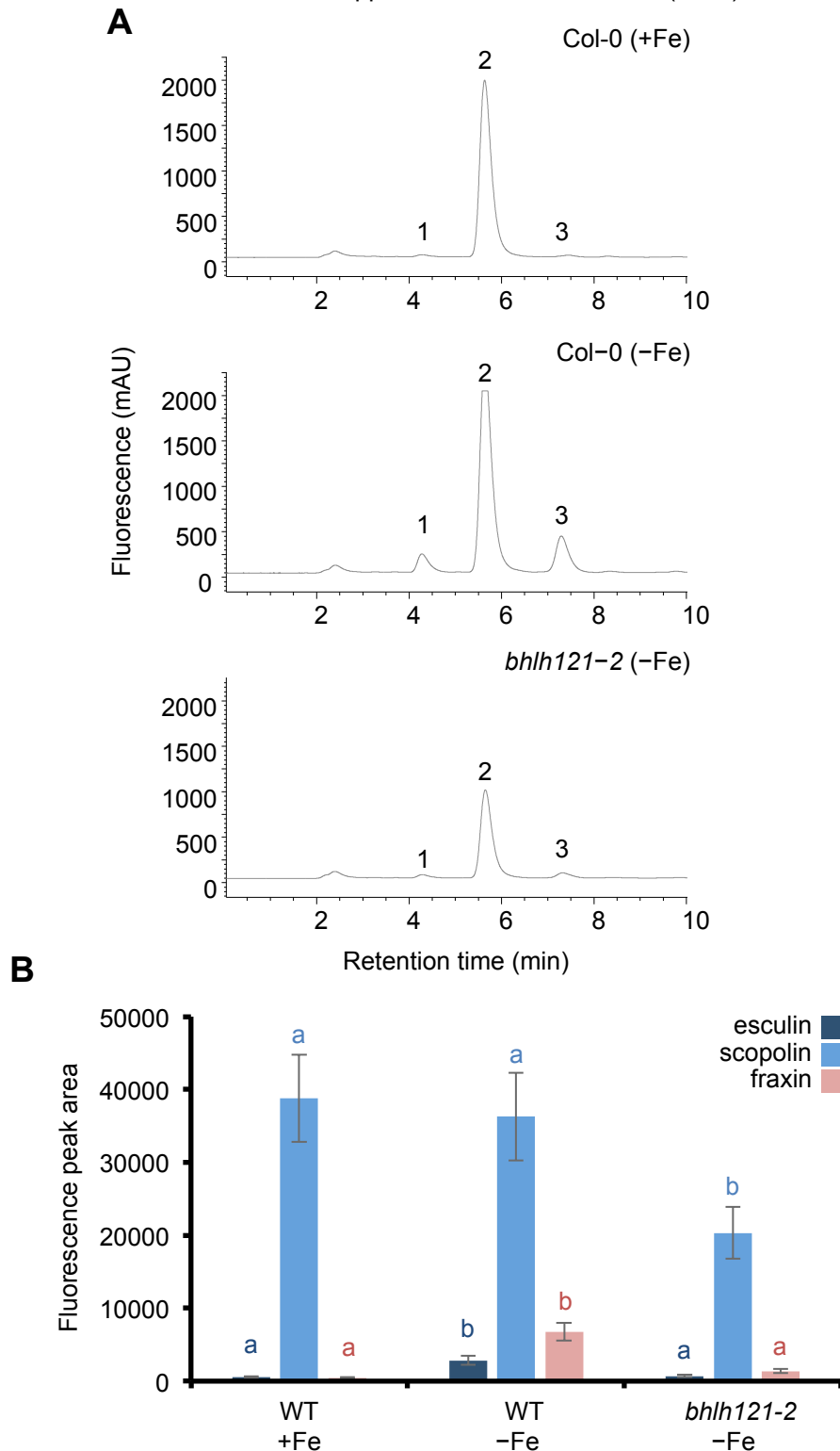
**Supplemental Figure 4. The *bhlh121* loss-of-function mutant plants have decreased accumulation of Fe in roots and shoots (Supports Figure 3).**

**(A)** Fe content WT and *bhlh121* roots grown for 5 weeks under control (50 µM Fe) and Fe deficient (0 µM Fe) hydroponic conditions. **(B)** Fe content in shoots of WT and *bhlh121* mutants grown as in panel A. **(A-B)** Means within each condition with the same letter are not significantly different according to one-way ANOVA followed by post-hoc Tukey test,  $p < 0.05$  ( $n = 3$  biological repeats from one representative experiment). Error bars show  $\pm$ SD. Each biological repeat comprised pooled samples from 3 plants and the experiment was repeated three times.



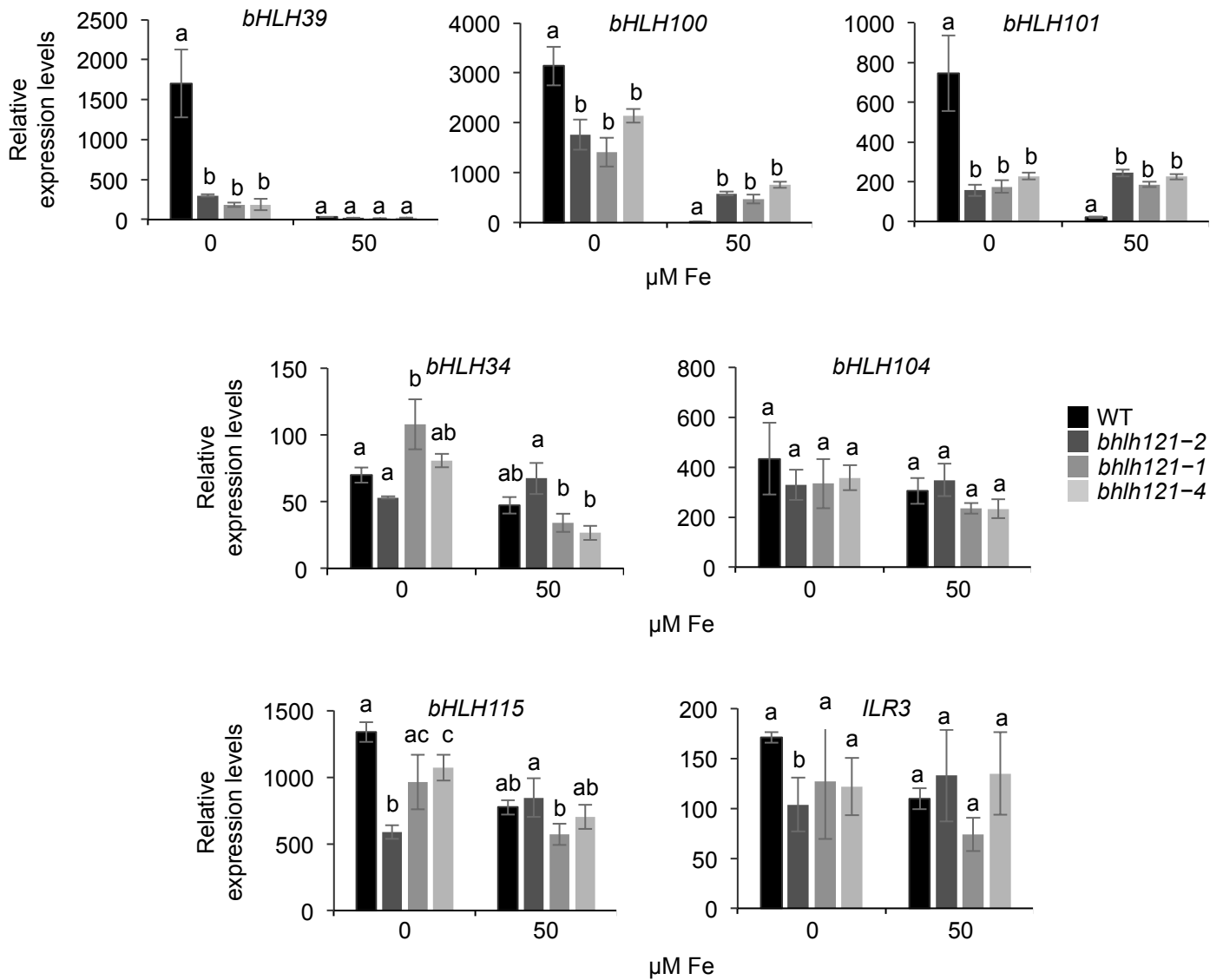
**Supplemental Figure 5. Coumarin accumulation in WT, *cyp8c24-1*, *f6'h1* and *bhlh121-2* (Supports Figure 4).**

Measurements of sideretin glycosides, scopolin (scopoletin glycoside), sideretin and fraxin (fraxetin glycoside) absorbance peak areas described in Figure 4E. Means for each coumarin type with the same letter are not significantly different between the genotypes according to one-way ANOVA followed by post-hoc Tukey test,  $p < 0.05$  ( $n = 3$  to 6 biological repeats from one representative experiment). The absence of a value indicates that the corresponding compound was not detected. Error bars show  $\pm$ SD. Each biological repeat comprised pooled roots from approximately 100 seedlings and the experiment was repeated three times.



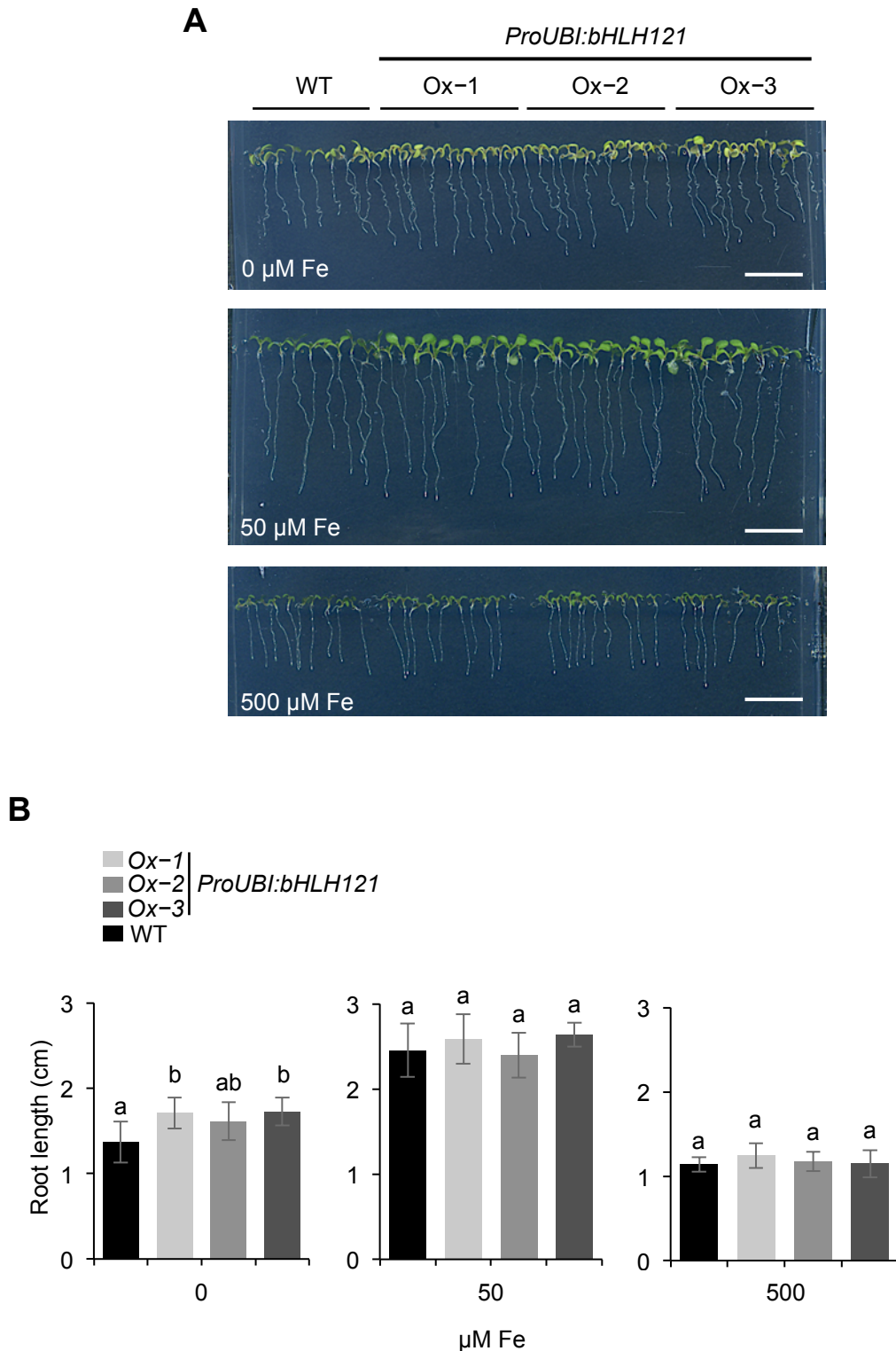
**Supplemental Figure 6. Coumarin accumulation in WT and *bhlh121-1* (Supports Figure 4).**

(A) Representative fluorescence chromatograms monitored using  $\lambda_{exc}$  365 and  $\lambda_{em}$  460 nm for root extracts of *Arabidopsis thaliana* WT and *bhlh121-2* seedlings grown for 7 days on MS/2 agar plates at pH 7. +Fe: control, -Fe: Fe deficiency. Numbered peaks correspond to esculin (1), scopolin (2) and fraxin (3). (B) Measurements of esculin, (scopoletin glycoside) and fraxin (fraxetin glycoside) fluorescence peak areas. Means for each coumarin type with the same letter are not significantly different between the genotypes according to one-way ANOVA followed by post-hoc Tukey test,  $p < 0.05$  ( $n = 3$  to 6 biological repeats from one representative experiment). The absence of a value indicates that the corresponding compound was not detected. Error bars show  $\pm$ SD. Each biological repeat comprised pooled roots from approximately 100 seedlings and was repeated three times.



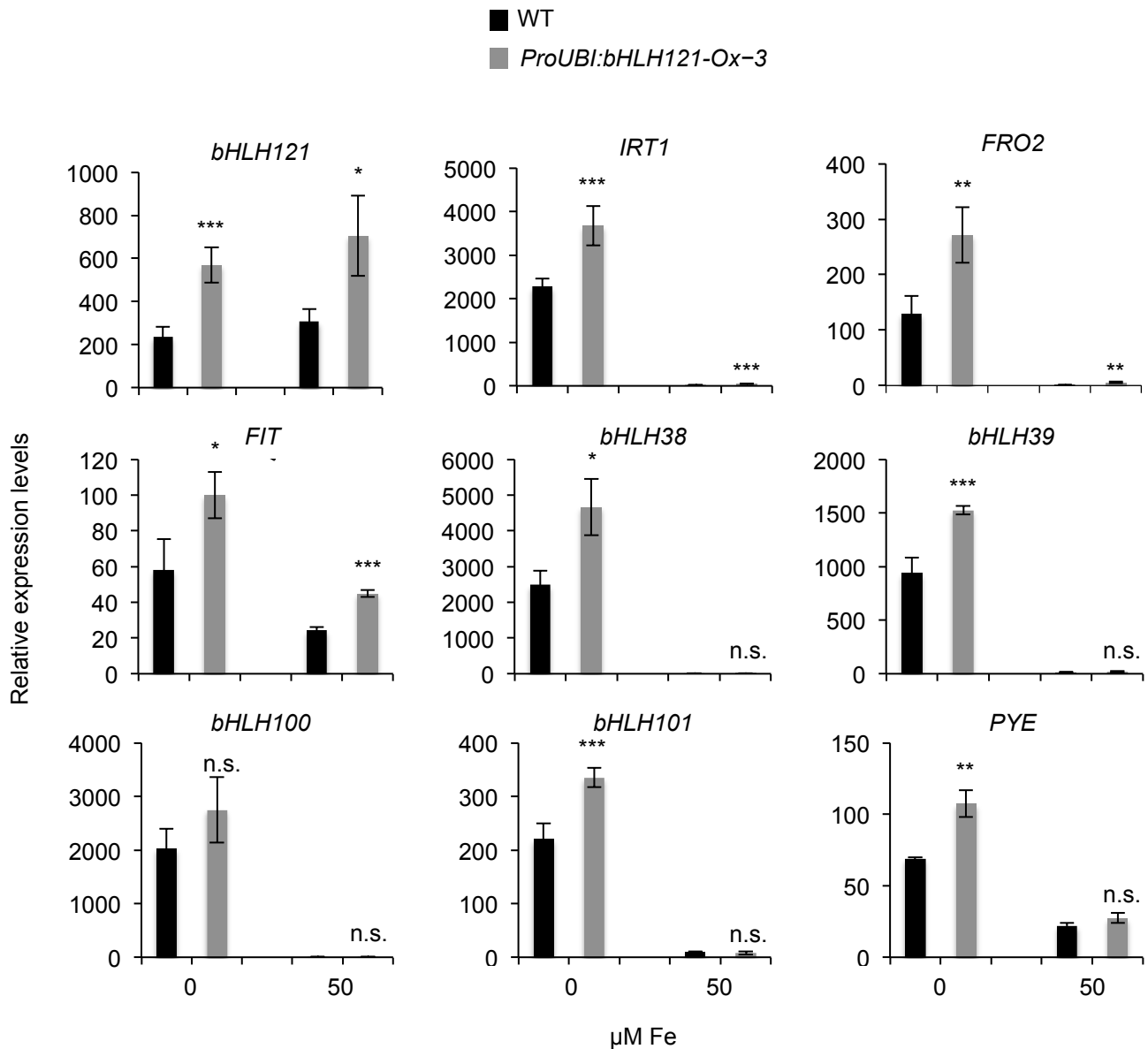
**Supplemental Figure 7. *bHLH34*, *bHLH104*, *bHLH115* and *ILR3* expression is not compromised in the *bhlh121* loss-of-function mutants (Supports Figure 5).**

Relative expression of *bHLH39*, *bHLH100*, *bHLH101*, *bHLH34*, *bHLH104*, *bHLH115* and *ILR3* was determined by qRT-PCR in 1-week-old *Arabidopsis thaliana* seedlings grown on Fe-sufficient (50 μM Fe) or Fe-deficient (0 μM Fe) medium. Means within each condition with the same letter are not significantly different according to one-way ANOVA followed by post-hoc Tukey test,  $p < 0.05$  ( $n = 3$  technical repeats from one representative experiment). Error bars show  $\pm$ SD. Each experiment (biological repeat) pools RNA extracted from approximately 30 seedlings and was independently repeated three times.



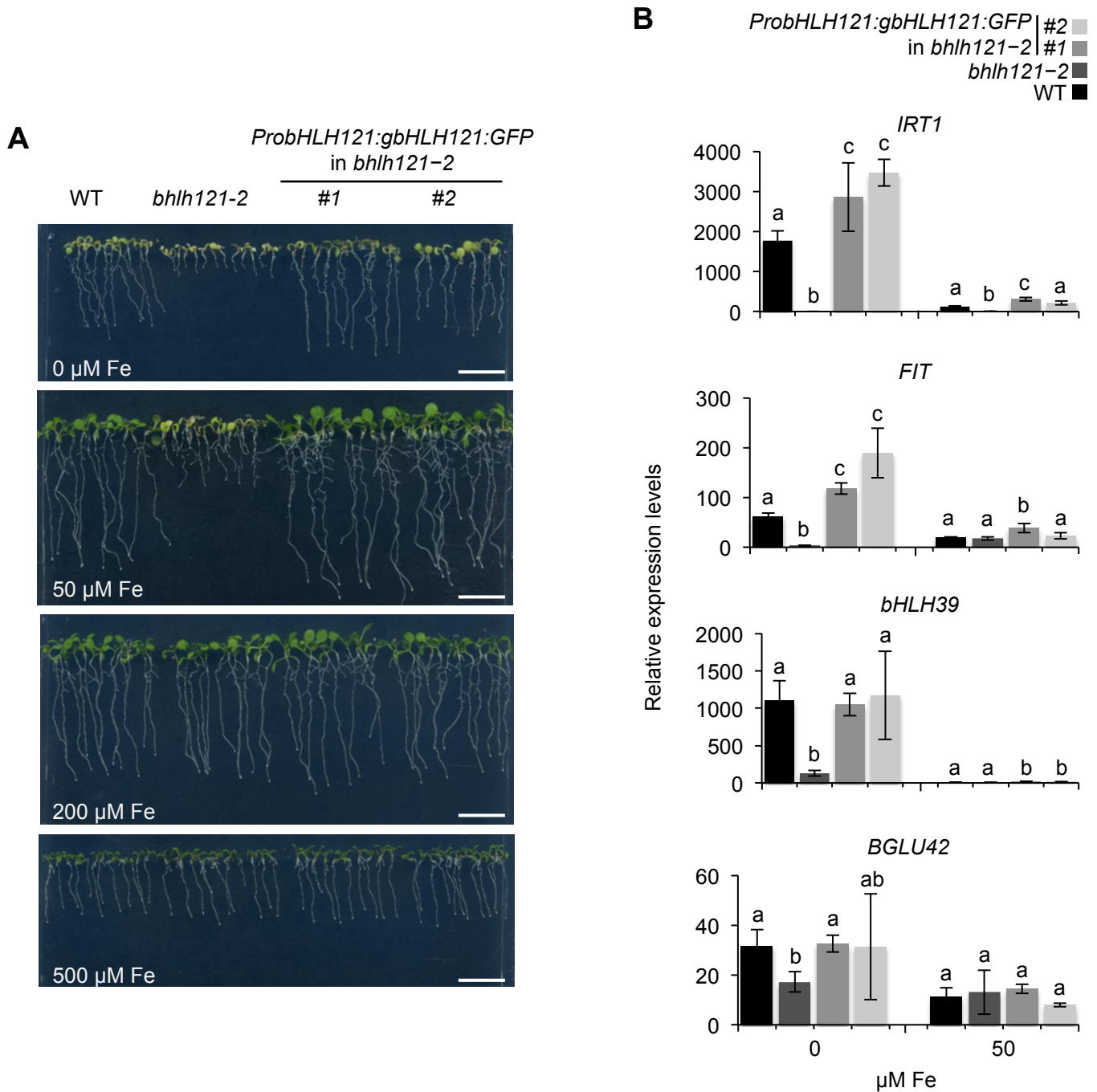
**Supplemental Figure 8. Phenotypes of *bHLH121* overexpressing lines (Supports Figure 5).**

**(A)** Phenotypes of the *Arabidopsis thaliana* WT and three *bHLH121* overexpressing lines (*ProUBI:bHLH121*-Ox) grown for 2 weeks on Fe-sufficient (50 μM Fe), Fe-deficient (0 μM Fe) or Fe-excess (500 μM Fe) medium. Bar = 1 cm. **(B)** Root length of WT and overexpressing lines shown in panel A. Means within each condition with the same letter are not significantly different according to one-way ANOVA followed by post-hoc Tukey test,  $p < 0.05$  ( $n = 3$  biological repeats from one representative experiment). Error bars show  $\pm$ SD. A biological repeat comprised 8 to 12 seedlings and was repeated three times.



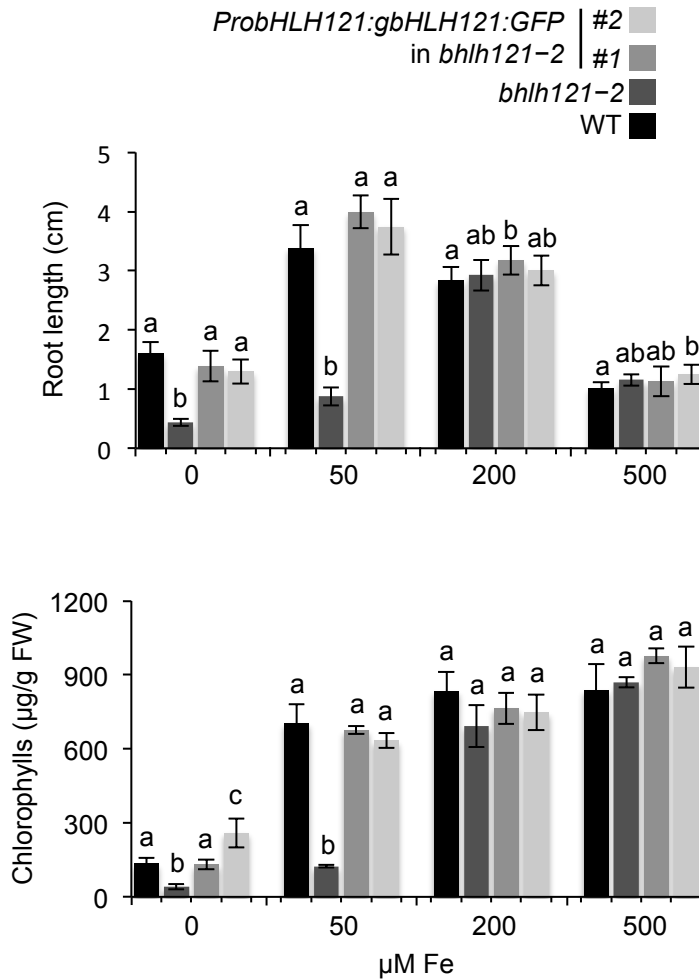
**Supplemental Figure 9. *bHLH121* overexpression induces the expression of several Fe homeostasis-related genes (Supports Figure 5).**

Relative expression of *bHLH121*, *IRT1*, *FRO2*, *FIT*, *bHLH38*, *bHLH39*, *bHLH100*, *bHLH101* and *PYE* was determined by qRT-PCR in 1-week-old *Arabidopsis thaliana* seedlings grown on Fe-sufficient (50 μM Fe) or Fe-deficient (0 μM Fe) medium. Error bars show ±SD. *t*-test significant difference: \*,  $p < 0.05$ ; \*\*,  $p < 0.01$ ; \*\*\*,  $p < 0.001$  ( $n = 3$  technical repeats from one representative experiment). Each experiment (biological repeat) comprised pooled RNA extracted from approximately 30 seedlings and was independently repeated three times.



**Supplemental Figure 10. Complementation of the *bhlh121-2* seedling defects with the *ProbHLH121:gbHLH121:GFP* transgene (Supports Figure 5).**

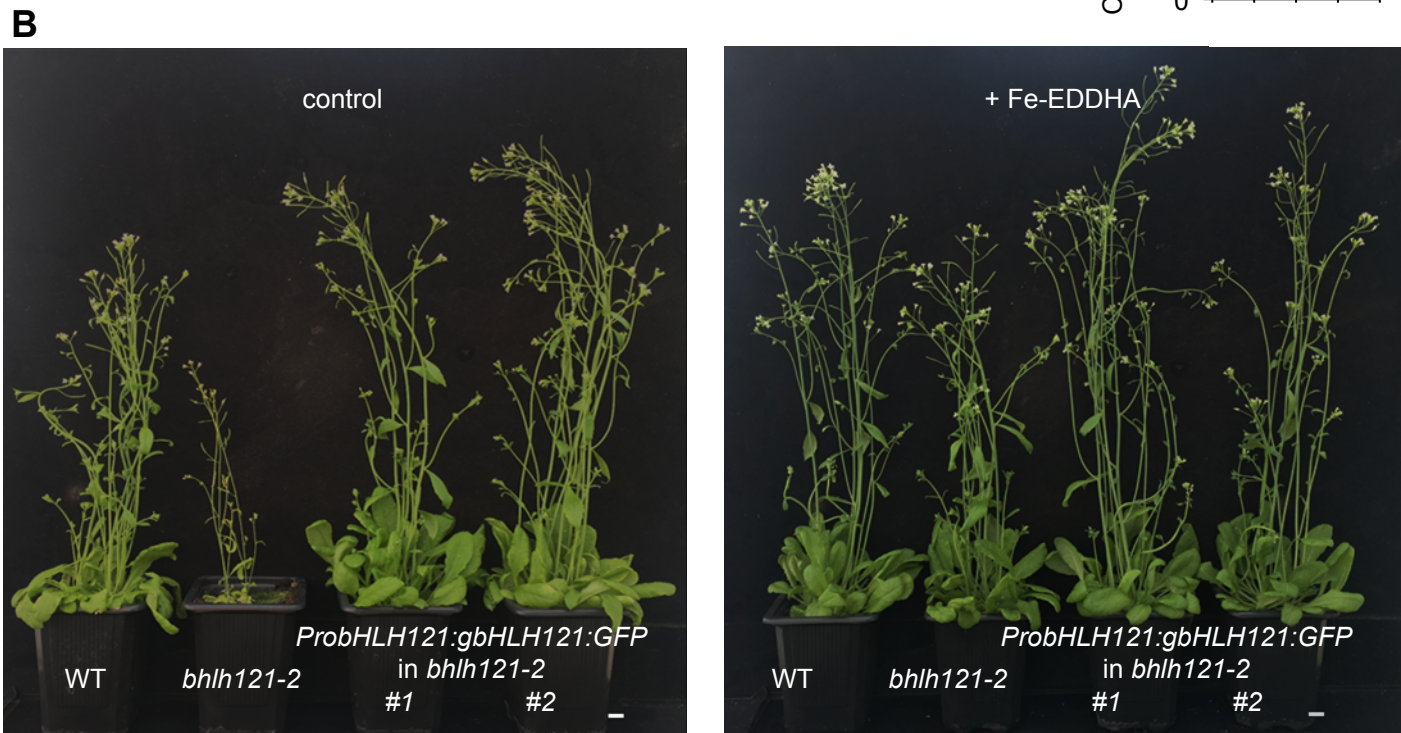
(A) Phenotypes of the *Arabidopsis thaliana* WT, *bhlh121-2* and two independent *bhlh121-2* lines complemented with the *ProbHLH121:gbHLH121:GFP* transgene. Plants were grown for 2 weeks on Fe-sufficient (50  $\mu\text{M Fe}$ ), Fe-deficient (0  $\mu\text{M Fe}$ ) or Fe-excess (200 and 500  $\mu\text{M Fe}$ ) medium. Bar = 1 cm. (B) Relative expression of *IRT1*, *FIT*, *bHLH39* and *BGLU42* as determined by qRT-PCR in two weeks old *Arabidopsis* seedlings grown on Fe-sufficient or Fe-deficient medium. Means within each condition with the same letter are not significantly different according to one-way ANOVA followed by post-hoc Tukey test,  $p < 0.05$  ( $n = 3$  technical repeats from one representative experiment). Error bars show  $\pm\text{SD}$ . Each experiment (biological repeat) pools RNA extracted from approximately 30 seedlings and was independently repeated three times.



**Supplemental Figure 11. Complementation of the *bhlh121-2* seedling defects with the *ProbHLH121:gbHLH121:GFP* transgene (Supports Figure 5).**

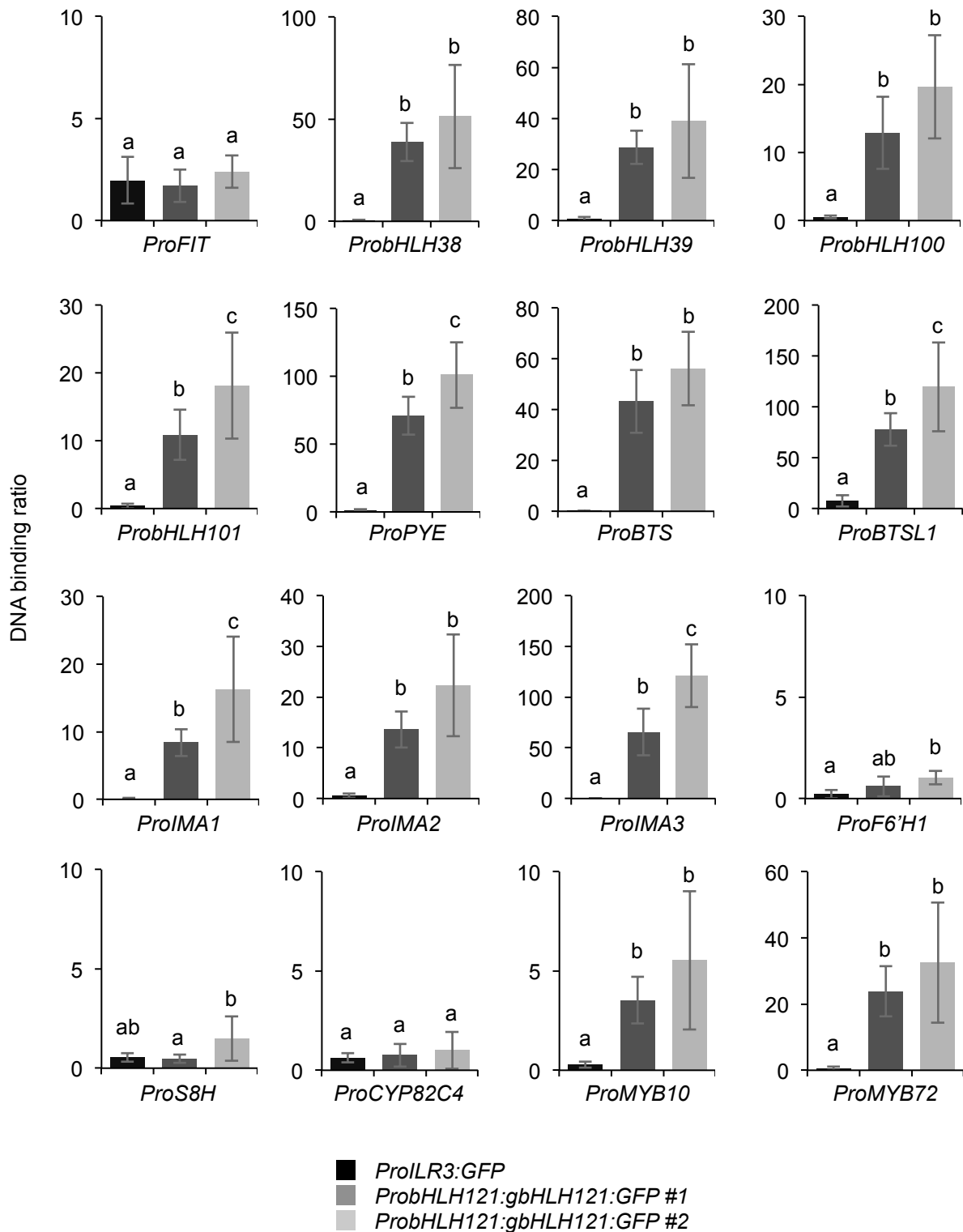
Root length and chlorophyll content of WT, *bhlh121-2* and two independent *bhlh121-2* lines complemented with the *ProbHLH121:gbHLH121:GFP* transgene. Plants were grown for 2 weeks on Fe-sufficient (50 μM Fe), Fe-deficient (0 μM Fe) or Fe-excess (200 and 500 μM Fe) medium. Means within each condition with the same letter are not significantly different according to one-way ANOVA followed by post-hoc Tukey test,  $p < 0.05$  ( $n = 3$  biological repeats from one representative experiment). Error bars show  $\pm$ SD. A biological repeat comprised approximately 8 to 12 seedlings for the root length measurements and 5 seedlings for chlorophyll measurements. Each experiment was repeated three times.





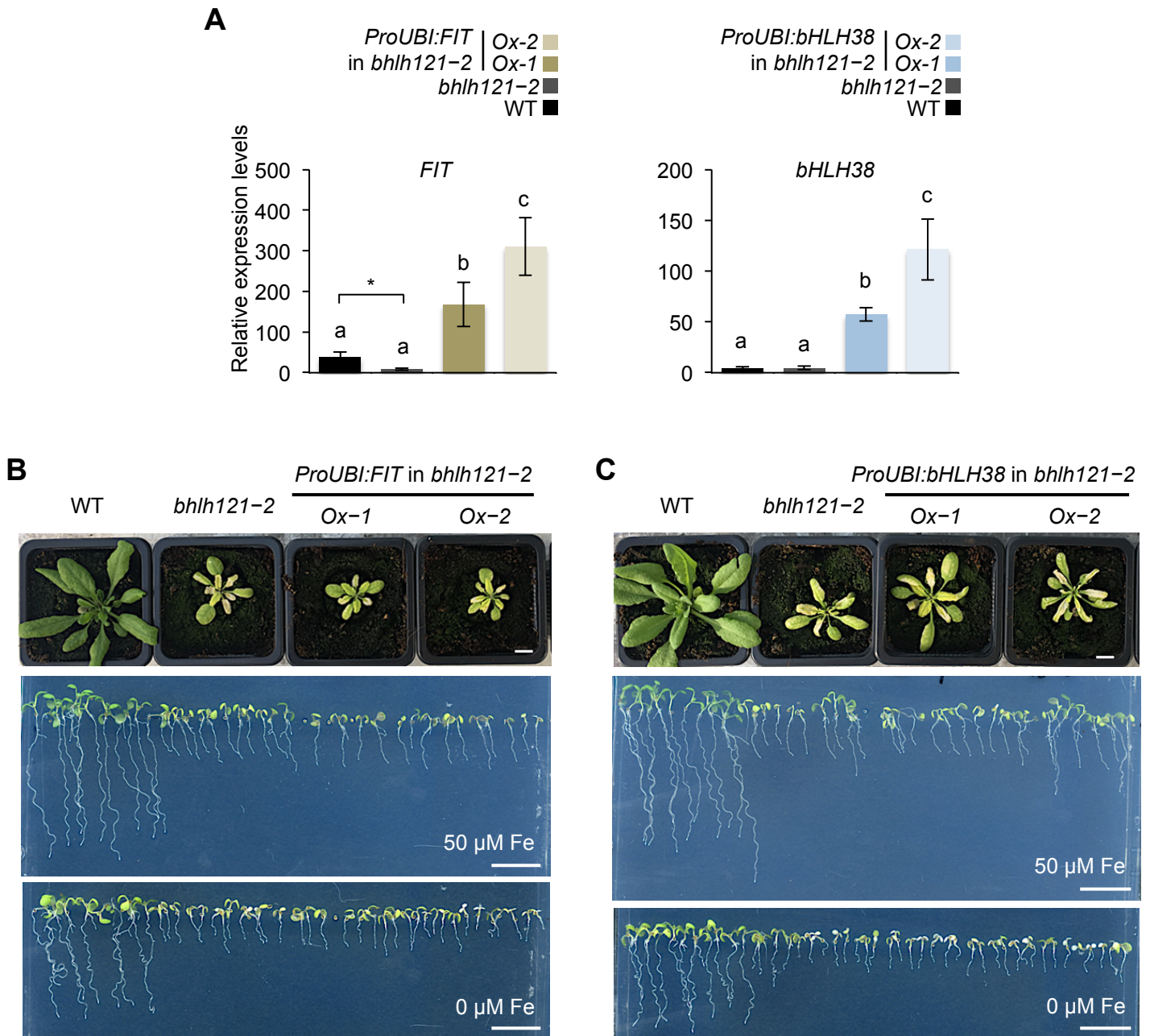
**Supplemental Figure 12. Complementation of the *bhlh121-2* defects with the *ProbHLH121:gbHLH121:GFP* transgene (Supports Figure 5).**

(A) Left panel: Phenotypes of WT, *bhlh121-2* and two independent *bhlh121-2* lines complemented with the *ProbHLH121:gbHLH121:GFP* transgene. Plants were grown in soil for 3 weeks and watered or not with Fe-EDDHA. Right panels: chlorophyll content in the leaves of the seedlings presented in the left panel. Means within each condition with the same letter are not significantly different according to one-way ANOVA followed by post-hoc Tukey test,  $p < 0.05$  ( $n = 3$  biological repeats from one representative experiment). Error bars show  $\pm$ SD. A biological repeat comprised pooled leaf samples from 3 to 10 seedlings. Each experiment was repeated three times. (B) Phenotypes of WT, *bhlh121-2* and two independent complemented *bhlh121-2* lines carrying the *ProbHLH121:gbHLH121:GFP* transgene grown in soil for 6 weeks and watered or not with Fe-EDDHA. (A and B) Bars = 1 cm.

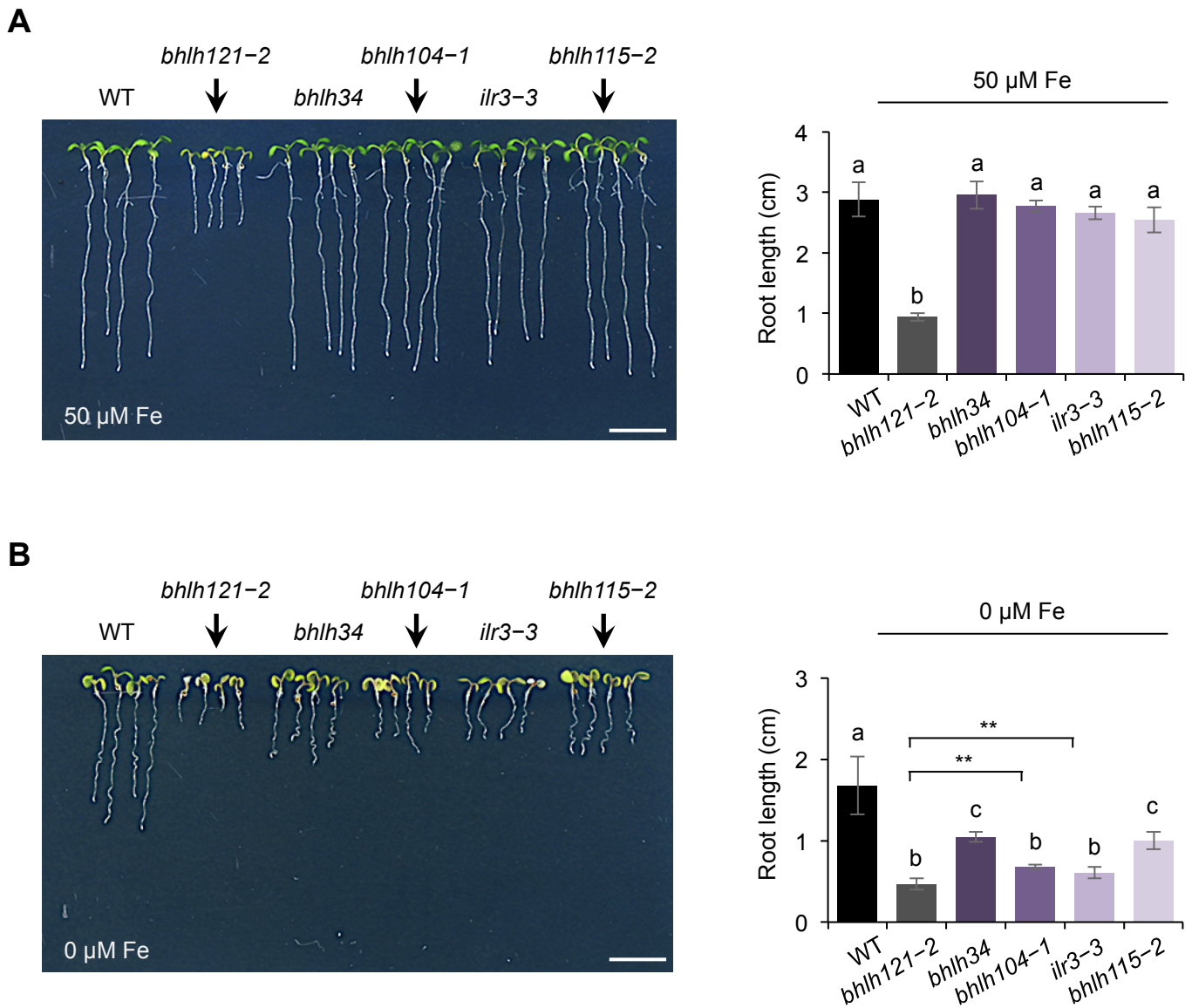


**Supplemental Figure 13. bHLH121 binding to the promoters of *FIT*, *bHLH38*, *bHLH39*, *bHLH100*, *bHLH101*, *PYE*, *BTS*, *BTSL1*, *IMA1*, *IMA2*, *IMA3*, *F6'H1*, *S8H*, *CYP82C4*, *MYB10* and *MYB72* by ChIP-qPCR (Supports Figure 5).**

Chromatin from the two complemented *bhlh121-2* lines carrying the *ProbHLH121:gbHLH121:GFP* transgene submitted to Fe deficiency was extracted using anti-GFP antibodies. Seedlings expressing GFP under the control of the *ILR3* promoter (*ProILR3:GFP*) were used as a negative control. qPCR was used to quantify enrichment of bHLH121 to the selected gene promoters. Means within each condition with the same letter are not significantly different according to one-way ANOVA followed by post-hoc Tukey test,  $p < 0.05$  ( $n = 4$  to 8 technical repeats). Error bars show  $\pm$ SD. Each experiment (biological repeat) pools chromatin immunoprecipitated from approximately 500 seedlings (2 g) and the experiment was independently repeated two times.

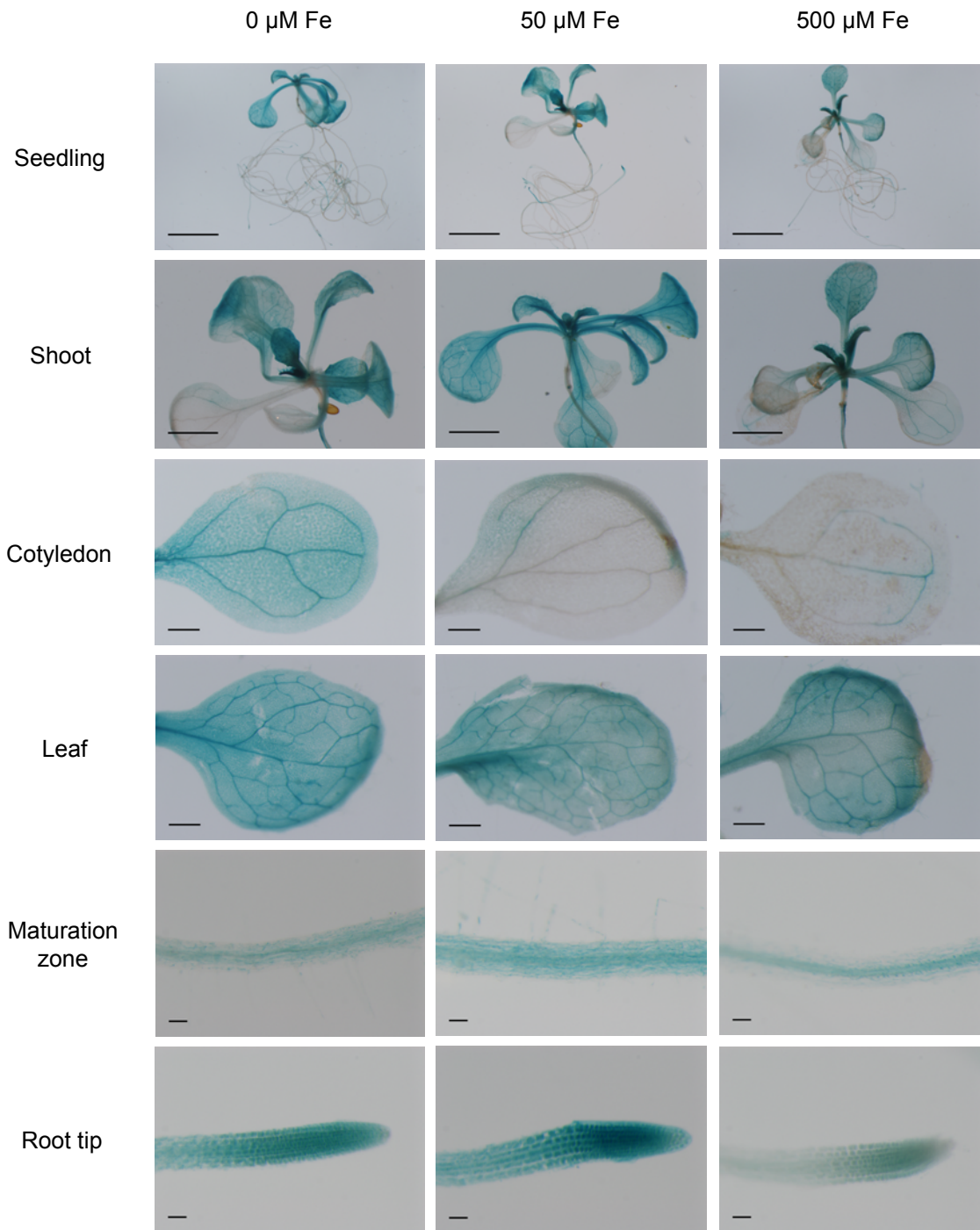


**Supplemental Figure 14. *bhlh121-2* complementation assays by overexpressing *FIT* and *bHLH38* (Supports Figure 5).** (A) Relative expression of *FIT* and *bHLH38* as determined by qRT-PCR in 2-weeks-old *bhlh121-2* seedlings carrying the *ProUBI:FIT* (left panel) or *ProUBI:bHLH38* (right panel) transgene grown on Fe-sufficient medium. Means within each condition with the same letter are not significantly different according to one-way ANOVA followed by post-hoc Tukey test,  $p < 0.05$  ( $n = 3$  technical repeats from one representative experiment). \*: significant differences between WT and *bhlh121-2*.  $t$ -test  $p < 0.05$ . Error bars show  $\pm$ SD. Each experiment (biological repeat) pools RNA extracted from approximately 30 seedlings and the experiment was independently repeated two times. (B) Top panel: Arabidopsis WT, *bhlh121-2* and three independent *bhlh121-2* lines overexpressing *FIT* (*ProUBI:FIT*) grown in soil for 3 weeks. Middle and bottom panels: Phenotypes of the same genotypes grown for 2 weeks on Fe-sufficient (50  $\mu$ M Fe) or Fe-deficient (0  $\mu$ M Fe) medium. (C) Same as in (B) with WT, *bhlh121-2* and three independent *bhlh121-2* lines overexpressing *bHLH38* (*ProUBI:bHLH38*). (B and C) Bar = 1 cm.



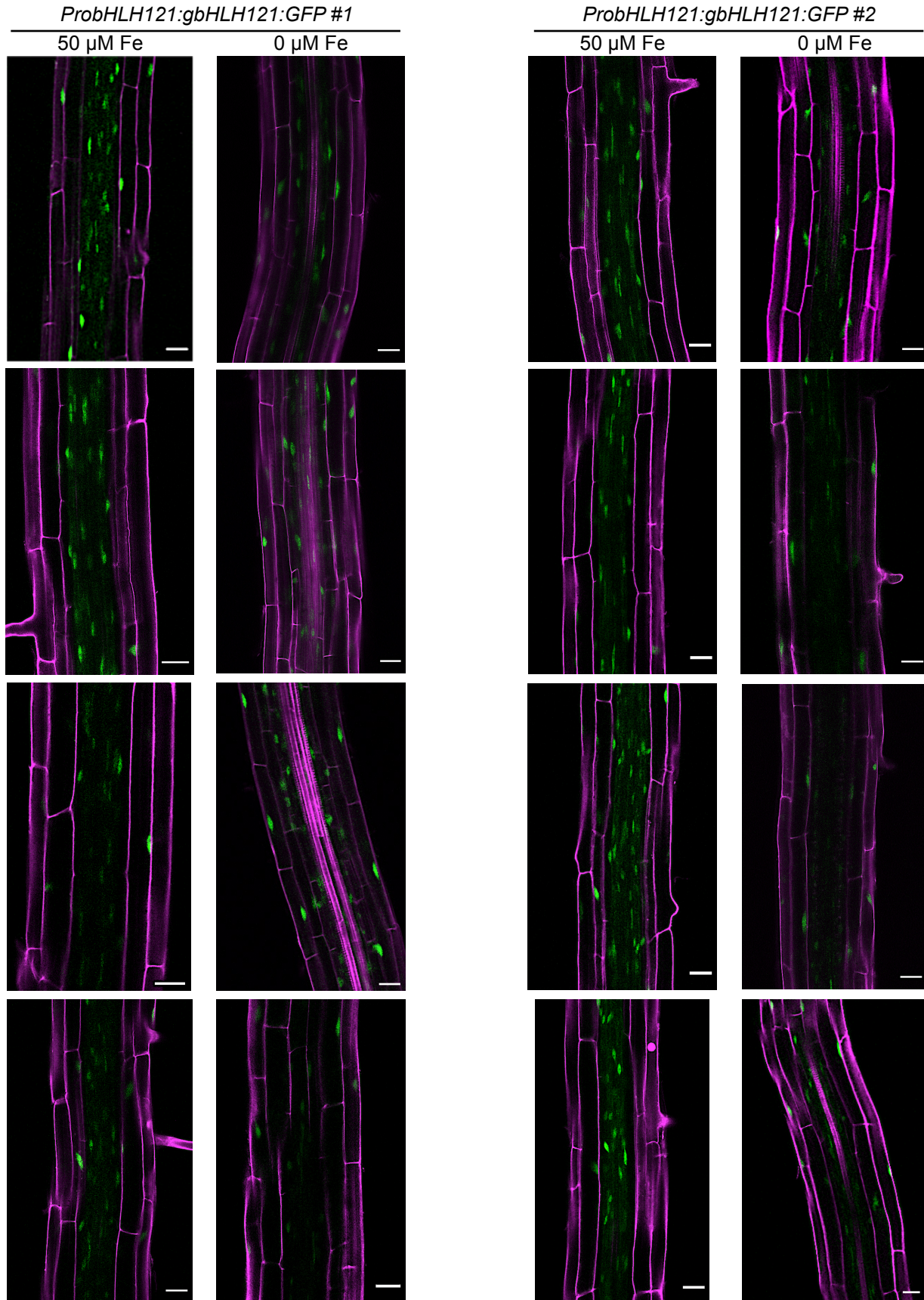
**Supplemental Figure 15. Root growth phenotypes of *bhlh121-2* compared to *bhlh121-2*, *bhlh34*, *bhlh104-1*, *ilr3-3* and *bhlh115-2* (Supports Figure 5).**

*Arabidopsis thaliana* WT, *bhlh121-2*, *bhlh34*, *bhlh104-1*, *ilr3-3* and *bhlh115-2* grown for 2 weeks in (A) control (50  $\mu$ M Fe) and (B) Fe deficiency (0  $\mu$ M Fe) conditions. Left panels: seedling phenotypes. Bar = 1 cm. Right panels: Root length. Means within each condition with the same letter are not significantly different according to one-way ANOVA followed by post-hoc Tukey test,  $p < 0.05$  ( $n = 8$  seedlings from one representative experiment). Error bars show SD. \*\*: significant differences between *bhlh121-2* and *bhlh34* or *ilr3-3*.  $t$ -test  $p < 0.01$ .

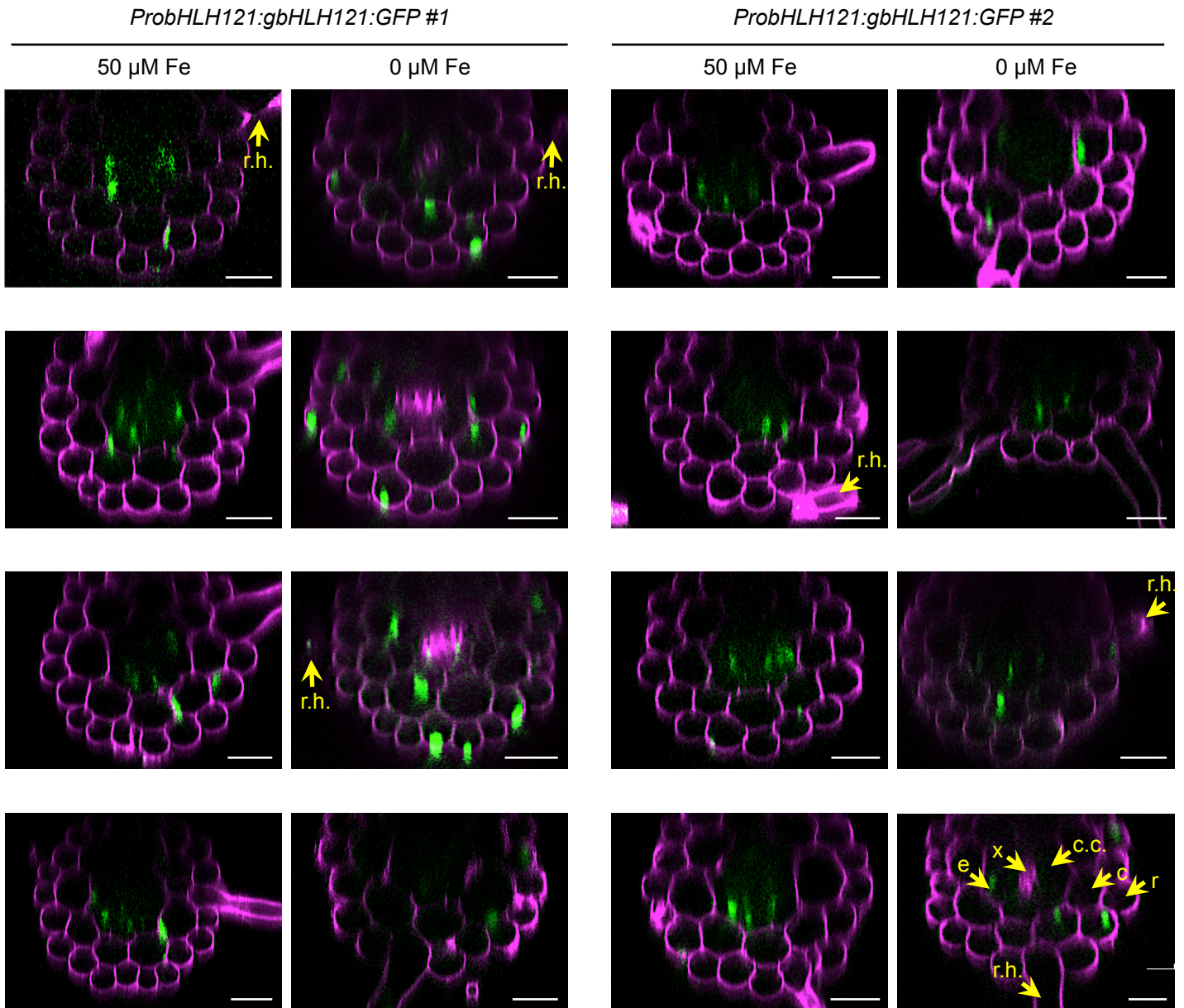


**Supplemental Figure 16. *bHLH121* promoter activity (Supports Figure 6).**

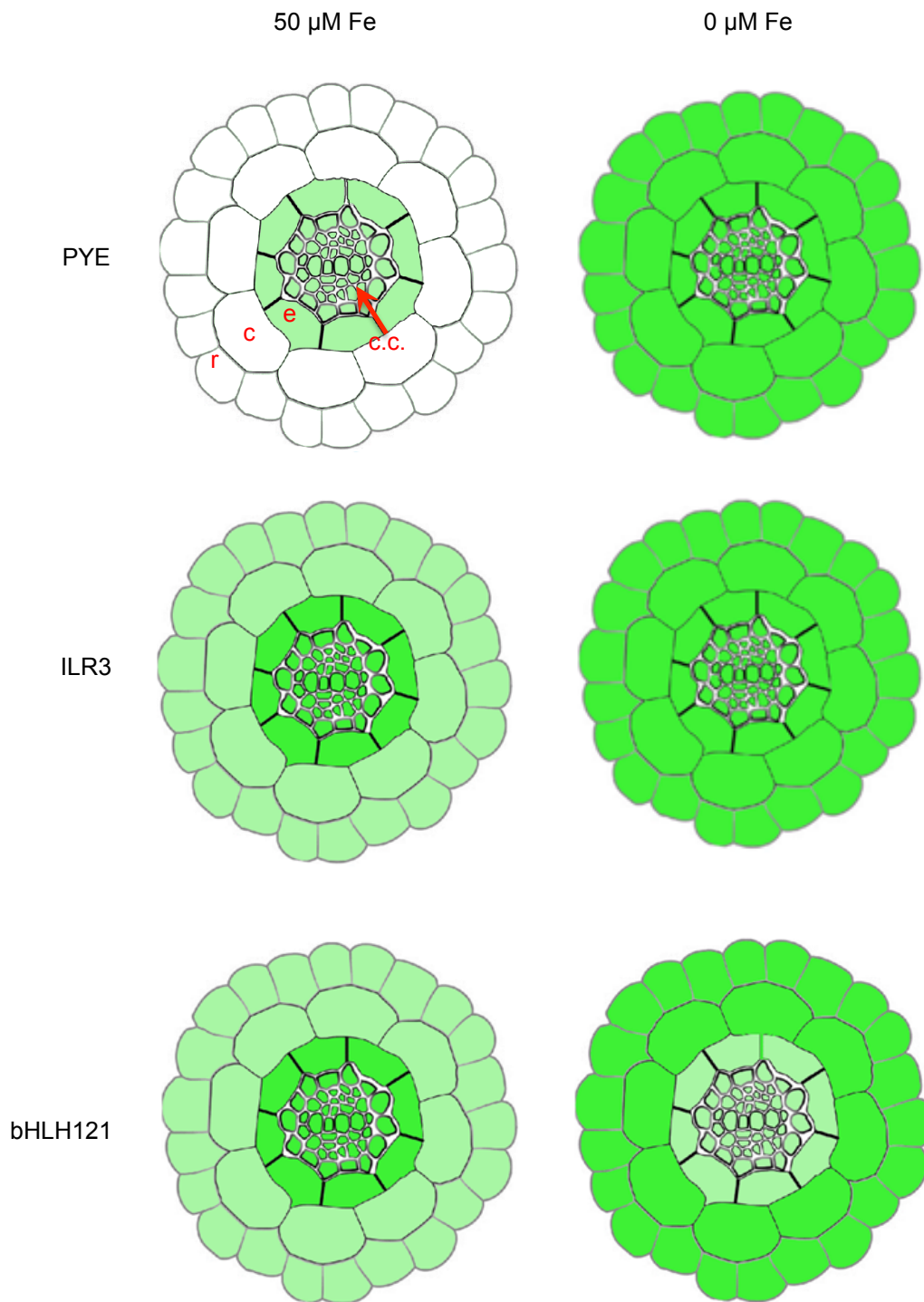
*Arabidopsis thaliana* WT seedlings expressing the promoter of *bHLH121* fused to the *GUS* reporter gene (*ProbHLH121:GUS*) were grown for 2 weeks on Fe-sufficient (50  $\mu\text{M}$  Fe), Fe-deficient (0  $\mu\text{M}$  Fe) or Fe-excess (500  $\mu\text{M}$  Fe) medium. Bars: seedling = 5 mm, shoot = 2 mm, cotyledon and leaf = 500  $\mu\text{m}$ , elongation zone and root tip = 100  $\mu\text{m}$ .



**Supplemental Figure 17. bHLH121 protein localization in longitudinal sections of roots (Supports Figure 6).** bHLH121:GFP localization in the roots (differentiation zone) of two complemented *bhlh121-2* lines (*ProbHLH121:gbHLH121:GFP* #1 and #2) subjected or not to Fe deficiency. Longitudinal sections (optical) from four independent seedlings are displayed. Bars: 25 μm.



**Supplemental Figure 17. bHLH121 protein localization in transverse sections of roots (Supports Figure 6).** bHLH121:GFP localization in the roots (differentiation zone) of two complemented *bhlh121-2* lines (*ProbHLH121:gbHLH121:GFP #1* and *#2*) subjected or not to Fe deficiency. Transverse sections (optical) from four independent seedlings are displayed. Bars: 25  $\mu\text{m}$ . r, rhizodermis; c, cortex; e, endodermis; c.c., central cylinder; x, xylem; r.h., root hair.



**Supplemental Figure 19. Schematic representation of the localization patterns of PYE, ILR3 and bHLH121 (GFP translational fusion) in the presence or absence of Fe in the maturation zone of the Arabidopsis roots (Supports Figure 6).**

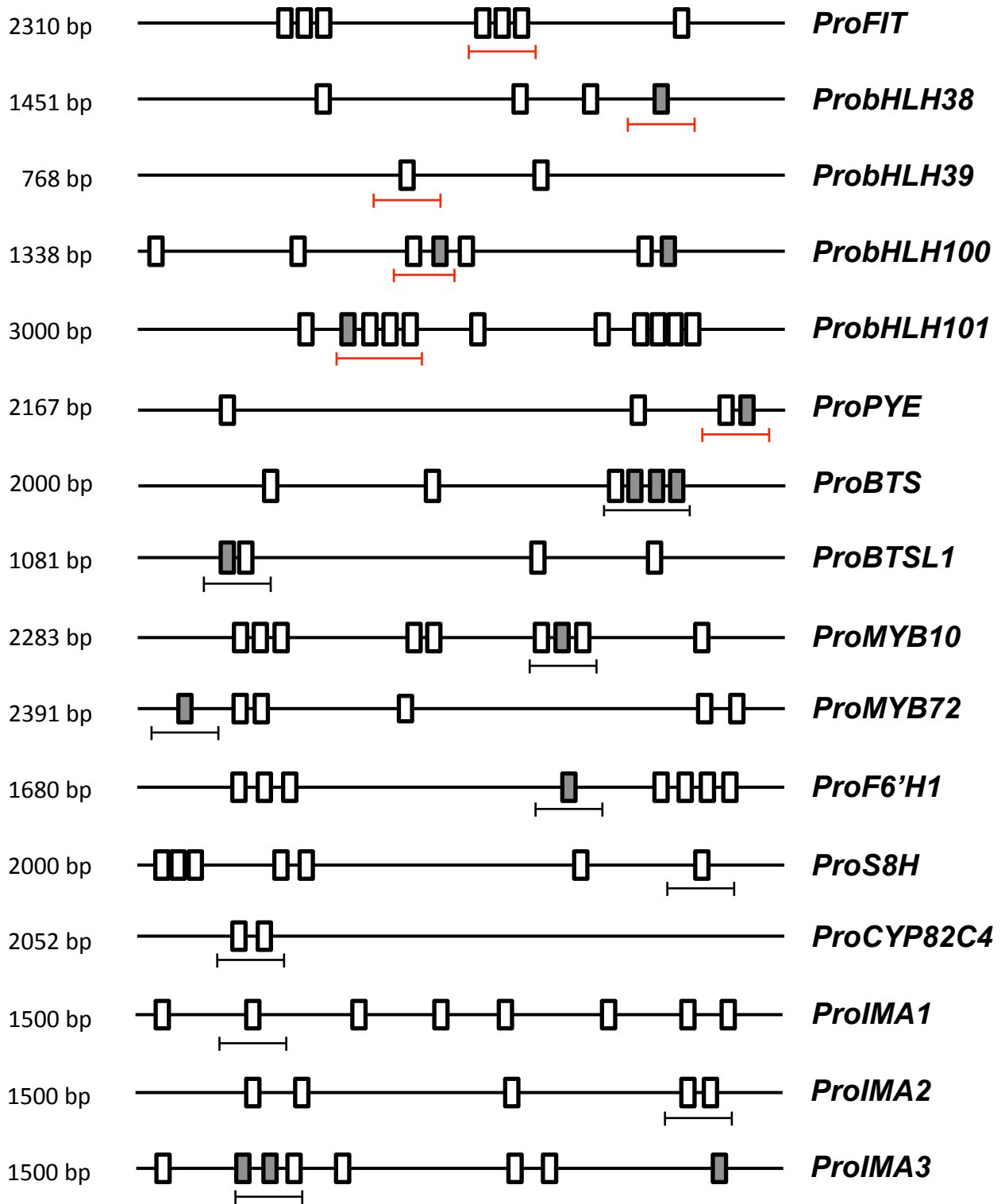
r, rhizodermis; c, cortex; e, endodermis; c.c., central cylinder. PYE and ILR3 protein patterns are based on the results presented in Long et al., 2010 and Samira et al., 2019, respectively. Pale green: tissues displaying a low level of GFP fluorescence, bright green: tissues displaying a high level of GFP fluorescence, white: no GFP fluorescence detected.











**Supplemental Figure 23. Promoter structure diagrams for the genes assayed in the CHIP-qPCR experiments (Supports Figure 5).**

White boxes, *E*-box (*CANNTG*); grey boxes, *G*-box (*CACGTG*). Lines under the boxes indicate sequences detected by CHIP-qPCR assays. Lines in red indicate previously described binding loci for ILR3 and its closet homologus. White boxes, *E*-box (*CANNTG*), grey boxes, *G*-box (*CACGTG*).

**Table S1: ILR3 interacting protein identified by CoIP-MS.**

Protein IDs	Fasta headers
AT5G24550	BGLU32   beta glucosidase 32
<a href="#">AT3G19860</a>	<a href="#">bHLH121</a>   <a href="#">basic helix-loop-helix (bHLH)</a>
AT2G18040	PIN1AT   peptidylprolyl cis/trans isomerase
AT1G24267	Protein of unknown function (DUF1664)
AT5G46800	BOU   Mitochondrial substrate carrier family protein
AT1G64160	Disease resistance-responsivefamily protein
AT2G29330	TRI   tropinone reductase
AT5G57490	VDAC4   voltage dependent anion channel 4
AT2G47380	Cytochrome c oxidase subunit Vc family protein
AT5G07460	PMSR2   peptidomethionine sulfoxide reductase 2
AT5G65970	MLO10   Seven transmembrane MLO family protein
AT1G56430	NAS4   nicotianamine synthase 4
AT3G11250	Ribosomal protein L10 family protein


**Article 4. Further insights into the role of bHLH121 in the regulation of iron homeostasis in *Arabidopsis thaliana***



SHORT COMMUNICATION



## Further insights into the role of bHLH121 in the regulation of iron homeostasis in *Arabidopsis thaliana*

Fei Gao, Kevin Robe, and Christian Dubos 

BPMP, Univ Montpellier, CNRS, INRAE, Institut Agro, Montpellier, France

### ABSTRACT

Iron (Fe) is an important micronutrient for plant growth and development but any excess of Fe is toxic because of the Fe-dependent generation of reactive oxygen species (ROS). Thus, Fe homeostasis must be tightly regulated. In *Arabidopsis thaliana*, a cascade of transcription factors has been identified as involved in the regulation of this process by modulating the expression of genes related to Fe uptake, transport, and storage. Recently, it was demonstrated that in response to Fe deficiency, bHLH121/URI (UPSTREAM REGULATOR OF IRT1) directly activates the expression of several genes involved in this regulatory network. It was also shown that bHLH121 interacts with ILR3 (bHLH105) and its homologs. Herein it is shown that bHLH121 is necessary for the expression of the main markers of the plant responses to Fe excess, the ferritin genes (i.e. *FER1*, *FER3*, and *FER4*). bHLH121 regulates ferritin genes expression by directly binding to their promoters, at the same locus than the ILR3-PYE repressive complex. Therefore, this study highlights that bHLH121, PYE, and ILR3 form a chain of antagonistic switches that regulate the expression of ferritin genes. The implication of this finding is discussed.

### ARTICLE HISTORY

Received 6 June 2020  
Revised 29 June 2020  
Accepted 30 June 2020

### KEYWORDS

*Arabidopsis thaliana*; basic helix-loop-helix; bHLH47; bHLH105; bHLH121; ferritins; ILR3; iron homeostasis; PYE; transcription factor

Iron (Fe) is an important micronutrient for plant growth and development, as it serves as cofactors for numerous enzymes involved in various cellular processes such as photosynthesis, respiration, or the synthesis of amino acids.<sup>1–3</sup> However, an excess of Fe is deleterious for plants because of its capacity to generate ROS.<sup>4</sup> Thus, the level of Fe in plant cells must be tightly regulated to avoid both Fe deficiency and Fe excess.

Fe uptake is the first limiting step for the maintenance of Fe homeostasis in plants. Non-grass species have evolved a reduction base mechanism allowing taking up the Fe present in the soil in the form of Fe(III)-chelates (Figure 1a).<sup>6–8</sup> Once into the plant, Fe is transported to the different organs to be assimilated in several metalloproteins or stored in different cell compartments. Part of the Fe is transiently stored into ferritins whose expression is strongly induced in response to Fe excess.<sup>9,10</sup> In *Arabidopsis thaliana*, there are four ferritin genes; three are expressed in vegetative tissues (i.e. *FER1*, *FER3*, and *FER4*) and one in seeds (i.e. *FER2*).<sup>9,11</sup>

Maintaining Fe homeostasis necessitates the activity of several transcription factors (TFs) organized into an intricate regulatory network.<sup>12,13</sup> In *Arabidopsis*, it involves 17 bHLH TFs, among which ILR3/bHLH105 (IAA-LEUCINE RESISTANT3) plays a dual role.<sup>13</sup> ILR3 physically interacts with its orthologs from the bHLH clade IVc (i.e. bHLH34, bHLH104, and bHLH115) to activate the Fe deficiency responses (Figure 1a).<sup>14–17</sup> ILR3 also acts as a transcriptional repressor when it interacts with PYE/bHLH47 (POPEYE).<sup>10</sup> Among the ILR3-PYE targets are the ferritin genes (i.e. *FER1*, *FER3*, and *FER4*), the main markers of the plant response to Fe excess.<sup>10</sup>

bHLH121 (URI, UPSTREAM REGULATOR OF IRT1) was identified as a novel TF that acts upstream the Fe homeostasis

regulatory network, together with ILR3 and its orthologs, as a transcriptional activator.<sup>15–18</sup> *bhlh121* mutants display severe Fe deficiency symptoms, even in control Fe condition, that can be rescued by providing extra Fe supply (Figure 1b).<sup>15–17</sup> In agreement with the upstream position of bHLH121 in the Fe homeostasis network, *bhlh121* mutants are affected in all the aspects of the Fe-deficiency responses and the expression of several regulatory proteins and peptides involved in this network is impaired.<sup>15–17</sup>

Since bHLH121 controls Fe uptake, one may hypothesize that bHLH121 might directly or indirectly regulate the expression of ferritin genes. In order to validate this hypothesis, the expression of *FER1*, *FER3*, and *FER4* was analyzed in wild type and three independent *bhlh121* mutant lines by qRT-PCR.<sup>16</sup> For this purpose, seedlings were first grown for 7 days in both Fe sufficient (50  $\mu$ M Fe) and Fe deficiency (0  $\mu$ M Fe) conditions. Under Fe deficiency condition, expression analysis revealed that *FER1* and *FER4* mRNA accumulation was similar between the wild type and the mutants whereas *FER3* mRNA accumulation was higher in the wild type than in the mutants (Figure 2a). These results suggest that bHLH121 has a positive effect on *FER3* expression when Fe availability is low. In contrast, under Fe sufficient condition, the mRNA levels of the three ferritin genes were lower in the mutants than in the wild type. These results indicate that bHLH121 is necessary to maintain ferritin gene expressions when Fe availability is not limiting. These observations are in contrast with a previous study, based on the analysis of microarray data, showing that ferritin genes expression is not affected in *bhlh121* mutants grown under Fe replete condition.<sup>19</sup> This apparent discrepancy



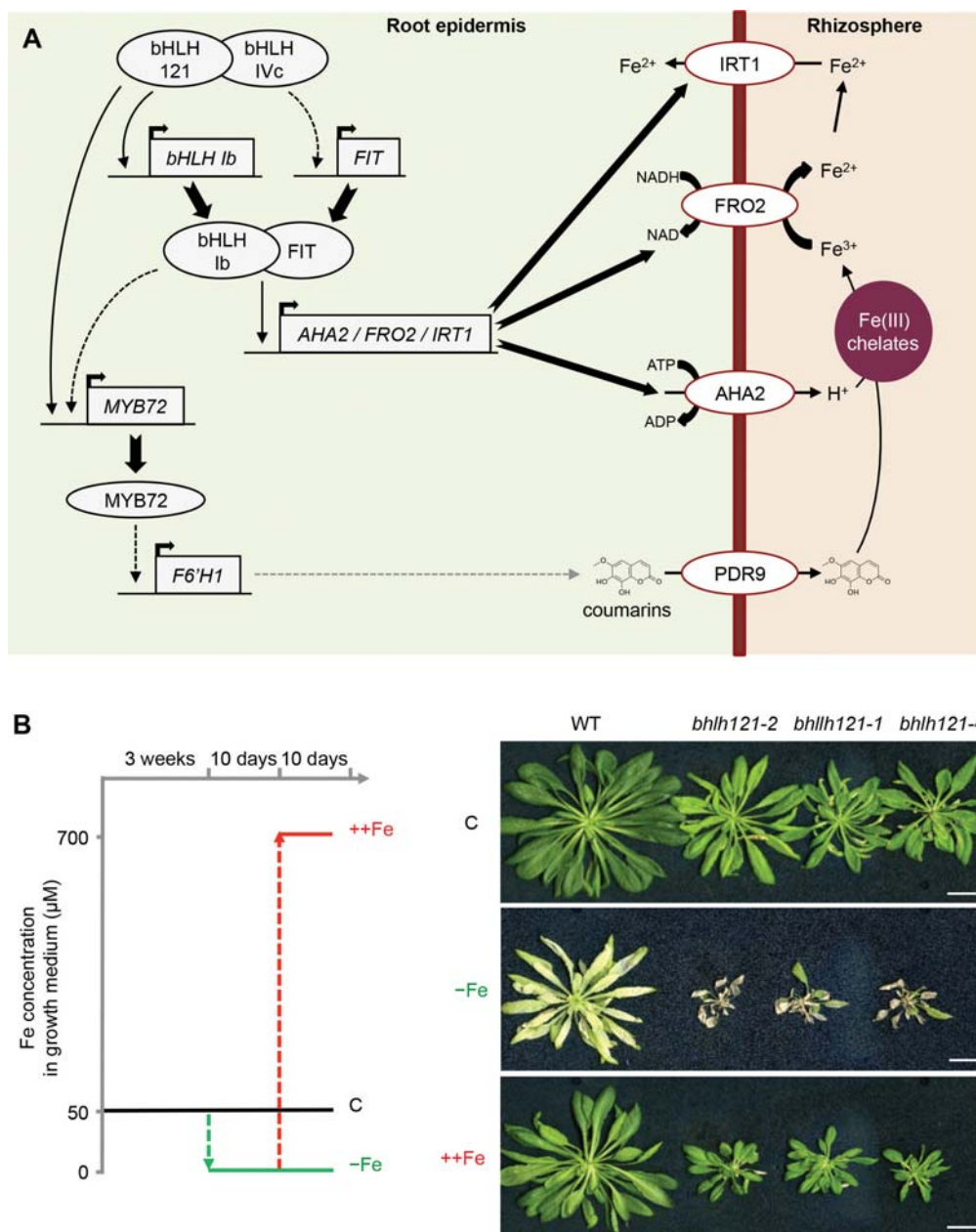


**Figure 1.** Loss-of-function of *bHLH121* leads to severe iron deficiency symptoms that can be rescued by extra iron supply. **(A)** *bHLH121* plays a central role in activating the iron (Fe) deficiency responses in *Arabidopsis thaliana*, in particular the Fe uptake machinery. *bHLH121* directly activates the expression of several transcription factors such as the clade lb *bHLH* (i.e. *bHLH38*, *bHLH39*, *bHLH100* and *bHLH101*) and *MYB72*. The activation of *FIT* (*FER-LIKE IRON DEFICIENCY-INDUCED TRANSCRIPTION FACTOR*) expression is most likely indirect even if one study suggests that it could be direct.<sup>5</sup> The activity of these transcription factors leads to the solubilization of  $\text{Fe}^{3+}$  via the secretion of protons and coumarins by the proton-ATPase *AHA2* and the *PDR9* (*PLEIOTROPIC DRUG RESISTANCE 9*) transporter, respectively. It also leads to the subsequent reduction of  $\text{Fe}^{3+}$  into  $\text{Fe}^{2+}$  that is insured by the reductase *FRO2* (*FERRIC REDUCTION OXIDASE2*) and to the transportation of  $\text{Fe}^{2+}$  into the roots by the *IRT1* (*IRON-REGULATED TRANSPORTER1*) transporter. Black line: direct induction, dashed black line: induction, gray-dashed line: indicate that several steps are involved for the biosynthesis of coumarins **(B)** Left panel: experimental design of hydroponic cultures (Hoagland medium). Plants were grown for 3 weeks under short-day conditions (8h/16h light/dark; light intensity: 120 mmol/cm<sup>2</sup>/s provided by a mix of sodium-vapor and metal halide 400-W lamps) in control condition (C, 50  $\mu\text{M}$  Fe). Plants were then grown for 10 more days under either C or iron deficiency (-Fe, 0  $\mu\text{M}$  Fe) conditions. Plants subjected to -Fe were then either kept in this condition or transferred to iron excess condition (++Fe, 700  $\mu\text{M}$  Fe-EDDHA, a form of Fe easily assimilated by plants) for another 10 days whereas the plants grown under C condition were kept in this condition until the end of the experiment. Right panels: rosette phenotype of wild type (WT) and loss-of-function *bhlh121-1*, *bhlh121-2* and *bhlh121-4* mutants (CRISPR/Cas9-induced mutation in *bHLH121* gene). C: plants grown in control condition for the whole duration of the experiment. -Fe: plants grown in control condition for 3 weeks and then grown under -Fe condition for 20 days. +Fe: plants grown in control condition for 3 weeks and then grown under -Fe condition for 10 days and an additional 10 days under +Fe condition.

might be explained by the higher sensitivity of the qRT-PCR method or to differences in the growth conditions.

Considering the decrease in ferritins mRNA abundance observed in *bhlh121* mutants when compared to the wild type (Figure 2a), it cannot be excluded that part of this diminution might be due to the reported differences in Fe accumulation

between both genotypes (i.e. a reduction of about one-third in the mutant when compared to the wild type).<sup>16</sup> Therefore, similar experiments were conducted with seedlings grown under two different Fe excess conditions: 200  $\mu\text{M}$  Fe (mid-Fe excess condition) and 500  $\mu\text{M}$  Fe (high Fe excess condition). Under mid excess condition, the mRNA levels of the three ferritin genes were lower

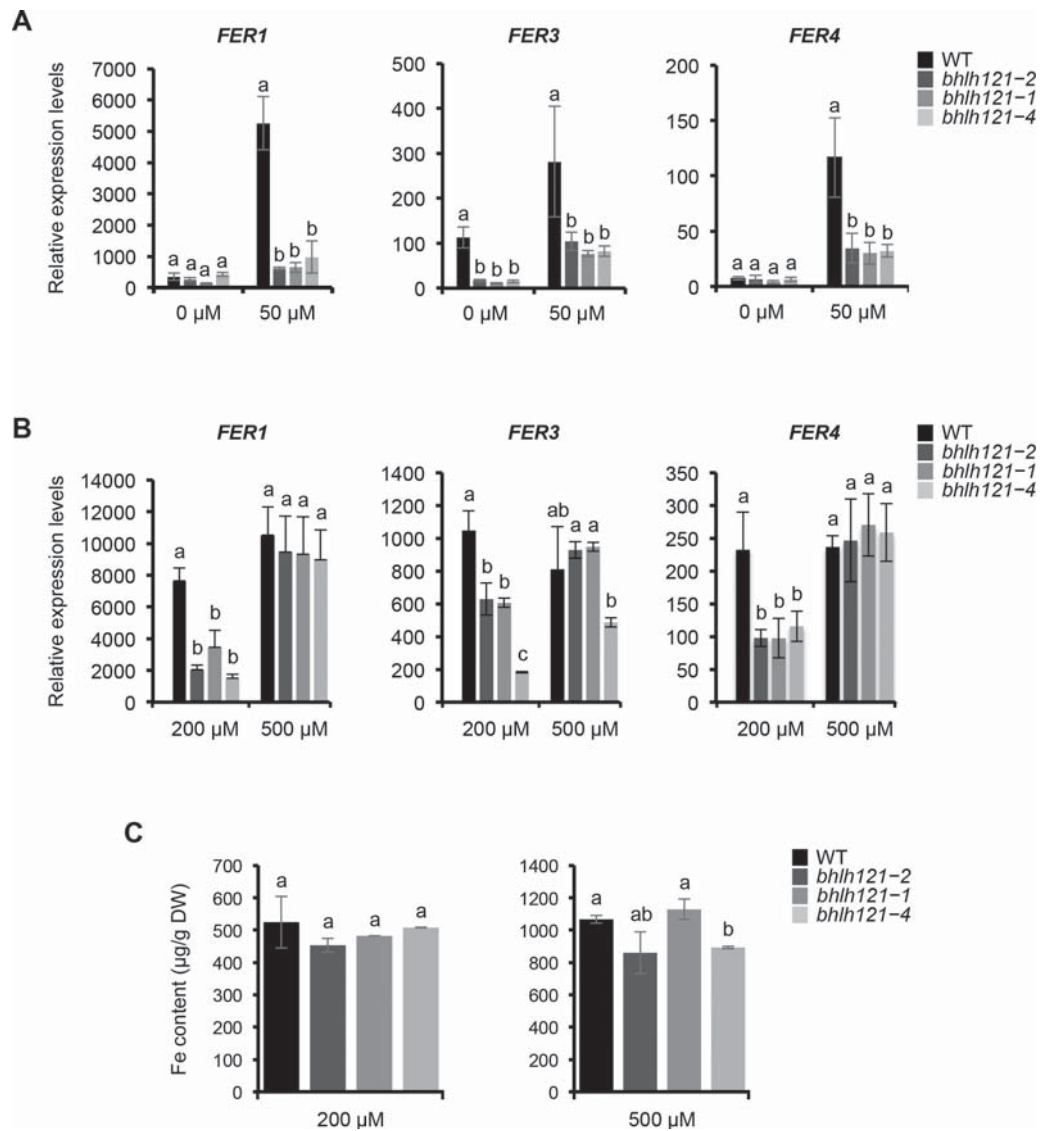


**Figure 2.** bHLH121 is an activator of the *Arabidopsis thaliana* *FER1*, *FER3* and *FER4* expression. **(A)** Relative expression levels of *FER1*, *FER3*, and *FER4*. Relative expression was determined by quantitative reverse transcription PCR (qRT-PCR) in 1-week-old *Arabidopsis* seedlings grown on iron-sufficient (50  $\mu$ M Fe) or iron-deficient (0  $\mu$ M Fe) medium. Seedlings were germinated and grown under long-day conditions (8h/16h light/dark; light intensity: 120 mmol/cm<sup>2</sup>/s provided by Osram 18-W 840 Lumilux neon tubes) on half-strength Murashige and Skoog medium containing 0.05% (w/v) MES, 1% (w/v) sucrose and 0.7% (w/v) agar. Iron was provided as Fe(III)-EDTA. **(B)** Relative expression levels of *FER1*, *FER3*, and *FER4* (qRT-PCR) in 1-week-old *Arabidopsis* seedlings grown as in A on two iron excess regimes: 200  $\mu$ M Fe (mid-Fe excess) and 500  $\mu$ M Fe (high Fe excess regime). **(C)** Fe contents of the wild type (WT) and the *bhlh121* mutants grown as in B. **(A-C)** Means within each condition with the same letter are not significantly different according to one-way ANOVA followed by post hoc Tukey test,  $p < .05$  ( $n = 3$  technical repeats). Error bars show  $\pm$ SD.

in the *bhlh121* mutants than in the wild type (Figure 2b) whereas Fe accumulation was similar between all genotypes (Figure 2c). This later result confirms that when Fe is not limiting bHLH121 is necessary for ferritin genes expression. Interestingly, under high Fe excess, the expression of ferritin genes was no longer different between the wild type and the *bhlh121* mutants (Figure 2b). Fe accumulation was also similar between all genotypes (Figure 2c). In addition, at the rosette stage, no chlorosis was observed on the leaves of *bhlh121* mutants submitted to Fe excess as it was previously reported for *Arabidopsis* plants deprived of ferritins (Figure 1b).<sup>10</sup> Taken together, these results indicate that bHLH121 is required to induce ferritin genes expression when Fe availability is in adequacy with the plant physiological needs. These data also suggest that under high Fe excess, ferritin genes expression relies on the IDRS (IRON-DEPENDENT REGULATORY SEQUENCE) signaling pathway.<sup>19</sup>

In order to confirm whether the regulation of ferritin genes expression by bHLH121 is direct or not, CHIP-qPCR experiments were conducted using two independent *bhlh121* mutant lines complemented with the whole *bHLH121* locus translationally fused to the *GFP* reporter gene (i.e. *pbHLH121:gbHLH121-GFP* in *bhlh121-2*).<sup>16</sup> This assay was centered on the promoter regions of the ferritin genes that contain the G-box motifs (CACGTG) known to be recognized by bHLH TFs. These loci were chosen for two reasons. First, because these G-boxes are directly targeted by the ILR3-PYE complex.<sup>10</sup> Second, because these G-boxes are located in nucleosome-free regions, suggesting the binding of regulatory proteins at the G-box loci.<sup>10</sup> CHIP-qPCR assays supported the *in vivo* binding of bHLH121 to the promoter of *FER1*, *FER3*, and *FER4* (Figure 3a), confirming previous results obtained by CHIP-seq analysis.<sup>19</sup> CHIP-qPCR experiments also showed that bHLH121 binds to the promoter

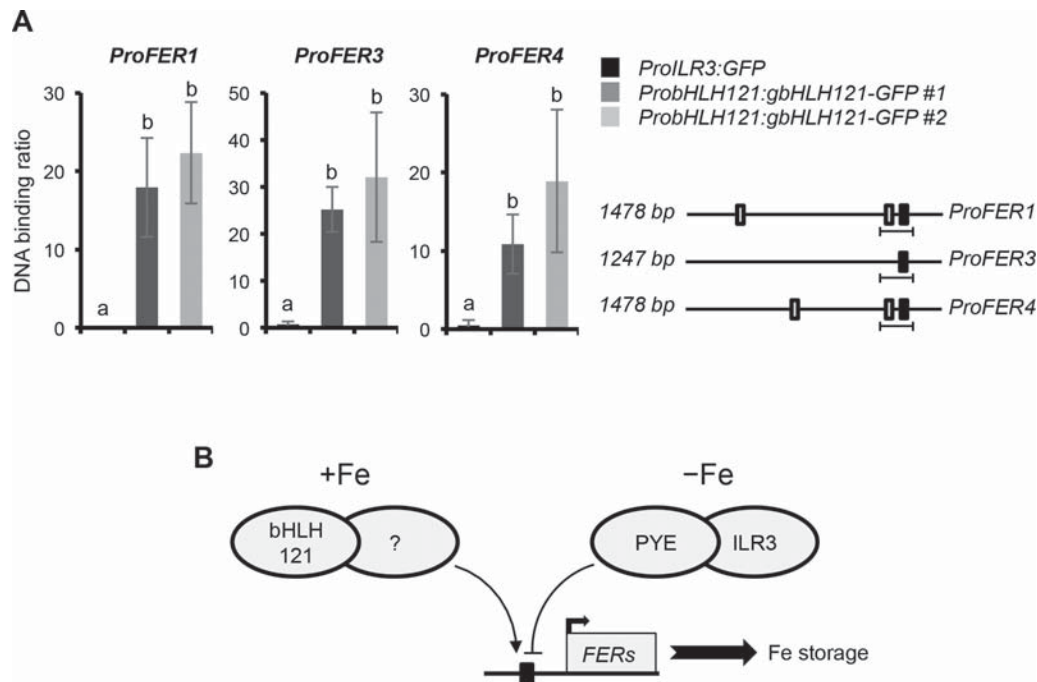


**Figure 3.** bHLH121 is a direct activator of the *Arabidopsis thaliana* *FER1*, *FER3* and *FER4* expression. **(A)** Left panels: chromatin immunoprecipitation coupled with qPCR (ChIP-qPCR) analysis of the binding of bHLH121 to the *FER1*, *FER3*, and *FER4* promoters (*ProFER1*, *ProFER3*, and *ProFER4*). Seedlings were germinated and grown under long-day conditions (8h/16h light/dark; light intensity: 120 mmol/cm<sup>2</sup>/s provided by Osram 18-W 840 Lumilux neon tubes) on half-strength Murashige and Skoog medium containing 0.05% (w/v) MES, 1% (w/v) sucrose and 0.7% (w/v) agar. Iron was provided as Fe(III)-EDTA. After 1 week of growth, seedlings were exposed to Fe deficiency for 3 days prior analysis. Chromatin from two complemented *bhlh121-2* lines expressing the *ProbHLH121:gbHLH121:GFP* construct was extracted using anti-GFP antibodies. Seedlings expressing GFP under the control of the *ILR3* promoter (*ProILR3:GFP*) were used as a negative control. qPCR was used to quantify enrichment of bHLH121 on ferritin gene promoters. Means within each condition with the same letter are not significantly different according to one-way ANOVA followed by post hoc Tukey test,  $p < .05$  ( $n = 3$  to 4 technical repeats). Error bars show  $\pm$ SD. Right panel: Promoter structure diagrams for the three ferritin genes assayed in ChIP-qPCR experiments. Grey boxes, E-box (CANNTG); black boxes, G-box (CACGTG). Lines under the boxes indicate sequences detected by ChIP-qPCR assays and correspond to known binding sites of ILR3 and PYE. **(B)** Schematic representation of the transcriptional regulation of ferritin genes expression in the stele by bHLH transcription factors. When Fe is not limiting (+Fe), bHLH121 localizes into the stele where it directly activates the expression of *FER1*, *FER3*, and *FER4* (*FERs*). The bHLH121 protein partner remains to be characterized. Under Fe deficiency condition (-Fe), bHLH121 localizes in the epidermis and the cortex where it activates the Fe deficiency response whereas the ILR3-PYE complex directly represses the expression of *FER1*, *FER3*, and *FER4* in the stele.

of ferritin genes at the same locus than the ILR3-PYE repressive complex.<sup>10</sup>

While the transcript level and protein abundance of bHLH121 are not significantly affected by the Fe status, Fe availability affects the cellular localization of bHLH121 in *Arabidopsis* roots.<sup>15,16</sup> Interestingly, the patterns of ILR3 and PYE accumulation in *Arabidopsis* root cells also depend on Fe availability. When Fe availability is not limiting, most bHLH121 accumulates in the stele, the site of ferritin gene expressions.<sup>20</sup> In this condition, ILR3 localizes in all root cells with higher abundance in the stele than in the epidermis and the cortex, whereas only traces of PYE are found in the stele.<sup>5,21</sup> These observations indicate that, under Fe sufficient condition, the repressive activity of the ILR3-PYE complex on ferritin genes expression is low.<sup>10,22</sup> It also supports that bHLH121 is a direct activator of ferritin genes expression. In contrast, when Fe availability is low, bHLH121 mainly localizes at the root epidermis and the cortex, the sites for Fe uptake, and ILR3 and PYE in all root cell types.<sup>5,16,21</sup> These observations are consistent with the repressive activity of the ILR3-PYE complex on ferritin genes expression and the positive role of bHLH121 on Fe uptake (Figure 3b).

The identification of the protein that interacts with bHLH121 to regulate ferritin genes expression is one of the main questions that remain to be solved (Figure 3b). It is unlikely that one of the clade IVc bHLH interact with bHLH121 to activate the expression

of ferritin genes since ILR3 is a repressor of ferritin gene expressions and since the expression of ferritin genes is not lowered in the *bhlh34*, *bhlh104*, and *bhlh115* loss-of-function mutants.<sup>10</sup> It is also unlikely that bHLH121 acts as homodimers since in vivo experiments suggest that bHLH121 cannot interact with itself.<sup>16</sup>

Interestingly, the phosphorylation state of bHLH121 also depends on Fe availability.<sup>15</sup> Under Fe deficiency, the phosphorylated form of bHLH121 accumulates in roots. It is proposed that this mechanism allows the heterodimerization of bHLH121 with ILR3 and its three homologs, and thus the transcriptional activation of their target genes to activate the Fe deficiency responses.<sup>15</sup> Whether the phosphorylation of bHLH121 is necessary to activate the expression of ferritin genes will have to be demonstrated. Firstly, because bHLH121 activates the expression of ferritin genes in the stele when Fe availability is not limiting, and thus when bHLH121 phosphorylation is low. Second, because the phosphorylated form of bHLH121 is degraded when plants are recovering from Fe deficiency, a growth condition that strongly induces ferritin genes expression.<sup>10,15</sup> The phosphorylation states of bHLH121 might rather be necessary to modify bHLH121 pattern of accumulation within the root cells in a Fe-dependent manner. In this hypothesis, which remains to be tested, there would be a balance between the phosphorylated bHLH121 form in the epidermis and the cortex and the non-phosphorylated form in the stele. The activity of FIT is also modulated by

phosphorylation via the activity of CIPK11 (CBL-INTERACTING PROTEIN KINASE 11).<sup>23,24</sup> Whether or not CIPK11 or closely related kinases, might also phosphorylate bHLH121 and thus function as a coordinating factor for different aspects of Fe homeostasis is an appealing hypothesis that will have to be investigated.

## Acknowledgments

FG is supported by a fellowship from the China Scholarship Council (CSC). KR was supported by fellowships from the ANR and the INRAE (department of “Biologie et Amélioration des Plantes”).

## Disclosure of potential conflicts of interest

No potential conflicts of interest were disclosed

## ORCID

Christian Dubos  <http://orcid.org/0000-0001-5486-3643>

## References

- Hänsch R, Mendel RR. Physiological functions of mineral micro-nutrients (Cu, Zn, Mn, Fe, Ni, Mo, B, Cl). *Curr Opin Plant Biol.* 2009;12:259–266. doi:10.1016/j.pbi.2009.05.006.
- Touraine B, Vignols F, Przybyla-Toscano J, Ischebeck T, Dhalleine T, Wu H-C, Magno C, Berger N, Couturier J, Dubos C, et al. Iron-sulfur protein NFU2 is required for branched-chain amino acid synthesis in Arabidopsis roots. *J Exp Bot.* 2019;70(6):1875–1889. doi:10.1093/jxb/erz050.
- Berger N, Vignols F, Przybyla-Toscano J, Roland M, Rofidal V, Touraine B, Zienkiewicz K, Couturier J, Feussner I, Santoni V, et al. Identification of client iron-sulfur proteins of the chloroplastic NFU2 transfer protein in Arabidopsis thaliana. *J Exp Bot.* 2020;71(14):4171–4187. doi: 10.1093/jxb/eraa166.
- Muckenthaler MU, Galy B, Hentze MW. Systemic iron homeostasis and the iron-responsive element/iron-regulatory protein (IRE/IRP) regulatory network. *Annu Rev Nutr.* 2008;28:197–213. doi:10.1146/annurev.nutr.28.061807.155521.
- Samira R, Li B, Kliebenstein D, Li C, Davis E, Gillikin JW, Long TA. The bHLH transcription factor ILR3 modulates multiple stress responses in Arabidopsis. *Plant Mol Biol.* 2018;97(4–5):297–309. doi:10.1007/s11103-018-0735-8.
- Tsai -H-H, Schmidt W. One way. Or another? Iron uptake in plants. *New Phytol.* 2017;214:500–505. doi:10.1111/nph.14477.
- Santi S, Schmidt W. Dissecting iron deficiency-induced proton extrusion in Arabidopsis roots. *New Phytol.* 2009;183:1072–1084. doi:10.1111/j.1469-8137.2009.02908.x.
- Brumbarova T, Bauer P, Ivanov R. Molecular mechanisms governing Arabidopsis iron uptake. *Trends Plant Sci.* 2015;20:124–133. doi:10.1016/j.tplants.2014.11.004.
- Briat J-F, Duc C, Ravet K, Gaymard F. Ferritins and iron storage in plants. *Biochimica Et Biophysica Acta (Bba)-gen Subj.* 2010;1800:806–814. doi:10.1016/j.bbagen.2009.12.003.
- Tissot N, Robe K, Gao F, Grant-Grant S, Boucherez J, Bellegarde F, Maghiaooui A, Marcelin R, Izquierdo E, Benhamed M, et al. Transcriptional integration of the responses to iron availability in Arabidopsis by the bHLH factor ILR3. *New Phytol.* 2019;223(3):1433–1446. doi:10.1111/nph.15753.
- Ravet K, Touraine B, Kim SA, Cellier F, Thomine S, Guerinot ML, Briat J-F, Gaymard F. Post-translational regulation of AtFER2 ferritin in response to intracellular iron trafficking during fruit development in Arabidopsis. *Mol Plant.* 2009;2:1095–1106. doi:10.1093/mp/ssp041.
- Connorton JM, Balk J, Rodríguez-Celma J. Iron homeostasis in plants—a brief overview. *Metallomics.* 2017;9:813–823. doi:10.1039/C7MT00136C.
- Gao F, Robe K, Gaymard F, Izquierdo E, Dubos C. The transcriptional control of iron homeostasis in plants: a tale of bHLH transcription factors? *Front Plant Sci.* 2019;10:6. doi:10.3389/fpls.2019.00006.
- Zhang J, Liu B, Li M, Feng D, Jin H, Wang P, Liu J, Xiong F, Wang J, Wang H-B, et al. The bHLH transcription factor bHLH104 interacts with IAA-LEUCINE RESISTANT3 and modulates iron homeostasis in Arabidopsis. *Plant Cell.* 2015;27(3):787–805. doi:10.1105/tpc.114.132704.
- Kim SA, LaCroix IS, Gerber SA, Guerinot ML. The iron deficiency response in Arabidopsis thaliana requires the phosphorylated transcription factor URI. *Proc National Acad Sci.* 2019;116:24933–24942. doi:10.1073/pnas.1916892116.
- Gao F, Robe K, Bettembourg M, Navarro N, Rofidal V, Santoni V, Gaymard F, Vignols F, Roschztardt H, Izquierdo E, et al. The transcription factor bHLH121 interacts with bHLH105 (ILR3) and its closest homologs to regulate iron homeostasis in Arabidopsis. *Plant Cell.* 2020;32(2):508–524. doi:10.1105/tpc.19.00541.
- Lei R, Li Y, Cai Y, Li C, Pu M, Lu C, Yang Y, Liang G. bHLH121 functions as a direct link that facilitates the activation of FIT by bHLH IVc transcription factors for maintaining Fe homeostasis in Arabidopsis. *Mol Plant.* 2020;3:634–649. doi:10.1016/j.molp.2020.01.006.
- Lockhart J. Personal trainer: BHLH121 functions upstream of a transcriptional network of heavy lifters involved in balancing iron levels. *Plant Cell.* 2020;32:293. doi:10.1105/tpc.19.00918.
- Briat J-F, Ravet K, Arnaud N, Duc C, Boucherez J, Touraine B, Cellier F, Gaymard F. New insights into ferritin synthesis and function highlight a link between iron homeostasis and oxidative stress in plants. *Ann Bot.* 2010;105(5):811–822. doi:10.1093/aob/mcp128.
- Reyt G, Boudouf S, Boucherez J, Gaymard F, Briat J-F. Iron- and ferritin-dependent reactive oxygen species distribution: impact on Arabidopsis root system architecture. *Mol Plant.* 2015;8:439–453. doi:10.1016/j.molp.2014.11.014.
- Long TA, Tsukagoshi H, Busch W, Lahner B, Salt DE, Benfey PN. The bHLH transcription factor POPEYE regulates response to iron deficiency in Arabidopsis roots. *Plant Cell.* 2010;22:2219–2236. doi:10.1105/tpc.110.074096.
- Ramsey RA, Woodward AW, Hobbs BN, Tierney MP, Lahner B, Salt DE, Bartel B. An Arabidopsis basic helix-loop-helix leucine zipper protein modulates metal homeostasis and auxin conjugate responsiveness. *Genetics.* 2006;174(4):1841–1857. doi:10.1534/genetics.106.061044.
- Gratz R, Manishankar P, Ivanov R, Köster P, Mohr I, Trofimov K, Steinhorst L, Meiser J, Mai H-J, Drerup M, et al. CIPK11-dependent phosphorylation modulates FIT activity to promote Arabidopsis iron acquisition in response to calcium signaling. *Dev Cell.* 2019;48(5):726–40. e10. doi:10.1016/j.devcel.2019.01.006.
- Gratz R, Brumbarova T, Ivanov R, Trofimov K, Tünnermann L, Ochoa-Fernandez R, Blomeier T, Meiser J, Weidtkamp-Peters S, Zurbriggen MD, et al. Phospho-mutant activity assays provide evidence for alternative phospho-regulation pathways of the transcription factor FER-LIKE IRON DEFICIENCY-INDUCED TRANSCRIPTION FACTOR. *New Phytol.* 2020;225:250–267. doi:10.1111/nph.16168.



# **CHAPTER IV**

**BHLH121 AND CLADE IVC BHLH TFS FUNCTION  
SYNERGISTICALLY TO REGULATE IRON HOMEOSTASIS**



**Article 5. bHLH121 and clade IVc bHLH transcription factors synergistically function to regulate iron homeostasis in *Arabidopsis thaliana***





1 **bHLH121 and clade IVc bHLH transcription factors synergistically function to**  
2 **regulate iron homeostasis in *Arabidopsis thaliana***

3  
4 Fei Gao<sup>1</sup> & Christian Dubos<sup>1,\*</sup>

5  
6 <sup>1</sup> BPMP, Univ Montpellier, CNRS, INRAE, Institut Agro, Montpellier, France

7 \* Corresponding author (Tel: 0033 (0)499 61 28 18)

8 **E-mails:** Fei Gao, fei.gao@supagro.fr; Christian Dubos, christian.dubos@inrae.fr

9 **Abstract**

10 Iron is an essential micronutrient for plant growth and development, and becomes a  
11 limiting factor when plants are grown in neutral or alkaline soil. To ensure the  
12 absorption of iron, plants have evolved sophisticated mechanisms to regulate iron  
13 homeostasis. To date, at least 16 bHLH proteins, are known to participate in the  
14 maintenance of iron homeostasis in Arabidopsis. Among them, bHLH121 plays a  
15 crucial role in controlling iron homeostasis. bHLH121 could interact with IVc bHLH  
16 subfamily transcription factors (TFs), and activate the expression of *FIT* and Ib *bHLH*  
17 subfamily TFs. However, how bHLH121 and IVc bHLHs function collectively and  
18 efficiently to regulate their shared target genes is still unclear. In this study, we found  
19 that double mutants of *bHLH121* and *IVc bHLHs* displayed more severe growth defects  
20 than those of single mutants under both iron sufficient and deficient conditions.  
21 Expression analysis demonstrated that the double mutants showed much more impaired  
22 iron deficiency response, in agreement with the lower iron accumulation in these double  
23 mutants. Overexpression of *bHLH34* and *bHLH105* could partially complement the  
24 iron-associated growth defects of *bhlh121* mutant by activating the expression of both  
25 *bHLH39* and *FIT* in the absence of *bHLH121*. Meanwhile, the different spatial  
26 expression patterns of *bHLH121* and *IVc bHLHs* implied that they may function in  
27 specific tissues. Taken together, these results indicated bHLH121 and clade IVc bHLH  
28 TFs function coordinately in the regulation of iron homeostasis.

29 **Key words:** Arabidopsis, iron homeostasis, transcription factors, bHLH121, bHLH IVc

30 **Introduction**

31 Iron is one of the most important microelements for almost all living organisms due to  
32 its key role in redox reactions. In plants, it serves as cofactor for many enzymatic  
33 reactions and plays an irreplaceable role in vital processes, including DNA synthesis,  
34 hormone biosynthesis, respiration, photosynthesis and nitrogen fixation (Hänsch and  
35 Mendel, 2009). Although iron is abundant on earth, it is generally poorly available to  
36 the plants because it often exists in insoluble forms as iron(III) oxide-hydroxides,  
37 especially in neutral to basic soils. Therefore, iron might become a scarce resource and  
38 a limiting factor for plant growth and development, subsequently altering crop  
39 productivity and the quality of their derived products (Briat *et al.*, 2015; Guerinot and  
40 Yi, 1994). However, redox-active iron can generate reactive oxygen species (ROS)  
41 through the Fenton reaction, which makes the plants also suffer from iron toxicity if  
42 iron availability is high (Briat *et al.*, 2010). Therefore, iron homeostasis in plants must  
43 be tightly controlled to integrate both the iron availability signals and the internal  
44 requirement.

45 To overcome the low iron solubility, plants have evolved two different strategies to  
46 acquire iron from the soil (Gao and Dubos, 2020; Marschner *et al.*, 1986). Non-  
47 graminaceous species, including the model plant *Arabidopsis thaliana*, employ the  
48 reduction-based strategy (Strategy I), in which ferric iron ( $\text{Fe}^{3+}$ ) is solubilized and  
49 mobilized through active proton ( $\text{H}^+$ ) extrusion and coumarins secretion, reduced at the  
50 root surface and then transported into the rhizodermis cells as ferrous iron ( $\text{Fe}^{2+}$ )  
51 (Brumbarova *et al.*, 2015; Connorton *et al.*, 2017; Kobayashi and Nishizawa, 2012). In  
52 *Arabidopsis*, these processes are ensured by the  $\text{H}^+$ -ATPase 2 (AHA2), the  
53 PLEIOTROPIC DRUG RESISTANCE (PDR9) transporter, the FERRIC  
54 REDUCTION OXIDASE 2 (FRO2) and the IRON-REGULATED TRANSPORTER 1  
55 (IRT1), respectively (Fourcroy *et al.*, 2014; Robe *et al.*, 2021; Robinson *et al.*, 1999;  
56 Santi and Schmidt, 2009; Vert *et al.*, 2002). In chelation-based strategy (Strategy II),  
57 graminaceous plants biosynthesize and secrete high-affinity iron chelators, the  
58 phytosiderophores of the mugineic acid (MA) family, to chelate and directly acquire  
59 Fe(III) from soil (Kobayashi *et al.*, 2014; Kobayashi and Nishizawa, 2012).

60 Iron deficiency can trigger the induction of genes responsible for iron uptake and

61 translocation. These genes are tightly regulated at the transcriptional level by several  
62 transcription factors (TFs), which are critical for the maintenance of iron homeostasis  
63 in plants (Gao and Dubos, 2020; Gao *et al.*, 2019a). Several bHLH TFs have been  
64 identified and characterized as regulators of iron homeostasis in the past two decades  
65 (Gao and Dubos, 2020). FIT (FER-like iron-deficiency-induced transcription factor),  
66 the functional homolog of the tomato FER TF, was identified as a key regulator in  
67 driving Strategy I iron uptake machinery in Arabidopsis (Colangelo and Guerinot, 2004;  
68 Jakoby *et al.*, 2004; Yuan *et al.*, 2005). FIT interaction with the members of the clade  
69 Ib bHLH subfamily (i.e. bhLH38, bHLH39, bHLH100 and bHLH101) is required for  
70 the activation of its target genes including *IRT1* and *FRO2* (Wang *et al.*, 2013; Yuan *et*  
71 *al.*, 2008). These interactions were also shown to enhance the stability of FIT (Cui *et al.*,  
72 2018).

73 Both *FIT* and clade Ib *bHLH* expression are induced by iron deficiency and their  
74 expression is down-regulated in the single mutants of clade IVc *bHLH* TFs (i.e.  
75 *bHLH34*, *bHLH104*, *bHLH105* and *bHLH115*) (Li *et al.*, 2016a; Liang *et al.*, 2017a;  
76 Zhang *et al.*, 2015a). Conversely, overexpression of clade IVc *bHLH* genes could  
77 constitutively activate the expression of *FIT* and clade Ib *bHLH* regardless of the iron  
78 status, resulting in iron overload in Arabidopsis (Li *et al.*, 2016a; Liang *et al.*, 2017a;  
79 Zhang *et al.*, 2015a). Chip-qPCR and transactivation assays demonstrated that clade  
80 IVc bHLH could directly bind to the promoter of clade Ib *bHLH* and activate their  
81 expression (Li *et al.*, 2016a; Liang *et al.*, 2017a; Zhang *et al.*, 2015a). Conversely, these  
82 studies highlighted that the clade IVc bHLH TFs regulate the expression of *FIT* via an  
83 indirect mechanism (Zhang *et al.*, 2015a). Although bHLH34, bHLH104, bHLH105,  
84 and bHLH115 shared the same target genes and showed similar molecular functions, it  
85 is likely they function in an additive and synergistic manner to regulate the iron  
86 homeostasis since multiple mutants show more severe iron deficiency symptoms than  
87 the single ones (Li *et al.*, 2016a; Liang *et al.*, 2017a).

88 Most recently, a bHLH transcription factor from the IVb clade, bHLH121, has been  
89 identified and characterized as a key regulator of iron deficiency responses by three  
90 different teams (Gao *et al.*, 2020; Kim *et al.*, 2019; Lei *et al.*, 2020). *bhlh121* loss-of-

91 function mutant displayed severe iron deficiency symptoms due to impaired iron  
92 deficiency responses and expression analysis indicated that bHLH121 is responsible for  
93 the induction of a set of iron-related genes including *bHLH38*, *bHLH39*, *bHLH100*,  
94 *bHLH101* and *FIT* under iron deficiency condition. Lei et al found that bHLH121 could  
95 directly bind to the promoter of clade *Ib bHLH* and *FIT* (Lei et al., 2020). However,  
96 different results reported by the two other studies only validated the interaction between  
97 bHLH121 and the promoter of clade *Ib bHLH* TFs (Gao et al., 2020; Kim et al., 2019).  
98 Although further investigation is required to clarify the relationship between bHLH121  
99 and *FIT*, it is definitely that clade *Ib bHLH* are directly targeted by bHLH121 and the  
100 clade IVc bHLH TFs (Gao et al., 2020; Kim et al., 2019; Lei et al., 2020; Li et al.,  
101 2016a; Liang et al., 2017a; Zhang et al., 2015a).

102 If it is clearly demonstrated that bHLH121 interacts with all the members of the IVc  
103 bHLH clade (Gao et al., 2020; Lei et al., 2020), it is also known that IVc bHLH TFs  
104 can homo and heterodimerize (Li et al., 2016a; Liang et al., 2017a; Zhang et al., 2015a).  
105 How bHLH121 and clade IVc bHLH proteins work collectively and efficiently to  
106 regulate the expression of their target genes, and thus iron homeostasis, still needs to be  
107 further investigated.

108 In this study, we found that double loss-of-function mutants between *bhlh121* and clade  
109 *IVc bhlhs* displayed more severe iron deficiency-associated growth defects compared  
110 to the single mutants. Consistent with this, expression analysis highlighted enhanced  
111 impaired iron deficiency responses in the double mutants when compared to single  
112 mutants. Constitutive expression of *bHLH34* and *bHLH105*, but not *bHLH104* or  
113 *bHLH115*, could partially complement the *bhlh121* iron deficiency symptoms notably  
114 by activating the expression of both *bHLH39* and *FIT*. Altogether, these results suggest  
115 a bHLH121-independent function for the four IVc bHLH members in regulating the  
116 iron deficiency responses. In addition, these data indicate that clade IVc bHLH play  
117 distinct roles in the regulation of iron homeostasis which might be related to their  
118 specific expression pattern.

119  
120

121 **Materials and methods**

122

123 **Plant materials**

124 *Arabidopsis thaliana* Columbia (Col-0) ecotype was used as the wild type in this study.

125 The *bhlh34* (GK-116E01), *bhlh104-1* (Salk\_099496C), *bhlh105/ilr3-3*

126 (Salk\_043690C), *bhlh115-2* (WiscDsLox384D9), *bhlh121-2* mutants have been

127 described previously (Gao *et al.*, 2020; Li *et al.*, 2016a; Liang *et al.*, 2017a; Zhang *et*

128 *al.*, 2015a). All the T-DNA insertion mutants were confirmed by PCR with gene-

129 specific primers and left border primers of the T-DNA insertion. The *bhlh121 bhlh104*,

130 *bhlh121 bhlh105 bhlh121 bhlh1115* double mutant plants were generated by crossing

131 *bhlh121-2* as the male parent to *bhlh104-1*, *bhlh105/ilr3-3* and *bhlh115-2*, respectively.

132 *bhlh121 bhlh34* double mutant was generated by CRISPR/Cas9 technology during the

133 study. All the mutants were confirmed by sequencing.

134

135 **Plant growth conditions**

136 For *in vitro* cultures, seeds were surface sterilized using 12.5% bleach for 5 mins and

137 rinsed 3 times with absolute ethanol. Sterilized seeds were plated on half-strength

138 Murashige and Skoog (MS/2) medium containing 0.05% (w/v) MES [2-(*N*-morpholino)

139 ethanesulfonic acid; pH 5.7], 1% (w/v) sucrose and 0.7% (w/v) agar with different

140 concentration of Fe-EDTA. For phenotypic analyses, plates were placed vertically in a

141 growth chamber at 22°C under a long-day photoperiod (16 h light / 8 h dark) for 7 days.

142 For the GUS staining assays, 7-day-old seedlings grown in presence of 50 µM iron

143 (control) conditions were transferred to 0 µM iron plates (Fe deficiency condition) for

144 another 7 days.

145 For hydroponic cultures, seeds were germinated on Hoagland medium containing 0.7%

146 (w/v) agar with 50 µM Fe-EDTA. Plants were transferred to liquid Hoagland medium

147 with 50 µM Fe-EDTA under short-day photoperiod (8 h light / 16 h dark) for 4 weeks

148 (Fourcroy *et al.*, 2016). For iron deficiency treatment, 5-week-old plants were rinsed

149 with Milli-Q water 3 times and then transferred to liquid Hoagland medium in absence

150 of iron for 1 week.

151

## 152 **Plasmid construction and plant transformation**

153 Arabidopsis ecotype Col-0 cDNA was used as the template to amplify the full length  
154 coding sequence (CDS) of *bHLH34*, *bHLH104*, *bHLH105*, and *bHLH115* (with stop  
155 codons). Purified PCR products were cloned into the entry vector pDONR207 by  
156 Gateway BP reaction (Invitrogen) and then recombined into the pUB-GFP Dest binary  
157 destination vector downstream of the strong, ubiquitous promoter of the Arabidopsis  
158 UBIQUITIN10 gene by Gateway LR reaction (Grefen *et al.*, 2010).

159 To construct the *probHLH34:bHLH34-GUS*, *probHLH104:bHLH104-GUS*,  
160 *probHLH105:bHLH105-GUS* and *probHLH115:bHLH115-GUS* plants, 4328 bp, 3466  
161 bp, 3557 bp, 3101 bp of the promoter and genomic region of *bHLH34*, *bHLH104*,  
162 *bHLH105*, and *bHLH115* were amplified and cloned into entry vector pDONR207,  
163 respectively, and then recombined into the pGWB3 destination vectors upstream from  
164 the GUS reporter gene (Nakagawa *et al.*, 2007).

165 *Agrobacterium tumefaciens* strain GV3101 was used for transformation into Col-0 or  
166 *bhlh121-2* plants through the floral dipping method (Clough and Bent, 1998). Seeds  
167 from T0 plants were selected on MS/2 agar plates containing 50 µg/ml hygromycin or  
168 12.5 µg/ml glufosinate-ammonium for pGWB3 and pUB-GFP Dest constructs,  
169 respectively. T3 homozygous lines were used for subsequent analyses. The primers  
170 used for cloning are described in Table S1.

171

## 172 **Gene expression analysis**

173 Total RNA was extracted from about 100 mg fresh weight of 7-day-old seedlings by  
174 using Trizol reagent (Invitrogen). 1 µg RNA was treated with DNase and then used for  
175 cDNA synthesis by using the RevertAid kit according to the manufacturer  
176 recommendations (Thermo Fisher Scientific). qRT-qPCR analyses were performed by  
177 using ONEGreen® FAST qPCR Premix (Ozyme) on a LightCycler 480 real-time PCR  
178 system (Roche). PROTEIN PHOSPHATASE 2A SUBUNIT A3 (PP2AA3) was used as  
179 internal control (Czechowski *et al.*, 2005). Expression levels were calculated using the  
180 comparative threshold cycle method. The primers used for gene expression analysis are

181 listed in Table S1.

182

### 183 **Histochemical GUS staining**

184 2-week-old seedlings expressing *probHLH34:bHLH34-GUS*, *probHLH104:bHLH104-*  
185 *GUS*, *probHLH105:bHLH105-GUS*, *probHLH115:bHLH115-GUS*, and  
186 *probHLH121:bHLH121-GUS* were collected and immersed immediately in 1 ml of  
187 GUS staining buffer [0.1 M phosphate buffer, pH 7.5, 10 mM Na<sub>2</sub>-EDTA, 0.1% (v/v)  
188 Triton X-100, 0.5 mM potassium ferricyanide, 0.5 mM potassium ferrocyanide and 2  
189 mM X-Gluc (5- bromo-4-chloro-3-indolyl-b-D-glucuronide).] The reaction was  
190 performed at 37°C overnight in the dark after a 1-hour vacuum treatment was applied  
191 at room temperature. After the reaction, samples were rinsed with distilled water and  
192 treated with 70% (v/v) ethanol to remove the chlorophylls. Images were captured by  
193 using a motorized fluorescence stereo zoom microscope (ZEISS).

194

### 195 **Iron measurement**

196 To measure iron content, leaves of 4-week-old plants grown in normal soils were  
197 harvested. Leaves and roots from plants grown in hydroponic culture were also  
198 harvested separately and used for iron measurement. Prior analysis, samples were dried  
199 at 65°C for 1 week in an oven. Ten milligrams of ground samples were homogenized  
200 with 750 µl of nitric oxide (65% [v/v]) and 250 µl of hydrogen peroxide (30% [v/v]).  
201 Following overnight incubation at room temperature, the samples were incubated at  
202 85°C for 48 hours in a HotBlock (Environmental Express). Samples were then diluted  
203 by adding 4 ml Milli-Q water. Analysis of iron content was performed by MP-AES  
204 (Microwave Plasma Atomic Emission Spectroscopy, Agilent Technologies).

205

### 206 **Chlorophyll measurement**

207 Twenty milligrams leaves (fresh weight) were collected and soaked overnight in 1 ml  
208 100% acetone in the dark with strong shaking. The absorbance (A) of the clear  
209 supernatant was measured at 661.8 and 644.8 nm using a spectrophotometer (Beckman).



210 Total chlorophyll contents were calculated as previously reported (Lichtenthaler, 1987).

211

### 212 **Ferric chelate reductase activity assays**

213 Ferric chelate reductase assays were performed as previously reported with slight  
214 modifications (Yi and Guerinot, 1996). Briefly, ten milligrams of fresh root tissues were  
215 soaked in 1 ml of FCR assays buffer (10 mM MES, pH 5.5, 100 mM Fe<sup>3+</sup>-EDTA and  
216 300 mM ferrozine) for 1 hour in the dark. An identical assay without any root tissues  
217 was used as a blank. Samples were measured at 560 nm using a microplate reader  
218 (Xenius).

219

### 220 **Accession Numbers**

221 Sequence data in this study can be found in the GenBank/EMBL databases under the  
222 following accession numbers: bHLH121 (At3g19860); IRT1 (At4g19690); FRO2  
223 (At1g01580); bHLH29/FIT (At2g28160); bHLH38 (At3g56970); bHLH39  
224 (At3g56980); bHLH100 (At2g41240); bHLH101 (At5g04150); bHLH34 (At3g23210);  
225 bHLH104 (At4g14410); bHLH105/ILR3 (At5g54680); bHLH115 (At1g51070);  
226 PP2AA3 (At1g13320).

227

### 228 **Results**

229

#### 230 **Generation of double mutants between bHLH121 and clade IVc bHLH TFs.**

231 bHLH121 was recently characterized, by three different teams, as a key regulator of the  
232 iron deficiency responses in Arabidopsis (Gao *et al.*, 2020; Kim *et al.*, 2019; Lei *et al.*,  
233 2020). Further studies indicated that bHLH121 activity relies on its interaction with the  
234 four members of clade IVc bHLH TFs (bHLH34, bHLH104, ILR3/bHLH105, and  
235 bHLH115), which are also reported to play a critical role in regulating the iron  
236 deficiency responses (Li *et al.*, 2016a; Liang *et al.*, 2017a; Tissot *et al.*, 2019; Zhang *et*  
237 *al.*, 2015a). Hypothesizing that additive functions might exist between bHLH121 and  
238 the four clade IVc bHLHs, we generated the double mutant *bhlh121 bhlh104*, *bhlh121*  
239 *bhlh105*, *bhlh121 bhlh115* by crossing the single mutant *bhlh121-2* (Gao *et al.*, 2020)

240 with *bhlh104-1* (Zhang *et al.*, 2015a), *ilr3-3* (Zhang *et al.*, 2015a) and *bhlh115-2* (Liang  
241 *et al.*, 2017a), respectively. We failed to obtain the double mutant *bhlh121-2 bhlh34* by  
242 crossing because of the close proximity of both genes on the same chromosome.  
243 Therefore, we constructed the double mutant *bhlh121 bhlh34* by editing the *BHLH121*  
244 gene in *bhlh34* mutant plants using the CRISPR/Cas9 technology. One representative  
245 allele was chosen for further investigation in this study. Sequencing analysis indicated  
246 that it contains a single nucleotide insertion (A) in exon 2 that is identical to the  
247 previously characterized *bhlh121-1* allele (Gao *et al.*, 2020). This frameshift mutation  
248 results in a truncated bHLH121 protein (Figure S1).

249

250 **bHLH121 and clade IVc bHLH TFs double mutants display enhanced iron**  
251 **deficiency symptoms compare to the single mutants.**

252 In normal soil, under greenhouse conditions, *bhlh121* mutant showed small stature and  
253 chlorotic leaves as previously reported (Gao *et al.*, 2020) (Figure 1A). The four double  
254 mutants *bhlh121 bhlh34*, *bhlh121 bhlh104*, *bhlh121 bhlh105* and *bhlh121 bhlh115*  
255 displayed enhanced growth defects compare to the *bhlh121* single mutant (Figure 1A).  
256 Both *bhlh121 bhlh104* and *bhlh121 bhlh105* double mutants withered and died early  
257 during their development when no extra iron was supplied (Figure 1A). Without extra  
258 iron supply, the *bhlh121 bhlh34* double mutant displayed leaves with necrosis  
259 symptoms whereas the *bhlh121 bhlh115* mutant showed only smaller leaves compare  
260 to the *bhlh121* single mutant. In soil watered with 1‰ Fe-EDDHA (ferric  
261 ethylenediamine di-(o-hydroxyphenylacetate), a form of iron easily assimilated by the  
262 plant), *bhlh121* and *bhlh121 bhlh115* were rescued and showed a similar phenotype  
263 compare to the wild type. *bhlh121 bhlh34* displayed slight chlorosis symptoms in young  
264 leaves (Figure 1A). The addition of Fe-EDDHA improved *bhlh121 bhlh104* and  
265 *bhlh121 bhlh105* survival, but both double mutants still showed severe growth defects  
266 associated with leaves chlorosis and necrosis, which were more pronounced for the  
267 *bhlh121 bhlh105* double mutant (Figure 1A).

268 Iron is indispensable for the biosynthesis of chlorophylls, and chlorophylls  
269 accumulation is a typical indicator of iron deficiency-associated leaves chlorosis (Terry,

270 1980). We measured the chlorophylls content of the different mutants grown in soil  
271 watered or not with exogenous iron (Figure 1B). Under the control condition, there was  
272 no significant difference between the wild type and the *bhlh34*, *bhlh104*, and *bhlh115*  
273 single mutants. In contrast, chlorosis of the *bhlh121* and *bhlh105* single mutants was  
274 correlated with a marked decline in chlorophylls content (Figure 1B). *bhlh121 bhlh34*,  
275 *bhlh121 bhlh104* and *bhlh121 bhlh105* showed a lower chlorophylls content compare  
276 to the *bhlh121* single mutant whereas no difference was observed with the *bhlh121*  
277 *bhlh115* double mutant. When the plants were watered with exogenous iron, only the  
278 two double mutants *bhlh121 bhlh104* and *bhlh121 bhlh105* showed lower chlorophyll  
279 contents compare to the other genotypes (Figure 1B).

280 We further investigated the phenotypes of plants grown on MS/2 medium containing  
281 different concentrations of iron. In the absence of iron (0  $\mu\text{M}$  Fe), all the single mutant  
282 were severely affected and showed shorter root length compare to the wild type (Figure  
283 S2). Although *bhlh121 bhlh34*, *bhlh121 bhlh104* and *bhlh121 bhlh105* showed similar  
284 root length compare to *bhlh121*, these double mutants displayed albinos cotyledons  
285 (Figure S2 and S3). When the plants were grown under normal conditions (50  $\mu\text{M}$  Fe),  
286 clade IVc bHLH single mutant grew and developed normally as the wild type. In  
287 contrast, *bhlh121* single mutant still showed chlorotic cotyledons and shorter root  
288 length compared to the wild type plants. The root growth defects of double mutants  
289 were partially rescued but still showed a shorter root length compare to *bhlh121*. When  
290 grown in the presence of 200  $\mu\text{M}$  iron, *bhlh121 bhlh34*, *bhlh121 bhlh104* and *bhlh121*  
291 *bhlh115* double mutants showed similar phenotype with *bhlh121* and had no significant  
292 difference in primary root length (Figure S2 and S3). By contrast, *bhlh121 bhlh105* still  
293 showed slight iron deficiency-associated phenotypes with chlorotic cotyledons and  
294 shorter primary roots. Even when the iron concentration was increased to 500  $\mu\text{M}$  Fe,  
295 the root length of *bhlh121 bhlh105* was still shorter than that of *bhlh121* (Figure S2 and  
296 S3).

297 Taken together, these results indicate that loss of function of IVc bHLH TFs in the  
298 *bhlh121* single mutant background enhanced its iron-associated phenotypes, implying  
299 that bHLH121 and clade IVc bHLHs TFs play an additive role in the iron deficiency

300 responses.

301

302 **Loss of function of clade IVc bHLH TFs in *bhlh121* mutant causes decreased iron**  
303 **accumulation.**

304 To determine whether the loss of function of IVc bHLH in *bhlh121* causes altered iron  
305 accumulation, we first measured the shoot iron contents in 5-week-old wild type and  
306 different mutant plants grown in normal soil under greenhouse conditions. As shown in  
307 Figure 1C, there was no significant difference between wild type and *bhlh34* or *bhlh115*  
308 single mutant. In contrast, *bhlh121* single mutant, *bhlh121 bhlh34* and *bhlh121 bhlh105*  
309 double mutants showed about 21.8 %, 42.3% and 31.7% lower iron contents than those  
310 of wild type plants, respectively. These results also indicated that the *bhlh121 bhlh34*  
311 and *bhlh121 bhlh105* double mutants showed significantly lower iron accumulation in  
312 the shoots compare to the *bhlh121* mutant (Figure 1C).

313 To further investigate how the loss of function of clade IVc bHLH TFs in *bhlh121*  
314 mutant affects iron accumulation in roots and shoots, wild type and mutant plants were  
315 grown in hydroponic condition for 5 weeks and then subjected to iron deficiency (0  $\mu$ M  
316 Fe) or kept in control (50  $\mu$ M Fe) conditions for one additional week. Under control  
317 conditions, *bhlh121*, *bhlh34*, *bhlh121 bhlh34* and *bhlh121 bhlh115* showed decreased  
318 iron accumulation compare to the wild type in both shoots and roots (Figure 2).  
319 Meanwhile, a significant decrease in iron accumulation was observed in the *bhlh121*  
320 *bhlh34* and *bhlh121 bhlh115* double mutants compared to the corresponding single  
321 mutants in both shoots and roots. Interestingly, when plants were grown under the iron  
322 deficiency condition, there was no significant difference between the wild type and the  
323 *bhlh121*, *bhlh34* and *bhlh115* mutants in the shoots. *bhlh121 bhlh34* and *bhlh121*  
324 *bhlh115* double mutants showed lower iron contents in the shoots when compared to  
325 the corresponding single mutants (Figure 2). By contrast, *bhlh121 bhlh34* and *bhlh121*  
326 *bhlh115* showed similar iron accumulation in the roots when compare to the *bhlh121*  
327 single mutant (Figure 2). These results further support the additive functions of  
328 bHLH121 and the clade IVc bHLH TFs, in particular for the uptake of iron.

329

330 **Loss of function of clade IVc bHLH TFs in *bhlh121* mutant enhances the impaired**  
331 **iron deficiency response.**

332 To determine whether the decreased iron deficiency tolerance observed for the *bhlh121*  
333 *bhlh34*, *bhlh121 bhlh104*, *bhlh121 bhlh105* and *bhlh121 bhlh115* double mutants was  
334 caused by the impaired expression of key iron deficiency-responsive genes, qRT-PCR  
335 experiments were conducted. For this purpose, seven-day-old seedlings were grown  
336 under iron deficient and sufficient conditions and transcript accumulation of *IRT1*, *FIT*  
337 and *bHLH39* was analyzed.

338 As expected, the expression of *IRT1* was lower in the *bhlh121*, *bhlh34*, *bhlh104* and  
339 *bhlh105* single mutants compare to that of the wild type under both iron deficient and  
340 sufficient conditions (Figure 3 and S4). Moreover, *IRT1* expression levels were  
341 decreased in the *bhlh121 bhlh34*, *bhlh121 bhlh104* and *bhlh121 bhlh105* double  
342 mutants when compared to the corresponding single mutants. In contrast, no difference  
343 in *IRT1* expression levels was found between *bhlh121* and *bhlh121 bhlh115* double  
344 mutant. These observations suggest that the observed reduction in iron accumulation in  
345 the double mutants is due to a decreased in iron uptake related to *IRT1* expression  
346 defects.

347 *bhlh121 bhlh104* and *bhlh121 bhlh105* double mutants showed considerably reduced  
348 transcript abundance for *bHLH39* compare to the *bhlh121* single mutant regardless of  
349 the iron status (Figure 3 and S4). *bHLH39* expression was also strongly diminished in  
350 the *bhlh121 bhlh34* double mutant when compared to the *bhlh121* single mutant when  
351 grown under the iron deficiency condition, but not in iron sufficient condition (Figure  
352 3 and S4). In contrast, *bhlh121 bhlh115* showed similar *bHLH39* expression level than  
353 *bhlh121* under both conditions.

354 Under iron deficiency condition, all the double mutant but *bhlh121 bhlh105* showed no  
355 significant difference in the transcript abundance of *FIT* with the *bhlh121* single mutant.  
356 When the plants were grown under the control condition, no variation in *FIT* expression  
357 was found between the *bhlh121*, *bhlh34*, *bhlh104*, *bhlh105*, and *bhlh115* mutants and  
358 the wild type. Interestingly, the expression of *FIT* was strongly diminished in all four  
359 double mutants.

360 Altogether, these results suggest that bHLH121 and the clade IVc bHLH TFs play an  
361 additive role in regulating the expression of *bHLH39* and *FIT*, and thus *IRT1* and the  
362 uptake of iron.

363

364 **Overexpression of *bHLH34* and *bHLH105* partially rescues the iron-deficiency**  
365 **phenotype of *bhlh121* mutant.**

366 Previous studies showed that the overexpression of clade IVc bHLH TFs in wild type  
367 plants could result in enhanced iron deficiency tolerance and over-accumulation of iron  
368 (Li *et al.*, 2016a; Liang *et al.*, 2017a; Zhang *et al.*, 2015a). To determine whether  
369 bHLH121 is required for these activities, the four clade IVc bHLH TFs were  
370 overexpressed in the *bhlh121* mutant. Two representative transgenic lines displaying  
371 elevated clade IVc bHLH expression levels were chosen for further study (Figure 4A).

372 When the plants were grown in soil under the greenhouse condition, the *bHLH104* and  
373 *bHLH115* overexpressing lines (*ProUBI::bHLH104/bhlh121* and  
374 *ProUBI::bHLH115/bhlh121*) displayed similar phenotype to that of *bhlh121* mutant,  
375 showing small stature and chlorotic leaves (Figure 4B). There was also no significant  
376 difference in chlorophyll contents (Figure 4C). In contrast, overexpression of *bHLH34*  
377 and *bHLH105* (*ProUBI::bHLH34/bhlh121* and *ProUBI::bHLH105/bhlh121*) partially  
378 rescued the iron-associated phenotypes of *bhlh121* mutant. For instance, both lines  
379 showed bigger leaves and higher chlorophylls content than those of *bhlh121* mutant  
380 (Figure 4B and C).

381 Similar results were observed when plants were grown *in vitro*.  
382 *ProUBI::bHLH34/bhlh121* and *ProUBI::bHLH105/bhlh121* lines showed stronger  
383 tolerance to iron deficiency than *bhlh121*. These overexpression lines had longer roots  
384 than the *bhlh121* mutant plants, but shorter roots than the wild type under low iron  
385 conditions (0, 10 and 25  $\mu$ M) (Figure S5 and S6). However, neither *bHLH104* nor  
386 *bHLH115* overexpression was able to overcome the *bhlh121* growth defects.  
387 *ProUBI::bHLH104/bhlh121* and *ProUBI::bHLH115/bhlh121* lines showed similar root  
388 length than *bhlh121* under the different iron conditions that were tested (0, 10, 25 and  
389 50  $\mu$ M) (Figure S5 and S6). These phenotypic analyses showed that the overexpression

390 of *bHLH34* and *bHLH105*, but not *bHLH104* and *bHLH115*, could partly complement  
391 the iron-associated phenotype of *bhlh121* mutant, indicating that the four clade IVc  
392 bHLH members play distinct roles in the regulation of iron homeostasis.

393 To further investigate how the overexpression of clade IVc bHLH TFs in *bhlh121*  
394 mutant affects iron accumulation in roots and shoots, we grew plants in hydroponic  
395 condition and subjected them or not to iron deficiency (Figure S7). In roots,  
396 overexpression of *bHLH34* and *bHLH105* increased the iron content in the *bhlh121*  
397 mutant regardless of whether the plants were grown in the presence or absence of iron  
398 (Figure 5). Such an increase was also observed in the shoots of these overexpression  
399 lines grown under control conditions, whereas no difference was detected in this tissue  
400 when grown under iron deficiency conditions. In accordance with the phenotypic  
401 analysis, overexpression of *bHLH104* and *bHLH115* showed no significant effect on  
402 the accumulation of iron neither in the roots nor in the shoots of *bhlh121*.

403 In addition, to further investigate how the overexpression of clade IVc bHLH TFs in  
404 *bhlh121* mutant affects iron homeostasis, the ferric-chelate reductase (FCR) activity  
405 was analyzed (Yi and Guerinot, 1996). As shown in Figure S8, overexpression of  
406 *bHLH34* and *bHLH105* increased the FCR activity in *bhlh121* mutant. These results  
407 suggest that bHLH34 and bHLH105 can partly reconstitute the iron uptake system to  
408 promote plant iron nutrition in the absence of bHLH121.

409

410 **Overexpression of *bHLH34* and *bHLH105* activates the expression of both *FIT* and**  
411 **clade Ib bHLH TFs in *bhlh121* mutant.**

412 Previous studies showed that overexpression of clade IVc bHLH in wild type plants  
413 could constitutively activate the iron deficiency response genes regardless of the iron  
414 status (Li *et al.*, 2016a; Liang *et al.*, 2017a; Zhang *et al.*, 2015a). In this study,  
415 overexpression of *bHLH34* and *bHLH105* partially complemented the iron deficiency  
416 phenotypes of *bhlh121*. Whether or not this observation was due to the activation of  
417 key downstream components of the iron deficiency regulatory network was still to be  
418 determined. For this purpose, the expression of *IRT1*, *bHLH39*, and *FIT* in these  
419 overexpression lines was analyzed by qRT-PCR.

420 Expression analyses indicated that the overexpression of *bHLH34* and *bHLH105*  
421 dramatically increased the expression of *IRT1* under iron sufficient condition (Figure  
422 S9). Under iron deficiency condition, the expression of *IRT1* was induced, although the  
423 expression level was still lower compared to the wild type (Figure 6). By contrast,  
424 overexpression of *bHLH104* and *bHLH115* did not affect *IRT1* expression in the absence  
425 of *bHLH121* (Figure 6 and S9). These expression results might explain the increased  
426 iron accumulation observed in the *ProUBI::bHLH34/bhlh121* and  
427 *ProUBI::bHLH105/bhlh121* lines but not in the *ProUBI::bHLH104/bhlh121* and  
428 *ProUBI::bHLH115/bhlh121* ones.

429 We also analyzed the expression of *bHLH39*, one representative gene of the Ib bHLH  
430 subfamily that is a direct target of clade IVc bHLH TFs (Li *et al.*, 2016b; Liang *et al.*,  
431 2017a; Zhang *et al.*, 2015b). Overexpression of each clade IVc bHLH TFs could restore  
432 the expression of *bHLH39* in *bhlh121* mutant under iron deficiency conditions,  
433 indicating that the *bHLH121* and clade IVc bHLH TFs play redundant roles, to a certain  
434 extent, in activating the expression of clade Ib bHLH TFs (Figure 6).

435 Overexpression of *bHLH34* and *bHLH105* rescued as well the expression of *FIT* in the  
436 *bhlh121* mutant background under both iron deficient and sufficient conditions (Figure  
437 6 and S9). In contrast, overexpression of *bHLH104* and *bHLH115* showed no effect on  
438 the *FIT* expression.

439 Taken together, these results suggest that the overexpression of *bHLH34* and *bHLH105*  
440 is sufficient activate both the *FIT* and *bHLH39* to induce the expression of genes  
441 involved in iron uptake such as *IRT1*, resulting in increased iron content in *bhlh121*  
442 mutant.

443

444 **The nuclear localization of *bHLH121* in roots is unaffected by the mutation of**  
445 **individual clade IVc *bHLH* genes.**

446 It was reported that clade IVc bHLH TFs could facilitate the nuclear accumulation of  
447 *bHLH121* (Lei *et al.*, 2020). To determine whether the absence of clade IVc bHLH TFs  
448 could affect the nuclear localization of *bHLH121* in Arabidopsis, we introduced the  
449 *ProbHLH121:gbHLH121-GFP* construct into the four clade IVc bHLH single mutants



450 (i.e. *bhlh34*, *bhlh104*, *bhlh105* and *bhlh115*). This was achieved by crossing these  
451 mutants with a *bhlh121-2* mutant line carrying the *ProbHLH121:gbHLH121-GFP*  
452 transgene (Gao *et al.*, 2020). As shown in Figure 7, the *bhlh121-2* lines carrying the  
453 *ProbHLH121:gbHLH121-GFP* transgene displayed bHLH121-GFP fluorescence in the  
454 nucleus of root cells regardless of the iron status. Similar results were observed when  
455 individual clade IVc bHLH genes were mutated, suggesting a redundant role for clade  
456 IVc bHLH TFs in promoting the nuclear localization of bHLH121 in roots.

457

458 **bHLH121 and clade IVc bHLH TFs show different but complementary expression**  
459 **patterns in roots.**

460 Given the potential additive roles of bHLH121 and clade IVc bHLH TFs in regulating  
461 the iron deficiency responses, we investigated whether the expression pattern of these  
462 TFs were different or not. To achieve this goal, we constructed the  
463 *probHLH121:bHLH121-GUS*, *probHLH34:bHLH34-GUS*, *probHLH104:bHLH104-*  
464 *GUS*, *probHLH105:bHLH105-GUS* and *probHLH115:bHLH115-GUS* transgenic lines.  
465 GUS staining results revealed that *bHLH121*, *bHLH34*, *bHLH104*, *bHLH105*, and  
466 *bHLH115* were expressed in both the roots and shoots and shared similar tissue  
467 expression patterns in the leaves (Figure 8). All these plants showed stronger expression  
468 strengths in the young leaves compare with the older ones. In the hypocotyls, strong  
469 GUS activities were detected for the *probHLH104:bHLH104-GUS* and  
470 *probHLH105:bHLH105-GUS* lines, but not for the *probHLH121:bHLH121-GUS*,  
471 *probHLH34:bHLH34-GUS* and *probHLH115:bHLH115-GUS* ones.

472 In the roots, GUS activity was observed for *bHLH121*, *bHLH104*, *bHLH105* and  
473 *bHLH115* in the root tips, the early lateral roots and the root maturation zone (Zone III),  
474 whereas for *bHLH34* GUS activity was only observed in the root tips and early lateral  
475 roots. *bHLH104*, *bHLH105* and *bHLH115* were also expressed in the upper maturation  
476 zone (Zone I and Zone II) (Figure 8). Strong GUS activities were detected in the stele  
477 of these zones for the *probHLH104:bHLH104-GUS* and *probHLH105:bHLH105-GUS*  
478 lines, whereas only a faint GUS staining was observed for *probHLH115:bHLH115-*  
479 *GUS* (Figure 8).

480 The different tissue-specific expression patterns observed for *bHLH121* and the clade  
481 IVc bHLH TFs in the roots indicate that each of these proteins might play specific role  
482 in the different tissues, which is in adequacy with the additive role observed for these  
483 TFs in the regulation of the plant iron deficiency responses.

484

## 485 **Discussion**

486 Iron is an essential microelement but also a potentially toxic heavy metal for plant  
487 growth and development. Its homeostasis is tightly regulated by an intricate regulatory  
488 network that involves several TFs (Gao and Dubos, 2020; Gao *et al.*, 2019b). In  
489 Arabidopsis, the 158 bHLH TFs are divided into 26 clades, which have been widely  
490 reported to regulate myriad metabolic processes (Bailey *et al.*, 2003; Carretero-Paulet  
491 *et al.*, 2010; Heim *et al.*, 2003; Pires and Dolan, 2010). Several studies indicate that  
492 bHLH TFs from the same clade are involved in the regulation of specific metabolic  
493 processes (Buti *et al.*, 2020; MacAlister and Bergmann, 2011; Sun *et al.*, 2018). This is  
494 for instance the case with clades Ib (i.e. bHLH38, bHLH39, bHLH100, and bHLH101),  
495 IVa (i.e. bHLH18, bHLH19, bHLH20 and bHLH25), IVb (i.e. bHLH11, bHLH47/PYE,  
496 bHLH121/URI) and IVc (i.e. bHLH34, bHLH104, bHLH105, and bHLH115) that are  
497 all involved in the regulation of iron homeostasis together with FIT (Gao and Dubos,  
498 2020).

499 The transcriptional activity of a given bHLH TF relies on its ability to form homo-  
500 and/or hetero-dimers. bHLH121, that is a key regulator of the iron deficiency responses,  
501 form heterodimers with the bHLH TFs belonging to clade IVc (Gao *et al.*, 2020; Lei *et al.*  
502 *et al.*, 2020). Each single loss-of-function mutant for bHLH121 and clade IVc bHLH TFs  
503 showed sensitivity to iron deficiency, including chlorotic leaves and defects in primary  
504 root development (Gao *et al.*, 2020; Kim *et al.*, 2019; Lei *et al.*, 2020; Li *et al.*, 2016a;  
505 Liang *et al.*, 2017b; Zhang *et al.*, 2015a). Multiple loss-of-function mutants for the  
506 clade IVc bHLH TFs (i.e. *bhlh34 bhlh104*, *bhlh104 bhlh115* and *bhlh105 bhlh115*)  
507 displayed stronger growth defects under iron deficiency than the parental single mutants,  
508 indicating the non-redundant but additive role of clade IVc bHLH TFs in the regulation  
509 iron homeostasis (Li *et al.*, 2016a; Liang *et al.*, 2017b).

510 In a previous studies, Lei et al showed that the phenotypes of *bhlh121 bhlh104* and  
511 *bhlh121 bhlh115* double mutants were similar to that of the *bhlh121-5* single mutant,  
512 and they concluded that bHLH121 acts downstream of clade IVc bHLH in the Fe  
513 homeostasis network (Lei *et al.*, 2020). In contrast, in the present study we found that  
514 *bhlh121 bhlh34*, *bhlh121 bhlh104*, *bhlh121 bhlh105* and *bhlh121 bhlh115* double  
515 mutants showed enhanced growth defects compare to the *bhlh121* (*bhlh121-2* and  
516 *bhlh121-1*) mutant under both iron deficiency and sufficient conditions. These  
517 discrepancies may be due to the different genetic backgrounds of the *bhlh121* mutant  
518 used in these two studies. The *bhlh121-5* mutant encodes a truncated bHLH121 protein  
519 that contains a complete bHLH domain that is required for the heterodimerization with  
520 other bHLH transcription factors, whereas *bhlh121-2* and *bhlh121-1* mutant  
521 backgrounds encode truncated bHLH121 protein with an incomplete bHLH domain.  
522 This hypothesis is further supported by the fact that *bhlh121-2* and *bhlh121-1* showed  
523 stronger growth defects than *bhlh121-5* when grown in soil (Gao *et al.*, 2020; Lei *et al.*,  
524 2020). In this study, we determined the iron-associated phenotypes of the double  
525 mutants under two different growth conditions (i.e. in soil and *in vitro* ), and provided  
526 compelling evidence to show that these double mutants presented stronger growth  
527 defects than *bhlh121* single mutant. (Figure 1, S2, and S3). Furthermore, we  
528 demonstrated that the iron contents are lower in *bhlh121 bhlh34* and *bhlh121 bhlh115*  
529 mutants compare to *bhlh121* single mutant (Figure 1,2).

530 bHLH121 and clade IVc bHLH TFs shared a set of target genes, including *FIT* and  
531 clade *Ib* bHLH (Gao *et al.*, 2020; Kim *et al.*, 2019; Li *et al.*, 2016a; Liang *et al.*, 2017b;  
532 Zhang *et al.*, 2015b). The expression of *FIT* and clade *Ib* bHLH was impaired in the  
533 *bhlh121*, *bhlh34*, *bhlh104*, *bhlh105* and *bhlh115* single mutants. Moreover, their  
534 expression levels in *bhlh34 bhlh104*, *bhlh34 bhlh105* and *bhlh104 bhlh115* double  
535 mutant was lower compared to the single mutants, suggesting the non-redundant but  
536 additive roles of clade IVc bHLH TFs in the transcriptional regulation of these genes  
537 (Li *et al.*, 2016a). Herein, we found the *bhlh121 bhlh34*, *bhlh121 bhlh104* and *bhlh121*  
538 *bhlh105* double mutants showed lower expression levels of *bHLH39* than those of the  
539 single mutant under iron deficiency, indicating that bHLH121 and clade IVc bHLH TFs

540 have a similar but different function in the regulation of clade Ib bHLH expression.  
541 However, the expression of *FIT* was only dramatically reduced in *bhlh121 bhlh105*, but  
542 not in the other double mutants compared to the single mutants under iron deficiency  
543 conditions. This observation indicates that bHLH105 and bHLH121 play an additive  
544 role in the activation of *FIT* expression under iron deficiency conditions.

545 Lei et al showed that overexpression of *bHLH104* and *bHLH115* could rescue the  
546 expression clade *Ib bHLH* TFs but not *FIT* in *bhlh121-5* mutant and concluded that  
547 bHLH121 is indispensable for the activation of *FIT* by bHLH IVc TFs (Lei *et al.*, 2020).  
548 In agreement with this conclusion, the same results were observed in this study.  
549 Overexpression of *bHLH105* and *bHLH115* could activate *bHLH39* expression but not  
550 *FIT* in the *bhlh121-2* mutant, which is not sufficient to activate *IRT1* expression to  
551 facilitate the uptake of iron. By contrast, overexpression of *bHLH34* and *bHLH105*  
552 could partially complement the iron-associated phenotype of *bhlh121* by up-regulating  
553 the expression of both *bHLH39* and *FIT*. It is noteworthy that *FIT* is not a direct target  
554 of clade IVc bHLH TFs (Li *et al.*, 2016a; Zhang *et al.*, 2015a). These results imply the  
555 existence of other transcription factors to connect *FIT* expression with bHLH34 and  
556 bHLH105 activity.

557 One possible mechanistic basis for the differential control of shared target genes by the  
558 individual above described bHLH TFs (i.e. bHLH121 and clade IVc bHLH TFs) is that  
559 each bHLH TF has a different spatial expression pattern within the plant body. Previous  
560 promoter-GUS analyses revealed that *bHLH038*, *bHLH039* and *bHLH100* were  
561 expressed in shoots and roots (Wang *et al.*, 2007). Within roots, GUS activity was  
562 detected in the epidermis and inside the root except near the root tip. In contrast to that,  
563 *FIT* was specifically expressed in roots near the root tip and also in the upper root zones  
564 under iron deficiency conditions (Colangelo and Guerinot, 2004; Jakoby *et al.*, 2004).  
565 Thus, the *FIT* expression patterns overlapped with clade *Ib bHLH* gene expression  
566 patterns within the root region except near the root tip (Jakoby *et al.*, 2004; Wang *et al.*,  
567 2007). We found that bHLH121 and clade IVc bHLH are also expressed in the roots  
568 with different spatial expression patterns (Figure 7). *bHLH121*, *bHLH104*, *bHLH105*  
569 and *bHLH115* are localized in the maturation zone (Zone III), where the *FIT* and clade

570 Ib bHLH TFs also showed strong expression under iron deficiency conditions. These  
571 observations support that bHLH121 and IVc bHLHs (except bHLH34) function  
572 coordinately to regulate the expression of *FIT* and clade *Ib bHLH* TFs within these  
573 regions. In addition, at the upper maturation zone (Zone I/II), only *bHLH104* and  
574 *bHLH105* are expressed in the stele, implying their putative specific roles in iron  
575 homeostasis beyond the uptake of iron. These results could partially explain why the  
576 *bhlh121 bhlh104* and the *bhlh121 bhlh105* double mutant showed the most severe  
577 growth defect among the four double mutants that were analyzed. It is noteworthy that  
578 bHLH121 and clade IVc bHLH TFs are also expressed in the shoots, especially in the  
579 veins (Lei *et al.*, 2020; Li *et al.*, 2016a; Liang *et al.*, 2017a) (Figure 7) even if little is  
580 known about their function in this tissue. Since *YSL3* (*YELLOW STRIPE LIKE 3*) and  
581 *OPT3* (*OLIGOPEPTIDE TRANSPORTER 3*), two iron transport and mobilization  
582 related genes, are highly expressed in the veins (Mendoza-Cózatl *et al.*, 2014; Stacey  
583 *et al.*, 2008; Waters *et al.*, 2006; Zhai *et al.*, 2014) and are direct targets of bHLH121,  
584 it might be that the function of bHLH121 and clade IVc bHLH TFs in aerial tissues  
585 would be to modulate iron transport and partitioning (Kim *et al.*, 2019).

586 Taken together, the data presented herein demonstrate that bHLH121 and clade IVc  
587 bHLH TFs play additive roles and function synergistically to regulate iron homeostasis.

588

## 589 Reference

590

591 **Bailey PC, Martin C, Toledo-Ortiz G, Quail PH, Huq E, Heim MA, Jakoby M, Werber M, Weisshaar B.**  
592 2003. Update on the basic helix-loop-helix transcription factor gene family in *Arabidopsis thaliana*. The  
593 *Plant Cell* **15**, 2497-2502.

594 **Briat J-F, Dubos C, Gaymard F.** 2015. Iron nutrition, biomass production, and plant product quality.  
595 *Trends in plant science* **20**, 33-40.

596 **Briat J-F, Duc C, Ravet K, Gaymard F.** 2010. Ferritins and iron storage in plants. *Biochimica et*  
597 *Biophysica Acta (BBA)-General Subjects* **1800**, 806-814.

598 **Brumbarova T, Bauer P, Ivanov R.** 2015. Molecular mechanisms governing *Arabidopsis* iron uptake.  
599 *Trends in plant science* **20**, 124-133.

600 **Buti S, Hayes S, Pierik R.** 2020. The bHLH network underlying plant shade-avoidance. *Physiologia*  
601 *Plantarum*.

602 **Carretero-Paulet L, Galstyan A, Roig-Villanova I, Martínez-García JF, Bilbao-Castro JR, Robertson**  
603 **DL.** 2010. Genome-wide classification and evolutionary analysis of the bHLH family of transcription factors

604 in Arabidopsis, poplar, rice, moss, and algae. *Plant Physiology* **153**, 1398-1412.

605 **Clough SJ, Bent AF**. 1998. Floral dip: a simplified method for Agrobacterium-mediated transformation of  
606 Arabidopsis thaliana. *The Plant Journal* **16**, 735-743.

607 **Colangelo EP, Guerinot ML**. 2004. The Essential Basic Helix-Loop-Helix Protein FIT1 Is Required for  
608 the Iron Deficiency Response. *The Plant Cell* **16**, 3400-3412.

609 **Connorton JM, Balk J, Rodríguez-Celma J**. 2017. Iron homeostasis in plants—a brief overview.  
610 *Metallomics* **9**, 813-823.

611 **Cui Y, Chen C-L, Cui M, Zhou W-J, Wu H-L, Ling H-Q**. 2018. Four IVa bHLH transcription factors are  
612 novel interactors of FIT and mediate JA inhibition of iron uptake in Arabidopsis. *Molecular plant* **11**, 1166-  
613 1183.

614 **Czechowski T, Stitt M, Altmann T, Udvardi MK, Scheible W-R**. 2005. Genome-wide identification and  
615 testing of superior reference genes for transcript normalization in Arabidopsis. *Plant Physiology* **139**, 5-  
616 17.

617 **Fourcroy P, Sisó-Terraza P, Sudre D, Savirón M, Reyt G, Gaymard F, Abadía A, Abadía J, Álvarez-  
618 Fernández A, Briat JF**. 2014. Involvement of the ABCG 37 transporter in secretion of scopoletin and  
619 derivatives by Arabidopsis roots in response to iron deficiency. *New Phytologist* **201**, 155-167.

620 **Fourcroy P, Tissot N, Gaymard F, Briat J-F, Dubos C**. 2016. Facilitated Fe nutrition by phenolic  
621 compounds excreted by the Arabidopsis ABCG37/PDR9 transporter requires the IRT1/FRO2 high-affinity  
622 root Fe<sup>2+</sup> transport system. *Molecular plant* **9**, 485-488.

623 **Gao F, Dubos C**. 2020. Transcriptional integration of the plant responses to iron availability. *Journal of*  
624 *experimental botany*.

625 **Gao F, Robe K, Bettembourg M, Navarro N, Rofidal V, Santoni V, Gaymard F, Vignols F,  
626 Roschztardt H, Izquierdo E, Dubos C**. 2020. The Transcription Factor bHLH121 Interacts with  
627 bHLH105 (ILR3) and Its Closest Homologs to Regulate Iron Homeostasis in Arabidopsis. *The Plant Cell*  
628 **32**, 508-524.

629 **Gao F, Robe K, Gaymard F, Izquierdo E, Dubos C**. 2019a. The Transcriptional Control of Iron  
630 Homeostasis in Plants: A Tale of bHLH Transcription Factors? *Frontiers in plant science* **10**.

631 **Gao F, Robe K, Gaymard F, Izquierdo E, Dubos C**. 2019b. The transcriptional control of iron  
632 homeostasis in plants: a tale of bHLH transcription factors? *Frontiers in plant science* **10**, 6.

633 **Grefen C, Donald N, Hashimoto K, Kudla J, Schumacher K, Blatt MR**. 2010. A ubiquitin-10 promoter-  
634 based vector set for fluorescent protein tagging facilitates temporal stability and native protein distribution  
635 in transient and stable expression studies. *The Plant Journal* **64**, 355-365.

636 **Guerinot ML, Yi Y**. 1994. Iron: Nutritious, Noxious, and Not Readily Available. *Plant Physiology* **104**, 815-  
637 820.

638 **Hänsch R, Mendel RR**. 2009. Physiological functions of mineral micronutrients (Cu, Zn, Mn, Fe, Ni, Mo,  
639 B, Cl). *Current Opinion in Plant Biology* **12**, 259-266.

640 **Heim MA, Jakoby M, Werber M, Martin C, Weisshaar B, Bailey PC**. 2003. The basic helix-loop-helix  
641 transcription factor family in plants: a genome-wide study of protein structure and functional diversity.  
642 *Molecular biology and evolution* **20**, 735-747.

643 **Jakoby M, Wang H-Y, Reidt W, Weisshaar B, Bauer P**. 2004. FRU (BHLH029) is required for induction  
644 of iron mobilization genes in Arabidopsis thaliana. *FEBS letters* **577**, 528-534.

645 **Kim SA, LaCroix IS, Gerber SA, Guerinot ML**. 2019. The iron deficiency response in Arabidopsis  
646 thaliana requires the phosphorylated transcription factor URI. *Proceedings of the National Academy of*  
647 *Sciences* **116**, 24933-24942.

648 **Kobayashi T, Itai RN, Nishizawa NK.** 2014. Iron deficiency responses in rice roots. *Rice* **7**, 27.

649 **Kobayashi T, Nishizawa NK.** 2012. Iron uptake, translocation, and regulation in higher plants. *Annual*

650 *Review of Plant Biology* **63**, 131-152.

651 **Lei R, Li Y, Cai Y, Li C, Pu M, Lu C, Yang Y, Liang G.** 2020. bHLH121 Functions as a Direct Link that

652 Facilitates the Activation of FIT by bHLH IVc Transcription Factors for Maintaining Fe Homeostasis in

653 *Arabidopsis*. *Molecular plant*.

654 **Li X, Zhang H, Ai Q, Liang G, Yu D.** 2016a. Two bHLH transcription factors, bHLH34 and bHLH104,

655 regulate iron homeostasis in *Arabidopsis thaliana*. *Plant Physiology* **170**, 2478-2493.

656 **Li XL, Zhang HM, Ai Q, Liang G, Yu DQ.** 2016b. Two bHLH Transcription Factors, bHLH34 and bHLH104,

657 Regulate Iron Homeostasis in *Arabidopsis thaliana*. *Plant Physiology* **170**, 2478-2493.

658 **Liang G, Zhang H, Li X, Ai Q, Yu D.** 2017a. bHLH transcription factor bHLH115 regulates iron

659 homeostasis in *Arabidopsis thaliana*. *Journal of experimental botany* **68**, 1743-1755.

660 **Liang G, Zhang HM, Li XL, Ai Q, Yu DQ.** 2017b. bHLH transcription factor bHLH115 regulates iron

661 homeostasis in *Arabidopsis thaliana*. *Journal of experimental botany* **68**, 1743-1755.

662 **Lichtenthaler HK.** 1987. [34] Chlorophylls and carotenoids: pigments of photosynthetic biomembranes.

663 *Methods in enzymology* **148**, 350-382.

664 **MacAlister CA, Bergmann DC.** 2011. Sequence and function of basic helix–loop–helix proteins required

665 for stomatal development in *Arabidopsis* are deeply conserved in land plants. *Evolution & development*

666 **13**, 182-192.

667 **Marschner H, Römheld V, Kissel M.** 1986. Different strategies in higher plants in mobilization and uptake

668 of iron. *Journal of plant nutrition* **9**, 695-713.

669 **Mendoza-Cózatl DG, Xie Q, Akmakjian GZ, Jobe TO, Patel A, Stacey MG, Song L, Demoin DW,**

670 **Jurisson SS, Stacey G.** 2014. OPT3 is a component of the iron-signaling network between leaves and

671 roots and misregulation of OPT3 leads to an over-accumulation of cadmium in seeds. *Molecular plant* **7**,

672 1455-1469.

673 **Nakagawa T, Kurose T, Hino T, Tanaka K, Kawamukai M, Niwa Y, Toyooka K, Matsuoka K, Jinbo T,**

674 **Kimura T.** 2007. Development of series of gateway binary vectors, pGWBs, for realizing efficient

675 construction of fusion genes for plant transformation. *Journal of bioscience and bioengineering* **104**, 34-

676 41.

677 **Pires N, Dolan L.** 2010. Origin and diversification of basic-helix-loop-helix proteins in plants. *Molecular*

678 *biology and evolution* **27**, 862-874.

679 **Robe K, Conejero G, Gao F, Lefebvre-Legendre L, Sylvestre-Gonon E, Rofidal V, Hem S, Rouhier**

680 **N, Barberon M, Hecker A.** 2021. Coumarin accumulation and trafficking in *Arabidopsis thaliana*: a

681 complex and dynamic process. *New Phytologist* **229**, 2062-2079.

682 **Robinson NJ, Procter CM, Connolly EL, Guerinot ML.** 1999. A ferric-chelate reductase for iron uptake

683 from soils. *Nature* **397**, 694-697.

684 **Santi S, Schmidt W.** 2009. Dissecting iron deficiency-induced proton extrusion in *Arabidopsis* roots. *New*

685 *Phytologist* **183**, 1072-1084.

686 **Stacey MG, Patel A, McClain WE, Mathieu M, Remley M, Rogers EE, Gassmann W, Blevins DG,**

687 **Stacey G.** 2008. The *Arabidopsis* AtOPT3 protein functions in metal homeostasis and movement of iron

688 to developing seeds. *Plant Physiology* **146**, 589-601.

689 **Sun X, Wang Y, Sui N.** 2018. Transcriptional regulation of bHLH during plant response to stress.

690 *Biochemical and biophysical research communications* **503**, 397-401.

691 **Terry N.** 1980. Limiting factors in photosynthesis: I. Use of iron stress to control photochemical capacity

692 in vivo. *Plant Physiology* **65**, 114-120.

693 **Tissot N, Robe K, Gao F, Grant-Grant S, Boucherez J, Bellegarde F, Maghiaoui A, Marcelin R,**  
694 **Izquierdo E, Benhamed M.** 2019. Transcriptional integration of the responses to iron availability in  
695 *Arabidopsis* by the bHLH factor ILR3. *New Phytologist* **223**, 1433-1446.

696 **Vert G, Grotz N, Dédaldéchamp F, Gaymard F, Guerinot ML, Briat J-F, Curie C.** 2002. IRT1, an  
697 *Arabidopsis* transporter essential for iron uptake from the soil and for plant growth. *The Plant Cell* **14**,  
698 1223-1233.

699 **Wang H-Y, Klatte M, Jakoby M, Bäumllein H, Weisshaar B, Bauer P.** 2007. Iron deficiency-mediated  
700 stress regulation of four subgroup Ib BHLH genes in *Arabidopsis thaliana*. *Planta* **226**, 897-908.

701 **Wang N, Cui Y, Liu Y, Fan H, Du J, Huang Z, Yuan Y, Wu H, Ling H-Q.** 2013. Requirement and functional  
702 redundancy of Ib subgroup bHLH proteins for iron deficiency responses and uptake in *Arabidopsis*  
703 *thaliana*. *Molecular plant* **6**, 503-513.

704 **Waters BM, Chu H-H, DiDonato RJ, Roberts LA, Easley RB, Lahner B, Salt DE, Walker EL.** 2006.  
705 Mutations in *Arabidopsis* yellow stripe-like1 and yellow stripe-like3 reveal their roles in metal ion  
706 homeostasis and loading of metal ions in seeds. *Plant Physiology* **141**, 1446-1458.

707 **Yi Y, Guerinot ML.** 1996. Genetic evidence that induction of root Fe (III) chelate reductase activity is  
708 necessary for iron uptake under iron deficiency. *The Plant Journal* **10**, 835-844.

709 **Yuan Y, Wu H, Wang N, Li J, Zhao W, Du J, Wang D, Ling H-Q.** 2008. FIT interacts with AtbHLH38 and  
710 AtbHLH39 in regulating iron uptake gene expression for iron homeostasis in *Arabidopsis*. *Cell research*  
711 **18**, 385.

712 **Yuan YX, Zhang J, Wang DW, Ling HQ.** 2005. AtbHLH29 of *Arabidopsis thaliana* is a functional ortholog  
713 of tomato FER involved in controlling iron acquisition in strategy I plants. *Cell research* **15**, 613-621.

714 **Zhai Z, Gayomba SR, Jung H-i, Vimalakumari NK, Piñeros M, Craft E, Rutzke MA, Danku J, Lahner**  
715 **B, Punshon T.** 2014. OPT3 is a phloem-specific iron transporter that is essential for systemic iron  
716 signaling and redistribution of iron and cadmium in *Arabidopsis*. *The Plant Cell* **26**, 2249-2264.

717 **Zhang J, Liu B, Li M, Feng D, Jin H, Wang P, Liu J, Xiong F, Wang J, Wang H-B.** 2015a. The bHLH  
718 transcription factor bHLH104 interacts with IAA-LEUCINE RESISTANT3 and modulates iron homeostasis  
719 in *Arabidopsis*. *The Plant Cell* **27**, 787-805.

720 **Zhang J, Liu B, Li MS, Feng DR, Jin HL, Wang P, Liu J, Xiong F, Wang JF, Wang HB.** 2015b. The  
721 bHLH Transcription Factor bHLH104 Interacts with IAA-LEUCINE RESISTANT3 and Modulates Iron  
722 Homeostasis in *Arabidopsis*. *Plant Cell* **27**, 787-805.

723

## 724 **Figure legends**

725

726 **Figure 1. *bhlh121* and clade IVc *bhlh* double loss-of-function mutants showed enhanced**  
727 **growth defects compare to single mutants.**

728 (A) Phenotype of the wild type (WT) and *bhlh121*, *bhlh34*, *bhlh104*, *bhlh105*, *bhlh115* loss-of-  
729 function mutants and *bhlh121 bhlh34*, *bhlh121 bhlh104*, *bhlh121 bhlh105* and *bhlh121 bhlh115*  
730 double mutants grown in soil for 5 weeks and watered or not with Fe-EDDHA [1‰(w/v)], a form  
731 of Fe easily assimilated by plants. (B) Chlorophyll content of WT, *bhlh121*, *bhlh34*, *bhlh104*,



732 *bhlh105*, *bhlh115*, *bhlh121 bhlh34*, *bhlh121 bhlh104*, *bhlh121 bhlh105* and *bhlh121 bhlh115* grown  
733 as in (A). (C) Iron contents in the leaves of WT, *bhlh121*, *bhlh34*, *bhlh115*, *bhlh121 bhlh34* and  
734 *bhlh121 bhlh115* grown as in (A). (B-C) Means within each condition with the same letter are not  
735 significantly different according to one-way ANOVA followed by post hoc Tukey test,  $p < 0.05$  ( $n$   
736 = 3 biological repeats). Error bars show  $\pm$ SD. n.d.: not determined. Asterisks indicate significant  
737 differences between samples (Student's t-test: \* \*  $P < 0.01$ ).

738

739 **Figure 2. Iron content in leaves and roots of *bhlh121* and clade *IVc bhlh* single and double**  
740 **mutant lines.**

741 Wild type (WT), *bhlh121*, *bhlh34*, *bhlh115*, *bhlh121 bhlh34* and *bhlh121 bhlh115* lines were grown  
742 under control hydroponic conditions (50  $\mu$ M Fe) for 5 weeks and then subjected to iron deficiency  
743 (0  $\mu$ M Fe) or kept in control (50 $\mu$ M Fe) condition for 1 additional week. Means within each  
744 condition with the same letter are not significantly different according to one-way ANOVA followed  
745 by post hoc Tukey test,  $p < 0.05$  ( $n = 3$  biological repeats). Error bars show  $\pm$ SD. n.d.: not determined.  
746 Asterisks indicate significant differences between two samples (Student's t-test: \*  $P < 0.05$ , \* \*  
747  $P < 0.01$ ).

748

749 **Figure 3. Expression of iron deficiency responsive genes in *bhlh121* and clade *IVc bhlh* single**  
750 **and double mutant lines grown under iron deficiency condition.**

751 Relative expression was determined by RT-qPCR in 7-day-old Arabidopsis seedlings grown on iron  
752 deficient MS/2 medium. Means within each condition with the same letter are not significantly  
753 different according to one-way ANOVA followed by post hoc Tukey test,  $p < 0.05$  ( $n = 3$  technical  
754 repeats). Error bars show  $\pm$ SD. Asterisks indicate significant differences between two samples  
755 (Student's t-test: \* \*  $P < 0.01$ ).

756

757 **Figure 4. Overexpression of *BHLH34* and *BHLH105* partly rescue the growth defect of *bhlh121***  
758 **mutant.**

759 (A) Relative expression of *BHLH34*, *BHLH104*, *BHLH105* and *BHLH115* in 7-day-old  
760 overexpression lines grown on iron sufficient MS/2 medium. (B) Phenotype of the wild type (WT),  
761 *bhlh121* and the overexpression lines grown in soil for 4 weeks. (C) Chlorophyll content of the WT,

762 *bhlh121* and the overexpression lines grown as in (A). (A and C) Means with the same letter are not  
763 significantly different according to one-way ANOVA followed by post hoc Tukey test,  $p < 0.05$  ( $n$   
764 = 3 technical repeats). Error bars show  $\pm$ SD.

765

766 **Figure 5. Overexpression of *bHLH34* and *bHLH105* in *bhlh121* mutant increases the iron**  
767 **content.**

768 (A-B) Iron contents in the leaves of *bhlh121* plants overexpressing *bHLH34* and *bHLH105*. Plants  
769 were grown in hydroponic condition (50  $\mu$ M Fe) for 5 weeks and then subjected to iron deficiency  
770 (0  $\mu$ M Fe, B) or kept in control condition (50  $\mu$ M Fe, A) for 1 additional week. (C-D) Iron contents  
771 in the roots of plants described in (A). Means within each condition with the same letter are not  
772 significantly different according to one-way ANOVA followed by post hoc Tukey test,  $p < 0.05$  ( $n$   
773 = 3 biological repeats). Error bars show  $\pm$ SD. n.d.: not determined. Asterisks indicate significant  
774 differences between two samples (Student's t-test: \*  $P < 0.05$ ).

775

776 **Figure 6. Expression of iron deficiency responsive genes in *bhlh121* mutant lines**  
777 **overexpressing clade IVc *bHLH* TFs grown under iron deficiency conditions.**

778 Relative expression was determined by RT-qPCR in 7-day-old Arabidopsis seedlings grown on iron  
779 deficient MS/2 medium. Means within each condition with the same letter are not significantly  
780 different according to one-way ANOVA followed by post hoc Tukey test,  $p < 0.05$  ( $n = 3$  technical  
781 repeats). Error bars show  $\pm$ SD. Asterisks indicate significant differences between two samples  
782 (Student's t-test: \*\*  $P < 0.01$ ).

783

784 **Figure 7. *bHLH121* protein localization in IVc *bhlh* mutant backgrounds.**

785 Seedlings were grown on iron sufficient (50  $\mu$ M Fe) or deficient (0  $\mu$ M Fe) MS/2 medium for 6  
786 days. Bars: 20  $\mu$ m.

787

788 **Figure 8. GUS staining of *pbHLH121:bHLH121-GUS*, *pbHLH34:bHLH34-GUS*,**  
789 ***pbHLH104:bHLH104-GUS*, *pbHLH105:bHLH105-GUS* and *pbHLH115:bHLH115-GUS***  
790 **transgenic plants.** Seedlings were grown on 50  $\mu$ M iron MS/2 medium for one week and then  
791 transferred to iron deficiency condition for another week.

792 **Figure S1. Generation of *bhlh121 bhlh34* double mutant by CRISPER-Cas9 system.**

793 Top part: schematic representation of *bHLH121* gene locus (grey box, exon; line, intron; red line:  
794 mutation site). Bottom part: localization of the RNA guides, within the second exon, selected for  
795 CRISPER-Cas9 gene editing. In red are the mutations produced in the coding sequence: single  
796 nucleotide insertions for *bhlh121 bhlh34* (A), which is same than the one in the *bhlh121-1* mutant  
797 allele. In green: *NGG* sequence.

798

799 **Figure S2. Phenotypes of wild type (WT), *bhlh121*, *bhlh34*, *bhlh104*, *bhlh105*, *bhlh115*, *bhlh121*  
800 *bhlh34*, *bhlh121 bhlh104*, *bhlh121 bhlh105* and *bhlh121bhlh115* mutants.** Seedlings were grown  
801 on iron sufficient (50  $\mu$ M Fe), iron deficient (0  $\mu$ M Fe) or iron excess (200 and 500  $\mu$ M Fe) MS/2  
802 medium. Bar: 1 cm.

803

804 **Figure S3. Root length of wild type (WT), *bhlh121*, *bhlh34*, *bhlh104*, *bhlh105*, *bhlh115*, *bhlh121*  
805 *bhlh34*, *bhlh121 bhlh104*, *bhlh121 bhlh105*, *bhlh121 bhlh115* mutants.**

806 Seedlings were grown on iron sufficient (50  $\mu$ M Fe), iron deficient (0  $\mu$ M Fe) or iron excess (200  
807 and 500  $\mu$ M Fe) MS/2 medium. Means within each condition with the same letter are not  
808 significantly different according to one-way ANOVA followed by post hoc Tukey test,  $P < 0.05$  ( $n$   
809 = 10-15 seedlings). Asterisks indicate significant differences between two samples (Student's t-test:  
810 \*  $P < 0.05$ ). Error bars show  $\pm$  SD.

811

812 **Figure S4. Expression of iron deficiency responsive genes in *bhlh121* and clade *IVc bhlh*  
813 *mutants* grown under iron sufficient condition.**

814 Relative expression was determined by RT-qPCR in 7-day-old Arabidopsis seedlings grown on iron  
815 sufficient MS/2 medium. Means within each condition with the same letter are not significantly  
816 different according to one-way ANOVA followed by post hoc Tukey test,  $p < 0.05$  ( $n = 3$  technical  
817 repeats). Error bars show  $\pm$ SD. Asterisks indicate significant differences between two samples  
818 (Student's t-test: \*\*  $P < 0.05$ , \* \*  $P < 0.01$ ).

819

820 **Figure S5. Overexpression of *bHLH34* and *bHLH105* partly rescue the growth defect of  
821 *bhlh121* mutant.**

822 Phenotype of the wild type (WT), *bhlh121* and *bhlh121* mutant lines overexpressing *bHLH34* and  
823 *bHLH105* grown on iron sufficient (50  $\mu$ M Fe) and iron deficient (0  $\mu$ M Fe, 10  $\mu$ M Fe and 25  $\mu$ M  
824 Fe) MS/2 medium. Bar: 1 cm.

825

826 **Figure S6. Root length of *bhlh121* mutant lines overexpressing clade IVc *bHLH* TFs.**

827 Seedlings were grown on iron sufficient (50  $\mu$ M Fe) and iron deficient (0  $\mu$ M Fe, 10  $\mu$ M Fe and 25  
828  $\mu$ M Fe) MS/2 medium. Means within each condition with the same letter are not significantly  
829 different according to one-way ANOVA followed by post hoc Tukey test,  $P < 0.05$  ( $n = 10-15$   
830 seedlings). Asterisks indicate significant differences between two samples (Student's t-test: \*  
831  $P < 0.05$ ). Error bars show  $\pm$  SD.

832

833 **Figure S7. Phenotype of *bhlh121* mutant lines overexpressing clade IVc *bHLH* TFs grown in**

834 **hydroponic conditions.** Plants were grown in hydroponic condition for 5 weeks and then subjected  
835 to iron deficiency (0  $\mu$ M Fe) or kept in control (50  $\mu$ M Fe) condition for 1 additional week.

836

837 **Figure S8. Ferric-chelate reductase activity of *bhlh121* mutant lines overexpressing clade IVc**

838 ***bHLH* TFs.** Plants were grown in hydroponic conditions for 5 weeks and then subjected to iron  
839 deficiency (0  $\mu$ M Fe) or kept in control (50  $\mu$ M Fe) condition for 1 additional week.

840

841 **Figure S9. Expression of iron deficiency responsive genes in *bhlh121* mutant lines**  
842 **overexpressing clade IVc *bHLH* TFs grown under iron sufficient conditions.**

843 Relative expression was determined by RT-qPCR in 7-day-old Arabidopsis seedlings grown on iron  
844 sufficient MS/2 medium (50  $\mu$ M Fe). Means within each condition with the same letter are not  
845 significantly different according to one-way ANOVA followed by post hoc Tukey test,  $p < 0.05$  ( $n$   
846 = 3 technical repeats). Error bars show  $\pm$ SD. Asterisks indicate significant differences between two  
847 samples (Student's t-test: \* \*  $P < 0.01$ ).

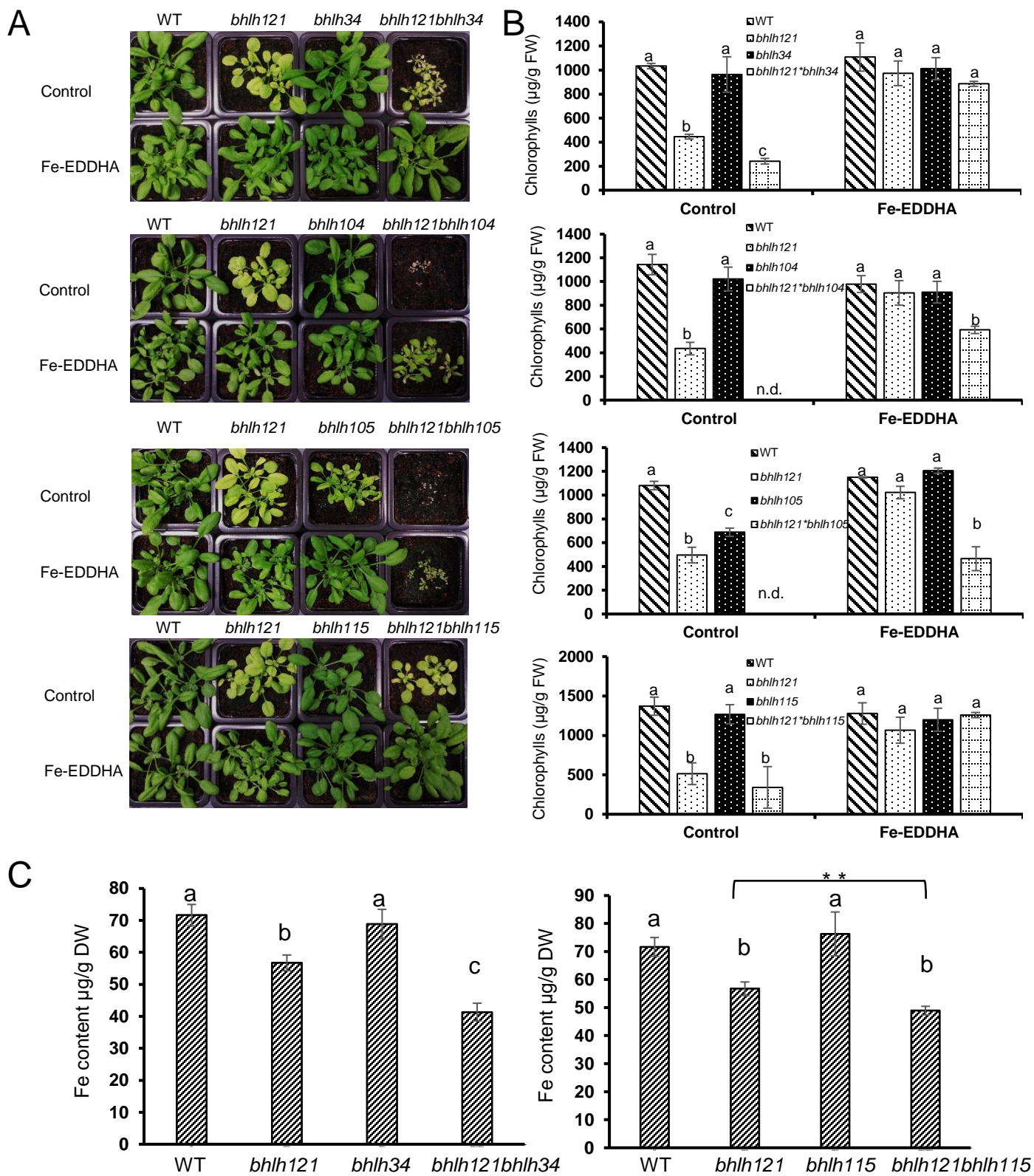


**Figure 1. Double mutants showed enhanced growth defects compare to single mutants.**

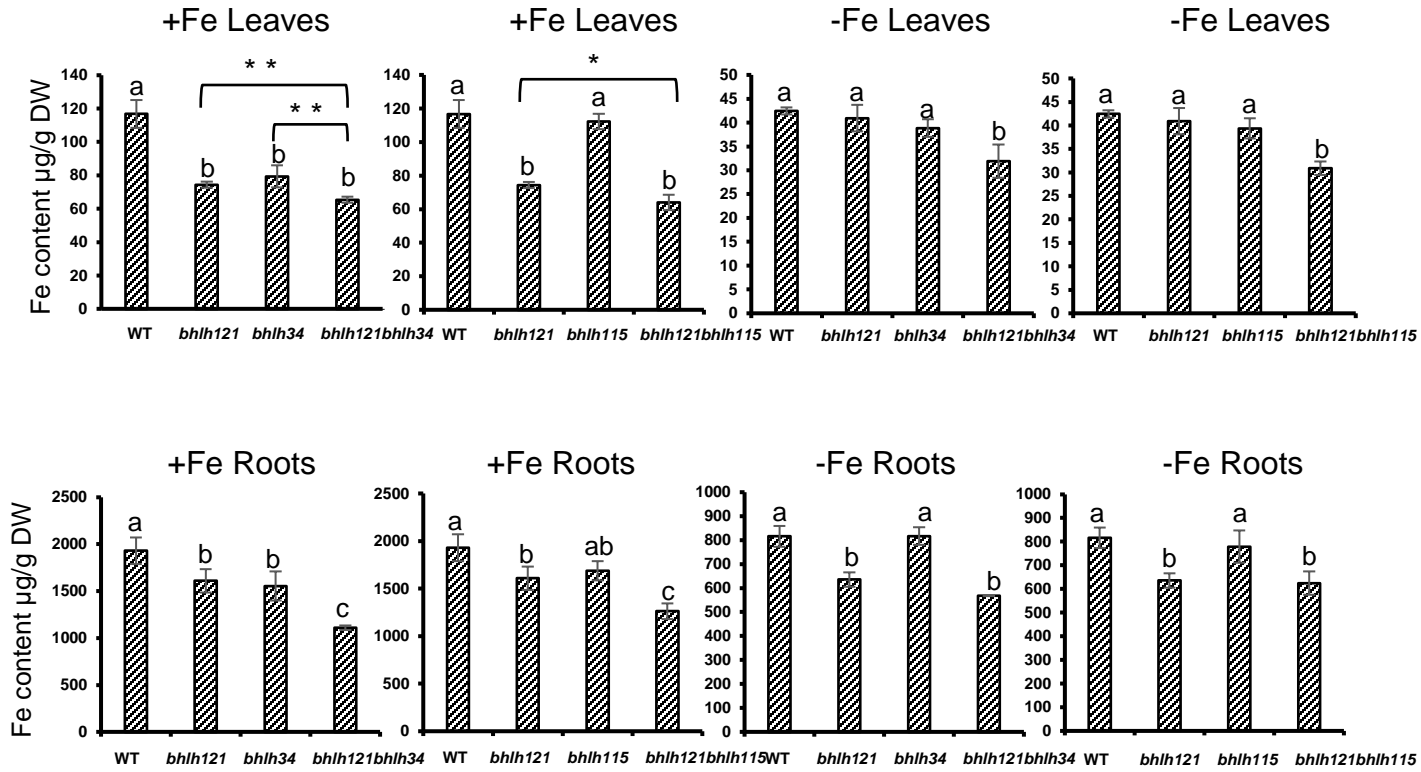


**Figure 2. Iron contents in the leaves and roots in wild type and mutants .**

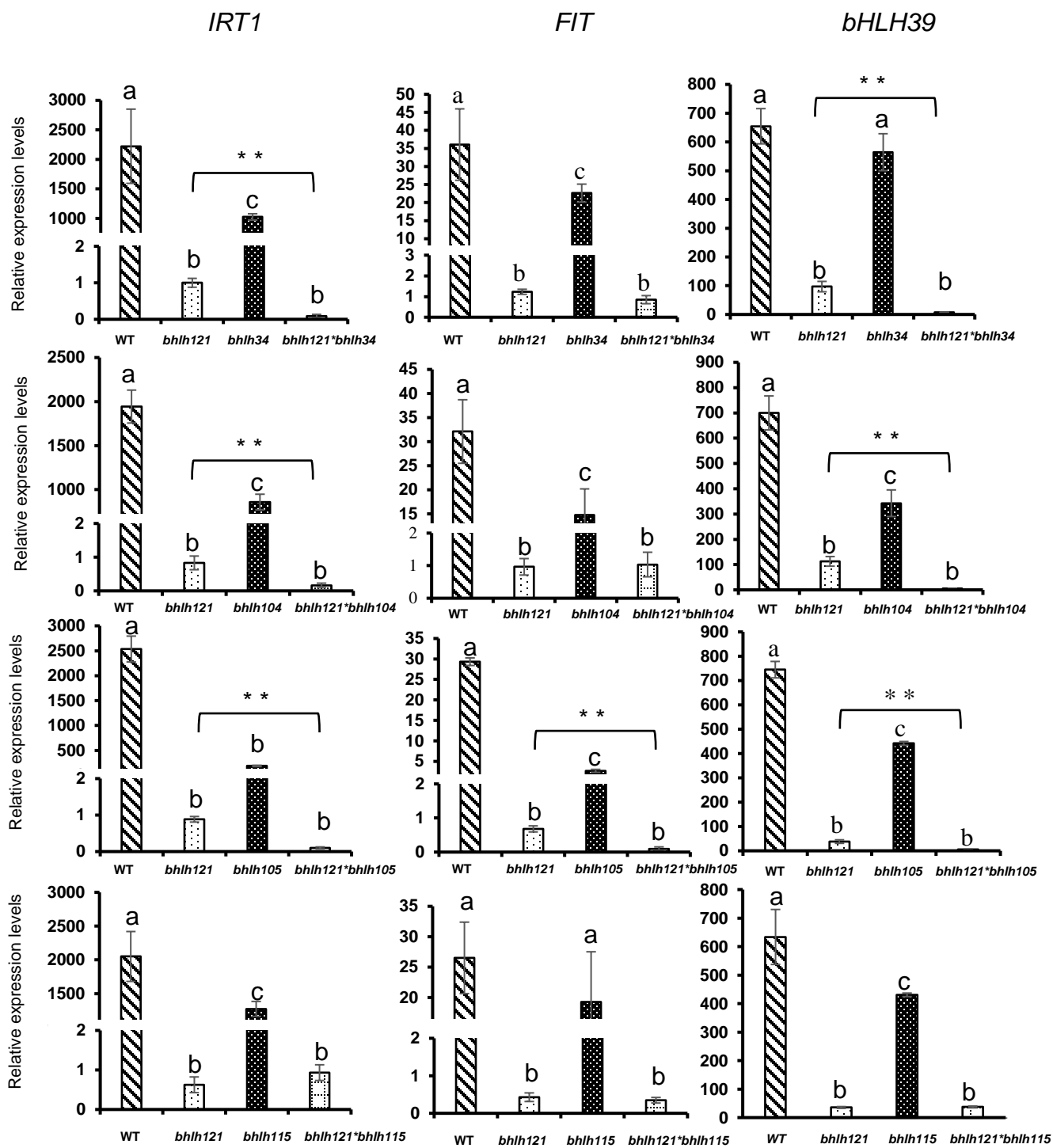
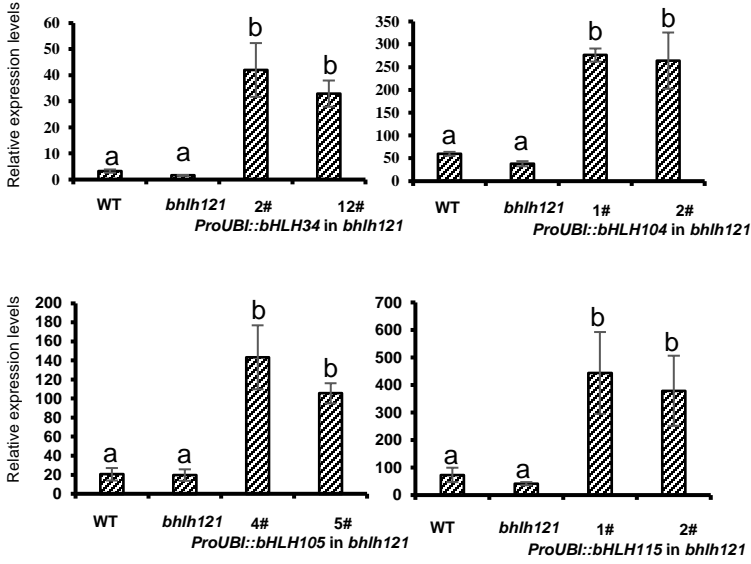
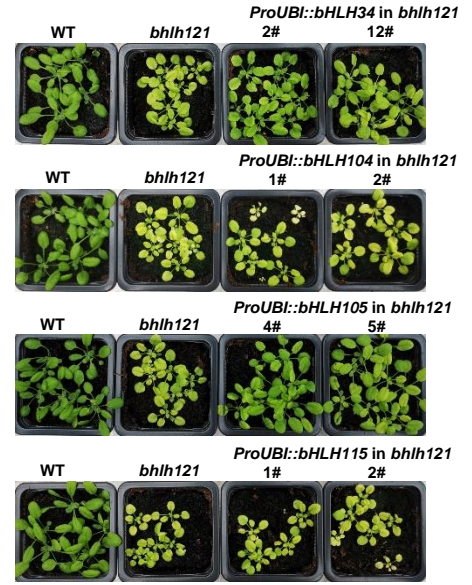


**Figure 3. Expression of Fe-deficiency-responsive genes in wild type and mutants under iron deficiency conditions.**

A



B



C

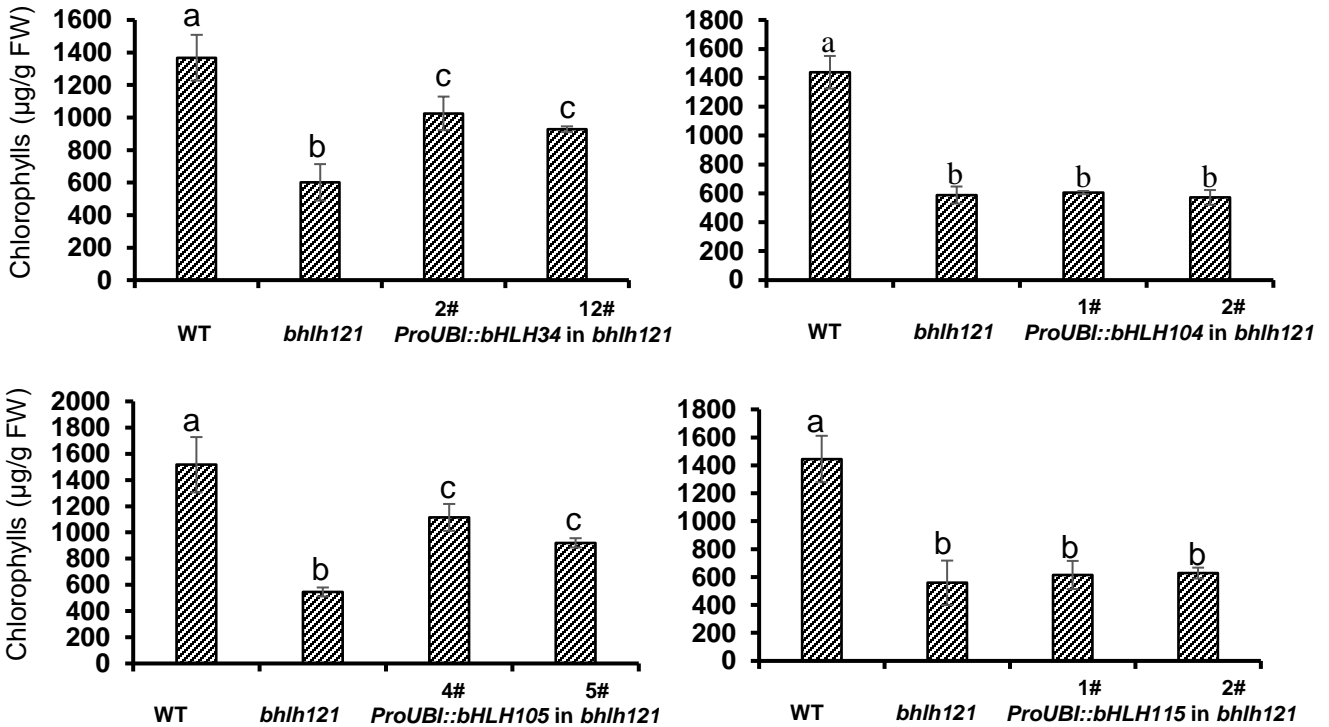


**Figure 4. Overexpression of *bHLH34* and *bHLH105* partly rescue the growth defect of *bhlh121* mutant.**



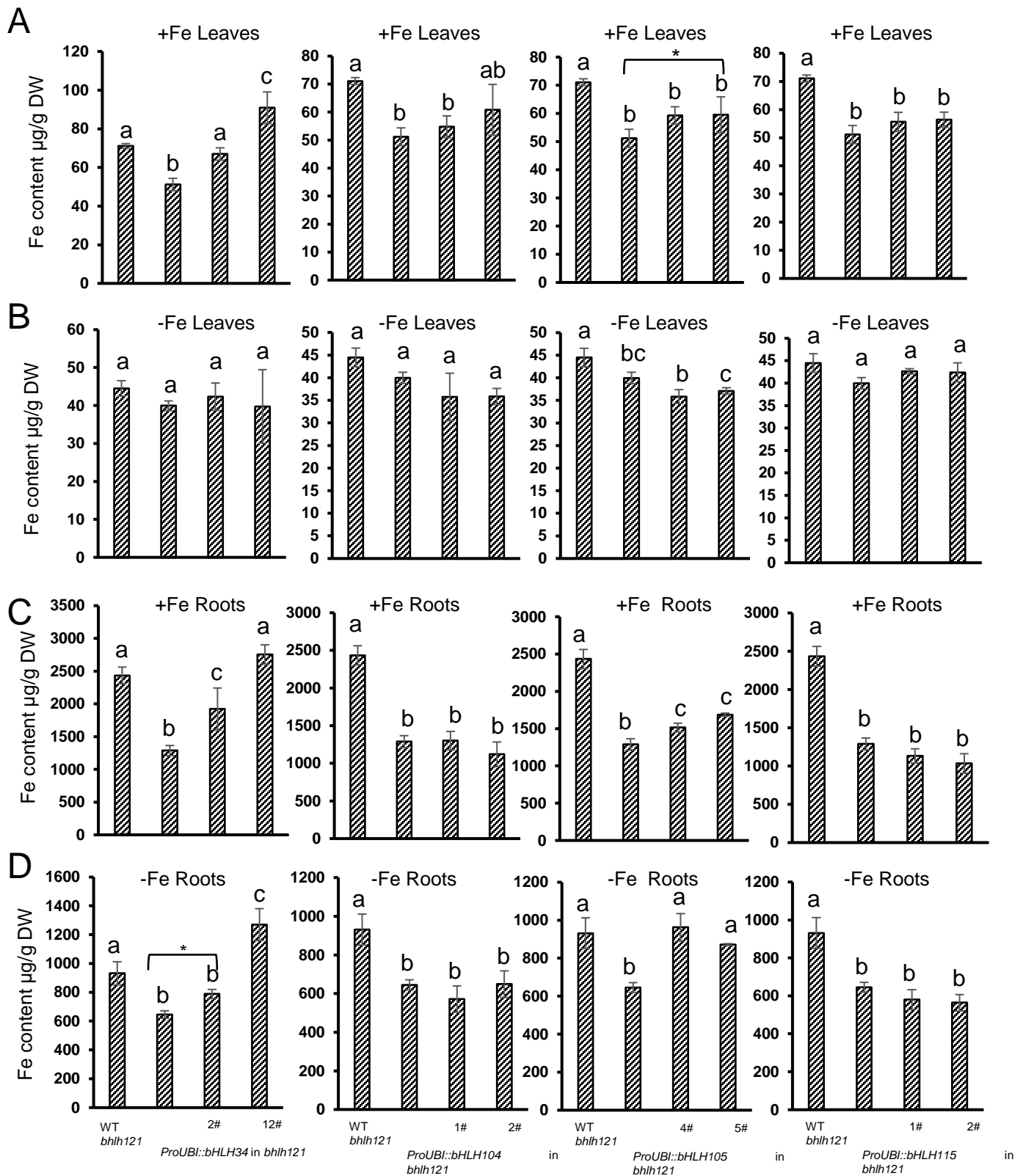


**Figure 5. Overexpression of *bHLH34* and *bHLH105* increased the iron accumulation in *bhlh121* mutant**

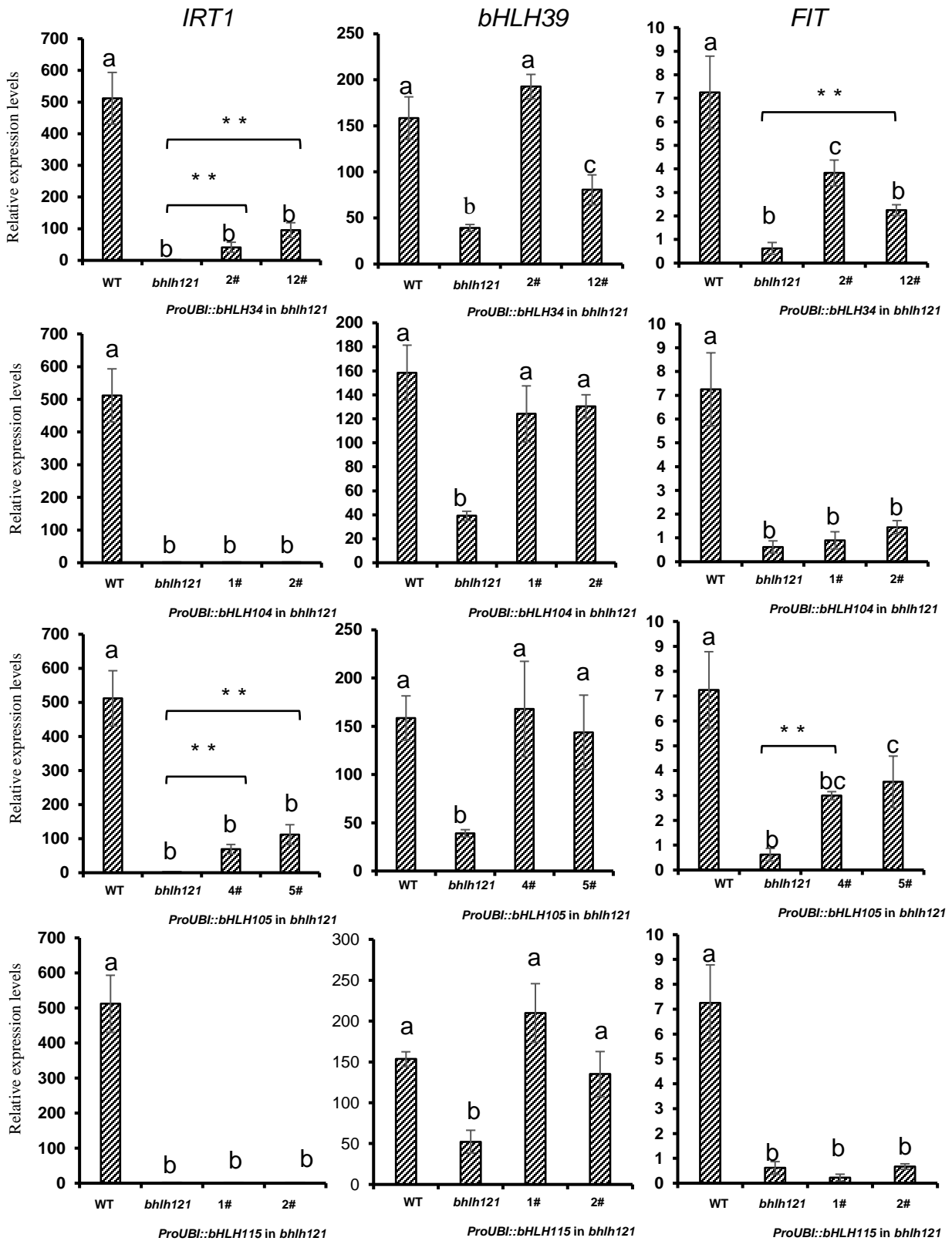


**Figure 6. Expression of Fe-deficiency-responsive genes in wild type, *bhlh121* mutant, and overexpression lines under iron deficiency conditions.**

*ProbHLH121:gbHLH121:GFP*

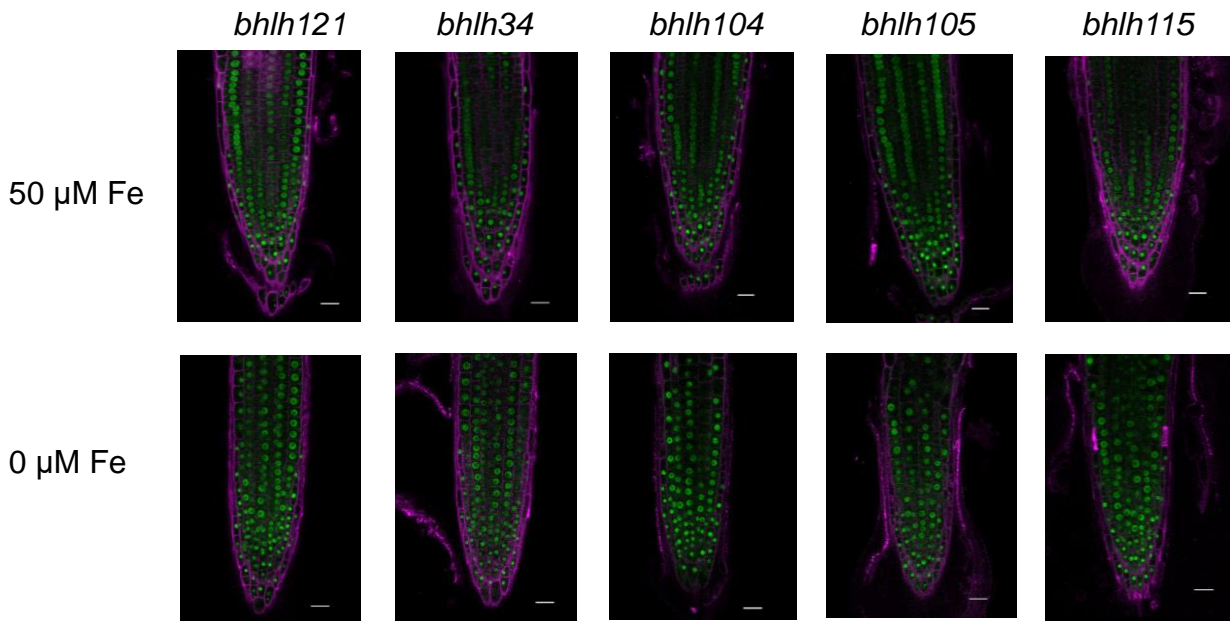


**Figure 7. bHLH121 protein localization in IVc bHLH mutant background.**

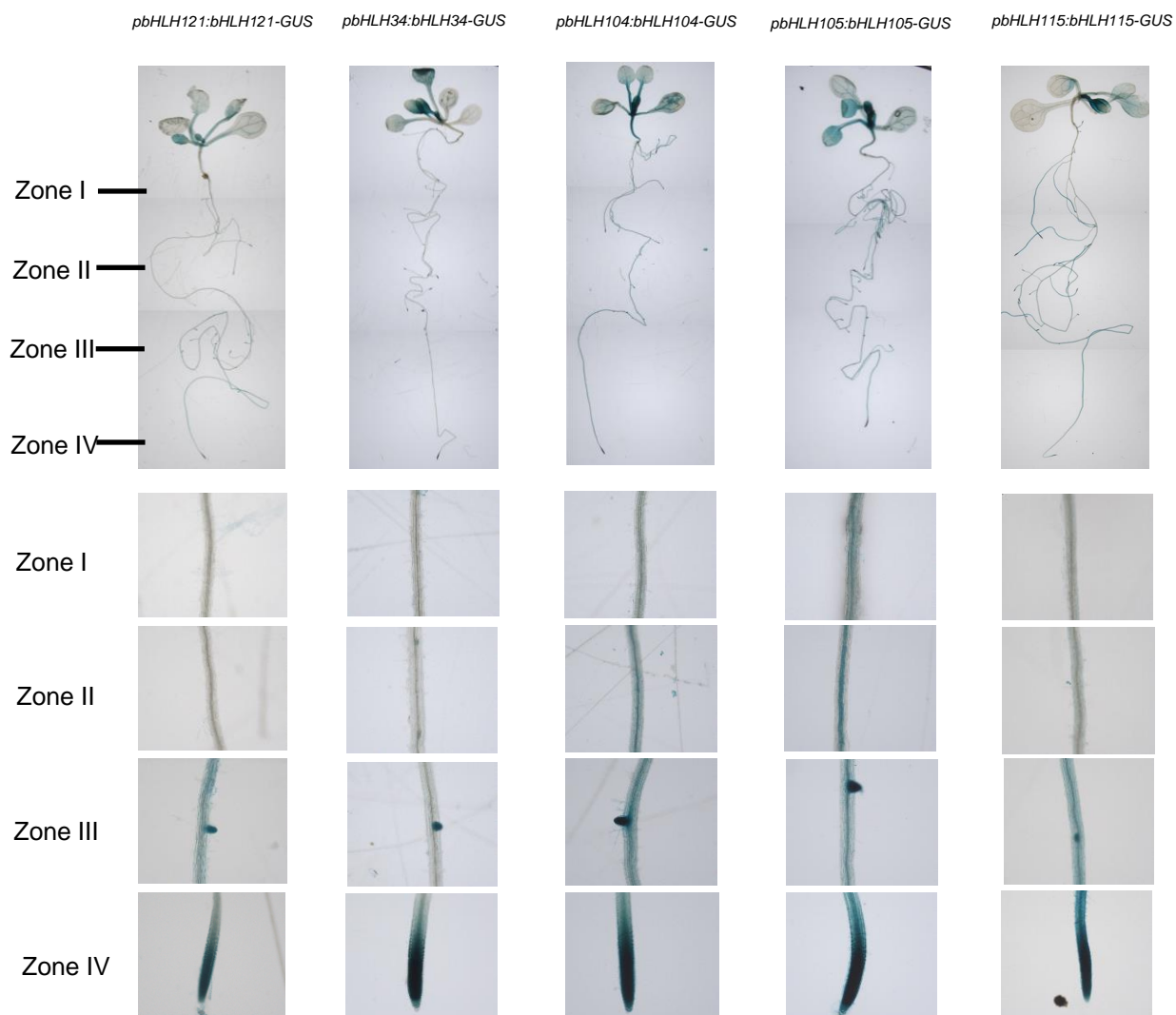


**Figure 8. GUS staining of *pbHLH121:bHLH121-GUS*, *pbHLH34:bHLH34-GUS*, *pbHLH104:bHLH104-GUS*, *pbHLH105:bHLH105-GUS* and *pbHLH115:bHLH115-GUS* transgenic plants.**

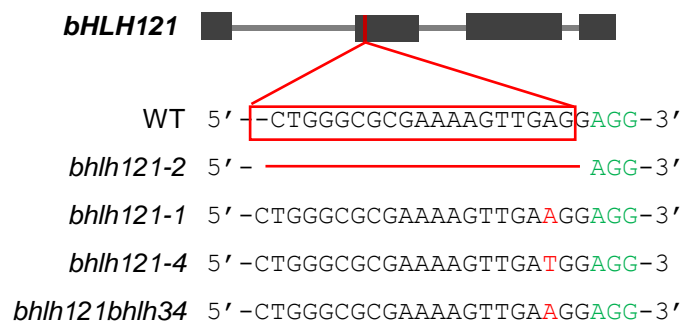


**Figure S1. Generation of *bhlh121bhlh34* double mutant by Crisper-CAS9 system.**

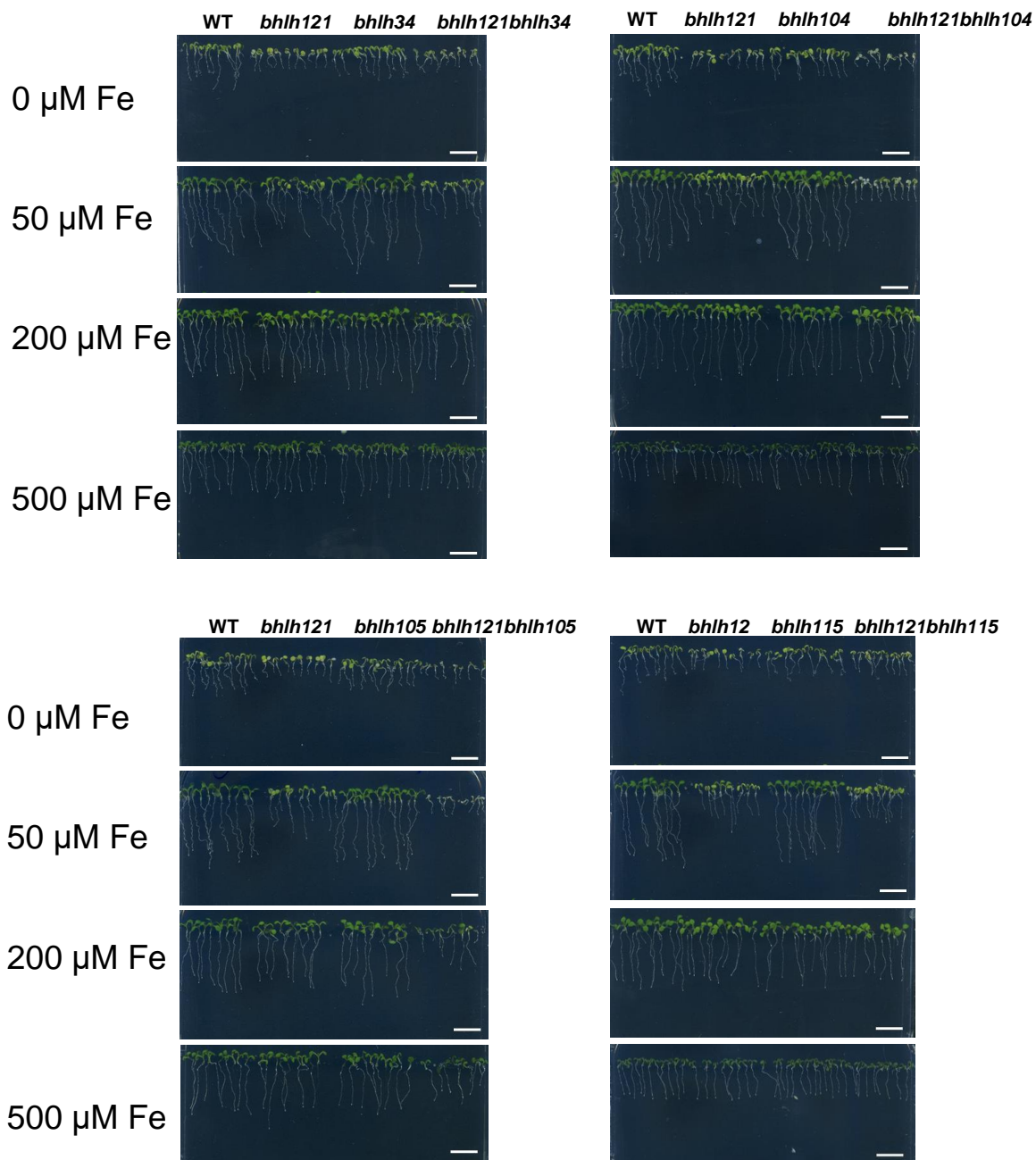


**Figure S2. Phenotypes of wild type (WT), *bhlh121*, *bhlh34*, *bhlh104*, *bhlh105*, *bhlh115* loss-of-function mutants and *bhlh121bhlh34*, *bhlh121bhlh104*, *bhlh121bhlh105*, *bhlh121bhlh115* double mutants.**

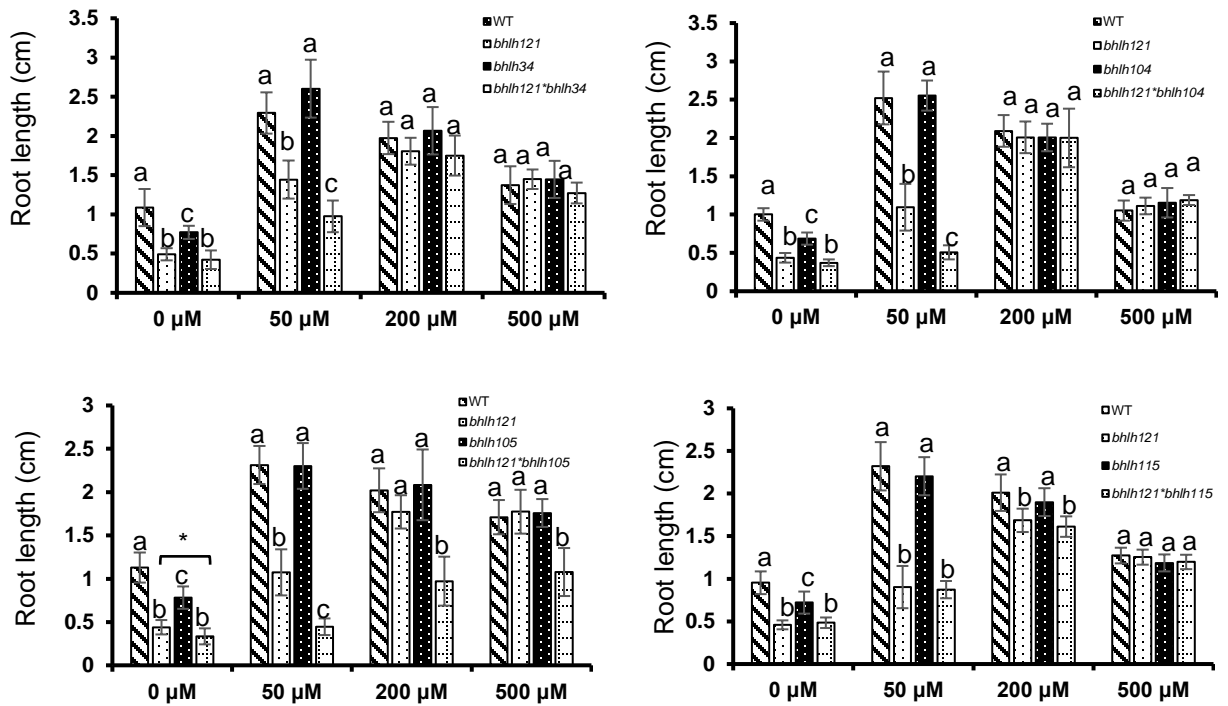


**Figure S3. Root length of wild type (WT), *bhlh121*, *bhlh34*, *bhlh104*, *bhlh105*, *bhlh115* loss-of-function mutants and *bhlh121bhlh34*, *bhlh121bhlh104*, *bhlh121bhlh105*, *bhlh121bhlh115* double mutants.**

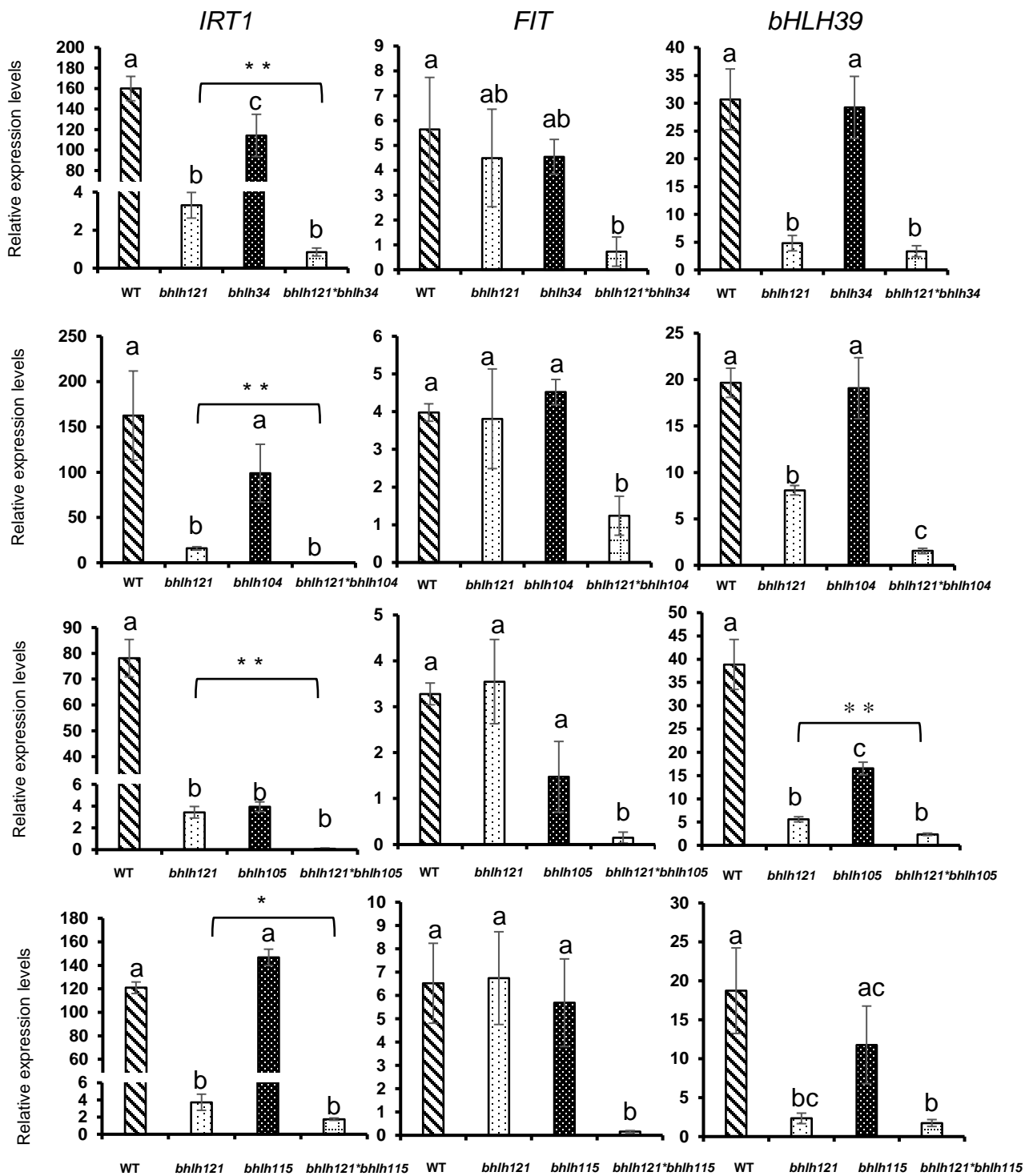


**Figure S4. Expression of Fe-deficiency-responsive genes in wild type and mutants under iron sufficient conditions**



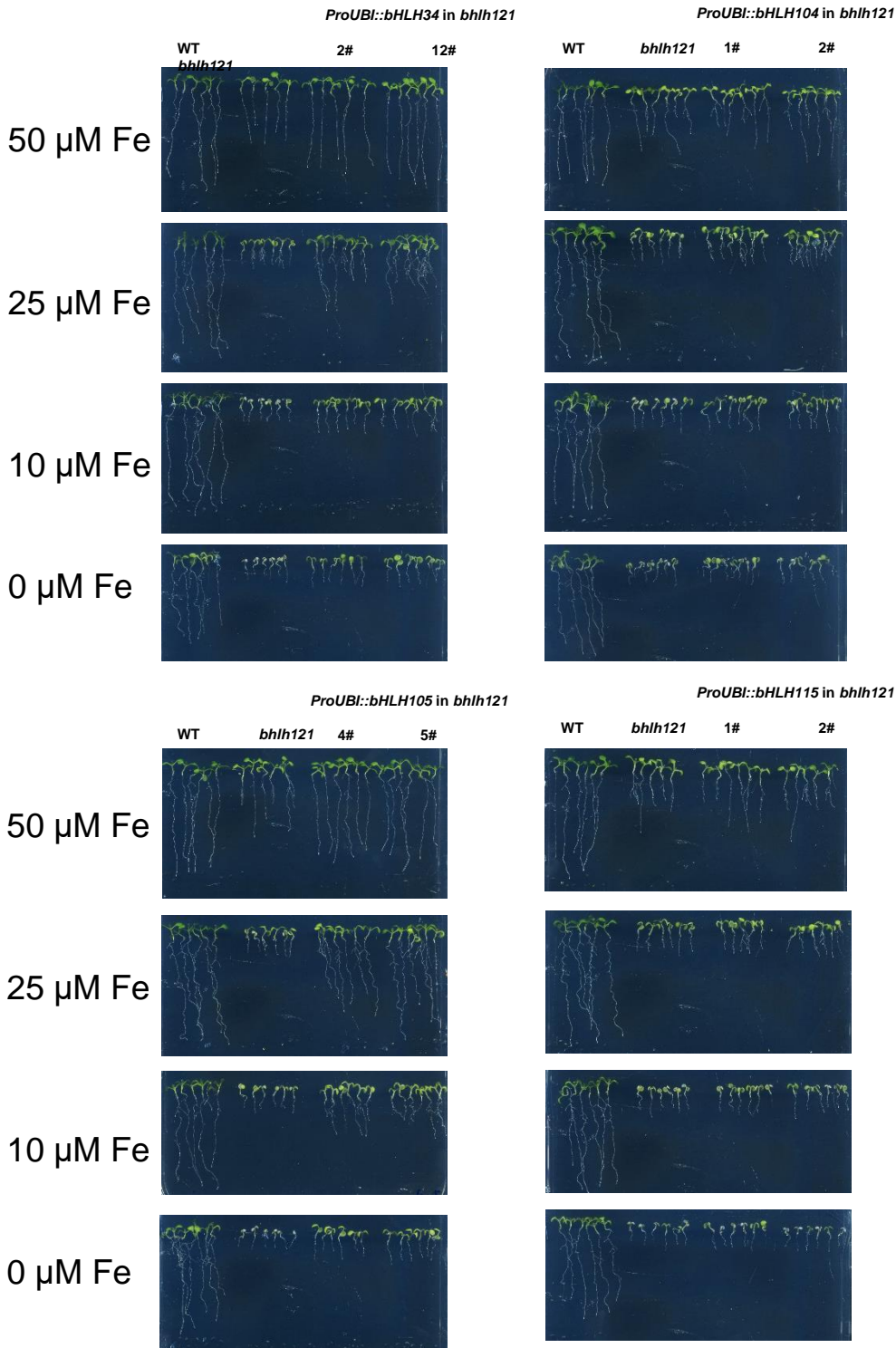


Figure S5. Overexpression of *bHLH34* and *bHLH105* partly rescue the growth defect of *bhlh121* mutant.

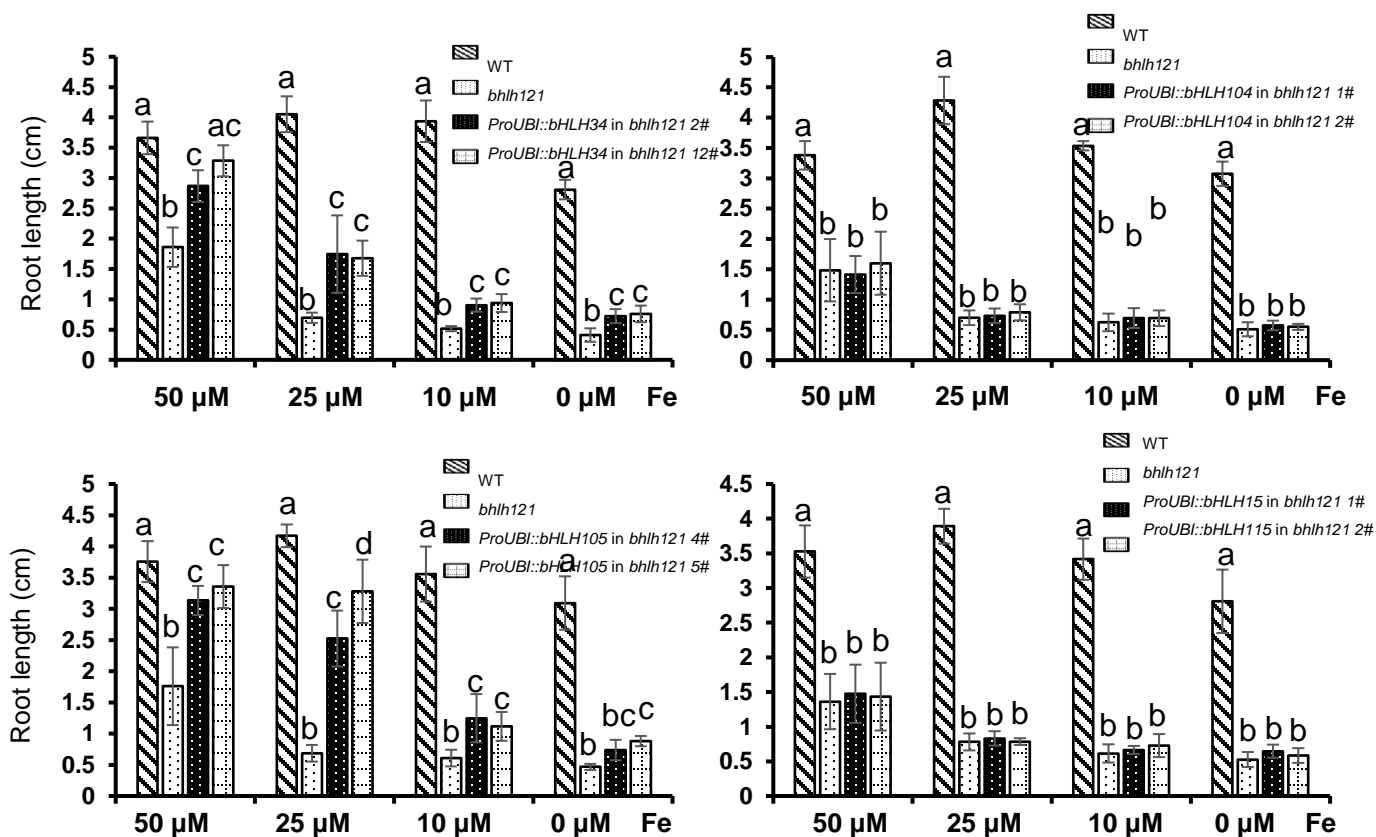
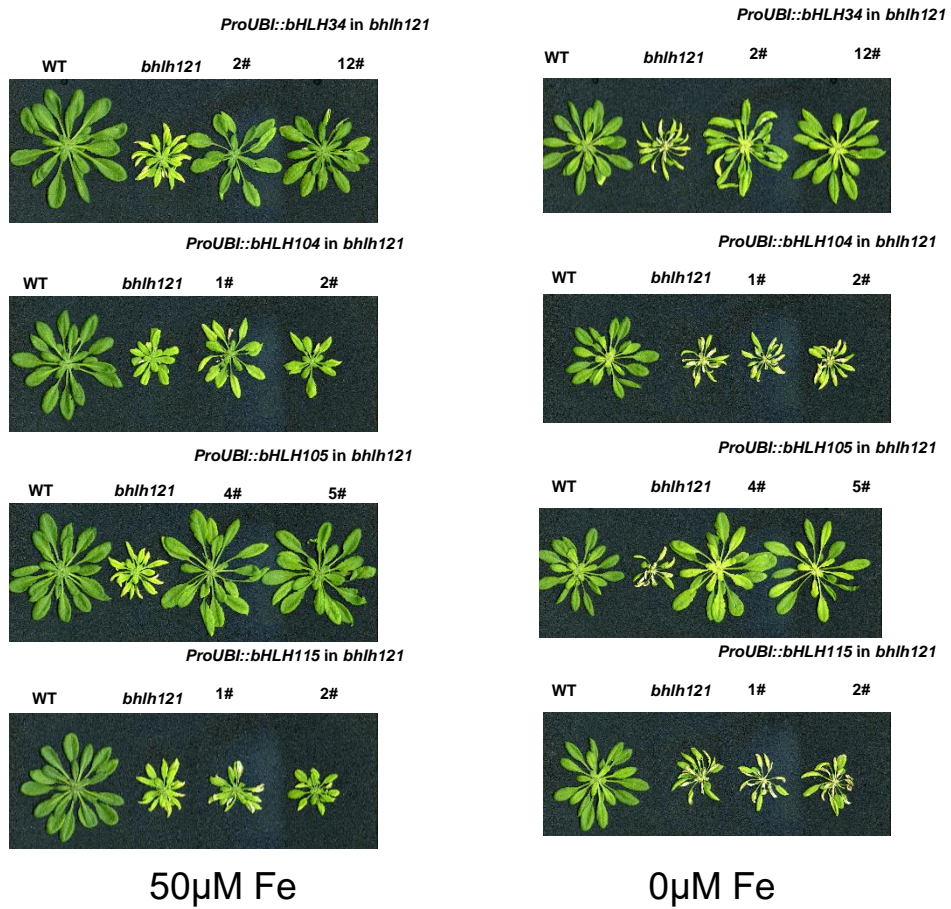


Figure S6. Root length of wild type (WT), *bhlh121* and overexpression lines.



**Figure S7. Phenotype of the wild type (WT), *bhlh121*, and overexpression transgenic plants under hydroponic conditions.**

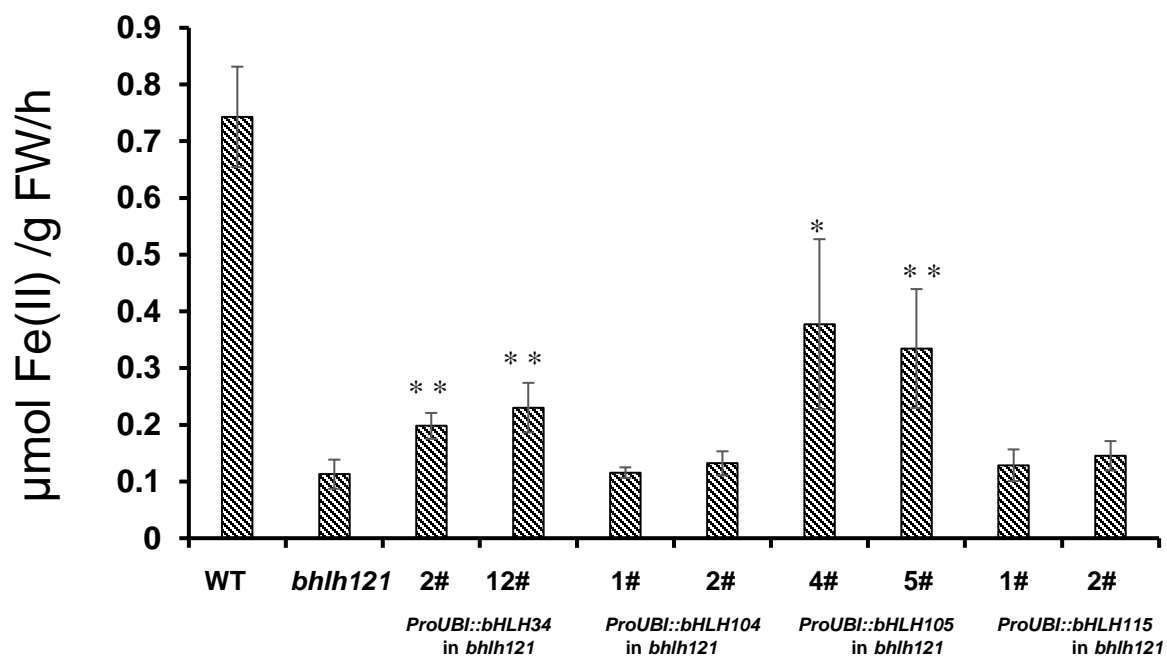
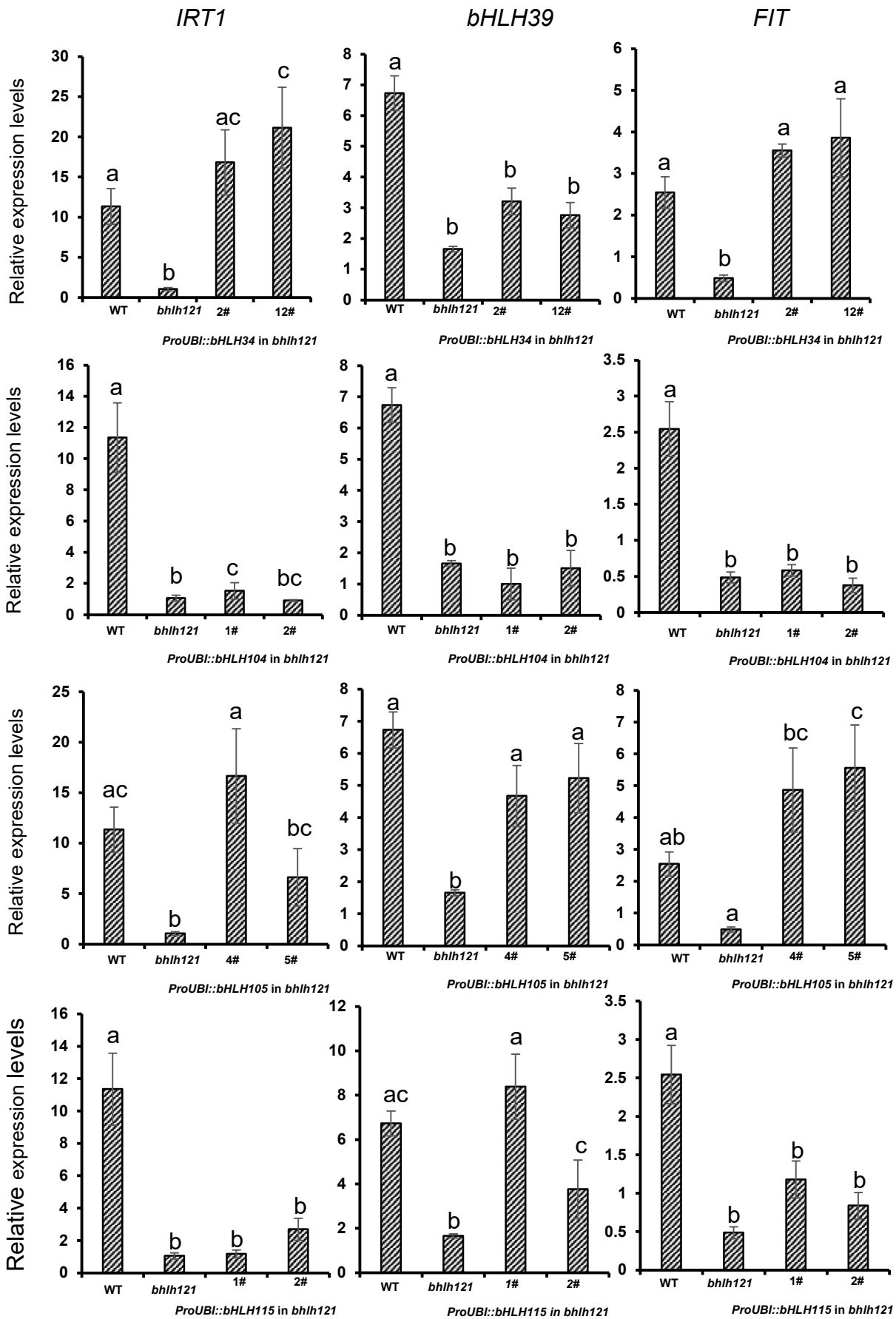


Figure S8. Ferric-chelate reductase activity of the wild type (WT), *bhlh121* and overexpression lines.



**Figure S9. Expression of Fe-deficiency-responsive genes in wild type, *bhlh121* mutant, and overexpression lines under iron sufficient conditions .**

Relative expression was determined by RT-qPCR in 6-day-old seedlings Arabidopsis seedlings grown on Fe-deficient MS/2 medium. Means within each condition with the same letter are not significantly different according to one-way ANOVA followed by post hoc Tukey test,  $p < 0.05$  ( $n = 3$  technical repeats). Error bars show  $\pm$ SD. Asterisks indicate significant differences between two samples (two-sample Student's t-test, \*  $P < 0.01$ ).

# **CHAPTER V**

## **MATERIALS AND METHODS**



## 5. Materials and Methods

### 5.1 Plant materials

*Arabidopsis thaliana* ecotype Columbia (Col-0) was used as the wild type in this study. All the mutant and transgenic plants are in the Col-0 genetic background. The *ilr3-1* seeds were kindly provided by Prof. Bonnie Bartel (Rice University, Houston, Texas, USA). The *fer1,3,4* triple mutant was generated in our group (Ravet *et al.*, 2009). Other T-DNA insertion mutants were ordered from the Nottingham Arabidopsis Stock Centre (NASC, <http://arabidopsis.info/>), and were confirmed by PCR with T-DNA and gene-specific primers (Annexes, Table 7). All the mutants used in this study are listed Table 8 (Annexes).

### 5.2 Plant growth conditions

#### 5.2.1 Greenhouse conditions

For seed amplifications, plant transformations and crosses, plants were grown in soil under long day conditions (16h light at 22°C / 8h dark at 19°C). For seed amplifications and crosses, plants were grown in 7×7 cm individual pots. For plant transformations, about 30 seeds were directly sown on 13×18 cm pots.

#### 5.2.2 *In vitro* cultures

Seeds were surface-sterilized using a bleach solution (12.5 % bleach and 50% ethanol) for 3 to 5 min, and rinsed 3 times with 96% ethanol. Once the seeds were dry, they were sowed on 1/2 MS medium (half-strength Murashige and Skoog) containing 0.05% (w/v) MES, 1% (w/v) sucrose, and 0.7% (w/v) agar in 12×12 cm square petri dishes. Fe was provided as Fe(III)-EDTA, and the concentration was 0 μM (deficiency), 10 μM, 25 μM, 50 μM (control), 200 μM (mild excess) or 500 μM (excess). Seedlings were germinated and grown under long-day conditions (16h light / 8h dark cycle; light intensity: 120 μmol/cm<sup>2</sup>/s). For RNA extraction and phenotypic analyses, seedlings were grown under the different iron conditions for 7 days. For ChIP-qPCR experiments, 7-day-old seedlings grown under control conditions were exposed to Fe deficiency for 3 days before analysis. For the GUS experiments, 7-day-old seedlings grown



under control conditions were exposed to Fe deficiency for 5 days or Fe excess for 1 day.

### 5.2.3 Hydroponic cultures

Seeds were germinated on Hoagland medium contains 0.7% agar in 0.2 ml PCR tubes under short day conditions (8h light at 22°C /16h dark at 20°C; light intensity: 120  $\mu\text{mol}/\text{cm}^2/\text{s}$ ) for 7 days. The bottom of the tubes was removed to allow root growth outside of the tubes. Fe was provided as Fe(III)-EDTA and the concentration was 0  $\mu\text{M}$  (deficiency), 50  $\mu\text{M}$  (control), or 500  $\mu\text{M}$  (excess) as described previously (Fourcroy *et al.*, 2016). Plants were transferred to liquid Hoagland medium containing 50  $\mu\text{M}$  Fe for 3 weeks. For Fe deficiency treatment, the roots of 4-week-old plants were rinsed 3 times with Milli-Q water (to remove the Fe adsorbed at the root surface) prior to their transfer to Hoagland medium deprived of Fe for 4 to 14 days depending on the experimental design.

## 5.3 Bacterial strains

### 5.3.1 DH5 $\alpha$

Genotype: F<sup>-</sup> *endA1 glnV44 thi-1 recA1 relA1 gyrA96 deoR nupG purB20  $\phi$ 80dlacZ $\Delta$ M15  $\Delta$ (lacZYA-argF)U169, hsdR17(rK<sup>-</sup>mK<sup>+</sup>),  $\lambda$ <sup>-</sup> (Hanahan 1985). The DH5 $\alpha$  is a versatile strain used for general cloning and sub-cloning applications.*

### 5.3.2 DB3.1

Genotype: F<sup>-</sup> *gyrA462 endA1 glnV44  $\Delta$ (sr1-recA) mcrB mrr hsdS20(rB<sup>-</sup>, mB<sup>-</sup>) ara14 galK2 lacY1 proA2 rpsL20(Sm<sup>r</sup>) xyl5  $\Delta$ leu mtl1*. DB3.1 is a HB101 derivative strain containing the *gyrA462* allele that confers this strain resistant to the toxic effects of the *ccdB* gene. This kind of bacteria are commonly used for propagating empty Gateway entry and destination vectors containing the *ccdB* gene on their recombination cassette.

### 5.3.3 GV3101::pMP90

GV3101::pMP90 (*Agrobacterium tumefaciens*) is described by (Koncz and Schell, 1986). The GV3101 strain has a C58 chromosomal background with rifampicin resistance and the Ti

plasmid pMP90 (pTiC58DT-DNA) with gentamicin resistance. This strain is widely used for *Agrobacterium*-mediated transformation in several dicots including *Arabidopsis thaliana* and *Nicotiana benthamiana*.

## 5.4 Yeast strains

### 5.4.1 AH109

Genotype: *MATa*, *trp1-901*, *leu2-3, 112*, *ura3-52*, *his3-200*, *gal4Δ*, *gal80Δ*, *LYS2::GAL1<sub>UAS</sub>-GAL1<sub>TATA</sub>-HIS3*, *GAL2<sub>UAS</sub>-GAL2<sub>TATA</sub>-ADE2*, *URA3::MEL1<sub>UAS</sub>-MEL1<sub>TATA</sub>-lacZ*. This strain is used to study protein-protein interactions by the yeast two hybrid method.

## 5.5 Vectors

### 5.5.1 pDNOR207

This 5585 bp entry vector was designed to generate attL flanked entry clones containing the gene of interest following recombination with an attB PCR product. It contains the attP1 and attP2 recombination cassette with the chloramphenicol resistance and *ccdB* genes. *ccdB* is a lethal gene that targets DNA gyrase in of *E. coli*, which is used as negative selection in the Gateway system (Figure 5-1).

### 5.5.2 pUBC-eGFP Dest

This binary destination vector contains the attR1/attR2 recombination cassette in the pBR322 backbone plasmid, and contains the spectinomycin and chloramphenicol resistance genes to make selections in *E. coli*. The T-DNA carries the gene phosphinothricin-N-acetyltransferase that confers resistance to the herbicide Basta that is used to verify the integration in plants. The expression cassette is under the control of the *Arabidopsis UBIQUITIN-10* promoter (At4g05320; 634bp). This binary destination vector is used for overexpression of interest genes in plants (Grefen *et al.*, 2010). (Figure 5-2).

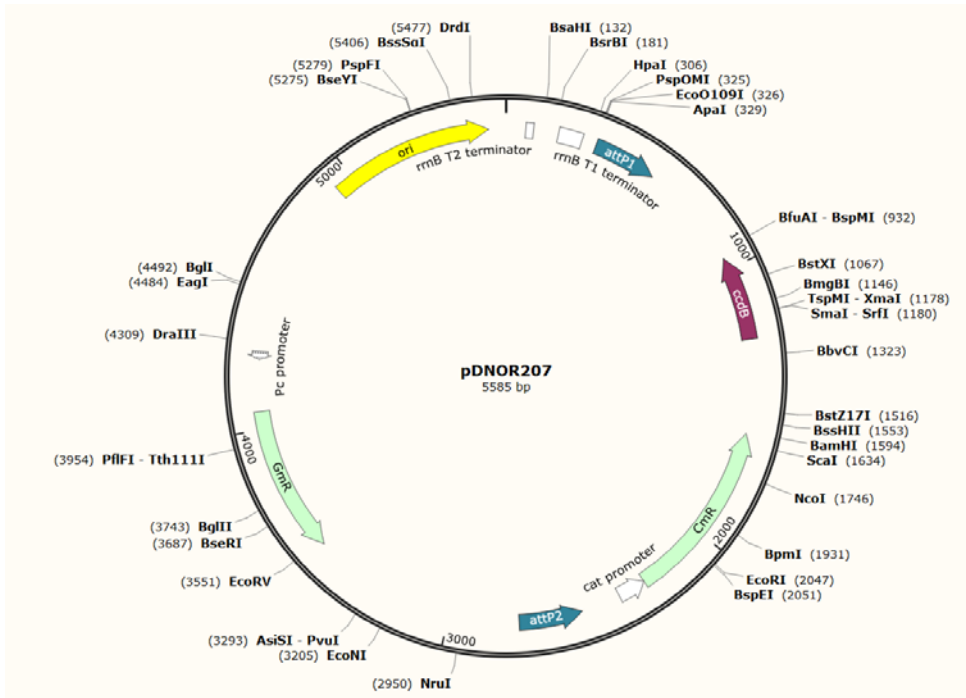


**Figure 5-1. Map of pDNOR207 vector**

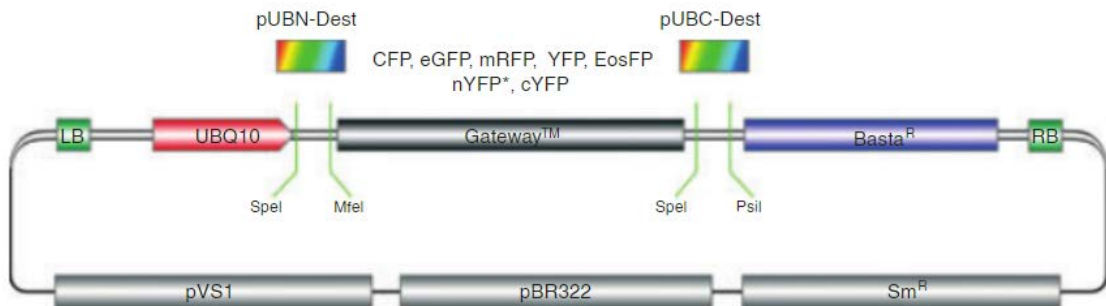


**Figure 5-2. Map of pUBC-Dest vector series**

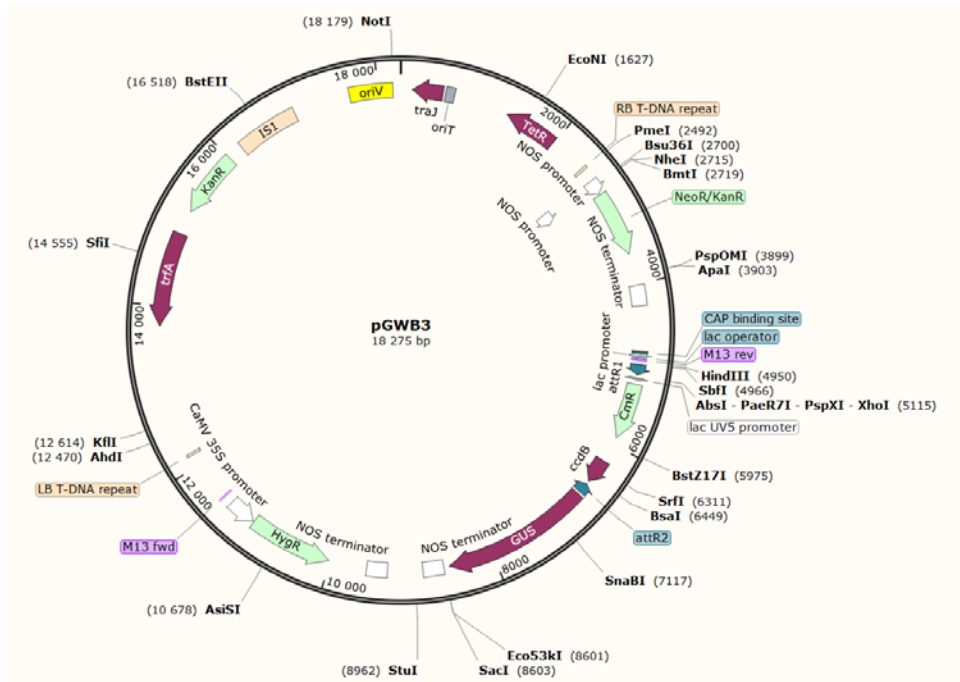


Figure 5-3. Map of pGWB3 destination vector

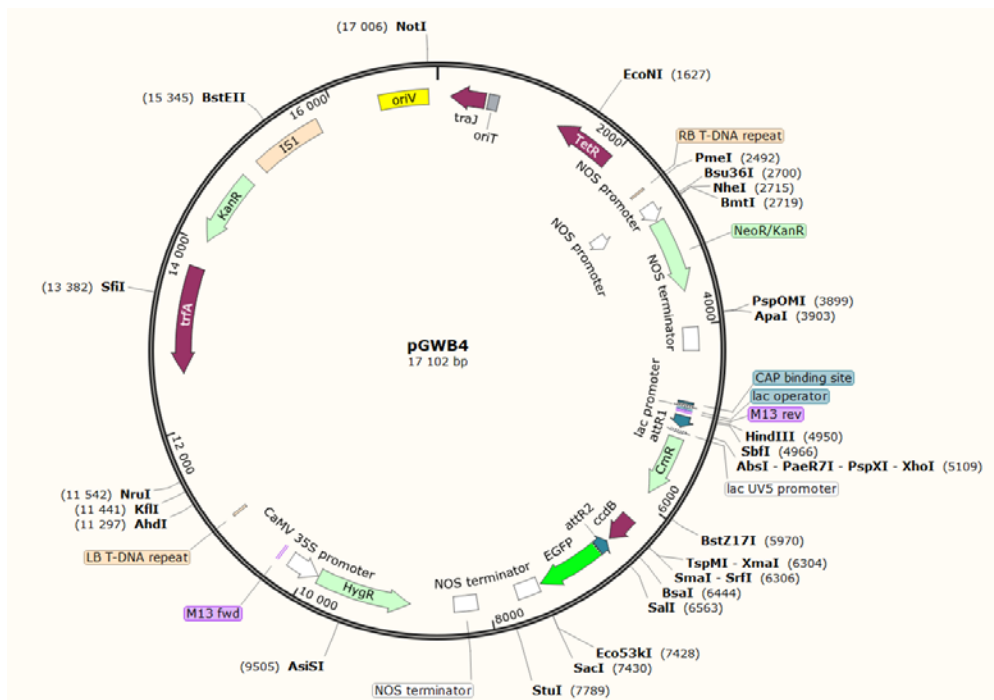


Figure 5-4. Map of pGWB4 destination vector

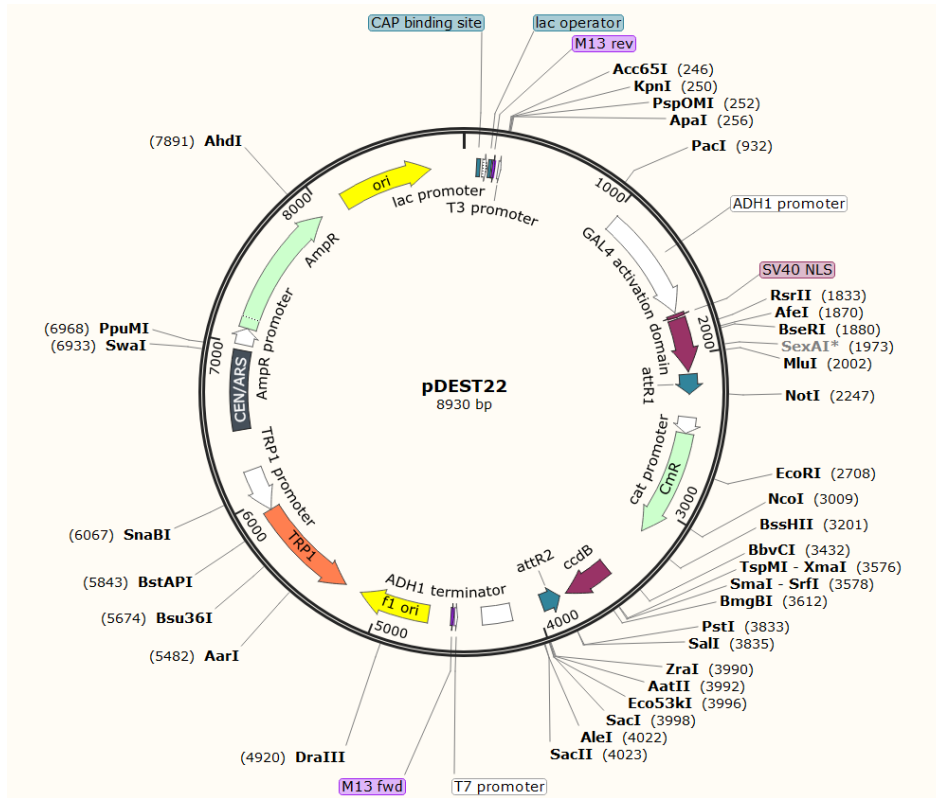


Figure 5-5. Map of pDEST22 destination vector

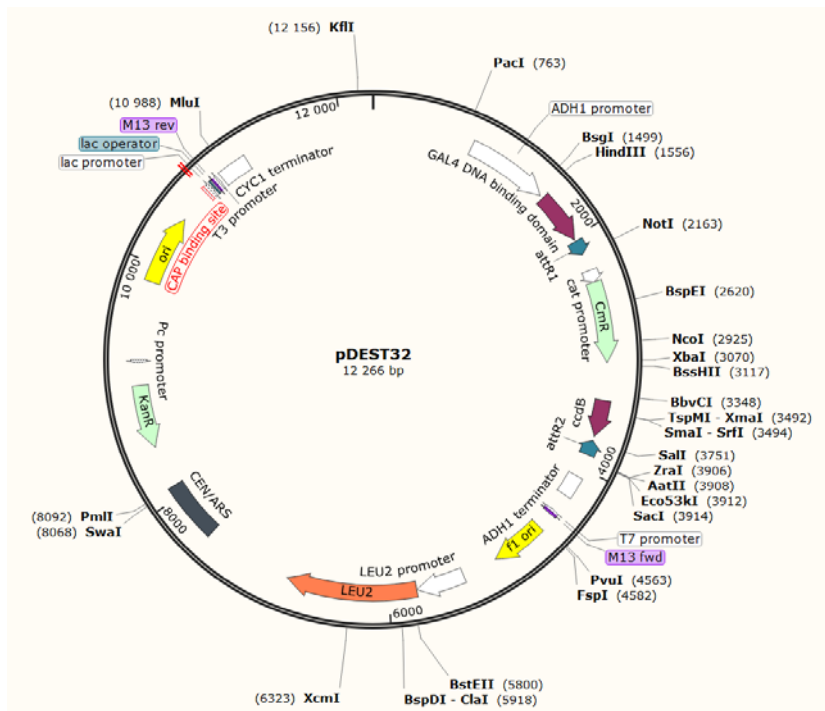


Figure 5-6. Map of pDEST32 destination vector

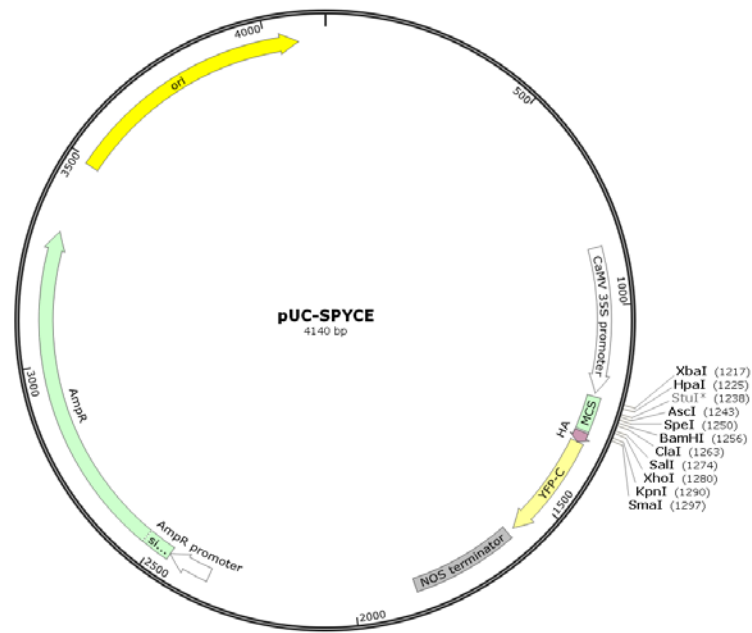


Figure 5-7. Map of pUC-SPYCE vector

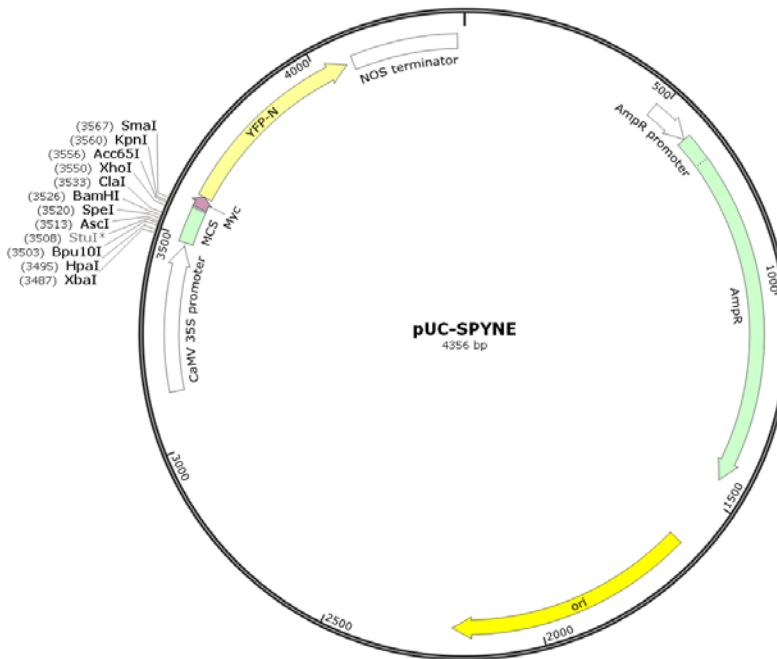


Figure 5-8. Map of pUC-SPYNE vector

### **5.5.3 pGWB3**

This 18275 bp binary destination vector contains the attR1/attR2 recombination cassette, used for C-terminal translational fusions with GUS (*uidA* reporter gene), contains the kanamycin and chloramphenicol resistance genes to make selections in *E. coli*. In planta, the integration is verified by hygromycin resistance (Nakagawa *et al.*, 2007). (Figure 5-3).

### **5.5.4 pGWB4**

This 17102 bp binary destination vector contains the attR1/attR2 recombination cassette, used for C-terminal translational fusions with eGFP (green fluorescent protein), contains the kanamycin and chloramphenicol resistance genes to make selections in *E. coli*. In planta, the integration is verified by hygromycin resistance (Nakagawa *et al.*, 2007). (Figure 5-4).

### **5.5.5 pDEST22**

This 8930 bp yeast expression vector contains the attR1/attR2 recombination cassette, used for generation of GAL4 Activation Domain fusion proteins (Invitrogen, Carlsbad, California). It contains the ampicillin resistance gene to make selections in *E. coli*, and contains the *TRP1* gene for selection in yeast on medium lacking tryptophan. (Figure 5-5).

### **5.5.6 pDEST32**

This 12266 bp yeast expression vector contains the attR1/attR2 recombination cassette, used for generation of GAL4 Binding Domain fusion proteins (Invitrogen, Carlsbad, California). It contains the kanamycin resistance genes to make selections in *E. coli* and the *LEU2* gene for selection in yeast on medium lacking leucine. (Figure 5-6).

### **5.5.7 pUC-SPYCE and pUC-SPYNE**

pUC-SPYCE and pUC-SPYNE are two pUC backbone based high copy plasmid vectors, encode the C-terminal and N-terminal regions of YFP (yellow fluorescent protein), respectively, under the control of the 35S promoter. They contain the same polylinker for cloning. They are used for Bimolecular Fluorescence Complementation (BiFC) experiments to check protein-

protein interactions in living plant cells (Walter *et al.*, 2004). (Figure 5-7, 5-8).

## 5.6 Arabidopsis transformation

*Agrobacterium tumefaciens* (GV3101::pMP90) mediated Floral-dip method was used for Arabidopsis stable transformation in this study (Clough and Bent, 1998; Zhang *et al.*, 2006). Briefly, an isolated agrobacterium colony is pre-cultured in 5 ml of LB liquid medium with the appropriate antibiotics (rifampicin, gentamicin and the antibiotic whose resistance is conferred by the binary vector) at 30°C for 24 hour with shaking (160 rpm). 1 ml of this pre-culture is mixed with 49 ml of liquid LB medium with antibiotics and cultured under the same conditions. When the OD<sub>600</sub> reach 0.8 (around 12 to 16 hours), the culture is centrifuged (5000 rpm, 5 min) to spin down the agrobacterium. The pellet is then resuspended to reach an OD<sub>600</sub> = 0.8 in freshly made liquid 1/2 MS medium containing 5% (w/v) sucrose and 0.05 MES (w/v) (pH 5.7). Before dipping, Silwet L-77 is added to a concentration of 0.03% (300 µl/l) and well mixed. To carry out the transformation, the inflorescences are dipped into the agrobacterium solution for 30 to 60 seconds with gentle agitation. The dipped plants are then placed under a dome or cover with plastic bags for 24 hours to maintain high humidity. To obtain good transformation efficiencies, fairly young Arabidopsis plants with many immature flower clusters and not many fertilized siliques should be used. Plants might be dipped two or three times with seven days' intervals. Once the siliques are dry, seeds are harvested and sown on selective 1/2 MS medium agar plates containing the antibiotic to which the transformed plants are resistant (i.e. hygromycin, basta).

## 5.7 Arabidopsis crossing

For most efficient crossings, it is better to sow the father plants 7 days earlier than mother plants in the greenhouse. When the mother plants have 5 to 6 inflorescences, and the father plants have formed siliques, this indicates the ovules and the pollen are fine. For the mother plants, remove mature siliques, open flowers, the buds with a white tip, as well as the meristem using fine forceps. Normally, 2 to 3 flower buds in each inflorescence have the right size and should be kept for crossing. Open the flower bud with fine forceps, remove all the petals, sepals and



immature anthers. Take an open, mature flower from the father plant with forceps. Tap the anther on the stigma and cover it with pollen grains as much as possible. Repeat by using a second male flower if necessary.

<b>Table 5-1. The typical PCR programs used in this study</b>				
	GoTaq® G2 DNA Polymerase		Phusion High-Fidelity PCR Kit	
Initial Denaturation	94 °C	3 minutes	98 °C	30 seconds
Denaturation	94 °C	30 seconds	98 °C	15 seconds
Primer Annealing	55 to 60 °C	30 seconds	55 to 60 °C	30 seconds
Extension (35-40 cycles)	72 °C	1 minute/kb	72 °C	30 seconds/kb
Final Extension	72 °C	7 minutes	72 °C	7 minutes
Hold	Room temperature			

### **5.8 Extraction of Arabidopsis genomic DNA**

This method is aimed for the extraction of DNA that is used as PCR template for genotyping and genomic amplification. Place the leaf sample in 1.5 ml eppendorf tube and smash it with a 1000 µl tip against the tube wall. Add 250 µl of Edward extraction buffer (200 mM Tris-HCl pH 7.5, 250 mM NaCl, 25 mM EDTA, 0.5% SDS) to the tube, mixed with pipette (Edwards *et al.*, 1991). Centrifuge for 5 min at 12000 rpm (room temperature), transfer 200 µl of supernatant to new a 1.5 ml eppendorf tube, and add 200 µl of isopropanol. Centrifuge for 10 min at 12000 rpm (room temperature), discard the supernatant and dry the pellet. Add 30µl of Milli-Q water in the tube, store at -20 °C until use.

### **5.9 DNA amplification by Polymerase Chain Reaction (PCR)**

The typical PCR (i.e. genotyping, colony PCR) amplification is carried out by using *Taq*

polymerase (GoTaq® G2 DNA Polymerase, Promega, USA), whereas the DNA amplification for cloning is carried out by using high-fidelity DNA polymerase (Phusion High-Fidelity PCR Kit, ThermoFischer Scientific, USA). For 20 µl reaction volume, 4 µl of 5X reaction buffer, 0.4 µl of dNTP mix (10 mM), 0.5 µl of each oligonucleotide primer (10 µM), 1 µl of DNA template and 0.1 µl of polymerase. The PCR programs used in this study are in the Table 5-1. All the PCR primers used in this study are listed in the Table 3 to 5 in Annexes.

## **5.10 Plasmid construction**

Plasmid vector construction is an essential step for plant molecular biology. In this PhD thesis, several genetic constructions were carried out by using the Gateway cloning system or restriction enzyme cloning system.

### **5.10.1 Gateway cloning by recombination**

The Gateway cloning system was invented and commercialized by Invitrogen since the late 1990s. This cloning system contains two steps of recombination: i) introduce the interest attB flanked PCR product into the donor vector by BP reaction to create the attL-flanked entry clone and ii) transfer the insert into a destination vector by LR reaction to create an expression clone with all of the components necessary for gene expression (Figure 5-9).

Gateway attB1 and attB2 sequences are added to the 5', and 3' end of a gene fragment, respectively, by PCR-amplification with gene specific PCR primers containing the attB1 and attB2 sequences. The PCR fragment obtained are then cloned into pDNOR207 by BP reaction following manufacturer's instruction. Briefly, 1 µl of PCR product, 1 µl of pDNOR207 plasmid, 1 µl of BP Clonase™ II Enzyme mix (ThermoFischer Scientific, USA), and 2 µl of Milli-Q water are mixed in 200 µl PCR tubes and incubated at 25°C for 2 h to overnight (depending of the size of the DNA fragment; the longer the fragment the longer the time of incubation). Add 0.5 µl of proteinase K and incubate for 10 min at 37°C to stop the recombination reaction. Then, 2 µl of this mix is used to transform 50 µl of DH5α ultra competent cells (Inoue *et al.*, 1990). The selection of clones containing recombined plasmid is made on LB agar plates with gentamycin. The recombined plasmids are check by colony PCR and sequencing. The correct

recombined plasmids are amplified for further use.

LR reaction makes it possible to transfer the interest fragment into a destination vector (i.e. binary vectors for plant stable transformation, yeast expression vector for yeast two hybrid). 1  $\mu$ l of plasmid pDNOR207 containing the insert, 1  $\mu$ l of destination plasmid, 1  $\mu$ l of LR Clonase™ II Enzyme mix (ThermoFischer Scientific, USA), and 2  $\mu$ l of Milli-Q water are mixed and incubated. The same procedure is followed as in BP reaction except for the selection antibiotic, the gentamicin is replaced by other appropriate antibiotics (i.e. kanamycin, spectinomycin, ampicillin).

### **5.10.2 Restriction enzyme cloning**

Restriction enzyme cloning method usually refers to the use of restriction endonucleases to generate DNA fragments with specific complementary end sequences that can be joined together with a DNA ligase, prior to transformation. In this study, restriction enzyme cloning method is used to clone the cDNA of several transcription factors into the pUC-SPYCE and pUC-SPYNE vectors for Bimolecular Fluorescence Complementation (BiFC) assays. Two unique enzyme sequences are added to the 5', and 3' end of a gene fragment, by PCR-amplification. Gene specific PCR primers containing the restriction sites are used. The PCR products and the destination plasmids are digested by two unique FastDigest restriction enzymes (ThermoFischer Scientific, USA) following the manufacturer's protocol. The digested DNA is purified by using Wizard® SV Gel and PCR Clean-Up System (Promega, USA). The digested insert and vector are ligated by using the T4 DNA Ligase (Promega, USA) following the manufacturer's protocol. Then, 5  $\mu$ l of the ligation is used transform 50  $\mu$ l of DH5 $\alpha$  ultra competent cells (Inoue *et al.*, 1990). The selection of clones containing recombined plasmid is made on LB agar plates with ampicillin. The recombined plasmids are check by colony PCR and sequencing. The correct recombined plasmids are amplified for further use.

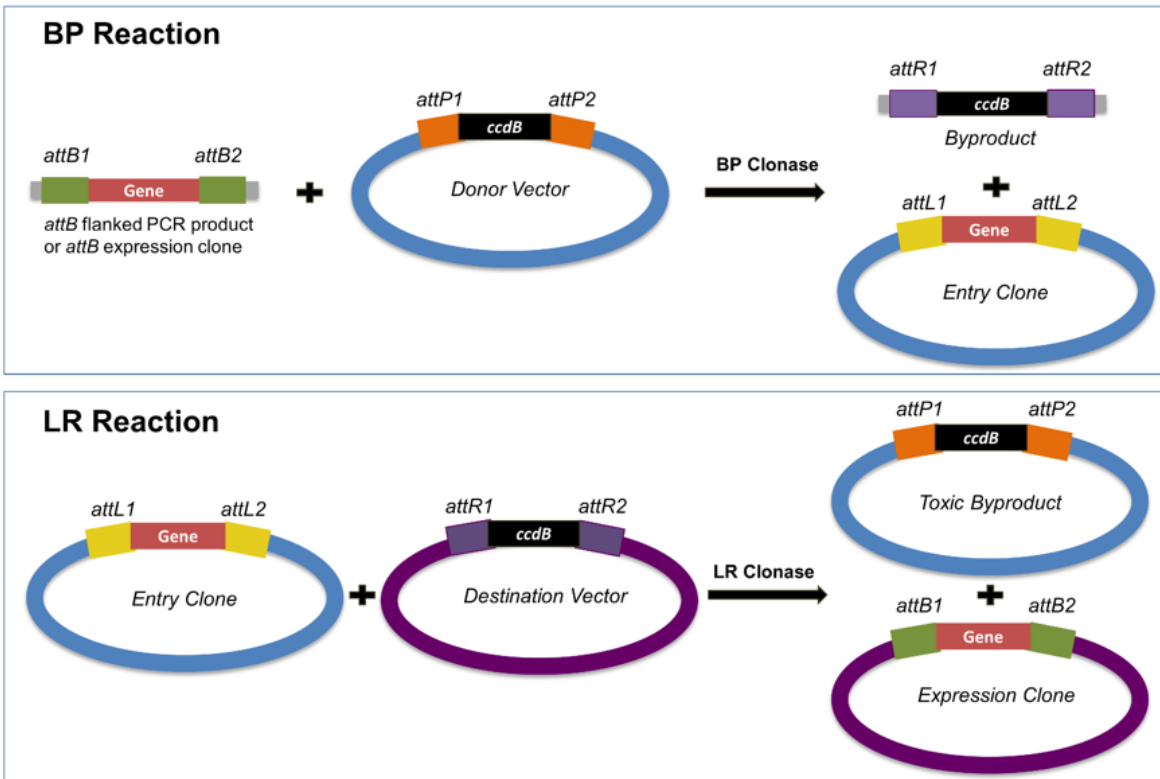


**Figure 5-9.** The Gateway methodology uses the bacteriophage lambda site-specific recombination system to insert in destination vectors DNA fragments of interest via **BP and LR reactions**. The BP reaction creates an attL-flanked entry clone. The LR reaction creates an expression clone with all of the components necessary for gene expression.

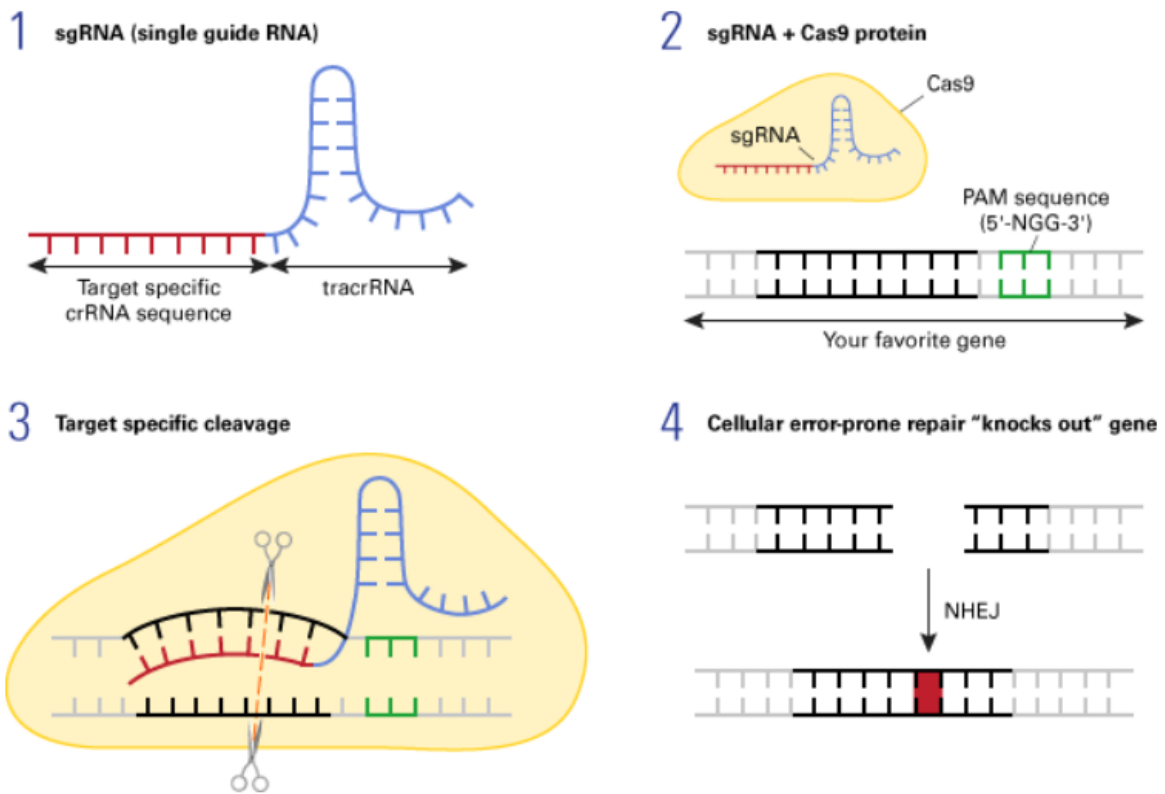


**Figure 5-10. The principle of CRISPR/Cas9 gene editing system.**

A single guide RNA (sgRNA), consisting of a crRNA sequence that is specific to the target DNA sequence and a tracrRNA that interacts with the Cas9 protein that has DNA endonuclease activity is designed (1). The Cas9 protein is directed to the genomic target sequence (2) and could cause target-specific double-strand break (3). The cleavage site will be repaired by the non-homologous end joining (NHEJ) DNA repair pathway, an error-prone process that may result in insertions/deletions (INDELs) that may disrupt gene function (4).

## **5.11 Generation of *bhlh121* mutant lines by CRISPR-Cas9 system**

CRISPR-Cas9 system is an effective tool to edit genes in plants. A single guide RNA (sgRNA), consisting of a crRNA sequence that specifically targets the DNA sequence and a tracrRNA that interacts with the Cas9 protein that has DNA endonuclease activity. The Cas9 protein is directed to the genomic target sequence and could cause target-specific double-strand break. The cleavage site will be repaired by the non-homologous end joining (NHEJ) DNA repair pathway, an error-prone process that may result in insertions/deletions (INDELs) that may disrupt gene function (Figure 5-10). In this study, this tool was used to generate the *bhlh121* mutants in the Col-0 genetic background. Two sgRNAs (sgRNA1 CTGGGCGCGAAAAGTTGAGG, sgRNA2 TCACCGGCGGGAAGAATCGA) were designed and cloned into the pRM-Cas9 binary vector prior to plant transformation (Eurofins, Luxembourg). For the design of the sgRNA, the results from four different web software were merged: CRISPRSCAN (<http://www.crisprscan.org/>), WU-Crispr (<http://crispr.wustl.edu/>), CHOP CHOP (<http://chopchop.cbu.uib.no/>), and CRISPR RGEN tool (<http://www.rgenome.net/cas-designer/>). The sgRNAs located in exons that were the most highly represented among these four databases and close to the translation initiation site (ATG) were manually selected. The number of potential off-targets of these selected sgRNAs was determined using the Cas-OFFinder tool of rgenome (<http://www.rgenome.net/cas-offfinder/>). Finally, the two sgRNAs presenting the smallest number of putative off-targets were chosen. The arabidopsis transformations were performed as described above. The mutants were identified by PCR and sequencing. Three different mutant lines without the CRISPR-Cas9 construct were chosen for further study.

## **5.12 Gene expression analysis by quantitative real time PCR**

### **5.12.1 RNA extraction**

RNA extraction was carried out by using the TRIzol method (Rio *et al.*, 2010). About 100 mg samples are frozen in liquid nitrogen and crushed using a ball mill. 800 µl of TRIzol (Invitrogen, USA) are added to the samples. After thoroughly mixing, 160 µl of chloroform are added to

each sample. After thoroughly mixing, samples are centrifuged at 16200 rpm for 10 min at 4°C. The supernatant is then transferred to a new 1.5 ml eppendorf tube. 400 µl of isopropyl alcohol are added and mixed by inversion, and then centrifuged at 16200 rpm for 10 min at 4°C. The supernatant is removed and the pellets are rinsed twice with 1 ml of 70% ethanol. Once the pellets are dried, 80 µl of autoclaved MiliQ water are added to dissolve the RNA.

### **5.12.2 Reverse-Transcription Reaction**

Before the reverse-transcription reaction, DNase (RQ1 RNase-Free DNase, Promega, USA) is used to remove the potential DNA contamination of RNA samples. 8 µl of RNA (1 µg) are mixed with 1 µl of DNase buffer and 1 µl of DNase in 200 µl PCR tubes. This mixture is incubated at 37°C for 35 min in a PCR machine. 1 µl of stop solution (25 mM EDTA) is added, and then the mixture is incubated at 65°C for 10 min to stop the reaction. The reverse-transcription reaction is carried out by using RevertAid First Strand cDNA Synthesis Kit (ThermoFischer Scientific, USA). Briefly, 1 µl of oligo(dT) is added to the RNAs after digestion with the DNase and then the mixture is incubated at 65°C for 5 min. After 5 min of incubation on the ice, 8 µl of pre-mixed reverse-transcription reaction solution are added (4 µl of 5X Reaction Buffer, 2 µl of 10 mM dNTP Mix, 1 µl of RiboLock RNase Inhibitor and 1 µl of RevertAid RT). The RT-PCR is performed at 42°C for 60 min, then the enzyme is inactivated by an incubation at 70°C for 10 min. The cDNA can be diluted up to 5 times for further use.

### **5.12.3 Quantitative real time PCR**

The relative expression of genes of interest are carried out by quantitative real time PCR that are performed using TB Green Premix Ex Taq (Tli RNase H Plus) (Takara, Japan) on a Roche LightCycler 480 real-time PCR machine, according to the manufacturer's instructions. For each sample, the following mixture is prepared: 3 µl of water, 0.5 µl of each primer (10 µM), 5 µl of TB Green Premix Ex Taq (Takara, Japan) and 1 µl of cDNA. The amplification program used is the following: denaturation (95°C, 5 min), then 45 cycles of denaturation (95°C, 15 sec), primer annealing (55 to 60°C, 10 sec) and extension (72°C, 10 sec). Then melting temperature of the amplified PCR product is determined by melting curve analysis to access

the identity and purity of amplified products. In a melting curve analysis, 30s of denaturation at 95°C, 30s of incubation at 65°C, then the temperature is gradually increased to 95°C. The temperature of primer annealing step is adapted according to the GC/AT ratio of the qPCR primer. PHOSPHATASE 2A SUBUNIT A3 (PP2AA3, At1g13320) was used as a reference gene (Czechowski *et al.*, 2005). Expression levels were calculated using the comparative threshold cycle method (Schmittgen and Livak, 2008). All the primers used in this study are listed in the Annexes (Table 1).

### **5.13 Yeast two-hybrid**

The yeast two-hybrid assay is a powerful tool to identify protein-protein interactions by using the properties of the yeast GAL4 transcription factor. In this system, the DNA-binding and activation domains of GAL4 are fused to the two proteins of interest in the pDEST32 and the pDEST22 vectors, respectively. If these two proteins could physically interact with each other, a functional GAL4 transcription factor is generated, thereby activating the reporter genes under the control of the GAL4-responsive promoter (Figure 5-11). In this study, the yeast strain AH109 that contains the *ADE2*, *HIS3*, *lacZ* and *MEL1* reporter genes under the control of distinct GAL4-responsive promoter, was used.

The LiAc/Single-Stranded Carrier DNA/PEG method is used for yeast transformation as previously described (Gietz and Woods, 2001; Gietz and Woods, 2006). The LiAc is used in combination with PEG to weaken yeast cell wall that becomes permeable for DNA and stimulate DNA uptake by intact yeast cells. The single-stranded carrier DNA is proposed to act as a carrier for the plasmid DNA to be transferred into the cell and it may also help to protect plasmid DNA from endonucleases.

#### **5.13.1 Preparation of yeast competent cells**

This protocol allows obtaining enough competent yeast cells for 20 transformations. AH109 yeast strain are cultured in 50 ml YPDA medium at 30°C under shaking (160 rpm). When the OD<sub>600</sub> reach to 0.8 to 1.2 (around 12 to 16 hours), the culture is centrifuged for 5 min at 5000 rpm, and the pellet is re-suspended in 10 ml of sterile distilled water. After a second



centrifugation, the pellet is re-suspended in 10 ml of 100 mM LiAc solution. After a third centrifugation, the pellet is re-suspended in 1 ml of 100 mM LiAc solution, and incubated at room temperature for further use.

### **5.13.2 Transformation of yeast**

The following components are added in a sterile 2 ml eppendorf tube, 500 ng DNA for each plasmid, 50 µg of denaturated carrier DNA of salmon sperm (10 mg/ml, Yeastmaker™ Carrier DNA, Clontech, USA), 50 µl of yeast competent cells and 300 µl of fresh made PEG-mix solution (40% PEG, 10 mM LiAc, 10mM Tris-HCl, pH 7.5, 1 mM EDTA).

After homogenization by inverting tubes, the yeasts are incubated at 30°C with gentle shaking for 30 min, then a heat shock is applied in a water bath at 42°C for 20 min. 1 ml of sterile distilled water is added to each tube to dilute PEG-mix. After a centrifugation at 13 000 rpm for 15 sec, the supernatant is carefully eliminated, and the pellet is re-suspended in 200 µl of sterile distilled water. 200 µl of the suspension are spread on the SD-Trp-Leu medium (Takara, Japan) that lacks tryptophan and leucine amino acids. The plates are incubated at 30 °C for 2-4 day.

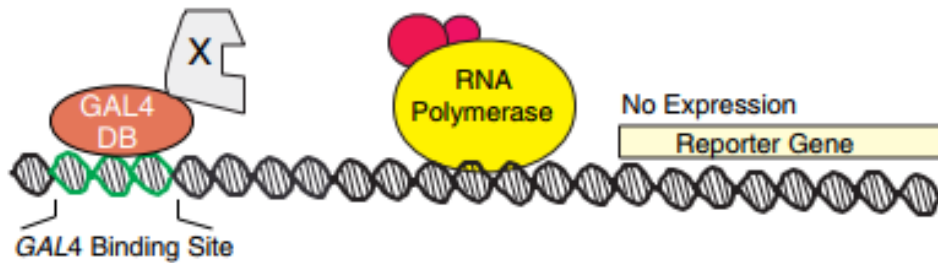
Interactions are visualized as cells growing on SD-Trp-Leu-His medium that lacks tryptophan leucine and histidine amino acids and in the presence of different concentration 3-Amino-1,2,4-triazole (3-AT). The 3-AT is a histidine biosynthesis inhibitor that is essential for reducing background of *HIS3* activation. It is used to evaluate the strength of each interaction after recording *HIS3* gene transactivation.

For this purpose, isolated yeast colony are cultured in 1 ml liquid SD-Trp-Leu medium at 30°C overnight under shaking (160 rpm). The culture are diluted to  $OD_{600} = 0.05$  with sterile distilled water and 7 µl of the dilution is dotted on the SD-Trp-Leu-His medium with different concentration of 3-AT. The plates are incubated at 30 °C and images are taken 2 to 4 days post-dotting.

Yeast cell expressing both the GAL4 DB-X fusion protein and the GAL4 AD-Y fusion protein.

X and Y do not interact.

The GAL4 AD-Y fusion protein does not localize to the promoter to activate transcription.



Yeast cell expressing both the GAL4 DB-X fusion protein and the GAL4 AD-Y fusion protein.

X and Y do interact.

The GAL4 AD-Y fusion protein is localized to the promoter and transcription is activated.

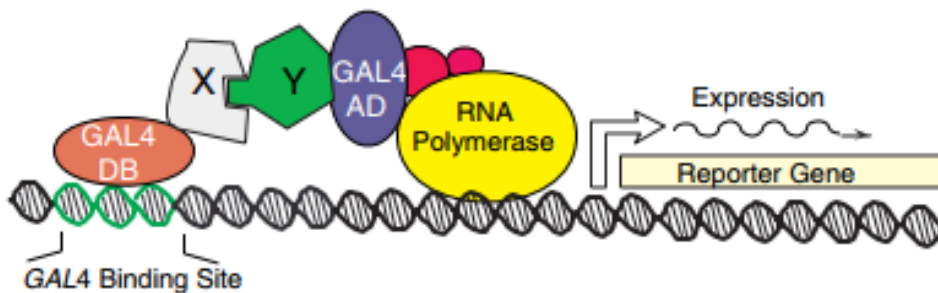
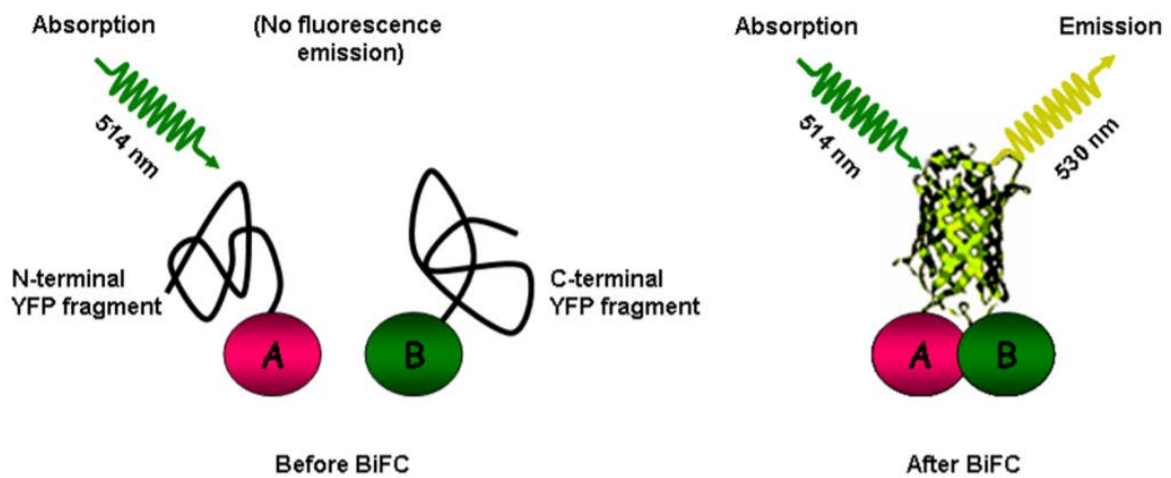


Figure 5-11. The basis of the yeast two-hybrid system.



**Figure 5-12: Principle of the bimolecular fluorescence complementation (BiFC) assay.** The N- and C-terminal fragments of the YFP (yellow fluorescent protein) reporter protein are fused with protein A and protein B, respectively, Interaction of protein A and protein B could bring the fluorescent fragments within proximity to reconstitute a functional fluorophore that could exhibit emission of fluorescence upon excitation with an appropriate wavelength (Bhat *et al.*, 2006).

## 5.14 Bimolecular fluorescence complementation (BiFC) Assays

To confirm protein-protein interaction *in vivo*, the bimolecular fluorescence complementation (BiFC) method was used in this study as described by (Couturier *et al.*, 2014). The N- and C-terminal fragments of YFP are fused with protein A and protein B, respectively. Interaction of protein A and protein B could bring the fluorescent fragments within proximity to reconstitute a functional fluorophore that could exhibit emission of fluorescence upon excitation with an appropriate wavelength (Bhat *et al.*, 2006) (Figure 5-12).

### 5.14.1 Arabidopsis protoplast isolation

Arabidopsis Col-0 are grown on soil under the short day conditions (8h light/16h dark cycle; light intensity: 120  $\mu\text{mol}/\text{cm}^2/\text{s}$ ). Well expanded leaves from 4-week-old plants are used to prepare protoplasts. Approximately 50 leaves are cut to 0.5-1 mm strips, and soaked in 10 ml of enzyme solution in a 12x12 cm petri plate. After a 3 to 4 hours of incubation in the dark at room temperature, the enzyme solution containing protoplasts are filtered with a 45  $\mu\text{m}$  nylon mesh. The filter-through are centrifuged at 900 rpm for 5 min to pellet the protoplasts (acceleration = 3, deceleration = 3). The protoplasts are then re-suspended in 10 ml of W5 solution, centrifuged at 900 rpm for 2 min, and then re-suspended in 2 ml of W5 solution. The cells are counted by using a counting chamber.

More W5 solution are added to the protoplasts to reach a cell density of  $5 \times 10^5/\text{ml}$ . The protoplasts are then incubated on ice for 30 min in W5 solution. After a centrifugation at 900 rpm for 5 min, protoplasts are re-suspended in the same volume of MMG solution.

### 5.14.2 Arabidopsis protoplast transfection

All the plasmids DNA used for protoplast transfection are extracted and purified using the QIAGEN Plasmid Plus Midi Kit (QIAGEN, Germany) following the manufacturer's procedure. 10  $\mu\text{l}$  of each plasmid DNA (1  $\mu\text{g}/\mu\text{l}$ ) and 100  $\mu\text{l}$  of protoplasts are added into a 2 ml Eppendorf tube. 120  $\mu\text{l}$  of PEG solution are added, gently mixed and then incubated at room temperature for 5 to 30 min. 1.8 ml of W5 solution are added (softly, drop by drop) and mixed well gently. After a centrifugation at 900 rpm for 5 min, the protoplasts are re-suspended gently in an

additional 1 ml of W5 solution. After another centrifugation at 900 rpm for 5 min, the protoplasts are re-suspended gently in 100  $\mu$ l MMG solution. In a 24-well cell culture plate, 900  $\mu$ l of WI solution are placed in each well and then 100  $\mu$ l of re-suspended protoplast are softly added over the WI solution. The protoplasts are incubated at 22°C in the dark for 16 to 20 hour until observation. After a centrifugation at 900 rpm for 5 min, most of the supernatant is eliminated to concentrate the protoplasts prior to microscope analyses. The pictures are taken by using the Leica TCS SP8 MP confocal microscope. The solution used in BiFC assay are listed in the Table 5-2.

<b>Table 5-2. The solutions for the BiFC assay used in this study</b>			
	<b>Stock</b>	<b>Volume/Mass</b>	<b>Final concentration</b>
<b>Enzyme solution (10ml)</b>	0.8M mannitol	5 ml	0.4 M
	0.2M KCl	1 ml	20 mM
	0.1M MES	2 ml	20 mM
	cellulase R10	0.1 g	1 %
	macerozyme R10	0.025 mg	0.25 %
	H <sub>2</sub> O	1.8 ml	
	1M CaCl <sub>2</sub>	0.1 ml	10 mM
	10% BSA	0.1 ml	0.1 %
<b>PEG Solution (10ml)</b>	PEG4000	4 g	40% w/v
	1 M mannitol	2 ml	200 mM
	1M CaCl <sub>2</sub>	1 ml	100 mM
	H <sub>2</sub> O	3.5 ml	
<b>W5 solution (50ml)</b>	3M NaCl	2.57 ml	154 mM
	1M CaCl <sub>2</sub>	6.25 ml	125 mM
	0.2M KCl	1.25 ml	5 mM
	0.1M MES	1 ml	2 mM
	0.1M glucose	2.5 ml	5 mM
	H <sub>2</sub> O	36.43 ml	
<b>MMG solution (50ml)</b>	0.8M mannitol	25 ml	0.4 M
	1M MgCl <sub>2</sub>	0.75 ml	15 mM
	0.1M MES	2 ml	4 mM
	H <sub>2</sub> O	22.25 ml	
<b>WI solution (50ml)</b>	0.8 M mannitol	31.25 ml	0.5 M
	0.1M MES	2 ml	4 mM
	0.2 M KCl	5 ml	20m M
	H <sub>2</sub> O	11.75 ml	

## 5.15 Co-immunoprecipitation (Co-IP)/ LC-MS/MS Analyses

Co-immunoprecipitation (Co-IP)/ LC-MS/MS has been used to screen for interacting proteins of ILR3. For this purpose, *ilr3-3* knockdown mutant plants complemented with the *ProILR3:gILR3:GFP* construct was used as bait, and the *ProILR3:GFP* was used as control.

### 5.15.1 Co-immunoprecipitation (Co-IP)

For protein extraction, approximately 700 mg of roots of plants grown under iron deficiency conditions are frozen in liquid nitrogen and crushed using a ball mill. 1.5 ml of pre-cooled lysis buffer (50 mM Tris-HCl, pH 7.5, 150 mM NaCl, 10% [v/v] glycerol, 5 mM MgCl<sub>2</sub>, 0.1% [w/v] IGEPAL CA-630, 2 mM DTT, 1X Complete Mini EDTA-Free Protease Inhibitor Cocktail Tablet [Roche], and 1X Phosphatase Inhibitor Cocktail 3 [Sigma]) are then added, and the mix is incubated on ice for 30 min. The samples are centrifuged at 16000 rpm at 4°C for 10 min. The supernatant is transferred to a new tube and centrifuged again at 16000 rpm at 4°C for 10 min. The Co-immunoprecipitation (Co-IP) are carried out by using an mMACS GFP isolation kit (MACS purification system, Milteny Biotech) according to the manufacturer's instructions. Briefly, 50 µl of anti-GFP microbeads are added to the supernatant, mixed well and incubated at 4°C for 1 hour with gently shaking. The magnetic microbeads are then retained in a µ column, and washed 4 times with 200 µl of lysis buffer. The proteins of interest are then eluted with 50 µl of 95°C Laemmli buffer (50 mM Tris-HCl, pH 6.8, 50 mM DTT, 1% SDS, 0.005% bromphenol blue, 10% glycerol).

Eluted samples from Co-IP are loaded on a 10% Mini-PROTEAN TGX pre-cast gel (Bio-Rad) for a short run (migration: about 1 cm) to eliminate the SDS. The gels with protein migration tracks were manually excised, cut to small cubes and then sequentially rinsed with Milli-Q water for 15 min, 25 mM ammonium bicarbonate for 30 min, and 50% (v/v) acetonitrile in 25 mM ammonium bicarbonate for 30 min, and then dehydrated with acetonitrile for 15 min and dried at room temperature. 100 µl of 10 mM DTT solution are added to the samples, and incubated at 56°C for 45 min to reduce the disulfide bonds of proteins. After removing the DTT solution, 100 µl of 55 mM iodoacetamide solution are added to the samples and the mix is

incubated for 30 min at room temperature in the dark to alkylate the cysteine residues. Once the iodoacetamide solution is removed, the gels are rinsed twice with 50% (v/v) acetonitrile in 25 mM ammonium bicarbonate for 30 min, dehydrated with acetonitrile for 15 min, and dried at room temperature. The digestion of the proteins in the gel is then carried out at 37°C for 12 hour by using 0.25 µg of trypsin (Sequencing Grade Modified, Promega) in a volume of 25 mM ammonium bicarbonate that is sufficient to completely submerge the gel slices. Peptides are extracted from the gel with 200 µl of 2% formic acid (FA) under shaking for 30 min. The supernatant is collected and two more extractions are done with 80% acetonitrile and 2% FA with shaking, for 30 min each. The three supernatants are pooled and vacuum dried. Each sample is then solubilized in 8 µl of 2% FA and 6 µl is injected for LC-MS/MS analysis.

### **5.15.2 LC-MS/MS analysis**

The LC-MS/MS analysis are carried out by using an Ultimate 3000 RSLC nano system (Thermo Fisher Scientific) interfaced online with a nano easy ion source and a Q Exactive™ Plus Orbitrap mass spectrometer (ThermoFisher Scientific). The samples are analyzed in data-dependent acquisition mode. 6 µl of each samples are loaded onto a C18 pre-column (PepMap 100 C18, 5 µm particle size, 100 Å pore size, 300 mm i.d.X, 5mm length; Thermo Fisher Scientific) at a flow rate of 10 µl/min for 3 min. The peptides were separated in a reverse-phase column (PepMap C18, 2 µm particle size, 100 Å pore size, 75 µm i.d. X, 50 cm length; Thermo Fisher Scientific) at a flow rate of 300 nl/min.

The loading buffer (solvent A) was 0.1% (v/v) formic acid in water and the elution buffer (solvent B) was 0.1% (v/v) formic acid in 80% (v/v) acetonitrile. The linear gradient used was 2 to 25% of solvent B in 103 min, followed by 25 to 40% of solvent B from 103 to 123 min and 40 to 90% of solvent B from 123 to 125 min. The total run time was 150 min, including high organic wash step and re-equilibration step.

The Q Exactive Plus mass analyzer is operated in positive ESI mode at 8 kV. In data-dependent acquisition mode, the top 10 precursors were acquired between 375 and 1500 m/z with a 2- Thomson selection window, dynamic exclusion of 40 s, normalized collision energy of 27, and resolutions of 70,000 for MS and 17,500 for MS2.

### 5.15.3 Data analysis

Spectra are recorded with Xcalibur software (Thermo Fisher Scientific). The raw data are analyzed in the Maxquant environment (Tyanova *et al.*, 2016). The minimal peptide length is set to 6. The criteria “Trypsin/P” is chosen as the digestion enzyme. Carbamidomethylation of cysteine is selected as a fixed modification and oxidation of methionine and acetylation (protein N terminus) as variable modifications. Up to two missed cleavages are allowed. The mass tolerance for the precursor is 20 and 4.5 ppm for the first and main searches, respectively, and that for the fragment ions is 20 ppm. The files are searched against an in-house modified Arabidopsis TAIR10 database (35,417 entries). Identified proteins are filtered according to the following criteria: at least one different trypsin peptide with at least one unique peptide and at least one razor peptide. Minimum score for modified peptides is set to 20. A peptide-spectrum match false discovery rate and a protein false discovery rate below 0.05 is required. Using the above-mentioned criteria, the rates of false peptide sequence assignment and false protein identification is lower than 5%. Proteins were selected as potential ILR3 interactors if they were identified in the three IP replicates (i.e. ILR3:GFP) and if they were not identified in any of the control IPs (i.e. GFP)

### 5.16 Chromatin immunoprecipitation qPCR (ChIP-qPCR) assays

Chromatin immunoprecipitation (ChIP) coupled with quantitative PCR can be used to investigate protein-DNA interaction at known genomic binding sites. In this study, this method is used to check if the bHLH121, ILR3 and PYE transcription factors could bind to the promoter region of their putative target genes (i.e. *bHLH38*, *bHLH39*, *FIT*, *FER1*, etc.). ChIP-qPCR experiments are performed as described by (Saleh *et al.*, 2008). Approximately 2 g of seedlings are harvested in a 50 ml Falcon tube. 20 ml of 1% formaldehyde are added and then the samples are placed under vacuum for 15 min for crosslink. Glycine is added to a final concentration of 0.125 M (1.3 ml of 2M glycine in 20ml 1% formaldehyde) to stop the crosslink. After 5 min of vacuum, samples are rinsed three times with 40 ml of water to remove all the formaldehyde. After the rinses, as much as possible water is removed by blotting between paper towels. The samples are frozen in liquid nitrogen and ground to fine powder with a mortar and pestle prior



transfer to a 50 ml Falcon tube. 7 ml of NIB (nuclei isolation buffer) solution are added and incubated on ice for 15 min. The samples are filtered with a 70 µm nylon mesh and filter again with a 45 µm nylon mesh. The filter-through are centrifuged at 1500 rpm at 4°C for 10 min. The supernatant is gently removed and the pellet is re-suspended in 1 ml NIB solution and then transferred to a 1.5 ml eppendorf tube. After a 10 min centrifugation at 1500 rpm at 4°C, the pellet is re-suspended in 220 µl of NLB (nuclei lysis buffer) solution. The re-suspended chromatin solution is sonicated using a Bioruptor (15 cycles of 30 second on/30 second off). The chromatin solution is centrifuged at full speed at 4°C for 5 min to pellet the debris. 200 µl of supernatant are transferred to a 2 ml eppendorf tube and diluted to 2 ml by adding 1.8 ml of ChIP dilution buffer. 20 µl of chromatin solution are stored as Input samples. The chromatin solution are pre-cleared by using 5 µl of beads (Dynabeads Protein G, ThermoFisher Scientific, USA). The chromatin solution is divided into two 2 tubes: one for no antibody control and one for IP. 5 µg of Anti-GFP antibody (Abcam, UK) are added to the IP tube and incubated at 4°C overnight on a rotating wheel. Then, 35 µl beads (Dynabeads Protein G, ThermoFisher Scientific, USA) washed by ChIP dilution buffer are added to each tube, incubated at 4°C for 2 hours. The immune complexes are collected by using a magnetic rack and then washed eight times using the sequence of four buffers (LSWB, HSWB, LiWB, TE buffer) with 2 washes per buffer. After the 8 washes, the protein-DNA complexes are eluted with 260 µl of Elution buffer at 65°C for 15 min. 10 µl of 5M NaCl are added to the elution buffer mix and reverse crosslink at 65°C overnight. The proteinase K treatment is performed by adding 6.5 µl of 0.5 M EDTA, 13 µl of Tris-HCl, pH 6.5 and 1.5 µl of proteinase K, and then incubated at 42°C for 2 hours. The DNA is purified with an IPURE Kit (Diagenode). The DNA is then analyzed by qPCR as described above. Data are presented as promoter target enrichment over input, using the following formula:  $2^{-(C_p \text{ IP} - C_p \text{ Input})} \times 100 \times 100$ . The solutions used this study are listed in Table 5-3. All primers used in this study are listed in Annexes (Table 2).

<b>Table 5-3. The solutions for the ChIP assay used in this study</b>			
	<b>Stock</b>	<b>Volume/Mass</b>	<b>Final concentration</b>
<b>NIB (50ml)</b>	0.5 M PIPES-KOH pH 7.6	2 ml	20 mM
	7.8 M Hexylene glycol	6.41 ml	1 M
	1M MgCl <sub>2</sub>	500 µl	10 mM
	0.5 M EGTA	10 µl	0.1 mM
	5 M NaCl	150 µl	15 mM
	1 M KCl	3.01 ml	60 mM
	20% Triton X100	1.25 ml	0.5 %
	β- mercaptoethanol	17.5 µl	5 mM
	Protease inhibitor(Roch)	1 tablet	
<b>NLB (2 ml)</b>	1 M tris-HCl, pH 8	100 µl	50 mM
	0.5 M EDTA	40 µl	10 mM
	20% SDS	100 µl	1 %
	Protease inhibitor(Roch)	1/5 mini tablet	
<b>CDB(25 ml)</b>	20% Triton X100	1.375 ml	1.1 %
	0.5 M EDTA	60 µl	1.2 mM
	1 M tris-HCl, pH 8	417.5µl	16.7 mM
	5 M NaCl	835 µl	167 mM
<b>LSWB(25 ml)</b>	5 M NaCl	750 µl	150 mM
	20% SDS	125 µl	0.1 %
	20% Triton X100	1.25 ml	1 %
	1 M tris-HCl, pH 8	500 µl	20 mM
	0.5 M EDTA	100 µl	2 mM
<b>HSWB(25 ml)</b>	5 M NaCl	2.5 ml	500 mM
	20% SDS	125 µl	0.1 %
	20% Triton X100	1.25 ml	1 %
	1 M tris-HCl, pH 8	500 µl	20 mM
	0.5 M EDTA	100 µl	2 mM
<b>LiWB(25 ml)</b>	4 M LiCl	1.563 ml	0.25 M
	10 % NP40(IGEPA CA-630)	2.5 ml	1 %
	10% Sodium deoxycholate	2.5 ml	1 %
	0.5 M EDTA	50 µl	1 mM
	1 M tris-HCl, pH 8	250 µl	10 mM
<b>TE(25 ml)</b>	1 M tris-HCl, pH 8	250 µl	10 mM
	0.5 M EDTA	50 µl	1 mM
<b>EB(10 ml)</b>	20% SDS	0.5 ml	1 %
	NaHCO <sub>3</sub>	0.084 g	0.1 M

### 5.17 HPLC analysis of coumarins

For HPLC analysis of coumarins, 30 mg of root material are frozen in liquid nitrogen and ground to fine powder using a ball mill in the presence of glass beads. 400  $\mu$ l of methanol: water [80:20 (v/v)] are added to the ground tissues, vortexed for 5 seconds and stored on ice. The mixture is then vortexed for another 10 seconds and filtered with a 0.45  $\mu$ m filter. 400  $\mu$ l of filtered extract is then evaporated in a speed-evaporator at -110°C in a vacuum. The dried samples are then re-suspended in 10  $\mu$ l of methanol and diluted to 100  $\mu$ l with water/acetonitrile mixture (90:10, v/v) containing 0.1% (v/v) of formic acid. Samples are always kept on ice throughout the extraction to limit degradation of coumarins. HPLC analysis was performed using a 1220 Infinity II LC system (Agilent Technologies) coupled with a ProStar 363 fluorescence detector (Varian) as described by (Gao *et al.*, 2020a; Robe *et al.*, 2020a). Separation was done on an analytical HPLC column (Aeris 3.6  $\mu$ m WIDEPOR XB-C8 200 Å, 100 X 2.1 mm; Phenomenex) with a gradient mobile phase made with 0.1% (v/v) formic acid in water (A) and 0.1% (v/v) formic acid in acetonitrile (B) and a flow rate of 0.25 ml/min. The gradient program started at 8% B for 2 min and increased linearly to 30% B in 13 min and then to 50% B in 1 min. This proportion was maintained for 4 min and returned linearly to initial conditions in 1 min. The column was allowed to stabilize for 9 min at the initial conditions. Absorbance was monitored at  $\lambda=338$  nm. Fluorescence was monitored at  $\lambda_{exc}=365$  and  $\lambda_{em}=460$  nm. For the quantification of coumarins, six-point calibration curve are made using commercial coumarins: esculin (Sigma), esculetin (Sigma), fraxetin (Sigma) scopoletin (Sigma), scopolin (TargetMol), and fraxin (TargetMol). Sideretin and sideretin-glycosides identification was confirmed by LC-MS/MS (Gao *et al.*, 2020a; Robe *et al.*, 2020a).

### 5.18 Chlorophyll measurement

20 mg of (fresh weight) leaves, seedlings or five leaf discs (diameter, 0.35 cm) were collected and soaked overnight in 1 ml 100% acetone in the dark with strong shaking. The absorbance (A) of the clear supernatant is then measured at 661.8 and 644.8 nm using a spectrophotometer. Total chlorophyll (Chl a +Chl b) contents are calculated as the following equation: Chl a +Chl b = 18.09 A<sub>644.8</sub> + 7.05 A<sub>661.6</sub> and is expressed as micrograms per gram fresh weight or

micrograms per square centimeter (Lichtenthaler, 1987).

### **5.19 Ferric chelate reductase (FCR) activity assays**

Ferric chelate reductase assays were performed as previously reported with modifications (Yi and Guerinot, 1996). Briefly, 10 mg fresh root tissues is soaked in 2 ml of FCR assays buffer (10 mM MES, pH 5.5, 100 mM Fe<sup>3+</sup>-EDTA and 300 mM ferrozine) for 1 hour in the dark with gentle shaking. An identical assay without any root tissues is used as a blank. The concentration of Fe<sup>2+</sup>-ferrozine complex (which displays a purple coloration) is measured at 560 nm using a microplate reader (Xenius).

### **5.20 Metal measurements**

For metal measurements, samples are harvested and dried at 65°C for one week in an oven. Samples are ground to fine powder with a mortar and pestle. 10 mg of ground samples are homogenized with 750 µl of nitric oxide (65% [v/v]) and 250 µl of hydrogen peroxide (30% [v/v]). Following an overnight incubation at room temperature, the samples are incubated at 85°C in HotBlock (Environmental Express) for 12 to 24 hours. Samples are then diluted by adding 4 ml Milli-Q H<sub>2</sub>O before the measurement. Analysis of iron content is performed using MP-AES (Microwave Plasma Atomic Emission Spectroscopy, Agilent Technologies).

### **5.21 Iron staining by Perls/DAB**

Perls blue staining is a powerful technique for visualization of iron localization in plants. This technique is based on the conversion of ferrocyanide to insoluble crystals of Prussian blue in the presence of Fe<sup>3+</sup> under acidic conditions. Iron signals could be enhanced by 3,3'-diaminobenzidine tetrahydrochloride (DAB).

The plant material is fixed with fixing solution (methanol:chloroform:glacial acetic acid [6:3:1]) for 1 to 2 hours under vacuum. For mature embryos, they are dissected from dry seeds that were previously imbibed in distilled water for 3 hours. After removing the fixing solution, plant materials are rinsed 3 times for 2 min each with distilled water. Fresh made staining solution

(2% HCl [v/v] and 2% potassium ferrocyanide [w/v]) are added to submerge the plant materials and incubated under vacuum for 15 min, and then incubated for 30 min at room temperature. After 3 washes with distilled water, plant material could be store in distilled water and is available for analysis and imaging.

For the DAB intensification, the plant material is incubated in preparation solution (10 mM  $\text{NaN}_3$  and 0.3%  $\text{H}_2\text{O}_2$  [v/v] in methanol) for 1 hour and then washed three times with 0.1 M Phosphate buffer (pH 7). The plant materials is then incubated with intensification solution (0.1 M phosphate buffer [pH 7] containing 0.025% DAB [w/v], 0.005%  $\text{H}_2\text{O}_2$  [v/v] and 0.005%  $\text{CoCl}_2$  [w/v]) for 5 to 30 min at room temperature. The reactions are stopped by three times washes with distilled water. The plant material is visualized under a stereoscopic microscope (Nikon SMZ800) and imaged with a Coolpix 4500 charge coupled device (CCD) digital camera (Nikon).

### **5.22 Histochemical detection of $\beta$ -glucoronidase (GUS) activity**

The GUS reporter gene system is a powerful tool for the assessment of promoter activity in transgenic plants (Jefferson *et al.*, 1987). In this study, the GUS staining method is used to study the expression patterns of *bHLH121* and other *bHLH* transcription factors. Seedlings were harvested and soaked immediately in 1 ml of GUS staining buffer (0.1 M phosphate buffer pH 7.5, 10 mM  $\text{Na}_2\text{-EDTA}$ , 0.1% [v/v] Triton X-100, 0.5 mM potassium ferricyanide, 0.5 mM potassium ferrocyanide and 2 mM X-Gluc [5-bromo-4-chloro-3-indolyl-b-D-glucuronide]) in 24-well plates. After 1 hour of vacuum at room temperature, the reaction was performed at 37°C overnight in the dark. After the reaction, samples were rinsed with distilled water and then treated with 70% (v/v) ethanol to remove the chlorophylls. Images were captured by using a motorized fluorescence stereo zoom microscope (ZEISS).

### **5.23 Measurement of root length**

After the growing period, roots are scanned with an Epson scanner and the roots length are measured using the ImageJ software (National Institutes of Health).

# DISCUSSIONS



## Discussion

In the past two decades, remarkable progress has been made in decrypting the molecular mechanisms that maintain iron homeostasis in plants. Research in this area has highlighted that iron homeostasis in plants is regulated at the transcriptional level and involves several bHLH TFs that function in a complex regulatory network (Gao and Dubos, 2020; Gao *et al.*, 2019a). Recent studies suggest that, in *Arabidopsis*, this intricate regulatory network is composed of two interconnected regulatory modules, with FIT (bHLH29) playing a predominant role in one module and ILR3 (bHLH105) in the other. Although overall the FIT and ILR3 regulatory modules have been well characterized (Colangelo and Guerinot, 2004; Jakoby *et al.*, 2004; Li *et al.*, 2016; Liang *et al.*, 2017; Wang *et al.*, 2007b; Yuan *et al.*, 2008; Zhang *et al.*, 2015), it remains unclear how these two subnetworks are synchronized to coordinately regulate iron homeostasis in plants.

### 1. ILR3 connects the plant responses to both iron deficiency and iron excess

In plants, both iron deficiency and excess are deleterious. Thus, the levels of iron in plant cells must be tightly regulated in response to iron availability and plant requirement (Briat *et al.*, 2015). Under iron deficiency, plants increase the root iron absorption and release iron from reservoir to satisfy the iron demand (Kobayashi and Nishizawa, 2012). By contrast, plants decrease the root iron absorption and sequester excess iron to avoid toxicity when iron concentration is high (Ravet *et al.*, 2009). Ferritins play pivotal roles in this process to maintain the intracellular iron balance. Expression of ferritins is down-regulated to decrease iron sequestration under low iron supply conditions, while with high iron supply, ferritins are up-regulated to increase iron sequestration to avoid the potential iron toxicity (Ravet *et al.*, 2009). Since iron absorption and sequestration show opposite effects on the intracellular iron homeostasis, it was expected that the regulation of these processes should be integrated (Kobayashi *et al.*, 2019; Kroh and Pilon, 2019).

In this study, to identify the key regulators that could coordinate the transcriptional regulatory cascade associated with plant responses to iron deficiency and iron excess, the *AtFER1*



promoter-based strategy was therefore chosen (Tissot *et al.*, 2019). We found that the basic helix-Loop-helix (bHLH) transcription factor, ILR3/bHLH105, which was known to positively regulate the iron deficiency responses, also could negatively regulate the expression of ferritin genes (*AtFER1*, *AtFER3*, and *AtFER4*), thus integrating the iron deficiency and iron excess responses. In the previous studies, ILR3 has been identified to act as an activator in iron deficiency responses *via* targeting clade *Ib* bHLH genes (Zhang *et al.*, 2015). Loss-of-function of *ILR3* in *Arabidopsis* caused impaired iron deficiency response, whereas overexpression of *ILR3* had the opposite effect and led to excess iron accumulation when grown in soil conditions (Zhang *et al.*, 2015). Nevertheless, some evidence implies that ILR3 function may extend beyond the induction of the iron uptake mechanism. Rampey *et al.* reported that the expression of three vacuolar iron transporter genes (*VTL1*, *VTL2*, and *VTL5*) and a gene encoding a chloroplastic iron-sulfur cluster transfer protein called *At-NEET* were down-regulated in the *ILR3* dominant mutant *ilr3-1* (Rampey *et al.*, 2006). Using CHIP-qPCR experiments we further demonstrated that ILR3 could bind to the promoter regions of *AtFER1*, *AtFER3*, *AtFER4*, *At-NEET*, *VTL2* as well as *NAS4*, suggesting that ILR3 is a direct transcriptional repressor of these target genes. PYE (POPEYE), a bHLH transcription factor belonging to clade IVb, was identified as a negative regulator of a set of genes involved in iron translocation and mobilization (Long *et al.*, 2010). PYE contains a typical EAR motif (DLNxxP), one of the most predominant form of transcriptional repression motif identified in plants, at its C-terminal region (Kagale and Rozwadowski, 2011). PYE was shown to interact *in vivo* with clade IVc bHLH proteins including ILR3 (Long *et al.*, 2010; Zhang *et al.*, 2015). In this study, we demonstrated that ILR3 and PYE can repress the expression of a common set of genes and directly bind to their promoter region at the same locus. Putting together our work with those from different laboratories, we proposed that the transcriptional repressor activity of ILR3 is likely conferred by its heterodimerization with PYE. Under iron deficiency conditions, ILR3-dependent complexes (bHLH34-ILR3, bHLH104-ILR3 and bHLH115-ILR3) act as activator to promote the iron uptake (Li *et al.*, 2016; Zhang *et al.*, 2015) and the ILR3-PYE complex act as repressor to inhibit iron sequestration, which is likely important to avoid reduced iron availability within the roots.

It is assumed that the relative protein abundance of clade IVc bHLH (i.e. bHLH34, bHLH104, bHLH115 and ILR3) and PYE could determine the amount of the two types of ILR3-dependent protein complexes (activator and repressor) within the different cell types depending on the iron status. Therefore, it would be interesting to investigate the cellular co-localization of these bHLH TFs within the root tissues under different iron conditions. Interestingly, PYE can also form heterodimers with bHLH104 and bHLH115. However, it remains unclear if these interacting complexes actually play a role in the regulation of iron homeostasis.

## **2. bHLH121 is required for the iron deficiency response in Arabidopsis**

ILR3 plays a critical role in regulating iron homeostasis (Tissot *et al.*, 2019; Zhang *et al.*, 2015). Therefore, we conducted Co-IP LC-MS/MS experiment to identify potential new actors involved in controlling iron homeostasis. In this study, bHLH121 (clade IVb) was identified as an ILR3-interacting TF. Loss-of-function of *bhlh121* causes severe iron deficiency symptoms that can be rescued by providing extra iron supply. Similar results were also reported by two other groups (Kim *et al.*, 2019; Lei *et al.*, 2020). These studies and our highlighted the upstream position of *bHLH121* in the iron homeostasis network since *bhlh121* mutants were affected in all the aspects of the iron deficiency responses and since the expression of several regulatory proteins involved in this network was impaired (Gao *et al.*, 2020a; Gao *et al.*, 2020b; Kim *et al.*, 2019; Lei *et al.*, 2020). All these three studies demonstrated that bHLH121 could directly bind to the promoter of the four clade Ib bHLH TFs (i.e. *bHLH38*, *bHLH39*, *bHLH100* and *bHLH101*) and activate their expression. However, some partially inconsistent results were reported in these three studies. First, Lei *et al.*, employed Y1H, ChIP-qPCR and EMSA to provide evidence that bHLH121 could bind to the promoter of *FIT*, whereas ChIP-qPCR experiment in our study did not show bHLH121 binding to the *FIT* promoter. Kim *et al.* reached a similar conclusion than us by using the ChIP-seq analysis (Kim *et al.*, 2019; Lei *et al.*, 2020). Kim *et al.* reported that the overexpression of subgroup Ib bHLH TFs, but not the overexpression of *FIT*, could rescue the *bhlh121* mutant (also called *uri*) and restore the induction of *IRT1* expression under iron deficiency conditions (Kim *et al.*, 2019). By contrast,

Lei *et al.* showed that overexpression of *FIT* could partially rescue the *bhlh121-5* mutant (Lei *et al.*, 2020). However, in our study, neither overexpression of *FIT* nor *bHLH38* could overcome the *bhlh121-2* growth defects. It is noteworthy that different *bhlh121* mutants were used in the three studies, which may account for the different results. Although, further investigation remains to be conducted to determine these inconsistent results, all these studies concluded that bHLH121 is required for the iron deficiency response in Arabidopsis.

### 3. Post-translational regulation of bHLH121

Post-translational modifications (i.e. sequestration, ubiquitination, or phosphorylation) can significantly affect the regulatory activities of TFs by controlling their active protein levels (Schütze *et al.*, 2008). Such mechanisms have been shown to play critical roles in the maintenance of iron homeostasis in plants (Kobayashi *et al.*, 2019; Rodríguez-Celma *et al.*, 2019a; Spielmann and Vert, 2020; Wu and Ling, 2019). Kim *et al.* and us demonstrated that *bHLH121* is expressed throughout the plant body and that its transcript and protein levels are not affected by iron availability (Gao *et al.*, 2020a; Kim *et al.*, 2019). By contrast, we found that iron availability was affecting the cellular localization of bHLH121 protein within roots. Under iron deficiency, bHLH121 was mainly detected in the root cortex and rhizodermis cells, whereas most bHLH121 was observed in the nuclei of cells in the stele when plants were grown under iron sufficient conditions. Several hypotheses might explain these observations. For example, some post-translational mechanism could modulate the stability of bHLH121 protein in a cell type- and iron-dependent manner to determine its localization. Although the precise mechanisms of these processes remain unknown and need to be investigated in the future, these results suggest that the genes that are targeted by bHLH121 differ depending on iron availability.

In fact, iron availability not only affect the cellular localization but also the subcellular localization of bHLH121. Lei *et al.* showed that bHLH121 is localized in both the endoplasmic reticulum and nucleus in the Arabidopsis protoplasts (Lei *et al.*, 2020). In the roots, Kim *et al.* and us showed that bHLH121 was localized in the nucleus under iron deficiency (0  $\mu$ M Fe) and iron sufficient conditions (50  $\mu$ M Fe) (Gao *et al.*, 2020a; Kim *et al.*, 2019). Interestingly, Lei *et*

*al.* reported that bHLH121-GFP was observed in both the cytoplasm and the nucleus when the iron concentration was increased to a higher level (100  $\mu$ M Fe)(Lei *et al.*, 2020). These results suggest that the lower iron availability could promote the bHLH121 nuclear accumulation. However, it is still unknown either the iron deficiency could facilitate the mobility of bHLH121 and redirects the protein toward the nucleus or the lower iron concentration could stabilize bHLH121 in the nucleus and destabilize it in the endoplasmic reticulum. The interaction of bHLH121 with clade IVc bHLH TFs has been determined through different approaches including Y2H, BiFC and Co-IP (Gao *et al.*, 2020a; Kim *et al.*, 2019; Lei *et al.*, 2020). Lei *et al.* further demonstrated that these interactions could facilitate the nuclear accumulation of bHLH121(Lei *et al.*, 2020). Previous studies revealed that iron deficiency could increase the protein levels of clade IVc bHLH TFs (Selote *et al.*, 2015; Tissot *et al.*, 2019). Therefore, it can be speculated that the increased protein levels of clade IVc bHLH TFs could facilitate the mobility of bHLH121 from the endoplasmic reticulum to the nucleus when iron is limiting. This post-translational mechanism for the intracellular partitioning of iron-responsive TFs has been reported. For instance, in Arabidopsis, Trofimov *et al.* demonstrated that the nuclear localization of bHLH39 depends on its interaction with FIT, since in cells lacking FIT, bHLH39 localizes predominantly in the cytoplasm (Trofimov *et al.*, 2019). Similar results have also been observed in rice for which it was shown that OsbHLH156/OsFIT could interact with the OsIRO2 and facilitate its accumulation in the nucleus (Liang *et al.*, 2020; Wang *et al.*, 2020). Thus, it is likely that this process is a common mechanism for the sequestration of TFs not immediately required by the plant cells.

Phosphorylation is one of the most widespread type of post-translational modification that affects the activity of proteins. In Arabidopsis, the iron-induced and calcium-dependent protein kinase CIPK11 can interact with FIT and phosphorylates it at Ser272, which positively regulates FIT activity by favoring its nuclear accumulation and dimerization capacity with bHLH39, thereby promoting the iron uptake under iron deficiency conditions (Gratz *et al.*, 2019). Similarly, Kim *et al.* reported that bHLH121 is phosphorylated under iron deficiency conditions (Kim *et al.*, 2019). When plants were grown under iron deficiency conditions, the phosphorylated form of bHLH121 is accumulated and enhanced its capacity to heterodimerize with clade IVc bHLH TFs and increased its ability to bind to the promoter of its target genes,

highlighting the positive role of phosphorylation on bHLH121 activity (Kim *et al.*, 2019). However, it is still unknown which kinase(s) are involved in the phosphorylation of bHLH121. Future studies to characterize the precise regulatory mechanism leading to the phosphorylation of bHLH121 proteins will help to shed light on how this TF respond to the iron deficiency and activate downstream regulatory network.

Recent studies have proposed that several hemerythrin (HHE) E3 ubiquitin ligases act as negative regulators of iron homeostasis to avoid toxic iron overload by directly targeting bHLH TFs (Rodríguez-Celma *et al.*, 2019a). In Arabidopsis, BTS (BRUTUS) has been reported to interact with ILR3 and bHLH115 and to facilitate their degradation *via* the 26S proteasome pathway, whereas BRUTUS LIKE 1 and 2 (BTSL1 and BTSL2) mediate FIT degradation, allowing fine tuning of the expression of downstream iron deficiency response genes (Hindt *et al.*, 2017; Long *et al.*, 2010; Rodríguez-Celma *et al.*, 2019a; Rodríguez-Celma *et al.*, 2019b; Selote *et al.*, 2015). Similarly, OsHRZ1 and OsHRZ2 (HAEMERYTHRIN MOTIF-CONTAINING REALLY INTERESTING NEW GENE [RING] AND ZINC-FINGER PROTEIN 1 and 2), two homologs of BTS in rice, have been reported to interact with OsPRI1/OsbHLH60, OsPRI2/OsbHLH58, and OsPRI3/ OsbHLH59 and mediate their degradation *via* the 26S proteasome pathway (Zhang *et al.*, 2020; Zhang *et al.*, 2017). As mentioned before, Kim *et al.* demonstrated that the phosphorylated form of bHLH121 only accumulates under iron deficiency conditions, whereas the phosphorylated bHLH121 are subject to proteasome-mediated degradation when iron is resupplied, likely mediated by the BTS E3 ligase (Kim *et al.*, 2019). This iron-dependent degradation of bHLH121 allows switching off iron deficiency signaling cascades and likely avoiding iron overload under iron sufficient conditions. However, Y2H failed to show the direct interaction between bHLH121 and BTS, BTSL1 and BTSL2 (Gao *et al.*, 2020a; Long *et al.*, 2010). Kim *et al.* employed an alternative approach and found that, unlike in the wild type, the phosphorylated form of bHLH121 is accumulated in the *bts-3* loss-of-function mutant under iron sufficient conditions, suggesting that the degradation of phosphorylated bHLH121 is dependent on BTS in the presence of iron (Kim *et al.*, 2019). More approaches are required to determine whether BTS could directly interact with bHLH121 or whether there is a scaffold protein that brings these two proteins together in plant cells.

#### **4. bHLH121 and clade IVc bHLH transcription factors function coordinately in the regulation of iron homeostasis**

As we have seen earlier, the four clade IVc bHLH TFs play a critical role upstream in the iron homeostasis regulatory network. These four TFs have been shown to interact *in vivo* in the form of homodimers or heterodimers and function similarly but additively in iron homeostasis regulation (Li *et al.*, 2016; Liang *et al.*, 2017; Zhang *et al.*, 2015). Single mutants of all the clade IVc bHLH TFs showed more sensitivity to iron deficiency compare to wild type and the high order mutants displayed increased iron deficiency associated symptoms (Li *et al.*, 2016; Liang *et al.*, 2017; Zhang *et al.*, 2015). In agreement with the phenotype, the induction of genes involved in iron uptake including clade *Ib bHLH* and *FIT* TFs are impaired in these mutants. Further analysis demonstrated that the clade IVc bHLH could directly bind to the promoter of the four clade *Ib bHLH* TFs but not the promoter of *FIT* (Li *et al.*, 2016; Liang *et al.*, 2017; Zhang *et al.*, 2015). Interestingly, bHLH121 and clade IVc bHLH TFs shared a set of known target genes, including the four clade *Ib bHLH* TFs (Gao *et al.*, 2020b; Kim *et al.*, 2019; Lei *et al.*, 2020). However, we still lack knowledge on the whole set of target genes of these TFs. Recently, Kim *et al.* employed the microarray and ChIP-seq approaches to reveal that bHLH121 could directly or indirectly regulate a set of target genes involved in both FIT-dependent and FIT-independent pathway (Kim *et al.*, 2019). Thus, given the importance of clade IVc bHLH TFs in this regulatory network, global gene expression analysis and ChIP-seq analysis would be required to decrypt the whole set of direct and indirect target genes of clade IVc bHLH TFs in the future, which is necessary to address the question of whether clade IVc bHLH and bHLH121 TFs display qualitative and/or quantitative functional divergence in regulating the shared target genes.

To further investigate the genetic interaction between bHLH121 and clade IVc bHLH TFs, Lei *et al.* generated the *bhlh104 bhlh121* and *bhlh115 bhlh121* double mutants and compared their phenotypes with the corresponding parental single mutants (Lei *et al.*, 2020). They showed that the phenotypes of *bhlh104 bhlh121* and *bhlh115 bhlh121* double mutants were similar to that of the *bhlh121* (*bhlh121-5*) single mutant and they concluded the bHLH121 acts downstream of clade IVc bHLH TFs in the iron homeostasis regulatory network (Lei *et al.*, 2020).

However, inconsistent results have been found in our study where *bhlh121 bhlh34*, *bhlh121 bhlh104*, *bhlh121 bhlh105* and *bhlh121 bhlh115* double mutants showed enhanced growth defects compare to the *bhlh121 (bhlh121-2)* single mutant under both the iron deficiency and sufficient conditions. Furthermore, we demonstrated that these double mutants showed decreased iron contents and enhanced impaired iron deficiency responses compare to *bhlh121-2* single mutant. It is therefore most likely that bHLH121 does not act downstream of the clade IVc bHLH TFs. Taken together, our data suggest that bHLH121 and clade IVc bHLH TFs play additive roles, at least partly, in iron homeostasis in Arabidopsis. Lei *et al.* showed that overexpression of *bHLH104* and *bHLH115* could completely rescue the expression of clade *lb bHLH* genes but not *FIT* in *bhlh121-5* mutant (Lei *et al.*, 2020). Similar results were observed in our study, where the overexpression of *bHLH105* and *bHLH115* could activate *bHLH39* expression but not the one of *FIT* in the *bhlh121-2* mutant, which is not sufficient to activate the downstream genes to facilitate the uptake of iron. These results suggested that bHLH121 is indispensable for the activation of *FIT* by bHLH104 and bHLH115. By contrast, overexpression of *bHLH34* and *bHLH105* could partially complement the iron-associated phenotype of *bhlh121* by inducing the expression of both *bHLH39* and *FIT*, which could partly reconstitute the iron uptake system to promote iron uptake in the absence of *bHLH121*. These results also indicated that distinct roles exist among the four clade IVc bHLH members in the regulation of iron homeostasis.

Zhang *et al.* employed Chip-qPCR to show that bHLH105 could not bind to the E-Box region on the promoter of *FIT* whereas Li *et al.* used reporter-effector transient expression assay to demonstrate that bHLH34 could not specifically activate the transcription of *FIT* (Li *et al.*, 2016; Zhang *et al.*, 2015). Liang *et al.* also concluded that *FIT* is not the direct target of clade IVc bHLH TFs (Liang *et al.*, 2017). Altogether these conclusions raise an important question, which protein(s) act as the direct linker to mediate the activation of *FIT* by clade IVc bHLH TFs. As described before, it is still disputed whether bHLH121 could directly associate with the promoter of *FIT* (Gao *et al.*, 2020a; Kim *et al.*, 2019; Lei *et al.*, 2020). Thus, further investigation is required to clarify the relationship between bHLH121 and *FIT* and to determine whether other proteins connect *FIT* with bHLH34 and ILR3.

## Conclusion

The major objective of this thesis was to study the transcriptional regulatory network that regulates iron homeostasis in plants using *Arabidopsis thaliana* as model. This work revealed that ILR3 is at the center of this regulatory network in which it acts as both transcriptional activator and repressor. The discovery of the novel bHLH TF, bHLH121, that plays critical roles in iron homeostasis substantially increased our understanding of the regulatory networks that controls iron homeostasis in plants and enables us to further explore how the known regulatory factors and their protein partners control the iron status. Finally, our work indicates that bHLH121 and clade IVc bHLH TFs play additive roles and function synergistically to regulate iron homeostasis. However, much work lies ahead to fully comprehend the transcriptional regulatory network of iron homeostasis in plants in particular if we aim at using these TFs for breeding crops to grow robustly in iron-limited soils and to produce high quality derived products.





# REFERENCES



- Aung MS, Masuda H.** 2020. How does rice defend against excess iron?: Physiological and molecular mechanisms. *Frontiers in plant science* **11**.
- Balk J, Lobréaux S.** 2005. Biogenesis of iron-sulfur proteins in plants. *Trends Plant Sci* **10**, 324-331.
- Balk J, Schaedler TA.** 2014. Iron cofactor assembly in plants. *Annual review of plant biology* **65**, 125-153.
- Bashir K, Inoue H, Nagasaka S, Takahashi M, Nakanishi H, Mori S, Nishizawa NK.** 2006. Cloning and characterization of deoxymugineic acid synthase genes from graminaceous plants. *Journal of Biological Chemistry* **281**, 32395-32402.
- Becker M, Asch F.** 2005. Iron toxicity in rice—conditions and management concepts. *Journal of Plant Nutrition and Soil Science* **168**, 558-573.
- Beinert H.** 2000. Iron-sulfur proteins: ancient structures, still full of surprises. *Journal of biological inorganic chemistry: JBIC: a publication of the Society of Biological Inorganic Chemistry* **5**, 2-15.
- Bhat RA, Lahaye T, Panstruga R.** 2006. The visible touch: in planta visualization of protein-protein interactions by fluorophore-based methods. *Plant methods* **2**, 1-14.
- Brear EM, Day DA, Smith PMC.** 2013. Iron: an essential micronutrient for the legume-rhizobium symbiosis. *Frontiers in plant science* **4**, 359.
- Briat J-F, Curie C, Gaymard F.** 2007. Iron utilization and metabolism in plants. *Current Opinion in Plant Biology* **10**, 276-282.
- Briat J-F, Dubos C, Gaymard F.** 2015. Iron nutrition, biomass production, and plant product quality. *Trends in plant science* **20**, 33-40.
- Briat J-F, Duc C, Ravet K, Gaymard F.** 2010. Ferritins and iron storage in plants. *Biochimica et Biophysica Acta (BBA)-General Subjects* **1800**, 806-814.
- Cassin G, Mari S, Curie C, Briat JF, Czernic P.** 2009. Increased sensitivity to iron deficiency in *Arabidopsis thaliana* overaccumulating nicotianamine. *J Exp Bot* **60**, 1249-1259.
- Chen S, Sánchez-Fernández R, Lyver ER, Dancis A, Rea PA.** 2007. Functional characterization of AtATM1, AtATM2, and AtATM3, a subfamily of *Arabidopsis* half-molecule ATP-binding cassette transporters implicated in iron homeostasis. *J Biol Chem* **282**, 21561-21571.
- Cho U-H, Seo N-H.** 2005. Oxidative stress in *Arabidopsis thaliana* exposed to cadmium is due to hydrogen peroxide accumulation. *Plant science* **168**, 113-120.
- Chu H-H, Chiecko J, Punshon T, Lanzirotti A, Lahner B, Salt DE, Walker EL.** 2010. Successful reproduction requires the function of *Arabidopsis* Yellow Stripe-Like1 and Yellow Stripe-Like3 metal-nicotianamine transporters in both vegetative and reproductive structures. *Plant Physiology* **154**, 197-210.
- Clough SJ, Bent AF.** 1998. Floral dip: a simplified method for *Agrobacterium*-mediated transformation of *Arabidopsis thaliana*. *The Plant Journal* **16**, 735-743.
- Colangelo EP, Guerinot ML.** 2004. The essential basic helix-loop-helix protein FIT1 is required for the iron deficiency response. *The Plant Cell* **16**, 3400-3412.
- Connolly EL, Campbell NH, Grotz N, Prichard CL, Guerinot ML.** 2003. Overexpression of the FRO2 ferric chelate reductase confers tolerance to growth on low iron and uncovers posttranscriptional control. *Plant Physiology* **133**, 1102-1110.
- Connorton JM, Balk J, Rodríguez-Celma J.** 2017. Iron homeostasis in plants—a brief

overview. *Metallomics* **9**, 813-823.

**Couturier J, Touraine B, Briat J-F, Gaymard F, Rouhier N.** 2013. The iron-sulfur cluster assembly machineries in plants: current knowledge and open questions. *Frontiers in plant science* **4**, 259.

**Couturier J, Wu H-C, Dhalleine T, Pégeot H, Sudre D, Gualberto JM, Jacquot J-P, Gaymard F, Vignols F, Rouhier N.** 2014. Monothiol glutaredoxin–BoIA interactions: redox control of *Arabidopsis thaliana* BoIA2 and SufE1. *Molecular plant* **7**, 187-205.

**Curie C, Cassin G, Couch D, Divol F, Higuchi K, Le Jean M, Misson J, Schikora A, Czernic P, Mari S.** 2009. Metal movement within the plant: contribution of nicotianamine and yellow stripe 1-like transporters. *Annals of botany* **103**, 1-11.

**Curie C, Panaviene Z, Loulergue C, Dellaporta SL, Briat JF, Walker EL.** 2001. Maize yellow stripe1 encodes a membrane protein directly involved in Fe(III) uptake. *Nature* **409**, 346-349.

**Czechowski T, Stitt M, Altmann T, Udvardi MK, Scheible W-R.** 2005. Genome-wide identification and testing of superior reference genes for transcript normalization in *Arabidopsis*. *Plant Physiology* **139**, 5-17.

**DiDonato Jr RJ, Roberts LA, Sanderson T, Eisley RB, Walker EL.** 2004. *Arabidopsis* Yellow Stripe-Like2 (YSL2): a metal-regulated gene encoding a plasma membrane transporter of nicotianamine–metal complexes. *The Plant Journal* **39**, 403-414.

**Divol F, Couch D, Conéjéro G, Roschzttardtz H, Mari S, Curie C.** 2013. The *Arabidopsis* YELLOW STRIPE LIKE4 and 6 transporters control iron release from the chloroplast. *The Plant Cell* **25**, 1040-1055.

**Durrett TP, Gassmann W, Rogers EE.** 2007. The FRD3-mediated efflux of citrate into the root vasculature is necessary for efficient iron translocation. *Plant Physiology* **144**, 197-205.

**Duy D, Wanner G, Meda AR, von Wirén N, Soll J, Philippar K.** 2007. PIC1, an ancient permease in *Arabidopsis* chloroplasts, mediates iron transport. *The Plant Cell* **19**, 986-1006.

**Eckhardt U, Mas Marques A, Buckhout TJ.** 2001. Two iron-regulated cation transporters from tomato complement metal uptake-deficient yeast mutants. *Plant Mol Biol* **45**, 437-448.

**Edwards K, Johnstone C, Thompson C.** 1991. A simple and rapid method for the preparation of plant genomic DNA for PCR analysis. *Nucleic acids research* **19**, 1349.

**Eide D, Broderius M, Fett J, Guerinot ML.** 1996. A novel iron-regulated metal transporter from plants identified by functional expression in yeast. *Proceedings of the National Academy of Sciences* **93**, 5624-5628.

**Fourcroy P, Sisó-Terraza P, Sudre D, Savirón M, Reyt G, Gaymard F, Abadía A, Abadía J, Álvarez-Fernández A, Briat JF.** 2014. Involvement of the ABCG 37 transporter in secretion of scopoletin and derivatives by *Arabidopsis* roots in response to iron deficiency. *New Phytologist* **201**, 155-167.

**Fourcroy P, Tissot N, Gaymard F, Briat J-F, Dubos C.** 2016. Facilitated Fe nutrition by phenolic compounds excreted by the *Arabidopsis* ABCG37/PDR9 transporter requires the IRT1/FRO2 high-affinity root Fe<sup>2+</sup> transport system. *Molecular plant* **9**, 485-488.

**Gao F, Dubos C.** 2020. Transcriptional integration of the plant responses to iron availability. *Journal of experimental botany*.

**Gao F, Robe K, Bettembourg M, Navarro N, Rofidal V, Santoni V, Gaymard F, Vignols F, Roschzttardtz H, Izquierdo E, Dubos C.** 2020a. The Transcription Factor bHLH121 Interacts

with bHLH105 (ILR3) and Its Closest Homologs to Regulate Iron Homeostasis in Arabidopsis. *The Plant Cell* **32**, 508-524.

**Gao F, Robe K, Dubos C.** 2020b. Further insights into the role of bHLH121 in the regulation of iron homeostasis in Arabidopsis thaliana. *Plant Signaling & Behavior*, 1795582.

**Gao F, Robe K, Gaymard F, Izquierdo E, Dubos C.** 2019a. The Transcriptional Control of Iron Homeostasis in Plants: A Tale of bHLH Transcription Factors? *Frontiers in plant science* **10**.

**Gao F, Robe K, Gaymard F, Izquierdo E, Dubos C.** 2019b. The transcriptional control of iron homeostasis in plants: a tale of bHLH transcription factors? *Frontiers in plant science* **10**, 6.

**Gayomba SR, Zhai Z, Jung H-i, Vatamaniuk OK.** 2015. Local and systemic signaling of iron status and its interactions with homeostasis of other essential elements. *Frontiers in plant science* **6**, 716.

**Gietz RD, Woods RA.** 2001. Genetic transformation of yeast. *Biotechniques* **30**, 816-831.

**Gietz RD, Woods RA.** 2006. Yeast transformation by the LiAc/SS Carrier DNA/PEG method. *Methods Mol Biol* **313**, 107-120.

**Gollhofer J, Timofeev R, Lan P, Schmidt W, Buckhout TJ.** 2014. Vacuolar-iron-transporter1-like proteins mediate iron homeostasis in Arabidopsis. *PLoS One* **9**, e110468.

**Gratz R, Manishankar P, Ivanov R, Köster P, Mohr I, Trofimov K, Steinhorst L, Meiser J, Mai H-J, Drerup M.** 2019. CIPK11-dependent phosphorylation modulates FIT activity to promote Arabidopsis iron acquisition in response to calcium signaling. *Developmental cell* **48**, 726-740. e710.

**Green LS, Rogers EE.** 2004. FRD3 controls iron localization in Arabidopsis. *Plant Physiology* **136**, 2523-2531.

**Grefen C, Donald N, Hashimoto K, Kudla J, Schumacher K, Blatt MR.** 2010. A ubiquitin-10 promoter-based vector set for fluorescent protein tagging facilitates temporal stability and native protein distribution in transient and stable expression studies. *The Plant Journal* **64**, 355-365.

**Grillet L, Mari S, Schmidt W.** 2014. Iron in seeds—loading pathways and subcellular localization. *Frontiers in plant science* **4**, 535.

**Guerinot ML, Yi Y.** 1994. Iron: nutritious, noxious, and not readily available. *Plant Physiology* **104**, 815.

**Hänsch R, Mendel RR.** 2009. Physiological functions of mineral micronutrients (Cu, Zn, Mn, Fe, Ni, Mo, B, Cl). *Current Opinion in Plant Biology* **12**, 259-266.

**Hell R, Stephan UW.** 2003. Iron uptake, trafficking and homeostasis in plants. *Planta* **216**, 541-551.

**Henriques R, Jásik J, Klein M, Martinoia E, Feller U, Schell J, Pais MS, Koncz C.** 2002. Knock-out of Arabidopsis metal transporter gene IRT1 results in iron deficiency accompanied by cell differentiation defects. *Plant Molecular Biology* **50**, 587-597.

**Hentze MW, Muckenthaler MU, Galy B, Camaschella C.** 2010. Two to tango: regulation of mammalian iron metabolism. *Cell* **142**, 24-38.

**Herbik A, Giritch A, Horstmann C, Becker R, Balzer H-J, Baumlein H, Stephan UW.** 1996. Iron and copper nutrition-dependent changes in protein expression in a tomato wild type and the nicotianamine-free mutant chloronerva. *Plant Physiology* **111**, 533-540.

- Higuchi K, Suzuki K, Nakanishi H, Yamaguchi H, Nishizawa N-K, Mori S.** 1999. Cloning of nicotianamine synthase genes, novel genes involved in the biosynthesis of phytosiderophores. *Plant Physiology* **119**, 471-480.
- Hindt MN, Akmakjian GZ, Pivarski KL, Punshon T, Baxter I, Salt DE, Guerinot ML.** 2017. BRUTUS and its paralogs, BTS LIKE1 and BTS LIKE2, encode important negative regulators of the iron deficiency response in *Arabidopsis thaliana*. *Metallomics* **9**, 876-890.
- Hoy JA, Hargrove MS.** 2008. The structure and function of plant hemoglobins. *Plant physiology and biochemistry* **46**, 371-379.
- Inoue H, Kobayashi T, Nozoye T, Takahashi M, Kakei Y, Suzuki K, Nakazono M, Nakanishi H, Mori S, Nishizawa NK.** 2009. Rice OsYSL15 is an iron-regulated iron(III)-deoxymugineic acid transporter expressed in the roots and is essential for iron uptake in early growth of the seedlings. *J Biol Chem* **284**, 3470-3479.
- Inoue H, Nojima H, Okayama H.** 1990. High efficiency transformation of *Escherichia coli* with plasmids. *Gene* **96**, 23-28.
- Ishimaru Y, Kim S, Tsukamoto T, Oki H, Kobayashi T, Watanabe S, Matsushashi S, Takahashi M, Nakanishi H, Mori S, Nishizawa NK.** 2007. Mutational reconstructed ferric chelate reductase confers enhanced tolerance in rice to iron deficiency in calcareous soil. *Proc Natl Acad Sci U S A* **104**, 7373-7378.
- Jain A, Dashner ZS, Connolly EL.** 2019. Mitochondrial iron transporters (MIT1 and MIT2) are essential for iron homeostasis and embryogenesis in *Arabidopsis thaliana*. *Frontiers in plant science* **10**, 1449.
- Jain A, Wilson GT, Connolly EL.** 2014. The diverse roles of FRO family metalloreductases in iron and copper homeostasis. *Frontiers in plant science* **5**, 100.
- Jakoby M, Wang H-Y, Reidt W, Weisshaar B, Bauer P.** 2004. FRU (BHLH029) is required for induction of iron mobilization genes in *Arabidopsis thaliana*. *FEBS letters* **577**, 528-534.
- Jean ML, Schikora A, Mari S, Briat JF, Curie C.** 2005. A loss-of-function mutation in AtYSL1 reveals its role in iron and nicotianamine seed loading. *The Plant Journal* **44**, 769-782.
- Jefferson RA, Kavanagh TA, Bevan MW.** 1987. GUS fusions: beta-glucuronidase as a sensitive and versatile gene fusion marker in higher plants. *The EMBO journal* **6**, 3901-3907.
- Jeong J, Cohu C, Kerkeb L, Pilon M, Connolly EL, Guerinot ML.** 2008. Chloroplast Fe(III) chelate reductase activity is essential for seedling viability under iron limiting conditions. *Proceedings of the National Academy of Sciences* **105**, 10619.
- Kagale S, Rozwadowski K.** 2011. EAR motif-mediated transcriptional repression in plants: an underlying mechanism for epigenetic regulation of gene expression. *Epigenetics* **6**, 141-146.
- Kim S-J, Kawaharada C, Suzuki T, Saito K, Hashimoto N, Takigawa S, Noda T, Matsuura-Endo C, Yamauchi H.** 2006a. Effect of natural light periods on rutin, free amino acid and vitamin C contents in the sprouts of common (*Fagopyrum esculentum* Moench) and tartary (*F. tataricum* Gaertn.) buckwheats. *Food science and technology research* **12**, 199-205.
- Kim SA, Guerinot ML.** 2007. Mining iron: iron uptake and transport in plants. *FEBS letters* **581**, 2273-2280.
- Kim SA, LaCroix IS, Gerber SA, Guerinot ML.** 2019. The iron deficiency response in *Arabidopsis thaliana* requires the phosphorylated transcription factor URI. *Proceedings of the National Academy of Sciences* **116**, 24933-24942.
- Kim SA, Punshon T, Lanzirotti A, Li L, Alonso JM, Ecker JR, Kaplan J, Guerinot ML.**

2006b. Localization of iron in Arabidopsis seed requires the vacuolar membrane transporter VIT1. *Science* **314**, 1295-1298.

**Klatte M, Schuler M, Wirtz M, Fink-Straube C, Hell R, Bauer P.** 2009. The analysis of Arabidopsis nicotianamine synthase mutants reveals functions for nicotianamine in seed iron loading and iron deficiency responses. *Plant Physiol* **150**, 257-271.

**Kobayashi T, Nishizawa NK.** 2012. Iron uptake, translocation, and regulation in higher plants. *Annual Review of Plant Biology* **63**, 131-152.

**Kobayashi T, Nozoye T, Nishizawa NK.** 2019. Iron transport and its regulation in plants. *Free Radical Biology and Medicine* **133**, 11-20.

**Koncz C, Schell J.** 1986. The promoter of TL-DNA gene 5 controls the tissue-specific expression of chimaeric genes carried by a novel type of Agrobacterium binary vector. *Molecular and General Genetics MGG* **204**, 383-396.

**Korshunova YO, Eide D, Clark WG, Guerinot ML, Pakrasi HB.** 1999. The IRT1 protein from Arabidopsis thaliana is a metal transporter with a broad substrate range. *Plant Molecular Biology* **40**, 37-44.

**Kroh GE, Pilon M.** 2019. Connecting the negatives and positives of plant iron homeostasis. *New Phytologist* **223**, 1052-1055.

**Kruger C, Berkowitz O, Stephan UW, Hell R.** 2002. A metal-binding member of the late embryogenesis abundant protein family transports iron in the phloem of *Ricinus communis* L. *J Biol Chem* **277**, 25062-25069.

**Kushnir S, Babiychuk E, Storozhenko S, Davey MW, Papenbrock J, De Rycke R, Engler G, Stephan UW, Lange H, Kispal G, Lill R, Van Montagu M.** 2001. A mutation of the mitochondrial ABC transporter *Sta1* leads to dwarfism and chlorosis in the Arabidopsis mutant *starik*. *Plant Cell* **13**, 89-100.

**Lanquar V, Lelièvre F, Bolte S, Hamès C, Alcon C, Neumann D, Vansuyt G, Curie C, Schröder A, Krämer U.** 2005. Mobilization of vacuolar iron by AtNRAMP3 and AtNRAMP4 is essential for seed germination on low iron. *The EMBO Journal* **24**, 4041-4051.

**Lee S, Chiecko JC, Kim SA, Walker EL, Lee Y, Guerinot ML, An G.** 2009. Disruption of *OsYSL15* Leads to Iron Inefficiency in Rice Plants. *Plant Physiology* **150**, 786.

**Lei R, Li Y, Cai Y, Li C, Pu M, Lu C, Yang Y, Liang G.** 2020. bHLH121 functions as a direct link that facilitates the activation of FIT by bHLH IVc transcription factors for maintaining Fe homeostasis in Arabidopsis. *Molecular plant* **13**, 634-649.

**Li L, Cheng X, Ling HQ.** 2004. Isolation and characterization of Fe(III)-chelate reductase gene *LeFRO1* in tomato. *Plant Mol Biol* **54**, 125-136.

**Li X, Zhang H, Ai Q, Liang G, Yu D.** 2016. Two bHLH transcription factors, bHLH34 and bHLH104, regulate iron homeostasis in Arabidopsis thaliana. *Plant Physiology* **170**, 2478-2493.

**Liang G, Zhang H, Li X, Ai Q, Yu D.** 2017. bHLH transcription factor bHLH115 regulates iron homeostasis in Arabidopsis thaliana. *Journal of experimental botany* **68**, 1743-1755.

**Liang G, Zhang H, Li Y, Pu M, Yang Y, Li C, Lu C, Xu P, Yu D.** 2020. *Oryza sativa* FER-LIKE FE DEFICIENCY-INDUCED TRANSCRIPTION FACTOR (*OsFIT/OsbHLH156*) interacts with *OsIRO2* to regulate iron homeostasis. *Journal of Integrative Plant Biology* **62**, 668-689.

**Lichtenthaler HK.** 1987. [34] Chlorophylls and carotenoids: pigments of photosynthetic



biomembranes. *Methods in enzymology* **148**, 350-382.

**Lill R, Dutkiewicz R, Freibert SA, Heidenreich T, Mascarenhas J, Netz DJ, Paul VD, Pierik AJ, Richter N, Stümpfig M.** 2015. The role of mitochondria and the CIA machinery in the maturation of cytosolic and nuclear iron–sulfur proteins. *European journal of cell biology* **94**, 280-291.

**Ling H-Q, Pich A, Scholz G, Ganai MW.** 1996. Genetic analysis of two tomato mutants affected in the regulation of iron metabolism. *Molecular and General Genetics MGG* **252**, 87-92.

**Long TA, Tsukagoshi H, Busch W, Lahner B, Salt DE, Benfey PN.** 2010. The bHLH transcription factor POPEYE regulates response to iron deficiency in Arabidopsis roots. *The Plant Cell* **22**, 2219-2236.

**Lubkowitz M.** 2011. The oligopeptide transporters: a small gene family with a diverse group of substrates and functions? *Molecular plant* **4**, 407-415.

**Ma JF, Taketa S, Chang Y-C, Iwashita T, Matsumoto H, Takeda K, Nomoto K.** 1999. Genes controlling hydroxylations of phytosiderophores are located on different chromosomes in barley (*Hordeum vulgare* L.). *Planta* **207**, 590-596.

**Marschner H.** 1995. Mineral nutrition of higher plants. 2nd. Edn. Academic Press.

**Marschner H.** 2011. *Marschner's mineral nutrition of higher plants*: Academic press.

**Mary V, Ramos MS, Gillet C, Socha AL, Giraudat J, Agorio A, Merlot S, Clairet C, Kim SA, Punshon T.** 2015. Bypassing iron storage in endodermal vacuoles rescues the iron mobilization defect in the natural resistance associated-macrophage protein3natural resistance associated-macrophage protein4 double mutant. *Plant Physiology* **169**, 748-759.

**Mendoza-Cózatl DG, Xie Q, Akmakjian GZ, Jobe TO, Patel A, Stacey MG, Song L, Demoin DW, Jurisson SS, Stacey G.** 2014. OPT3 is a component of the iron-signaling network between leaves and roots and misregulation of OPT3 leads to an over-accumulation of cadmium in seeds. *Molecular plant* **7**, 1455-1469.

**Miller JL.** 2013. Iron deficiency anemia: a common and curable disease. *Cold Spring Harbor perspectives in medicine* **3**, a011866.

**Mori S, Nishizawa N.** 1987. Methionine as a dominant precursor of phytosiderophores in Gramineae plants. *Plant and Cell Physiology* **28**, 1081-1092.

**Morrissey J, Baxter IR, Lee J, Li L, Lahner B, Grotz N, Kaplan J, Salt DE, Guerinot ML.** 2009. The ferroportin metal efflux proteins function in iron and cobalt homeostasis in Arabidopsis. *The Plant Cell* **21**, 3326-3338.

**Morrissey J, Guerinot ML.** 2009. Iron uptake and transport in plants: the good, the bad, and the ionome. *Chemical reviews* **109**, 4553-4567.

**Murata Y, Ma JF, Yamaji N, Ueno D, Nomoto K, Iwashita T.** 2006. A specific transporter for iron(III)-phytosiderophore in barley roots. *Plant J* **46**, 563-572.

**Murgia I, Tarantino D, Soave C, Morandini P.** 2011. Arabidopsis CYP82C4 expression is dependent on Fe availability and circadian rhythm, and correlates with genes involved in the early Fe deficiency response. *Journal of plant physiology* **168**, 894-902.

**Nakagawa T, Kurose T, Hino T, Tanaka K, Kawamukai M, Niwa Y, Toyooka K, Matsuoka K, Jinbo T, Kimura T.** 2007. Development of series of gateway binary vectors, pGWBs, for realizing efficient construction of fusion genes for plant transformation. *Journal of bioscience and bioengineering* **104**, 34-41.

- Nozoye T, Nagasaka S, Kobayashi T, Takahashi M, Sato Y, Sato Y, Uozumi N, Nakanishi H, Nishizawa NK.** 2011. Phytosiderophore efflux transporters are crucial for iron acquisition in graminaceous plants. *Journal of Biological Chemistry* **286**, 5446-5454.
- Ortiz de Montellano PR.** 2010. Hydrocarbon hydroxylation by cytochrome P450 enzymes. *Chemical reviews* **110**, 932-948.
- Pottier M, Oomen R, Picco C, Giraudat J, Scholz-Starke J, Richaud P, Carpaneto A, Thomine S.** 2015. Identification of mutations allowing Natural Resistance Associated Macrophage Proteins (NRAMP) to discriminate against cadmium. *The Plant Journal* **83**, 625-637.
- Przybyla-Toscano J, Boussardon C, Law S, Rouhier N, Keech O.** Gene atlas of iron-containing proteins in *Arabidopsis thaliana*. *The Plant Journal*.
- Rampey RA, Woodward AW, Hobbs BN, Tierney MP, Lahner B, Salt DE, Bartel B.** 2006. An *Arabidopsis* basic helix-loop-helix leucine zipper protein modulates metal homeostasis and auxin conjugate responsiveness. *Genetics* **174**, 1841-1857.
- Ravet K, Touraine B, Boucherez J, Briat JF, Gaymard F, Cellier F.** 2009. Ferritins control interaction between iron homeostasis and oxidative stress in *Arabidopsis*. *The Plant Journal* **57**, 400-412.
- Rellán-Álvarez R, El-Jendoubi H, Wohlgemuth G, Abadía A, Fiehn O, Abadía J, Álvarez-Fernández A.** 2011. Metabolite Profile Changes in Xylem Sap and Leaf Extracts of Strategy I Plants in Response to Iron Deficiency and Resupply. *Frontiers in plant science* **2**.
- Rellán-Alvarez R, Giner-Martínez-Sierra J, Orduna J, Orera I, Rodríguez-Castrillón JA, García-Alonso JI, Abadía J, Álvarez-Fernández A.** 2010. Identification of a tri-iron(III), tri-citrate complex in the xylem sap of iron-deficient tomato resupplied with iron: new insights into plant iron long-distance transport. *Plant Cell Physiol* **51**, 91-102.
- Rio DC, Ares M, Jr., Hannon GJ, Nilsen TW.** 2010. Purification of RNA using TRIzol (TRI reagent). *Cold Spring Harb Protoc* **2010**, pdb.prot5439.
- Robe K, Conejero G, Gao F, Lefebvre-Legendre L, Sylvestre-Gonon E, Rofidal V, Hem S, Rouhier N, Barberon M, Hecker A.** 2020a. Coumarin accumulation and trafficking in *Arabidopsis thaliana*: a complex and dynamic process. *New Phytologist*.
- Robe K, Izquierdo E, Vignols F, Rouached H, Dubos C.** 2020b. The Coumarins: Secondary Metabolites Playing a Primary Role in Plant Nutrition and Health. *Trends in Plant Science*.
- Robinson NJ, Procter CM, Connolly EL, Guerinot ML.** 1999. A ferric-chelate reductase for iron uptake from soils. *Nature* **397**, 694-697.
- Rodríguez-Celma J, Chou H, Kobayashi T, Long TA, Balk J.** 2019a. Hemerythrin E3 ubiquitin ligases as negative regulators of iron homeostasis in plants. *Frontiers in plant science* **10**, 98.
- Rodríguez-Celma J, Connorton JM, Kruse I, Green RT, Franceschetti M, Chen Y-T, Cui Y, Ling H-Q, Yeh K-C, Balk J.** 2019b. *Arabidopsis* BRUTUS-LIKE E3 ligases negatively regulate iron uptake by targeting transcription factor FIT for recycling. *Proceedings of the National Academy of Sciences* **116**, 17584-17591.
- Rogers EE, Guerinot ML.** 2002. FRD3, a member of the multidrug and toxin efflux family, controls iron deficiency responses in *Arabidopsis*. *The Plant Cell* **14**, 1787-1799.
- Römheld V, Marschner H.** 1983. Mechanism of iron uptake by peanut plants : I. Fe reduction, chelate splitting, and release of phenolics. *Plant Physiol* **71**, 949-954.

- Römheld V, Marschner H.** 1986. Evidence for a specific uptake system for iron phytosiderophores in roots of grasses. *Plant Physiology* **80**, 175-180.
- Roschzttardtz H, Conéjéro G, Curie C, Mari S.** 2009. Identification of the endodermal vacuole as the iron storage compartment in the Arabidopsis embryo. *Plant Physiology* **151**, 1329-1338.
- Roschzttardtz H, Séguéla-Arnaud M, Briat J-F, Vert G, Curie C.** 2011. The FRD3 citrate effluxer promotes iron nutrition between symplastically disconnected tissues throughout Arabidopsis development. *The Plant Cell* **23**, 2725-2737.
- Saleh A, Alvarez-Venegas R, Avramova Z.** 2008. An efficient chromatin immunoprecipitation (ChIP) protocol for studying histone modifications in Arabidopsis plants. *Nature protocols* **3**, 1018.
- Santi S, Cesco S, Varanini Z, Pinton R.** 2005. Two plasma membrane H(+)-ATPase genes are differentially expressed in iron-deficient cucumber plants. *Plant Physiol Biochem* **43**, 287-292.
- Santi S, Schmidt W.** 2009. Dissecting iron deficiency-induced proton extrusion in Arabidopsis roots. *New Phytologist* **183**, 1072-1084.
- Schaaf G, Honsbein A, Meda AR, Kirchner S, Wipf D, von Wirén N.** 2006. AtIREG2 encodes a tonoplast transport protein involved in iron-dependent nickel detoxification in Arabidopsis thaliana roots. *J Biol Chem* **281**, 25532-25540.
- Schaaf G, Schikora A, Häberle J, Vert G, Ludewig U, Briat J-F, Curie C, von Wirén N.** 2005. A putative function for the Arabidopsis Fe-phytosiderophore transporter homolog AtYSL2 in Fe and Zn homeostasis. *Plant and Cell Physiology* **46**, 762-774.
- Schaedler TA, Thornton JD, Kruse I, Schwarzländer M, Meyer AJ, Van Veen HW, Balk J.** 2014. A conserved mitochondrial ATP-binding cassette transporter exports glutathione polysulfide for cytosolic metal cofactor assembly. *Journal of Biological Chemistry* **289**, 23264-23274.
- Schmid NB, Giehl RF, Döll S, Mock H-P, Strehmel N, Scheel D, Kong X, Hider RC, von Wirén N.** 2014. Feruloyl-CoA 6'-Hydroxylase1-dependent coumarins mediate iron acquisition from alkaline substrates in Arabidopsis. *Plant Physiology* **164**, 160-172.
- Schmittgen TD, Livak KJ.** 2008. Analyzing real-time PCR data by the comparative C T method. *Nature protocols* **3**, 1101.
- Schütze K, Harter K, Chaban C.** 2008. Post-translational regulation of plant bZIP factors. *Trends in plant science* **13**, 247-255.
- Selote D, Samira R, Matthiadis A, Gillikin JW, Long TA.** 2015. Iron-binding E3 ligase mediates iron response in plants by targeting basic helix-loop-helix transcription factors. *Plant physiology* **167**, 273-286.
- Shenker M, Chen Y.** 2005. Increasing iron availability to crops: fertilizers, organo-fertilizers, and biological approaches. *Soil Science & Plant Nutrition* **51**, 1-17.
- Shojima S, Nishizawa N-K, Fushiya S, Nozoe S, Irifune T, Mori S.** 1990. Biosynthesis of phytosiderophores: in vitro biosynthesis of 2'-deoxymugineic acid from L-methionine and nicotianamine. *Plant Physiology* **93**, 1497-1503.
- Siwinska J, Siatkowska K, Olry A, Grosjean J, Hehn A, Bourgaud F, Meharg AA, Carey M, Lojkowska E, Ichnatowicz A.** 2018. Scopoletin 8-hydroxylase: a novel enzyme involved in coumarin biosynthesis and iron-deficiency responses in Arabidopsis. *Journal of experimental botany* **69**, 1735-1748.

**Sperotto RA, Ricachenevsky FK, Stein RJ, Waldow V, Fett JP.** 2010. Iron stress in plants: dealing with deprivation and overload. *Plant Stress* **4**, 57-69.

**Spielmann J, Vert G.** 2020. The many facets of protein ubiquitination and degradation in plant root iron deficiency responses. *Journal of experimental botany*.

**Stacey MG, Patel A, McClain WE, Mathieu M, Remley M, Rogers EE, Gassmann W, Blevins DG, Stacey G.** 2008. The Arabidopsis AtOPT3 protein functions in metal homeostasis and movement of iron to developing seeds. *Plant Physiology* **146**, 589-601.

**Stassen MJ, Hsu S-H, Pieterse CM, Stringlis IA.** 2020. Coumarin communication along the microbiome–root–shoot axis. *Trends in Plant Science*.

**Stoltzfus RJ.** 2011. Iron interventions for women and children in low-income countries. *The Journal of nutrition* **141**, 756S-762S.

**Suzuki M, Takahashi M, Tsukamoto T, Watanabe S, Matsushashi S, Yazaki J, Kishimoto N, Kikuchi S, Nakanishi H, Mori S.** 2006. Biosynthesis and secretion of mugineic acid family phytosiderophores in zinc-deficient barley. *The Plant Journal* **48**, 85-97.

**Takahashi M, Yamaguchi H, Nakanishi H, Shioiri T, Nishizawa N-K, Mori S.** 1999. Cloning two genes for nicotianamine aminotransferase, a critical enzyme in iron acquisition (Strategy II) in graminaceous plants. *Plant Physiology* **121**, 947-956.

**Terry N, Abadía J.** 1986. Function of iron in chloroplasts. *Journal of Plant Nutrition* **9**, 609-646.

**Tissot N, Robe K, Gao F, Grant-Grant S, Boucherez J, Bellegarde F, Maghiaoui A, Marcelin R, Izquierdo E, Benhamed M, Martin A, Vignols F, Roschttardt H, Gaymard F, Briat JF, Dubos C.** 2019. Transcriptional integration of the responses to iron availability in Arabidopsis by the bHLH factor ILR3. *New Phytologist* **223**, 1433-1446.

**Tottey S, Block MA, Allen M, Westergren T, Albrieux C, Scheller HV, Merchant S, Jensen PE.** 2003. Arabidopsis CHL27, located in both envelope and thylakoid membranes, is required for the synthesis of protochlorophyllide. *Proceedings of the National Academy of Sciences* **100**, 16119-16124.

**Trofimov K, Ivanov R, Eutebach M, Acaroglu B, Mohr I, Bauer P, Brumbarova T.** 2019. Mobility and localization of the iron deficiency-induced transcription factor bHLH039 change in the presence of FIT. *Plant direct* **3**, e00190.

**Tsai H-H, Rodríguez-Celma J, Lan P, Wu Y-C, Vélez-Bermúdez IC, Schmidt W.** 2018. Scopoletin 8-hydroxylase-mediated fraxetin production is crucial for iron mobilization. *Plant Physiology* **177**, 194-207.

**Tyanova S, Temu T, Cox J.** 2016. The MaxQuant computational platform for mass spectrometry-based shotgun proteomics. *Nature protocols* **11**, 2301.

**Vanholme R, Sundin L, Seetso KC, Kim H, Liu X, Li J, De Meester B, Hoengenaert L, Goeminne G, Morreel K.** 2019. COSY catalyses trans–cis isomerization and lactonization in the biosynthesis of coumarins. *Nature plants* **5**, 1066-1075.

**Vasconcelos M, Eckert H, Arahana V, Graef G, Grusak MA, Clemente T.** 2006. Molecular and phenotypic characterization of transgenic soybean expressing the Arabidopsis ferric chelate reductase gene, FRO2. *Planta* **224**, 1116-1128.

**Vert G, Grotz N, Dédaldéchamp F, Gaymard F, Guerinot ML, Briat J-F, Curie C.** 2002. IRT1, an Arabidopsis transporter essential for iron uptake from the soil and for plant growth. *The Plant Cell* **14**, 1223-1233.

- Vignais P.** 2002. The superoxide-generating NADPH oxidase: structural aspects and activation mechanism. *Cellular and Molecular Life Sciences CMLS* **59**, 1428-1459.
- von Wiren N, Klair S, Bansal S, Briat JF, Khodr H, Shioiri T, Leigh RA, Hider RC.** 1999. Nicotianamine chelates both FeIII and FeII. Implications for metal transport in plants. *Plant Physiol* **119**, 1107-1114.
- Walter M, Chaban C, Schütze K, Batistic O, Weckermann K, Näke C, Blazevic D, Grefen C, Schumacher K, Oecking C.** 2004. Visualization of protein interactions in living plant cells using bimolecular fluorescence complementation. *The Plant Journal* **40**, 428-438.
- Wang H-Y, Klatte M, Jakoby M, Baumlein H, Weisshaar B, Bauer P.** 2007a. Iron deficiency-mediated stress regulation of four subgroup Ib BHLH genes in *Arabidopsis thaliana*. *Planta* **226**, 897-908.
- Wang HY, Klatte M, Jakoby M, Baumlein H, Weisshaar B, Bauer P.** 2007b. Iron deficiency-mediated stress regulation of four subgroup Ib BHLH genes in *Arabidopsis thaliana*. *Planta* **226**, 897-908.
- Wang S, Li L, Ying Y, Wang J, Shao JF, Yamaji N, Whelan J, Ma JF, Shou H.** 2020. A transcription factor OsbHLH156 regulates Strategy II iron acquisition through localising IRO2 to the nucleus in rice. *New Phytologist* **225**, 1247-1260.
- Waters BM, Chu H-H, DiDonato RJ, Roberts LA, Easley RB, Lahner B, Salt DE, Walker EL.** 2006. Mutations in *Arabidopsis* yellow stripe-like1 and yellow stripe-like3 reveal their roles in metal ion homeostasis and loading of metal ions in seeds. *Plant Physiology* **141**, 1446-1458.
- Waters BM, Lucena C, Romera FJ, Jester GG, Wynn AN, Rojas CL, Alcántara E, Pérez-Vicente R.** 2007. Ethylene involvement in the regulation of the H(+)-ATPase CsHA1 gene and of the new isolated ferric reductase CsFRO1 and iron transporter CsIRT1 genes in cucumber plants. *Plant Physiol Biochem* **45**, 293-301.
- White MD, Flashman E.** 2016. Catalytic strategies of the non-heme iron dependent oxygenases and their roles in plant biology. *Current opinion in chemical biology* **31**, 126-135.
- Winterbourn CC.** 1995. Toxicity of iron and hydrogen peroxide: the Fenton reaction. *Toxicology letters* **82**, 969-974.
- Wu H, Ling H-Q.** 2019. FIT-binding proteins and their functions in the regulation of Fe homeostasis. *Frontiers in plant science* **10**, 844.
- Yi Y, Guerinot ML.** 1996. Genetic evidence that induction of root Fe (III) chelate reductase activity is necessary for iron uptake under iron deficiency. *The Plant Journal* **10**, 835-844.
- Yuan Y, Wu H, Wang N, Li J, Zhao W, Du J, Wang D, Ling H-Q.** 2008. FIT interacts with AtbHLH38 and AtbHLH39 in regulating iron uptake gene expression for iron homeostasis in *Arabidopsis*. *Cell research* **18**, 385.
- Yuan YX, Zhang J, Wang DW, Ling HQ.** 2005. AtbHLH29 of *Arabidopsis thaliana* is a functional ortholog of tomato FER involved in controlling iron acquisition in strategy I plants. *Cell research* **15**, 613-621.
- Zhai Z, Gayomba SR, Jung H-i, Vimalakumari NK, Piñeros M, Craft E, Rutzke MA, Danku J, Lahner B, Punshon T.** 2014. OPT3 is a phloem-specific iron transporter that is essential for systemic iron signaling and redistribution of iron and cadmium in *Arabidopsis*. *The Plant Cell* **26**, 2249-2264.
- Zhang H, Li Y, Pu M, Xu P, Liang G, Yu D.** 2020. *Oryza sativa* POSITIVE REGULATOR

OF IRON DEFICIENCY RESPONSE 2 (OsPRI2) and OsPRI3 are involved in the maintenance of Fe homeostasis. *Plant, cell & environment* **43**, 261-274.

**Zhang H, Li Y, Yao X, Liang G, Yu D.** 2017. Positive regulator of iron homeostasis1, OsPRI1, facilitates iron homeostasis. *Plant physiology* **175**, 543-554.

**Zhang J, Liu B, Li M, Feng D, Jin H, Wang P, Liu J, Xiong F, Wang J, Wang H-B.** 2015. The bHLH transcription factor bHLH104 interacts with IAA-LEUCINE RESISTANT3 and modulates iron homeostasis in Arabidopsis. *The Plant Cell* **27**, 787-805.

**Zhang X, Henriques R, Lin S-S, Niu Q-W, Chua N-H.** 2006. Agrobacterium-mediated transformation of Arabidopsis thaliana using the floral dip method. *Nature protocols* **1**, 641.



# ANNEXES





**Table 1. Primers used for qRT-PCR experiments**

Primer name	Sequence (5'->3')
<b>bHLH121-Q1</b>	CCAACGAAGTTGCAACACAACCTCG
<b>bHLH121-Q2</b>	CTGGAAGAAGTGTGGTCTCGTACG
<b>FIT-Q1</b>	CAGTCACAAGCGAAGAAACTCA
<b>FIT-Q2</b>	CTTGTAAGAGATGGAGCAACACC
<b>bHLH34-Q1</b>	TCGTCATCTGTTGGAGCTGT
<b>bHLH34-Q2</b>	GTTTCTCGCGACAGGCTTTG
<b>bHLH104-Q1</b>	CCAGCTGCATTTAACCACAACA
<b>bHLH104-Q2</b>	TTAAGCAGCAGGAGGCCTGAG
<b>bHLH115-Q1</b>	TCAAGCAAGAGATGAAGCGC
<b>bHLH115-Q2</b>	GACAAGCTTGCTTCCAGGAG
<b>ILR3-Q1</b>	GCAACCTATTGGTGTCTTCTTAACCTC
<b>ILR3-Q2</b>	CCAGGTTCTTTGCTAGCTTCTGA
<b>bHLH38-Q1</b>	AGGAGAGAGGCTCTTCTACACTT
<b>bHLH38-Q2</b>	TGAGAAGTAGTGGATAAACACACCA
<b>bHLH39-Q1</b>	GACGGTTTCTCGAAGCTTG
<b>bHLH39-Q2</b>	GGTGGCTGCTTAACGTAACAT
<b>bHLH100-Q1</b>	CTCCCACCAATCAAACGAAGAAG
<b>bHLH100-Q2</b>	TGTTTTGGTCGGTGTAACGAG
<b>bHLH101-Q1</b>	AAGAAGATCGAGGAGCGGTG
<b>bHLH101-Q2</b>	AGAGGCAAGAGAGCACGAAG
<b>PYE-Q1</b>	CAGGACTTCCCATTTTCCAA
<b>PYE-Q2</b>	CTTGTGTCTGGGGATCAGGT
<b>MYB10-Q1</b>	GGGGAAATCTTGGTGGAGCA
<b>MYB10-Q2</b>	AGGAGGAACCTGGCTATCGT
<b>MYB72-Q1</b>	TCGAGAGGTAACCAAATCGCA
<b>MYB72-Q2</b>	CAGCTGTCTCCTCAAGTCGG
<b>BTS-Q1</b>	GCTCTGGCACAAGTCAATCA
<b>BTS-Q2</b>	CGTTCATCAAATGCCGATAA
<b>BTSL1-Q1</b>	GGCAATGAAGATGGATTTGG
<b>BTSL1-Q2</b>	TCATATGGAACCGTTGCTGA
<b>BTSL2-Q1</b>	CGGGGCAGAATCCATCTTAT
<b>BTSL2-Q2</b>	GTTGCAACAAGGAGCAAGAAG
<b>IRT1-Q1</b>	CGGTTGGACTTCTAAATGC
<b>IRT1-Q2</b>	CGATAATCGACATTCCACCG
<b>FRO2-Q1</b>	AGTACGCCACAAGAATCGCT
<b>FRO2-Q2</b>	CCACACTCGAACCTTCCACA
<b>F6'H1-Q1</b>	TGATATCTGCAGGAATGAAACG
<b>F6'H1-Q2</b>	GGGTAGTAGTTAAGGTTGACTC
<b>S8H-Q1</b>	CCGAGACACTTGGCTTCTT
<b>S8H-Q2</b>	CAGCAGCTCCACCGAAACA
<b>CYP82C4-Q1</b>	AGGCTCAGTATCGTCGGAG

<b>CYP82C4-Q2</b>	TTTCTATGTCTGAATCCTCGACG
<b>PDR9-Q1</b>	GTCTTGGACACTCAACGGGT
<b>PDR9-Q2</b>	ATCTTGCAACCGTCGTGGAT
<b>BGLU42-Q1</b>	ATGGCCTGGGAAGTGAAGTC
<b>BGLU42-Q2</b>	ATTTGTCCAACCTCCGATTG
<b>FER1-Q1</b>	TCGTTGAGAGTGAATTTCTGG
<b>FER1-Q2</b>	ACCCCAACATTGGTCATCTG
<b>FER3-Q1</b>	AGAGTGTGTTTCTGAACGAAC
<b>FER3-Q2</b>	CCAAACTGCGAGATTACAGC
<b>FER4-Q1</b>	AGAGCGAGTTTCTGACAGAG
<b>FER4-Q2</b>	CTTACCCTTCCAGAAGCATCTG
<b>NAS4-Q1</b>	GGCTTCGACGTTGTGTTCTT
<b>NAS4-Q2</b>	AGCAAAGCACCAGGAGACAT
<b>VTL2-Q1</b>	GATGGGAGTTGGAGCTGTGAA
<b>VTL2-Q2</b>	CCTGCGAATCCGGAGAGAA
<b>NEET-Q1</b>	CCTGCGAATCCGGAGAGAA
<b>NEET-Q2</b>	CCTGCGAATCCGGAGAGAA
<b>APX1-Q1</b>	GGTGCATGGACATCAAACCC
<b>APX1-Q2</b>	ACAGGGTCGTCCAATAGTGC
<b>PP2AA3-Q1</b>	TAAGGTGGCCAAAATGATGC
<b>PP2AA3-Q2</b>	GTTCTCCACAACCGCTTGGT

**Table 2. Primers used for ChIP-qPCR experiments**

Primer name	Sequence (5'->3')
<b>ProFIT-F</b>	GCTTGTGACAACCTAAACCAGTTGAC
<b>ProFIT-R</b>	ATCGATCAGACCGTATTAATAAAGGT
<b>ProbHLH38-F</b>	CGAATGTTGGAACTTCATTGATTC
<b>ProbHLH38-R</b>	TTTTAATTCCACAATGACGATGGTC
<b>ProbHLH39-F</b>	CCAGTCTACTTGTGACTAGACCTTG
<b>ProbHLH39-R</b>	AACCAAACTTTAAAAATTCGCAAA
<b>ProbHLH100-F</b>	AAGAACATTAGGATATTAATGCCTG
<b>ProbHLH100-R</b>	TAAATTAATAACATTGGGTCACGA
<b>ProbHLH101-F</b>	ACAGCAAACATAAACTTCATGTGG
<b>ProbHLH101-R</b>	GTTATATTTTGAACATGTGAACGCA
<b>ProPYE-F</b>	GAGATGAGCTTTAGTGGCACGC
<b>ProPYE-R</b>	GAAGGTCCGAAGTTGAGGAGGG
<b>ProMYB10-F</b>	GCATAATACATTACCTTCCAACCTCAAC
<b>ProMYB10-R</b>	GAATTCAACTGTGGCCTGTGGG
<b>ProMYB72-F</b>	CAATAAAGTTGGTGGACGATATTTTACG
<b>ProMYB72-R</b>	CGCGACGTCGTGTTACTTG
<b>ProBTS-F</b>	TCCATGTCTCGCGACCAAATG
<b>ProBTS-R</b>	GTGGGTGTTTCTATACATAGGTTTTG
<b>ProBTS1-F</b>	CCTCGTTCGGTCTTCTCTCTTCC
<b>ProBTS1-R</b>	GGTATGGGCTCATTAGTTATAGAAC
<b>ProIMA1-F</b>	GCGGCTTTACAAGTACTGGAC
<b>ProIMA1-R</b>	TATTTGCGTTTGCTGAGCGG
<b>ProIMA2-F</b>	TCTTTGTTTTGCTCGGGGAAG
<b>ProIMA2-R</b>	GGCTTTTATAGGTGGAAGTTAAAGG
<b>ProIMA3-F</b>	TATTCACACTCACGTATGGTAATGG
<b>ProIMA3-R</b>	CCCTTTGTGAAAAGCAAAGAGA
<b>ProF6'H1-F</b>	CAACATGTACAATTTTTTATGTATC
<b>ProF6'H1-R</b>	CCTCAATTTAAAAATATCAATTTG
<b>ProS8H-F</b>	GGTTGGTAAATGAGAAGATATGT
<b>ProS8H-R</b>	CACTTGGTAAACTAGTCGTCGA
<b>ProCYP82C4-F</b>	CTTGTCTCCCTCATCTATCTACTTC
<b>ProCYP82C4-R</b>	GCTCCTCCGCATCAGGTATC
<b>ProFER1-a-F</b>	TGCACTATTCTGCAGCCAA
<b>ProFER1-a-R</b>	AGTTGTAATGTTGGCAAGGACA
<b>ProFER1-b-F</b>	TCCGATTTCTATGTCAATATGTGT
<b>ProFER1-b-R</b>	ATTTCCGGTTCCTACTCTCGC
<b>ProFER1-c-F</b>	CCTCACGTTACACTATCCCA
<b>ProFER1-c-R</b>	GATAGTGTTGAGCCGCCTGA
<b>ProFER3-a-F</b>	TCTCTGTCTTTTGGAGCACAGTGA
<b>ProFER3-a-R</b>	TGTGTGAGCATTTTCATTCTTTACA
<b>ProFER3-b-F</b>	GCCAAAATTACACAAATACCAACGG

<b>ProFER3-b-R</b>	TGTGCGACGAAATTGGAGGA
<b>ProFER4-a-F</b>	TCTTCAATTTGAGGAATGTGCCA
<b>ProFER4-a-R</b>	AGAGTGCATAAGGAAAACAATTTGGT
<b>ProFER4-b-F</b>	AGTGAAAGAGATTTTGAAGCTGCA
<b>ProFER4-b-R</b>	AGGAAAGTTTTCTTCGCGAGA
<b>proNEET-a-F</b>	GCCTATGACCAAATCCTTTGCA
<b>proNEET-a-R</b>	TTGTTCTCAAATTCGTCTAACTAAGT
<b>proNEET-b1-F</b>	ACTTAGTTAGACGAATTTGAGAACAA
<b>proNEET-b1-R</b>	AGCGTGTGTATGAGATGGAAGA
<b>ProNAS4-b-F</b>	GCGACTTCTGTGCATGTGAT
<b>ProNAS4-b-R</b>	TCGTGTCATATCGTGTCTGTG
<b>ProNAS4-a-F</b>	TCAATGTTATTGTTTTCTTGAAATGG
<b>ProNAS4-a-R</b>	ATTTAAATTTTATAACCAAGTGATCGAG
<b>ProNAS4-c-F</b>	TGAGAGTACACGTGCCATCG
<b>ProNAS4-c-R</b>	CGAAATATGAAGACAACACATGC
<b>ProVTL2-b-F</b>	CAGTGTACAAAGTGATGTACAAACGA
<b>ProVTL2-b-R</b>	CGGTGTAGAAGGTGATTTATGG
<b>ProVTL2-a-F</b>	TGTGTGCAAACAAGTGACGA
<b>ProVTL2-a-R</b>	TGATGGATTGGTGAATTGGA

**Table 3. Primers used for yeast two-hybrid experiments**

<b>Primer name</b>	<b>Sequence (5'-&gt;3')</b>
<b>bHLH121-AD/BD-B1</b>	ggggacaagtttgtacaaaaaagcaggctTCATGGGGATAAGAGAAAATGG
<b>bHLH121-AD/BD-B2</b>	ggggaccacttttgtacaagaaagctgggtcTCATTTTGCATCATCAGGTTTTTGG
<b>bHLH11-AD/BD-B1</b>	ggggacaagtttgtacaaaaaagcaggctTCATGGATCAACCAATGAAACC
<b>bHLH11-AD/BD-B2</b>	ggggaccacttttgtacaagaaagctgggtcTTATGGCTTCAACATGTCATTTAC
<b>bHLH34-AD/BD-B1</b>	ggggacaagtttgtacaaaaaagcaggctTCATGTATCCATCAATCGAAGAC
<b>bHLH34-AD/BD-B2</b>	ggggaccacttttgtacaagaaagctgggtcTTAAGCAACAGGAGGAAGAT
<b>bHLH104-AD/BD-B1</b>	ggggacaagtttgtacaaaaaagcaggctTCATGTATCCTTCTCTCGACGATG
<b>bHLH104-AD/BD-B2</b>	ggggaccacttttgtacaagaaagctgggtcTTAAGCAGCAGGAGGCCTGAG
<b>bHLH115-AD/BD-B1</b>	ggggacaagtttgtacaaaaaagcaggctTCATGGTGTCTCCGGAGAATACG
<b>bHLH115-AD/BD-B2</b>	ggggaccacttttgtacaagaaagctgggtcTTAAGCAACTGGAGGACGAAG
<b>ILR3-AD/BD-B1</b>	ggggacaagtttgtacaaaaaagcaggctTCATGGTGTACCCGAAAACGC
<b>ILR3-AD/BD-B2</b>	ggggaccacttttgtacaagaaagctgggtcTTAAGCAACAGGAGGACGAAGG
<b>PYE-AD/BD-B1</b>	ggggacaagtttgtacaaaaaagcaggctTCATGGTATCGAAAACCTCCTTC
<b>PYE-ADBD-B2</b>	ggggaccacttttgtacaagaaagctgggtcTCATTCACTGGCTTTTCAGCC

**Table 4. Primers used for BiFC experiments**

Primer name	Sequence (5'->3')
<b>bHLH121-N/Cter-B1</b>	CGCGGATCCATGGGGATAAGAGAAAATGG
<b>bHLH121-N/Cter-B2</b>	CGGGGTACCTTTTGCATCATCAGGTTTTTGG
<b>bHLH11-Nter-B1</b>	CGCGGATCCATGGATCAACCAATGAAACC
<b>bHLH11-Nter-B2</b>	CGGGTCGACTGGCTTCAACATGTCATTTAC
<b>bHLH34-Nter-B1</b>	CGCGGATCCATGTATCCATCAATCGAAGAC
<b>bHLH34-Nter-B2</b>	CGGGGTACCAGCAACAGGAGGAAGATTTTTGAG
<b>bHLH104-Nter-B1</b>	CGCGGATCCATGTATCCTTCTCTCGACGATG
<b>bHLH104-Nter-B2</b>	CGGGGTACCAGCAGCAGGAGGCCTGAGTTC
<b>bHLH115-Nter-B1</b>	CGCGGATCCATGGTGTCTCCGGAGAATACG
<b>bHLH115-Nter-B2</b>	CGGGGTACCAGCAACTGGAGGACGAAGGAC
<b>ILR3-Nter-B1</b>	GGACTAGTATGGTGTCAACCGAAAACGC
<b>ILR3-Nter-B2</b>	CGGGGTACCAGCAACAGGAGGACGAAGGAC

**Table 5. Primers used for cDNA cloning**

Primer name	Sequence (5'->3')
<b>cbHLH121-Stop-B1</b>	ggggacaagtttgtacaaaaaagcaggctTCATGGGGATAAGAGAAAATGG
<b>cbHLH121- Stop-B2</b>	ggggaccactttgtacaagaaagctgggtcTCATTTTGCATCATCAGGTTTTTT GG
<b>cbHLH121-B1</b>	ggggacaagtttgtacaaaaaagcaggctTCATGGGGATAAGAGAAAATGG
<b>cbHLH121-B2</b>	ggggaccactttgtacaagaaagctgggtcTTTTGCATCATCAGGTTTTTTGG
<b>cFIT- Stop-B1</b>	ggggacaagtttgtacaaaaaagcaggctTCATGGAAGGAAGAGTCAACGC
<b>cFIT- Stop-B2</b>	ggggaccactttgtacaagaaagctgggtcTCAAGTAAATGACTTGATGAATT C
<b>cbHLH39- Stop-B1</b>	ggggacaagtttgtacaaaaaagcaggctTCATGTGTGCATTAGTACCTCC
<b>cbHLH39- Stop-B2</b>	ggggaccactttgtacaagaaagctgggtcTCATATATATGAGTTTCCACATT C
<b>cbHLH34-B1</b>	ggggacaagtttgtacaaaaaagcaggctTCATGTATCCATCAATCGAAGAC
<b>cbHLH34-B2</b>	ggggaccactttgtacaagaaagctgggtcAGCAACAGGAGGAAGATTTTTTGA G
<b>cbHLH104-B1</b>	ggggacaagtttgtacaaaaaagcaggctTCATGTATCCTTCTCTCGACGATG
<b>cbHLH104-B2</b>	ggggaccactttgtacaagaaagctgggtcAGCAGCAGGAGGCCTGAGTTCTT G
<b>cbHLH105-B1</b>	ggggacaagtttgtacaaaaaagcaggctTCATGGTGTACCCGAAAACGC
<b>cbHLH105-B2</b>	ggggaccactttgtacaagaaagctgggtcAGCAACAGGAGGACGAAGGACAT G
<b>cbHLH115-B1</b>	ggggacaagtttgtacaaaaaagcaggctTCATGGTGTCTCCGGAGAATACG
<b>cbHLH115-B2</b>	gggaccactttgtacaagaaagctgggtcAGCAACTGGAGGACGAAGGACATG G
<b>cFER1- Stop-B1</b>	ggggacaagtttgtacaaaaaagcaggcttcTATGTTGGAAACGCTATCATC
<b>cFER1- Stop-B2</b>	gggaccactttgtacaagaaagctgggtcCTACAATCTTATTAGTCC



**Table 6. Primers used for promoter and genomic DNA cloning**

<b>Primer name</b>	<b>Sequence (5'-&gt;3')</b>
<b>pbHLH121-B1</b>	ggggacaagtttgtacaaaaaagcaggctAATAGTTATCACATGGAAACGGC
<b>pbHLH121-B2</b>	ggggaccactttgtacaagaaagctgggtcTTTTTCAATTATTTAATTA
<b>cbHLH121-B2</b>	ggggaccactttgtacaagaaagctgggtcTTTTGCATCATCAGGTTTTTGG
<b>pbHLH34-B1</b>	ggggacaagtttgtacaaaaaagcaggctTCACCAAAGATACTCTCAGCCTCTCAC
<b>cbHLH34-B2</b>	ggggaccactttgtacaagaaagctgggtcAGCAACAGGAGGAAGATTTTTGAG
<b>pbHLH104-B1</b>	ggggacaagtttgtacaaaaaagcaggctTCGTGATCTAGCACTCATCCTCAAATCC
<b>cbHLH104-B2</b>	ggggaccactttgtacaagaaagctgggtcAGCAGCAGGAGGCTGAGTTCTTG
<b>cbHLH105-B1</b>	ggggacaagtttgtacaaaaaagcaggctTCATGGCAAATTCATGCCTTCA
<b>cbHLH105-B2</b>	ggggaccactttgtacaagaaagctgggtcAGCAACAGGAGGACGAAGGACATG
<b>pbHLH115-B1</b>	ggggacaagtttgtacaaaaaagcaggctTCAAGCGGAACAAAACCTTGGGG
<b>cbHLH115-B2</b>	gggaccactttgtacaagaaagctgggtcAGCAACTGGAGGACGAAGGACATGG

**Table 7. Primers used for mutant screening**

<b>Primer name</b>	<b>Sequence (5'-&gt;3')</b>
<b>bhlh121-F</b>	ATGGGGATAAGAGAAAATGGAATAATGC
<b>bhlh121-R</b>	GAACAGTATCAGTCAGAATCGTGGCT
<b>bhlh34-LP</b>	TGGAAATCTTGAGCAAGTTTGT
<b>bhlh34-RP</b>	ATCACATCAAACAACGAAATGG
<b>bhlh104-1-LP</b>	GGGGAAAGGTTGTGTCTTTTG
<b>bhlh104-1-RP</b>	GCCTGAGTTCTTGATCACGAG
<b>irl3-1-LP</b>	AGAAATCGCTATGGAATTGTTTATGGTTCT
<b>irl3-1-RP</b>	CATTGTTCAACAGATAACAGTTACGATGAT
<b>irl3-3-LP</b>	TCAATCAATTCCTGAATCAAG
<b>irl3-3-RP</b>	CTTGCCACTATACCGATTTTG
<b>bhlh115-LP</b>	CGCTGAGGTAATTCCTCTTCC
<b>bhlh115-RP</b>	CAGAGGAACGTAAGCAAAACG

**Table 8. Mutants used in this study**

<b>Locus Name</b>	<b>Mutant name</b>	<b>Source</b>
AT3G19860	<i>bhlh121-1,bhlh-2,bhlh-4</i>	Crisper -CAS9 lines
AT3G23210	<i>bhlh34-1</i>	CS411089
AT4G14410	<i>bhlh104</i>	Salk_099496C
AT5G54680	<i>irl3-1</i>	Rampey et al., 2006
AT5G54680	<i>irl3-3</i>	Salk_043690C
AT1G51070	<i>bhlh115</i>	WiscDsLox384D9
AT3G13610	<i>f6'h1-1</i>	SALK_132418C
AT4G31940	<i>cyp82c4-1</i>	SALK_001585
AT5G01600	<i>fer1,3,4</i>	SALK_055487
AT3G56090		GABI-KAT_496A08
AT2G40300		SALK_068620



# The Transcriptional Control of Iron Homeostasis in Plants: A Tale of bHLH Transcription Factors?

Fei Gao<sup>†</sup>, Kevin Robet, Frederic Gaymard, Esther Izquierdo and Christian Dubos\*

BPMP, CNRS, INRA, Montpellier SupAgro, University of Montpellier, Montpellier, France

## OPEN ACCESS

### Edited by:

Thomas J. Buckhout,  
Humboldt-Universität zu Berlin,  
Germany

### Reviewed by:

Takanori Kobayashi,  
Ishikawa Prefectural University, Japan  
Tzvetina Brumbarova,  
Heinrich-Heine-Universität Düsseldorf,  
Germany

### \*Correspondence:

Christian Dubos  
christian.dubos@inra.fr

<sup>†</sup>These authors have contributed  
equally to this work

### Specialty section:

This article was submitted to  
Plant Nutrition,  
a section of the journal  
Frontiers in Plant Science

**Received:** 16 November 2018

**Accepted:** 07 January 2019

**Published:** 18 January 2019

### Citation:

Gao F, Robe K, Gaymard F,  
Izquierdo E and Dubos C (2019) The  
Transcriptional Control of Iron  
Homeostasis in Plants: A Tale  
of bHLH Transcription Factors?  
Front. Plant Sci. 10:6.  
doi: 10.3389/fpls.2019.00006

Iron is one of the most important micronutrients in plants as it is involved in many cellular functions (e.g., photosynthesis and respiration). Any defect in iron availability will affect plant growth and development as well as crop yield and plant product quality. Thus, iron homeostasis must be tightly controlled in order to ensure optimal absorption of this mineral element. Understanding mechanisms governing iron homeostasis in plants has been the focus of several studies during the past 10 years. These studies have greatly improved our understanding of the mechanisms involved, revealing a sophisticated iron-dependent transcriptional regulatory network. Strikingly, these studies have also highlighted that this regulatory web relies on the activity of numerous transcriptional regulators that belong to the same group of transcription factors (TF), the bHLH (basic helix-loop-helix) family. This is best exemplified in Arabidopsis where, to date, 16 bHLH TF have been characterized as involved in this process and acting in a complex regulatory cascade. Interestingly, among these bHLH TF some form specific clades, indicating that peculiar function dedicated to the maintenance of iron homeostasis, have emerged during the course of the evolution of the green lineage. Within this mini review, we present new insights on the control of iron homeostasis and the involvement of bHLH TF in this metabolic process.

**Keywords:** basic helix loop helix, bHLH, iron, homeostasis, *Arabidopsis thaliana*

## INTRODUCTION

Iron (Fe) is one of the most important micronutrient elements in plants as it is involved in many cellular functions (e.g., photosynthesis and respiration). Any defect in Fe availability will impact plant growth and development as well as crop yield and plant product quality (Briat et al., 2015).

In order to cope with Fe shortage and recover Fe from soil, where it is in poorly available forms, plants have evolved two strategies. The first one, strategy I, is used by all dicots and non-graminaceous monocots. This strategy consists in rhizosphere acidification via proton extrusion in order to promote Fe solubility and involves proton-ATPase such as AHA2. The secretion by the root of Fe-mobilizing phenolic compounds facilitates this process (Fourcroy et al., 2014, 2016). Fe<sup>3+</sup> is thus reduced into Fe<sup>2+</sup> by ferric chelate reductases, such as FRO2 (FERRIC REDUCTION OXIDASE 2), prior to being transported across the rhizodermis cell membranes by IRT1 (IRON-REGULATED TRANSPORTER 1) (Brumbarova et al., 2015). The second strategy, strategy II, is used by graminaceous species. This strategy consists in releasing phytosiderophores into the rhizosphere to chelate Fe<sup>3+</sup> (Nozoye et al., 2011). Fe<sup>3+</sup>-phytosiderophores chelates are then transported into the roots by the YELLOW STRIPE 1 transporter (Curie et al., 2001). If the machinery

allowing plant Fe uptake from the soil is central for the maintenance of Fe homeostasis, this is indeed not the sole mechanism involved in this process. It also necessitates several genes encoding proteins involved in Fe transport, compartmentation and storage, at the cellular and subcellular levels, throughout the entire plant body. Such complex mechanism must thus be tightly regulated in order to avoid any physiological situation that would be deleterious to the plant.

How, at the molecular level, plants control Fe homeostasis has thus been a critical question for several years. This question has been mostly addressed by studying plant response to Fe deficiency, in particular in the model plant *Arabidopsis thaliana*. These studies have highlighted that such response involves an intricate network of basic helix-loop-helix (bHLH) transcription factors (TF) (**Figure 1**). bHLH proteins form one of the largest family of TFs found in plants that act as homo- or heterodimers to regulate the expression of their target genes. In *Arabidopsis*, 133 members have been identified and divided into 12 clades (Heim et al., 2003). From what is known on the role played by several members of this family of TFs in plants, it appears that their participation in the control of Fe homeostasis is unique by the number of individual TFs and different clades that are involved as well as by the intricacy of the network they form.

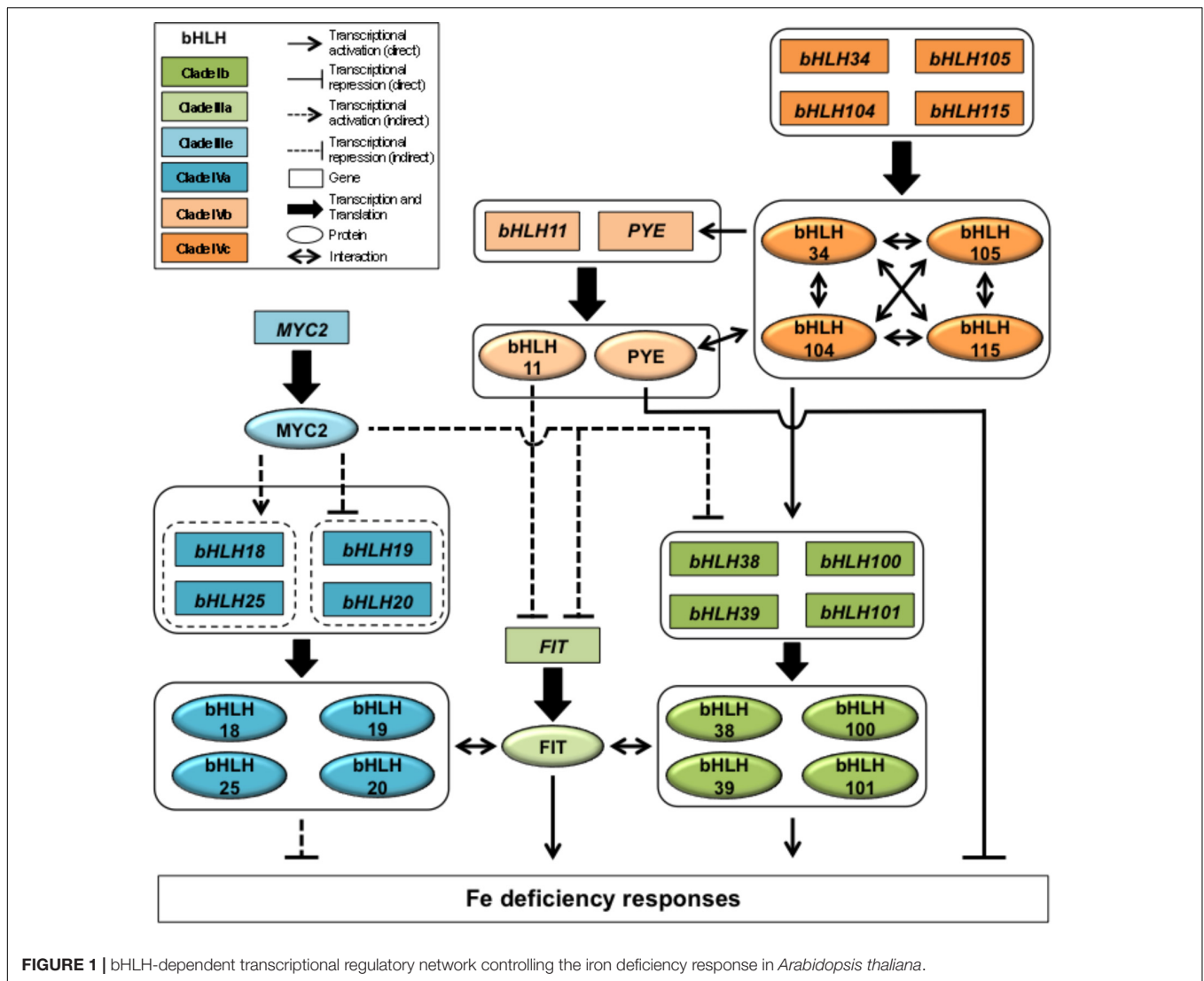
## THE MOLECULAR REGULATION OF PLANT IRON HOMEOSTASIS

### The bHLH Regulatory Network

Upstream from the regulatory network involved in *Arabidopsis* Fe deficiency response are four bHLH TFs belonging to the clade IVc, namely bHLH34, bHLH104, bHLH105/ILR3 (IAA-LEUCINE RESISTANT3), and bHLH115 (**Figure 1**). These four TFs, shown to interact *in vivo* in the form of homo- or heterodimers, act as transcriptional activators of the plant response to Fe deficiency and display partial redundant activities (Zhang et al., 2015; Li et al., 2016; Liang et al., 2017). Clade IVc bHLH targets consist of *bHLH47/PYE* (*POPEYE*; clade IVb) and four clade Ib bHLH genes (*bHLH38*, *bHLH39*, *bHLH100*, and *bHLH101*) (Colangelo and Gueriot, 2004; Wang et al., 2007; Yuan et al., 2008; Wang N. et al., 2013; Zhang et al., 2015). *PYE* acts as a transcriptional repressor. For example, *PYE* was shown to inhibit the expression of *NAS4* (*NICOTIANAMINE SYNTHASE 4*), a key gene involved in phloem-based transport of Fe to sink organs, and *FRO3*, a Fe reductase located in root vasculature mitochondria (Jeong and Connolly, 2009; Klatte et al., 2009; Long et al., 2010). Interestingly, *PYE* can interact *in vivo* with bHLH104, ILR3, and bHLH115 (Long et al., 2010; Zhang et al., 2015). Whether or not these interactions play a role in the plant response to Fe deficiency or in the control of Fe homeostasis is an important question that remains to be elucidated. In contrast, bHLH38, bHLH39, bHLH100, and bHLH101 are partially redundant proteins that function at the root epidermis as positive regulators of *FRO2* and *IRT1*. This activity relies on their interaction with FIT (Fe-deficiency induced transcription factor), a clade IIIa bHLH (Colangelo and Gueriot, 2004;

Yuan et al., 2008; Wang N. et al., 2013; Maurer et al., 2014). *FIT* expression is likely controlled, at least in part, by a feed forward regulatory loop involving bHLH39 (Naranjo-Arcos et al., 2017). bHLH6/MYC2 (clade IIIe) is a master regulator of the jasmonic acid (JA) signaling pathway whose activity differentially affects the expression clade IVa bHLH (bHLH18, bHLH19, bHLH20, and bHLH25) genes to modulate FIT protein accumulation (Cui et al., 2018). This mechanism relies on the direct interaction of clade IVa bHLHs with FIT in order to promote its degradation via the 26S proteasome pathway (Cui et al., 2018). In addition, MYC2 is a JA-dependent repressor of *FIT* and clade Ib bHLH genes expression, hence inhibiting FIT-dependent Fe uptake machinery at the transcriptional and posttranslational levels (Cui et al., 2018). Interestingly, *bHLH11*, another clade IVb bHLH, was recently proposed to be a negative regulator of FIT-dependent Fe uptake mechanism effecting Fe levels in *Arabidopsis* plants (Tanabe et al., 2018).

Altogether, this is 16 bHLH TFs out of the 133 present in *Arabidopsis* that have been identified as involved in the control of the Fe deficiency response, which represent more than 12% of the members of this large family of TFs (Heim et al., 2003). Indeed, orthologous members from the above-described clades were identified in other strategy I plant species such as tomato, apple, or soybean (Ling et al., 2002; Du et al., 2015; Zhao et al., 2016b; Li et al., 2018). In soybean, it is likely that the orthologs of *FIT* (*GmbHLH57*) and clade Ib bHLH (*GmbHLH300*) genes may also play a role in nodules, a tissue where several enzymes involved in symbiotic nitrogen fixation require Fe for their activity (Tang et al., 1990; O'Hara, 2001; Li et al., 2018). With the exception of FIT, which is specific to strategy I plants, orthologs of several bHLH are present in strategy II plants, indicating that the regulatory cascade controlling plant response to Fe deficiency is mostly conserved within the plant kingdom. For instance, orthologs of clade Ib (*OsIRO2*), IVc (*OsPRI1*), *PYE* (*OsIRO3*) and *MYC2* (*OsMYC2*) genes have been characterized in rice (Ogo et al., 2007; Zheng et al., 2010; Ogawa et al., 2017; Zhang et al., 2017). However, no orthologous bHLH TF in strategy I plants has been described so far for *OsbHLH133*, another regulator of the Fe deficiency response in rice (Wang L. et al., 2013). Is *OsbHLH133* function specific to strategy II plants as it is the case for FIT in strategy I plants? Protein sequence analysis tends to indicate that *OsbHLH133* is closely related to the bHLH clade VIIIc and thus it might be that this clade plays a role in the control of Fe homeostasis in both strategy I and II plants. If this hypothesis is verified, it will certainly render more complicated our understanding of this transcriptional regulatory network. Indeed, it is not the complexity of this network that is intriguing considering that any defect in the control of Fe homeostasis might be deleterious to the plants. The main question is why so many bHLHs are involved in this process? If it is difficult to answer this question, the involvement of a large number of TFs from one family in a specific process has already been described. This is the case with the R2R3-MYB family where at least 19 members out of 122 (about 16%) are involved in the control of the phenylpropanoid pathway (Dubos et al., 2010; Zamioudis et al., 2014; Xu et al., 2015). From these observations it would be tempting to speculate that during the course of the evolution



of the green lineage, TF families have evolved specialized roles, in which plant Fe homeostasis would be mostly regulated by TFs belonging to the bHLH gene family.

How these bHLH TFs interact with the *cis*-regulatory sequences usually present in the promoter of their target genes is an important question considering that (i) each bHLH must specifically recognize its own target and (ii) the number of bHLH involved in this complex network. Indeed, it is well known that bHLH TFs bind to specific DNA motifs (*CANNTG*) named *E-box*, and in particular to the canonical *CACGTG* sequence, named *G-box* (De Masi et al., 2011). For instance, chromatin immunoprecipitation assays showed that PYE, bHLH104, bHLH115, ILR3, and FIT preferentially bound to the promoter of their target genes in regions that contain *E-box* or *G-box* (Long et al., 2010; Zhang et al., 2014, 2015; Liang et al., 2017). Similar observations were made, using biochemical approaches, for MbHLH104 and OsPRI1 (Zhao et al., 2016a; Zhang et al., 2017). Interestingly, it was demonstrated that the genomic regions flanking *E-box* binding sites influence the DNA

binding specificity of TFs (Gordan et al., 2013; Ezer et al., 2017). This is for example the case for OsIRO2 that binds preferentially to *CACGTGG* motif (Ogo et al., 2007). Hence, despite the fact that several direct target genes have been identified for most of the bHLH involved in the transcriptional control of Fe homeostasis and the fact that it is possible to infer the *E-box* sequence recognized by a given bHLH dimer based on bHLH domain compositions (De Masi et al., 2011), very little is known on the actual bHLH/DNA interactions.

### The Other Actors Involved in the Transcriptional Control of Plant Fe Homeostasis

Additional TFs, from several gene families, involved in the control of Fe homeostasis in both strategy I and strategy II plant species, have also been characterized.

MYB10 and MYB72, two R2R3-MYB TFs whose expression is partially dependent on FIT, are involved in Fe acquisition

and distribution by notably regulating the expression of *BGLU42* and *NAS4* (Palmer et al., 2013; Stringlis et al., 2018). A closely related apple R2R3-MYB, MdMYB58, was recently reported as potentially involved in the control of Fe transport and tissue partitioning. It is proposed that MdMYB58 activity is repressed by its heterodimerization with MdSAT1, a clade IVa bHLH (Wang et al., 2018). WRKY46 plays a critical role in Fe translocation from root to shoot by directly repressing the expression of *VITL1/VTL1* (*vacuolar iron transporter like 1*) (Yan et al., 2016). ERF4 and ERF72 (AP2/ERF TFs) play negative roles in plant response to Fe deficiency by inhibiting the expression of genes involved in Fe uptake such as *IRT1* or *AHA2* (Liu et al., 2017a,b). Two TFs (EIL family) involved in ethylene signaling (EIN3, ETHYLENE INSENSITIVE 3 and EIL1, ETHYLENE INSENSITIVE 3 LIKE 1) and ZAT12 (a C2H2-type plant-specific zinc finger TF) are also involved by modulating FIT stability (Lingam et al., 2011; Le et al., 2016). Two MYB-CC TFs (PHR1, PHOSPHATE STARVATION RESPONSE 1 and PHL1, PHR1-LIKE 1), that play a central role in the phosphate deficiency response, regulate the expression of the main Fe storage ferritin gene in Arabidopsis (*AtFER1*), indicating that they act as integrators of both the phosphate and Fe signaling pathways (Bournier et al., 2013).

IDEF1 (ABI3/VP1 family) is an early regulator of Fe deficiency response in rice that directly binds to divalent metals suggesting that IDEF1 is a cellular sensor of metal ion balance caused by changes in Fe availability (Kobayashi et al., 2009, 2012). IDEF2 (NAC family) and OsARF16 (ARF family) play also critical roles in the control of Fe homeostasis in rice by modulating the expression of Fe-related genes and by integrating auxin signals, respectively (Ogo et al., 2008; Shen et al., 2015).

## THE MOLECULAR REGULATION OF THE TRANSCRIPTIONAL REGULATORY CASCADE CONTROLLING IRON HOMEOSTASIS

### Post-translational Regulation of bHLH TFs

Iron deficiency results in a transcriptional response that leads to the activation of the Fe uptake machinery, which could lead to a Fe overload if it becomes suddenly available or to a toxic overaccumulation of other divalent metals (e.g., Zn, Mn, and Cd) due to the low specificity of *IRT1*. To cope with this, plants have developed posttranslational mechanisms such as the continuous recycling of *IRT1* (Barberon et al., 2011, 2014). In addition, in Arabidopsis, *IRT1* phosphorylation and ubiquitination leads to its internalization and subsequent degradation, a process that is triggered by direct binding of *IRT1* to non-Fe metals (Ivanov et al., 2014; Dubeaux et al., 2018). However, maintaining Fe homeostasis requires also to tightly regulating, at the posttranslational level, the TFs involved in this process.

Fe-deficiency induced TF posttranslational regulation has been extensively investigated in Arabidopsis. For instance, it

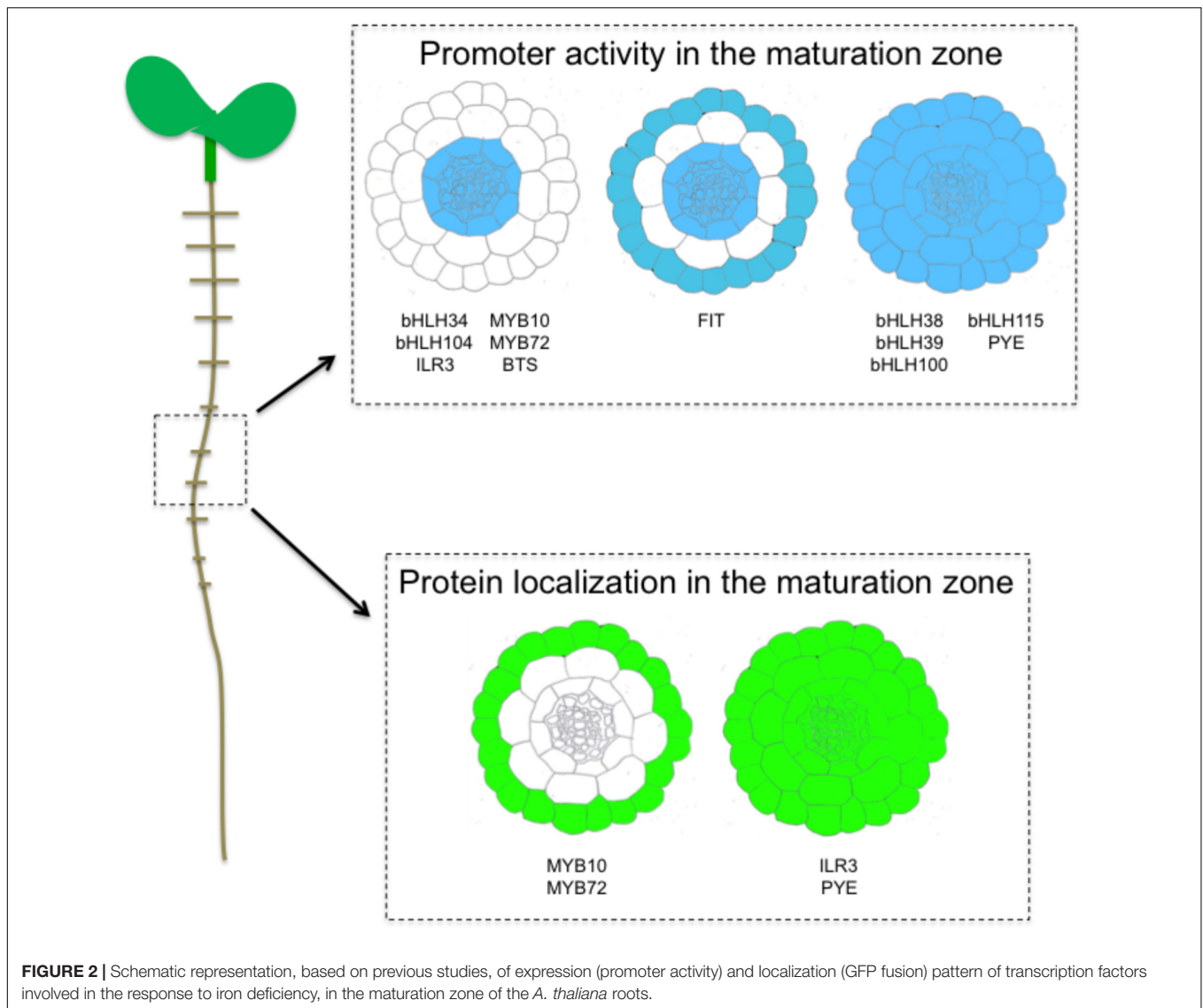
was shown that FIT heterodimerization with clade IVa bHLH promotes its degradation via the 26S proteasome pathway, whereas its interaction with clade Ib bHLH promotes its stability (Cui et al., 2018). FIT interaction with EIN3 or EIL1 also promotes its stability and contributes to Fe acquisition during the early stage of Fe deficiency (Lingam et al., 2011). In contrary, FIT interaction with ZAT12 has an inhibitory effect on its function when plants are grown under Fe sufficiency or prolonged Fe deficiency conditions (Le et al., 2016).

Several ubiquitin E3 ligases targeting bHLH TFs involved in the response to Fe deficiency have been characterized. *BRUTUS* (*BTS*), whose expression is induced upon Fe deficiency, is thought to be a Fe-sensing negative regulator in Arabidopsis (Selote et al., 2015). *In vitro* analyses suggest that *BTS* restricts the accumulation of *ILR3* and *bHLH115* through its RING E3 ligase activity and mediates their 26S proteasomal degradation (Selote et al., 2015). Whether the interaction of *bHLH104* with *BTS* participate to its degradation remains to be demonstrated (Selote et al., 2015). The identification of two *BTS* orthologues in rice, namely *OsHRZ1* [HEMERYTHRIN MOTIF-CONTAINING REALLY INTERESTING NEW GENE (RING) AND ZINC-FINGER PROTEIN 1] and *OsHRZ2*, suggests that *BTS* function is conserved in strategy II plants (Kobayashi et al., 2013). In addition to *BTS*, two closely related RING E3 ligases named *BTSL1* and *BTSL2* (*BRUTUS LIKE 1* and *2*) are proposed to negatively regulate the Fe deficiency responses by directly targeting FIT, leading to its degradation (Sivitz et al., 2011; Hindt et al., 2017; Rodriguez-Celma et al., 2018). Interestingly, it was shown in apple that a cullin-based E3 ligase mechanism, involving two BTB-TAZ proteins (*MdbT1* and *MdbT2*) and *MdCUL3*, target *MdbHLH104* for ubiquitin-dependent degradation via the 26S proteasome (Zhao et al., 2016a). Unlike *BTS* and the E3 ligase degrading FIT, *MdbT* expression and protein accumulation is induced when Fe availability is not limiting, leading to *MdbHLH104* degradation (Zhao et al., 2016a). In addition, *MdbHLH104* sumoylation, by the SUMO E3 ligase *MdSIZ1*, promotes *MdbHLH104* stability, especially when Fe availability is scarce (Zhou et al., 2018). These findings suggest that the degradation of the bHLHs involved in the plant response to Fe availability may require two types of ubiquitin E3 ligases and that sumoylation may also have an important role in this process.

### bHLH Promoter Activity and Protein Localization

Iron uptake and translocation to the whole plant body requires coordinating the expression of several structural genes within and between the different cell types of roots that is achieved by the involvement of several TFs, in particular bHLHs (Figure 2).

Clade IVc bHLHs analysis of promoter activity revealed a specific expression in the stele (pericycle) of the root in the maturation zone (Li et al., 2016; Liang et al., 2017). Root tip expression was also detected except for *bHLH115*, whereas *ILR3* was the sole bHLH from this clade to be expressed in the elongation zone of root tips and early lateral roots. These differences suggest that non-redundant biological functions may



exist between the members of this clade (Liang et al., 2017). For instance, ILR3 was shown to participate in the plant response to biotic and abiotic stresses (Samira et al., 2018). Perivascular expression has also been observed in the aerial part of the plants (i.e., hypocotyl and leaves) (Rampey et al., 2006; Zhang et al., 2015; Li et al., 2016; Liang et al., 2017). Promoter activity of *PYE* is similar in roots to that of *bHLH115*. In these cells *PYE* represses the expression of *NAS4* and *FRO3*, modulating Fe translocation to the above ground part of the plant (Long et al., 2010). Clade Ib bHLHs (except *bHLH101* whose promoter is not active in roots) were expressed throughout the root including the stele cells, which was in contrast with the expression pattern of their regulators, the clade IVc bHLH TFs (Wang et al., 2007). Clade Ib bHLHs promoter activity was essentially detected in the epidermis in the maturation zone, in the epidermis and inside the roots in the upper part zone (but not in the stele), and at the lateral root emergence site. However, a comparable pattern of expression with clade IVc bHLHs was observed in leaves. The

apparent discrepancy observed in roots between the expression of clade Ib bHLHs and their transcriptional regulators suggests that clade IVc bHLH TFs may act in various cell types and thus have the ability to move from one cell type to another. In a recent study, it was shown that ILR3 protein is present in all root cell type when Fe availability is scarce (Samira et al., 2018). If this observation supports the hypothesis that ILR3 may move from the stele to other cell layers, it cannot be excluded that the promoter of *ILR3* is not sufficient for proper *ILR3* expression, and that sequences present in the coding region (e.g., introns) might be required. Interestingly, the pattern of *PYE* accumulation in root cells is similar to that of *ILR3* (Long et al., 2010). The fact that *ILR3* and *PYE* are present in the same cell layers and interact *in vivo* suggest that *PYE* function in the plant response to Fe deficiency might be tightly connected to *ILR3* activity (Long et al., 2010; Selote et al., 2015). What would be the role of such heterodimers is still a matter of debate. Nevertheless, if the inter cellular trafficking of these two TFs was proven to be



true, decrypting the underlying mechanisms would be the next challenge.

Fe-deficiency induced TF expression is mostly restricted to root tissues. At the rhizodermis, *FIT* expression overlaps those of its bHLH interacting partners from clade Ib (Colangelo and Gueriot, 2004; Jakoby et al., 2004). This is in agreement with the heterodimerization of FIT with clade Ib bHLHs to regulate the expression of Fe mobilization genes such as *IRT1* and *FRO2*. Two other TFs whose expression is partly regulated by FIT in response to Fe deficiency, namely MYB10 and MYB72, are mainly localized at the rhizodermis where they control the expression of *BGLU42* (Zamioudis et al., 2014). In the maturation zone, *FIT* is expressed in the epidermis and throughout the stele (Jakoby et al., 2004). Clade IVa bHLHs promoter activity is specific to the stele, a tissues where the repressive role of the encoded proteins on FIT stability is counteracted by FIT heterodimerization with clade Ib bHLHs (Cui et al., 2018). In the aerial part of the plant, clade IVa expression follows the vasculature as it is the case for ILR3 or clade Ib bHLHs.

## CONCLUSION

To date several TFs involved in the control of Fe homeostasis have been characterized and several molecular connections have been identified. However we still do not know how the expression of the most upstream TFs of this network is regulated (i.e., FIT,

clade IVc bHLH), indicating that we still do not have the full set of TFs involved in this network. Whether or not the Fe deficiency and Fe excess responses are controlled by an integrated pathway involving common players is still an open question that remains to be addressed. Last, deciphering the precise localization, at the protein level, of all the TFs involved in the control of Fe homeostasis is an important task that should be achieved if one aims at fully decrypting the functioning of this intricate molecular network.

## AUTHOR CONTRIBUTIONS

FeG, KR, FrG, EI, and CD wrote the manuscript. FeG, KR, and CD made the figures.

## FUNDING

KR and FeG were supported by a fellowship from the Agence Nationale pour la Recherche (ANR-17-CE20-0008-01) and from the China Scholarship Council (CSC), respectively.

## ACKNOWLEDGMENTS

We thank Dr. N. Berger for help in preparing this manuscript.

## REFERENCES

- Barberon, M., Dubeaux, G., Kolb, C., Isono, E., Zelazny, E., and Vert, G. (2014). Polarization of IRON-REGULATED TRANSPORTER 1 (IRT1) to the plant-soil interface plays crucial role in metal homeostasis. *Proc. Natl. Acad. Sci. U.S.A.* 111, 8293–8298. doi: 10.1073/pnas.1402262111
- Barberon, M., Zelazny, E., Robert, S., Conejero, G., Curie, C., Friml, J., et al. (2011). Monoubiquitin-dependent endocytosis of the iron-regulated transporter 1 (IRT1) transporter controls iron uptake in plants. *Proc. Natl. Acad. Sci. U.S.A.* 108, E450–E458. doi: 10.1073/pnas.1100659108
- Bournier, M., Tissot, N., Mari, S., Boucherez, J., Lacombe, E., Briat, J. F., et al. (2013). *Arabidopsis* ferritin 1 (AtFer1) gene regulation by the phosphate starvation response 1 (ATPHR1) transcription factor reveals a direct molecular link between iron and phosphate homeostasis. *J. Biol. Chem.* 288, 22670–22680. doi: 10.1074/jbc.M113.482281
- Briat, J. F., Dubos, C., and Gaymard, F. (2015). Iron nutrition, biomass production, and plant product quality. *Trends Plant Sci.* 20, 33–40. doi: 10.1016/j.tplants.2014.07.005
- Brumbarova, T., Bauer, P., and Ivanov, R. (2015). Molecular mechanisms governing *Arabidopsis* iron uptake. *Trends Plant Sci.* 20, 124–133. doi: 10.1016/j.tplants.2014.11.004
- Colangelo, E. P., and Gueriot, M. L. (2004). The essential basic helix-loop-helix protein FIT1 is required for the iron deficiency response. *Plant Cell* 16, 3400–3412. doi: 10.1105/tpc.104.024315
- Cui, Y., Chen, C. L., Cui, M., Zhou, W. J., Wu, H. L., and Ling, H. Q. (2018). Four IVa bHLH transcription factors are novel interactors of FIT and mediate JA inhibition of iron uptake in *Arabidopsis*. *Mol. Plant* 11, 1166–1183. doi: 10.1016/j.molp.2018.06.005
- Curie, C., Panaviene, Z., Loulergue, C., Dellaporta, S. L., Briat, J. F., and Walker, E. L. (2001). Maize yellow stripe1 encodes a membrane protein directly involved in Fe(III) uptake. *Nature* 409, 346–349. doi: 10.1038/35053080
- De Masi, F., Grove, C. A., Vedenko, A., Alibes, A., Gisselbrecht, S. S., Serrano, L., et al. (2011). Using a structural and logics systems approach to infer bHLH-DNA binding specificity determinants. *Nucleic Acids Res.* 39, 4553–4563. doi: 10.1093/nar/gkr070
- Du, J., Huang, Z., Wang, B., Sun, H., Chen, C., Ling, H. Q., et al. (2015). SlbHLH068 interacts with FER to regulate the iron-deficiency response in tomato. *Ann. Bot.* 116, 23–34. doi: 10.1093/aob/mcv058
- Dubeaux, G., Neveu, J., Zelazny, E., and Vert, G. (2018). Metal sensing by the IRT1 transporter-receptor orchestrates its own degradation and plant metal nutrition. *Mol. Cell* 69, 953.e5–964.e5. doi: 10.1016/j.molcel.2018.02.009
- Dubos, C., Stracke, R., Grotewold, E., Weisshaar, B., Martin, C., and Lepiniec, L. (2010). MYB transcription factors in *Arabidopsis*. *Trends Plant Sci.* 15, 573–581. doi: 10.1016/j.tplants.2010.06.005
- Ezer, D., Shepherd, S. J. K., Brestovitsky, A., Dickinson, P., Cortijo, S., Charoensawan, V., et al. (2017). The G-Box transcriptional regulatory code in *Arabidopsis*. *Plant Physiol.* 175, 628–640. doi: 10.1104/pp.17.01086
- Fourcroy, P., Siso-Terraza, P., Sudre, D., Saviron, M., Rey, G., Gaymard, F., et al. (2014). Involvement of the ABCG37 transporter in secretion of scopoletin and derivatives by *Arabidopsis* roots in response to iron deficiency. *New Phytol.* 201, 155–167. doi: 10.1111/nph.12471
- Fourcroy, P., Tissot, N., Gaymard, F., Briat, J. F., and Dubos, C. (2016). Facilitated Fe nutrition by phenolic compounds excreted by the *Arabidopsis* ABCG37/PDR9 transporter requires the IRT1/FRO2 high-affinity root Fe(2+) transport system. *Mol. Plant* 9, 485–488. doi: 10.1016/j.molp.2015.09.010
- Gordan, R., Shen, N., Dror, I., Zhou, T., Horton, J., Rohs, R., et al. (2013). Genomic regions flanking E-box binding sites influence DNA binding specificity of bHLH transcription factors through DNA shape. *Cell Rep.* 3, 1093–1104. doi: 10.1016/j.celrep.2013.03.014
- Heim, M. A., Jakoby, M., Werber, M., Martin, C., Weisshaar, B., and Bailey, P. C. (2003). The basic helix-loop-helix transcription factor family in plants: a genome-wide study of protein structure and functional diversity. *Mol. Biol. Evol.* 20, 735–747. doi: 10.1093/molbev/msg088
- Hindt, M. N., Akmakjian, G. Z., Pivarski, K. L., Punshon, T., Baxter, I., Salt, D. E., et al. (2017). BRUTUS and its paralogs, BTS LIKE1 and BTS LIKE2, encode important negative regulators of the iron deficiency response in *Arabidopsis thaliana*. *Metallomics* 9, 876–890. doi: 10.1039/c7mt00152e

- Ivanov, R., Brumbarova, T., Blum, A., Jantke, A. M., Fink-Straube, C., and Bauer, P. (2014). SORTING NEXIN1 is required for modulating the trafficking and stability of the *Arabidopsis* IRON-REGULATED TRANSPORTER1. *Plant Cell* 26, 1294–1307. doi: 10.1105/tpc.113.116244
- Jakoby, M., Wang, H. Y., Reidt, W., Weisshaar, B., and Bauer, P. (2004). FRU (BHLH029) is required for induction of iron mobilization genes in *Arabidopsis thaliana*. *FEBS Lett.* 577, 528–534. doi: 10.1016/j.febslet.2004.10.062
- Jeong, J., and Connolly, E. L. (2009). Iron uptake mechanisms in plants: functions of the FRO family of ferric reductases. *Plant Sci.* 176, 709–714. doi: 10.1016/j.plantsci.2009.02.011
- Klatte, M., Schuler, M., Wirtz, M., Fink-Straube, C., Hell, R., and Bauer, P. (2009). The analysis of *Arabidopsis* nicotianamine synthase mutants reveals functions for nicotianamine in seed iron loading and iron deficiency responses. *Plant Physiol.* 150, 257–271. doi: 10.1104/pp.109.136374
- Kobayashi, T., Itai, R. N., Aung, M. S., Senoura, T., Nakanishi, H., and Nishizawa, N. K. (2012). The rice transcription factor IDEF1 directly binds to iron and other divalent metals for sensing cellular iron status. *Plant J.* 69, 81–91. doi: 10.1111/j.1365-313X.2011.04772.x
- Kobayashi, T., Itai, R. N., Ogo, Y., Kakei, Y., Nakanishi, H., Takahashi, M., et al. (2009). The rice transcription factor IDEF1 is essential for the early response to iron deficiency, and induces vegetative expression of late embryogenesis abundant genes. *Plant J.* 60, 948–961. doi: 10.1111/j.1365-313X.2009.04015.x
- Kobayashi, T., Nagasaka, S., Senoura, T., Itai, R. N., Nakanishi, H., and Nishizawa, N. K. (2013). Iron-binding haemerythrin RING ubiquitin ligases regulate plant iron responses and accumulation. *Nat. Commun.* 4:2792. doi: 10.1038/ncomms3792
- Le, C. T., Brumbarova, T., Ivanov, R., Stoof, C., Weber, E., Mohrbacher, J., et al. (2016). Zinc finger of *Arabidopsis thaliana* 12 (ZAT12) interacts with FER-LIKE Iron Deficiency-Induced Transcription Factor (FIT) linking iron deficiency and oxidative stress responses. *Plant Physiol.* 170, 540–557. doi: 10.1104/pp.15.01589
- Li, L., Gao, W., Peng, Q., Zhou, B., Kong, Q., Ying, Y., et al. (2018). Two soybean bHLH factors regulate response to iron deficiency. *J. Integr. Plant Biol.* 60, 608–622. doi: 10.1111/jipb.12651
- Li, X., Zhang, H., Ai, Q., Liang, G., and Yu, D. (2016). Two bHLH transcription factors, bHLH34 and bHLH104, regulate iron homeostasis in *Arabidopsis thaliana*. *Plant Physiol.* 170, 2478–2493. doi: 10.1104/pp.15.01827
- Liang, G., Zhang, H., Li, X., Ai, Q., and Yu, D. (2017). bHLH transcription factor bHLH115 regulates iron homeostasis in *Arabidopsis thaliana*. *J. Exp. Bot.* 68, 1743–1755. doi: 10.1093/jxb/erx043
- Ling, H. Q., Bauer, P., Berezcky, Z., Keller, B., and Ganai, M. (2002). The tomato fer gene encoding a bHLH protein controls iron-uptake responses in roots. *Proc. Natl. Acad. Sci. U.S.A.* 99, 13938–13943. doi: 10.1073/pnas.212448699
- Lingam, S., Mohrbacher, J., Brumbarova, T., Potuschak, T., Fink-Straube, C., Blondet, E., et al. (2011). Interaction between the bHLH transcription factor FIT and Ethylene Insensitive3/Ethylene Insensitive 3-Like1 reveals molecular linkage between the regulation of iron acquisition and ethylene signaling in *Arabidopsis*. *Plant Cell* 23, 1815–1829. doi: 10.1105/tpc.111.084715
- Liu, W., Karemera, N. J. U., Wu, T., Yang, Y., Zhang, X., Xu, X., et al. (2017a). The ethylene response factor AtERF4 negatively regulates the iron deficiency response in *Arabidopsis thaliana*. *PLoS One* 12:e0186580. doi: 10.1371/journal.pone.0186580
- Liu, W., Li, Q., Wang, Y., Wu, T., Yang, Y., Zhang, X., et al. (2017b). Ethylene response factor AtERF72 negatively regulates *Arabidopsis thaliana* response to iron deficiency. *Biochem. Biophys. Res. Commun.* 491, 862–868. doi: 10.1016/j.bbrc.2017.04.014
- Long, T. A., Tsukagoshi, H., Busch, W., Lahner, B., Salt, D. E., and Benfey, P. N. (2010). The bHLH transcription factor POPEYE regulates response to iron deficiency in *Arabidopsis* roots. *Plant Cell* 22, 2219–2236. doi: 10.1105/tpc.110.074096
- Maurer, F., Naranjo Arcos, M. A., and Bauer, P. (2014). Responses of a triple mutant defective in three iron deficiency-induced Basic Helix-Loop-Helix genes of the subgroup Ib(2) to iron deficiency and salicylic acid. *PLoS One* 9:e99234. doi: 10.1371/journal.pone.0099234
- Naranjo-Arcos, M. A., Maurer, F., Meiser, J., Pateyron, S., Fink-Straube, C., and Bauer, P. (2017). Dissection of iron signaling and iron accumulation by over expression of subgroup Ib bHLH039 protein. *Sci. Rep.* 7:10911. doi: 10.1038/s41598-017-11171-7
- Nozoye, T., Nagasaka, S., Kobayashi, T., Takahashi, M., Sato, Y., Uozumi, N., et al. (2011). Phytosiderophore efflux transporters are crucial for iron acquisition in graminaceous plants. *J. Biol. Chem.* 286, 5446–5454. doi: 10.1074/jbc.M110.180026
- Ogawa, S., Kawahara-Miki, R., Miyamoto, K., Yamane, H., Nojiri, H., Tsujii, Y., et al. (2017). OsMYC2 mediates numerous defence-related transcriptional changes via jasmonic acid signalling in rice. *Biochem. Biophys. Res. Commun.* 486, 796–803. doi: 10.1016/j.bbrc.2017.03.125
- Ogo, Y., Itai, R. N., Nakanishi, H., Kobayashi, T., Takahashi, M., Mori, S., et al. (2007). The rice bHLH protein OsIRO2 is an essential regulator of the genes involved in Fe uptake under Fe-deficient conditions. *Plant J.* 51, 366–377. doi: 10.1111/j.1365-313X.2007.03149.x
- Ogo, Y., Kobayashi, T., Nakanishi Itai, R., Nakanishi, H., Kakei, Y., Takahashi, M., et al. (2008). A novel NAC transcription factor, IDEF2, that recognizes the iron deficiency-responsive element 2 regulates the genes involved in iron homeostasis in plants. *J. Biol. Chem.* 283, 13407–13417. doi: 10.1074/jbc.M708732200
- O'Hara, G. (2001). Nutritional constraints on root nodule bacteria affecting symbiotic nitrogen fixation: a review. *Anim. Prod. Sci.* 41, 417–433. doi: 10.1071/EA00087
- Palmer, C. M., Hindt, M. N., Schmidt, H., Clemens, S., and Guerinot, M. L. (2013). MYB10 and MYB7 are required for growth under iron-limiting conditions. *PLoS Genet.* 9:e1003953. doi: 10.1371/journal.pgen.1003953
- Rampey, R. A., Woodward, A. W., Hobbs, B. N., Tierney, M. P., Lahner, B., Salt, D. E., et al. (2006). An *Arabidopsis* basic helix-loop-helix leucine zipper protein modulates metal homeostasis and auxin conjugate responsiveness. *Genetics* 174, 1841–1857. doi: 10.1534/genetics.106.061044
- Rodriguez-Celma, J., Green, R. T., Connorton, J. M., Kruse, I., Cui, Y., Ling, H. Q., et al. (2018). BRUTUS-LIKE proteins moderate the transcriptional response to iron deficiency in roots. *bioRxiv* [Preprint]. doi: 10.1101/231365
- Samira, R., Li, B., Kliebenstein, D., Li, C., Davis, E., Gillikin, J. W., et al. (2018). The bHLH transcription factor ILR3 modulates multiple stress responses in *Arabidopsis*. *Plant Mol. Biol.* doi: 10.1007/s11103-018-0735-8 [Epub ahead of print].
- Selote, D., Samira, R., Matthiadis, A., Gillikin, J. W., and Long, T. A. (2015). Iron-binding E3 ligase mediates iron response in plants by targeting basic helix-loop-helix transcription factors. *Plant Physiol.* 167, 273–286. doi: 10.1104/pp.114.250837
- Shen, C., Yue, R., Sun, T., Zhang, L., Yang, Y., and Wang, H. (2015). OsARF16, a transcription factor regulating auxin redistribution, is required for iron deficiency response in rice (*Oryza sativa* L.). *Plant Sci.* 231, 148–158. doi: 10.1016/j.plantsci.2014.12.003
- Sivitz, A., Grinvalds, C., Barberon, M., Curie, C., and Vert, G. (2011). Proteasome-mediated turnover of the transcriptional activator FIT is required for plant iron-deficiency responses. *Plant J.* 66, 1044–1052. doi: 10.1111/j.1365-313X.2011.04565.x
- Stringlis, I. A., Yu, K., Feussner, K., de Jonge, R., Van Bentum, S., Van Verk, M. C., et al. (2018). MYB72-dependent coumarin exudation shapes root microbiome assembly to promote plant health. *Proc. Natl. Acad. Sci. U.S.A.* 115, E5213–E5222. doi: 10.1073/pnas.1722335115
- Tanabe, N., Noshi, M., Mori, D., Nozawa, K., Tamoi, M., and Shigeoka, S. (2018). The basic helix-loop-helix transcription factor, bHLH11 functions in the iron-uptake system in *Arabidopsis thaliana*. *J. Plant Res.* doi: 10.1007/s10265-018-1068-z [Epub ahead of print].
- Tang, C., Robson, A., and Dilworth, M. J. (1990). The role of iron in nodulation and nitrogen fixation in *Lupinus angustifolius* L. *New Phytol.* 114, 173–182. doi: 10.1111/j.1469-8137.1990.tb00388.x
- Wang, F. P., Wang, X. F., Zhang, J., Ma, F., and Hao, Y. J. (2018). MdMYB58 modulates Fe homeostasis by directly binding to the MdMATE43 promoter in plants. *Plant Cell Physiol.* 59, 2476–2489. doi: 10.1093/pcp/pcy168
- Wang, H. Y., Klatte, M., Jakoby, M., Baumlein, H., Weisshaar, B., and Bauer, P. (2007). Iron deficiency-mediated stress regulation of four subgroup Ib bHLH genes in *Arabidopsis thaliana*. *Planta* 226, 897–908. doi: 10.1007/s00425-007-0535-x
- Wang, L., Ying, Y., Narsai, R., Ye, L., Zheng, L., Tian, J., et al. (2013). Identification of OsbHLH133 as a regulator of iron distribution between roots and shoots in *Oryza sativa*. *Plant Cell Environ.* 36, 224–236. doi: 10.1111/j.1365-3040.2012.02569.x

- Wang, N., Cui, Y., Liu, Y., Fan, H., Du, J., Huang, Z., et al. (2013). Requirement and functional redundancy of Ib subgroup bHLH proteins for iron deficiency responses and uptake in *Arabidopsis thaliana*. *Mol. Plant* 6, 503–513. doi: 10.1093/mp/sss089
- Xu, W., Dubos, C., and Lepiniec, L. (2015). Transcriptional control of flavonoid biosynthesis by MYB-bHLH-WDR complexes. *Trends Plant Sci.* 20, 176–185. doi: 10.1016/j.tplants.2014.12.001
- Yan, J. Y., Li, C. X., Sun, L., Ren, J. Y., Li, G. X., Ding, Z. J., et al. (2016). A WRKY transcription factor regulates Fe translocation under Fe deficiency. *Plant Physiol.* 171, 2017–2027. doi: 10.1104/pp.16.00252
- Yuan, Y., Wu, H., Wang, N., Li, J., Zhao, W., Du, J., et al. (2008). FIT interacts with AtbHLH38 and AtbHLH39 in regulating iron uptake gene expression for iron homeostasis in *Arabidopsis*. *Cell Res.* 18, 385–397. doi: 10.1038/cr.2008.26
- Zamioudis, C., Hanson, J., and Pieterse, C. M. (2014). beta-Glucosidase BGLU42 is a MYB72-dependent key regulator of rhizobacteria-induced systemic resistance and modulates iron deficiency responses in *Arabidopsis* roots. *New Phytol.* 204, 368–379. doi: 10.1111/nph.12980
- Zhang, H., Li, Y., Yao, X., Liang, G., and Yu, D. (2017). Positive regulator of iron homeostasis1, OsPRI1, facilitates iron homeostasis. *Plant Physiol.* 175, 543–554. doi: 10.1104/pp.17.00794
- Zhang, J., Liu, B., Li, M., Feng, D., Jin, H., Wang, P., et al. (2015). The bHLH transcription factor bHLH104 interacts with IAA-LEUCINE RESISTANT3 and modulates iron homeostasis in *Arabidopsis*. *Plant Cell* 27, 787–805. doi: 10.1105/tpc.114.132704
- Zhang, Y., Wu, H., Wang, N., Fan, H., Chen, C., Cui, Y., et al. (2014). Mediator subunit 16 functions in the regulation of iron uptake gene expression in *Arabidopsis*. *New Phytol.* 203, 770–783. doi: 10.1111/nph.12860
- Zhao, Q., Ren, Y. R., Wang, Q. J., Wang, X. F., You, C. X., and Hao, Y. J. (2016a). Ubiquitination-related MdbT scaffold proteins target a bHLH transcription factor for iron homeostasis. *Plant Physiol.* 172, 1973–1988. doi: 10.1104/pp.16.01323
- Zhao, Q., Ren, Y. R., Wang, Q. J., Yao, Y. X., You, C. X., and Hao, Y. J. (2016b). Overexpression of MdbHLH104 gene enhances the tolerance to iron deficiency in apple. *Plant Biotechnol. J.* 14, 1633–1645. doi: 10.1111/pbi.12526
- Zheng, L., Ying, Y., Wang, L., Wang, F., Whelan, J., and Shou, H. (2010). Identification of a novel iron regulated basic helix-loop-helix protein involved in Fe homeostasis in *Oryza sativa*. *BMC Plant Biol.* 10:166. doi: 10.1186/1471-2229-10-166
- Zhou, L. J., Zhang, C. L., Zhang, R. F., Wang, G. L., Li, Y. Y., and Hao, Y. J. (2018). The SUMO E3 ligase MdSIZ1 targets MdbHLH104 to regulate plasma membrane H<sup>+</sup>-ATPase activity and iron homeostasis. *Plant Physiol.* 179, 88–106. doi: 10.1104/pp.18.00289

**Conflict of Interest Statement:** The authors declare that the research was conducted in the absence of any commercial or financial relationships that could be construed as a potential conflict of interest.

Copyright © 2019 Gao, Robe, Gaymard, Izquierdo and Dubos. This is an open-access article distributed under the terms of the Creative Commons Attribution License (CC BY). The use, distribution or reproduction in other forums is permitted, provided the original author(s) and the copyright owner(s) are credited and that the original publication in this journal is cited, in accordance with accepted academic practice. No use, distribution or reproduction is permitted which does not comply with these terms.